Technische Universität Kaiserslautern

Fachbereich Chemie

Hydroamidierung und Carboxylierung terminaler Alkine

Entwicklung effizienter Katalysatorsysteme, Anwendung in der Naturstoffsynthese und mechanistische Studien

vom Fachbereich Chemie der Technischen Universität Kaiserslautern zur Verleihung des akademischen Grades

„Doktor der Naturwissenschaften“

D 386

genehmigte Dissertation

vorgelegt von

Dipl.-Chem. Matthias Arndt

angefertigt im Arbeitskreis von

Prof. Dr. Lukas J. Gooßen

Termin der wissenschaftlichen Aussprache: Freitag, 08. Juni 2012

Für meine Frau

Inga

"Auch aus Steinen, die einem in den Weg gelegt werden, kann man Schönes bauen."

Johann Wolfgang von Goethe

Die vorliegende Arbeit wurde im Zeitraum von Februar 2009 bis Mai 2012 im Arbeitskreis von Prof. Dr. Lukas J. Gooßen am Fachbereich Chemie der Technischen Universität Kaiserslautern angefertigt.

Promotionskommission

Vorsitzender: Prof. Dr. H. Sitzmann

Berichterstatter: Prof. Dr. L. J. Gooßen

Berichterstatter: Prof. Dr. Dr. G. Niedner-Schatteburg

Termin der wissenschaftlichen Aussprache: Freitag, 08. Juni 2012

Eidesstattliche Erklärung

Hiermit versichere ich, dass ich die vorliegende Arbeit eigenständig verfasst und keine anderen als die angegebenen Quellen und Hilfsmittel verwendet, sowie Literaturzitate kenntlich gemacht habe. Kooperationsprojekte sind ausdrücklich als solche gekennzeichnet und die Mitarbeiter genannt. Die Arbeit liegt weder in gleicher noch in ähnlicher Form in einem anderen Prüfungsverfahren vor.

Kaiserslautern, den_____ _____

Matthias Arndt

Danksagung

Herrn Prof. Dr. Lukas J. Gooßen gebührt mein großer Dank für die interessanten Aufgabenstellungen, seine kompetente Betreuung und ambitionierte Förderung, die lehrreiche Zusammenarbeit und die großen Freiräume bei der Bearbeitung der Themen. Für das entgegengebrachte Vertrauen und die Unterstützung bin ich Herrn Gooßen sehr verbunden.

Dr. Käthe Gooßen danke ich für die unentbehrliche Hilfestellung beim Anfertigen wissenschaftlicher Texte und für das Korrekturlesen vieler Manuskripte und Anträge.

Herrn Prof. Dr. Dr. Gereon Niedner-Schatteburg danke ich für das Erstellen des Zweitgutachtens, die erfolgreiche und stets motivierende Zusammenarbeit bei den mechanistischen Arbeiten sowie der Geduld und Wertschätzung bei der gemeinsamen Beantragung des SFB. Der gesamten Clustergruppe danke ich für die stets freundliche und tatkräftige Unterstützung während meiner Promotion. Besonders Fabian Menges, Lars Barzen und Frau Hilde Seelos danke ich für die Durchführung der ESI-MS-Messungen und die Hilfe bei der SFB-Organisation.

Herrn Prof. Dr. Helmut Sitzmann danke ich herzlich für die Übernahme des Prüfungsvorsitzes und die Unterstützung während meiner Diplomarbeit.

Dem gesamten Arbeitskreis Gooßen danke ich für die gute Zusammenarbeit. Besonders hervorheben möchte ich Martin Rudzki, Andreas Fromm, Annette Buba, Corneliu Stanciu, Patrizia Mamone, Christian Kerner, Bingrui Song, Wojciech Dzik, Florence Collet, Mathieu Blanchot, Bettina Zimmermann, Matthias Grünberg, Sabrina Baader und Christoph Oppel, die mir immer hilfreich zur Seite standen und durch ihre nette und freundschaftliche Art mir die tägliche Arbeit erleichtert haben.

Meiner Frau Inga und Herrn Andreas Fromm danke ich für das Korrekturlesen dieser Arbeit.

Den Mitarbeitern der anderen beiden Arbeitskreise der organischen Chemie, deren Gruppenleitern Prof. Dr. Ing. Jens Hartung und Prof. Dr. Stefan Kubik, der ehemaligen Sekretärin Edith Müller und der jetzigen Sekretärin Frau Zeigner danke ich für die

problemlose und hilfreiche Zusammenarbeit und den stets respektvollen und freundlichen Umgang.

Christiane Müller und Harald Kelm danke ich für das Messen der Magnetresonanzspektren und der Analytikabteilung, Frau Biel, Frau Dusch, Frau Ellmer und Frau Bergsträßer, für die Elementaranalysen und HRMS-Analysen. Den Mitarbeitern der Chemikalienausgabe, Ludvik Napast, Jürgen Rahm und Frank Schröer sowie Herrn Tömör und Frau Eggert von der Glasbläserei danke ich für die Versorgung mit Chemikalien und Glasgeräten und für den stets hilfsbereiten und herzlichen Umgang. Frau Heike Schramm danke ich für die Unterstützung bei allen organisatorischen Angelegenheiten.

Meiner ehemaligen Diplomandin Annette Buba und meinen Forschungspraktikanten Eugen Risto, Thilo Krause, Sandra Schäfer, Alexander Jones und Christian Matheis und meinen Studienprojektteilnehmerinnen Stephanie Brühl und Maike Weiland danke ich für die tatkräftige Unterstützung bei der Bearbeitung der Forschungsprojekte und die tolle Atmosphäre im Labor.

Meiner Familie und meinen Freunden danke ich für die Unterstützung und für den Rückhalt. Ohne dieses Vertrauen, die aufmunternden und motivierenden Worte und kleinen entscheidenden Gesten hätte ich diese Arbeit wohl nicht zu einem erfolgreichen Ende gebracht.

Für die finanzielle Unterstützung bedanke ich mich bei der Stipendienstiftung des Landes Rheinland-Pfalz, der BASF SE, der Deutschen Forschungsgemeinschaft und der Umicore AG & Co. KG.

Abkürzungsverzeichnis

Ac	Acetyl	[Kat.]	Katalysator
AcOH	Essigsäure	L	Ligand
AgI	Silberiodid	LDA	Lithiumdiisopropylamid
$AgBF_4$	Silbertetrafluoroborat	LM	Lösungsmittel
$AgNO_3$	Silbernitrat	MALDI	Matrix-unterstützte Laser-Desorption/
Äquiv.	Äquivalent		Ionisation
Ar	Arylrest	MeCN	Acetonitril
BASF	Badische Anilin- & Soda-Fabrik	Me	Methyl
BOC	Di-*tert*-butyldicarbonat	MeOH	Methanol
Bz	Benzoyl	Mes	Mesityl
CID	collision-induced dissociation	NVP	*N*-Vinylpyrrolidon
COD/cod	1,5-Cyclooctadien	^{n}Bu	*n*-Butyl
Cy	Cyclohexyl	NHC	*N*-heterocyclischer Carbenligand
CuCl	Kupfer(I)chlorid	NMP	*N*-Methyl-2-pyrrolidon
CuCN	Kupfer(I)cyanid	^{n}Pr	*n*-Propyl
CuI	Kupfer(I)iodid	Nu	Nukleophil
δ	Chemische Verschiebung	org.	organisch
DCM	Dichlormethan	O^{t}Bu	*tert*.-Butanolat
DBN	1,5-Diazabicyclo(4.3.0)non-5-en	PCy_3	Tricyclohexylphosphin
DBU	1,8-Diazabicyclo[5.4.0]undec-7-en	P$^{n}Bu_3$	Tri-*n*-butylphosphin
DMAC	*N*,*N*-Dimethylacetamid	Ph	Phenyl
DMAP	4-*N*,*N*-Dimethylaminopyridin	P(*p*-F-C6H4)	Tris(4-Fluorophenyl)phosphin
DMF	*N*,*N*-Dimethylformamid	PPh_3	Triphenylphosphin
DCYPB	Bis(dicyclohexylphosphino)butan	ppm	parts per million
DMSO	Dimethylsulfoxid	PVP	Polyvinylpyrrolidon
Et	Ethyl	R	organischer Rest
GC	Gaschromatograph	RT	Raumtemperatur
GBL	γ-Butyrolacton	$(cod)Ru(met)_2$	Bis(2-methallyl)(cyclookta-1,5-dien) Ruthenium(II)
^{n}Hex	*n*-Hexyl	^{t}Bu	*tert*-Butyl
HEP	*N*-Hydroxyethylpyrrolidon	TFA	Trifluoressigsäure
HIV	Humane Immundefizienz-Virus	THF	Tetrahydrofuran
HTP	Hochtemperatur-Pyrolyse	TMEDA	*N*,*N*,*N*',*N*'-Tetramethylethylendiamin
i. Vak.	im Vakuum	TMS	Trimethylsilyl
^{i}Pr	Isopropyl	TOF	Massenspektrometrie mit Flugzeitanalysator
IPr	1,3-Bis(2,6-diisopropylphenyl)-	Tol.	Toluol
	imidazol-2-yliden	Tos	4-Tolylsulfonyl
J	Kopplungskonstante	X	Halogenid

Nummerierung der Verbindungen

Die vorliegende Arbeit besteht zu einem großen Teil aus originalen Veröffentlichungstexten, in denen alle vorkommenden Verbindungen unabhängig voneinander nummeriert wurden. Alle nicht aus originalen Veröffentlichungstexten stammenden Verbindungen wurden daher auch in jedem Kapiteln neu nummeriert. Die Bezeichnung setzt sich jeweils zusammen aus der Nummer der zweiten Überschriftsebene und einer durchlaufenden Nummer. Beispielsweise trägt die 2. Verbindung aus Kapitel III.1 die Nummer **III.1-2**. Für stark verallgemeinerte Strukturen aus Schemata, die z.B. Reaktionsprinzipien verdeutlichen, wurde auf eine Nummerierung verzichtet. Alle Zwischenstufen aus Katalysezyklen wurden mit römischen Zahlen bezeichnet und die Nummerierung nur für das jeweilige Kapitel fortlaufend weitergeführt. Um Doppelbenennungen vor allem im experimentellen Teil zu vermeiden, wurden die Verbindungen mit einem Kürzel des Fachjournals und der publizierten Nummer bezeichnet. Beispielsweise bezeichnet **JACS-3a** die Verbindung **3a** aus dem Journal of the American Chemical Society.

Veröffentlichungen

Einige Ergebnisse dieser Arbeit wurden bereits in folgenden Publikationen veröffentlicht:

I. L. J. Gooßen, M. Blanchot, M. Arndt, K. S. M. Salih, *Synlett* **2010**, 1685-1687: *Synthesis of Botryllamides and Lansiumamides via Ruthenium-Catalyzed Hydroamidation of Alkynes.*

II. A. E. Buba, M. Arndt, L. J. Gooßen, *J. Organomet. Chem.* **2011**, *696*, 170-178: *Z-Selective Hydroamidation of Terminal Alkynes with Secondary Amides and Imides Catalyzed by a Ru/Yb-System.*

III. M. Arndt, K. S. M. Salih, A. Fromm, L. J. Goossen, F. Menges, G. Niedner-Schatteburg, *J. Am. Chem. Soc.* **2011**, *133*, 7428-7449: *Mechanistic Investigation of the Ru-Catalyzed Hydroamidation of Terminal Alkynes*.

IV. M. Arndt, E. Risto, T. Krause, L. J. Gooßen, *ChemCatChem* **2012**, *4*, 484-487: *C–H Carboxylation of Terminal Alkynes Catalyzed by Low Loadings of Silver(I)/DMSO at Ambient CO_2 Pressure.*

V. M. Arndt, L. J. Gooßen, *Chem. Rev.* **2012**, *Manuskript in Bearbeitung*: *Ruthenium-catalyzed hydroamination and hydroamidation reactions: atom-economic and environmentally benign processes*.

Patente

Ergebnisse aus Forschungs- und Entwicklungs- Kooperationen mit der Umicore AG & Co. KG und der BASF SE wurden in den folgenden Patenten veröffentlicht:

I. L. J. Gooßen, M. Arndt, P. Mamone, M. F. Grünberg, *Patentanmeldung*, **2011**: *Method for the preparation of a palladium catalyst dimer and process for its use in isomerization reactions*.

II. Patentanmeldung mit der BASF SE in Bearbeitung.

Inhaltsverzeichnis

I. Struktur der Doktorarbeit

Die vorliegende kumulative Doktorarbeit gliedert sich in zwei große Themengebiete auf; die Ruthenium-katalysierte Hydroamidierung und die Silber-katalysierte Carboxylierung terminaler Alkine. Aufgrund der kumulativen Promotionsform enthält diese Ausarbeitung vier englische Originaltexte sowie einen Manuskriptentwurf eigener wissenschaftlicher Veröffentlichungen und ergänzende deutschsprachige Passagen, die die Publikationen thematisch miteinander verbinden und wichtige, unveröffentlichte Ergebnisse darlegen.

In der Einleitung werden Alkine als wertvolle Startmaterialien für die organische Synthese eingeführt und ihre traditionelle Reaktivität, Vorkommen und Herstellung beschrieben (Kap. II.1). Anschließend werden nacheinander die Hydroamidierung (Kap. II.2) und die Carboxylierung (Kap. II.3) terminaler Alkine als moderne atomökonomische Methoden zur Synthese von Enamiden und Propiolsäurederivaten vorgestellt und deren Vorkommen, Anwendungen sowie traditionelle Herstellungsverfahren diskutiert. Der Stand der Forschung bezüglich Hydroamidierungs- und Carboxylierungsreaktionen terminaler Alkine sowie deren Vorteile gegenüber traditionellen Synthesewegen werden beschrieben und aufbauend auf den verbleibenden Schwachpunkten bestehender Katalysatorsysteme die Motivation für das Projekt vermittelt und die Aufgabenstellung (Kap. III) dieser Doktorarbeit abgeleitet.

Im Ergebnis- und Diskussionsteil werden die im Rahmen dieser Arbeit erzielten Fortschritte in der Ruthenium-katalysierten Hydroamidierung und der Silber-katalysierten Carboxylierung terminaler Alkine getrennt voneinander vorgestellt und kritisch diskutiert. Es werden die Ergebnisse umfassender mechanistischer Studien präsentiert (Kap. IV.1.1) und die Entwicklungen effizienterer Katalysatorsysteme (Kap. IV.1.2 und IV.2.1-2) und deren Anwendung für die Naturstoffsynthese (Kap. IV.1.3) bzw. der großtechnischen Synthese einer wichtigen Basischemikalie (Kap. IV.2.3) beschrieben. Die beiden Themengebiete werden in Kapitel V zusammengefasst und es werden Vorschläge für zukünftige Arbeiten vorgestellt.

Der experimentelle Teil (Kap. VI) enthält alle verwendeten Versuchsvorschriften, vollständige Charakterisierungen der erhaltenen Verbindungen sowie sämtliche spektroskopischen Daten und die Spezifikationen eingesetzter Messinstrumente. Das Kapitel wurde auf Englisch verfasst, da es zum größten Teil aus dem Material der englischsprachigen Supporting Information besteht.

II. Einleitung

II.1. Die Chemie der Alkine

Alkine gehören den chemischen Verbindungen der aliphatischen Kohlenwasserstoffe an, die mindestens eine C-C-Dreifachbindung als charakteristische funktionelle Gruppe im Molekül tragen.[1] Die Alkine bilden eine homologe Reihe mit der allgemeinen Summenformel C_nH_{2n-2} (mit n = 2, 3, 4, ...), derselben wie für Cycloalkene. Alkine werden häufig noch mit Trivalnamen benannt, z. B. Acetylen für Ethin, das einfachste Alkin der homologen Reihe mit der Summenformel C_2H_2, oder als Derivate von Acetylen mit z. B. Phenylacetylen.

II.1.1. Vorkommen, Verwendung und Herstellung von Alkinen

Vorkommen von Alkinen

Alkine kommen in der Natur nicht sehr häufig vor; man spricht von etwas mehr als 1000 bekannten Verbindungen, bei denen es sich vorwiegend um Polyine handelt. Nur wenige davon sind physiologisch aktiv (Abbildung 1).[2]

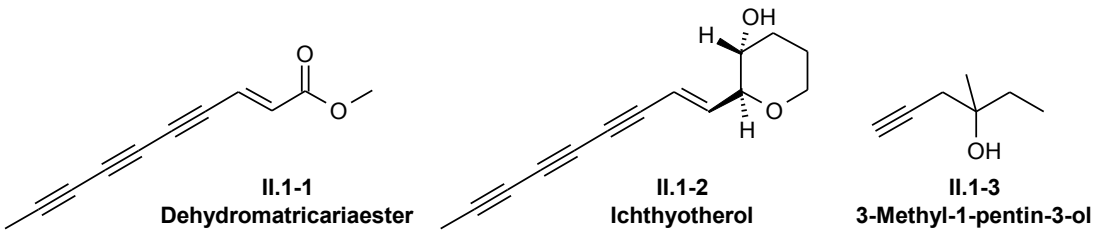

II.1-1 Dehydromatricariaester | **II.1-2** Ichthyotherol | **II.1-3** 3-Methyl-1-pentin-3-ol

Abbildung 1. Beispiele natürlich vorkommender Alkine und für Alkine als Wirkstoff.

Im Jahr 1826 konnte Bohlmann mit Dehydromatricariaester (**II.1-1**) erstmals ein natürliches Alkin aus einer *Artemisia*-Spezies isolieren. Daraufhin wurden weitere Alkine isoliert, die meistens Wirkung als Fungizid, Verteidigungsgift oder Schleimhautreizstoff zeigten. Ichthyotherol (**II.1-2**) ist ein natürlich vorkommendes Alkin, das bei Säugetieren Krämpfe verursacht und daher von Indianern des Niederen Amazonasbecken als Pfeilgift eingesetzt wurde. Durch die synthetische Einbettung von Dreifachbindungen in medizinische

Wirkstoffe kann oft die Aufnahme in den Körper erleichtert werden. So findet 3-Methyl-1-pentin-3-ol (**II.1-3**) in den USA Anwendung als rezeptfreies Schlafmittel.[1]

Ethin hat kein natürliches Vorkommen auf der Erde, konnte jedoch in der Atmosphäre des Jupiter und im intergalaktischen Raum nachgewiesen werden. Es wurde erstmals 1836 von Edmund Davy als Nebenprodukt bei der Herstellung metallischen Kaliums beobachtet. Mittels Umsetzung von Calciumcarbid mit Wasser gelang Friedrich Wöhler 1862 die erste gezielte Synthese von Ethin, und noch im gleichen Jahr konnte Pierre Eugène Marcelin Berthelot Ethin erfolgreich aus den Elementen synthetisieren.[3]

Anwendung von Alkinen

Ethin und Propin sind die einzigen Alkine, die eine direkte Verwendung in der Industrie finden. Aufgrund ihrer hohen Verbrennungstemperaturen von bis zu 3100 °C werden Sie unter anderem zum autogenen Schneiden und Schweißen von Stahlteilen benutzt.

Ethin zählte lange Zeit zu den wichtigsten Grundstoffen der industriellen organischen Chemie (siehe Kap. II.1.3, Reppe-Chemie), bis die Petrochemie leichter zugängliche und damit preiswertere Ausgangsstoffe verfügbar machte. In kürzester Zeit wurde die Produktion zahlreicher industrieller Basisprodukte ausgehend von Ethin auf Olefine wie z. B. Ethen, Propen und Butadien umgestellt.[1]

Es wird prognostiziert, dass die Erdölreserven im Laufe des 21. Jahrhundert erschöpft sein werden, sodass Ethin wieder zu einem der wichtigsten Rohstoffe der chemischen Industrie werden könnte. Ethin kann im Gegensatz zu den genannten Olefinen direkt aus Kohle oder Koks hergestellt werden. Die Kohlereserven sind deutlich größer als die Erdölreserven und sollten daher weit über das 21. Jahrhundert hinaus zur Verfügung stehen.[1]

Für viele Prozesse ist Ethin auch heute noch von großer Bedeutung. So wird es z. B. zur Herstellung von Butan-1,4-diol, sowie von Vinylester und -ether höherer Alkohole, zum Härten von Stahl und ausgehend von Ethin-Ruß in Batterien verwendet. Ethin wird als Dissousgas in Stahlflaschen verkauft, die mit porösen Massen (Bimsstein) sowie mit Aceton befüllt sind.[3]

Herstellung von Alkinen

Ethin kann heute besonders effektiv aus Leichtbenzin bzw. Rohöl durch das Hochtemperatur-Pyrolyse-Verfahren (HTP-Verfahren) hergestellt werden. Dieses zweistufige Verfahren wurde von der Firma Hoechst entwickelt und wird seit 1960 angewendet. Durch

rasches Erhitzen in einem Wärmeträgergas von ca. 2500 °C Anfangstemperatur wird das Leichtbenzin oder Rohöl gecrackt und nach lediglich 2 ms Verweilzeit bei einer Spaltendtemperatur von 1300 °C durch Eindüsen von Spaltöl auf 300 °C gequencht.[4] Das älteste großtechnische Herstellungsverfahren von Ethin verläuft über Calciumcarbid. Durch Umsetzung von Koks und Calciumoxid bei ca. 2000 °C entsteht Calciumcarbid, das durch Reaktion mit Wasser bei Raumtemperatur zu Ethin und Calciumhydroxid umgesetzt werden kann.[5] Ausgehend von Kohle kann Ethin durch Umsetzung mit Wasserstoff in einem elektrischen Lichtbogen bei einigen tausend Grad hergestellt werden.[1] Ferner kann Ethin durch Dimerisierung und Dehydrierung von Methan oder durch partielle Methanoxidation dargestellt werden.

Propin kann durch Dehydrohalogenierung von Dihalogenpropanen oder durch Isomerisierung von Allenen hergestellt werden, außerdem kann es aus der C3-Fraktion von Crackgasen gewonnen werden.[6]

Alle höheren Alkine **II.1-6** können durch eine Reaktionsfolge aus Halogenierung und doppelter Dehydrohalogenierung von Olefinen **II.1-4** oder durch Alkylierung von Alkinyl-Anionen **II.1-10** dargestellt werden (Schema 1).[1]

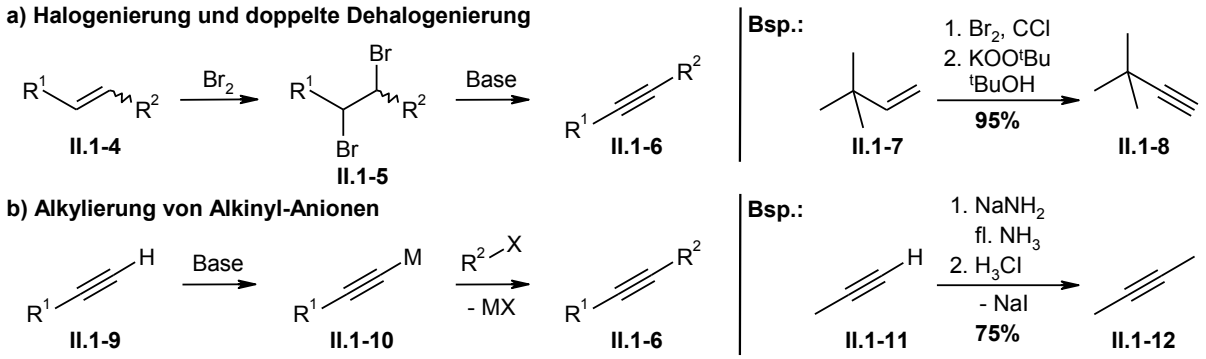

Schema 1. Darstellung von Alkinen II.1-6 durch Halogenierung und doppelte Dehydrohalogenierung oder Alkylierung von Alkinyl-Anionen II.1-10.

II.1.2. Physikalische und chemische Eigenschaften von Alkinen

Ab 2-Butin (Sdp. 27 °C) sind Alkine bei Raumtemperatur flüssige destillierbare Verbindungen. Ethin, Propin (Sdp. -23.2 °C) und 1-Butin (Sdp. 8.1 °C) liegen gasförmig vor, wobei Ethin keinen Siedepunkt besitzt und bei -84 °C sublimiert. Die physikalischen und chemischen Eigenschaften der Alkine werden durch die Dreifachbindung und deren sp-Hybridisierung bestimmt (Abbildung 2).[1]

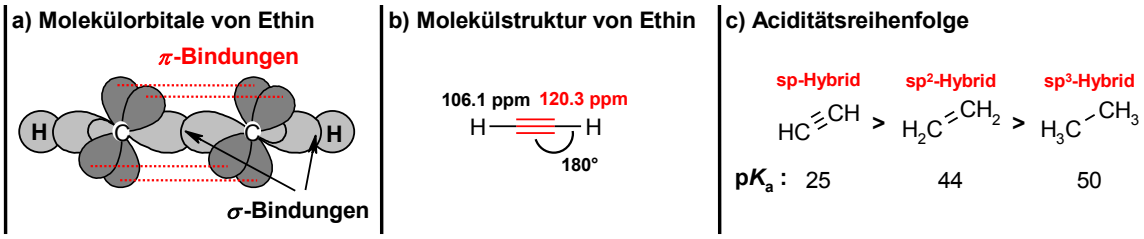

Abbildung 2. Physikalische und chemische Eigenschaften von Ethin.

Alkine zeichnen sich durch eine starke Bindung, eine lineare Struktur, eine verhältnismäßig hohe Acidität der C(sp)-H-Bindung terminaler Alkine und die Ausbildung von Dipolmomenten in asymmetrischen Alkinen aus.

Die C-C-Dreifachbindung ist aufgrund der beiden π-Bindungen extrem stark (Dissoziationsenergie von Ethin, $\Delta H°$ = 962 kJ/mol) und gleichzeitig sehr elektronenreich, wodurch sie leicht mit Elektrophilen reagieren kann.

Die relativ hohe Acidität der C(sp)-H-Bindung ermöglicht die Deprotonierung in Gegenwart starker Basen (z. B. Natriumamid oder Alkyllithiumverbindungen) zum entsprechendem Alkinyl-Anion, das als Nukleophil weiter umgesetzt werden kann.

II.1.3. Klassische Reaktivität von Alkinen

Alkine sind wertvolle Ausgangsverbindungen für die organische Synthese und können auf vielerlei Wegen umgesetzt werden. In Schema 2 sind die vier klassischen Reaktionstypen von Alkinen allgemein dargestellt.[1]

Alkine **II.1-6** können vollständig zu Alkanen **II.1-13** oder partiell zu Alkenen **II.1-14** und **II.1-15** hydriert werden (Schema 2, Reaktionstypen 1a-c). In Gegenwart von Platin oder Palladium auf Aktivkohle können Alkine **II.1-6** analog zu Alkenen durch Einleiten von Wasserstoff zu den entsprechenden Alkanen **II.1-13** umgesetzt werden. Durch Verwendung weniger aktiver Lindlar-Katalysatoren ist es möglich die Hydrierung gezielt auf der Stufe des Alkens zu stoppen, wobei diastereoselektiv das *Z*-Alken **II.1-14** hergestellt werden kann, da diese Reaktion *syn*-selektiv verläuft. Das *E*-Alken **II.1-15** kann selektiv aus Alkinen **II.1-6** durch doppelte Ein-Elektronen-Reduktion mit Natrium in flüssigem Ammoniak dargestellt werden.

Es gibt zahlreiche Möglichkeiten Alkine **II.1-6** mit elektrophilen Reagenzien umzusetzen (Schema 2, Reaktionstypen 2a-e). Alkine **II.1-6** reagieren mit Halogenwasserstoffen über Vinylhalogenide **II.1-16** zu C(n),C(n)-Dihalogen-substituierten Alkanen **II.1-17**. Mit

Halogenen reagieren sie über *trans*-Dihalogenalkene **II.1-18** zu vierfach Halogen-substituierten Alkanen **II.1-19**. Im Gegensatz zu Alkenen reagieren Alkine trotz der höheren Elektronendichte der Dreifachbindung deutlich langsamer, weil das intermediär gebildete Vinyl-Kation deutlich instabiler ist als ein Carbenium-Ion. So ist es möglich Doppelbindungen selektiv in Gegenwart einer Dreifachbindung mit Halogenen oder Halogenwasserstoffen umzusetzen.

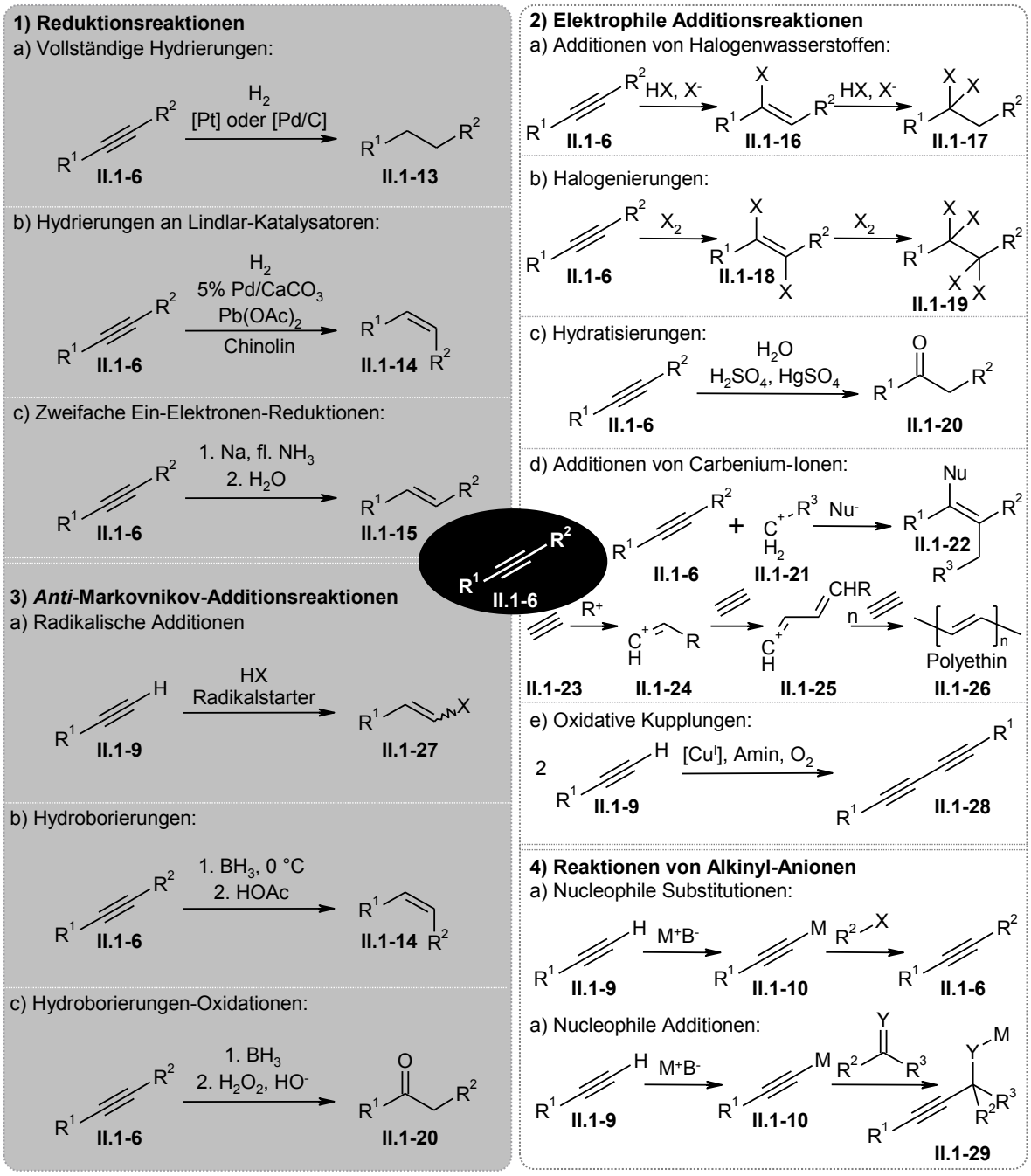

Schema 2. Übersicht der klassischen Reaktionstypen von Alkinen.

Traditionelle Hydratisierungen von Alkinen **II.1-6** verlaufen in Gegenwart von Quecksilbersulfat Markovnikov-selektiv unter Bildung von Ketonen **II.1-20**. Carbenium-Ionen **II.1-21** addieren ebenfalls Markovnikov-selektiv an Alkine **II.1-6**, wobei erneut intermediär ein Carbenium-Ion generiert wird. Dieses kann entweder mit einem Nukleophil abgefangen werden oder mit weiteren Alkinen **II.1-6** zu Polymerverbindungen wie z.B. Polyethin **II.1-26** weiterreagieren. Die auch als Glaser-Kupplung bekannte oxidative Kupplung terminaler Alkine **II.1-9** in Gegenwart eines Kupfer(I)-salzes sowie einer Base und Sauerstoff führt zur Bildung von Diinen **II.1-28** und wird oft als unerwünschte Nebenreaktion beobachtet, z.B. bei Sonogashira-Kupplungen.

Eine Umkehr der Regioselektivität zu Gunsten der *anti*-Markovnikov Additionsprodukte kann durch radikalische Addition von Halogenwasserstoffen an Alkine **II.1-6** oder durch Hydroborierung von Alkinen **II.1-6** erreicht werden (Schema 2, Reaktionstypen 3a-c). Die Hydroborierung liefert nach Hydrolyse selektiv *Z*-Alkene **II.1-14** und in Gegenwart von Oxidationsmitteln Ketone **II.1-20**.

Ferner können terminale Alkine durch starke Basen wie z.B. Alkyllithiumverbindungen oder Grignard-Reagenzien deprotoniert und in zahlreichen nukleophilen Substitutions- oder Additionsreaktionen eingesetzt werden (Schema 2, Reaktionstypen 4a-b).

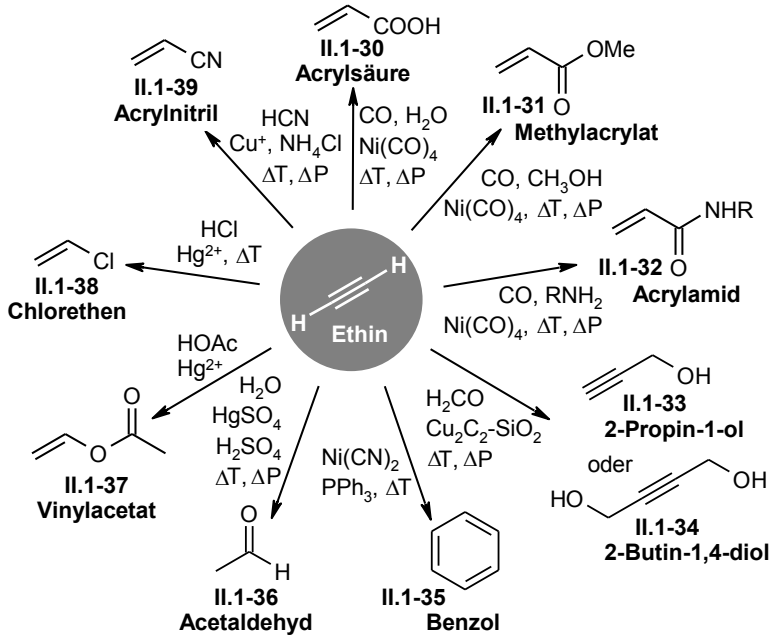

Schema 3. Beispiele für Reppe-Synthesen: Ethin als Rohstoff für die chemische Industrie.

Für großtechnische Prozesse hat sich Ethin als besonders wertvolle Ausgangsverbindung bewährt. In den dreißiger und vierziger Jahren des letzten Jahrhunderts wurden von Reppe für

die BASF zahlreiche Ethin-basierte Prozesse entwickelt und im großtechnischen Maßstab verwirklicht. Die Explosionsgefahr durch Metallacetylid-Bildung bei erhöhtem Reaktionsdruck und hohen Reaktionstemperaturen konnte dabei erfolgreich minimiert werden. Die Hauptreaktionen dieser Reppe-Chemie sind die Carbonylierung, Ethinylierung, Vinylierung sowie die Cyclisierung (Schema 3).[7]

Durch Carbonylierungen von Ethin mit z.B. Wasser, Methanol oder primären Aminen können mit Hilfe von Nickel-Katalysatoren die wertvollen Basischemikalien Acrylsäure, Methylacrylat und verschiedene Acrylamide (**II.1-30-32**) hergestellt werden. Die Kupfer-katalysierte Ethinylierung von z.B. Formaldehyd liefert 2-Propin-1-ol oder 2-Butin-1,4-diol (**II.1-33-34**). Durch Vinylierungsprozesse können unter anderem Vinylacetat, Chlorethen und Acrylnitril (**II.1-37-39**) erhalten werden und durch Cyclisierung z.B. Benzol (**II.1-35**). Acetaldehyd ist durch Quecksilber-katalysierte Hydratisierung zugänglich (**II.1-36**).

Aufgrund der enormen Anzahl moderner Methoden zur Umsetzung von Alkinen werden im Rahmen dieser Doktorarbeit ausschließlich die Hydroamidierung und die Carboxylierung terminaler Alkine betrachtet. Neuere Methoden zur Umsetzung von Alkinen haben oft die Zielsetzung, bekannte Reaktivitäten unter deutlich milderen Reaktionsbedingungen zu verwirklichen und dabei umweltfreundlichere und atomökonomischere Reaktionsführungen zu ermöglichen, um so möglichst viele der zwölf idealen Prinzipien der “Green Chemistry“ zu erreichen.[8]

Dafür werden Katalysatorsysteme benötigt, die in der Lage sind durch Koordination an das Alkin dieses zu acidifizieren oder für den Angriff eines Nukleophils zu aktivieren. So können heute terminale Alkine ohne zusätzliche Basen oder erhöhtem Druck in Hydroamidierungsreaktionen mit wenig nukleophilen Amiden zu Enamiden oder in Additionsreaktionen mit anderen Heteroatom-Wasserstoff-Nukleophilen zu einer Vielzahl an Heteroatom-Vinylverbindungen umgesetzt werden (Kap. II.2). Ausserdem können terminale Alkine in Gegenwart von Kupfer- oder Silberkatalysatoren schon mit milden Carbonatbasen anstelle von z.B. Alkyllithiumverbindungen deprotoniert werden und in Carboxylierungsreaktionen mit CO_2 zu Propiolsäurederivaten umgesetzt werden (Kap. II.3).

In den nächsten beiden Kapiteln werden Methoden zur Hydroamidierung und Carboxylierung terminaler Alkine vorgestellt und hinsichtlich der erforderlichen Reaktionsbedingungen, ihrer katalytischen Aktivität und Anwendungsbreite diskutiert. Ferner werden die auf diese Weise zugänglichen Verbindungsklassen vorgestellt, sowie ihre Vorkommen, Anwendungen und traditionelle Herstellungsverfahren beschrieben.

II.2. Hydroamidierungsreaktionen terminaler Alkine

Das im Rahmen dieser Doktorarbeit entstandene Manuskript soll als Review-Artikel veröffentlicht werden und gibt einen umfassenden Überblick über Ruthenium-katalysierte Hydroaminierungs- und Hydroamidierungsreaktionen von Alkenen und Alkinen. Die auf diesem Weg zugänglichen Verbindungsklassen, namentlich die Amine, Amide, Imine, Enamine, Enamide, Enimide sowie Thioamide, werden vorgestellt und Beispiele für deren traditionelle Herstellungsverfahren, ihre Anwendung und ihr Vorkommen in biologisch aktiven Verbindungen beschrieben. Außerdem wird die Herausforderungen bei der Entwicklung katalytischer Additionsreaktionen an Alkene und Alkine diskutiert und gegenübergestellt, welche Metallkatalysatoren für die Synthese welcher Verbindungsklassen geeignet sind.

Der vorliegende Manuskriptentwurf soll noch 2012 in *Chemical Reviews* der American Chemical Society zur Veröffentlichung eingereicht werden.

Ruthenium-catalyzed hydroamination and hydroamidation reactions: atom-economic and environmentally benign processes

*Matthias Arndt, and Lukas J. Gooßen**

Department of Chemistry, TU Kaiserslautern, Erwin-Schrödinger-Straße Geb. 54, 67663 Kaiserslautern, Germany. Fax: (+49) 631-205-3921; Tel: (+49) 631-205-2046

goossen@chemie.uni-kl.de

RECEIVED DATE (to be automatically inserted after your manuscript is accepted if required according to the journal that you are submitting your paper to)

Keywords. alkynes, addition reaction, ruthenium, hydroamination, hydroamidation.

Contents

1. Introduction

The abundance of amine, enamine, imine, (thio)enamide, and imide functionalities in natural products, biologically active compounds, synthetic drugs, and building blocks explains the profound interest in developing increasingly efficient, selective, and environmentally benign methods for C-N bond formation. In this context, the discovery of catalyst systems that mediate the addition of heteroatom-hydrogen nucleophiles including amines, amides, O-H, S-H, Se-H, and P-H derivatives across C-C multiple bonds has opened up new synthetic opportunities.[1] Such catalytic additions are effective and atom-economic provided that the regio-, stereo-, and chemoselectivity can be controlled by the catalyst system. Due to the advances made in recent years related to metal-catalyzed addition reactions of N-nucleophiles to C-C multiple bonds, these have evolved into broadly applicable tools for the selective construction of enamine, imine, and enamide moieties. Some of the most effective protocols make use of ruthenium catalysts, which have a particularly high functional group tolerance.

This article comprehensively reviews the use of ruthenium catalysts for hydroamination and hydroamidation reactions of alkynes i.e. the addition of amines and amides across C-C triple bonds. As can be seen in Scheme 1, this synthetic concept has been used to access a huge variety of substrate classes.

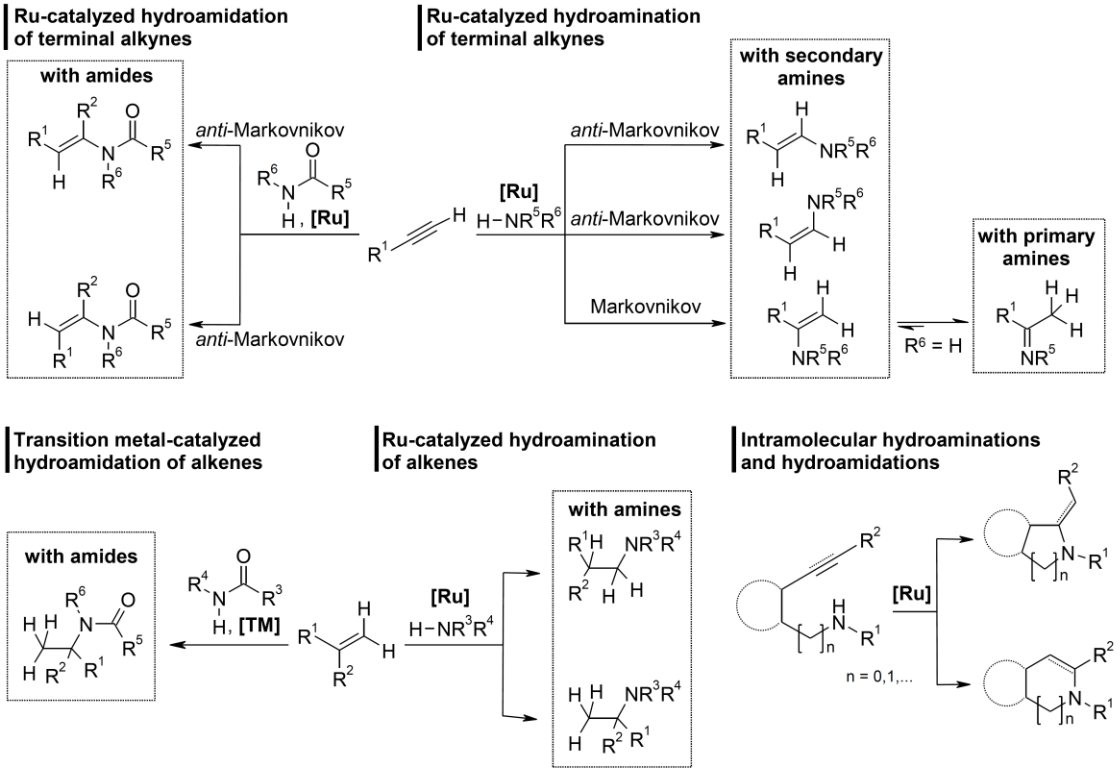

Scheme 1. Reaction pathways and product classes of this review. TM = transition metal.

The addition of primary amines to terminal alkynes yields imines, whereas the addition of secondary amines furnishes *E*- or *Z*-configured enamines. Known Ru-catalyzed hydroamidations of terminal alkynes provide *E*- or *Z*-configured *anti*-Markovnikov enamides. Hydroaminations of terminal alkenes catalyzed by ruthenium yield linear or branched amines. Intramolecular hydroaminations and hydroamidations give access to aliphatic or aromatic nitrogen-containing heterocycles, e.g. indoles. Interestingly, Ru-catalyzed hydroamidations of alkenes have not yet been reported, while this reaction - when mediated by other late transition metal catalysts - gives rise to Markovnikov *N*-alkylamides.

Among these known reactions, the addition of amines to non-activated alkenes and the addition of amides to alkynes are synthetically particularly attractive. The first reaction provides valuable alkylamines starting from easily available alkenes and amines. The second gives a regio- and stereoselective entry to enamides, which are key functionalities in biologically active compounds, and synthetic intermediates e.g. for

polymerization reactions, asymmetric hydrogenation reactions, the synthesis of heterocycles, cross-coupling reactions, Heck reactions, and enantioselective addition reactions.

Additions of N-H nucleophiles across multiple bonds have partially been covered in previous review articles. Doye et al. have reviewed the early transition metal-catalyzed hydroamination chemistry of alkynes, with a particular focus on titanium, up to the end of 2006.[2] In this context, they briefly outlined the progress made in late transition metal-catalyzed hydroamination reactions. Alonso et al. reviewed early and late transition metal-catalyzed hydroamination reactions of alkynes until 2004 with a focus on palladium-based methods.[1a] Two reviews by Müller et al. published in 1998 and 2008 give an overview on homogeneously and heterogeneously catalyzed hydroaminations of alkenes and alkynes, and focus on rare earths, early transition metals, and palladium, as well as Brønstedt acid- and base-catalyzed hydroamination protocols.[1b,c]

This review comprehensively covers catalytic hydroamidations, i.e. additions of amides to alkenes and alkynes. Among the vast field of hydroamination chemistry, i.e. reactions involving additions of amines to alkynes and alkenes, only ruthenium-catalyzed methods are comprehensively covered, whereas protocols with different catalyst metals are only briefly summarized to set the results achieved with ruthenium systems into a general context.

2. Products accessible via hydroamination or hydroamidation processes

2.1. Importance of hydroamination and hydroamidation products

Amine, enamine/imine, or enamide moieties are often encountered in natural products or synthetic drugs with sedative, cytotoxic, antiviral, *anti*-cancer, or *anti*-inflammatory properties. Figure 1 displays a selection of natural products containing such functionalities as substructures.

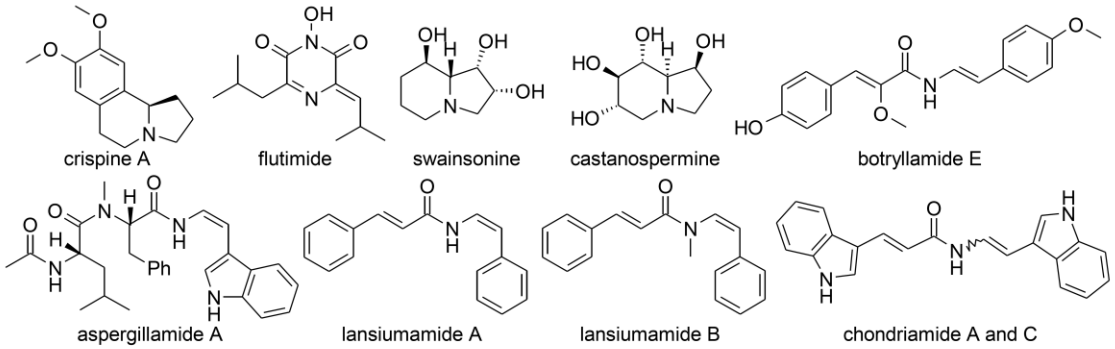

Figure 1. Examples of natural products and bioactive compounds accessible via hydroamination reactions.

In Chinese folk medicine, extracts of the plant *Carduus crispus* are used for the treatment of cold, stomach ache, and rheumatism. A recently characterized active ingredient from this plant, crispine A, displays cytotoxic activity and inhibits the growth of some human cancer cells.[3] Flutimide has been isolated from dung of the Namibian dassie beetle *Delitschia confertaspora*. This natural product is a selective endonuclease inhibitor and shows antiviral activity in cell culture.[4] The two polyhydroxylated indolizidines swainsonine and castanospermine, found in the genera *Polygonatum* and *Prosopis*, are potent inhibitors of several glycosidase enzymes, resulting in *anti*-HIV, antimetastatic, immunoregulating, and *anti*-cancer activities.[5] The marine ascidian *Botryllus tyreus* is the source of a mixture of ten structurally related enamide derivatives. These botryllamides selectively inhibit the ABCG2 multidrug transporter.[6] Aspergillamide A is a peptide produced by the cultured marine fungus *Aspergillus sp.* and exhibits modest *in vitro* cytotoxicity against the HCT-116 human colon tumor cell line.[7] Lansiumamides A and B are compounds from the leaves and fruits of *Clausena lansium*, which are used in Chinese medicine for the treatment of asthma and viral hepatitis.[8] The two indole derivatives chondriamide A and C, originating from extracts of Argentinean *Chondria sp.*, were found to show moderate anthelmintic activity.[9]

In addition to their relevance as part of bioactive naturally occurring products, enamines/imines or enamides are of substantial interest to the chemical industry as building blocks for the synthesis of more complex structures. For example, they can be used in asymmetric hydrogenations, the synthesis of heterocycles, polymerization reactions, enantioselective additions, cross-couplings, and Heck reactions (Figure 2).

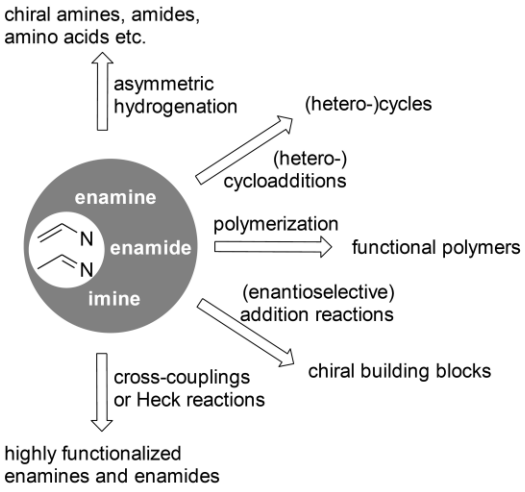

Figure 2. Enamines/imines and amides as building blocks.

Since the addition of N-H nucleophiles to alkenes is harder to accomplish (see section 1.3), the asymmetric hydrogenation of enamines/imines or enamides represents an efficient alternative for the straightforward synthesis of chiral amines, amides or amino acids. Many metal complexes[10] as well as organocatalysts[11] are known to promote such stereoselective hydrogenation reactions.

For example, Zhou et al. synthesized crispine A and other tertiary cyclic amines via iridium-catalyzed asymmetric enamine hydrogenations in 97% yield and with 90% enantiomeric excess (*ee*) (Scheme 2).[12]

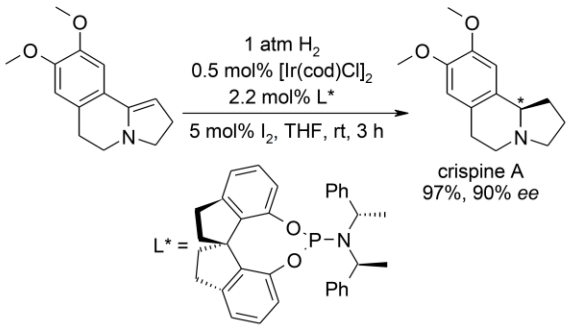

Scheme 2. Iridium-catalyzed asymmetric hydrogenation of enamines.

The rhodium-catalyzed asymmetric hydrogenation of enamides leads to chiral *N*-protected amino acids in high *ee* (Scheme 3).[13]

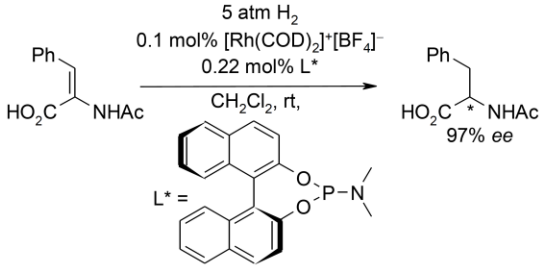

Scheme 3. Rhodium-catalyzed hydrogenation of enamides.

The organocatalytic asymmetric hydrogenation of enamines with trichlorosilane as the hydride donor represents an effective option for the enantioselective synthesis of *β*-amino acids. When Lewis-basic formamides such as sigamide are used as the organocatalyst, (*S*)-configured acid derivatives are formed in high yields and *ee* (Scheme 4).[14]

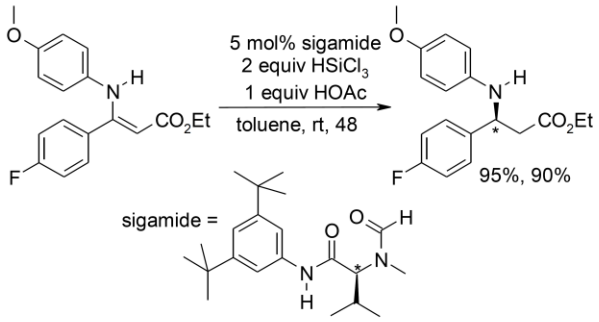

Scheme 4. Organocatalytic hydrogenation of enamines with sigamide/$HSiCl_3$.

Enamines/imines and enamides are important building blocks also for cycloadditions. They can be used as dienophiles in [4+2]-(hetero-)cycloadditions. Such cycloadditions can be used for the synthesis of highly functionalized carbocycles or heterocycles.[15]

For example, Stevenson et al. described an yttrium-catalyzed Povarov reaction with 3-substituted imines and acyclic enamides (Scheme 5).[16]

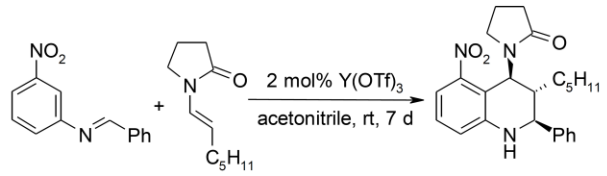

Scheme 5. Regioselective Povarov reaction of imines and enamides.

In this [4+2]-heterocycloaddition, the tetrahydroquinoline product is formed as a single regio- and diastereoisomer, when stirring the 3-nitro-substituted imine with the *trans*-configured enamide at room temperature.

N-Vinyloxazolidinones can be used as chiral dienophiles in [4+2]-hetero-Diels-Alder reactions with inverse electron demand with this *β*,*γ*-unsaturated *α*-ketoesters as the heterodienes, Eu(fod)$_3$-catalyzed reaction proceeds with high diastereoselectivity to the corresponding *endo* product. The (*2S*,*4S*)-adduct is exclusively formed starting form the (*4S*)-dienophile (Scheme 6, right), and the (*2R*,*4R*)-adduct starting from the (*4R*)-dienophile (Scheme 6, left).[17]

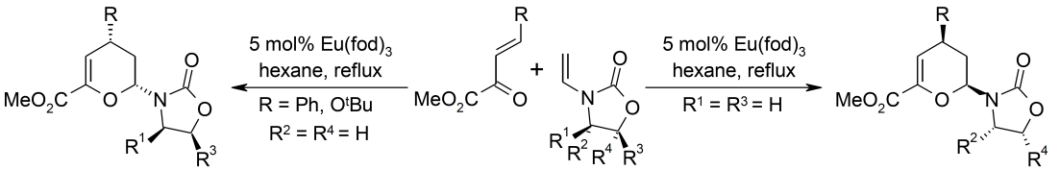

Scheme 6. Eu(fod)$_3$-catalyzed hetero-Diels-Alder reaction of enamides. fod = 6,6,7,7,8,8,8-heptafluoro-2,2-dimethyl-3,5-octanedionato.

Conjugated enamides are electron-rich dienes and react with acroleins to substituted cyclohexenes. This transformation proceeds in the presence of Jacobsen's Lewis-acidic Cr(III)-salen complex, and gives a single product in up to 95% yield and 97% *ee* (Scheme 7).[18]

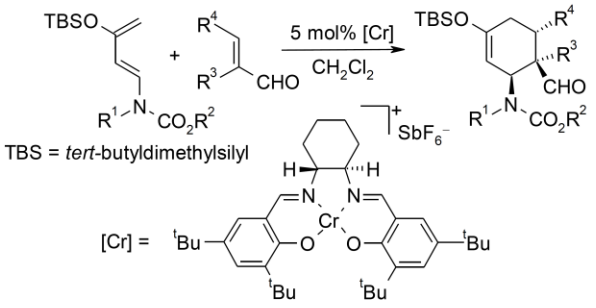

Scheme 7. Enantioselective chromium-catalyzed Diels-Alder reaction.

Like many other unsaturated compounds, enamides can be used in polymerization processes. Thousands of tons of functional polymers are produced each year starting from enamides. One economically important building block for such polymerizations is *N*-vinylpyrrolidone (NVP), which is produced on a technical scale via the addition of 2-pyrrolidone to acetylene under high pressure since 1939 (Scheme 8).[19]

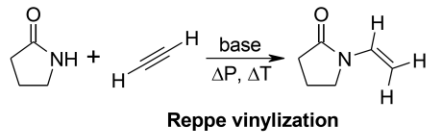

Scheme 8. Technical synthesis of NVP via vinylization of 2-pyrrolidinone.

Radical polymerization of NVP allows the synthesis of numerous many functional polymers and coplymers (Scheme 9),[20] e.g. Kollidon®, Luviskol®, Sokalan® and Luvitec®.[21] In 2006, the world market for PVP had a capacity of approximately 31,000 tons.[22] These polymers show remarkable physical properties. For example, they are hygroscopic, dispersing, adhesive, binding, biological compatible, toxicologically safe, stable in a wide pH range, and soluble in hydrophilic as well as lipophilic systems. Furthermore, they exhibit good stabilizing and solubilizing capacity, crosslink ability and tend to film and complex formation.

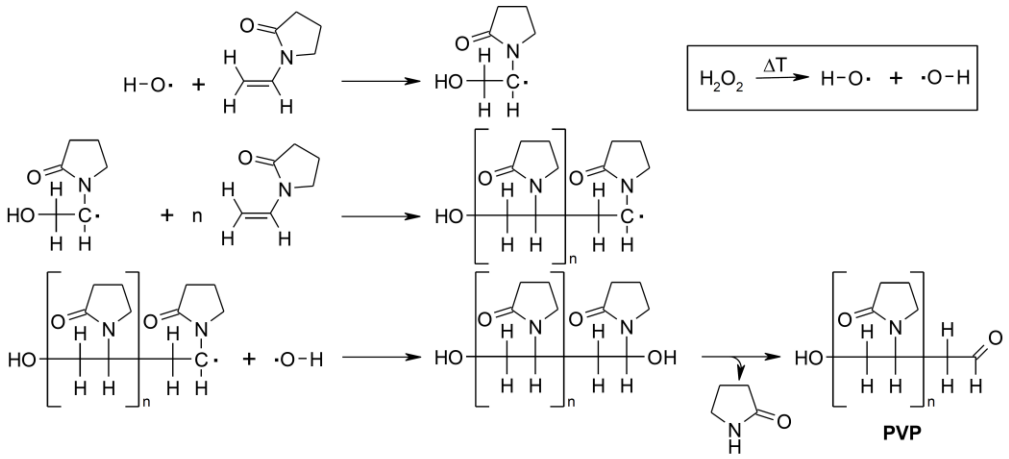

Scheme 9. General reaction mechanism for the radical polymerization of NVP.

A further application for enamines and enamides is their addition to electrophiles (Scheme 10). The electrophilic attack generally proceeds at the vinologous carbon rather than the enamine nitrogen. Enamines are strong nucleophiles due to the electron-donating ability of the nitrogen, which increases the electron density at the C-C double bond. The nucleophilicity of enamides is reduced because of the electron-withdrawing effect of the carbonyl group. Imines, in contrast, exhibit electrophilic properties. Nucleophilic attack occurs in the α-C-position and is usually catalyzed by acids or Lewis-acidic metals.[23]

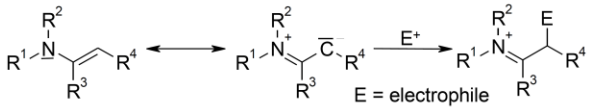

Scheme 10. Reactions of enamines with electrophiles.

Thus, Matsubara et al. described an aza-ene-type copper-catalyzed asymmetric addition of enamides to electrophiles.[24] Using imines as the electrophiles, this method enantioselectively affords *N*-protected *β*-amino imines in high yields and *ee*. These *β*-amino imines can subsequently be hydrolyzed to *β*-amino ketones by treatment with acid, or reduced to diamines using $LiAlH(O^tBu)_3$ and LiI (Scheme 11).[24a,b]

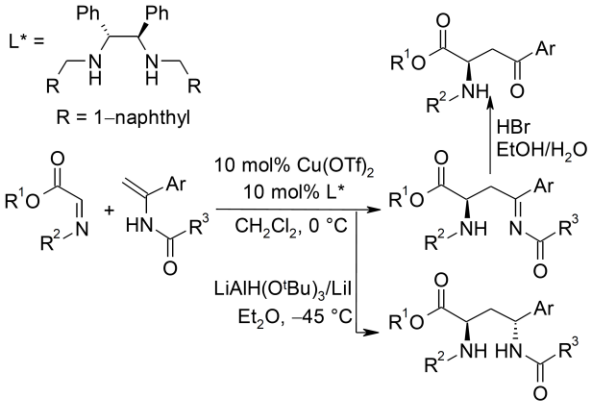

Scheme 11. Copper-catalyzed asymmetric addition of enamides to imines.

This method can also be applied to the addition of enamides and enecarbamates to α-oxo aldehydes to give *syn* and *anti* α-alkyl-β-hydroxy imines, ketones, and amides.[24c,d]

The enantioselective aza-Henry or Mannich-type reaction of imines with silyl nitronates or silyl ethers leads to the formation of *N*-protected α-amino esters (Scheme 12).[25]

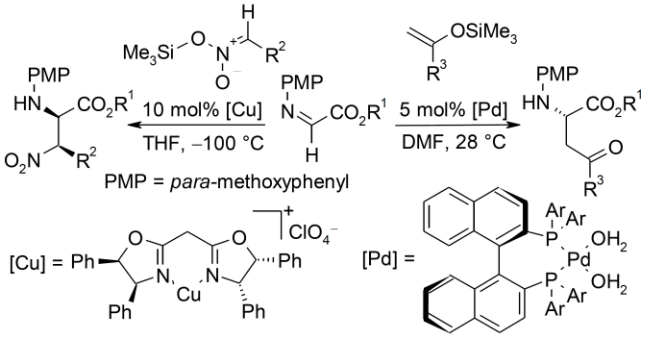

Scheme 12. Enantioselective aza-Henry and Mannich-type reaction.

Finally, enamides undergo metal-catalyzed Heck-olefinations, cross-coupling reactions and co-dimerizations.[26] Willans et al. developed a ligand-free palladium-catalyzed Heck reaction of enamides and aryl bromides with formation of *cis*-functionalized enamides (Scheme 13, equation 1). The cross-coupling of vinyl iodide derivatives and aryl boronic acids leads to the same products and tolerates further substitution at the enamide double bond (Scheme 13, equation 2). The ruthenium-catalyzed co-dimerization

of *N*-vinyl amides and acrylates or alkynes is a mild method to derivatize a non-substituted enamide in the *trans* position (Scheme 13, equation 3).

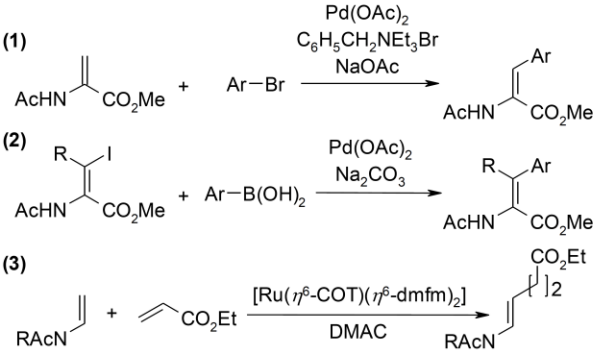

Scheme 13. Palladium-catalyzed Heck- and cross coupling-reaction.

2.2. Traditional syntheses of enamines, imines and enamides

The versatile applications of enamines/imines and enamides described above explain the afford made towards finding general, stereoselective and environmentally benign access to these substance classes. Early approaches are based on condensation, substitution or cross-coupling techniques. In each case, one functional group, e.g. a halide, is substituted by an amine or amide group. Most of these methods suffer from harsh reaction conditions, low yields, the formation of mixtures of isomers and/or a limited tolerance of functional groups. Cross-coupling reactions are the exception, reaching high yields, regio- and stereoselectivities, as well as tolerating a range of functional groups if, e.g., palladium is used as the catalyst metal. However, expensive coupling reagents have to be used, and the regio- and stereoselectivity is controlled by the starting material, which in most cases has to be synthesized in isomerically pure form beforehand. A selection of established protocols for the formation of enamines/imines and enamides is illustrated in Scheme 14.

Traditionally, such compounds are synthesized via a simple acid mediated condensation of aldehydes or ketones with amines and amides (Scheme 14, equation 1). In most cases, the conversion of primary amines results in the formation of imines (R^5 = H), whereas the conversion of secondary amines and amides leads to enamines ($R^5 \neq$ H), or enamides (R^5 = C(O)R^6) respectively.[23a,27] As a consequence of the forcing reaction

conditions, the products are generally obtained as mixtures of diastereoisomers, in which the thermodynamically favored *E*-enamines or *E*-enamides predominate. To achieve high yields, the water generated during the condensation must completely be removed. Advanced condensation methods employ benzotriazole as organocatalysts,[28] alkyl- or phenylaluminum dichloride as mediators,[29] trimethylsilyltriflate as the catalyst,[30] or use microwave irradiation[31] to enhance the yields and scope of this type of transformation.

Very efficient ways to synthesize such compounds are palladium-catalyzed cross-coupling reactions between vinyl halides or vinyl pseudo-halides and amines or amides (Scheme 14, equation 2).[32] Similar to condensation reactions, the coupling of primary amines results in the formation of imines (R^5 = H), and the coupling of secondary amines and amides leads to enamines ($R^5 \neq$ H), or enamides (R^5 = C(O)R^6) respectively. High yields and high selectivities can be reached under mild conditions, but these methods suffer from high costs and a low availability of the vinyl compounds. Moreover, a high stereoselectivity can only be obtained when the vinyl compound is used in diastereomerically pure form.

Wittig reactions of amides or imides and phosphoranes or phosphonates result in the formation of enamines and enamides in good to excellent yields (Scheme 14, equation 3).[33] However, the stereochemical outcome of the reaction is driven by the substituents of the starting materials. Another drawback of this method is their low atom economy, resulting in the formation of large amounts of toxic by-products.

The pyrolysis of *α*,*β*-unsaturated acyl azides induces a Curtius rearrangement to the isocyanates (Scheme 14, equation 4). At a temperature of -78 °C, these intermediates react with Grignard reagents to form *Z*-enamides in moderate to good yields.[34] Starting from alkyl azides, imines can be synthesized analogously.[23a] This method leads to the thermodynamically disfavored *Z*-isomer, but is unsuitable for large scale application because of the use of explosive azides.

The addition of Grignard reagents to *N*,*N*-dialkyl formamides gives enamines in good yields (Scheme 14, equation 5).[35] The reaction proceeds under mild conditions, but the scope is limited to *N*,*N*-dialkyl formamides.

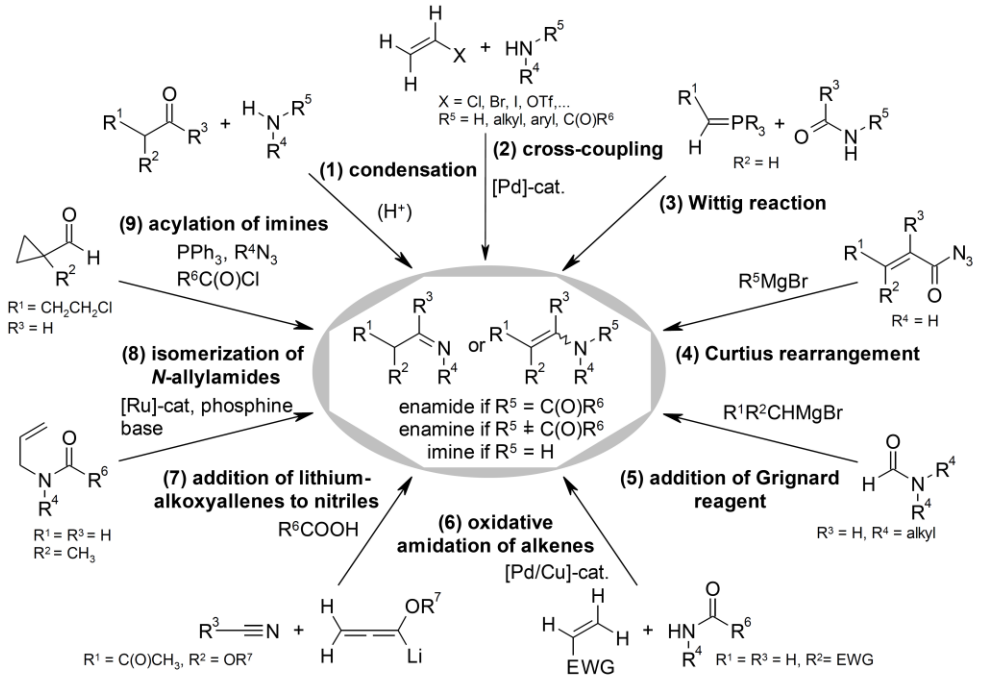

Scheme 14. Syntheses of enamines/imines and enamides.

E-configured enamides can be obtained as the major products in palladium/copper-catalyzed oxidative amidations of acrylates (Scheme 14, equation 6).[36] In a modified procedure, Lee et al. were able to reverse the stereoselectivity in favor of the *Z*-isomer by using non-polar solvents and tetraethyl methylenediphosphonate as an additive.[37] Recently, Panda et al. developed a copper-free palladium-catalyzed protocol for the *E*/*Z*-selective oxidative amidation of acrylates.[38]

Reißig et al. described an alternative access to *β*-alkoxy *β*-keto enamides using alkoxyallenes as precursors in a multi-component reaction with nitriles and carboxylic acids (Scheme 14, equation 7).[39] Moderate yields, cryogenic conditions and the sensitivity of lithiated alkoxyallenes restrict this method to the small-scale synthesis of a narrow range of enamides.

With specialized Ruthenium catalysts, *N*-allylamides can be isomerized to enamides in high yields (Scheme 14, equation 8).[40] The *Z*-enamide is preferentially formed due to steric effects in the transition state, so that the stereoselectivity is determined by the starting material.

The acylation of in situ-generated imines produces a mixture of diastereoisomers with an excess of the thermodynamically favored *E*-enamides (Scheme 14, equation 9).[41] Again the scope is limited by the availability of the starting materials, and yields are only moderate.

None of the methods to synthesize enamines/imines and enamides presented in this chapter satisfy the requirements of atom-economy and selectivity. They suffer from low yields, low stereoselectivities, forcing reaction conditions, formation of large amounts of by-products, or limited availability or toxicity of the starting materials.

In contrast, the addition of *N*-nucleophiles across C-C double or triple bonds represents an efficient and safe way of synthesizing enamines, imines and enamides. Such hydroamination and hydroamidation reactions have the inherent advantage of optimal atom-economy. By using readily available and inexpensive starting materials and avoiding huge amounts of salts or other coupling reagents, these transformations are attractive for small-scale and industrial applications alike. However, full control of their chemo-, regio- and stereoselectivity is essential to establish them as synthetic "green" alternatives to established transformations in the spirit of Anastas, who coined the term "Green Chemistry".[42] These challenges need to be mastered to succeed in developing efficient hydroamination protocols, in order to benefit from the obvious advantages of this transformation. The next sections will demonstrate the advantages of late transition metal-catalyzed hydroamination reactions over established methods, and discuss improvements still required.

3. The development of hydroamination chemistry

3.1. Development milestones

Ruthenium is neither the first nor the only metal that has been used in hydroaminations and hydroamidations.[1,2] Already in 1930, a French patent describes thermal processes for the addition of ammonia to acetylene. In the presence of supported zinc compounds and using optimized gas flows, the typical formation of pyridine bases could be reduced, and acetonitrile as well as ethyl amines were formed at 350 °C (Scheme 15).[43]

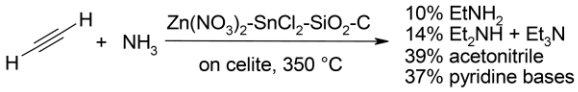

Scheme 15. Addition of ammonia to acetylene.

The first addition of amines to alkenes was reported in 1954.[44] Howk and co-workers found that ammonia also adds to ethylene in the presences of metallic sodium or lithium, or the corresponding alkali-metal hydrides. At 200 °C and with pressures up to 1000 bar a mixture of ethyl-, diethyl-, and triethylamines can be isolated in up to 66% (Scheme 16).

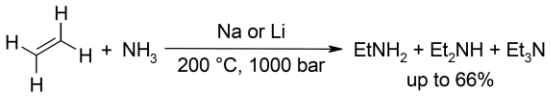

Scheme 16. Addition of ammonia to ethylene.

The first experimental evidence for a homogeneously catalyzed hydroamination of alkynes was provided by Kozlov in 1936. He postulated that the addition of aniline to acetylene in the presence of mercury(II) chloride leads to the intermediate formation of ethylidene aniline as reaction. However, this intermediate is transient and under reaction conditions, diethylidene aniline is the main product, formed via an aldol-type condensation. Based on these findings, Loritsch et al. developed a mercury oxide-catalyzed hydroamination of 1-heptyne and 3-octyne with aniline and ethyl aniline (Scheme 17).[45]

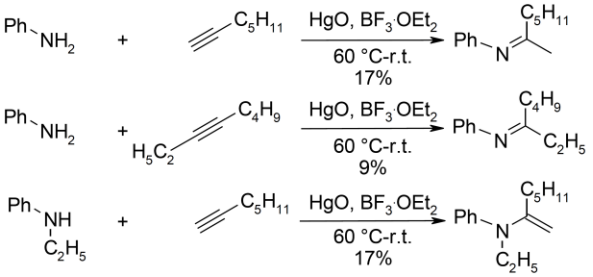

Scheme 17. Mercury-catalyzed hydroamination of 1-heptyne.

At the same time, Reppe et al. filed several patents for the synthesis of *N*-vinyl compounds from N-H nucleophiles and acetylene in the presence of strong bases, as well as their polymerization (see Scheme 8).[19,20]

In 1969 Möhrle et al. discovered that the sodium salts of cyclic lactams, methyl acetamide and acetanilide can be added to phenylacetylene with formation of *Z*-enamides (Scheme 18).[46]

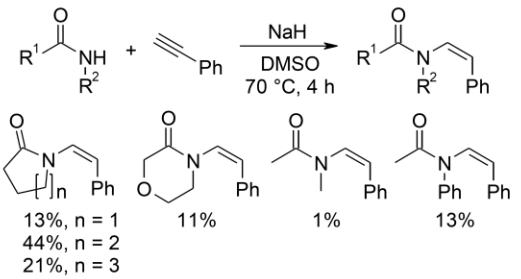

Scheme 18. Base-mediated hydroamidation of phenylacetylene.

Even before the first Ru-catalyzed hydroamination protocol was developed, Heider et al. and Watanabe et al. had reported methods for the homogeneously catalyzed addition of amides across alkynes.

One of the first examples of a Ru-catalyzed intermolecular addition of *N*-nucleophiles across alkynes was described in 1995 by Heider et al. in a patent for BASF.[47] In their process cyclic *N*-nucleophiles (e.g., 2-pyrrolidone, imidazole or succinimide) dissolved in toluene are treated with 20 bar of a 1 : 3 mixture of N_2/acetylene in the presence of 0.3-3 mol% of $RuCl_3$ as catalyst. After 7 to 24 h at 150-160 °C, the corresponding enamides, enimides, or enamines are obtained in good yields (Scheme 19).

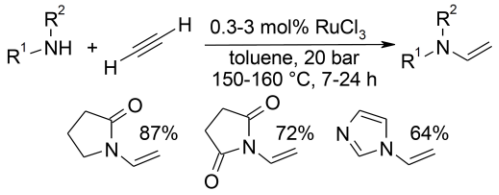

Scheme 19. First ruthenium-catalyzed hydroamidation protocol.

Only months later, Watanabe et al. published another high pressure method for the hydroamidation of terminal alkynes with *N*-aryl substituted amides.[48] Their catalyst system, derived from previous work on the addition of carboxylic acids to alkynes, is formed in situ from $Ru_3(CO)_{12}$ and tricyclohexylphosphine (PCy_3). The *E*-configured *anti*-Markovnikov enamides were isolated in up to 67% after 15 h at 180 °C in an autoclave (Scheme 20). This pioneering protocol was limited to 1-octyne in combination with a

restricted range of 4-substituted *N*-acylanilines, and the high pressure/ high reaction temperatures conditions.

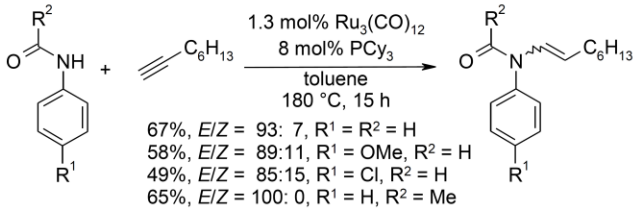

Scheme 20. Ru-catalyzed hydroamidation of 1-octyne.

The regioselective formation of the *anti*-Markovnikov enamide was explained by Watanabe with the mechanism displayed in Scheme 21. The oxidative addition of the amide to the active ruthenium species is facilitated by coordination of the carbonyl oxygen to the metal center. In the next step, a Ru-amide-hydride intermediate forms and coordinates the alkyne. The π-coordinated alkyne is able to insert into either the Ru-H or the Ru-N bonds, leading to an amide-ruthenium-vinyl or a hydride-ruthenium-enamide complex. From either complex, the *anti*-Markovnikov product may be cleaved by reductive elimination, regenerating the catalytic active Ru-species.

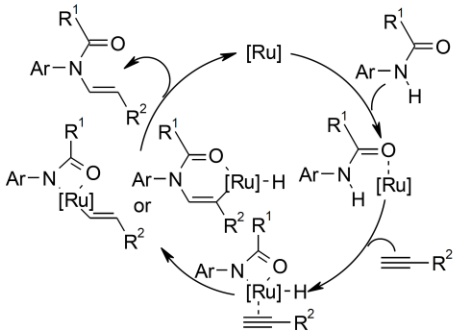

Scheme 21. Mechanism for the addition of amides to terminal alkynes.

The first protocol for the hydroamidation of alkenes, developed by Widenhoefer and co-workers, used platinum(II) rather than ruthenium(II) as the catalyst. A platinum chloride and triphenylphosphine system catalyzed the addition of benzamides and carbamates to non-activated ethylene and propylene (Scheme 22).[49] In the presence of only 2.5 mol% of $[PtCl_2(H_2C{=}CH_2)]_2$ and 5 mol% of PPh_3, a variety of primary aromatic and aliphatic amides were successfully added to ethylene in good to excellent yields. The

methodology was also suitable for the addition to propylene at pressures of 100 bar. Other late transition metal catalyst such as palladium are also able to promote the addition of amides to alkenes, but in contrast to platinum, enamides are formed in this oxidative amidation process, due to *β*-hydride eliminations.

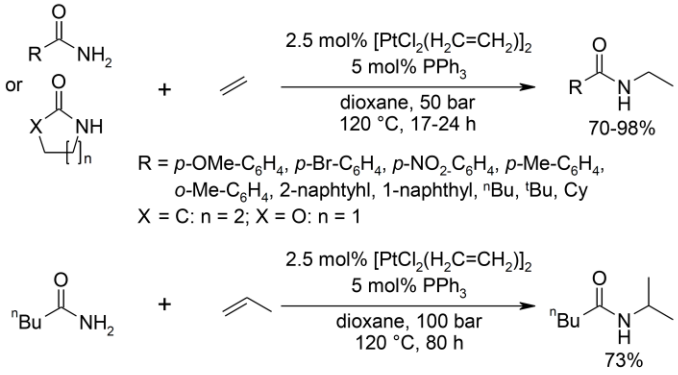

Scheme 22. Platinum-catalyzed hydroamidation of non-activated olefins.

Based on these pioneering studies, a number of catalyst systems could be developed for homogeneously catalyzed inter- as well as intramolecular hydroaminations and hydroamidations of internal or terminal alkenes and alkynes.[1,2]

3.2. Challenges in catalytic additions of *N*-nucleophiles across multiple bonds

The development of catalyst systems for efficient and environmentally benign addition processes encounters many challenges. On the one hand, high conversion rates have to be reached, and on the other, the chemo-, regio-, and stereoselectivity must be controlled so that only the desired product is produced (Figure 3).

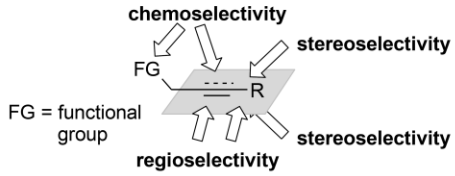

Figure 3. Chemo-, regio-, and stereocontrol of addition reactions.

The addition of a nucleophile such as an amine across a C-C multiple bond is thermodynamically feasible because it is slightly exothermic. Kinetically, it is difficult, since the high electron density of the nucleophile

and the π-electrons of the multiple bond repel each other. Therefore, a large activation barrier needs to be overcome for conversion to occur. Moreover, the high temperatures required to cross this barrier induce a shift of the equilibrium towards the starting materials because of the generally negative reaction entropy $\Delta S°$ of this reaction type.[50,2a] This problem may be overcome by employing a catalyst to lower the activation barrier.

Despite the fact that alkynes have more π-electrons than alkenes, which could be expected to increase the electrostatic repulsion of the nucleophile, a metal-catalyzed addition reaction across C-C triple bonds is much easier to accomplish than across C-C double bonds. This can be explained by the formation of substantially weaker π-bonds between most catalysts and alkynes compared to alkenes. The intermediate strength of this interaction between the alkyne and the catalyst allows activating the C-C triple bond towards nucleophilic attack without inhibiting the reaction by a strong π-coordination to the metal center. Furthermore, alkynes are sterically less hindered towards attack of the nucleophile.[2b] Even though huge advances in developing more efficient and broadly applicable methods for the addition of amines and amides to alkenes, the scope remains limited to certain substrates.[51]

The first feature to be controlled in addition reactions is their chemoselectivity. The nucleophile needs to interact selectively with the C-C double or triple bond and rather than with other reactive centers. Good functional group tolerance is the key to the broad applicability of a new method, and the presence of functional groups opens up opportunities for further derivatization. Late transition metals such as ruthenium and palladium tend to score better in terms of functional group tolerance than most early transition metals and the conditions employed are usually milder (see also section 3.3).

Secondly, the regioselectivity is influenced by the reaction mechanism. Alkenes and alkynes can be activated by Lewis-acidic metals (Scheme 23, equation **a**). π-Coordination of the metal to the C-C double or triple bond decreases its electron density and facilitates nucleophilic attack. For terminal alkenes or alkynes (R^1 = H), this activation mode leads to the regioselective formation of the Markovnikov addition product. The same regioselectivity can result from insertion of an alkene or alkyne into the M-Nu or M-H bond of reaction intermediates, formed by oxidative addition of the nucleophile to the metal catalyst (Scheme 23,

equation **b**). According to Dixneuf and co-workers the *anti*-Markovnikov product may be obtained whenever metal vinylidene species are involved, which are very reactive in the α-C position and can only be formed starting from terminal alkynes (R^1 = H) (Scheme 23, equation **c**).[52]

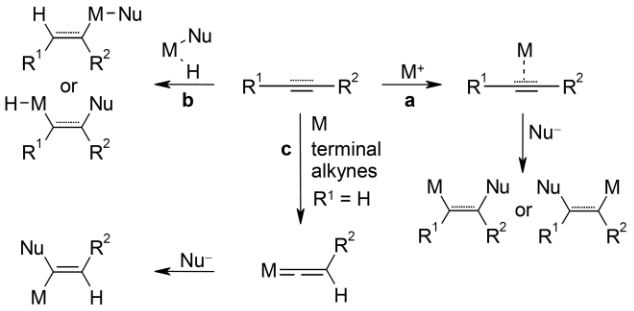

Scheme 23. Alkene and alkyne activation towards nucleophilic attack.

Finally, the stereochemical outcome of the reaction is influenced mainly by the electronic and steric properties of the transition metal complex used, the acidity of the hydrogen bound to the nucleophile, as well as the electronic properties of the alkene or alkyne. There is thus ample room for stereocontrol by appropriately choosing the catalyst/ligand system.

Only well-optimized catalyst systems capable of overcoming the activation barrier as well as of controlling the chemo-, regio- and stereoselectivities are alternatives to established C-N bond forming reactions. The subsequent sections demonstrate the benefits of Ru-catalyzed hydroamination and hydroamidation reactions, and their value for atom-economic and selective syntheses of diverse building blocks, bioactive compounds and natural products. The scope and limitations of such addition reactions in comparison to established methods will be presented and critically evaluated.

3.3. Choice of the catalyst metal for hydroamination and hydroamidation reactions

Early efforts were directed at improving mercury and thallium-based methods.[53] Though effective mercury and thallium-based methods should no longer be considered for use because of the toxicity of these metals.[53]

Alternative catalytic hydroamination/hydroamidation methods use bases,[54] or metals such as lanthanides (neodymium, samarium, lutetium),[55] actinides (uranium, thorium),[56] early (titanium, zirconium)[57] and late transition metals (ruthenium, rhodium, iridium, palladium, gold, silver and copper).[1,2]

The choice of an appropriate catalyst metal may be guided by the properties of each metal. Early and late transition metals are generally less toxic than Hg or Tl and more readily available than lanthanides or actinides. While early transition metals tend to be less expensive than late transition metals, they are also less stable towards air and water.

Many titanium complexes bearing two labile ligands have been used as catalysts for the hydroamidation of symmetrically and unsymmetrically substituted internal and terminal alkynes with primary amines. However, the low functional group tolerance resulting from the high oxophilicity of titanium had not yet been overcome.[2,57]

Palladium complexes are by far the most widely used catalysts in intramolecular hydroamination and hydroamidation reactions of alkynes.[1] The intramolecular hydroamination of aminoalkynes via η^2-alkyne-organopalladium complexes is a well-established method for the synthesis of heterocyclic compounds, in particular of indoles.[58] Aniline derivates and alkynes have been employed directly in the synthesis of indoles via a C-C-coupling/intramolecular hydroamination cascade reaction.[59] Only a few selective Pd-catalyzed intermolecular hydroamination reactions have been reported because allenes tend to intermediately form whenever β-hydride elimination is possible.[60] Allene intermediates then lead to mixtures of regioisomers or allylic amine products.

Several Rh- , Ir- or Cu-catalyzed hydroamination reactions have been described,[61] whereas Au and Ag catalysts have increasingly been used for intra- and intermolecular hydroamination reactions.[62] These methods suffer mostly from high costs for often in stoichiometric amounts required metal sources. The high loadings of these expensive metals, however, preclude widespread use of Au- or Ag-based protocols.

Among the metals capable of mediating hydroamination and hydroamidation reactions, ruthenium catalysts seem to present the most balanced profile of properties. The high activity and functional group tolerance of Ru-catalysts in addition reactions is further demonstrated by related reactions such as

hydrations with formation of aldehydes,[63] carboxylations to give enol esters,[64] hydrothiolations to vinyl sulfides,[65] and additions of alcohols to form vinyl ethers.[66]

The subsequent sections will demonstrate that Ru-complexes provide a good compromise between catalyst performance, cost, toxicity, and functional group tolerance. For clarity, hydroamination and hydroamidation reactions will be discussed separately. Since hydroamidation reactions have not previously been reviewed, advances in hydroamidations without metal catalysts and catalyzed by other late transition metals will also be discussed.

4. Ruthenium-catalyzed hydroamination

The first Ru-catalyzed hydroamination reactions were reported independently in 1999 by the groups of Wakatsuki and Uchimaru. Based on this pioneering work, many Ru-catalyzed hydroamination protocols have been developed that allow the synthesis of imines, enamines, amines, indoles, indenes, benzoxazoles and quinoline derivatives. The hydroamination of terminal alkynes with secondary (section 4.1) and primary amines (section 4.2) will be discussed, followed by hydroaminations of alkenes (section 4.3), intramolecular hydroaminations, and hydroamination cascade reactions (section 4.4).

4.1. Hydroamination of terminal alkynes with secondary amines

The first method for the addition of secondary amines to terminal alkynes was developed by Uchimaru et al.[67] It involves a triruthenium dodecacarbonyl-catalyzed regioselective hydroamination of aryl and cycloalkenyl alkynes with *N*-methyl aniline or -toluidine . Under solvent-free reaction conditions, several Markovnikov addition products were formed in good yields based on the alkyne (Scheme 24). The main drawback of this method is the use of a ten-fold excess of the amine derivative to suppress alkyne oligomerization and isomerization of the enamine product.

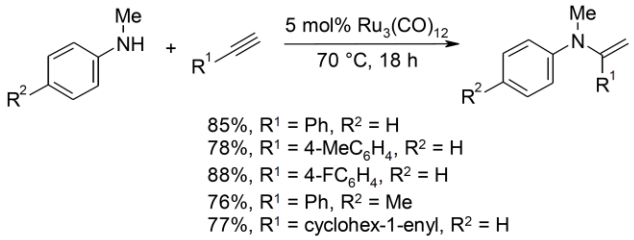

Scheme 24. $Ru_3(CO)_{12}$-catalyzed hydroamination protocol by Uchimaru.

A plausible mechanism for this transformation, as was postulated by Uchimaru, is displayed in Scheme 25. The catalytic cycle starts with an oxidative addition of the amine to a ruthenium(0) center with formation of a ruthenium-amido-hydride complex. Coordination of an alkyne to the resulting complex followed by its insertion into the Ru-N bond gives rise to an ruthenium-enamine intermediate, which releases the product via reductive elimination, regenerating the active ruthenium(0) species.

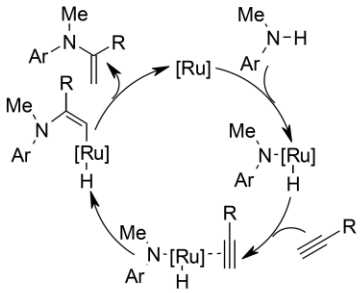

Scheme 25. Reaction mechanism for the Ru-catalyzed hydroamination.

The only other published example of a Ru-catalyzed hydroamination of terminal alkynes with secondary amines, which leads to *anti*-Markovnikov products selectively. Thus, Lau and co-workers reported a hydro(trispyrazolyl)borato-ruthenium(II) diphosphinoamino-catalyzed addition of secondary amines to aromatic 1-alkynes (Scheme 26).[68] In the presence of 1 mol% of the Ru-catalyst, *E*-configured enamines could be isolated in moderate to good yields. The same catalyst was more effective mediating the addition of *β*-diketones to 1-alkynes. The high cost and complexity of the catalyst and the limited scope of enamines constitute the major drawbacks of this method.

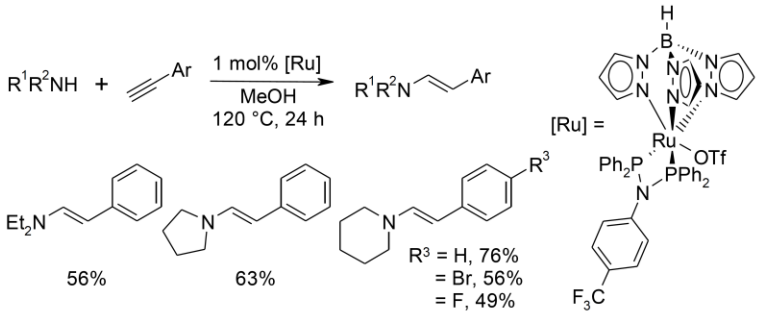

Scheme 26. Ru-catalyzed *anti*-Markovnikov selective addition of secondary amines to terminal alkynes.

4.2. Hydroamination of terminal alkynes with primary amines

Wakatsuki and co-workers introduced the first method for the addition of primary amines to terminal alkynes in parallel to the work of Uchimaru.[69] They found that a combination of $Ru_3(CO)_{12}$ with acids is effective in catalyzing hydroaminations (Scheme 27). Beside aliphatic and aromatic alkynes, methoxy-substituted alkynes were also converted. Additives such as HPF_6 or HBF_4 or their ammonium salts dramatically enhanced the reaction rates and yields of the desired ketimines. For example, with 0.1 mol% $Ru_3(CO)_{12}$ and 0.3 mol% NH_4PF_6, the addition of aniline to phenylacetylene yielded 84% of the Markovnikov product after 12 h at 100 °C, while only 3% yield were obtained without the additive. The role of the acids was not elucidated, but the authors suggest that according to studies by Lavigne, halides and related salts promote substitution reactions at $Ru_3(CO)_{12}$.[70]

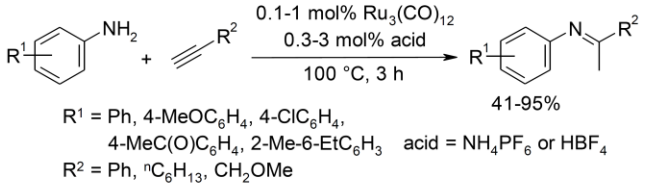

Scheme 27. Ruthenium/acid-catalyzed hydroamination of terminal alkynes.

The activity of the first $Ru_3(CO)_{12}$-based catalyst system of Wakatsuki et al. for the hydroamination of terminal alkynes with primary amines is still competitive compared to the more recent, highly engineered preformed Ru-complexes. Three additional Ru-based catalyst systems have been reported to date.

Klein et al. introduced a dinuclear ruthenium complex with a rigid double-bridged dicyclopentadienyl ligand to catalyze the Markovnikov selective hydroamination of phenylacetylenes with anilines (Scheme 28).[71] In spite of the low catalyst efficiency, this work is the first report of a hydroamination catalyzed by a dinuclear Ru-complex, and includes a detailed elucidation of the reaction mechanism. The low yields obtained (up to 29%) are due to low catalyst turnover numbers (up to six), rather than side reactions the unreacted alkyne and amine could be isolated.

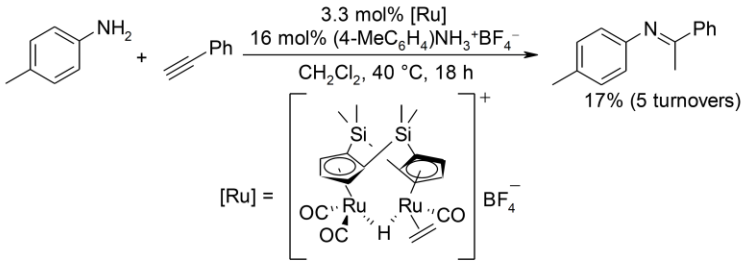

Scheme 28. First dinuclear hydroamination protocol.

The catalytically active species was characterized as $\{(\eta^5\text{-}C_5H_3)_2(SiMe_2)_2\}Ru_2(CO)_3\{NH_2(4\text{-}MeC_6H_4)\}$, and arises by in situ exchange of an ethylene ligand and proton for 4-toluidine from $\{(\eta^5\text{-}C_5H_3)_2(SiMe_2)_2\}Ru_2(CO)_3(C_2H_4)H^+BF_4^-$. Despite the fact that this active species and all other postulated reaction intermediates are unstable, most of have unambiguously been characterized by crystal structure or NMR. The authors verified that the corresponding non-bridged Ru-dimer exhibited no catalytic activity and concluded that the unique bridging nature of $(\eta^5\text{-}C_5H_3)_2(SiMe_2)_2$ was responsible for the hydroamination activity.

A new Ru-styrylphosphine complex $[Ru(CO)_2(PPh_3)(SP)]$ was synthesized by the group of Mizushima, and used for the hydroamination of phenylacetylene with aniline (Scheme 29).[72] A catalyst system containing of 0.3 mol% of $[Ru(CO)_2(PPh_3)(SP)]$ and 0.6 mol% of NH_4PF_6 yielded 72% of the desired ketimine; other Ru-sources such as $[Ru(CO)(PPh_3)_2(SP)]$, $[Ru(CO)_2(PPh_3)_3]$, $[Ru(CO)_3(PPh_3)_2]$ and $[RuH_2(CO)(PPh_3)_3]$ led to only moderate yields. Further improvement of the catalyst activity could be achieved by using tungstophosphoric acid ($H_3PW_{12}O_{40}$) as the additive instead of NH_4PF_6, so that only 0.1 mol% $[Ru(CO)(PPh_3)_2(SP)]$ and 0.2 mol% $H_3PW_{12}O_{40}$ were needed for the hydroamination of equimolar

mixtures of phenylacetylene and different arylanilines in up to 99%. Compared to the catalyst system reported by Wakatsuki et al.[69] (see Scheme 19), the use of more expensive Ru-sources and additives as well as longer reaction times is justified by the gain in overall atom economy, because no excess of the alkyne is needed to reach full conversion.

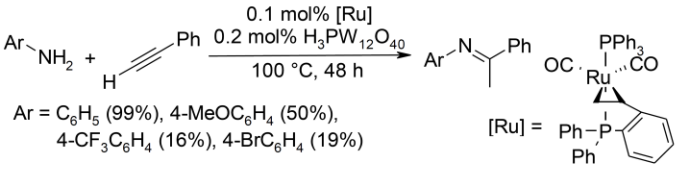

Scheme 29. Ru-styrylphosphine complex as a catalyst for the hydroamination of phenylacetylene.

Following the Method described by Fukomoto et al.[73] nitriles can regioselectively be synthesized via the addition of hydrazines to terminal alkynes. This $TpRuCl(PPh_3)_2$-catalyzed (Tp = tris-pyrazolyl borate) reaction involves an intermolecular attack of the unsubstituted hydrazine nitrogen at the α-carbon atom of a ruthenium-vinylidene species, followed by elimination of dimethylamine (Scheme 30). While the full mechanism of vinylidene formation has not been supported by data, the authors have shown that isolated ruthenium-vinylidene complexes react with *N*,*N*-dimethylhydrazine to the corresponding nitrile. This method allows converting various alkynes bearing functional groups such as ethers, silyl ethers, amines, nitriles, chlorides, tosylates, thiophenes, and pyridines in high yields.

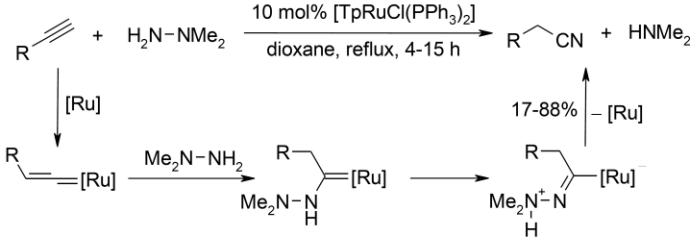

Scheme 30. Synthesis of nitriles via addition of hydrazines to alkynes.

4.3. Hydroamination of alkenes

Only two years after the first Ru-catalyzed methods for the hydroamination of terminal alkynes were published, the groups of Keim and Hartwig developed Ru-based protocols for the hydroamination of less reactive alkenes.

Keim et al. described a ruthenium-catalyzed hydroamination of ethylene with piperidine (Scheme 31).[74]

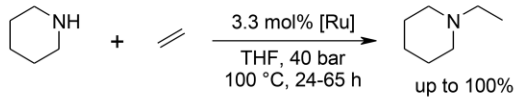

[Ru] = $RuCl_2(PPh_3)_3$, $[\eta^6\text{-}C_6H_6)RuCl_2]_2$,
$[\eta^5\text{-}C_5H_5)Ru(PPh_3)_2(C_2H_4)]^+BF_4^-$, $[\eta^5\text{-}C_9H_7)Ru(PPh_3)(C_2H_4)]^+BF_4^-$

Scheme 31. Hydroamination of ethylene and piperidine catalyzed by Ru^{II}-complexes.

Several Ru^{II}-complexes were able to provide quantitative yields in this reaction using 40 bar ethylene pressure at 100 °C. Other alkenes, such as propene or pent-1-ene, could not be converted analogously, and among several other amines tested, only morpholine reacted and gave 50% yield. Even though this method is limited in scope, it is the first example demonstrating that Ru is able to catalyze the intermolecular hydroamination of olefins.

Hartwig and co-workers showed in a high-throughput screening of transition metal catalysts for the addition of piperidine to methacrylonitrile that beside palladium complexes, $[RuCl_2(p\text{-cymene})]_2$ is also a good hydroamination catalyst.[75] They later found that a catalyst system consisting of 5 mol% $(cod)Ru(met)_2$, 7 mol% 1,5-bis-diphenylphosphinopentane (DPPPent) and 10 mol% TfOH is able to mediate the *anti*-Markovnikov addition of alkyl amines to vinylarenes (Scheme 32).[76] The scope includes electron-rich and -poor vinylarenes as well as cyclic and acyclic dialkyl amines bearing several functional groups, e.g., ether, ester, methoxy or phenyl groups.

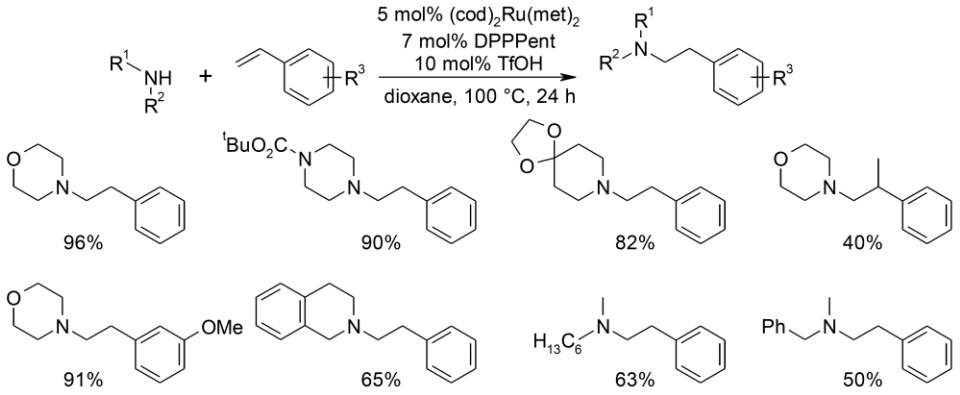

Scheme 32. Intermolecular hydroamination of vinylarenes and alkyl amines.

Mechanistic studies revealed that π-arene complexes are key intermediates in this hydroamination (Scheme 33).[77] The authors were able to isolate (η^6-styrene)- and (η^6-(2-phenylethyl)morpholine)ruthenium complexes which are formed in situ from (cod)Ru(met)$_2$, DPPPent, and TfOH, and demonstrated that they are intermediates in the catalytic cycle. Nucleophilic addition of an amine to the (η^6-styrene)-ruthenium complex affords the *anti*-Markovnikov adduct, still π-coordinated to the ruthenium center. The product is then released via arene exchange and regeneration of the catalytically active species.

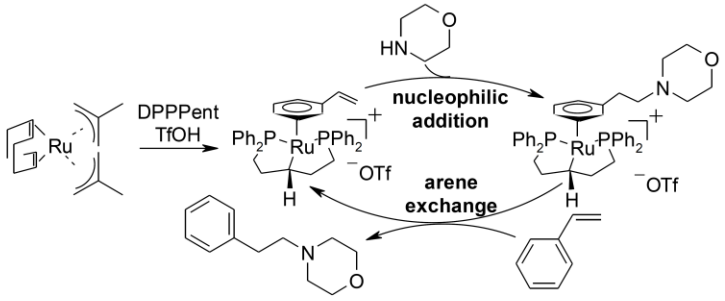

Scheme 33. Postulated reaction mechanism via Ru-π-arene complexes.

Additional examples for Ru-catalyzed intermolecular hydroaminations of ethylene and 1,3-dienes were reported by Yi et al. (Scheme 34).[78] With Ru-alkylidene-species as the hydroamination catalysts, predominantly Markovnikov products are obtained in moderate to excellent yields. However, the regioselectivity is low, the scope is limited with regard to functional groups, and benzene is used as the solvent. Moreover, the hydroamination of ethylene mainly yields 2-methylquinoline, which presumably

arises through a series of steps involving *ortho*-arene C-H bond activation, double ethylene insertion and oxidation.

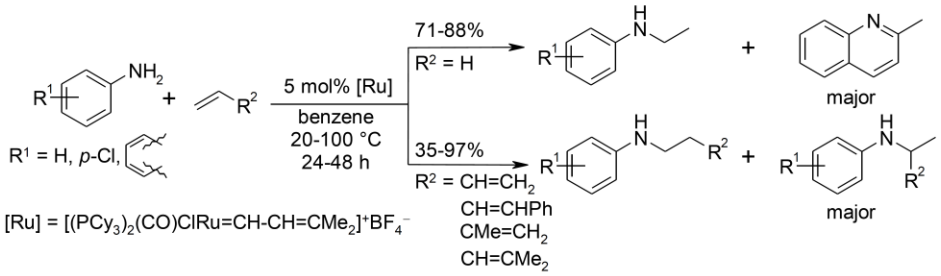

Scheme 34. Addition of primary amines to ethylene and 1,3-dienes.

4.4. Intramolecular hydroaminations and cascade reactions

The Ru-catalyzed hydroamination is an efficient tool to synthesize nitrogen heterocycles, when starting from aminoalkynes, or when using the hydroamination as a part of a cascade reaction sequence.

Wakatsuki and co-workers applied their $Ru_3(CO)_{12}$-catalyzed hydroamination to the Bischler-type synthesis of indoles.[79] Starting from commercially available propargylic alcohols and anilines, a hydroamination/cyclization cascade leads to the synthesis of substituted 3-methylindoles in good yields and selectivities (Scheme 35). The first step of the reaction represents a Markovnikov-selective Ru-catalyzed hydroamination of the propargylic alcohol. This is followed by rearrangement to an α-aminoketone and cyclization to the indole.

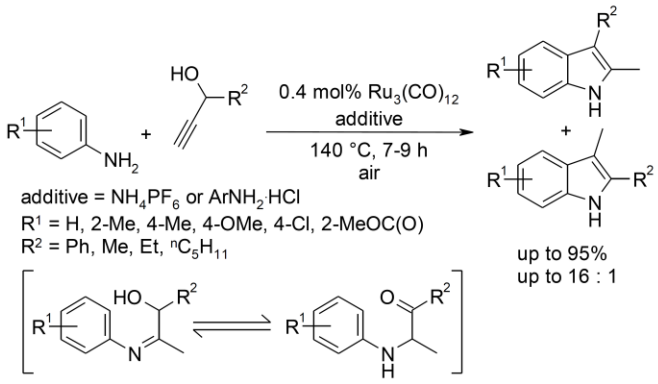

Scheme 35. Cascade hydroamination/Bischler-type indole synthesis by Wakatsuki et al.

A broader product spectrum is obtained by the method of Ackermann et al., consisting of a one-pot Ru-catalyzed hydroamination and Pd-catalyzed intramolecular Heck reaction sequence.[80] Substituted indoles were isolated in up to 89% yield starting from 2-chloroanilines and internal or terminal alkynes (Scheme 36).

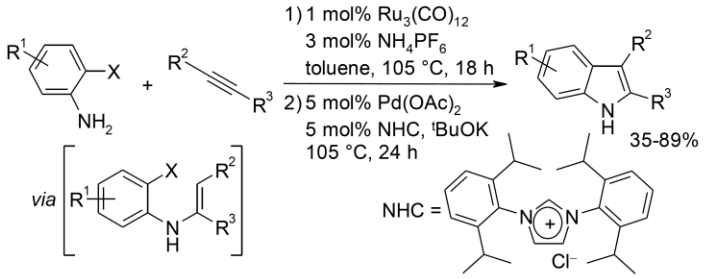

Scheme 36. Synthesis of indoles via hydroamination/Heck reaction.

The group of Kondo developed a Ru-catalyzed intramolecular hydroamination protocol for the synthesis of indole and aliphatic nitrogen heterocycles.[81] In the presence of $Ru_3(CO)_{12}$ as the catalyst and without further additives internal and terminal aminoalkynes could be converted in good yields after 4 h at 110 °C (Scheme 37). Drawbacks of this intramolecular method are the availability of the starting materials, the high reaction temperatures required and a low functional group tolerance.

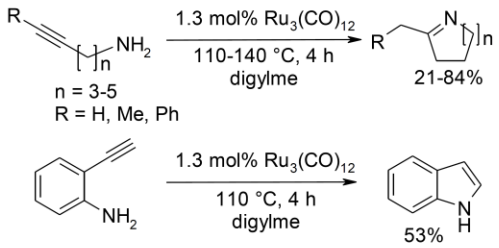

Scheme 37. Ruthenium-catalyzed intramolecular hydroamination.

Chang and co-workers described an intramolecular hydroamination of aminoalkynes followed by an in situ-addition of azides.[82] This tandem reaction proceeds at room temperature and gives access to diversly functionalized cyclic amidines in good yield and regioselectivities (Scheme 38).

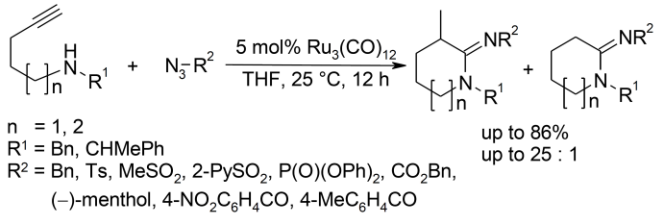

Scheme 38. Synthesis of amidines via tandem hydroamination of aminoalkynes and cycloaddition with azides.

The following mechanism was presented for this tandem process (Scheme 39). A Markovnikov-selective ruthenium-catalyzed intramolecular hydroamination leads to the formation of an enamine with an exocyclic (n=1) or endocyclic (n=2) C-C double bond. The *exo*-methylene pyrrolidine adduct undergoes [3+2] cyclization with azides to give a spiro triazoline, which rearranges to the cycloamidine product, releasing diazomethane (Scheme 39, top). A fused bicyclic triazoline results from the [3+2] cycloaddition of the azide to the six-membered enamine (Scheme 39, bottom). 1,2-Methyl shift and N_2 elimination furnish the product.

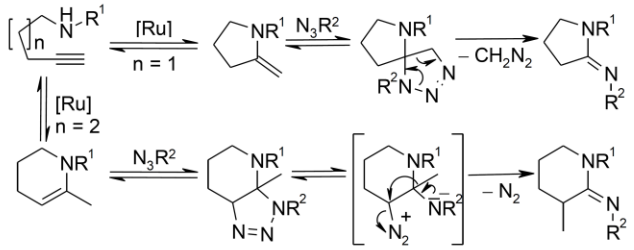

Scheme 39. Reaction mechanism for the synthesis of cyclic amidines.

Kuninobu et al. reported an indene synthesis that proceeds via ruthenium-catalyzed intermolecular hydroamination of alkynes to imines, followed by a rhenium-catalyzed [3+2] anulation with C-H activation. Aniline is eliminated in the process (Scheme 40).[83] Despite the elevated temperatures required for the Re-catalyzed step, several [3+2] anulation products were obtained regioselectively in up to 97%, starting from a variety of arylalkynes. *ortho*-Substituted arylalkynes results in low yields, whereas arylalkynes bearing electron-donating groups in the *para*-position showed the best results. No conversion was observed for arylalkynes with electron-withdrawing groups in the *para*-position.

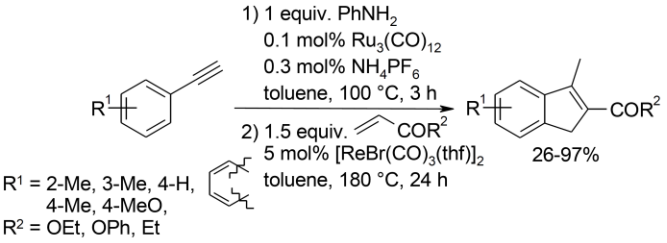

Scheme 40. Synthesis of indenes via intermolecular hydroamination-anulation.

The reaction starts with a Ru-catalyzed Markovnikov selective hydroamination of the terminal aryl alkyne. The resulting ketimine directs the Re-catalyst into the *ortho*-position for C–H bond activation, leading to the formation of a Re-aryl intermediate. Heck-type insertion of the α,β-unsaturated carbonyl compound into the Re-aryl bond, followed by cyclization, reductive elimination, and cleavage of the aniline generates the product along with the active Re-catalyst (Scheme 41).

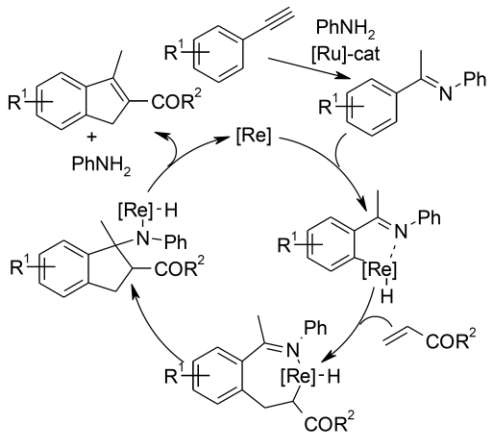

Scheme 41. Mechanism for the Re-catalyzed [3+2] anulation.

Shimada et al. observed that the Ru-catalyzed hydroamination of diynes with aminophenols does not lead to the expected enamines. Instead, a benzoxazole product resulting from cyclization and C-C bond cleavage is obtained (Scheme 42).[84]

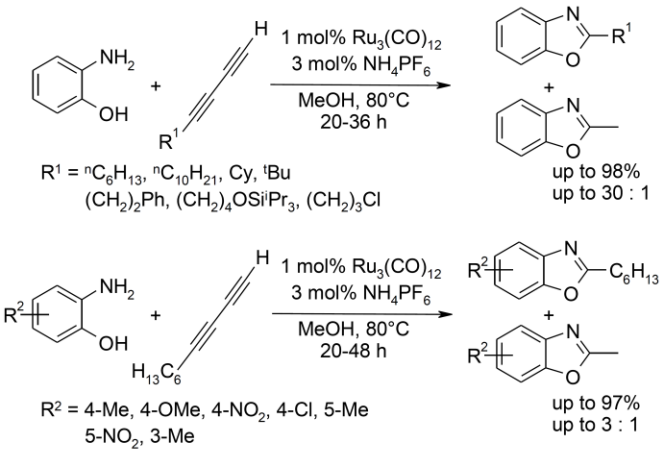

Scheme 42. Synthesis of benzoxazoles via hydroamination of diynes.

This method furnishes a mixture of the two possible 2-substituted benzoxazoles under mild reaction conditions in good to excellent yields. The degree of selectivity for the substituted product depends on the steric demand of the substituent R^1 on the alkyne. Ratios of up to 30 : 1 were obtained. Many functional groups, such as halogens, ethers, silyl ethers and nitro-groups are tolerated. A palladium-catalyzed variant of this protocol was also shown to promote the addition of aminophenols to symmetrical internal diynes at more elevated temperatures and gives comparable yields and selectivities. The poor availability and high cost of the diynes limit synthetic applications of this protocol.

A plausible mechanism is illustrated in Scheme 43. In the first step of the reaction cascade, one aminophenol adds to the sterically less hindered C-C triple bond of the diyne, resulting in the formation of an α,β-unsaturated imine. The addition of a second aminophenol to this intermediate provides two tautomeric β-aminoenimines (Scheme 24, upper and lower reaction pathway). Intramolecular cyclization of the iminophenol moiety gives rise to two different aminoketals, which finally undergo retro-Mannich-type C-C bond cleavage to form the corresponding benzoxazoles. The product selectivity depends on the relative size of the R^1- and the R^2CH_2-fragments. When R^1 is sterically more demanding than R^2CH_2, the formation of the R^1-substituted product is favored because the steric repulsion between R^1 and Ar of the sp^2 plane becomes stronger than that between R^2CH_2 and Ar in the corresponding β-aminoenimine intermediates.

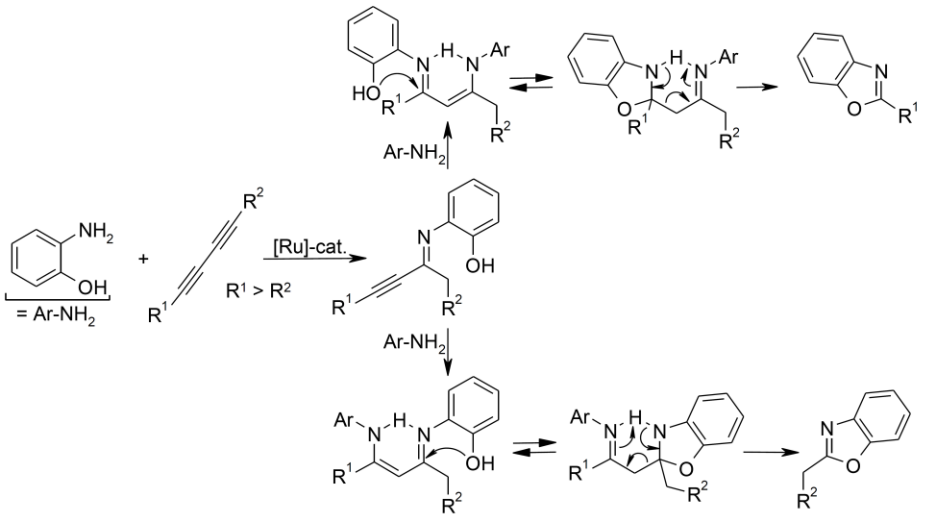

Scheme 43. Mechanism for the diyne hydroamination-carbon-carbon bond cleavage sequence.

Yi and co-workers described a one-pot synthesis of bi- and tricyclic quinolines from terminal alkynes and aromatic amine derivatives via a reaction cascade involving hydroamination and C-H activation steps (Scheme 44).[85] Various substituted quinoline derivatives were obtained in good to excellent yields and regioselectivities. The catalyst system tolerates many different functional groups such as hydroxy, halogen, ether, and thiophene groups. A three to six-fold excess of the alkyne is required for good conversions, and there is no differentiation between the two alkyne molecules incorporated into the product.

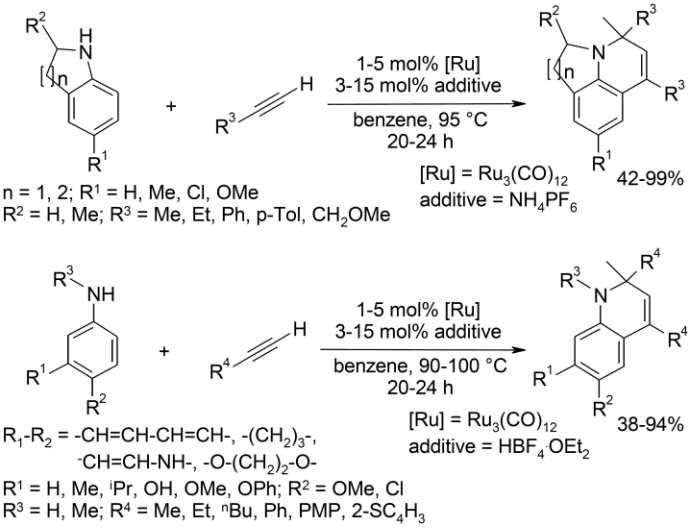

Scheme 44. Ru-catalyzed hydroamination/C-H activation sequence.

The proposed mechanism for this reaction is outlined in Scheme 45. The catalytic cycle starts with the addition of the aryl amine to a cationic Ru-acetylide complex, which is generated in situ from the reaction of two equivalents of alkyne with a Ru-hydride complex. This results in a cationic Ru-amino-vinyl species, which undergoes Ru-migration to the arene ring by a sequence of *ortho*-C-H bond activation and reductive elimination of the vinyl group to and form an *ortho*-metalated intermediate. The insertion of a second alkyne into the Ru-aryl bond leads to another Ru-vinyl species. Heck-type *endo*-cyclization yields a cationic Ru-alkyl species. Since no hydrides are present in the *β*-position to the ruthenium, the product may be released either via oxidative alkyne addition/reductive elimination, or via *σ*-bond metathesis of the terminal alkyne. Each would regenerate the active Ru-acetylide species.

This mechanistic pathway is supported by kinetic studies, which showed that the arene C-H bond activation is the rate-determining step. Additional Hammett studies with different alkynes affirmed that the alkyne C-H activation is not rate-limiting. Deuteration experiments with labeled alkynes revealed that at the end of the reaction, deuterium remains bound to the original carbon atom, so that no proton shift takes place during the reaction.

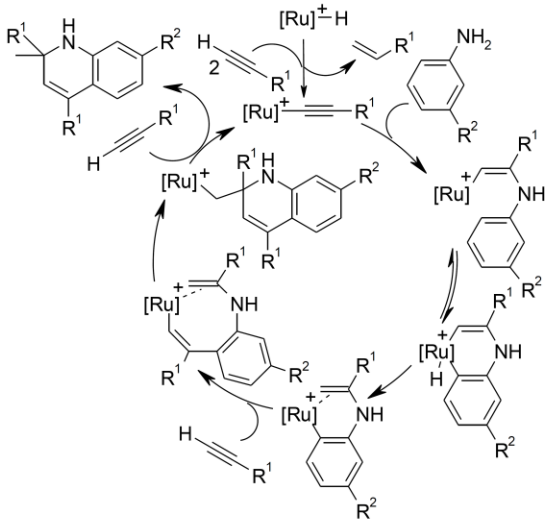

Scheme 45. Mechanism for the cascade synthesis of quinolines.

4.5. Addition of related *N*-nucleophiles to alkynes

The Ru-catalyzed addition of sulfenamides to alkynes represents an efficient method for the *Z*-selective synthesis of polyfunctional alkenes (Scheme 46).[86]

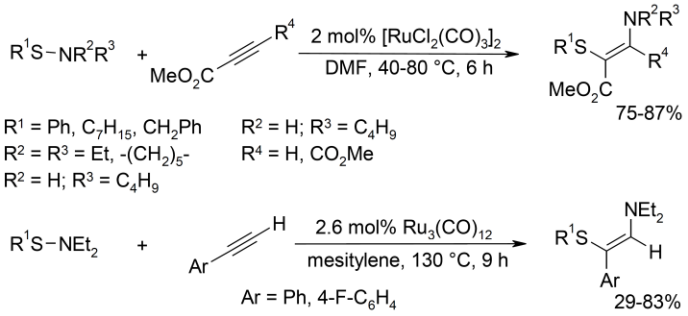

Scheme 46. Ru-catalyzed addition of sulfenamides to alkynes.

Activated alkynes, substituted with a Michael accepting group were converted in high yields and under relatively mild conditions. The authors suggest that the catalyst simply acts as an effective Lewis acid, which activates the Michael system by coordinating to the carbonyl group and thereby facilitating attack of the nucleophile onto the alkyne. Subsequent 1,3-shift of the sulfur group furnishes the product (Scheme 47).

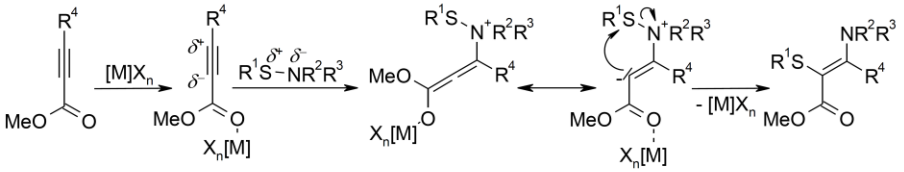

Scheme 47. Postulated mechanism for the addition of sulfenamides to activated alkynes.

For the addition to less activated phenylacetylenes, a different catalyst system and higher reaction temperatures were required. A different reaction mechanism may come into play.

5. Ruthenium-catalyzed hydroamidation

5.1. Hydroamidation of terminal alkynes with secondary amides

Eight years after the pioneering work of Watanabe and co-workers (see section 3.1) an alternative method for the hydroamidation of alkynes was published in our group. Based on previous experience with the

addition of carboxylic acids to terminal alkynes,[64f] an efficient protocol for the *anti*-Markovnikov addition of various secondary amides across terminal C-C triple bonds was identified in our group.[87] The catalyst system generated in situ from bis(2-methallyl)(cycloocta-1,5-diene)ruthenium(II) [(cod)Ru(met)$_2$], tri-*n*-butylphosphine (P^{n}Bu$_3$), and dimethylaminopyridine (DMAP), allows the synthesis of *E*-enamides in high yields and diastereoselectivities (Scheme 48).

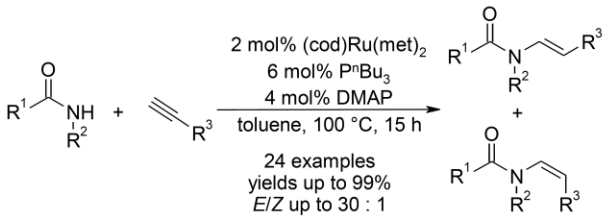

Scheme 48. Ru-catalyzed addition of secondary amides to terminal alkynes.

The reaction proceeds smoothly even in the presence of reactive functional groups, such as esters, ethers, ketones, halides or silanes. Various amides, anilides, ureas, bislactams, carbamates, and chiral auxiliaries can be used, but imides gave poor yields and primary amides could not be converted. Compared to the method of Watanabe, this reaction requires substantially lower temperatures, results in higher yields and diastereoselectivities, and gives access to a broader product range.

A first *Z*-selective protocol consisting of bis(dicyclohexylphosphino)methane (dcypm) and water instead of P^{n}Bu$_3$ and DMAP, was introduced in the same publication. This did not, however, reach the same level of performance and selectivity.

Subsequently, we demonstrated by ESI-MS that the same active Ru-catalyst may be generated in situ from rutheniumtrichloride hydrate ($RuCl_3$•3 H_2O), P^{n}Bu$_3$, DMAP, K_2CO_3 and water.[88] The initiation step involves a phosphine-mediated reduction of the ruthenium(III) (see Scheme 50). The scope of this protocol was somehow improved over that of the costly first-generation catalyst systems, and includes thioamides as well as improved yields for some *E*-enamides.

The original protocols provided *anti*-Markovnikov selective access to *E*-enamide products derived from secondary amides and terminal alkynes. The stereoselectivity was successfully inverted by using a bimetallic catalyst system (Scheme 49).[89] Thus, we showed that a catalyst composed of (cod)Ru(met)$_2$, 1,4-

bis(dicyclohexylphosphino) butane (dcypb), and ytterbium triflate ($Yb(OTf)_3$) was able to promote this transformation at 60 °C in chlorobenzene. Several enamides were synthesized in good yields and a *Z*/*E*-selectivity greater than 20 : 1. Beyond vary amides, the substrate range extended to ureas, carbamates, and a number of imides, which were added selectively across numerous aliphatic and aromatic alkynes.

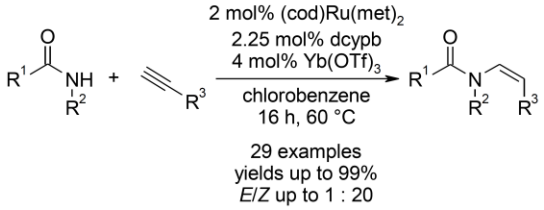

Scheme 49. Z-selective Ru-catalyzed addition of secondary amides to terminal alkynes.

The mechanism of the hydroamidation of alkynes was elucidated by our group using a combination of deuterium-labeling and control experiments, as well as kinetic and spectroscopic studies (Scheme 50).[90]

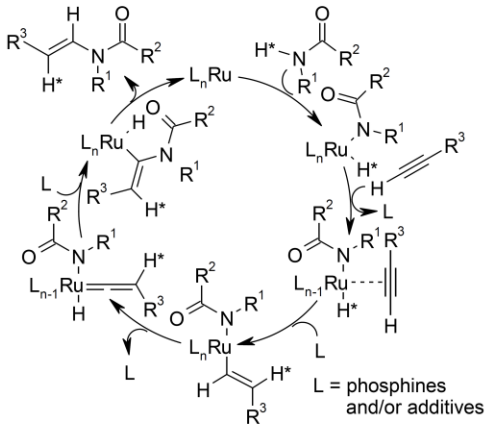

Scheme 50. Mechanism for the Ru-catalyzed hydroamidation of terminal alkynes.

The catalytic cycle starts with the oxidative addition of an amide to an active Ru(0) species, generated via phosphine-mediated reduction of the Ru(II) precursor and ligand exchange reactions. An alkyne coordinates to the resulting Ru(II)-hydride species with cleavage of one neutral ligand, followed by insertion of the alkyne into the Ru-H bond and refilling of the empty coordination site with one neutral ligand. In a slow step, an intermediate ruthenium(II)-vinyl complex rearranges to a Ru(IV)-hydride-vinylidene species with α-hydride transfer. This intermediate is susceptible to nucleophilic attack at the electropositive α-C-position.

An internal attack of the amide ligand in this position results in the formation of a Ru(II)-enamide intermediate. The neutral ligand cleaved during the rearrangement step refills the coordination site of the amide. Finally, reductive elimination releases the enamide and regenerates the original catalytically active Ru(0) species. The stereochemistry is controlled by the steric bulk of the phosphine ligands. Bulky, chelating phosphines lead to the formation of *Z*-enamides, whereas the use of smaller monodentate phosphines results in *E*-configured products.

5.2. Hydroamidation of terminal alkynes with primary amides

Primary amides are challenging substrates because of their weakly nucleophilic character and the greater reactivity of the secondary enamide products towards a second alkyne hydroamidation (Scheme 51).

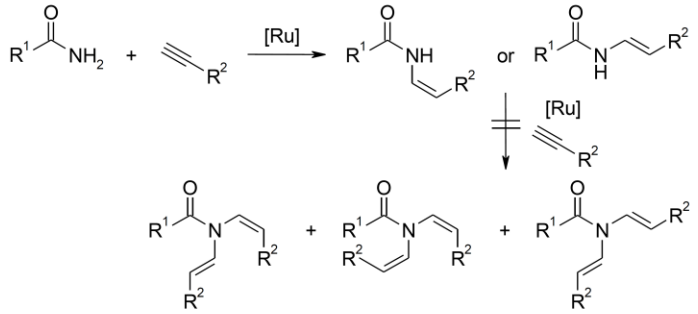

Scheme 51. Challenges in additions of primary amides to terminal alkynes.

The first catalyst system capable of overcoming these hurdles was developed in our group in 2008.[91] The catalyst system is formed in situ from (cod)Ru(met)$_2$, 1,4-bis(dicyclohexylphosphino) butane (dcypb), ytterbium triflate (Yb(OTf)$_3$) and water. The Lewis acid is crucial in facilitating the oxidative addition to the ruthenium center, whereas the electron-rich and sterically demanding bidentate ligand dcypb suppresses a second vinylation of the product and controls the reaction stereochemistry (Scheme 52).

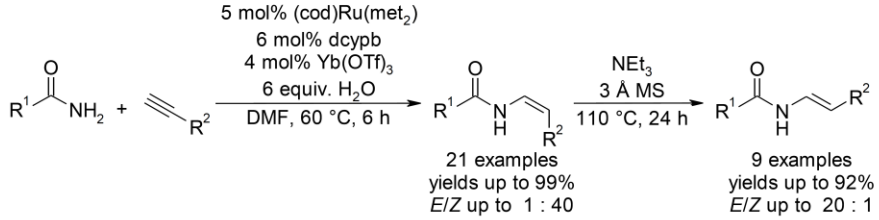

Scheme 52. *Anti*-Markovnikov addition of primary amides to alkynes.

The *Z*-enamides were obtained in good yields and selectivities. Moreover, the corresponding *E*-enamides are accessible by in situ double-bond isomerization following the hydroamidation, by adding triethylamine (NEt_3) and molecular sieves (3 Å) and increasing the temperatures to 110 °C. Representative examples for the wide scope are illustrated in Figure 4, and include the natural product alatamide[92] and a key intermediate in Castedo's total synthesis of aristolactam.[93]

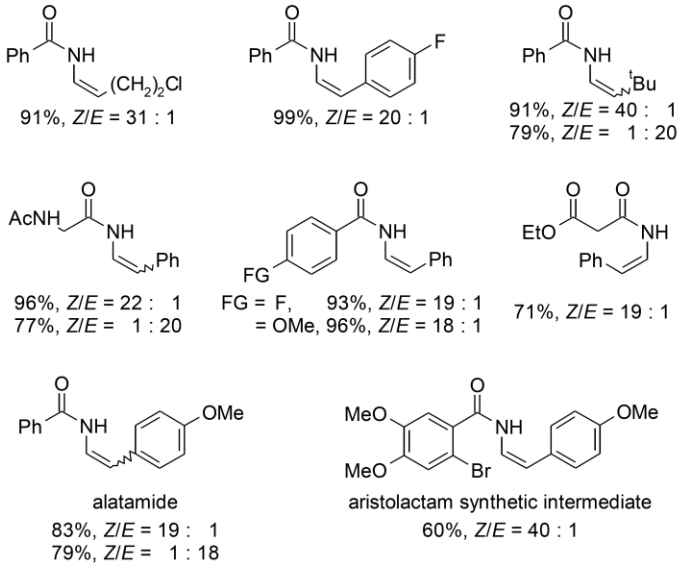

Figure 4. Representative examples for the hydroamidation of terminal alkynes with primary amides.

The value of this bimetallic system was further demonstrated by the synthesis of five bioactive natural products, namely botryllamides C and E, lansiumamides A and B, and lansamide I.[94] Starting from simple, commercially available precursors the desired products were obtained in 1 to 3 reaction steps in 57–98% overall yield (Scheme 53 and Scheme 54).

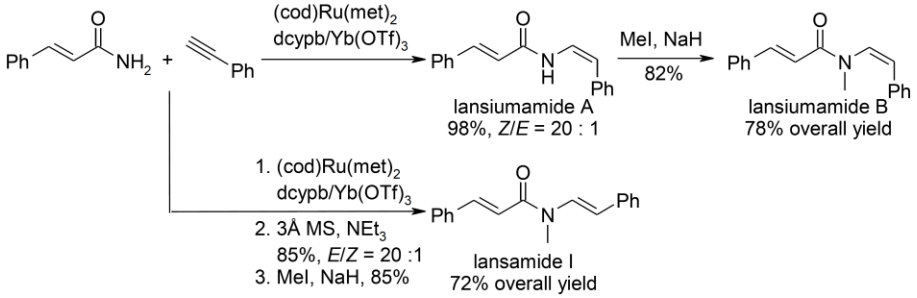

Scheme 53. Syntheses of lansiumamides via hydroamidation.

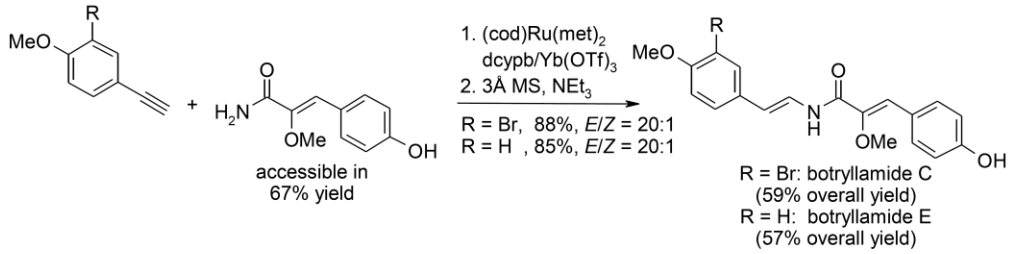

Scheme 54. Syntheses of botryllamides C and E via hydroamidation.

5.3. Addition of related *N*-nucleophiles to terminal alkynes

Related *N*-nucleophiles that have successfully been used in hydroamidations include imides and thioamides. The reactivity of these substrates is particularly low because of the substantially higher acidity of imides and thioamides compared to secondary amides (pK_a(DMSO) of 2-pyrrolidone, 24.2; succinimide 14.6; pyrrolidine-2-thione, 18.1).[95] Additionally, imides are less nucleophilic than secondary amides because of the more favorable electron-pair delocalization of two carbonyl-groups next to the nitrogen and thioamides are ambident nucleophiles. They can react at the nitrogen or sulfur terminus depending on the electrophile used (HSAB concept) and they are known catalyst poisons because of their strong interaction with many late transition metals.

The *anti*-Markovnikov addition of imides to terminal alkynes was achieved with a bimetallic catalyst system generated in situ from (cod)Ru(met)$_2$, P^{n}Bu$_3$ and scandium(III) trifluoromethanesulfonate (Sc(OTf)$_3$) (Scheme 55).[96] The replacement of auxiliary bases by Lewis acid co-catalysts was crucial for a high catalyst activity because this way the N-H acidity rather than the nucleophilicity of the N-H component determined the reaction outcome. Sc(OTf)$_3$ acidifies the N-H bond via interaction with the carbonyl oxygens, which efficiently facilitates the oxidative addition of the imide, allowing the reaction to proceed at a reduced reaction temperature of 60 °C in DMF as solvent. This new protocol gives access to *Z*-configured enimides in good yields and high selectivities. Alternatively, using higher catalyst loadings and triisopropylphosphine (P^{i}Pr$_3$) in place of P^{n}Bu$_3$, the *E*-configured isomer can be synthesized as the major product. The generality of the two complementary reaction protocols was tested with regard to both coupling partners.

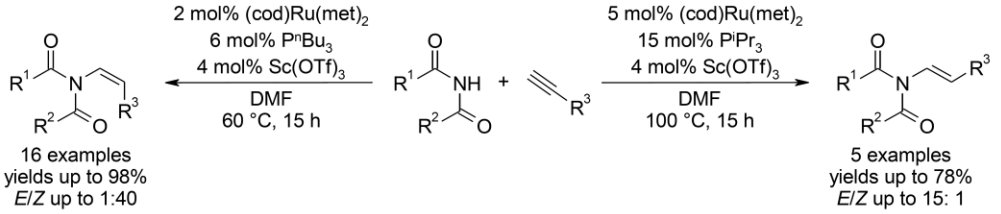

Scheme 55. *Anti*-Markovnikov addition of imides to alkynes.

We were able to modify our first catalyst system and to broaden the scope of hydroamidations to the *anti*-Markovnikov addition of secondary thioamides across terminal alkynes (Scheme 56).[97] An in situ system using tri-*n*-octylphosphine (P^nOc_3) and molecular sieves (3 Å) instead of P^nBu_3 and DMAP lead to the formation of *E*-configured thioenamides in up to 98% yield and a *E*/*Z*-selectivity up to 30 : 1. The diastereoselectivity could be reversed in favor of the corresponding *Z*-configured isomer when dcypm and potassium *tert*-butoxide were used instead of P^nOc_3 and molecular sieves (MS). The presented scope contained a total of 19 representative examples; e.g. pyrrolidine-2-thione added smoothly to various alkynes, among them alkyl and aryl-substituted alkynes, conjugated enynes and trimethylsilylacetylene. A range of secondary thioamides could be converted as well, bearing aromatic or aliphatic substituents.

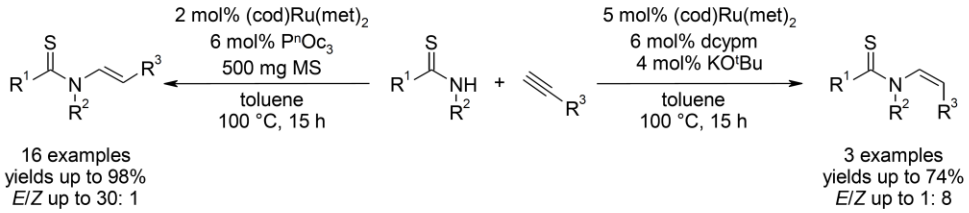

Scheme 56. *Anti*-Markovnikov addition of secondary thio amides to alkynes.

6. Hydroamidations with catalysts other than ruthenium

6.1. Hydroamidation of terminal alkynes

Since the development of the first (cod)Ru(met)$_2$-based methods for the *anti*-Markovnikov intermolecular addition of amides to terminal alkynes, other late transition metal complexes have been introduced as catalysts for such hydroamidation processes.

Sun et al. reported the $AgNTf_2$-catalyzed (silver bis(trifluoromethylsulfonyl) imide) hydroamidation of electron-rich siloxy alkynes with secondary amides and carbamates (Scheme 57).[98] This method allows the *E*-selective synthesis of *α*-siloxy enamides in good to excellent yields within only 30 minutes at ambient temperature. However, the scope is limited to aliphatic or aromatic siloxy alkynes, which are not readily available and.

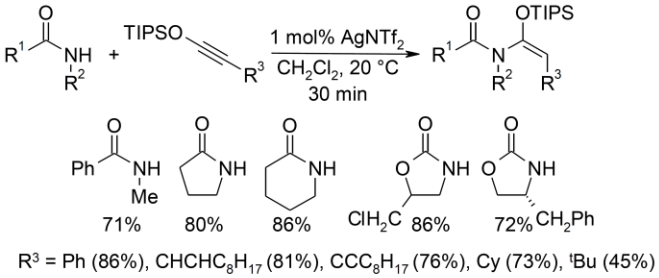

Scheme 57. Silver-catalyzed hydroamidation of siloxy alkynes.

The proposed mechanism is illustrated in Scheme 58.

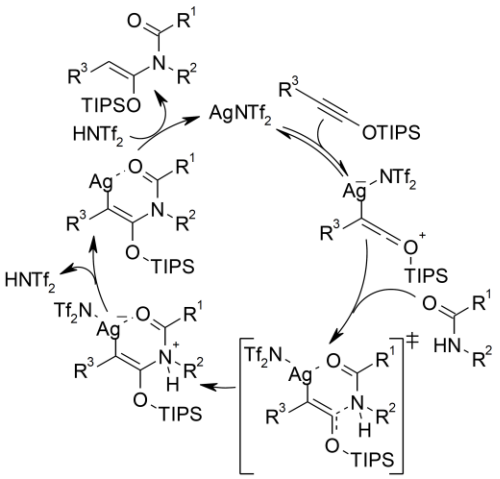

Scheme 58. Mechanism for the Ag-catalyzed hydroamidation.

According to the authors, that the reaction starts with a fast and reversible complexation between the siloxy alkyne and $AgNTf_2$ to give a silver–alkyne complex. The equilibrium can be shifted towards the silver–alkyne complex by higher concentrations of the alkyne. The subsequent attack of the activated by the amide alkyne is presumed to be rate-determining. It proceeds via a six-membered transition state and results

in a highly *syn*-selective addition. Subsequent release of a proton from this intermediate and protodemetallation of the alkenyl–silver compound releases the observed product and regenerates the active silver catalyst.

In 2007, Yudha et al. described the first example of a rhenium-catalyzed intermolecular hydroamidation of terminal alkynes (Scheme 59).[99] In the presence of dirheniumdecacarbonyl, cyclic lactames undergo *anti*-Markovnikov addition to terminal alkynes, yielding *E*-configured enamides in up to 80%. The mechanism is assumed to involve Re-vinylidene intermediates, in analogy to those observed in Ru-based protocols. This first Re-based protocol was not attained the high efficiency and functional group tolerance of Ru-catalyzed methods.

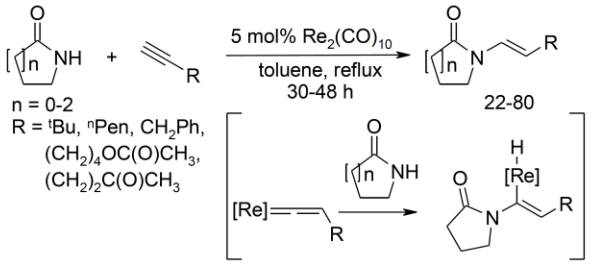

Scheme 59. Rhenium-catalyzed hydroamidation of terminal alkynes with cyclic lactams.

The cobalt-mediated regio- and stereoselective synthesis of dienamides via hydroaminative alkyne coupling of α,ω-diynes was reported by Vollhardt and co-workers (Scheme 61). In the presence of one equivalent of (η^5-cyclopentadienyl)bis(η^2-ethene)cobalt(I) ($CpCo(C_2H_4)_2$) several dienamides could be synthesized in good yields and regioselectivities after 24 h at room temperature. The reaction proceeds via oxidative coupling of the α,ω-diynes to form a cobaltcyclopentadiene followed by proton transfer from the amide with formation of a *N*-coordinated cobaltacyclopentene complex. Reductive valence tautomerization and removal of the cobalt-mediator with iron(III)nitrate furnishes the product.

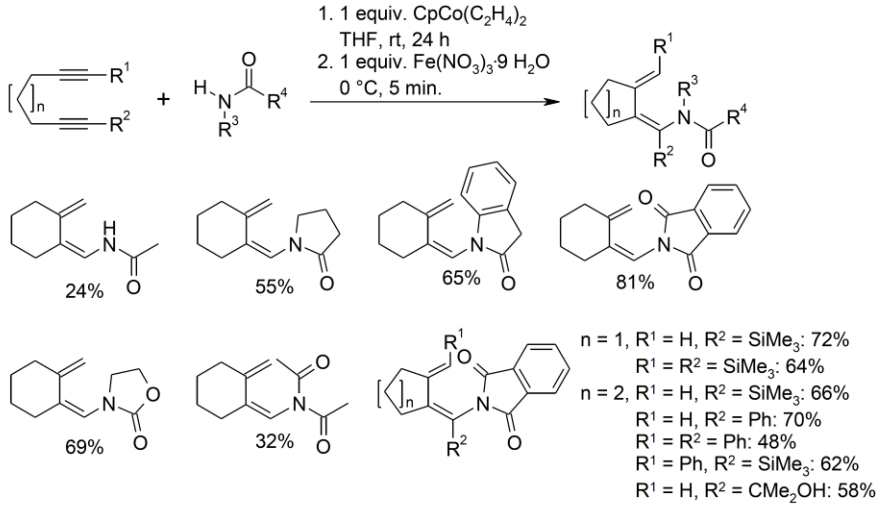

Scheme 60. Cobalt-mediated syntheses of dienamides via hydroaminative alkyne coupling.

A synthesis of *N*-alkenynes via copper/phenanthroline-catalyzed hydroamidation of 1,3-diynes was published in 2011 by Kundu and co-workers (Scheme 61).[100] Fair to good yields of *N*-alkenynes and high *E*-selectivities were obtained in the addition of acylic amides with 10 mol% of catalyst. Under the same reaction conditions, many acyclic secondary amines also underwent addition to 1,3-diynes in good to excellent yields and in high stereoselectivity. In contrast to the Ru-catalyzed method of Shimada et al. (see Scheme 42), the copper catalyst is only able to mediate the addition of one amide to the diyne, therefore no C-C bond cleavage takes place and *N*-alkenynes can be isolated.

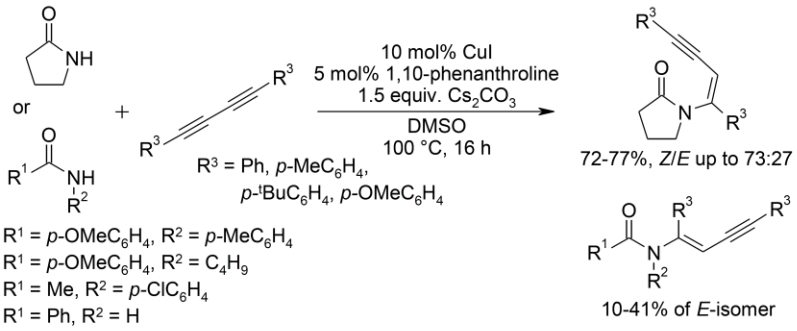

Scheme 61. Copper/phenanthroline-catalyzed hydroamidation of 1,3-diynes.

6.2. Hydroamidation of alkenes

The first protocol for the platinum-catalyzed hydroamidation of olefins (see Scheme 22) could be further extended to vinyl arenes by Widenhoefer and co-workers. They used tri-4-trifluoromethylphenylphosphine instead of PPh_3 and performed the reaction in mesitylene at 140 °C and ambient pressure (Scheme 62).[101]

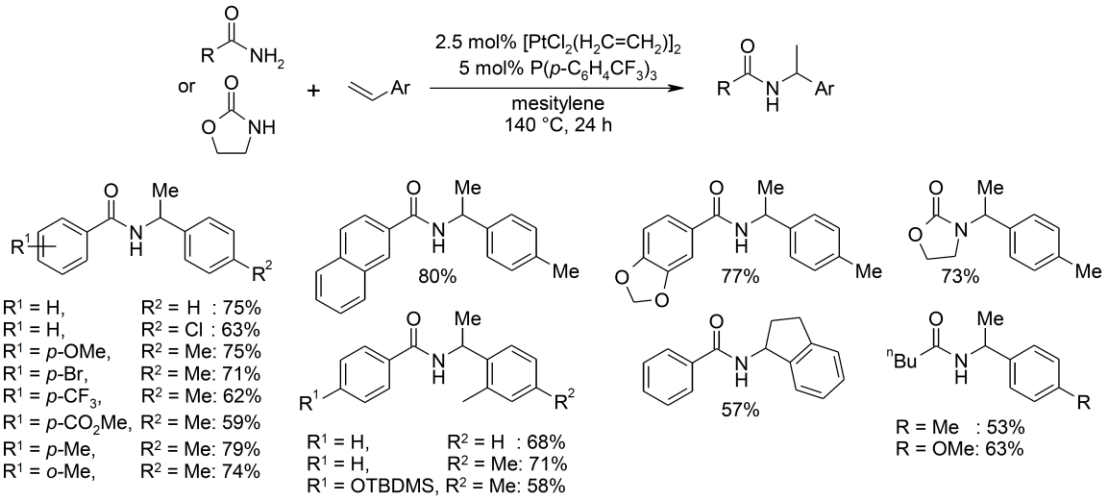

Scheme 62. Scope of the platinum-catalyzed hydroamidation of vinyl arenes.

The proposed reaction mechanism is illustrated in Scheme 63. The catalytic cycle starts with an outer-sphere attack of the amide to a platinum-olefin π-complex, resulting in the formation of a zwitterionic platinum-alkyl intermediate. Loss of HCl from this intermediate followed by protonolysis of the Pt-C bond releases the *N*-alkyl-amide with regeneration of the catalytically active Pt-species. The authors reasoned that the high Markovnikov selectivity of the platinum-catalyzed hydroamination of vinyl arenes might result from the zwitterionic character of the M-olefin interaction, which places substantial positive charge on the benzylic carbon atom.

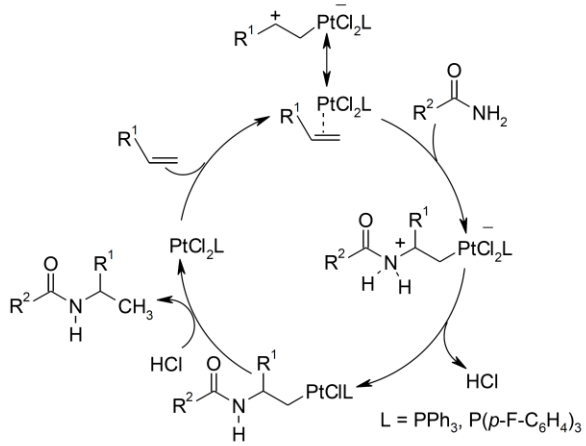

Scheme 63. Postulated mechanism for the platinum-catalyzed hydroamidation of ethylene and vinyl arenes.

A gold-catalyzed intramolecular addition of amides to terminal olefins was developed by Che and co-workers (Scheme 64).[102] This method furnishes several lactams in moderate to good yields under mild reaction conditions. Furthermore, thermal or microwave-assisted conditions allowed the use of this method for the intramolecular addition of various sulfonamides to terminal olefins.

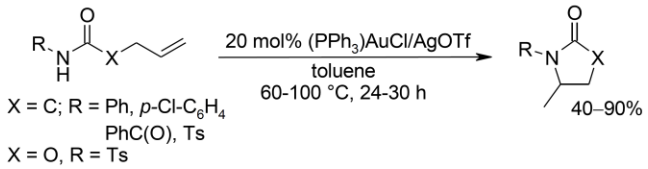

Scheme 64. Gold-catalyzed intramolecular hydroamidation of terminal olefins.

6.3. Intramolecular hydroamidation of alkynes

The palladium-catalyzed intramolecular hydroamidation of internal or terminal alkynes to yield indoles or other aromatic or aliphatic heterocycles has intensively been investigated since 1985. Intramolecular hydroamidation methods start from pre-formed, amido-functionalized terminal or internal alkynes[103] or, alternatively, involve cascade cross-coupling/hydroamidation reactions of *ortho*-iodo-benzamides and internal alkynes (Scheme 65).[104]

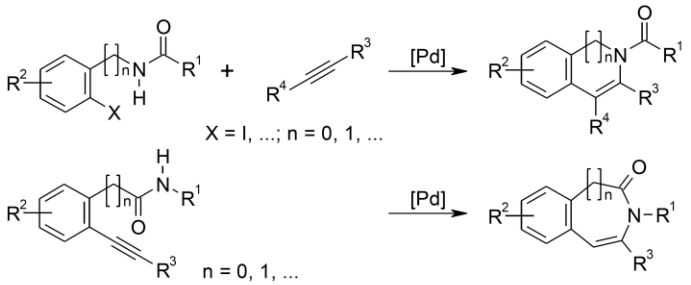

Scheme 65. Palladium-catalyzed intramolecular hydroamidation reaction pathways to indoles and heterocycles.

MacDonald and co-workers showed that group VI metals are able to promote intramolecular hydroamidation reactions of alkynyl amides (Scheme 66).[105] In the presence of stoichiometric and catalytic amounts of molybdenum, chromium and tungsten, fair to good yields of BOC-protected heterocycles were obtained. These results show that especially molybdenum is an active catalyst for intramolecular hydroamidation reactions.

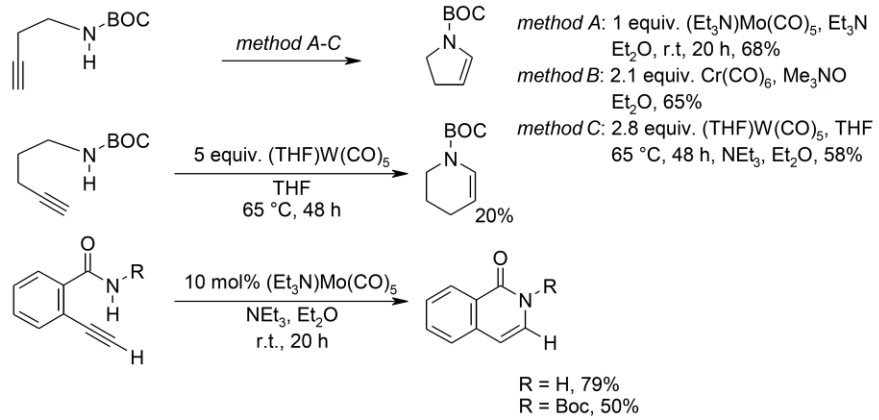

Scheme 66. Group VI metal-catalyzed intramolecular hydroamidation of alkynyl amides.

A domino C-N coupling/hydroamidation cascade was described by Buchwald and co-workers.[106] This combination of copper-catalyzed processes represents a straightforward synthesis of pyrroles and pyrazoles, starting from haloenynes (Scheme 67). In the presence of 5 mol% copper iodide, 20 mol% *N*,*N*'-dimethylethylenediamine and 2 equivalents of cesium carbonate, a broad range of pyrroles and pyrazoles

were synthesized in good to excellent yield. Drawbacks of this method are the costs as well as the limited availability of the required haloenynes and the restriction to carbamates as nucleophiles.

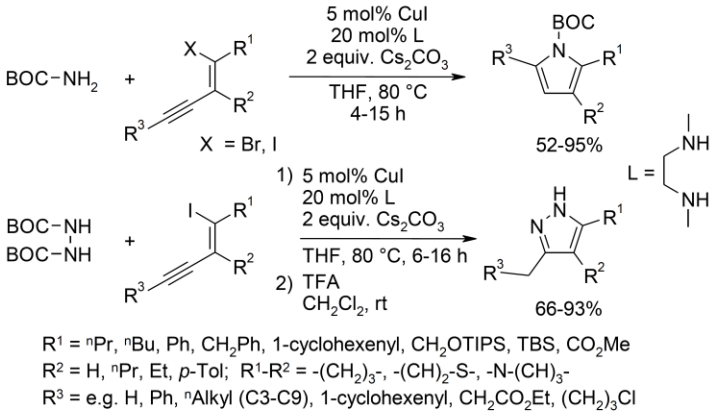

Scheme 67. Synthesis of pyrroles and pyrazoles via domino C-N coupling/hydroamidation cascade.

Further Rh-, Au-, or Au/Ag-catalyzed intramolecular hydroamidations are the key step in the synthesis of complex heterocycles such as tetracyclic heterocycles (e.g. dihydronitidine),[107] cyclic guanidines,[108] 4-alkylidene-2-oxazolidinones,[109] benzodiazepines,[110] tetrahydropyrroles,[111] polysubstituted 2-aminoimidazole alkaloids,[112] or CDE ring system of tetrahydroisoquinoline alkaloids.[113] Intramolecular Au/Ag-catalyzed hydroamidations proceed in aqueous media, and lead to indole derivatives in high yields.[114]

6.4. Hydroamidation without transition metal catalysts

It is also worth mentioning that several late transition metal-free hydroamidation protocols had been reported over the last decades.

Trost et al. introduced a phosphine-catalyzed hydroamidation of alkynoates that proceeds via Michael-addition of the phosphine to the alkyne and protonation to an ylide-type intermediate.[115] This undergoes attack by the imide or sulfonamide α to the ester, followed by proton shift and elimination of the phosphine organocatalyst. This process gives access to *E*-configured dehydro-α-aminoacids in up to 95% yield (Scheme 68).

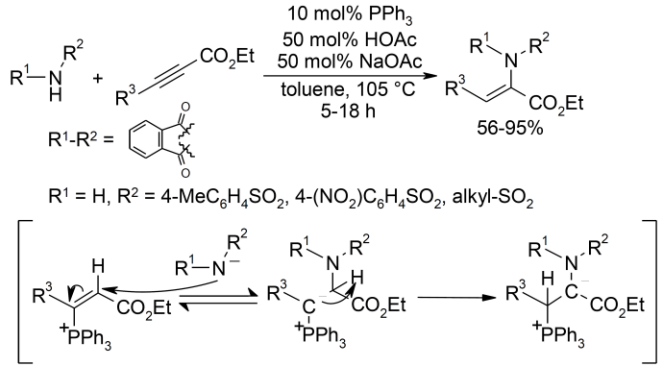

Scheme 68. Phosphine-catalyzed hydroamidation of alkynoates.

Further transition metal-free hydroamidation methods are mediated by bases or Brønstedt acids. The former involve caesium carbonate for the selective addition of amides to activated 1-alkynylphosphine sulfides to generate *E*-2-amino-1-thiophosphinyl-1-alkenes,[116] potassium phosphate for the addition of cyclic lactams to ynamides to give ketene *N*,*N*-acetals,[117] and potassium carbonate as well as palladium acetate in a two-step synthesis of polycyclic indoles via intramolecular hydroamidation/annulation tandem reaction.[118] Kundu et al. reported an iodine-mediated three-component domino reaction synthesis of iodo-indoloazepinones via a regioselective 7-endo-dig iodo-cyclization pathway.[119] Sudalei and co-workers described an *N*-bromosuccinimide-catalyzed addition of carbamates to activated styrenes.[120] Brønstedt acid-catalyzed hydroamidations include triflic acid-mediated cyclization of amidoalkenes,[121] and the triflic acid-promoted sequential hydroarylation–hydroamidation of arene-tethered 1-(2-alkynylphenyl)ureas yielding 4,4-spiro-3,4-dihydro-2-(1H)-quinazolinones.[122]

7. Conclusions

The late transition metal-catalyzed addition of N-H nucleophiles across alkenes and alkynes is in fact a highly efficient and atom-economic reaction pathway for the synthesis of enamines/imines and enamides, which are valuable bulk and fine chemicals or important building blocks in organic synthesis and often incorporated in biologically active, naturally occurring compounds.

Compared to most established methods for the synthesis of those substance classes, hydroamination/hydroamidation reactions offer many significant advantages. As starting materials alkynes

and amines/amides are used, which are readily available, can be handled in air and are cheaper than most coupling reagents or specialized nitrogen-containing compounds, e.g. needed for cross-couplings, Wittig-reactions or Curtius-rearrangements. Besides the formation of alkyne oligomers for some hydroamination/hydroamidation protocols, the addition reaction proceeds atom-economically without the formation of further by-products such as stoichiometric amounts of inorganic salts or coupling reagent residues. The reaction can be achieved at temperatures below 100 °C and in less than 6 h, whereas condensation reactions of ketones and amines/amides were often performed in boiling toluene or other high boiling solvents for more then 24 h. The main advantage of transition metal-catalyzed addition reactions across alkenes and alkynes is the possibility to control the regio- and stereoselectivity of the reaction by the electronic and steric properties of the metal complex used. In most alternative methods the thermodynamically favored *E*-configured products or mixtures of *E*- and *Z*-isomers are obtained, or the stereoselectivity problem is passed on to the configuration of the starting materials.

Ruthenium complexes proved to be very efficient catalysts for the inter- and intramolecular hydroamination of internal and terminal alkenes and alkynes, but the performance of these systems is similar to e.g. those of titanium- or palladium-based methods. High catalyst loadings and an excess of the alkene or alkyne are often required to achieve high conversions, due to relatively low turn-over numbers and oligomerization side reactions. The main advantage of Ru-based methods is the fact that more functional groups are tolerated, such as ethers, silylethers, esters, halogens, sulfonates, phosphonates, thiophenes and nitro-groups, expanding the synthetic applicability of this transformation. Palladium-based methods were mainly used for intramolecular hydroamination reactions or in cascade reactions with a variety of other Pd-catalyzed transformations, while titanium-catalyzed hydroamination protocols are often limited to aliphatic and aromatic compounds and must be carried out under strictly anaerobic conditions since the metal center is air-sensitive.

In contrast to hydroamination processes the Ru-catalyzed hydroamidation of terminal alkynes exhibits superior catalyst activity and unprecedented stereo- and regioselectivity as well as functional group tolerance. Other transition metal-catalyzed or transition metal-free processes are limited to activated alkynes

or intermolecular reaction pathways or reach only moderate conversion levels and therefore can simply be seen as proof of concept.

The most efficient hydroamidation catalyst systems are simply formed in situ from air-stable Ru(II) or Ru(III) precursors, phosphine ligands and additional basic or Lewis-acidic additives. Despite the fact that a two-fold excess of the alkyne is needed to reach a high conversion due to Ru-catalyzed oligomerization side reactions, and also the fact that substrate class-dependent modifications of the in situ formed catalyst system were required to expand the scope, a huge variety of valuable enamides can be synthesized via addition of amides to terminal alkynes. The requirement of substrate-adopted hydroamidation methods originates in the significant electronic and steric differences between primary as well as secondary amides, imides and thioamides because of the influence of a second substituent or a second electron withdrawing group next to the nitrogen or the influence of the bigger sulfur instead of the oxygen atom of the carbonyl group. So far only terminal alkynes can be converted and only *anti*-Markovnikov addition products can be synthesized. Both limitations are based on the formation of Ru-vinylidene species as catalytically active intermediates, which require terminal alkynes to be generated and selectively induce an *anti*-Markovnikov attack of the nucleophile in α-position to the Ru center.

The high catalyst loadings of 2 to 5 mol% and the resulting costs could be dramatically reduced by using $RuCl_3$ instead of $(cod)Ru(met)_2$ for the addition of secondary amides and thioamides to terminal alkynes. The addition of primary amides and imides could not be accomplished using $RuCl_3$ as Ru source; in return the reaction conditions of the bimetallic catalyst systems are much milder, allowing the hydroamidation reaction to proceed at 60 instead of 100 °C. Still, the slightly lower functional group tolerance for the bimetallic catalyst systems and in general the need of a second costly transition metal prevent a big-scale industrial application of this method. In order to use such methods in a sustainable, profitable and completely atom-economic process, the catalyst loadings must be reduced considerably below 1 mol%, the alkyne oligomerization must be minimized, and less toxic and easier removable solvents must be employed.

Recently new reaction intermediates of the Ru-catalyzed hydroamidation could be identified, leading to a better mechanistic understanding and resulting in a new reaction mechanism. These new insights of the catalytic process represent an ideal starting point for further optimizations of the catalyst systems as well as

the development of a universally applicable hydroamidation method. However, it also showed that ruthenium might not be the metal center of choice for the development of a Markovnikov-selective hydroamidation protocol, because electron-rich Ru complexes are required to achieve the addition of amides to alkynes, which are know to form Ru-vinylidene species in the presence of terminal alkynes with and without the involvement of Ru-hydride species. These Ru-vinylidene complexes always induce the formation of an *anti*-Markovnikov addition product.

Consequently, alternative metal centers such as gold or silver should be further investigated regarding their catalytic activity in intermolecular hydroamidation reactions. First Au- and Ag-based hydroamidation methods were successfully developed and could even be performed in aqueous reaction media, but so far they remain limited to intramolecular processes or the use of activated alkynes. Platinum-based methods allowed for the first time the hydroamidation of non-activated alkenes and might also be interesting alternatives for the development of Markovnikov selective hydroamidation processes. Additional studies are required to possibly outperform the Ru-based hydroamidation protocols or to accomplish the first Markovnikov selective hydroamidation.

8. Acknowledgements

We thank the Landesgraduiertenförderung Rheinland Pfalz for a scholarship to M. Arndt.

9. References

(1) For a review see: (a) Alonso, F.; Beletskaya, I. P.; Yus, M. *Chem. Rev.* **2004**, *104,* 3079. (b) Müller, T. E.; Beller, M. *Chem. Rev.* **1998**, *98*, 675. (c) Müller, T. E.; Hultzsch, K. C.; Yus, M.; Foubelo, F.; Tada, M. *Chem. Rev.* **2008**, *108,* 3795.

(2) (a) Pohlki, F.; Doye, S. *Chem. Soc. Rev.* **2003**, *32*, 104. (b) Severin, R.; Doye, S. *Chem. Soc. Rev.* **2007**, *36*, 1407.

(3) (a) Knoelker, H.-J.; Agarwal, S. *Tetrahedron Lett.* **2005**, *46*, 1173. (b) Zhang, Q.; Tu, G.; Zhaoa, Y.; Cheng, T. *Tetrahedron* **2002**, *58*, 6795.

(4) Hensens, O. D.; Goetz, M. A.; Liesch, J. M.; Zink, D. L.: Raghoobar, S. L.; Helms, G. L.; Singh, S. B. *Tetrahedron Lett.* **1995**, *36*, 2005.

(5) (a) Michael, J. P. *Nat. Prod. Rep.* **2005**, *22*, 603. (b) Jiang, X.-P.; Cheng, Y.; Shi, G.-F.; Kang, Z.-M. *J. Org. Chem.* **2007**, *72*, 2212.

(6) (a) Rao, M. R.; Faulkner, D. J. *J. Nat. Prod.* **2004**, *67*, 1064. (b) Henrich, C. J.; Robey, R. W.; Takada, K.; Bokesch, H. R.; Bates, S. E.; Shukla, S.; Ambudkar, S. V.; McMahon, J. B.; Gustafson, K. R. *ACS Chem. Biol.* **2009**, *4*, 637. (c) Takada, K.; Imamura, N.; Gustafson, K. R.; Henrich, C. *J. Bioorg. Med. Chem. Lett.* **2010**, *20*, 1330. (d) McDonald, L. A.; Swersey, J. C.; Ireland, C. M. *Tetrahedron* **1995**, *51*, 5237.

(7) Toske, S. G.; Jensen, P. R.; Kauffman, C. A.; Fenical, W. *Tetrahedron* **1998**, *54*, 13459.

(8) Lin, J.-H. *Phytochemistry* **1989**, *28*, 621.

(9) Davyt, D.; Entz, W.; Fernandez, R.; Mariezcurrena, R.; Mombrú, A. W.; Saldaña, J.; Domínguez, L.; Coll, J.; Manta, E. *J. Nat. Prod.* **1998**, *61*, 1560.

(10) For a review of metal-catalyzed asymmetric hydrogenations see: Tang, W.; Zhang, X. *Chem. Rev.* **2003**, *103*, 3029.

(11) For recent examples of organo-catalyzed asymmetric hydrogenations see: (a) Malkov, A. V.; Stewart-Liddon, A. J. P.; Ramírez-López, P.; Bendová, L.; Haigh, D.; Kočovský, P. *Angew. Chem.* **2006**, *118*, 1460; *Angew. Chem. Int. Ed.* **2006**, *45*, 1432. (b) Malkov, A. V.; Stončius, S.; Kočovský, P. *Angew. Chem.* **2007**, *119*, 3796; *Angew. Chem. Int. Ed*. **2007**, *46*, 3722. (c) Iwasaki, F.; Omonura, O.; Mishima, K.; Kanematsu, T.; Maki, T.; Matsumura, Y. *Tetrahedron Lett.* **2001**, *42*, 2525. (d) Wang, Z.; Ye, K.;

Wei, S.; Wu, P.; Zhang, A.; Sun, J. *Org. Lett*. **2006**, *8*, 999. (e) Rueping, M.; Sugiono, E.; Azap, C.; Theissmann, T.; Bolte, M. *Org. Lett*. **2005**, *7*, 3781. (f) Hoffman, S.; Seayad, A. M.; List, B. *Angew. Chem*. **2005**, *117*, 7590; *Angew. Chem., Int. Ed.* **2005**, *44*, 7424. (g) Storer, R. I.; Carrera, D. E.; Ni, Y.; MacMillan, D. W. C. *J. Am. Chem. Soc.* **2006**, *128*, 84.

(12) Hou, G.-H.; Xie, J.-H.; Yan, P.-C.; Zhou, Q.-L. *J. Am. Chem. Soc.* **2009**, *131*, 1366.

(13) (a) Sell, T.; Meiswinkel, A.; Mehler, G.; Reetz, M. T. *Tetrahedron Lett.* **2002**, *43*, 7941. (b) van den Berg, M.; Minnaard, A. J.; Haak, R. M.; Leeman, M.; Schudde, E. P.; Meetsma, A.; Feringa, B. L.; de Vries, H. M.; Maljaars, E. P.; Wilians, C. E.; Hyett, D.; Boogers, A. F.; Hendricks, J. W.; de Vries, J. G. *Adv. Synth. Catal.* **2003**, *345*, 308.

(14) Malkov, A. V.; Stončius, S.; Vranková, K.; Arndt, M.; Kočovský, P. *Chem. Eur. J.* **2008**, *14*, 8082.

(15) For reviews see: (a) Nicolaou, K. C.; Snyder, S. A.; Montagnon, T.; Vassilikogiannakis, G. *Angew. Chem.* **2002**, *114*, 1742; *Angew. Chem. Int. Ed.* **2002**, *41*, 1668. (b) Desimoni, G.; Tacconi, G. *Chem. Rev.* **1975**, *75*, 651.

(16) Stevenson, P. J.; Graham, I. *Arkivoc* **2003**, *VII*, 139.

(17) Gaulon, C.; Dhal, R.; Chapin, T.; Maisonneuve, V.; Dujardin, G. *J. Org. Chem.* **2004**, *69*, 4192.

(18) Huang, Y.; Iwama, T.; Rawal, V. H. *J. Am. Chem. Soc.* **2000**, *122*, 7843.

(19) (a) Reppe, W.; Krzikalla, H.; Dornheim, O. Verfahren zur Herstellung von *N*-Vinylverbindungen aus stickstoffhaltigen Verbindungen und Acetylen. Ger. Patent DE000000890508B, January 17, 1939. (b) Reppe, W.; Krzikalla, H. Verfahren zur Herstellung stickstoffhaltiger Derivate aromatischer Oxyverbindungen. Ger. Patent DE000000851197B, April 18, 1944. (c) Reppe, W. *Justus Liebigs Ann. Chem.* **1956**, *601*, 81.

(20) (a) Reppe, W.; Schuster, C., Hartmann, A. Verfahren zur Herstellung von polymeren Vinylverbindungen. Ger. Patent DE000000737663A, January 17, 1939. (b) Reppe, W.; Herrle, K.; Fikentscher, H. Verfahren zur Herstellung von Polymerisationsprodukten aus N-Vinyllactamen. Ger. Patent DE000000922378B, November 21, 1943. (c) Bühler, V. *Kollidon® - Polyvinylpyrrolidone excipients for pharmaceutical industry*; BASF SE: Ludwigshafen, 2008; p 12.

(21) Kollidon®, Luviskol®, Sokalan® and Luvitec® are registered trademarks of the BASF SE.

(22) Fischer, F.; Bauer, S. *Chem. Unserer Zeit*, **2009**, *43*, 376.

(23) For reviews of the reactivity of enamines/imines and enamides see: (a) Layer, R. W. *Chem. Rev.* **1963**, *63*, 489. (b) Granik, V. G. *Russ. Chem. Rev.* **1984**, *53*, 383. (c) Adams, J. P.; Robertson, G. *Contemp. Org. Synth.* **1997**, *3*, 183. (d) Carbery, D. R. *Org. Biomol. Chem.* **2008**, *6*, 3455.

(24) (a) Matsubara, R.; Nakamura, Y.; Kobayashi, S. *Angew. Chem.* **2004**, *116*, 1711; *Angew. Chem., Int. Ed.* **2004**, *43*, 1679. (b) Matsubara, R.; Kobayashi, S. *Acc. Chem. Res.* **2008**, *41*, 292. (c) Matsubara, R.; Nakamura, Y.; Kobayashi, S. *Angew. Chem.* **2004**, *116*, 3319; *Angew. Chem. Int. Ed.* **2004**, *43*, 3257. (d) Matsubara, R.; Kawai, N.; Kobayashi, S. *Angew. Chem.* **2006**, *118*, 3898; *Angew. Chem. Int. Ed.* **2006**, *45*, 3814.

(25) (a) Rahbek Knudsen, K.; Risgaard, T.; Nishiwaki, N.; Gothelf, K. V.; Anker Jørgensen, K. *J. Am. Chem. Soc.* **2001**, *123*, 5843. (b) Hagiwara, E.; Fujii, A.; Sodeoka, M. *J. Am. Chem. Soc.* **1998**, *120*, 2474. (c) Hamada, T.; Manabe, K.; Kobayashi, S. *J. Am. Chem. Soc.* **2004**, *126*, 7768.

(26) (a) Willans, C. E.; Mulders, J. M. C. A.; de Vries, J. G.; de Vries, A. H. M. *J. Organomet. Chem.* **2003**, *687*, 494. (b) Roff, G. J.; Lloyd, R. C.; Turner, N. J. *J. Am. Chem. Soc.* **2004**, *126*, 4098. (c) Tsujita, H.: Ura, Y.; Matsuki, S.; Wada, K.; Mitsudo, T.-A.; Kondo, T. *Angew. Chem.* **2007**, *119*, 5252; *Angew. Chem., Int. Ed.* **2007**, *46*, 5160.

(27) (a) Haynes, L. W.; Cook, A. G. Methods and Mechanisms of Enamine Formation. In: Enamines: *Synthesis, Structure and Reactions*, (Ed. A G. Cook), Marcel Dekker: New York, **1988**, pp. 103–164; (*b*) Becker, H. G. O. et al., *Organikum*, 22 Ed., Wiley-VCH, Weinheim, **2004**, pp. 462–468. (c) Dulou, R.; Elkik, E.; Veillard, A. *Bull. Soc. Chim. France* **1960**, *967*. (d) Dupau, P.; Le Gendre, P.; Bruneau, C.; Dixneuf, P. H. *Synlett* **1999**, 1832. (e) Wang, X. Jr; Porco, J. A. *J. Org. Chem*. **2001**, *66*, 8215. (f) Bayer, A.; Maier, M. E. *Tetrahedron* **2004**, *60*, 6665. (g) Adam, W.; Bosio, S. G.; Turro, N. J. *J. Org. Chem*. **2004**, *69*, 1704. (h) Burk, M. J.; Casy, G.; Johnson, N. B. *J. Org. Chem*. **1998**, *63*, 6084.

(28) Katritzky, A. R.; Long, Q.-H.; Lue, P.; Jozwiak, A. *Tetrahedron* **1990**, *46*, 8153.

(29) Eisch, J. J.; Sanchez, R. *J. Org. Chem.* **1986**, *51*, 1848.

(30) Morimoto, T.; Skiya, M. *Chem. Lett.* **1985**, 1371.

(31) Varma, R. S.; Dahiya, R.; Kumar, S. *Tetrahedron Lett.* **1997**, *38*, 2039.

(32) (a) Kozawa, Y.; Mori, M. *Tetrahedron Lett.* **2002**, *43*, 111. (b) Barluenga, J.; Fernández, M A.; Aznar, F.; Valdés, C. *Chem. Commun.* **2002**, 2362. (c) Lebedev, A. Y.; Izmer, V. V.; Kazyul'kin, D. N.; Beletskaya, I. P.; Voskoboynikov, A. Z. *Org. Lett.* **2002**, *4*, 623. (d) Kozawa, Y.; Mori, M. *J. Org. Chem.* **2003**, *68*, 3064. (e) Wallace, D. J.; Klauber, D. J.; Chen, C.-y.; Volante, R. P. *Org. Lett.* **2003**, *5*, 4749. (f) Brice, J. L.; Meerdink, J. E.; Stahl, S. S. *Org. Lett.* **2004**, *6*, 1845. (g) Pan, X.; Cai, Q.; Ma, D. *Org. Lett.* **2004**, *6*, 1809. (h) Barluenga, J.; Fernández, M. A.; Aznar, F.; Valdés, C. *Chem. Eur. J.* **2004**, *10*, 494. (i) Reddy, C. R. V.; Urgaonkar, S.; Verkade, J. G. *Org. Lett.* **2005**, *7*, 4427. (j) Barluenga, J.; Valdés, C. *Chem. Commun.* **2005**, 4891. (k) Barluenga, J.; Jiménez-Aquino, A.; Fernández, M. A.; Aznar, F.; Valdés, C. *Tetrahedron* **2008**, *64*, 778. (l) Bolshan, Y.; Batey, R. A. *Angew. Chem.* **2008**, *120*, 2139; *Angew. Chem. Int. Ed.* **2008**, *47*, 2109.

(33) (a) Flitsch, W.; Schindler, S. R. *Synthesis* **1975**, 685. (b) Murphy, P. J.; Brennan, J. Chem. Soc. Rev. **1988**, *17*, 1.

(34) (a) Brettle, R.; Mosedale, A. J. *J. Chem. Soc. Perkin Trans. 1* **1988**, 2185. (b) Kuramochi, K.; Watanabe, H.; Kitahara, T. *Synlett* **2000**, 397.

(35) Hansson, C.; Wickberg, B. *J. Org. Chem.* **1973**, *38*, 3074.

(36) Hosokawa, T.; Takano, M.; Kuroki, Y.; Murahashi, S.-I. *Tetrahedron Lett.* **1992**, *33*, 6643.

(37) Lee, J. M.; Ahn, D.-S.; Jung, D. Y.; Lee, J.; Do, Y.; Kim, S. K.; Chang, S. *J. Am. Chem. Soc.* **2006**, *128*, 12954.

(38) Panda, N.; Jena, A. K.; Raghavender, M. *ACS Catal.* **2012**, *2*, 539.

(39) (a) Brasholz, M.; Reißig, H.-U.; Zimmer, R. *Acc. Chem. Res.* **2009**, *42*, 45. (b) Fögel, O.; Dash, J.; Brüdgam, I.; Hartl, H.; Reißig, H.-U. *Chem. Eur. J.* **2004**, *10*, 4283. (c) Lechel, T.; Dash, J.; Eidamshaus, C.; Brüdgam, I.; Lentz, D.; Reißig, H.-U. *Org. Biomol. Chem.* **2010**, *8*, 3007.

(40) Krompiec, S.; Pigulla, M.; Kuźnik, N.; Krompiec, M.; Marciniec, B.; Chadyniak, D.; Kasperczyk, J. *J. Mol. Catal. A: Chem.* **2005**, *225*, 91.

(41) Bolshan, Y.; Batey, R. A. *Angew. Chem.* **2008**, *120*, 2139; *Angew. Chem., Int. Ed.* **2008**, *47*, 1.

(42) (a) Anastas, P. T.; Warner, J. C. *Green Chemistry: Theory and Practise*, Oxford University Press, Oxford, **1998**. (b) Poliakoff, M.; Fitzpatrick, J. M.; Farren, T. R.; Anastas P. T. *Science* **2002**, *297*, 807.

(43) I. G. Farbenind. AG., Fr. Patent 38.072, January 3, 1930.

(44) Howk, B. W.; Little, E. L.; Scott, S. L.; Whitman, G. M. *J. Am. Chem. Soc.* **1954**, *76*, 1899.

(45) Loritsch, J. A.; Vogt, D. R. R. *J. Am. Chem. Soc.* **1939**, *61*, 1462 and references therein.

(46) Möhrle, H.; Kilian, R. *Tetrahedron* **1969**, *25*, 5745.

(47) Heider, M.; Henkelmann, J.; Ruehl, T. EP 646571, **1995**; *Chem. Abstr.* **1995**, *123*, 229254.

(48) Kondo, T.; Tanaka, A.; Kotachi, S.; Watanabe, Y. *Chem. Commun.* **1995**, 413.

(49) Wang, X.; Widenhoefer, R. A. *Organometallics* **2004**, *23*, 1649.

(50) Haggins, J. *Chem. Eng. News* **1993**, *71*, 23.

(51) Only hydroamidation and Ru-catalyzed hydroamination reactions of alkenes are in the scope of this review. For examples of non ruthenium-catalyzed hydroaminations of alkenes see: (a) Beller, M.; Trauthwein, H.; Eichberger, M.; Breindl, C.; Herwig, J.; Müller, T. E.; Thiel, O. R. *Chem. Eur. J.* **1999**, *5*, 1306. (b) Takasu, K.; Nishida, N.; Ihara, M. *Synlett* **2004**, 1844. (c) Müller, C.; Loos, C.; Schulenberg, N.; Doye, S. *Eur. J. Org. Chem.* **2006**, 2499. (d) Baudequin, C.; Brunet, J.-J.; Rodriguez-Zubiri, M. *Organometallics* **2007**, *26*, 5264. (e) Liu, Z.; Hartwig, J. F. *J. Am. Chem. Soc.* **2008**, *130*, 1570. (f) Leitch, D. C.; Payne, P. R.; Dunbar, C. R.; Schafer, L. L. *J. Am. Chem. Soc.* **2009**, *131*, 18246. (g) Reznichenko, A. L.; Nguyen, H. N.; Hultzsch, K. C. *Angew. Chem.* **2010**, *122*, 9168; *Angew. Chem. Int. Ed.* **2010**, *49*, 8984. (h) Toups, K. L.; Widenhoefer, R. A. *Chem. Commun.* **2010**, *46*, 1712. (i) Hesp, K. D.; Stradiotto, M. *ChemCatChem* **2010**, *2*, 1192. (j) Liu, G.-Q.; Li, Y.-M. *Tetrahedron Lett.* **2011**, *52*, 7168. (k) MacDonald, M. J.; Schipper, D. J.; Ng, P. J.; Moran, J.; Beauchemin, A. M. *J. Am. Chem. Soc.* **2011**, *133*, 20100. (l) Zhang, X.; Emge, T. J.; Hultzsch, K. C. *Angew. Chem.* **2012**, *124*, 406; *Angew. Chem. Int. Ed.* **2012**, *51*, 394. (m) Giner, X.; Nájera, C.; Kovács, G.; Lledós, A.; Ujaque, G. *Adv. Synth. Catal.* **2011**, *353*, 3451.

(52) (a) Bruneau, C.; Dixneuf, P. H. *Angew. Chem.* **2006**, *118*, 2232; *Angew. Chem. Int. Ed.* **2006**, *45*, 2176. (b) Rigaut, S.; Touchard, D.; Dixneuf, P. H. *Coord. Chem. Rev.* **2004**, *248*, 1585.

(53) (a) Barluenga, J.; Aznar, F. *Synthesis* **1977**, 195. (b) Barluenga, J.; Aznar, F.; Liz, R.; Rodes, R. *J. Chem. Soc., Perkin Trans. 1* **1980**, 2732. (c) Barluenga, J.; Jiménez, C.; Nájera, C.; Yus, M. *J. Chem. Soc., Perkin Trans. 1* **1983**, 591. (d) Barluenga, J.; Ferrera, C.; Nájera, C.; Yus, M. *Synthesis* **1984**, 831. (e) Sakamuri, S. *Tetrahedron Lett.* **2001**, *42*, 4317.

(54) For reviews see: (a) Seayad, J.; Tillack, A.; Hartung, C. G.; Beller, M. *Adv. Synth. Catal.* **2002**, *344*, 795. (b) Godoi, B.; Schumacher, R. F.; Zeni, G. *Chem. Rev.* **2011**, *111*, 2937. For a recent example see: (c) Verma, A. K.; Joshi, M.; Singh, V. P. *Org. Lett.* **2011**, *13*, 1630.

(55) For example: (a) Li, Y.; Marks, T. J. *Organometallics* **1996**, *15*, 3770. (b) Li, Y.; Marks, T. J. *J. Am. Chem. Soc.* **1998**, *120*, 1757.

(56) For example: (a) Straub, T.; Haskel, A.; Neyroud, T. G.; Kapon, M.; Botoshansky, M.; Eisen, M. S. *Organometallics* **2001**, *20*, 5017. (b) Haskel, A.; Straub, T.; Eisen, M. S. *Organometallics* **1996**, *15*, 3773.

(57) For example: (a) Walsh, P. J.; Baranger, A. M.; Bergman, R. G. *J. Am. Chem. Soc.* **1992**, *114*, 1708. (b) McGrane, P. L.; Jensen, M.; Livinghouse, T. *J. Am. Chem. Soc.* **1992**, *114*, 5459. (c) Haak, E.; Bytschkov, I.; Doye, S. *Angew. Chem.* **1999**, *111*, 3584; *Angew. Chem., Int. Ed.* **1999**, *38*, 3389. (d) Johnson, J. S.; Bergman, R. G. *J. Am. Chem. Soc.* **2001**, *123*, 2923. (e) Pohlki; F.; Doye, S. *Angew. Chem.* **2001**, *113*, 2361; *Angew. Chem., Int. Ed.* **2001**, *40*, 2305. (f) Straub, B. F.; Bergman, R. G. *Angew. Chem.* **2001**, *113*, 4768; *Angew. Chem., Int. Ed.* **2001**, *40*, 4632. (g) Tillack, A.; Khedkar, V.; Jiao, H.; Beller, M. *Eur. J. Org. Chem.* **2005**, 5001. (h) Heutling, A.; Pohlki, F.; Bytschkov, I.; Doye, S. *Angew. Chem.* **2005**, *117*, 3011, *Angew. Chem., Int. Ed.* **2005**, *44*, 2951. (i) Buil, M. L.; Esteruelas, M. A.; López, A. M.; Concepción Mateo, A. C.; Oñate, E. *Organometallics* **2007**, *26*, 554. (j) Gräbe, K.; Pohlki, F.; Doye, S. *Eur. J. Org. Chem.* **2008**, 4815. (k) Weitershaus, K.; Ward, B. D.: Kubiak, R.; Müller, C.; Wadepohl, H.; Doye, S.; Gade, L. H. *Dalton Trans.* **2009**, 4586. (l) Leitch, D. C.; Turner, C. S.; Schafer, L. L. *Angew. Chem.* **2010**, *122*, 6526; *Angew. Chem. Int. Ed.* **2010**, *49*, 6382.

(58) For example: (a) Utimoto, K.; Miwa, H.; Nozaki, H. *Tetrahedron Lett.* **1981**, *22*, 4277. (b) Richmond, M. K.; Scott, S. L.; Alper, H. *J. Am. Chem. Soc.* **2001**, *123*, 10521. (c) Wolf, L. B.; Tjen, K. C. M. F.; ten Brink, H. T.; Blaauw, R. H.; Hiemstra, H.; Schoemaker, H. E.; Rutjesa, F. P. J. T. *Adv. Synth. Catal.* **2002**, *344*, 70. (d) Arcadi, A. *Synlett* **1997**, 941. (e) Bouyssi, D.; Cavicchioli, M.; Balme, G. *Synlett*

1997, 944. (f) Cacchi, S.; Fabrizi, G.; Carangio, A. *Synlett* **1997**, 959. (g) Iritani, K.; Matsubara, S.; Utimoto, K. *Tetrahedron Lett.* **1988**, *29*, 1799. (h) Bian, Y.-J.; Liu, X.-Y.; Ji, K.-G.; Shu, X.-Z; Guo, L.-N.; Liang, Y.-M. *Tetrahedron* **2009**, *65*, 1424.

(59) For example: (a) Larock, R. C.; Yum, E. K. *J. Am. Chem. Soc.* **1991**, *113*, 6689. (b) Arcadi, A.; Cacchi, S.; Fabrizi, G.; Marinelli, F. *Synlett* **2000**, 394. (c) Chaplin, J. H.; Flynn, B. L. *Chem. Commun.* **2001**, 1594. (d) Alonso, D. A.; Nájera, C.; Pacheco, M. C. *Adv. Synth. Catal.* **2002**, *344*, 172. (e) Ujjainwalla, F.; Warner, D. *Tetrahedron Lett.* **1998**, *39*, 5355. (f) Dai, G.; Larock, R. C. *J. Org. Chem.* **2002**, *67*, 7042. (g) Cao, H.; McNamee, L.; Alper, H. *Org. Lett.* **2008**, *10*, 5281. (h) Ackermann, L.; Sandmann, R.; Kondrashov, M. V. *Synlett* **2009**, 1219. (i) Chena, L.; Xu, M.-H. *Adv. Synth. Catal.* **2009**, *351*, 2005. (j) Severin, R.; Reimer, J.; Doye, S. *Eur. J. Org. Chem.* **2010**, 51.

(60) (a) Kadota, I.; Shibuya, A.; Mpaka Lutete, L.; Yamamoto, Y. *J. Org. Chem.* **1999**, *64*, 4570. (b) Shimada, T.; Yamamoto, Y. *J. Am. Chem. Soc.* **2002**, *124*, 12670. (c) Fix, S. R.; Brice, J. L.; Stahl, S. S. *Angew. Chem.* **2002**, *114*, 172; *Angew. Chem. Int. Ed.* **2002**, *41*, 164. (d) Shimada, T.; Bajracharya, G. B.; Yamamoto, Y. *Eur. J. Org. Chem.* **2005**, 59. (e) Iglesias, Á.; Pérez, E. G.; Muñiz, K. *Angew. Chem.* **2010**, *122*, 8286; *Angew. Chem. Int. Ed.* **2010**, *49*, 8109.

(61) (a) Burling, S.; Field, L. D.; Messerle, B. A. *Organometallics* **2000**, *19*, 87. (b) Hartung, C. G.; Tillack, A.; Trauthwein, H.; Beller, M. *J. Org. Chem.* **2001**, *66*, 6339. (c) Field, L. D.; Messerle, B. A.; Vuong, K. Q.; Turner, P.; Failes, T. *Organometallics* **2007**, *26*, 2058. (d) Fukumoto, Y.; Asai, H.; Shimizu, M.; Chatani, N. *J. Am. Chem. Soc.* **2007**, 129, 13792. (e) Burling, S.; Field, L. D.; Messerle, B. A.; Rumble, S. L. *Organometallics* **2007**, *26*, 4335. (f) Lai, R.-Y.; Surekha, K.; Hayashi, A.; Ozawa, F.; Liu, Y.-H.; Peng, S.-M.; Liu, S.-T. *Organometallics* **2007**, *26*, 1062. (g) Dabb, S. L.; Messerle, B. A. *Dalton Trans.* **2008**, 6368. (h) Dabb, S. L.; Ho, J. H. H.; Hodgson, R.; Messerle, B. A.; Wagler, J. *Dalton Trans.* **2009**, 634. (i) Field, L. D.; Messerle, B. A.; Vuonga, K. Q.; Turner, P. *Dalton Trans.* **2009**, 3599. (j) Alonso-Moreno, C.; Carrillo-Hermosilla, F.; Romero-Fernández, J.; Rodríguez, A. M.; Otero, A.;

Antiñolo, A. *Adv. Synth. Catal.* **2009**, *351*, 881. (k) Gupta, S.; Agarwal, P. K.; Saifuddin, M.; Kundu, B. *Tetrahedron Lett.* **2011**, *52*, 5752.

(62) For reviews see: (a) Widenhoefer, R. A.; Han, X. *Eur. J. Org. Chem.* **2006**, 4555. (b) Corma, A.; Leyva-Pérez, A.; Sabater, M. J. *Chem. Rev.* **2011**, *111*, 1657. For recent examples see: (c) Kang, J.-E.; Kim, H.-B.; Lee, J.-W.; Shin, S. *Org. Lett.* **2006**, *8*, 3537. (d) Lingaiah, N.; Seshu Babu, N.; Mohan Reddy, K.; Sai Prasad, P. S.; Suryanarayana, I. *Chem. Commun.* **2007**, 278. (e) Zhang, Y.; Donahue, J. P.; Li; C.-J. *Org. Lett.* **2007**, *9*, 629. (f) Carney, J. M.; Donoghue, P. J.; Wuest, W. M.; Wiest, O.; Helquist, P. *Org. Lett.* **2008**, *10*, 3903. (g) Corma, A.; González-Arellano, C.; Iglesias, M.; Navarroa, M. T.; Sánchez, F. *Chem. Commun.* **2008**, 6218. (h) Lavallo, F.; Frey, G. D.; Donnadieu, B.; Soleilhavoup, M.; Bertrand, G. *Angew. Chem.* **2008**, *120*, 5302; *Angew. Chem. Int. Ed.* **2008**, *47*, 5224. (i) Duan, H.; Sengupta, S.; Petersen, J. L.; Akhmedov, N. G.; Shi, X. *J. Am. Chem. Soc.* **2009**, *131*, 12100. (j) Leyvaa, A.; Cormaa, A. *Adv. Synth. Catal.* **2009**, *351*, 2876. (k) Liu, X.-Y.; Che, C.-M. *Org. Lett.* **2009**, *11*, 4204. (l) Cui, D.-M.; Zheng, J.-Z.; Yang, L.-Y.; Zhang, C. *Synlett* **2010**, 809. (m) Hirano, K.; Inaba, Y.; Watanabe, T.; Oishi, S.; Fujii, N.; Ohno, H. *Adv. Synth. Catal.* **2010**, *352*, 368. (n) Kramer, S.; Madsen, J. L. H.; Rottländer, M.; Skrydstrup, T. *Org. Lett.* **2010**, *12*, 2758. (o) Dash, C.; Shaikh, M. M.; Butcher, R. J.; Ghosh, P. *Inorg. Chem.* **2010**, *49*, 4972. (p) Leyva-Pérez, A.; Cabrero-Antonino, J. R.;ı Cantín, A.; Corma, A. *J. Org. Chem.* **2010**, *75*, 7769.

(63) (a) Tokunaga, M.; Wakatsuki, Y. *Angew. Chem.* **1998**, *110*, 3024; *Angew. Chem. Int. Ed.* **1998**, *37*, 2867; (b) Tokunaga, M.; Suzuki, T.; Koga, N.; Fukushima, T.; Horiuchi, A.; Wakatsuki, Y. *J. Am. Chem. Soc.* **2001**, *123*, 11917; (c) Grotjahn, D. B.; Incarvito, C. D.; Rheingold, A. L. *Angew. Chem.* **2001**, *113*, 4002; *Angew. Chem. Int. Ed.* **2001**, *40*, 3884; (d) Chevallier, F.; Breit, B. *Angew. Chem.* **2006**, *118*, 1629; *Angew. Chem. Int. Ed.* **2006**, *45*, 1599. (e) Labonne, A.; Kribber, T.; Hintermann, L. *Org. Lett.* **2006**, *8*, 5853. (f) Hintermann, L.; Kribber, T.; Labonne, A.; Paciok, E. *Synlett* **2009**, 2412.

(64) (a) Rotem, M.; Shvo, Y. *Organometallics* **1983**, *2*, 1689. (b) Mitsudo, T.; Hori, Y.; Yamakawa, Y.; Watanabe, Y. *J. Org. Chem.* **1987**, *52*, 2230. (c) Ruppin, C.; Dixneuf, P. H. *Tetrahedron Lett.* **1986**, *27*, 6323. (d) Philippot, K.; Devanne, D.; Dixneuf, P. H. *J. Chem. Soc. Chem. Commun.* **1990**, 1199. (e) Neveux, M.; Seiller, B.; Hagedorn, F.; Bruneau, C.; Dixneuf, P. H. *J. Organomet. Chem.* **1993**, *451*, 133. (f) Goossen, L. J.; Paetzold, J.; Koley, D. *Chem. Commun.* **2003**, 706.

(65) Koelle, U.; Rietmann, C.; Tjoe, J.; Wagner, T.; Englert, U. *Organometallics* **1995**, *14*, 703.

(66) (a) Gemel, C.; Trimmel, G.; Slugovc, C.; Kremel, S.; Mereiter, K.; Schmid, R.; Kirchner, K. *Organometallics* **1996**, *15*, 3998. (b) Varela-Fernández, A.; González-Rodríguez, C.; Varela, J. A.; Castedo, L.; Saá, C. *Org. Lett.* **2009**, *11*, 5350. (c) Liu, P. N.; Su, F. H.; Wen, T. B.; Sung, H. H.-Y. *Chem. Eur. J.* **2010**, *16*, 7889.

(67) Uchimaru, Y. *Chem. Commun.* **1999**, 1133.

(68) Cheung, H. W.; So, C. M.; Pun, K. H.; Zhou, Z.; Lau, C. P. *Adv. Synth. Catal.* **2011**, *353*, 411.

(69) (a) Tokunaga, M.; Eckert, M.; Wakatsuki, Y. *Angew. Chem.* **1999**, *111*, 3416; *Angew. Chem., Int. Ed.* **1999**, *38*, 3222. (b) Tokunaga, M.; Eckert, M.; Wakatsuki, Y. JP Patent 2000, 2000256284; *Chem. Abstr.* **2000**, *133*, 237674.

(70) Lavigne, G. *Eur. J. Inorg. Chem.* **1999**, 917.

(71) Klein, D. P.; Ellern, A.; Angelici, R. J. *Organometallics* **2004**, *23*, 5662.

(72) Mizushima, E.; Chatani, N.; Kakiuchi, F. *J. Organomet. Chem.* **2006**, *691*, 5739.

(73) Fukumoto, Y.; Dohi, T.; Masaoka, H.; Chatani, N.; Murai, S. *Organometallics* **2002**, *21*, 3845.

(74) Schaffrath, H.; Keim, W. *J. Mol. Catal. A: Chem.* **2001**, *168*, 9.

(75) Kawatsura, M.; Hartwig, J. F. *Organometallics* **2001**, *20*, 1960.

(76) (a) Utsunomiya, M. Hartwig, J. F. *J. Am. Chem. Soc.* **2004**, *126*, 2702. (b) Hartwig, J. F.; Utsunomiya, M.; Takaya, J. WIPO *patent application* WO/2005/077885, **2005**.

(77) Takaya, J.; Hartwig, J. F. *J. Am. Chem. Soc.* **2005**, *127*, 5756.

(78) (a) Yi, C. S.; Yun, S. Y. *Org. Lett.* **2005**, *7*, 2181. (b) Yi, C. S. *J. Organomet. Chem.* **2011**, *696*, 76.

(79) Tokunaga, M.; Ota, M.; Haga, M.-A.; Wakatsuki, Y. *Tetrahedron Lett.* **2001**, *42*, 3865.

(80) Ackermann, L.; Althammer, A. *Synlett* **2006**, 3125.

(81) Kondo, T.; Okada, T.; Suzuki, T.; Mitsudo, T.-a. *J. Organomet. Chem.* **2001**, *622*, 149.

(82) Chang, S.; Lee, M.; Jung, D. Y.; Yoo, E. J.; Cho, S. H.; Han, S. K. *J. Am. Chem. Soc.* **2006**, *128*, 12366.

(83) Kuninobu, Y.; Nishina, Y.; Takai, K. *Org. Lett.* **2006**, *8*, 2891.

(84) Shimada, T.; Yamamoto, Y. *J. Am. Chem. Soc.* **2003**, *125*, 6646.

(85) (a) Yi, C. S.; Yun, S. Y.; Guzei, I. A. *J. Am. Chem. Soc.* **2005**, *127*, 5782. (b) Yi, C. S.; Yun, S. Y. *J. Am. Chem. Soc.* **2005**, *127*, 17000.

(86) Kondo, T.; Baba, A.; Nishi, Y.; Mitsudo, T.-a. *Tetrahedron Lett.* **2004**, *45*, 1469.

(87) Gooßen, L. J.; Rauhaus, J. E.; Deng, G. *Angew. Chem.* **2005**, *117*, 4110; *Angew. Chem. Int. Ed.* **2005**, *44*, 4042.

(88) Gooßen, L. J.; Arndt, M.; Blanchot, M.; Rudolphi, F.; Menges, F.; Niedner-Schatteburg, G. *Adv. Synth. Catal.* **2008**, *350*, 2701.

(89) Buba, A. E.; Arndt, M.; Goossen, L. J. *J. Organomet. Chem.* **2010**, *696*, 170.

(90) Arndt, M.; Salih, K. S. M.; Fromm, A.; Gooßen, L. J.; Menges, F.; Niedner-Schatteburg G. *J. Am. Chem. Soc.* **2011**, *133*, 7428.

(91) (a) Gooßen, L. J.; Salih, K. S. M.; Blanchot, M. *Angew. Chem.* **2008**, *120*, 8620; *Angew. Chem. Int. Ed.* **2008**, *47*, 8492. (b) Gooßen, L. J.; Blanchot, M.; Salih, K. S. M.; Gooßen, K. *Synthesis* **2009**, 2283.

(92) (a) Ghosh, S.; Datta, D. B.; Sen, N. *Synth. Commun.* **1987**, *17*, 299. (b) Maxwell, A.; Rampersad, D. *J. Nat. Prod.* **1989**, *52*, 411. (c) Estévez, J. C.; Villaverde, M. C.; Estévez, R. J.; Seijas, J. A.; Castedo, L. *Synth. Commun.* **1990**, *20*, 503.

(93) Estévez, J. C.; Estévez, R. J.; Castedo, L. *Tetrahedron* **1995**, *51*, 10801.

(94) Gooßen, L. J.; Blanchot, M.; Arndt, M.; Salih, K. S. M. *Synlett* **2010**, 1685.

(95) (a) Bordwell, F. G. *Acc. Chem. Res.* **1988**, *21*, 456. (b) Bordwell, F. G.; Fried, H. E. *J. Org. Chem.* **1991**, *56*, 4218.

(96) Gooßen, L. J.; Blanchot, M.; Brinkmann, C.; Gooßen, K.; Karch, R.; Rivas-Nass, A. *J. Org. Chem.* **2006**, *71*, 9506.

(97) Goossen, L. J.; Blanchot, M.; Salih, K. S. M.; Karch, R.; Rivas-Nass, A. *Org. Lett.* **2008**, *10*, 4497.

(98) Sun, J.; Kozmin, S. A. *Angew. Chem.* **2006**, *118*, 5113; *Angew. Chem. Int. Ed.* **2006**, *45*, 4991.

(99) Yudha S., S.; Kuninobu, Y.; Takai, K. *Org. Lett.* **2007**, *9*, 5609.

(100) Gupta, S.; Agarwal, P. K.; Saifuddin, M.; Kundu, B. *Tetrahedron Lett.* **2011**, *52*, 5752.

(101) Qian, H.; Widenhoefer, R. A. *Org. Lett.* **2005**, *7*, 2635.

(102) Liu, X.-Y.;Li, C.-H.; Che C.-M. *Org. Lett.* **2006**, *8*, 2707.

(103) (a) Taylor, E. C.; Katz, A. H.; Salgado-Zamora, H. *Tetrahedron Lett.* **1985**, *26*, 5963. (b) Iritani, K.; Matsubara, S.; Utimoto, K. *Tetrahedron Lett.* **1988**, *29*, 1799. (c) Arcadi, A.; Cacchi, S.; Marinelli, F. *Tetrahedron Lett.* **1992**, *33*, 3915. (d) Kondo, Y.; Shiga, F.; Murata, N.; Sakamoto, T.; Yamanaka, H. *Tetrahedron* **1994**, *50*, 11803. (e) Arcadi, A.; Cacchi, S.; Carnicelli, V.; Marinelli, F. *Tetrahedron* **1994**, *50*, 437. (f) Bouyssi, D.; Cavicchioli, M.; Balme, G. *Synlett* **1997**, 944. (g) Kimura, M.; Wakamiya, Y.; Horino, Y.; Tamaru, Y. *Tetrahedron Lett.* **1997**, *38*, 3963. (h) Mahanty, J. S.; De, M.; Das, P.; Kundu, N. G. *Tetrahedron* **1997**, *53*, 13397. (i) Cacchi, S.; Fabrizi, G.; Marinelli, F.; Moro, L.; Pace, P. *Synlett* **1997**, 1363. (j) Bacchi, A.; Chiusoli, G. P.; Costa, M.; Sani, C.; Gabriele, B.; Salerno, G. *J. Organomet. Chem.* **1998**, *562*, 35. (k) Yasuhara, A.; Kaneko, M.; Sakamoto, T. *Heterocycles* **1998**, *48*, 1793. (l) Sashida, H.; Kawamukai, A. *Synthesis* **1999**, 1145. (m) Jacobi, P. A.; Liu, H. *Org. Lett.* **1999**, *1*, 341. (n) Cacchi, S.; Fabrizi, G.; Pace, P.; Marinelli, F. *Synlett* **1999**, 620. (o) Lei, A.; Lu, X. *Org. Lett.* **2000**, *2*, 2357. (p) Arcadi, A.; Cacchi, S.; Fabrizi, G.; Marinelli, F. *Synlett* **2000**, 394. (q) Karstens, W. F. J.; Stol, M.; Rutjes, F. P. J. T.; Kooijman, H.; Spek, A. L.; Hiemstra, H. *J. Organomet. Chem.* **2001**, *624*, 244. (r) Yu, Y.; Stephenson, G. A.; Mitchell, D. *Tetrahedron Lett.* **2006**, *47*, 3811. (s) Wu, J.; Jiang, Y.; Dai, W.-M. *Synlett* **2009**, 1162.

(104) (a) Larock, R. C.; Yum, E. K. *J. Am. Chem. Soc.* **1991**, *113*, 6689. (b) Wensbo, D.; Eriksson, A.; Jeschke, T.; Annby, U.; Gronowitz, S.; Cohen, L. A. *Tetrahedron Lett.* **1993**, *34*, 2823. (c) Jeschke, T.; Wensbo, D.; Annby, U.; Gronowitz, S.; Cohen, L. A. *Tetrahedron Lett.* **1993**, *34*, 6471. (d) Larock, R. C.; Yum, E. K.; Doty, M. J.; Sham, K. K. C. *J. Org. Chem.* **1995**, *60*, 3270. (e) Fagnola, M. C.; Candiani, I.; Visentin, G.; Cabri, W.; Zarini, F.; Mongelli, N.; Bedeschi, A. *Tetrahedron Lett.* **1997**, *38*, 2307. (f) Zhang, H.-C. Brumfield, K. K.; Maryanoff, B. E. *Tetrahedron Lett.* **1997**, *38*, 2439. (g) Khan, M. W.; Kundu, N. G. *Synlett* **1997**, 1435. (h) Larock, R. C.; Yum, E. K.; Refvik, M. D. *J. Org. Chem.* **1998**, *63*, 7652. (i) Xu, L.; Lewis, I. R.; Davidsen, S. K.; Summers, J. B. *Tetrahedron Lett.* **1998**, *39*, 5159. (j) Chaplin, J. H.; Flynn, B. L. *Chem. Commun.* **2001**, 1594.

(105) McDonald, F. E.; Chatterjee, A. K. *Tetrahedron Lett.* **1997**, *38*, 7687

(106) Martín, R.; Rodríguez Rivero, M.; Buchwald, S. L. *Angew. Chem.* **2006**, *118*, 7237; *Angew. Chem. Int. Ed.* **2006**, *45*, 7079.

(107) Enomoto, T.; Girard, A.-L.; Yasui, Y.; Takemoto, Y. *J. Org. Chem.* **2009**, *74*, 9158.

(108) Gainer, M. J.; Bennett, N. R.; Takahashi, Y.; Looper, R. E. *Angew. Chem.* **2011**, *123*, 710; *Angew. Chem. Int. Ed.* **2011**, *50*, 684.

(109) Ritter, S.; Horino, Y.; Lex, J.; Schmalz, H.-G. *Synlett* **2006**, 3309.

(110) Zhang, L.; Ye, D.; Zhou, Y.; Liu, G.; Feng, E.; Jiang, H.; Liu, H. *J. Org. Chem.* **2010**, *75*, 3671.

(111) de Haro, T; Nevado, C. *Angew. Chem.* **2011**, *123*, 936; *Angew. Chem. Int. Ed.* **2011**, *50*, 906

(112) Ermolat'ev, D. S.; Bariwal, J. B.; Steenackers, H. P. L.; De Keersmaecker, S. C. J.; Van der Eycken, E. V. *Angew. Chem.* **2010**, *122*, 9655; *Angew. Chem. Int. Ed.* **2010**, *49*, 9465

(113) Obika, S.; Yasui, Y.; Yanada, R.; Takemoto, Y. *J. Org. Chem.* **2008**, *73*, 5206.

(114) Ye, D.; Wang, J.; Zhang, X.; Zhou, Y.; Ding, X.; Feng, E.; Sun, H.; Liu, G.; Jiang, H.; Liu, H. *Green Chem.* **2009**, *11*, 1201.

(115) Trost, B. M.; Dake, G. R. *J. Am. Chem. Soc.* **1997**, *119*, 7595.

(116) Kondoh, A.; Yorimitsu, H.; Oshima, K. *Org. Lett.* **2008**, *10*, 3093.

(117) Coste, A.; Couty, F.; Evano, G. *Org. Lett.* **2009**, *11*, 4454.

(118) Liu, J.; Zhang, Y.; Li, G.; Roschangar, F.; Farina, V.; Senanayake, C. H.; Lub, B. Z. *Adv. Synth. Catal.* **2010**, *352*, 2667.

(119) Sharma, S. K.; Mandadapu, A. K.; Kumar, B.; Kundu, B. *J. Org. Chem.* **2011**, *76*, 6798.

(120) Talluri, S. K.; Sudalai, A. *Org. Lett.* **2005**, *7*, 855.

(121) Schlummer, B.; Hartwig, J. F. *Org. Lett.* **2002**, *4*, 1471.

(122) Wang, H.; Zhao, J.; Zhang, J.; Zhu, Q. *Adv. Synth. Catal.* **2011**, *353*, 2653.

II.3. Direkte Carboxylierung terminaler Alkine mit Kohlenstoffdioxid

Der Begriff "Carboxylierung" beschreibt die Herstellung von Carbonsäuren durch die Einführung einer Carboxy-Gruppe (COOH) in eine organische Verbindung.[9] Im Gegensatz zu einer Oxidationsreaktion wird dabei die Anzahl der C-Atome um eins erhöht. Als Carboxylierungsreagenzien können neben Kohlenstoffdioxid auch andere Metallkomplexe eingesetzt werden, wie z. B. Nickeltetracarbonyl oder Phosgen.

Kohlenstoffdioxid ist zu 0,039% in der Erdatmosphäre enthalten und jährlich fallen weitere 29 Milliarden Tonnen CO_2 als Folge menschlichen Handelns an.[10] Unter führenden Wissenschaftlern wird derzeit kontrovers diskutiert, welche genauen Auswirkungen die Anreicherung von CO_2 in der Atmosphäre haben könnte. Oft wird es als Hauptursache für die Erderwärmung angesehen, weil die von der Erdoberfläche ausgehende Wärmestrahlung durch CO_2-Schichten in der Atmosphäre zurückgehalten wird und somit die Temperatur langsam ansteigt. Es werden derzeit mehrere Ansätze erforscht, um dieser negativen Entwicklung Herr zu werden, z. B. die Kohlenstoffabscheidung oder die Kohlenstoffspeicherung (CCS Carbon capture and storage, CCR carbon capture and reuse). Stellt man jedoch die technischen Möglichkeiten dieser oder anderer Methoden dem jährlichen stark ansteigenden CO_2-Ausstoß gegenüber, so wird sehr schnell deutlich, dass mit dem derzeitigen Stand der Technik die Anreicherung von CO_2 in der Atmosphäre nur durch eine deutliche Verringerung des CO_2-Ausstoßes erreicht werden kann.

Völlig andere Ansätze zur Verringerung des CO_2-Ausstoßes oder zumindest Möglichkeiten zur wertschöpfenden Verwendung von CO_2 liefert die Chemie. CO_2 ist ein interessanter Ausgangsstoff für die organische Synthese, und die Einführung dieses C1-Bausteins in organische Moleküle ermöglicht durch die schon bestehenden Heteroatombindungen einen direkten Zugang zu wertvollen Sauerstoff-funktionalisierten Verbindungsklassen, wie die der Alkohole und der Carbonsäuren.[11] CO_2 ist ein lineares, thermodynamisch sehr stabiles Molekül, daher kann es lediglich mit starken Nukleophilen eine direkte Additionsreaktion eingehen oder mit Hilfe von Katalysatoren für den Angriff von weniger starken Nukleophilen aktiviert werden.[12]

Der Einsatz von Kohlendioxid in der chemischen Industrie kann derzeit noch keinen großen Beitrag zur Reduzierung des CO_2-Ausstoßes leisten, aber die Anwendungsmöglichkeiten steigen stetig, und CO_2 gehört zu den preiswertesten und ökologisch wertvollsten Kohlenstoffquellen. Jegliche Verwendung von CO_2 in der

chemischen Synthese führt nicht nur zu einer Wertschöpfung durch das entstandene Produkt, sondern zusätzlich können Kosten, die durch den EU-Emissionshandel in Form von Umweltzertifikaten entstehen, reduziert werden oder sogar Gewinne durch den Verkauf von überschüssigen Umweltzertifikaten erwirtschaftet werden.

In den letzten Jahren konnten zahlreiche Methoden zur direkten CO_2-Fixierung entwickelt werden.[12, 13] Darunter sind einige katalytische Verfahren, wie z. B. die Carboxylierung von organometallischen Verbindungen sowie von Epoxiden, die carboxylierende Zyklisierung von Propargylaminen und -alkoholen, die reduktive Carboxylierung von Alkinen und Alkenen, und die Hydrosilylierung von CO_2. Besonders große Fortschritte konnten bei der Münzmetall-katalysierten direkten C–H Carboxylierung erzielt werden.[14] Auf diese Weise kann ausgehend von terminalen Alkinen ein direkter Zugang zu Propiolsäuren eröffnet werden, die vielfach Einsatz als wertvolle Synthesebausteine für die chemische Industrie finden.

II.3.1. Verwendung von Propiolsäurederivaten

Propiolsäurederivate sind vielseitige synthetische Intermediate und finden Anwendung zum Beispiel in decarboxylierenden Kreuzkupplungsreaktionen zur Darstellung von Arylalkinen oder Aminoalkinen[15] und in Cycloadditionen oder Hydroarylierungsreaktionen, wodurch eine Vielzahl heterocyclischer Derivate, beispielsweise Cumarine (**II.3-1**), Flavone (**II.3-4**) oder 3-Aryliden-2-oxindole (**II.3-7**), synthetisiert werden können (Schema 4).[16]

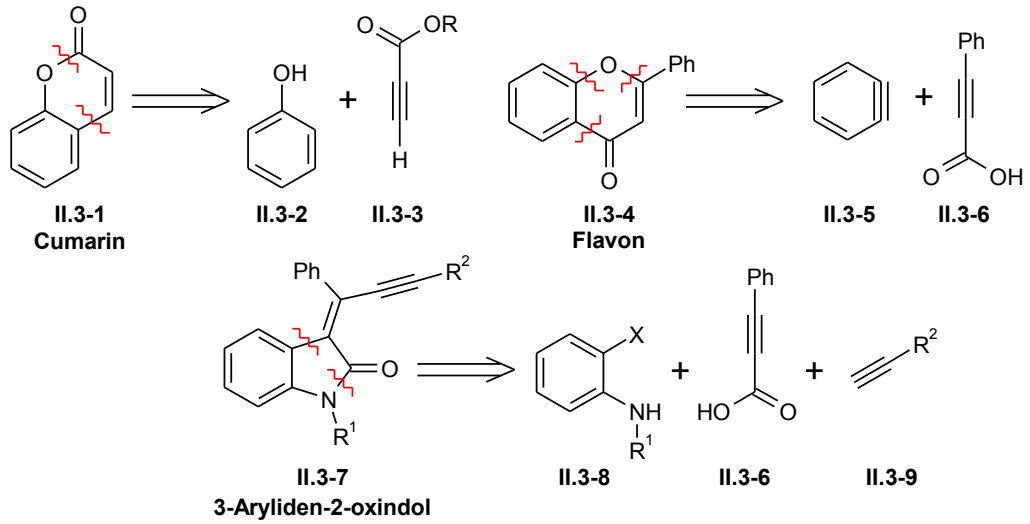

Schema 4. Retrosynthetischer Ansatz zur Darstellung von Cumarinen (II.3-1), Flavonen (II.3-4) und 3-Aryliden-2-oxindolen (II.3-7) ausgehend von Propiolsäurederivaten.

Arylalkine sind wichtige Leitstrukturen für die pharmazeutische Industrie [17] und wichtige Bausteine für die Polymerforschung.[18] Cumarin wurde erstmals aus der namensgebenden Tonkabohne (*Coumarouna odorata* Aubl., Leguminosae) isoliert, und es ist außerdem z. B. im Steinklee, im Waldmeister, in Datteln, im Lavendelöl oder in Pfefferminzöl enthalten.[19] Cumarin und dessen Derivate zeigen interessante biologische Eigenschaften. Sie wirken blutgerinnungshemmend sowie antibiotisch und sind wirksam gegen HIV und Tumore.[16a+b] Flavone kommen z. B. in Beeren-, Kern- und Steinobst vor und weisen eine Vielzahl biologischer Aktivitäten auf. Sie wirken unter Anderem entzündungshemmend, antimikrobiell und zytotoxisch und sind deshalb wirksam gegen Tumore.[20] In der Antiangiogenese oder Antitumortherapie kommen 3-Aryliden-2-oxindol-Derivate zum Einsatz.[21]

Als industriell besonders interessantes Beispiel sei die Acetylendicarbonsäure genannt. Es handelt sich dabei um ein wichtiges chemisches Zwischenprodukt für einen alternativen Zugang zu 2-Butin-1,4-diol sowie zu Butan-1,4-diol durch Hydrierung und als Vorstufe zur Synthese von Propinsäure durch Mono-Decarboxylierung. In Form eines Dialkylester ist die Acetylendicarbonsäure ein wichtiges Intermediat für die Herstellung von Heterozyklen, und als Dienophil wird es vielfach in Diels-Alder-Reaktionen umgesetzt.[22]

II.3.2. Traditionelle Verfahren zur Herstellung von Propiolsäurederivaten

Das einfachste Propiolsäurederivat ist die Propinsäure (**II.3-14**, Propiolsäure); sie wird entweder durch anodische Oxidation von Propargylalkohol oder ausgehend von Maleinsäure (**II.3-10**) in einer mehrstufigen Synthese über Mono-Decarboxylierung von Butindisäure (**II.3-13**, Acetylendicarbonsäure) hergestellt (Schema 5).[23]

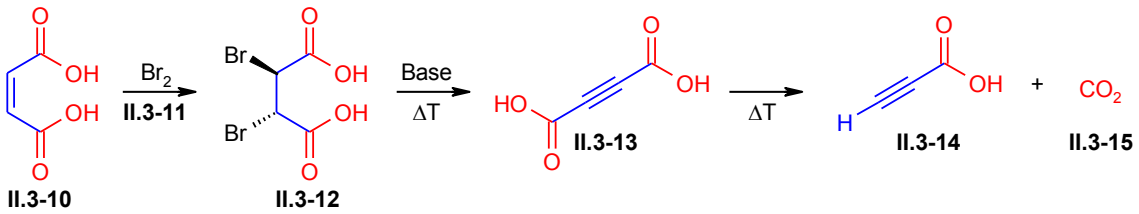

Schema 5. Darstellung von Acetylendicarbonsäure (II.3-13) und Propiolsäure (II.3-14) ausgehend von Maleinsäure (II.3-10).

Dieser Reaktionsweg liefert sowohl die Butindisäure (**II.3-13**) als auch die Propiolsäure (**II.3-14**) lediglich in sehr geringen Ausbeuten. Die Bromierung der Maleinsäure (**II.3-10**) und die doppelte Eliminierung in Gegenwart starker Basen sind aus sicherheitstechnischen

Gründen und aufgrund der schlechten Atomökonomie sowie der anfallenden Nebenprodukte aus ökologischen Gründen sehr bedenklich.

Langkettige Propiolsäurederivate werden traditionell in einer zweistufigen Reaktion aus terminalen Alkinen dargestellt. Dabei hat sich sowohl die Addition terminaler Alkine **II.3-16** an Formaldehyd (**II.3-17**) mit anschließender Oxidation der entstanden Propargylalkohole **II.3-18** als auch die oxidative Carboxylierung terminaler Alkine **II.3-16** bewährt (Schema 6).[24,25]

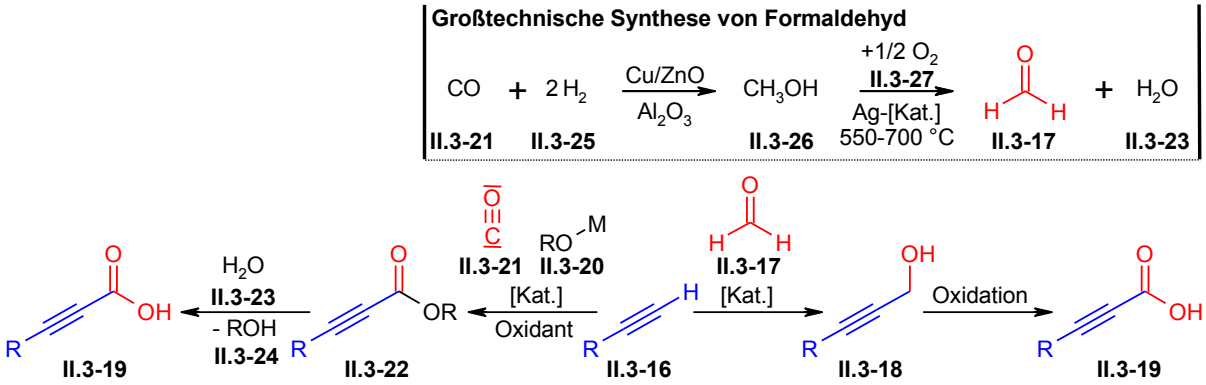

Schema 6. Synthese langkettiger Propiolsäurederivate (II.3-19) durch nukleophile Addition an Formaladehyd (II.3-17) oder an Kohlenmonoxid (II.3-21).

Nachteilig an diesen Reaktionspfaden sind die hohen Kosten von Formaldehyd (**II.3-17**), die durch die Auftrennung der Formaldehyd-Wasser-Gemische aus der großtechnischen Produktion entstehen, und der Umgang mit toxischen Gasen sowie starken Basen. Alternative synthetische Methoden beinhalten die Lithiierung endständiger Alkine und anschließender Umsetzung mit Chloroformat,[26] die Carboxylierung instabiler und kommerziell nicht verfügbarer Alkinhalogenide,[27] die direkte Carboxylierung von Alkin-Magnesium oder Lithium-Reagenzien mit CO_2,[26] und die Nickel- oder Palladium-katalysierte Carboxylierung in Gegenwart von Organozink-Reagenzien unter CO_2-Atmosphäre.[14a]

Alle in diesem Abschnitt vorgestellten Synthesewege zu Propiolsäurederivaten sind der direkten Carboxylierung terminaler Alkinen hinsichtlich der Atomökonomie der Reaktion, der Anzahl benötigter Reaktionsschritte, der Anwendungsbreite sowie der Kosten und der Verfügbarkeit der Startmaterialien unterlegen. Im nächsten Abschnitt werden die großen Fortschritte der letzten Jahre in der Entwicklung hocheffizienter Katalysatorsysteme für die Carboxylierung terminaler Alkine mit CO_2 beschrieben.

Es stellt sich die Frage, ob diese Systeme bewährte großtechnische Verfahren zur Herstellung von Propiolsäurederivaten ersetzen können.

II.3.3. Darstellung von Propiolsäurederivaten durch katalytische Carboxylierung terminaler Alkine mit Kohlenstoffdioxid

Im Jahre 1974 wurde erstmals von Saegusa *et al.* die Kupfer(I)- bzw. Silber(I)-vermittelte Umsetzung von Kohlenstoffdioxid mit Phenylacetylen beobachtet.[28] Die intermediär gebildeten Cu(I)- oder Ag(I)-Phenylpropiolate mussten jedoch durch Zugabe von Methyliodid in die Phenylpropiolsäuremethylester überführt werden, um Ausbeuten von 50 bzw. 70% zu erreichen. Ferner konnte gezeigt werden, dass präformierte Cu(I)-Phenylpropiolat-Komplexe beim Erwärmen von -10 °C auf 35 °C unter Bildung von Cu(I)-phenylacetyliden decarboxylieren, jedoch durch Zugabe von Überschüssen eines Liganden (z. B. P^nBu_3) erneut in den Cu(I)-Phenylpropiolat-Komplex überführt werden können.[29] Das Gleichgewicht dieser Reaktion war dabei abhängig von der Menge und der σ-Donor-Fähigkeit der eingesetzten Liganden. Je höher beide Faktoren waren, desto weniger freies CO_2 lag im Gleichgewicht vor.

20 Jahre später beschrieben Inoue und Mitarbeiter die Cu(I)- oder Ag(I)-katalysierte Synthese von Propiolsäurealkylestern **II.3-29** durch Umsetzung terminaler Alkine **II.3-27** mit CO_2 (**II.3-15**) und Bromalkanen **II.3-28** (Schema 7).[30]

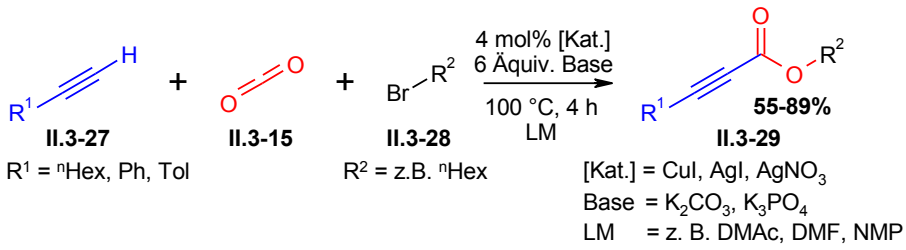

Schema 7. Kupfer- oder Silber-katalysierte Synthese von Propiolsäurealkylestern (II.3-29) durch Carboxylierung terminaler Alkine (II.3-16).

Mit diesen Arbeiten konnte zum ersten Mal gezeigt werden, dass terminale Alkine durch geeignete Katalysatoren in Gegenwart schwacher Basen deprotoniert und erfolgreich zu den gewünschten Propiolsäureestern umgesetzt werden können. Nachteile dieser Methode sind, dass nur die Ester, nicht aber die freien Propiolsäurederivate zugänglich sind und dass nur wenige unfunktionalisierte Alkine carboxyliert werden können.

Weitere 16 Jahre später erschienen fast zeitgleich drei verschiedene Methoden zur direkten Carboxylierung terminaler Alkine (Schema 8).[31]

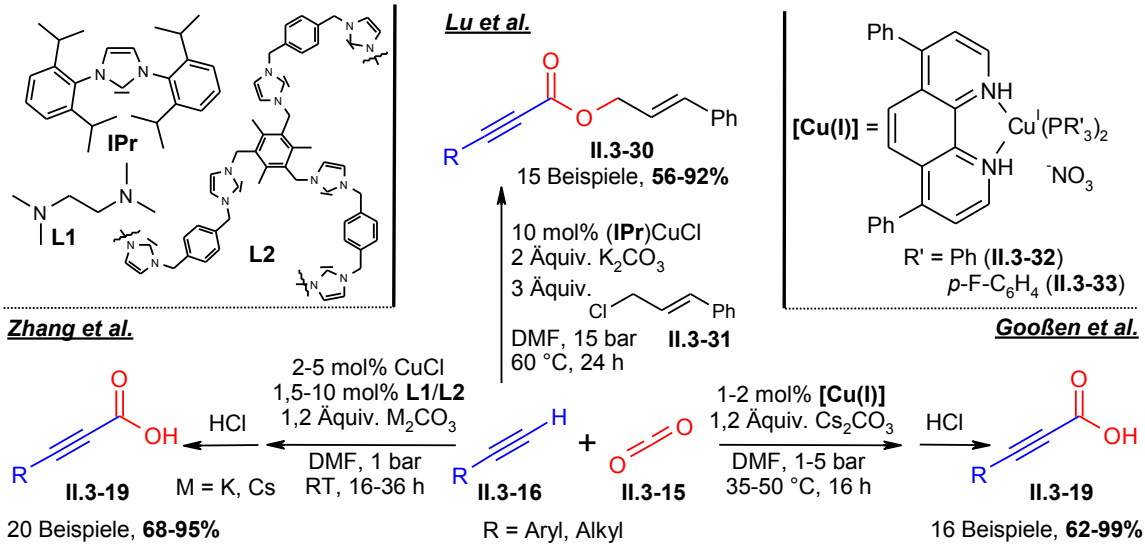

Schema 8. Zeitgleich erschienene Methoden zur Carboxylierung terminaler Alkine (II.3-16) von Gooßen, Zhang und Lu *et al*.

Das hocheffiziente Verfahren von Gooßen *et. al.* wird von luftstabilen und leicht zugänglichen Kupfer(I)-Phenanthrolin-Phosphin-Komplex **II.3-32** und **II.3-33** katalysiert (Schema 8, rechter Reaktionspfad).[31a] Viele verschiede Substrate werden in DMF und in Gegenwart von 1,2 Äquivalenten Cs_2CO_3 zu den gewünschten freien Propiolsäurederivaten **II.3-19** umgesetzt. Für aliphatische Alkine hat sich der PPh_3-substituierte Cu(I)-Katalysator **II.3-32** bei einer Reaktionstemperatur von 50 °C und einen CO_2-Druck von 1 bar bewährt, während für aromatische Alkine der P(*p*-F-C_6H_4) abgeleitete Cu(I)-Komplex **II.3-33** bei 35 °C und 5 bar Druck die besten Ausbeuten liefert. Aufgrund der milden Reaktionsbedingungen des Verfahrens werden zahlreiche funktionellen Gruppen toleriert, wie z. B. Ether, Halogene, Trifluoromethyl- und Alkenylgruppen. Nachteile der Methode sind der stöichiometrische Einsatz von teuerem Cs_2CO_3 und die hohen Katalysatorbeladungen, die benötigt werden, um hohe Umsätze zu erreichen.

Das von *Lu et al.* entwickelte Verfahren zur Synthese von Propiolsäurecinnamylestern **II.3-30** verläuft mit 10 mol% eines präformierten *N*-heterozyklischen Carben-Cu(I)-Komplexes und bei 15 bar CO_2-Druck in guten bis exzellenten Ausbeuten (Schema 8, oberer Reaktionspfad).[31b] Auch mit dieser Methode können zahlreiche funktionalisierte Alkyl- und Arylalkine **II.3-16** umgesetzt werden, jedoch können unter den Reaktionsbedingungen nicht

die freien Säuren isoliert werden. Zudem verhindern die sehr hohen Mengen an Katalysator eine großtechnische Anwendung.

Zhang *et. al.* ist es gelungen, die katalytische Carboxylierung terminaler Alkine **II.3-16** bereits unter CO_2-Normaldruck und bei Raumtemperatur durchzuführen, mit Katalysatorsystemen bestehend aus einfachem Cu(I)-chlorid und Stickstoffliganden (Schema 7, linker Reaktionspfad).[31c] Als Ligand werden 1,5 mol% TMEDA (**L1**) oder 5-10 mol% eines polymeren *N*-heterozyklischen Carbenliganden (**L2**) eingesetzt und die Basenwahl fällt bei aromatischen Alkinen auf K_2CO_3 und bei aliphatischen Alkinen auf Cs_2CO_3. So können gute bis sehr gute Ausbeuten divers funktionalisierter Propiolsäurederivate **II.3-19** nach 16 bis 36 h Reaktionszeit erhalten werden. Nachteile dieser Methode sind die teueren Liganden und die langen Reaktionszeiten. In späteren Arbeiten gelang es Zhang *et al.* Silber-Nanopartikel auf den polymeren *N*-heterozyklischen Carbenliganden (**L2**) aufzutragen und als effektiven, wieder verwendbaren Carboxylierungs-Katalysator einzusetzen.[32]

Die Arbeitsgruppe von Lu *et al.* griff als Erste die frühen Ergebnisse von Saegusa *et al.* auf und entwickelte eine breit anwendbare Silber-katalysierte Methode zur Carboxylierung terminaler Alkine **II.3-16** (Schema 9).[33]

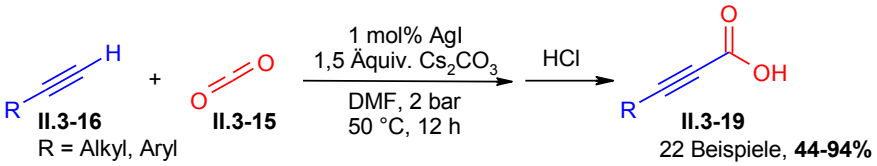

Schema 9. Silberiodid-katalysierte Synthese von Propiolsäurederivaten (II.3-19)nach Lu *et al.*

Schon 1 mol% von AgI sind ausreichend, um ohne zusätzliche Liganden in Gegenwart von 1,5 Äquivalenten Cs_2CO_3 und nach 12 h bei 50 °C und 2 bar CO_2 Druck zahlreiche freie Propiolsäurederivate **II.3-19** in guten bis exzellenten Ausbeuten zu synthetisieren.

Diese Methode erreicht eine hohe katalytische Aktivität mit einfachem Silberiodid-Salz ohne Zugabe von Liganden; allerdings ist ein Druck von 2 bar notwendig. Dadurch wird die Reaktionsführung aufwendiger und im größeren Maßstab aufgrund der Gefahr der Silberacetylid-Bildung riskanter.

Im Rahmen dieser Arbeiten wurden erste mechanistische Studien durchgeführt, um einen vorgeschlagenen Reaktionsmechanismus zu bekräftigen. So wurden präformierte Silber(I)phenylacetylide und Silber(I)phenylpropiolate dargestellt, die als Intermediate des Katalysezyklus vorgeschlagen wurden und direkt in einer Carboxylierungsreaktion eingesetzt.

Ausgehend von diesen Schlüsselintermediaten konnten unter ansonsten identischen Reaktionsbedingungen 80% beziehungsweise 86% Ausbeute an Phenylpropiolsäure erzielt werden. Ferner wurden Markierungsexperimente mit ^{13}C-angereichertem CO_2 durchgeführt. Die auf diese Weise in Gegenwart nichtmarkierter Base dargestellte Phenylpropiolsäure zeigte eine vollständige Anreicherung des ^{13}C-Isotops in der Carboxy-Gruppe. So kann ausgeschlossen werden, dass die Base die Quelle für die Carboxy-Gruppe der Phenylpropiolsäure ist.

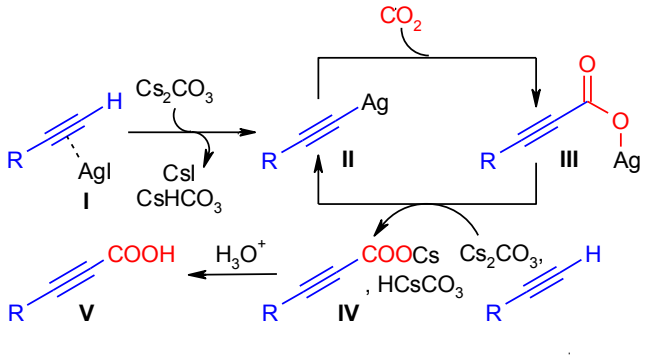

Schema 10. Postulierter Mechanismus für die Silberiodid-katalysierte Carboxylierung terminaler Alkine.

Der postulierte Mechanismus beginnt mit einem Katalysator-Präformierungsschritt, bei dem das Silber(I)-Salz an das Alkin unter Erhöhung der Azidität der terminalen C(sp)-H–Bindung koordiniert (Schema 10). Die schwache Base Cs_2CO_3 ist dadurch in der Lage das Alkin zu deprotonieren, um die Bildung eines katalytisch aktiven Silberacetylids **II** zu vermitteln. Die Insertion von CO_2 in die Ag-C-Bindung des Silberacetylids **II** liefert ein Silberpropiolat **III**. Der Katalysezyklus wird durch die Freisetzung eines Cäsiumpropiolats **IV** und der Regenerierung des Silberacetylids **II** geschlossen, indem ein weiteres Alkin in Gegenwart von Cs_2CO_3 deprotoniert und transmetalliert wird. Das Cäsiumpropiolat **IV** liefert nach saurer Aufarbeitung das gewünschte Propiolsäurederivat **V**.

Neben der Kupfer(I)-katalysierten Carboxylierung terminaler Alkine **II.3-16** konnte die Arbeitsgruppe von Zhang auch eine Katalysator-freie Methode zur Darstellung freier Propiolsäurederivate **II.3-19** verwirklichen (Schema 11).[34]

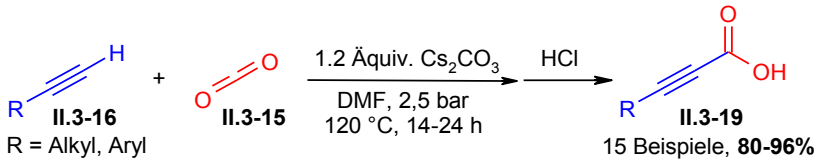

Schema 11. Basen-katalysierte Carboxylierung terminaler Alkine (II.3-16).

Um hohe Ausbeuten zu erreichen, sind jedoch ein erhöhter CO_2-Druck von 2,5 bar und Reaktionstemperaturen von 120 °C nötig. Außerdem sind bis auf zwei Ausnahmen nur aromatische Alkine umgesetzt worden, was auf Schwierigkeiten bei der Umsetzung aliphatischer Alkine schließen lässt. Ansonsten können exzellente Ausbeuten vielseitig funktionalisierter Propiolsäurederivate **II.3-19** erhalten werden.

Die in diesem Abschnitt vorgestellten Verfahren zur direkten Carboxylierung terminaler Alkine in Gegenwart von CO_2 verdeutlichen das große Potential dieser Reaktionsführung und die Tatsache, dass durch einen Katalysator die Acidität des Alkins erhöht werden kann. Im Vergleich zu traditionellen Verfahren können höhere Ausbeuten ausgehend von günstigeren und besser verfügbaren Startmaterialien erzielt werden. Die Carboxylierungsreaktionen verlaufen mit einer Atomökonomie von hundert Prozent und unter deutlich milderen Bedingungen ab und tolerieren daher deutlich mehr funktionelle Gruppen. Dennoch erscheint eine großtechnische Nutzung dieser Verfahren bisher nicht möglich. Besonders die hohen Kosten der in großen Mengen benötigten Münzmetall-Katalysatoren und des oftmals verwendeten Cäsiumcarbonats verhindern die industrielle Anwendung. Umsatzzahlen von maximal 100 sind viel zu gering, um die Produktionskosten zu decken. Ferner bergen diese Verfahren die Gefahr der Bildung explosiver Metallacetylide, vor allem wenn Silber-Katalysatoren eingesetzt werden und bei erhöhtem CO_2-Druck gearbeitet werden muss, obwohl mit CO_2 bereits ein Löschgas im Reaktor vorhanden wäre.

Nur eine deutliche Erhöhung der Umsatzzahl und der Einsatz katalytischer Mengen der Base oder günstigerer Alternativen können dazu führen, dass eine großtechnische Anwendung eines solchen Verfahrens möglich wird.

II.4. Exkurs: Synthese des Funktionspolymers Polyvinylpyrrolidon

Wie die Industrie elementare Schritte der zuvor beschriebenen Reppe-Synthesen (siehe Kapitel II.1.3) einsetzen kann, um komplexe, hoch funktionalisierte Verbindungen darzustellen und wie neue Methoden zur Carboxylierung und Hydroamidierung terminaler Alkinen dazu beitragen können, alternative Reaktionspfade zu ermöglichen, belegt das Synthesebeispiel Polyvinylpyrrolidon (PVP).

Der Weltmarkt des Funktionspolymers PVP lag 2006 bei ca. 31.000 Tonnen.[35] Handelsübliches PVP ist ein weißes, hygroskopisches Pulver, mit einer mittleren Molmasse von ca. 2.000 – 2.500.000 g/mol. Es kann durch K-Werte klassifiziert werden, die ein Maß für die Eigenviskositäten darstellen und für PVP von K-12 bis K-115 reichen. Durch die polaren Pyrrolidoneinheiten ist PVP in der Lage starke Wasserstoffbrückenbindungen auszubilden, wodurch es eine hohe Löslichkeit in Wasser und vielen polaren Lösungsmitteln besitzt. PVP zeichnet sich weiterhin durch eine außerordentlich gute Klebrigkeit und Haftung auf unterschiedlichen Materialien aus. PVP ist aus toxikologischer Sicht völlig unbedenklich und biologisch sehr gut verträglich. Hauptanwendungen findet es daher mit einem Anteil von ca. 47 % in der Kosmetik, insbesondere in Shampoos, Haargelen und –sprays, sowie mit 25 % im Pharmabereich, wo es hauptsächlich als Bindemittel und Sprengmittel für Tabletten verwendet wird. Des Weiteren findet es Anwendung in Waschmitteln und bei der Wein- und Bierfiltration. Historisch wurde Polyvinylpyrrolidon zunächst als Blutplasmaersatzstoff im Zweiten Weltkrieg eingesetzt.

Nach dem in Schema 12 illustrierten Syntheseweg, der von Prof. Reppe vor mehr als 70 Jahren entwickelt wurde, kann PVP in sechs Schritten dargestellt werden (linker Reaktionspfad).[36]

Im ersten Prozessschritt, einer Ethinylierung, wird Ethin (**II.4-1**) an Formaldehyd (**II.4-2**) unter Bildung von 2-Butin-1,4-diol (**II.4-4**) addiert. Nach der Hydrierung der C-C-Dreifachbindung wird das entstandene Butan-1,4-diol (**II.4-7**) durch oxidative Cyclisierung zu *γ*-Butyrolacton (**II.4-8**) umgesetzt. Im Folgenden kann *N*-Vinylpyrrolidon (**II.4-14**) auf zwei Wegen hergestellt werden: entweder durch Aminierung des Lactons **II.4-8** mit Ammoniak (**II.4-9**) und anschließender Vinylierungsreaktion zwischen Ethin (**II.4-1**) und Pyrrolidon (**II.4-11**) oder durch Aminierung mit Ethanolamin (**II.4-10**) zu *N*-Hydroxyethylpyrrolidon (**II.4-12**) und anschließender Eliminierung von Wasser (**II.4-13**).

Eine radikalische Lösungspolymerisation in Wasser oder organischen Lösungsmitteln liefert letztlich das gewünschte PVP (**II.4-15**).

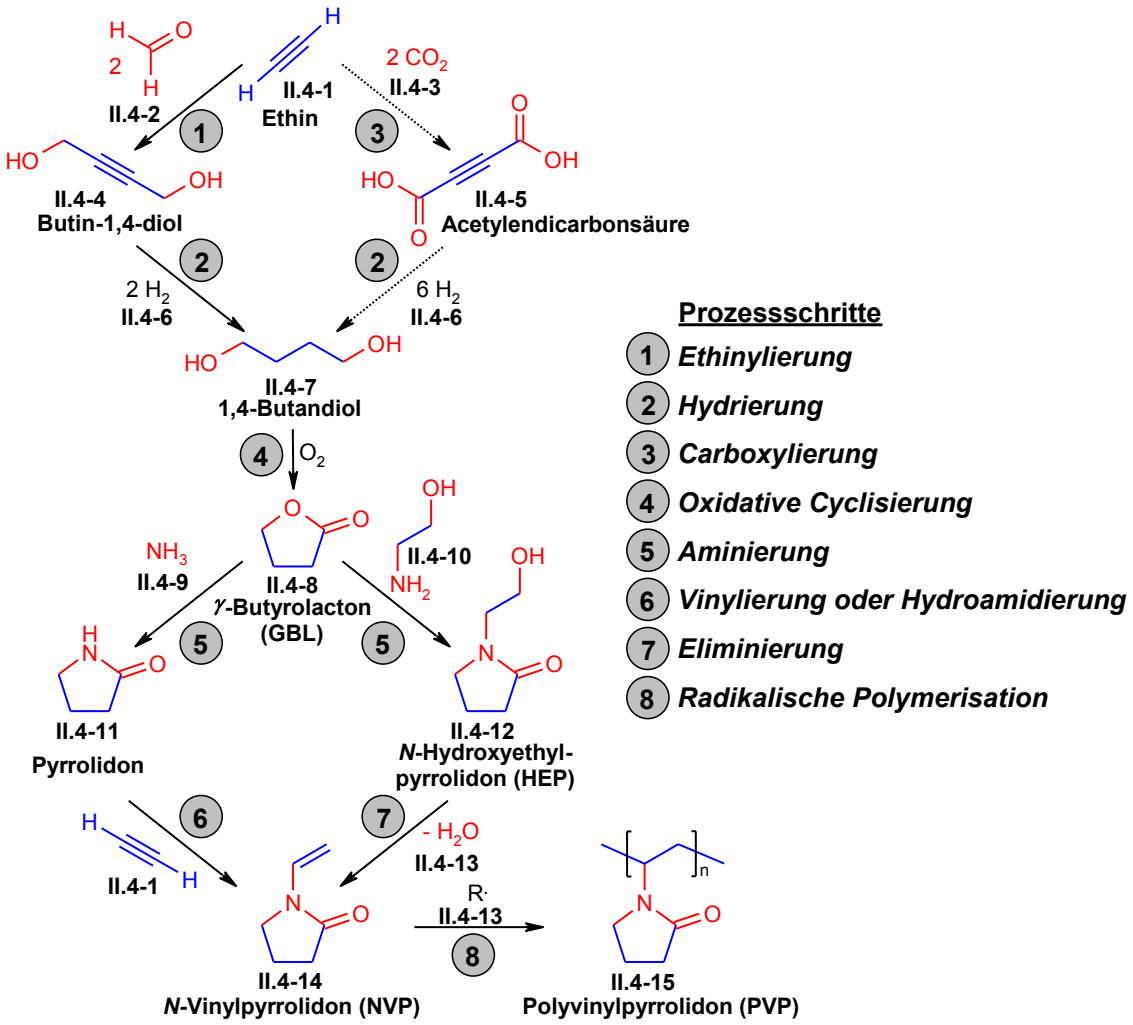

Schema 12. Großtechnische Synthese von PVP (II.4-15) nach Reppe sowie ein alternativer Zugang über Acetylendicarbonsäure (II.4-5).

Nachteilig bei dem großtechnischen Reaktionspfad sind die hohen Kosten von reinem Formaldehyd, die durch die teuere Auftrennung der Formaldehyd-Wasser-Gemische aus der industriellen Produktion entstehen, sowie der hohe Reaktionsdruck und die hohen Reaktionstemperaturen, die für die Carbonylierungs- und Ethinylierungs-Schritte erforderlich sind.

Ausgehend von konkurrenzlos günstigen und im Überschuss vorhandenen Startmaterialien könnte durch Carboxylierung von Ethin (**II.4-1**) mit CO_2 (**II.4-3**) in einem hundertprozentig atomökonomischen Prozess Acetylendicarbonsäure (**II.4-5**) zugänglich gemacht werden (Schema 12, Prozessschritt 3). Diese kann direkt durch gleichzeitige Hydrierung der C-C-

Dreifachbindung und der beiden Carboxy-Gruppen in Butan-1,4-diol (**II.4-7**) umgewandelt werden und ohne weiteren technischen Aufwand nach den bekannten Prozessschritten zu PVP (**II.4-15**) weiterverarbeitet werden.

Die Ruthenium-katalysierte Hydroamidierung bietet eine deutlich mildere Alternative zur etablierten Vinylierung von Pyrrolidon (**II.4-11**). Hydroamidierungsreaktionen laufen schon bei Normaldruck und 60 °C ab. Durch diese Verringerung der Temperatur und des Druckes könnte der Energieverbrauch gesenkt und die Reaktionsführung vereinfacht werden.

Sowohl die Carboxylierung als auch die Hydroamidierung von Ethin (**II.4-1**) könnten signifikante Beiträge zur Optimierung großtechnischer Synthesen beispielsweise von PVP (**II.4-15**) leisten. Dafür müssten jedoch die Umsatzzahlen der bestehenden Katalysatorsysteme deutlich gesteigert und viel einfachere sowie preiswerte Katalysatoren eingesetzt werden.

II.5. Literatur der Einleitung

[1] K. P. C. Vollhardt, N. E. Schore, in *Organische Chemie*, 3. Aufl. (H. Butenschön), Wiley-VCH, Weinheim, **2000**, pp. 563–603.

[2] a) F. Bohlmann, *Angew. Chem.* **1955**, *67*, 389–394; b) F. Bohlmann, H. Burkhardt, C. Zdero, *Naturally Occurring Acetylenes*, Academic Press, New York, **1973**; c) A. L. K. Shi Shun, R. R. Tykwinski, *Angew. Chem.* **2006**, *118*, 1050–1073; *Angew. Chem. Int. Ed.* **2006**, *45*, 1034–1057.

[3] Eintrag zu Acetylen. In: *Thieme Römpp Online*. URL http://www.roempp.com. Letzter Zugriff 23.02.2012.

[4] Eintrag zu Hochtemperatur-Pyrolyse-Verfahren. In: *Thieme Römpp Online*. URL http://www.roempp.com. Letzter Zugriff 23.02.2012.

[5] Eintrag zu Calciumcarbid. In: *Thieme Römpp Online*. URL http://www.roempp.com. Letzter Zugriff 23.02.2012.

[6] Eintrag zu Propin. In: *Thieme Römpp Online*. URL http://www.roempp.com. Letzter Zugriff 23.02.2012.

[7] a) W. Reppe *et al*., *Justus Liebigs Ann. Chem.* **1953**, *582*, 1–161; b) W. Reppe *et al*., *Justus Liebigs Ann. Chem.* **1955**, *596*, 1–224; c) W. Reppe *et al*., *Justus Liebigs Ann. Chem.* **1956**, *601*, 81–138; d) W. Reppe, O. Schlichting, K. Klager, T. Toepel, *Justus Liebigs Ann. Chem.* **1948**, *560*, 1–116; e) W. Reppe, N. v. Kutepow, A. Magin, *Angew. Chem.* **1969**, *81*, 717–723; *Angew. Chem. Int. Ed.* **1969**, *8*, 727–733; f) Eintrag zu Reppe-Synthesen. In: *Thieme Römpp Online*. URL http://www.roempp.com. Letzter Zugriff 27.02.2012.

[8] a) P. T. Anastas, J. C. Warner, *Green Chemistry: Theory and Practice*, Oxford University Press, Oxford, **1998**. b) M. Poliakoff, J. M. Fitzpatrick, T. R. Farren, P. T. Anastas, *Sciences* **2002**, *297*, 807-810.

[9] Eintrag zu Carboxylierung. In: *Thieme Römpp Online*. URL http://www.roempp.com. Letzter Zugriff 16.02.2012.

[10] a) C. Federsel, R. Jackstell, M. Beller, *Angew. Chem.* **2010**, *122*, 6392–6395; *Angew. Chem. Int. Ed.* **2010**, *49*, 6254–6257; b) A. Bazzanella, D. Krämer, M. Peters, *Nachr. Chem.* **2010**, *58*, 1226–1230; c) D. M. Dalton, T. Rovis, *Nat. Chem.* **2010**, *2*, 710–711; d) L. Ackermann, *Angew. Chem.* **2011**, *123*, 3926–3928; *Angew. Chem. Int. Ed.* **2011**, *50*, 3842–3844.

[11] a) R. Zevenhoven, S. Eloneva, S. Teir, *Catalysis Today* **2006**, *115*, 73–79; b) M. Aresta, A. Dibenedetto, I. Tommasi, *Energy & Fuels* **2001**, *15*, 269–273; c) P. Tundo, M. Selva, *Acc. Chem. Res.* **2002**, *35*, 706–716; d) G. A. Olah, *Angew. Chem.* **2005**, *117*, 2692–2696; *Angew. Chem. Int. Ed.* **2005**, *44*, 2636–2639; e) T. Aida, S. Inoue, *Acc. Chem. Res.* **1996**, *29,* 39–48; f) M. Mori, *Eur. J. Org. Chem.* **2007**, 4981–4993; g) M. Aresta, A. Dibenedetto, *Dalton Trans.* **2007**, 2975–2992.

[12] T. Sakakura, J.-C. Choi, H. Yasuda, *Chem. Rev.* **2007**, *107*, 2365–2387.

[13] a) H. Arakawa *et al.*, *Chem. Rev.* **2001**, *101*, 953–996; b) D. J. Darensbourg, *Chem. Rev.* **2007**, *107*, 2388–2410; c) N. Eghbali, C.-J. Li, *Green Chem.* **2007**, *9*, 213–215; d) S. N.

Riduan, Y. Zhang, J. Y. Ying*, Angew. Chem.* **2009**, *121*, 3372–3375; *Angew. Chem. Int. Ed.* **2009**, *48*, 3322–3325; e) T. Sakakura, K. Kohno, *Chem. Commun.* **2009**, 1312–1330; f) L. Gu, Y. Zhang, *J. Am. Chem. Soc.* **2010**, *132*, 914–915; g) A. Correa, R. Martín, *Angew. Chem.* **2009**, *121*, 6317–6320; *Angew. Chem. Int. Ed.* **2009**, *48*, 6201–6204; h) I. Omae, *Catalysis Today* **2006**, *115*, 33–52; i) T. Kubota, I. Hayakawa, H. Mabuse, K. Mori, K. Ushikoshi, T. Watanabe, M. Saito, *Appl. Organometal. Chem.* **2001**, *15*, 121–126; j) M. Cokoja, C. Bruckmeier, B. Rieger, W. A. Herrmann, F. E. Kühn, *Angew. Chem.* **2011**, *123*, 8662–8690; *Angew. Chem. Int. Ed.* **2011**, *50*, 8510–8537.

[14] a) S. N. Riduan, Y. Zhang, *Dalton Trans.* **2010**, *39*, 3347–3357; b) K. Huang, C.-L. Sun, Z.-J. Shi, *Chem. Soc. Rev.* **2011**, *40*, 2435–2452.

[15] a) J. Moon, M. Jeong, H. Nam, J. Ju, J. H. Moon, H. M. Jung, S. Lee, *Org. Lett.* **2008**, *10*, 945–948; b) J. Moon, M. Jang, S. Lee, *J. Org. Chem.* **2009**, *74*, 1403–1406; c) W. Jia, N. Jiao, *Org. Lett.* **2010**, *12*, 2000–2003.

[16] a) B. M. Trost, F. D. Toste, K. Greenman, *J. Am. Chem. Soc.* **2003**, *125*, 4518–4526; b) T. Kitamura, *Eur. J. Org. Chem.* **2009**, 1111–1125; c) M. Bararjanian, S. Balalaie, F. Rominger, B. Movassagh, H. R. Bijanzadeh, *J. Org. Chem.* **2010**, 75, 2806–2812. d) A. V. Dubrovskiy, R. C. Larock, *Org. Lett.* **2010**, *12*, 3117–3119.

[17] a) F. Mitzel, S. FitzGerald, A. Beeby, R. Faust, *Eur. J. Org. Chem.* **2004**, 1136–1142; b) D. Falcone, J. Li, A. Kale, G. B. Jones, *Bioorg. Med. Chem. Lett.* **2008**, *18*, 934–937.

[18] J. Boukouvalas, S. Cote, B. Ndzi, *Tetrahedron Lett.* **2007**, *48*, 105–107.

[19] Eintrag zu Cumarin. In: *Thieme Römpp Online*. URL http://www.roempp.com. Letzter Zugriff 16.02.2012.

[20] a) S. Martens, A. Mithofer, *Phytochemistry* **2005**, *66*, 2399–2407; b) N. C. Veitch, R. J. Grayer, *Nat. Prod. Rep.* **2008**, *25*, 555–611; c) A. Crozier, I. B. Jaganath, M. N. Clifford, *Nat. Prod. Rep.* **2009**, *26*, 1001–1043; d) U. Sequin, *Fortschr. Chem. Naturst.* **1986**, *50*, 57–122; e) M. R. Hansen, L. H. Hurley, *Acc. Chem. Res.* **1996**, *29*, 249–258; e) Eintrag zu Flavone. In: *Thieme Römpp Online*. URL http://www.roempp.com. Letzter Zugriff 16.02.2012.

[21] a) D. B. Mendel, A. D. Laird, B. D. Smolich, R. A. Blake, C. Liang, A. L. Hannah, R. M. Shaheen, L. M. Ellis, S. Weitman, L. K. Shawver, J. M. Cherrington, *Anti-Cancer Drug Des.* **2000**, *15*, 29–41; b) C. Le Tourneau, E. Raymond, S. Faivre, *Ther. Clin. RiskManage* **2007**, *3*, 341–346.

[22] a) L. Mandell, W. A. Blanchard, *J. Am. Chem. Soc.* **1957**, *79*, 6198–6201; b) N. W. Gabel, *J. Org. Chem.* **1962**, *27*, 301–303; c) C. K. Lee, C. S. Hahn*, J. Org. Chem.* **1978**, *43*, 3727–3729; d) K. Ando, M. Kankake, T. Suzuki, H. Takayama, *Tetrahedron* **1995**, *51*, 129–138; e) P. A. Wender, H. Rieck, M. Fuji, *J. Am. Chem. Soc.* **1998,** *120,* 10976–10977; f) Z. Xu, X. Lu, *J. Org. Chem.* **1998**, *63*, 5031–5041; g) V. Nair, A. U. Vinod, J. S. Nair, A. R. Sreekanth, N. P. Rath, *Tetrahedron Lett.* **2000**, *41*, 6675–6679; h) Y. Tominaga, K. Ueda, *J. Heterocyclic Chem*. **2005**, *42*, 337–352.

[23] a) E. Bandrowski, *Chem. Ber.* **1877**, *10*, 838–842; b) W. Lossen, *Justus Liebigs Ann. Chem.* **1893**, *272*, 127–139; c) W. Lossen, *Justus Liebigs Ann. Chem.* **1906**, *348*, 261–346; d) T. W. Abbott, R. T. Arnold, R. B. Thompson, *Org. Synth.* **1938**, *18*, 3.

[24] a) W. Reppe, *Justus Liebigs Ann. Chem.* **1955**, *596*, 25–32; b) J. Stohrer, E. Fritz-langhals, C. Brüninghaus, U.S. Patent 7,173,149B2, **2007**.

[25] a) J. Tsuji, M. Takahashi, T. Takahashi, *Tetrahedron Lett.* **1980**, *21*, 849–850; b) E. R. H. Jones, G. H. Whitham, M. C. Whiting, *J. Chem. Soc.* **1957**, 4628–4633; c) N. Satyanarayana, H. Alper, *Organometallics*, **1991**, *10*, 804–807; d) J. Li, H. Jiang, M. Chen, *Synth. Commun.*, **2001**, *31*, 199–202; e) Y. Izawa, I. Shimizu, A. Yamamoto, *Bull. Chem. Soc. Jpn.* **2004**, *77*, 2033–2045; f) L. Kollár, *Modern Carbonylation Reactions*, Wiley-VCH, Weinheim, **2008**, 276–280.

[26] L. Brandsma, *Preparative Acetylenic Chemistry*, 2nd , Elsevier, Amsterdam, **1998**.

[27] a) T. Mizuno, H. Alper, *J. Mol. Catal. A: Chemical* **1997**, *123*, l–24; b) H. Arzoumanian, F. Cochini, D. Nuel, J. F. Petrignani, N. Rosas, *Organometallics* **1992**, *11*, 493–495.

[28] T. Tsuda, K. Ueda, T. Saegusa, *J. Chem. Soc., Chem. Commun.* **1974**, 380–381.

[29] T. Tsuda, Y. Chujo, T. Saegusa, *J. Chem. Soc., Chem. Commun.* **1975**, 963–964.

[30] Y. Fukue, S. Oi, Y. Inoue, *J. Chem. Soc. Chem. Commun.* **1994**, 2091.

[31] a) L. J. Gooßen, N. Rodríguez, F. Manjolinho, P. P. Lange, *Adv. Synth. Catal.* **2010**, *352*, 2913–2917; b) W.-Z. Zhang, W.-J. Li, X. Zhang, H. Zhou, X.-B. Lu, *Org. Lett.* **2010**, *12*, 4748–4751; c) D. Yu, Y. Zhang, *Proc. Natl. Acad. Sci.* 2010, *107*, 20184–20189.

[32] D. Yu, M. X. Tan, Y. Zhang, *Adv. Synth. Catal.* **2012**, *354*, 969–974.

[33] X. Zhang, W.-Z. Zhang, X. Ren, L.-L. Zhang, X.-B. Lu, *Org. Lett.* **2011**, *13*, 2402–2405.

[34] Y. Dingyi, Z. Yugen, *Green Chem.* **2011**, *13*, 1275–1279.

[35] F. Fischer, S. Bauer, *Chem. Unserer Zeit*, **2009**, *43*, 376–383.

[36] a) W. Reppe, H. Krzikalla, O. Dornheim, Ger. Patent DE000000890508B, **1939**; b) W. Reppe, H. Krzikalla, Ger. Patent DE000000851197B, **1944**, c) W. Reppe, C. Schuster, A. Hartmann, Ger. Patent DE000000737663A, **1939**; d) W. Reppe, K. Herrle, H. Fikentscher, Ger. Patent DE000000922378B, **1943**; e) V. Bühler, *Kollidon® - Polyvinylpyrrolidone excipients for pharmaceutical industry*; BASF SE: Ludwigshafen, **2008**; p 12ff.

III. Aufgabenstellung

Die Zielsetzung dieser Arbeit bestand in der Entwicklung effizienter und nachhaltiger Verfahren zur Addition von Nukleophilen an terminale Alkine und für die Insertion von CO_2 in die C-H Bindung terminaler Alkine.

Im ersten Teil dieser Dissertation sollte der Mechanismus der Ruthenium-katalysierten Addition von Amiden an terminale Alkine durch eine Kombination von Kontrollexperimenten, kinetischen Studien, spektroskopischen Untersuchungen und theoretischen Berechnungen untersucht werden. Auf einem besseren mechanistischen Verständnis aufbauend sollten als nächstes effizientere und selektivere Verfahren für die Hydroamdierung terminaler Alkine entwickelt werden und deren Anwendungsbreite anhand ausreichend vieler Synthesebeispiele belegt werden. Das synthetische Potential sollte durch die Darstellung der biologisch aktiven Naturstoffe Lansiumamid A und B, Lansamid I sowie Botryllamid C und E demonstriert werden.

Bei den mechanistischen Studien sollte wie folgt vorgegangen werden: Zunächst sollten literaturbekannte Katalysezyklen identifiziert werden, die plausible Mechanismen für die Hydroamidierung terminaler Alkine darstellen. Ferner sollte überprüft werden, ob aufbauend auf nachgewiesenen Elementarschritten chemisch verwandter Reaktionen neue Mechanismen für die Hydroamidierung entwickelt werden können. Anschließend sollten Kontrollexperimente durchgeführt werden, mit deren Hilfe einzelne Elementarschritte der Katalysezyklen verifiziert oder falsifiziert werden können und somit Mechanismen ausgeschlossen werden können. Um herauszufinden, ob die Hydroamidierung mit einem der verbleibenden Mechanismen zutreffend beschrieben werden kann, sollte versucht werden, postulierte Intermediate des Katalysezyklus nachzuweisen. Dafür sollten spektroskopische Untersuchungen vor, während und nach Hydroamidierungsreaktionen durchgeführt werden. Zusätzlich sollte die Stabilität vorgeschlagener Reaktionsintermediate durch theoretische Berechnungen von Diplom-Chemiker Andreas Fromm überprüft werden.

Im zweiten Teil dieser Dissertation sollten effizientere Methoden für die Carboxylierung terminaler Alkine mit CO_2 entwickelt werden. Ausgehend von bekannten Carboxylierungsverfahren sollte ein Katalysatorsystem entwickelt werden, das in Gegenwart geringer Mengen einfacher Metallsalze und unter milden, druckfreien Bedingungen sowohl Alkyl- als auch Arylalkine zu den entsprechenden Propiolsäurederivaten umsetzen kann.

Dabei sollten deutlich höhere Umsatzzahlen erzielt und so ein neuer Benchmark für die katalytische Carboxylierung terminaler Alkine gesetzt werden. Die Anwendungsbreite der neuen Methode sollte an einer hinreichend großen Anzahl von Synthesebeispielen aufgezeigt werden.

Als nächstes sollte das Carboxylierungsverfahren hinsichtlich einer industriellen Anwendung optimiert werden. Dafür sollte unter anderem Cäsiumcarbonat durch günstigere und bevorzugt organische Basen ersetzt und ein höherer CO_2-Druck eingesetzt werden, um die Prozesskosten zu senken und höhere Raum-Zeit-Ausbeuten zu ermöglichen. Ausserdem sollte versucht werden, die Menge der eingesetzten Base zu reduzieren.

In einem Kooperationsprojekt mit der BASF SE sollte dieses Verfahren abschließend auf die Umsetzung von Ethin mit CO_2 erweitert werden. Dadurch sollte ein neuer, atomökonomischer Syntheseweg zur Acetylendicarbonsäure ausgehend von preiswerten und leicht verfügbaren Startmaterialien ermöglicht werden. Durch einen anschließenden Hydrierungsschritt könnte so die industriell bedeutende Basischemikalie Butan-1,4-diol auf besonders nachhaltige Weise hergestellt werden, wobei zwei Moleküle CO_2 als C1-Bausteine eingesetzt würden.

IV. Ergebnisse und Diskussion

IV.1. Ruthenium-katalysierte Hydroamidierung terminaler Alkine

IV.1.1. Umfassende mechanistische Untersuchungen der Ruthenium-katalysierten Hydroamidierung terminaler Alkine

Die Forschungsarbeiten der Arbeitsgruppe von Professor Dr. L. J. Gooßen auf dem Gebiet der Ruthenium-katalysierten Hydroamidierung terminaler Alkine waren sehr erfolgreich und führten zur Entwicklung effektiver und diastereoselektiver Methoden zur Darstellung einer Vielzahl von Enamiden und zahlreichen Veröffentlichungen in hochrangigen Fachzeitschriften. Im Rahmen dieser Arbeiten mussten jedoch vielfach mechanistische Überlegungen und Annahmen aufgrund widersprüchlicher Ergebnisse sorgfältig geplanter Kontrollexperimente verworfen werden. Literaturbekannte Mechanismen für Additionsreaktionen von Alkinen können zwar prinzipiell auf die Hydroamidierung übertragen werden, sind jedoch nicht mit allen experimentellen Befunden vereinbar. So konnte bisher nicht geklärt werden, warum die Hydroamidierung auf terminale Alkine und die Synthese von *anti*-Markovnikov Produkten limitiert ist und wie die Diastereoselektivität der Reaktion kontrolliert wird. Weiter war unklar, welcher Schritt des Katalysezyklus geschwindigkeitsbestimmend ist. Nur durch Aufklärung dieser essentiellen mechanistischen Problemstellungen kann die Entwicklung noch effizienterer Katalysatorsysteme und die Umkehr der Regioselektivität ermöglicht werden. Daher wurden umfassende Studien zur Aufklärung des Reaktionsmechanismus durchgeführt.

Die Ergebnisse der nachfolgenden Veröffentlichung wurden über einen Zeitraum von mehreren Jahren gesammelt und durch zahlreiche verschiedene spektroskopische und kinetische Methoden bestätigt. Die Arbeiten wurden in Kooperation mit dem Arbeitskreis von Professor Dr. Dr. G. Niedner-Schatteburg durchgeführt. Die Experimente zur Bestimmung kinetischer Isotopeneffekte und die Deuterium-Markierungsexperimente wurden von Dr. Kifah S. M. Salih und alle DFT-Rechnungen von Diplom-Chemiker Andreas Fromm durchgeführt. Die ESI-MS-Experimente wurden in Zusammenarbeit mit Diplom-Chemiker Fabian Menges durchgeführt. Alle anderen Experimente wurden im Rahmen dieser Dissertation geplant, durchgeführt, ausgewertet und ganzheitlich zum Ausschluss von vier

möglichen Mechanismen und zur Entwicklung eines neuen Mechanismus für die Hydroamidierung terminaler Alkine genutzt.

JACS
JOURNAL OF THE AMERICAN CHEMICAL SOCIETY

ARTICLE

pubs.acs.org/JACS

Mechanistic Investigation of the Ru-Catalyzed Hydroamidation of Terminal Alkynes

Matthias Arndt, Kifah S. M. Salih, Andreas Fromm, Lukas J. Goossen,* Fabian Menges, and Gereon Niedner-Schatteburg*

Fachbereich Chemie and State Reaserch Center OPTIMAS, TU Kaiserslautern, Erwin-Schrödinger-Strasse 52−54, 67663 Kaiserslautern, Germany

Supporting Information

ABSTRACT: The ruthenium-catalyzed hydroamidation of terminal alkynes has evolved to become a broadly applicable tool for the synthesis of enamides and enimides. Depending on the catalyst system employed, the reaction leads chemo-, regio-, and stereoselectively to a single diastereoisomer. Herein, we present a comprehensive mechanistic study of the ruthenium-catalyzed hydroamidation of terminal alkynes, which includes deuterium-labeling, in situ IR, in situ NMR, and in situ ESI−MS experiments complemented by computational studies. The results support the involvement of ruthenium−hydride and ruthenium−vinylidene species as the key intermediates. They are best explained by a reaction pathway that consists of an oxidative addition of the amide, followed by insertion of a π-coordinated alkyne into a ruthenium−hydride bond, rearrangement to a vinylidene species, nucleophilic attack of the amide, and finally reductive elimination of the product.

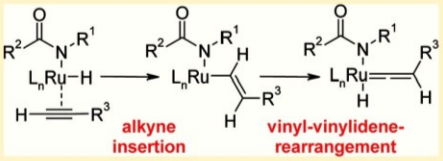

INTRODUCTION

Enamides are valuable structural elements in natural products with interesting biological activities and in pharmaceutical drug lead compounds[1] showing antibiotic,[2] antitumor,[3] anthelmintic,[4] antifungal, and cytotoxic activities (Figure 1).[5]

In addition, enamides can serve as versatile synthetic intermediates, particularly in pericyclic and photochemical reactions for the formation of heterocycles,[6] [4 + 2]-cycloadditions,[7] cross-coupling reactions,[8] Heck olefinations,[9] enantioselective additions,[10] or asymmetric hydrogenations.[11]

Traditional syntheses include the condensation of aldehydes and ketones with amides or dehydration of hemiaminals,[12] the Curtius rearrangement of α,β-unsaturated acyl azides,[13] and the elimination of β-hydroxy-α-silylamides (Peterson reaction).[14] Several metal-catalyzed approaches have also been investigated, such as the isomerization of *N*-allylamides[15] and catalytic cross-coupling reactions of amides and vinyl halides, pseudohalides or enol ethers.[16] Problems often encountered using these methods are the harsh reaction conditions, the formation of (*E*)- and (*Z*)-product mixtures, or the use of expensive or poorly available starting materials.

Over the last years, a particularly convenient synthetic entry to this important substrate class has emerged, namely, the addition of amides to terminal alkynes (Scheme 1).

This reaction mode is the most atom-economic transformation of all the catalytic reactions based on carboxylic acid derivatives that we have investigated over the last years.[17] On the basis of pioneering studies by Heider et al.[18] and Watanabe et al.,[19] who were the first to observe that ruthenium complexes mediate the addition of certain amides to terminal alkynes, we have developed efficient Ru catalysts and established the addition of amide-type nucleophiles to terminal alkynes as a general method for the synthesis of enamide derivatives. The same reaction principle is the basis for a number of preparatively useful Ru-catalyzed addition reactions to alkynes, for example, their hydration with formation of aldehydes,[20] the addition of carboxylic acids to give enol esters,[21] their hydroamination with formation of imines or enamines,[22] their hydrothiolation to vinyl sulfides,[23] and the addition of alcohols to form vinyl ethers.[24]

Over the last years, a range of customized protocols were disclosed for the *anti*-Markovnikov addition of various *N*-nucleophilic amides, thioamides, and imides across terminal C−C triple bonds. They provide an expedient and chemo-, regio-, and stereoselective synthetic entry to enamides, thioenamides, and enimides (Scheme 2).

With a catalyst system generated in situ from bis(2-methallyl)-(cycloocta-1,5-diene)ruthenium(II) [(cod)Ru(met)$_2$], tri-*n*-butylphosphine (P(*n*-Bu)$_3$), and 4-dimethylaminopyridine (DMAP), tertiary (*E*)-enamides can be synthesized in high yields and selectivities from terminal alkynes and secondary amides.[25] The stereoselectivity can be reversed in favor of the corresponding (*Z*)-enamides when employing bis-(dicyclohexylphosphino)methane (dcypm) and water instead of P(*n*-Bu)$_3$ and DMAP. The reaction proceeds smoothly even in the presence of sensitive functional groups such as esters, ethers, ketones, halides, or silanes. Various amides, anilides, ureas, bislactams, carbamates, and even amide-type chiral auxiliaries can be

Received: January 3, 2011
Published: April 26, 2011

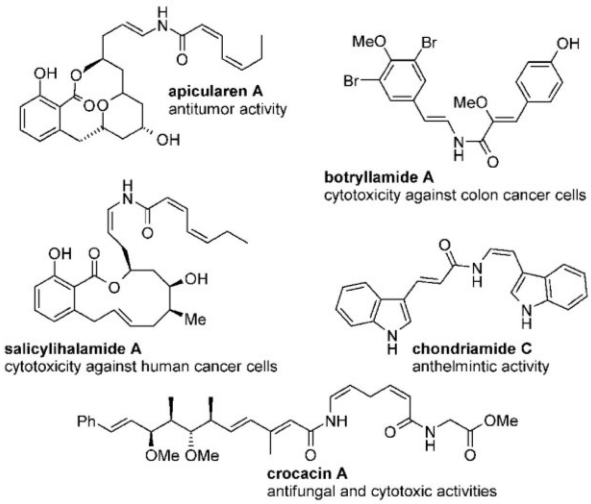

Figure 1. Enamide substructure in bioactive or functional molecules.

Scheme 1. Addition of Amides to Terminal Alkynes

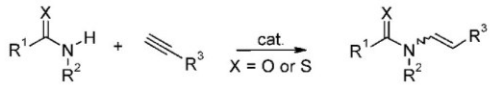

used as N−H nucleophiles. Recently, we have shown that for many substrates, a similar level of activity can be achieved when the catalytically active species is generated in situ from inexpensive ruthenium trichloride hydrate ($RuCl_3 \cdot 3H_2O$), P(*n*-Bu)$_3$, DMAP, K_2CO_3, and water.[26]

Subsequently, modified catalyst systems were developed that allowed extending the substrate scope to thioamides[27] and imides.[28] In this context, we made the discovery that for imides, which are acidic N−H nucleophiles, the addition of a Lewis acid rather than an auxiliary base is essential for achieving turnover of the catalyst.

The conversion of primary amides into secondary enamides is challenging due to the higher nucleophilicity of secondary over primary amides, leading to double vinylation products. However, a catalyst system consisting of the Lewis acid ytterbium(III) triflate in combination with (cod)Ru(met)$_2$ and an electron-rich, sterically demanding bidentate ligand (dcypb, 1,4-bis(dicyclohexylphosphino)butane) allowed the selective conversion of primary amides to secondary enamides.[29] This protocol gives access to (*Z*)-enamides in high yields and selectivities, whereas the (*E*)-enamides can be prepared by subsequent in situ double-bond isomerization with triethylamine at higher reaction temperatures in the same pot. Furthermore, after minor modifications, the same bimetallic system can be used for the *Z*-selective addition of secondary amides and imides to terminal alkynes in the absence of the primary amide functionality, yielding the corresponding enamides and enimides with *Z*/*E*-selectivities greater than 20:1.[30]

The applicability of Ru-catalyzed hydroamidation reactions is illustrated in Figure 2. The examples include the natural products alatamide, lansiumamides A and B, lansamide I, and botryllamides C and E.[29,31] They demonstrate that the hydroamidation of alkynes has meanwhile reached a high level of maturity and can be widely applied in organic synthesis. However, the reaction mechanism has so far remained speculative.

The aims of the present study were to investigate the coordination type of the alkyne during the reaction, to clarify how the regio- and stereochemistry is controlled, and to identify the rate-determining step of the catalytic cycle.

MECHANISTIC CONSIDERATIONS

Numerous potential reaction mechanisms have to be evaluated with appropriately designed mechanistic studies and control experiments.

Several catalytic cycles have previously been proposed for the Ru-catalyzed addition of nucleophiles such as amides, amines, carboxylic acids, and water to C−C triple bonds. The first mechanism for *anti*-Markovnikov-selective hydroamidations was postulated by Watanabe but was not supported by experimental data (Scheme 3).[19]

This mechanism will further be referred to as *Mechanism A*. It involves the oxidative addition of an amide, insertion of a π-coordinated alkyne into the Ru−N or Ru−H bond, and reductive elimination of the enamide product. Stabilizing interactions between the oxygen atom of the carbonyl group and the Ru center in a four- or six-membered intermediate (**17** and **18**) that forms following alkyne insertion were used to explain the regioselectivity, in both cases leading to the formation of the *anti*-Markovnikov product. Uchimaru proposed a similar mechanism for the Markovnikov-selective Ru-catalyzed hydroamination of terminal alkynes,[22a] in which a π-coordinated alkyne inserts into the Ru−N bond of a Ru-amine species. The Markovnikov selectivity is explained by the formation of a sterically less hindered Ru-enamine intermediate.

Indications for *Mechanism A* would be provided by a dependence of the rate-determining step on the acidity of the amide and the electronic and steric properties of the Ru-complex. Moreover, Ru-hydride species may be detectable via ^{1}H NMR or electrospray ionization mass spectroscopy (ESI−MS) investigations if concentrations are high enough, and the reaction of 1-deuterioalkynes should give rise to a product deuterated exclusively in the 1-position.

Dixneuf proposed a different mechanism to explain the selective formation of *anti*-Markovnikov addition products in the addition of carboxylic acids to alkynes. His pathway can directly be translated to hydroamidation reactions (Scheme 4).[32]

This mechanism will further be referred to as *Mechanism B*. Its key step is the formation of a Ru−vinylidene complex **20** via a 1,2-proton shift at the alkyne moiety, followed by an attack of a nucleophile in the α-position to the ruthenium center. After protonolysis of the ruthenium intermediate **25** and regeneration of the active ruthenium species **19**, an *anti*-Markovnikov enol ester **26** or enamide **6**−**13** is formed. In contrast, the alternative direct addition of a nucleophile to a coordinated alkyne should result in the formation of the Markovnikov product. This mechanism provides a sound explanation for the *anti*-Markovnikov selectivity of the reaction and its limitation to terminal alkynes. Experiments with isolated Ru−vinylidene complexes confirmed that their reaction with nucleophiles will indeed lead to the addition product. As an alternative to vinylidene formation via a 1,2-proton shift, a sequence consisting of an oxidative addition of the alkyne C(sp)−H bond to ruthenium followed by a 1,3-proton shift was also proposed as an entry to this mechanism.

Mechanism B would again predict a dependence of the reaction rate on the electronic and steric properties of the Ru-complex,

Journal of the American Chemical Society ARTICLE

Scheme 2. Ru-catalyzed Addition of *N*-Nucleophiles to Terminal Alkynes

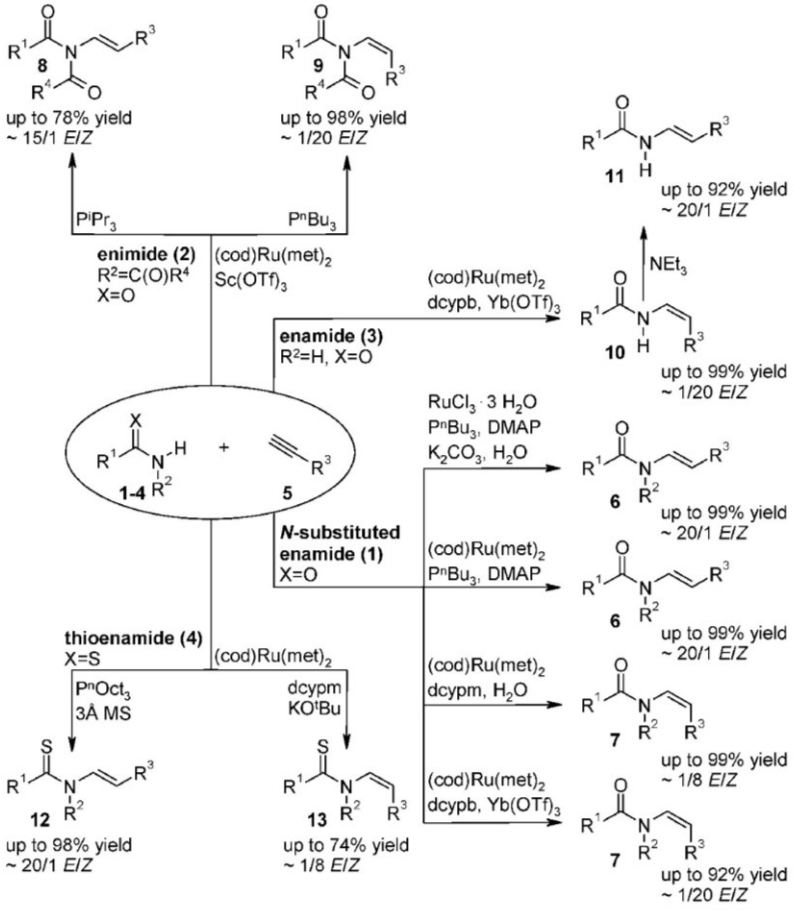

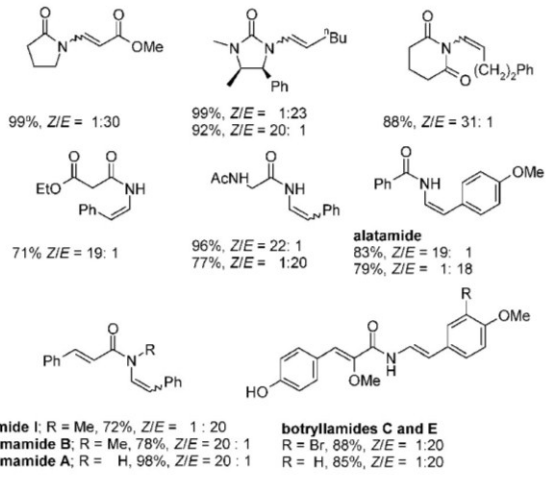

Figure 2. Representative example for the addition of terminal alkynes.

Scheme 3. *Mechanism A*: Hydroamidation Pathway Postulated by Watanabe

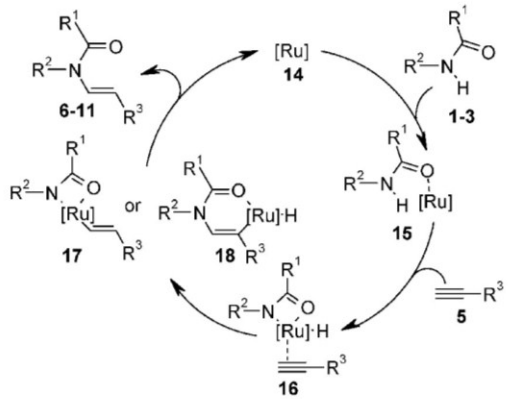

and the reaction would benefit from the stabilizing effect of electron-donating ligands on the high oxidation state of the ruthenium center. We assume the vinylidene formation to be a relatively slow reaction step. Therefore, in contrast to *Mechanism A*, the acidity of the alkyne C(sp)−H bond rather than that of the amide N−H bond should have an additional influence on the C−H bond cleaving vinylidene formation step. Therefore,

dx.doi.org/10.1021/ja111389r |J. Am. Chem. Soc. 2011, 133, 7428–7449

Scheme 4. *Mechanism B:* **Hydroamidation in Analogy to Dixneuf's Carboxylation of Terminal Alkynes**

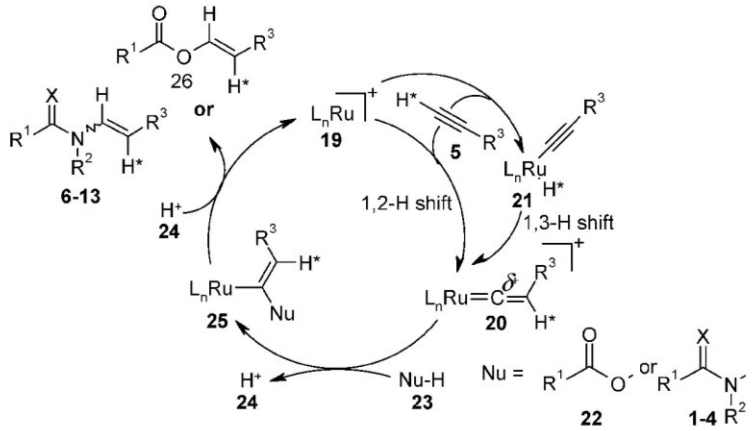

Scheme 5. *Mechanism C*: **Hydroamidation in Analogy to Wakatsuki's Hydration of Terminal Alkynes**

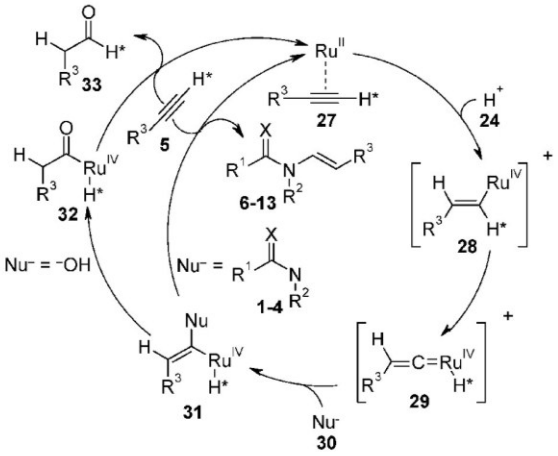

Scheme 6. *Mechanism D*: **Hydroamidation via Oxidative Addition of the Amide, Insertion of the Alkyne, and Ru−Vinyl/−Vinylidene Rearrangement**

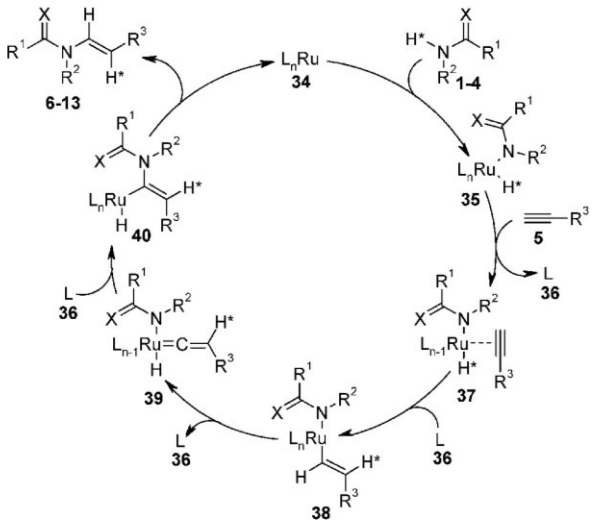

kinetic isotope effects should be measurable in experiments with 1-deuterioalkynes, and the resulting product should exclusively be deuterated in the 2-position, because proton shifts to the internal alkyne C-atom are postulated. ESI−MS and in situ IR experiments could help to verify reactive intermediates.

Vinylidene intermediates have been confirmed for other ruthenium-catalyzed addition reactions.[32] One example is the addition of alcohols to alkynes, where a 1,2-proton shift was observed in isotopic labeling experiments.[24b] However, the intermediacy of vinylidene intermediates does not necessarily call for proton shifts, and alternative mechanisms for Ru−vinylidene formation have been proposed for the hydration of terminal alkynes[20b] and for stoichiometric reactions of terminal alkynes with ruthenium−hydride complexes.[33] On the basis of computational studies, Wakatsuki and Caulton concluded that vinylidene intermediates are formed via rearrangement of Ru-vinyl species for these reactions, whereas pathways via 1,2- or 1,3-proton shifts are energetically unfavorable (see Schemes 5 and 6).

For the hydration of terminal alkynes, the absence of proton shifts was corroborated by deuterium-labeling experiments. Wakatsuki et al. thus derived a different mechanism involving Ru−vinylidene intermediates.[20b] Again, this may be translated to hydroamidation reactions (Scheme 5).

The key step in this mechanism, which will further be referred to as *Mechanism C*, is the protonation of a π-coordinated alkyne resulting in the formation of a cationic Ru^{IV}−vinyl intermediate **28**. Its rearrangement to the Ru−H−vinylidene species **29** was proposed to be the rate-determining step. Addition of a nucleophile and reductive elimination gives the aldehyde **33** or the enamide **6**−**13**, respectively. In this mechanism, the alkyne C(sp)-proton is transferred to the metal center and subsequently reattached to its original carbon atom. For the hydration of alkynes, 1,2-proton shifts were indeed not observed in deuteration studies. This mechanism offers an explanation for the *anti*-Markovnikov selectivity and the limitation to terminal alkynes. However, it involves cationic intermediates in the high oxidation states of +4 or even +6, depending on whether the Ru═C bond in species **29** is

viewed as a covalent bond or a as the coordination of a neutral carbene ligand to the metal center. This may be reasonable for hydration reactions in aqueous solvents, but is less likely for hydroamidations under almost neutral conditions in toluene.

If the hydroamidation proceeded via *Mechanism C*, the use of protic and more polar solvents should result in a higher reaction rate. Again, electron-donating ligands should enhance the catalyst activity due to their stabilizing effect on higher oxidation states of the ruthenium center, and sterically demanding ligands should facilitate the reductive elimination of the product. During the slow vinylidene formation step, the C(sp) proton is transferred to the ruthenium center. This proton may be detectable via ^{1}H NMR. When comparing the reactions of alkynes and 1-deuterioalkynes, a primary kinetic isotope effect is expected, as a C−D rather than a C−H bond has to be cleaved. The resulting product should be deuterated exclusively in the 1-position.

Caulton and co-workers investigated pathways leading to the formation of Ru−vinylidene intermediates.[33] They found that π-coordinated alkynes readily insert into Ru−H bonds to form Ru−vinyl complexes. The Ru−vinyl species then rearrange to Ru−H−vinylidene complexes. They isolated all postulated Ru intermediates and confirmed the pathways by DFT calculations. These showed reasonable energy barriers for the proposed pathway, and substantially higher barriers for an oxidative addition of the alkyne followed by a 1,3-proton shift. It is possible to incorporate this alternative route to vinylidene species into a new catalytic cycle for hydroamidations, which will further be referred to as *Mechanism D* (Scheme 6).

This catalytic cycle starts with the oxidative addition of an amide to an active Ru^0 species (**34**). After insertion of the alkyne into the Ru−hydride bond and rearrangement to the vinylidene species **39**, the amide attacks the carbon atom α to the ruthenium center, leading to the *anti*-Markovnikov enamide product (**6**−**13**) via reductive elimination. The oxidation state of the Ru center changes from 0 via +2 to +4 during the catalytic cycle, or only from 0 to +2 if the vinylidene ligand is interpreted as neutral carbene. The vinylidene formation proceeds without proton shifts, and at the end of the reaction, the alkyne proton is linked to the original C-atom.

For *Mechanism D*, a dependence of the reaction rate on the acidity of the N−H group of the amide as well as the C(sp)−H function of the alkyne should be detectable, resulting in measurable kinetic isotope effects both when *N*-deuterated amides or 1-[*D*]-alkynes are used as starting materials. Electron-rich ligands will stabilize the high oxidation state of the ruthenium center, and the use of sterically demanding ligands should facilitate the reductive elimination step. Reaction intermediates might be identifiable via ESI−MS and in situ IR experiments. It might also be interesting to investigate by in situ NMR whether the Ru-complexes are capable of activating N−H bonds.

In our previous work, we had excluded reaction mechanisms starting from Ru^0 species because no coupling product of the methylallyl ligands from the (cod)Ru(met)$_2$ precursor could be detected, and instead, free isobutene was observed via GC−MS and ^{1}H NMR spectroscopy, which appeared to support a redox-neutral ligand-exchange reaction.[29] A control experiment with 1-[*D*]-hex-1-yne showed no 1,2-proton shift during the reaction.[28] In situ NMR and ESI−MS experiments of the catalyst preformation step confirmed that all ligands of (cod)Ru(met)$_2$ are exchanged, and that cationic Ru-amide-phosphine and Ru-amide-phosphine-DMAP species are formed in the addition of secondary amides to terminal alkynes.[26] On the basis of these

Scheme 7. Redox-Neutral *Mechanism E* for the Hydroamidation of Terminal Alkynes

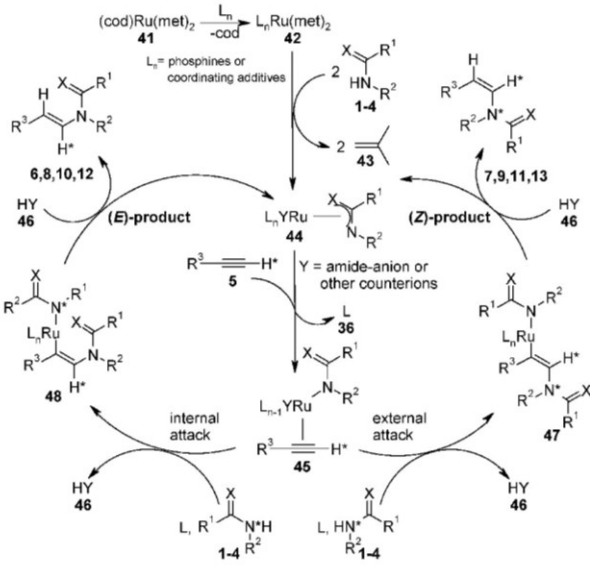

experiments, we postulated a redox-neutral ligand exchange mechanism, which will further be referred to as *Mechanism E* (Scheme 7).

In the catalyst preformation step, all ligands initially bound to the Ru-precursor are exchanged, with formation of ruthenium^{II}−amide complexes **44**. In the first step of the catalytic cycle, the alkyne coordinates to the ruthenium center (**45**). Depending on the steric bulk of the phosphines, the amide attacks from either the inner or the outer coordination resulting in the formation of *E*- or *Z*-configured enamides (**6**−**13**). Bulky ligands are likely to favor an external attack resulting in the formation of an (*E*)-Ru−enamide complex **47**, which releases the corresponding (*Z*)-enamide (**7**, **9**, **11**, or **13**) after protonolysis, along with a regenerated active Ru^{II}-species **44**. In contrast, an insertion of the alkyne into the Ru−N-bond of a coordinated amide is favorable in the presence of smaller ligands, giving rise to (*E*)-enamides (**6**, **8**, **10**, or **12**). Over the entire cycle, the Ru center remains in the oxidation state +2. A likely driving force behind the reaction is the continuous exchange of basic for more acidic ligands at the metal center.[34] *Mechanism E* offers an explanation for the stereochemistry of the hydroamidation, but cannot adequately address the limitation to terminal alkynes and selectivity for the *anti*-Markovnikov products.

If *Mechanism E* holds true, an inverse secondary kinetic isotope effect should be detectable for 1-deuterioalkynes, because it involves a rehybridization from sp to sp^2, which is more favorable for the stronger C−D bond.[35] Furthermore, no ruthenium−hydride species should be detectable via ^{1}H NMR. The nucleophilicity of the amide should have a strong influence on the reaction rate, and additives that increase the nucleophilic character of the amide should enhance the reaction rate. The ruthenium center remains in the oxidation state of +2 and merely activates the alkyne for nucleophilic attack by removing electron-density from the π-system. Therefore, less electron-rich phosphines should lead to a higher catalyst activity, whereas sterically demanding phosphines should lead to a reduced activity because the

Table 1. Overview of Experimental Findings for a Set of Control Experiments

Experimental finding	Expected outcome for *Mechanism*				
	A	*B*	*C*	*D*	*E*
1,2-proton shift in experiments with 1-[*D*]-alkynes	No	Yes	No	No	No
Primary kinetic isotope effect in hydroamidation competition experiments with 1-[*H/D*]-alkynes	No	Yes	Yes	Yes	No
Primary kinetic isotope effect in hydroamidation competition experiments with *N*-[*H/D*]-amides	Yes	Yes	Yes	Yes	Yes
Inverse secondary kinetic isotope effect in hydroamidation competition experiments with 1-[*H/D*]-alkynes	Yes	No	No	No	Yes
Detection of Ru-hydride species in ^{1}H-NMR hydroamidation experiments in absence of the alkyne	Yes	No	No	Yes	No
Detection of Ru-hydride species in ^{1}H-NMR hydroamidation experiments in absence of the amide	No	Yes	Yes	No	No
Detection of Ru-amide species in ESI-MS hydroamidation experiments in absence of the alkyne	Yes	No	No	Yes	Yes
Intermediacy of cationic species in the catalytic cycle	No	Yes	Yes	No	No

ligand-exchange reactions and the formation of the ruthenium−enamide intermediate are disfavored.

An overview of all predictions we made in this paragraph for *Mechanisms A*−*E* in a set of control experiments is presented in Table 1. These predictions are made under the assumption that the concentrations of all characteristic intermediates are high enough for detection and that the reaction steps leading to possible kinetic isotope effects (KIE) are slow.

All mechanisms presented above are in principle feasible, but give contradictory predictions for the outcome of simple control experiments and spectroscopic studies. The combined experimental findings presented herein provide strong evidence that the reaction proceeds via *Mechanism D*.

■ DEUTERATION STUDIES OF HYDROAMIDATIONS

We started our mechanistic investigation with hydroamidation experiments using 1-deuterioalkynes. *Mechanisms A*, *C*, *D*, and *E* predict that the deuterium should end up in the geminal position to the amide nitrogen, whereas *Mechanism B* predicts that the deuterium should be transferred to the vicinal carbon. In the inverse experiment, with *N*-deuterioamides and nondeuterated alkynes, the deuterium should be incorporated to the geminal position to the amide nitrogen for *Mechanism B* and bind to the vicinal atom for *Mechanisms A*, *C*, *D*, and *E*.

Deuteration studies were carried out for the additions of primary and secondary amides as well as imides, using both the *E*- and the *Z*-selective methods. The results are summarized in Table 2.

The addition of 2-pyrrolidone (**1a**) to 1-[*D*]-hex-1-yne (**5a**, Deuteration grade, DG = 92%) using the *E*-selective protocol (2 mol % (cod)Ru(met)$_2$, 6 mol % P(*n*-Bu)$_3$, 4 mol % DMAP) led to incorporation of the deuterium almost exclusively in the 1′-position of the corresponding enamide (**6aa**), that is, in geminal position to the amide (entry 1). The 2′-deuterated product (**6ab**) was detected in traces only. In the analogous reaction of 1-[*D*]-2-pyrrolidone (**1b**, DG = 85%) and 1-hexyne (**5b**), the deuterium was transferred to the 2′-position of **6ab** in very high selectivity (entry 2). These results indicate that the predominant mechanism does not involve proton shifts. The trace formation of 2′-deuterated product can be accounted for by H−D exchange reactions at a relatively acidic site of the hydroamidation product, possible competing mechanisms, or unproductive vinylidene rearrangements.

The reaction of 2-pyrrolidone (**1a**) and 1-[*D*]-hex-1-yne (**5a**) under *Z*-selective conditions (2 mol % (cod)Ru(met)$_2$, 3 mol % $Cy_2PCH_2PCy_2$, 2 equiv H_2O) also proceeded mostly without proton shift (entry 3). The ratio between 2′-deuterated (**7ab**) versus 1′-deuterated product (**7aa**) dropped to a moderate value of 4:1 for the inversely deuterated starting materials (entry 4). In both reactions, the deuteration grades in the products were only moderate, which we attribute to the presence of water in the reaction mixture responsible for background H−D exchange reactions. Indeed, when we replaced the water, which is essential for an effective hydroamidation protocol, by deuterium oxide, the deuteration rates in the products (**7aa** and **7ab**) were high (entries 5 and 6). However, the regioselectivity of the deuteration was only moderate, and in the reaction of 1-[*D*]-hex-1-yne (**5a**), a doubly deuterated product was observed. All these findings suggest that background H−D exchange overlays regioselective deuterium incorporation in the presence of water.

The catalytic addition of succinimide (**2a**) to 1-[*D*]-hex-1-yne (**5a**) under *E*-selective conditions (5 mol % (cod)Ru(met)$_2$, 15 mol % P(*i*-Pr)$_3$, 4 mol % Sc(OTf)$_3$) proceeds without proton shift and leads exclusively to the incorporation of the deuterium in the 1′-position of the corresponding enimide product (**8aa**, entry 7). When using the inversely deuterated starting materials, the deuterium is mainly incorporated in the 2′-position of the enimide product (**8ab**, entry 8). In addition to the expected products, traces of the product deuterated in the α-position to the imide carbonyl group were detected, which can be rationalized by H/D exchange at this acidic position.[36]

Journal of the American Chemical Society ARTICLE

Table 2. Hydroamidation with Deuterated Starting Materials[a]

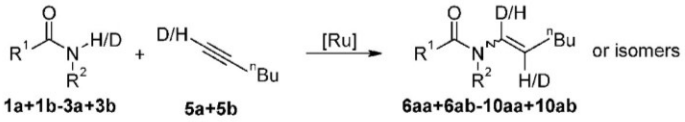

1a+1b-3a+3b 5a+5b 6aa+6ab-10aa+10ab

Entry	Amide	Alkyne	Products	Yield Ratio **6aa**:**6ab**
1	 **1a**	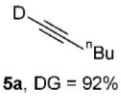 **5a**, DG = 92%	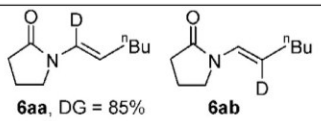 **6aa**, DG = 85% **6ab**	92% >30:1
2	 **1b**, DG = 85%	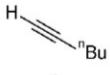 **5b**	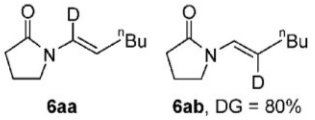 **6aa** **6ab**, DG = 80%	91% <1:30
3[b]	 **1a**	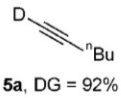 **5a**, DG = 92%	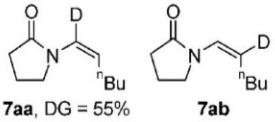 **7aa**, DG = 55% **7ab**	89% 12:1
4[b]	 **1b**, DG = 85%	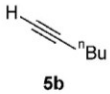 **5b**	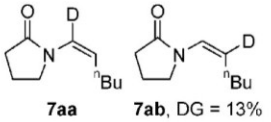 **7aa** **7ab**, DG = 13%	90% 1:4
5[c]	 **1a**	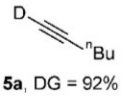 **5a**, DG = 92%	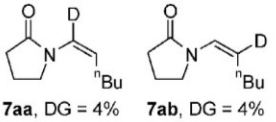 **7aa**, DG = 4% **7ab**, DG = 4%	80% 1:1[d]
6[c]	 **1b**, DG = 85%	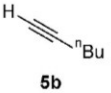 **5b**	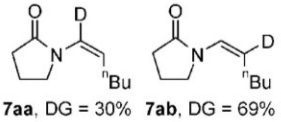 **7aa**, DG = 30% **7ab**, DG = 69%	91% 1:2
7[e]	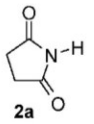 **2a**	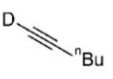 **5a**, DG = 92%	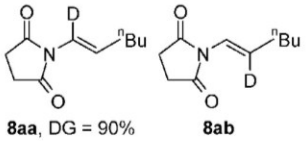 **8aa**, DG = 90% **8ab**	75% >30:1
8[e,f]	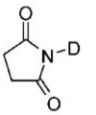 **2b**, DG = 81%	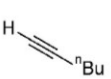 **5b**	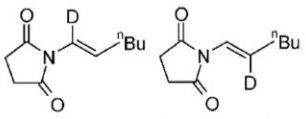 **8aa** **8ab**, DG = 56%	92% <1:30[g]
9[h]	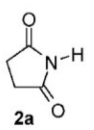 **2a**	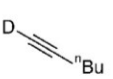 **5a**, DG = 92%	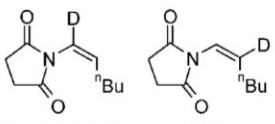 **9aa**, DG = 84% **9ab**	92% >30:1

dx.doi.org/10.1021/ja111389r |J. Am. Chem. Soc. 2011, 133, 7428–7449

Table 2. Continued

Entry	Amide	Alkyne	Products	Yield Ratio **6aa**:**6ab**
10[h]	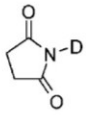 **2b**, DG = 81%	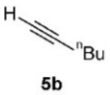 **5b**	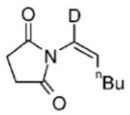 **9aa** 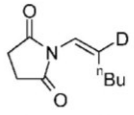 **9ab**, DG = 83%	91% <1:30[g]
11[i]	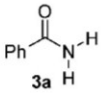 **3a**	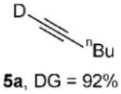 **5a**, DG = 92%	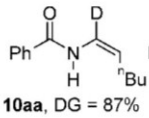 **10aa**, DG = 87% 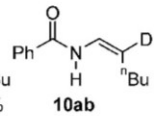 **10ab**	89% >30:1
12[i]	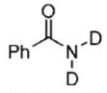 **3b**, DG = 75%	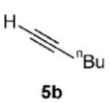 **5b**	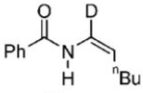 **10aa** 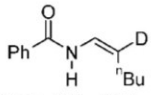 **10ab**, DG = 62%	87% <1:30

[a] *Reaction conditions*: Amide or imide (1.00 mmol), alkyne (2.00 mmol), (cod)Ru(met)$_2$ (2 mol %), P(*n*-Bu)$_3$ (6 mol %), DMAP (4 mol %), toluene (3 mL), 100 °C, 15 h, selectivity determined by ^{1}H NMR; DG = deuteration grade. [b] $Cy_2PCH_2PCy_2$ (3 mol %) instead of P(*n*-Bu)$_3$, H_2O (2.00 equiv) instead of DMAP. [c] $Cy_2PCH_2PCy_2$ (3 mol %) instead of P(*n*-Bu)$_3$, D_2O (2.00 equiv) instead of DMAP. [d] The doubly deuterated product was mainly formed with a DG of 91%. [e] (cod)Ru(met)$_2$ (5 mol %), P(*i*-Pr)$_3$ (15 mol %), Sc(OTf)$_3$ (4 mol %), DMF-d_7 (3 mL), 60 °C, 15 h, isolated yields, selectivities determined by ^{1}H NMR. [f] DMF (3 mL) instead of DMF-d_7. [g] A product deuterated in the 3-position of the imide was detected in traces. [h] (cod)Ru(met)$_2$ (2 mol %), P(*n*-Bu)$_3$ (6 mol %), Sc(OTf)$_3$ (4 mol %), DMF (3 mL), 60 °C, 15 h, isolated yields, selectivities determined by ^{1}H NMR. [i] (cod)Ru(met)$_2$ (5 mol %), dcypb (6 mol %), Yb(OTf)$_3$ (4 mol %), DMF (3 mL), 60 °C, 6 h, isolated yields, selectivity determined by ^{1}H NMR.

Similar results were observed also for the *Z*-selective protocol (2 mol % (cod)Ru(met)$_2$, 6 mol % P(*n*-Bu)$_3$, 4 mol % Sc(OTf)$_3$). Thus, the reaction of succinimide (**2a**) with 1-[*D*]-hex-1-yne (**5a**) yielded the enimide mainly deuterated in the 1′-position (**9aa**, entry 9), whereas the addition of *N*-[*D*]-succinimide (**2b**, DG = 81%) to 1-hexyne (**5b**) led to the formation of the product with near-quantitative deuterium incorporation in the 2′-position (**9ab**, entry 10). The hydroamidation therefore also proceeded without proton shift, as did the reaction of the secondary amides **1a** and **1b**.

The reaction of benzamide (**3a**) with 1-[*D*]-hex-1-yne (**5a**) under *Z*-selective conditions (5 mol % (cod)Ru(met)$_2$, 6 mol % dcypb, 4 mol % Yb(OTf)$_3$) furnished the corresponding enamide **10aa** deuterated exclusively in the 1′-position (entry 11). Analogously, the deuterium was selectively incorporated in the reaction of *N*,*N*-[D_2]-benzamide (**3b**, DG = 75%) and 1-hexyne (**5b**) under otherwise identical conditions (**10ab**, entry 12). It is worth mentioning that, in contrast to the previously reported hydroamidation protocol for the addition of primary amides,[29] we had to perform these two deuteration experiments without water, because in the presence of water H−D exchange reactions overlaid regioselective deuterium incorporation.

On the basis of these results, the formation of vinylidene intermediates via a 1,2-proton shift or via oxidative addition of the alkyne followed by a 1,3-proton shift as postulated in *Mechanism B* can be ruled out for both *E*- and *Z*-selective hydroamidation reactions. *Mechanisms A*, *C*, *D*, and *E* are all in agreement with the results of the present deuteration studies.

KINETIC INVESTIGATIONS OF HYDROAMIDATIONS

We next investigated the kinetics of hydroamidations by means of in situ IR spectroscopy. Using a ReactIR 45 m FT-IR spectrometer (3.2 scans/s, 8 cm^{-1} resolution), we monitored the hydroamidation of 2-pyrrolidinone (**1a**) and 1-hexyne (**5b**) by the disappearance of the C−C triple bond valence oscillation of 1-hexyne (**5b**) at 2122 cm^{-1} and the appearance of a C═O valence oscillation of the enamide product (**6a**) at 1725 cm^{-1}. Figure 3 illustrates the starting material consumption as well as the product formation and the temperature inside the reaction vessel over a period of 30 min. The reaction starts almost immediately after the reaction vessel is placed in an aluminum block preheated to 100 °C and is complete within several minutes.

Evaluation of the spectroscopic data with the iC IR software using the ConcIRT algorithm also allowed to detect the appearance of short-lived reaction intermediates by their C═C vibration stretches at 1607 cm^{-1} (see Supporting Information). This frequency is in an area typical for ruthenium−vinylidene species.[37] However, in-depth studies under carefully optimized conditions would be required to unambiguously confirm these species.

Attempts to slow down the reaction by lowering the temperature were unsuccessful. Below 100 °C, the hydroamidation was sluggish, and undesired alkyne dimerization became the predominant process. Even at the optimum reaction temperature, the catalyst preformation did not always proceed at the same speed, so that the variability of overall reaction rates was rather high.

It was therefore unfeasible to perform comparative kinetic studies with deuterated and nondeuterated substrates in separate vessels to determine kinetic isotope effects. Instead, we performed

Journal of the American Chemical Society ARTICLE

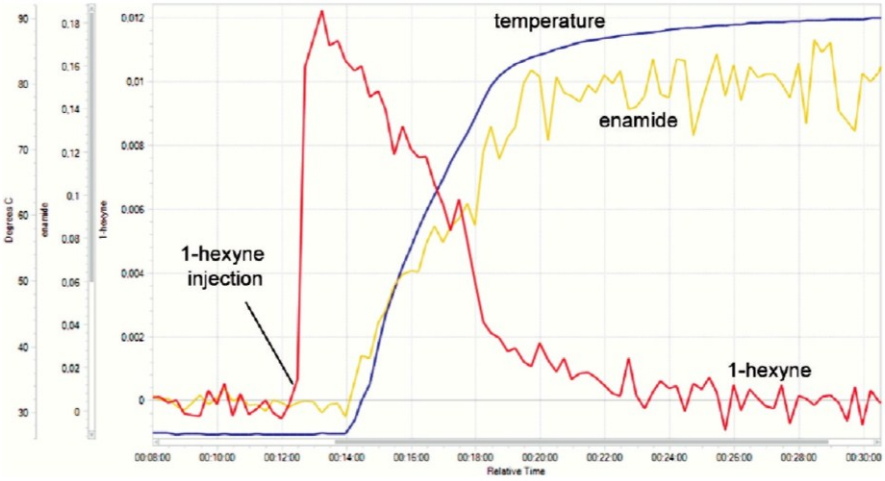

Figure 3. In situ IR-experiment: Concentration trends for the hydroamidation of 1-hexyne (**5b**) with 2-pyrrolidinone (**1a**).

competition experiments in which one of the starting materials was added in large excess as a 1:1 mixture of its deuterated and nondeuterated form (Table 3). From the ratio of hydrogen versus deuterium incorporation in the enamide product, we calculated the relative reaction rates.

In the reaction of 2-pyrrolidinone (**1a**) with 1-hexyne (4 equiv, DG adjusted to 50%), the enamide (**6a**/**6aa**) was obtained with a DG of 39% (entry 1). This translates to a kinetic isotope effect (KIE) of 1.6. Similarly, the reaction of succinimide (**2a**) with 1-hexyne (4 equiv, DG adjusted to 50%) gave a product (**9a**/**9aa**) with 30% DG, translating to a KIE of 2.3 (entry 2). In the analogous reaction of benzamide (**3a**), the product DG was 40% (**10a**/**10aa**), corresponding to a KIE of 1.5 (entry 3).

In all cases, normal kinetic isotope effects (KIE = $k_H/k_D = n_H/n_D$) greater than 1 were observed. During the reaction, the hybridization of the C(1) carbon changes from sp to sp^2 and any intermediate should thus have a higher or the same p-character as the starting material. However, a reaction step during which the p-character of a C−H bond increases is known to lead to an inverse secondary KIE. Thus, the KIE should always have a value smaller than 1, unless the sp C−H bond is cleaved in a slow reaction step, and a sp^2 C−H bond is reinstated at the same carbon atom in a later, non rate-determining step.[35] This implies that, despite their relatively small magnitudes, the values must result from a primary KIE. *Mechanism A*, which does not involve a bond cleavage but rather an insertion of the alkyne into a Ru−H or Ru−N bond with sp to sp^2 rehybridization, can thus be excluded as the main reaction pathway. *Mechanism E* is also incompatible with the observed KIE > 1, as in this process, the C−H bond is also not cleaved.

In *Mechanisms C* and *D*, a rearrangement step from a ruthenium−vinyl to a ruthenium−hydride−vinylidene species takes place, during which the C(sp)−H/D bond is cleaved. The KIE values greater than 1 are in good agreement with these pathways. Although primary KIEs for deprotonation processes usually have values of 4−7, the relatively low values of 1.5−2.3 observed here are easily rationalized when considering that the overall catalytic process consists of several steps. For example, if one reaction step is slower by a factor of 5 because of an isotope effect, but this individual reaction step requires only one-forth of the catalyst turnover time, the overall KIE would be 2 rather than 5.

Table 3. Determination of KIE Values by Competition Experiments[a]

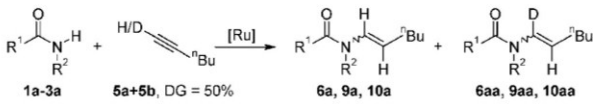

Entry	Amide	Main Product	Ratio **a**/**aa**	KIE
1	 **1a**	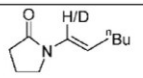 DG = 39%, **6a/6aa**	1.6:1	1.6
2[c]	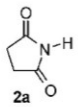 **2a**	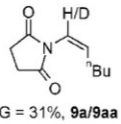 DG = 31%, **9a/9aa**	2.3:1	2.3
3[d]	 **3a**	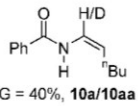 DG = 40%, **10a/10aa**	1.5:1	1.5

[a] *Reaction conditions*: Amide (1.00 mmol), 1-hexyne (2.00 mmol), 1-[*D*]-hex-1-yne (2.00 mmol), (cod)Ru(met)$_2$ (2 mol %), P(*n*-Bu)$_3$ (6 mol %), DMAP (4 mol %), toluene (3 mL), 100 °C, 15 h, product ratio determined by ^{1}H NMR. [b] Determined by the ratio of nondeuterated to deuterated product yields. [c] Sc(OTf)$_3$ (4 mol %) instead of DMAP, DMF (3 mL) instead of toluene, 60 °C, 15 h. [d] (cod)Ru(met)$_2$ (5 mol %), dcypb (6 mol %), Yb(OTf)$_3$ (4 mol %), DMF (3 mL), 60 °C, 6 h.

Indeed, in the reaction of 2-pyrolidinone (4 equiv, DG adjusted to 50%) and hex-1-yne (**5b**) (Scheme 8), the enamide (**6a**/**6ab**) was obtained with a DG of 30%, translating to a KIE of 2.3. The fact that a noticeable KIE is again observed reveals that this step is also relatively slow. The KIE value for each individual step is thus probably larger than 4, resulting in a smaller observed KIE for the overall reaction because the catalytic cycle involves at least two slow steps.

Scheme 8. Competition Hydroamidation Experiment with 1-[*D*]-2-Pyrrolidinone (1b)

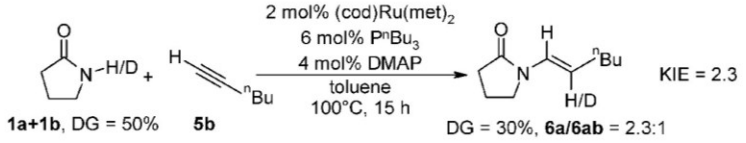

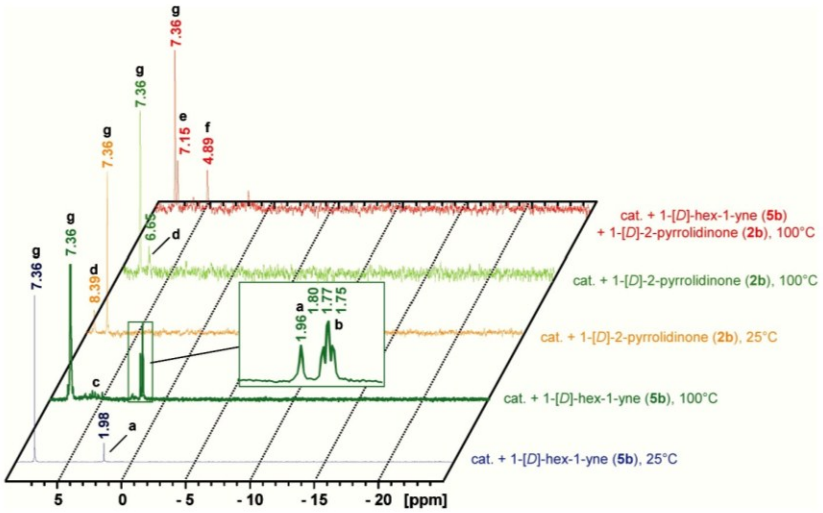

Figure 4. In situ ^{2}H NMR experiments with 1-[*D*]-hex-1-yne (**5b**) and 1-[*D*]-2-pyrrolidinone (**1b**). (a) Free 1-[*D*]-hex-1-yne; (b) triplet signal; (c) oligomerization products; (d) free 1-[*D*]-2-pyrrolidinone; (e) 1′-deuterium of the enamide; (f) 2′-deuterium of the enamide; (g) benzene-d_6.

Another possible explanation for the relatively small values is that the transition state is a nonlinear one.[38]

Overall, only *Mechanisms C* and *D*, both involving Ru−vinylidene intermediates formed without proton shifts, are in agreement with the outcome of both the deuteration studies and the kinetic investigations.

■ NMR STUDIES OF HYDROAMIDATIONS

We next performed in situ NMR studies with the goal of identifying potential Ru-bound organic fragments. However, the reaction proceeds very rapidly when using increased amounts of Ru catalyst, and the spectra contained numerous signals pertaining to ligands, additives, and byproducts that often obscured relevant species. To specifically monitor species derived from the alkyne and amide starting materials, we used deuterated derivatives and followed the reaction by ^{2}H NMR. This greatly simplified the NMR spectra obtained (Figure 4). Unfortunately, the sensitivity of this spectroscopic method was determined to be rather low.

^{2}H NMR spectra of a mixture containing the catalyst (20 mol % (cod)Ru(met)$_2$, 60 mol % P(*n*-Bu)$_3$, 40 mol % DMAP) and 1-[*D*]-hex-1-yne (**5a**) only were recorded in toluene, using benzene-d_6 as an internal standard (Figure 4 and Supporting Information).

At room temperature, only the signal pertaining to the starting material was visible (a), confirming that the catalyst activation requires elevated temperatures. Indeed, at 100 °C, a new broad triplet (b) was detected at δ = 1.77 ppm (J = 2.2 Hz). Moreover, a series of signals in the range of 4.89−6.20 ppm (c) rapidly appeared and increased in intensity with concomitant consumption of the alkyne, which can be attributed to alkyne oligomerization products. Some of them might also originate from Ru−vinyl species, but an unambiguous assignment of signals to such intermediates was not possible. When both 1-[*D*]-hex-1-yne (**5b**) and 2-pyrrolidinone (**1a**) were present, the same triplet (b) was detected along with a strong signal for the C(1)-deuterated enamide product (e). Alkyne oligomerization products (c) and C(2)-deuterated enamide (f) were detected only in traces.

This triplet (b) was not in good agreement with literature NMR data for ruthenium alkyne and vinyl complexes (Figure 5). Terminal protons of coordinated alkynes should appear around 5 ppm and have a large H−P coupling.[39] Ru−H and Ru−vinyl species should also appear at chemical shifts different than 1.77 ppm.[33] Considering the small value of D−H couplings in ^{2}H NMR spectra[40] and the broad shape of triplet b, this signal might be assigned to the vinylic proton of a Ru−vinylidene−phosphine species. For a known *trans*-[(dppm)$_2$(Cl)Ru=C=CH^{n}Bu]PF$_6$ complex (dppe = bisdiphenylphosphino methane) with the identical 1-hexyne-derived vinylidene ligand, Dixneuf et al. reported a triplet of quintets at 2.5 ppm in the ^{1}H NMR spectrum (Figure 5).[41] Coupling constants of 7.9 and 2.8 Hz for the vinylic proton at the vinylidene entity could be determined, resulting from a coupling to two neighboring protons and a long-range coupling to four phosphine atoms. The chemical shift of triplet b is in good range for such a vinylic proton, considering that the Ru center should be more electron-rich because of the stronger donor capacity of alkyl phosphine compared with the aryl phosphine ligands. That should lead to an upfield shift of the proton signal. The observed coupling constant of 2.2 Hz is in agreement with a long-range

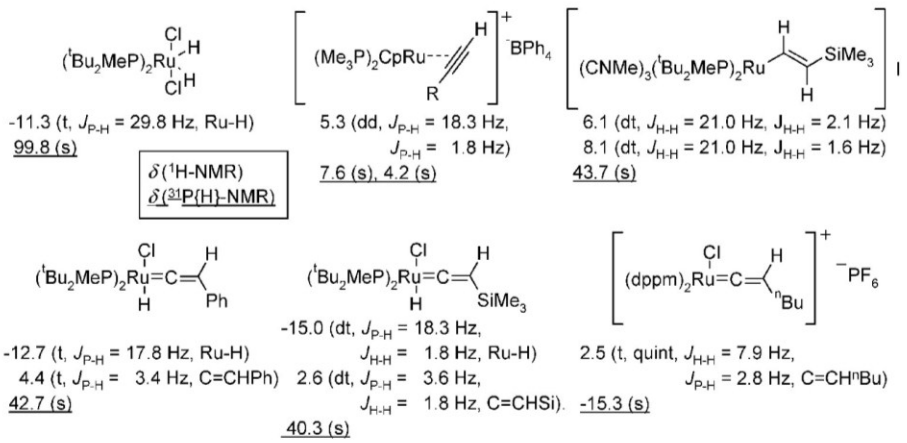

Figure 5. ^{1}H- and ^{31}P NMR chemical shifts for selected ruthenium−phosphine complexes.

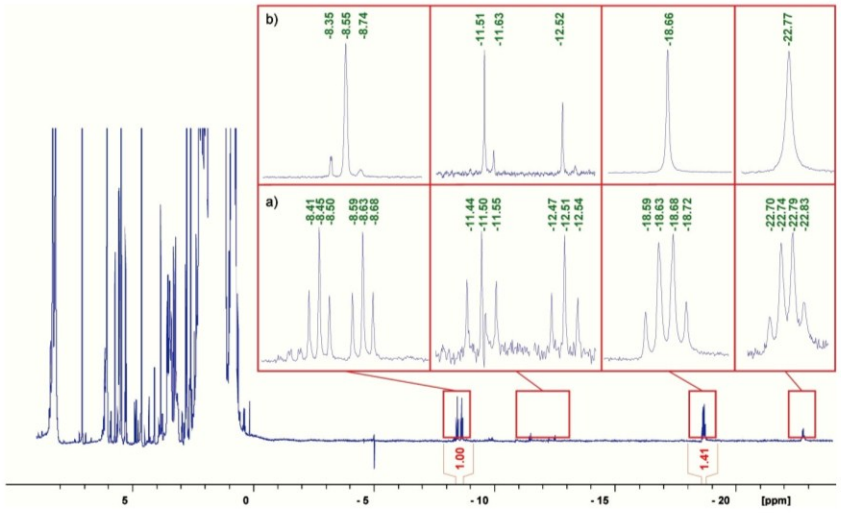

Figure 6. In situ ^{1}H NMR experiments with 2-pyrrolidinone (**1a**) at ambient temperature after heating to 100 °C for 5 min. (a) ^{1}H NMR experiment; (b) ^{1}H{^{31}P}-NMR experiment.

coupling to two phosphine atoms. The broad shape might indicate that the coupling to the neighboring protons, which is expected to be arround 1 Hz for such a D−H coupling,[40] could not be resolved in this in situ ^{2}H NMR experiment. These results suggest that, in the absence of the amide, a Ru−vinylidene species is formed, possibly via 1,2-proton shift. This is in agreement with the observation by Dixneuf that alkyne oligomerization reactions proceed via vinylidene species.[32,42]

In an attempt to find evidence for Ru−H species resulting from the oxidative addition of amides, we recorded the ^{2}H NMR spectrum for a mixture of 1-[*D*]-2-pyrrolidinone (**1b**) with the catalyst system (40 mol % (cod)Ru(met)$_2$, 120 mol % P(*n*-Bu)$_3$, 80 mol % DMAP) in toluene using benzene-d_6 as an internal standard (Figure 4). However, it contained only the signal for the free amide (d). Subsequent addition of 1-[*D*]-hex-1-yne (**5a**) led to a rapid disappearance of this signal with concomitant appearance of the signals for vinylic deuterium atoms of the enamide product (e and f). The reaction simply proceeded too rapidly to allow a detection of any intermediates by ^{2}H NMR.

We next investigated the reaction mixtures with the help of ^{1}H NMR, as this is more sensitive than ^{2}H NMR. In the ^{1}H NMR spectrum of a mixture containing the catalyst (20 mol % (cod)Ru(met)$_2$, 60 mol % P(*n*-Bu)$_3$, 40 mol % DMAP) and 1-hexyne (**5b**) but no amide (see Supporting Information), multiple signals in the range of 4.66−6.12 ppm were observed, but none were detected below 0 ppm in the region characteristic for Ru−H species. Such signals would have been expected for *Mechanisms B* and *C*. A corresponding signal for triplet b observed in the ^{2}H NMR experiment at 1.77 ppm could not be found in the ^{1}H NMR spectrum since the area from 0 to 3 ppm was overlaid with multiple broad proton signals of alkyl groups, for example, from the phosphine ligands.

In contrast, after briefly heating a mixture of the catalyst and 2-pyrrolidinone (**1a**) to 100 °C, the ^{1}H NMR spectrum showed several new signals below 0 ppm (Figure 6): A group of peaks consisting of a duplet of triplets, two triplets and two quartets appeared between −8 and −23 ppm with coupling constants between 22 and 33 Hz for the triplets and quartets and 108 Hz for

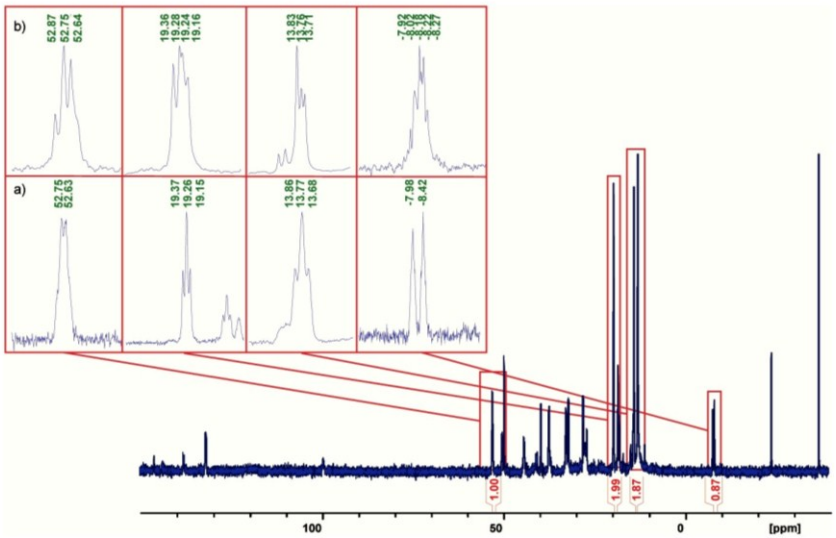

Figure 7. In situ ^{31}P NMR experiments with 2-pyrrolidinone (**1a**) measured at 22 °C after heating to 100 °C for 5 min. (a) ^{31}P NMR experiment; (b) $^{31}P\{^{1}H\}$-NMR experiment.

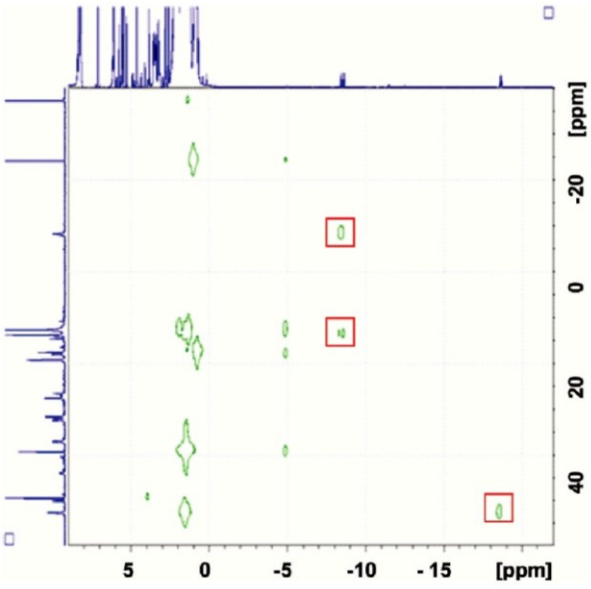

Figure 8. In situ H,P-HMQC experiments with 2-pyrrolidinone (**1a**) at ambient temperature after heating to 100 °C for five minutes.

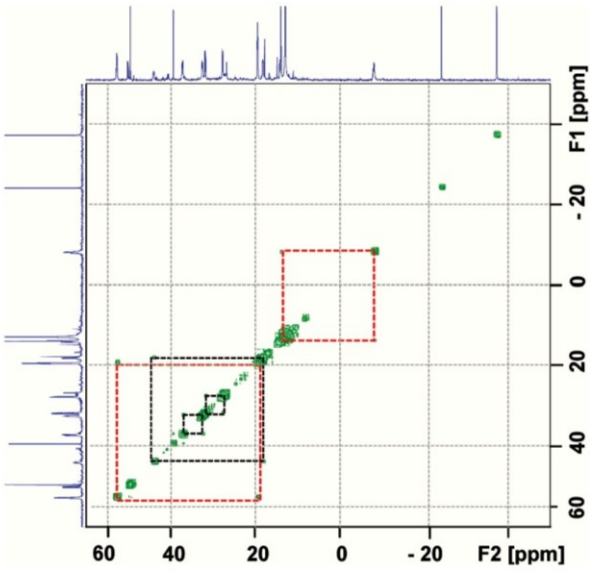

Figure 9. In situ P,P-COSY experiments with 2-pyrrolidinone (**1a**) at ambient temperature after heating to 100 °C for 5 min.

the duplet. Because of the extreme upfield shift of these signals, they are likely to originate from Ru−H species.[33] Coupling constants of 20−30 Hz are typical for *cis* H−Ru−P couplings in ruthenium hydride species stabilized by phosphines. The observed coupling constants of 108 Hz are in the expected range for *trans* H−Ru−P coupling in such complexes.[43] That the observed couplings indeed resulted from H−Ru−P interactions could be verified by phosphorus-decoupled ^{1}H NMR experiments with the same sample. Here, all signals changed to singlets.

The ^{31}P-spectrum revealed that many different phosphine species are present in the reaction mixture (Figure 7). Only the signal at −37.26 ppm could unambiguously be assigned to free tri-*n*-butylphosphine.

H,P-HMQC (Heteronuclear Multiple Quantum Coherence) and P,P-COSY (Correlation spectroscopy) experiments were used to elucidate which of these phosphine signals correspond to the Ru−H species (Figures 8 and 9).

The intensity of the proton signals at −8.55 and −18.66 ppm species was sufficient to detect them in the 2D NMR experiments. The H,P-HMQC (Figure 8) showed cross-peaks between the Ru−H-signal at −8.55 and phosphorus signals at −8.20 ppm and 13.77 ppm, which are in a reasonable range for Ru-coordinated phosphines. The signal at −8.20 ppm integrates as

Scheme 9. In Situ Formation of Ru−H-Phosphine Complexes Starting from (Cod)Ru(met)$_2$ and the Resulting ^{1}H-NMR Coupling Patterns

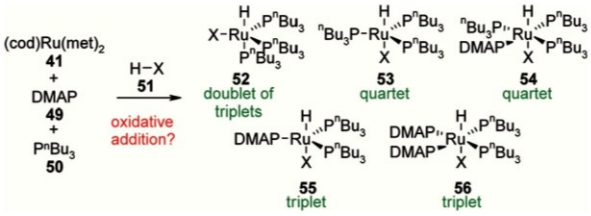

one, the signal at 13.77 ppm as two P-atoms in the ^{31}P- spectrum. In the P,P-COSY spectrum (Figure 9), a cross-peak between the two phosphorus signals is observed, confirming that all signals belong to a single Ru-species likely to contain one hydride and three phosphine ligands. The best interpretation for the H−P coupling constants for the proton signal at −8.55 ppm (J_{H-P} = 27 and 108 Hz) is that two of the phosphines are in *cis*- and one is in *trans*-position to the Ru−H bond (Scheme 9, **52**).

The H,P-HMQC (Figure 8) also showed a cross-peak for the proton signal at −18.66 ppm and the phosphorus signal at 52.69 ppm. A quartet was observed for this proton in the ^{1}H NMR which merged to a singlet in the P-decoupled ^{1}H NMR spectrum. In addition, the P,P-COSY (Figure 9) showed a clear cross-peak between the phosphorus signals at 52.69 and 19.26 ppm. The signal at 52.69 ppm integrates as one P-atom, and the signal at 19.26 ppm as two P-atoms in the ^{31}P- spectrum. These combined findings indicate an octahedral Ru-species with three phosphine ligands and one DMAP ligand in plane (Scheme 9, **54**). Two phosphorus signals are expected for species **54**, one for the two P-atoms next to, and one for the P-atom in *trans* position to the DMAP ligand. Therefore, the observed quartet in the ^{1}H NMR spectrum must actually be a duplet of triplets with nearly identical *cis* H−P couplings, which leads to an overlay of two triplets to one quartet.

The remaining upfield signals in the ^{1}H NMR showed very similar splitting patterns that disappear in the P-decoupled proton spectrum and are also likely to originate from Ru−H phosphine complexes. Beside the duplet of triplets at −8.55 ppm and the pseudo quartet at −18.66 ppm, two triplets at −11.50 and −12.51 ppm and one quartet at −22.77 ppm were detected in the ^{1}H NMR. Their coupling patterns and coupling constants in the range of 24−36 Hz also suggest Ru−H−phosphine complexes with, respectively, two and three phosphines coordinated in *cis*-position to the hydride. Scheme 9 provides for an overview of possible Ru−H species that would be in agreement with the spectroscopic data obtained.

We next added phenylacetylene-2-^{13}C (**5c**) to the NMR sample containing 2-pyrrolidinone (**1a**), 40 mol % (cod)Ru(met)$_2$, 120 mol % P(*n*-Bu)$_3$, 80 mol % DMAP and toluene-d_8 which had shown the signals for Ru−H species, and performed further ^{13}C- and ^{1}H NMR experiments (see Supporting Information).

The proton-decoupled ^{13}C NMR spectrum showed multiple signals below 200 ppm. A triplet detected at 214 ppm and a duplet of duplets of duplets at 216 ppm seemed to originate from Ru−alkyne intermediates, since no signals of an organic fragment should appear at chemical shifts higher than 200 ppm.

It is not straightforward to assign these signals. The coupling constants between 8 and 28 Hz seem to result from carbon−Ru−phosphorus couplings. However, Ru−vinylidene species should appear at chemical shifts higher than 300 ppm, Ru−vinyl species between 120 and 170 ppm, and Ru−alkyne π-complexes around 75 ppm.[44]

The corresponding ^{1}H NMR spectrum showed a duplet of triplets at around −7.4 ppm and a duplet of triplets of duplets at around −8.7 ppm. Before the addition of phenylacetylene-2-^{13}C (**5c**), the signal at −8.7 ppm appeared as a duplet of triplets with H−P couplings of 108 and 27 Hz, whereas after the addition of phenylacetylene-2-^{13}C (**5c**), the H−P couplings changed in part to 87 and 27 Hz and an additional coupling of 7 Hz appeared which must result from a proton-carbon coupling. The H−C coupling might originate from a π-coordination of phenylacetylene-2-^{13}C (**5c**) to species **52** (Scheme 9), the formation of a Ru−vinylidene−hydride such as **29** and **39**, or a Ru−hydride−enamide species such as **31** and **40**.

After heating the reaction mixture briefly to 100 °C, the spectra revealed that the reaction was already complete, as expected for this highly reactive alkyne.

We continued our in situ NMR studies with the investigation of the *Z*-selective hydroamidation of secondary amides (see Supporting Information). The first generation catalyst system for the *Z*-selective hydroamidation of secondary amides proved to be unsuitable for NMR investigations because of the high amount of water (8 equiv) required for this catalyst system,[25] causing massive solubility problems and preventing an effective shimming during the measurements. Therefore, we used a modified protocol of the second generation catalyst system.[30] The experiments were performed in DMF-d_7 instead of chlorobenzene and the paramagnetic Yb(OTf)$_3$ was substituted by diamagnetic Sc(OTf)$_3$. Because of the high catalyst loading (40 mol % (cod)Ru(met)$_2$, 45 mol % dcypb, 80 mol % Sc(OTf)$_3$, 2-pyrrolidinone (**1a**), DMF-d_7) only broad signals were detected in the ^{1}H NMR spectrum. After centrifugation of the suspension in the NMR tube and briefly heating to 100 °C, the ^{1}H NMR spectrum showed several signals between −15 and −25 ppm. These signals below 0 ppm confirm the formation of Ru−hydride species under *Z*-selective reaction conditions, indicating a similar reaction mode for this protocol. Unfortunately, no characteristic H−P couplings could be determined. The corresponding ^{31}P NMR spectrum showed several low intensity phosphorus signals between −20 and 70 ppm.

The results from these NMR studies strongly suggest that Ru−H−phosphine complexes are present in the reaction mixtures of hydroamidation reactions. The experiments also show how readily Ru−H species are formed when an amide is added to a Ru−phosphine catalyst, presumably via oxidative insertion into the N−H bond.[19,22,45] These observations, in combination with the findings of Caulton et al., who reported that Ru−H-complexes rapidly react with alkynes under formation first of Ru−vinyl and then of Ru−vinylidene complexes,[33] all point in the direction of *Mechanism D*. After all, *Mechanisms A* and *D* are the only ones that involve Ru−H species formed via an oxidative addition of N−H nucleophiles. In *Mechanisms E*, Ru−H species are not involved at all and can be ruled out. In *Mechanisms B* and *C*, Ru−H species are formed in the reaction of a Ru-precursor with an alkyne without participation of the amide. However, in the NMR experiments, the fact that Ru−H species were observed in the presence of amide but not in the presence of alkyne contributes to the evidence against *Mechanisms B* and *C*. Considering that the results of the labeling experiments and the kinetic studies are incompatible with

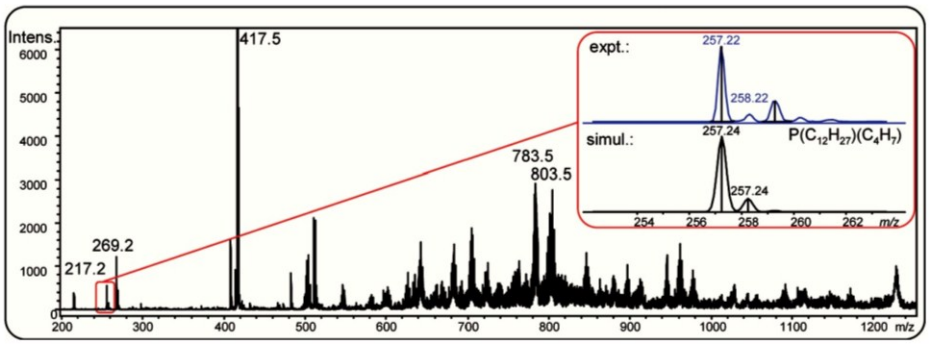

Figure 10. Assignment of $[(n\text{-Bu})_3\text{P}-\text{C}_4\text{H}_7]^+$ (m/z = 257.2) as the product of an allylic substitution reaction of methylallyl ligands with tri-*n*-butylphosphine.

Mechanisms A, B, and *E*, *Mechanism D* at this stage appears to be most likely.

■ IN SITU ESI–MS EXPERIMENTS

The electronspray ionization mass spectroscopy (ESI–MS) has evolved as a key technology in the investigation of reaction mechanism. In pioneering work, Chen et al., for example, used ESI–MS to identify key intermediates for the Ru-catalyzed olefin metathesis,[46] and Pfaltz et al. and di Lena et al. used ESI–MS technology to develop more efficient and more selective catalyst systems.[47] Intrigued by the predictive power of these investigations, we performed a series of in situ ESI–MS experiments with the goals of investigating the catalyst preformation step and identifying reaction intermediates that further support any of the proposed catalytic cycles.

There is ample literature evidence that the cod ligand is immediately replaced by more strongly coordinating phosphine and/or DMAP ligands, giving rise to a $L_nRu(met)_2$ species (L = phosphine, DMAP).[26,29] To differentiate between the proposed mechanisms, the decisive question to be addressed is whether the methylallyl ligands remain bound to Ru^{II} (consistent with *Mechanisms B* and *C*), become protonated and replaced by another ligand (consistent with *Mechanisms B, C* and *E*), or are cleaved via a reductive elimination step leading to Ru^0 species (consistent with *Mechanisms A* and *D*).

In this context, we investigated several combinations of $(\text{cod})\text{Ru}(\text{met})_2$, $\text{P}(n\text{-Bu})_3$ and DMAP by ESI–MS, both at room temperature and after briefly heating to 100 °C. The spectra obtained at room temperature from all possible solutions showed low overall intensities and no clear assignment to Ru-species was possible (see Supporting Information). This is not surprising, as the expected neutral Ru(II) complexes with strongly coordinating counterions would be hard to detect. However, after briefly heating the solutions to 100 °C, the overall intensities increased and clear signals for Ru^{II} species could be detected in all cases, except for the toluene solution of $(\text{cod})\text{Ru}(\text{met})_2$ alone.

The solution of $(\text{cod})\text{Ru}(\text{met})_2$ and DMAP showed three signals at m/z = 371.1, 625.2, and 716.3 which could only be matched with the calculated pattern for $[\text{Ru}(\text{met})(\text{DMAP})(\text{tol})]^+$ (met = C_4H_7^-, DMAP = $\text{C}_7\text{H}_{10}\text{N}_2$, tol = toluene, C_7H_8), $[\text{Ru}(\text{met})_2(\text{cod-H}_2)(\text{DMAP})(\text{tol})_2] + \text{H}^+$ (cod-H_2 = C_8H_{10}) and $[\text{Ru}(\text{met})_2(\text{cod-H}_2)(\text{DMAP})(\text{tol})_3]^+$, illustrating that DMAP indeed coordinates to the Ru center and is able to replace the cod ligand. The dehydrogenation of the cod ligand leading to cyclooctatriene (C_8H_{10}) or anionic cyclooctadienyl fragments ($\text{C}_8\text{H}_{10}^{2-}$) provides a simple explanation for the observed signal patterns. During the electrospray process, several toluene molecules seemed to condense to the detected cationic Ru-fragments. Such species are highly unstable and unlikely to exist in the reaction solution in significant abundances.

For the toluene solution of $\text{P}(n\text{-Bu})_3$ and $(\text{cod})\text{Ru}(\text{met})_2$, three signals of Ru species at m/z = 505.3, 761.5, and 779.5 were detected matching the calculated patterns of $[\text{Ru}(\text{cod})(\text{P}(n\text{-Bu})_3)(\text{tol})(\text{H})]^+$ ($\text{P}(n\text{-Bu})_3 = \text{PC}_{12}\text{H}_{27}$), $[\text{Ru}(\text{met})(\text{cod})(\text{P}(n\text{-Bu})_3)_2(\text{tol})]^+$ and $[\text{Ru}(\text{cod})(\text{P}(n\text{-Bu})_3)(\text{tol})_4)] + \text{H}^+$.

For the toluene solution of $(\text{cod})\text{Ru}(\text{met})_2$, $\text{P}(n\text{-Bu})_3$ and DMAP, two strong signals at m/z = 783.5 and 803.5 were detected, that matched the calculated patterns for $[\text{Ru}(\text{P}(n\text{-Bu})_3)_2(\text{tol})_3(\text{H})]^+$ and $[\text{Ru}(\text{P}(n\text{-Bu})_3)_3(\text{tol})(\text{H})_2] + \text{H}^+$.

Whenever $\text{P}(n\text{-Bu})_3$ was present the reaction solution, a series of three signals at m/z = 217.2, 257.2, and 417.5 was detected matching the calculated patterns of $[\text{OPC}_{12}\text{H}_{26}]^+$, $[(n\text{-Bu})_3\text{P}-\text{C}_4\text{H}_7]^+$ and $[\text{O}(\text{PC}_{12}\text{H}_{26})_2]^+$ fragments (Figure 10). The signals for $[\text{OPC}_{12}\text{H}_{26}]^+$ and $[\text{O}(\text{PC}_{12}\text{H}_{26})_2]^+$ fragments might have been caused by partial oxidation of $\text{P}(n\text{-Bu})_3$, but $[(n\text{-Bu})_3\text{P}-\text{C}_4\text{H}_7]^+$ fragment must be seen as evidence for a reduction process at the Ru center, in which a phosphine reacts with a methylallyl ligand with formation of a phosphonium salt that can be further deprotonated to the corresponding phosphorus ylide species ($(n\text{-Bu})_3\text{P}{=}\text{CH}(\text{C}_3\text{H}_5)$). This coupling is known to occur in the reaction of bis(2-methylallyl)palladium chloride dimer with phosphines giving rise to Pd^0–phosphine complexes such as $\text{Pd}(\text{P}(n\text{-Bu})_3)_4$.[48]

This suggests that during catalyst preformation, the nucleophilic $\text{P}(n\text{-Bu})_3$ attacks one of the methylallyl ligands with formation of a phosphonium salt. In this process, Ru^{II} is reduced to Ru^0 while the second methylallyl ligand is protonated, for example, by the acidic proton of the phosphonium salt, with formation of isobutene. The resulting phosphorus ylide species are known to decompose to the corresponding phosphine oxide and the alkene. Indeed, upon heating the reaction mixture to 100 °C, the intensity of the signal at m/z = 257.2 decreased and a signal at m/z = 217.2 was detected, which is characteristic for tri*n*-butylphosphine oxide ($(n\text{-Bu})_3\text{P}{=}\text{O}$). The formation of isobutene as well as $(n\text{-Bu})_3\text{P}{=}\text{O}$ in hydroamidation reactions was previously confirmed via GC- and NMR-spectroscopy.[29a]

We had previously dismissed mechanisms starting from Ru^0 intermediates (*Mechanisms A* and *D*), because we had never detected byproducts resulting from the reductive elimination of

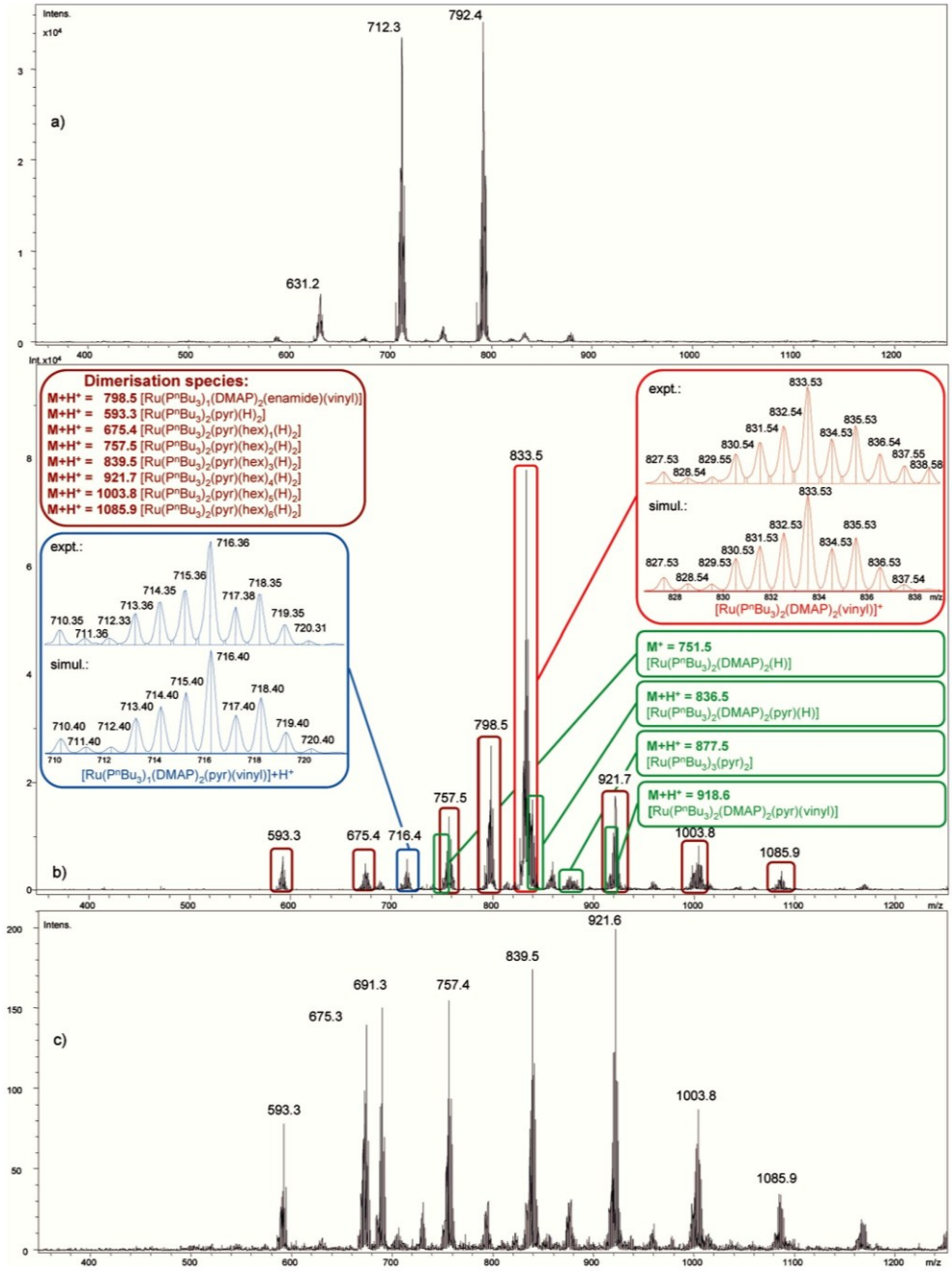

Figure 11. ESI−MS spectra for the *E*-selective hydroamidation of 2-pyrrolidinone (**1a**) and 1-hexyne (**5b**). (a) Heating to 100 °C for 5 min without 1-hexyne; (b) 40 min reaction time; (c) 150 min reaction time.

allyl fragments and had thus favored *Mechanism E*. However, this new experimental data gives at least indirect evidence for the formation of L_nRu^0 species, which unfortunately are particularly hard to detect by ESI−MS, because such species cannot be ionized by ligand dissociation.

We attempted to overcome this hurdle by using charged phosphine ligands. Unfortunately, the spectra obtained using [2-(dicyclohexylphosphino)ethyl] trimethylammonium chloride $[(C_6H_{11})_2P(C_2H_4)N(CH_3)_3Cl]$ instead of P(*n*-Bu)$_3$ were inconclusive. Only few signals of ruthenium intermediates were detected, and they resulted mostly from ruthenium chloride species. In fact, we observed a strong signal at $m/z = 225.2$, which could unambiguously be assigned to a $[(cy)_2P(C_2H_4)]^+$ fragment (cy = cyclohexyl = C_6H_{11}), indicating that the trimethylamine entity is cleaved under the reaction conditions. The exchange of chloride by other counterions, for example, hexafluorophosphate, did not have any beneficial effect on the complexity of the resulting spectra. We also tried to induce a ligand

dx.doi.org/10.1021/ja111389r |*J. Am. Chem. Soc.* 2011, 133, 7428–7449

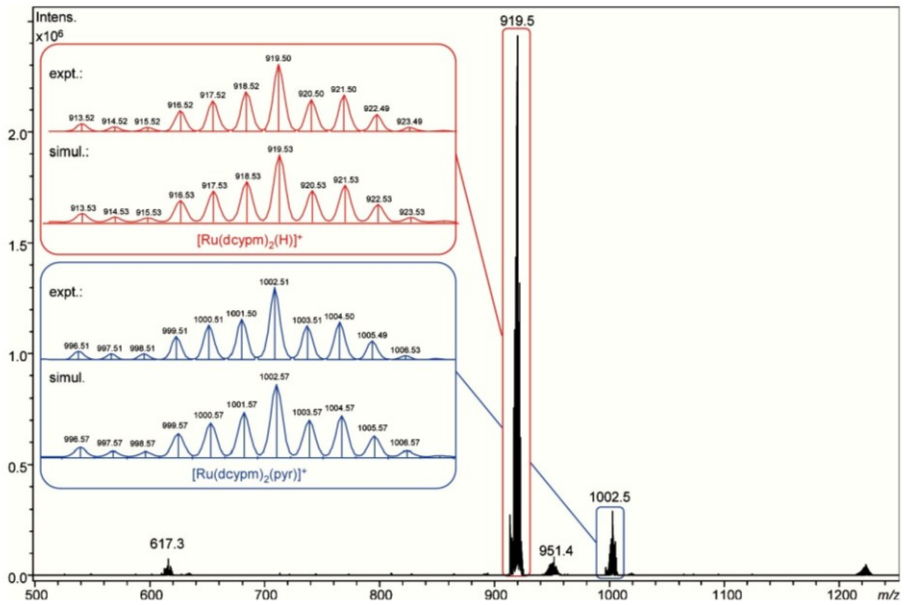

Figure 12. ESI−MS spectrum of a mixture of the catalyst and 2-pyrrolidinone (**1a**) under *Z*-selective hydroamidation conditions and after 5 min at 100 °C.

exchange of P(*n*-Bu)$_3$ by $[(C_6H_{11})_2P(C_2H_4)N(CH_3)_3]^+$ in a preformed catalyst solution (2 mol % (cod)Ru(met)$_2$, 6 mol % P(*n*-Bu)$_3$, 4 mol % DMAP) by adding the charged phosphine ligand afterward. Unfortunately, we could not observe any new Ru species in the corresponding ESI−MS spectra. The charged amonium phosphine ligand was simply not stable enough for in situ ESI−MS experiments. The syntheses of other non-amonium-based charged phosphine ligands, which are also suitable for hydroamidation reactions, are underway.

Next, we added 2-pyrrolidinone (**1a**) to the catalyst system consisting of 2 mol % of (cod)Ru(met)$_2$, 6 mol % of P(*n*-Bu)$_3$ and 4 mol % of DMAP at 100 °C. At this stage, signals at m/z = 712.3 and 792.4 appeared, which, based on their location and exact isotope pattern, could be assigned to $[Ru(P(n\text{-}Bu)_3)_2(DMAP)(pyr)]^+$ (pyr =2-pyrrolidinyl anion, $C_4H_6NO^-$) and $[Ru(P(n\text{-}Bu)_3)_3(pyr)]^+$ (Figure 11, Spectrum a).[26]

These species can result from the dissociation of a 2-pyrrolidinyl anion ($[M\text{-}(pyr)]^+$) of $[Ru(P(n\text{-}Bu)_3)_2(DMAP)(pyr)_2]$ and $[Ru(P(n\text{-}Bu)_3)_3(pyr)_2]$ (*Mechanisms B, C* and *E*) but also from $[Ru(P(n\text{-}Bu)_3)_2(DMAP)(pyr)(H)]$ and $[Ru(P(n\text{-}Bu)_3)_3(pyr)(H)]$ by protonation and H_2 release ($[M + H]^+\text{-}H_2$)[49] during the ionization process (*Mechanisms A* and *D*).

1-Hexyne (**5b**) was then injected to the mixture and further samples were taken after 5, 15, 30, 40, 150, and 470 min at 100 °C (Figure 11, Spectra b and c, and Supporting Information).

Already after 5 min, the signals at m/z = 712.3 and 792.4 disappeared. Strong signals appeared at m/z = 798.4 and 833.5 and weaker signals at m/z = 593.3, 675.4, 716.4, 757.5, 880.5, 921.7, 1003.8, and 1085.9.

The signals at m/z = 833.5 and 918.6 matched the calculated patterns for Ru−vinyl species $[Ru(P(n\text{-}Bu)_3)_2(DMAP)_2(vinyl)]^+$ (vinyl = $C_6H_{11}^-$) and $[Ru(P(n\text{-}Bu)_3)_2(DMAP)_2(pyr)(vinyl)] + H^+$ (Figure 11, Spectrum b). They are both likely to result from the ionization of the $[Ru(P(n\text{-}Bu)_3)_2(DMAP)_2(pyr)(vinyl)]$ complex. Further fragmentation of this species via ESI−MS−CID−MS (CID = collision-induced dissociation) was in agreement with the assignment and showed mainly the cleavage or the gradual decay of DMAP and P(*n*-Bu)$_3$ ligands. This intermediate is in agreement with all postulated mechanisms.

The signal at m/z = 716.4 matched the calculated pattern for $[Ru(P(n\text{-}Bu)_3)(DMAP)_2(pyr)(hex)(H)] + H^+$ (hex = C_6H_{10}) and the weak signal at m/z = 631.3 that of $[Ru(P(n\text{-}Bu)_3)(DMAP)_2(hex)(H)]^+$. Both species are likely to result from the ionization of a $[Ru(P(n\text{-}Bu)_3)(DMAP)_2(pyr)(hex)(H)]$ complex. This might result from a Ru−vinyl complex such as **28** or **38** with a suitable ligand sphere (m/z = 833.5), via vinyl/vinylidene rearrangement with concomitant dissociation of a P(*n*-Bu)$_3$ ligand (consistent with *Mechanisms C* and *D*). The weak signals at m/z = 751.5, 836.5, and 918.6 might be explained by $[Ru(P(n\text{-}Bu)_3)_2(DMAP)_2(H)]^+$, $[Ru(P(n\text{-}Bu)_3)_2(DMAP)_2(pyr)(H)] + H^+$ and $[Ru(P(n\text{-}Bu)_3)_2(DMAP)_2(enamide)(H)] + H^+$ fragments (enamide = $C_{10}H_{16}NO^-$) resulting from the ionization of $[Ru(P(n\text{-}Bu)_3)_2(DMAP)_2(pyr)(H)]$ (*Mechanisms A* and *D*) and $[Ru(P(n\text{-}Bu)_3)_2(DMAP)_2(enamide)(H)]$ (*Mechanisms A* to *E*).

The species at m/z = 798.4 matched the pattern calculated for $[Ru(P(n\text{-}Bu)_3)(DMAP)_2(enamide)(vinyl)] + H^+$ and might result from ionization of $[Ru(P(n\text{-}Bu)_3)(DMAP)_2(enamide)(vinyl)]$. The CID-fragmentation of this species showed the dissociation of a P(*n*-Bu)$_3$ ligand and of a fragment with the mass of the enamide product (**6a**). As it contains two 1-hexyne (**5b**) molecules, this species is likely to be an intermediate in the formation of double alkyne insertion enamide products, which are observed as minor side products in hydroamidations. Its intensity decreases sharply after the first minutes of the reaction, while all other signals discussed above increased and the signal at m/z = 833.5 remained at a high level.

After the hydroamidation reaction was complete (150 min) the intensity of the signals pertaining to hydroamidation intermediates decreased, and a set of signals that had been detected at

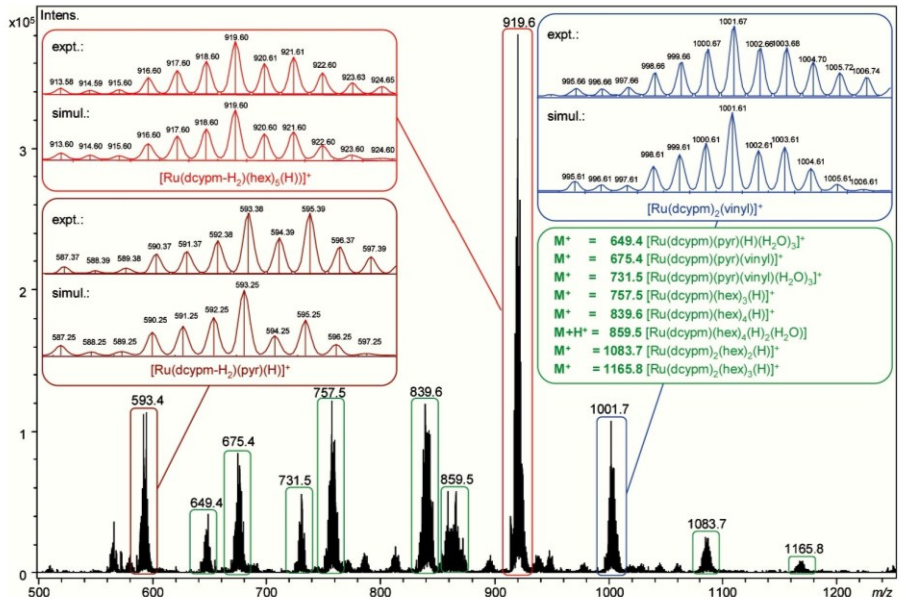

Figure 13. ESI−MS spectrum of a mixture of the catalyst, 2-pyrrolidinone (**1a**) and 1-hexyne (**5b**) under *Z*-selective hydroamidation conditions and after 5 min at 100 °C.

very low intensities earlier on, now became predominant. The signals at m/z = 593.4, 675.4, 757.4, 839.5, 921.6, 1003.7, and 1085.5 (Figure 11, Spectrum c) matched the calculated pattern for a series of Ru^{III} complexes with the chemical composition of $[Ru(P(n\text{-}Bu)_3)_2(pyr)(hex)_x(H)_2] + H^+$ bearing up to six 1-hexyne molecules (**5b**, x = 0−6). These species seem to be intermediates of alkyne oligomerization, which becomes the main reaction once most of the amide is consumed.

Next, we investigated the *Z*-selective hydroamidation of 2-pyrrolidinone (**1a**) and 1-hexyne (**5b**) in an analogous set of ESI−MS experiments.

A reaction mixture of the catalyst (2 mol % (cod)Ru(met)$_2$, 3 mol % dcypm, 8 equiv water) and 2-pyrrolidinone (**1a**) in toluene was heated to 100 °C for 5 min. The spectrum obtained at this stage showed two major signals at m/z = 919.5 and 1002.5, which, based on their location and exact isotope pattern, could be assigned to $[Ru(dcypm)_2(H)]^+$ (dcypm = bis-(dicyclohexylphosphino)methane, $P_2C_{25}H_{46}$) and $[Ru(dcypm)_2(pyr)]^+$ fragments (Figure 12).

Both cationic species seem to result from the same Ru-intermediate $[Ru(dcypm)_2(pyr)(H)]$. The formation of a Ru-intermediate such as **16** and **35** with a suitable ligand sphere can be explained best via oxidative addition of an amide to a neutral Ru^0-phosphine species (consistent with *Mechanisms A* and *D*). It is most likely that the cationic species are formed via dissociation of a 2-pyrrolidinyl anion ($[M\text{-}(pyr)]^+$) or protonation and H_2 release ($[M + H]^+\text{-}H_2$)[49] of $[Ru(dcypm)_2(pyr)(H)]$ during the ionization process. Further fragmentation of both species via ESI−MS−CID−MS (see Supporting Information) was in good agreement with this assignment and showed the same fragmentation species formed via gradual decay of dcypm and additionally via the cleavage of one 2-pyrrolidinyl anion from $[Ru(dcypm)_2(pyr)]^+$ in the case of the species at m/z = 1002.5.

We next injected 1-hexyne (**5b**) to the mixture and further samples were taken after 5, 25, 130, and 360 min at 100 °C (Figure 13 and Supporting Information).

After 5 min of heating in the presence of 1-hexyne (**5b**), the signals at m/z = 919.5 and 1002.5 disappeared and strong signals at m/z = 593.4, 757.5, 839.6, 919.6, and 1001.7 as well as weaker signals at m/z = 649.4, 675.4, 731.5, 859.5, 1083.7, and 1165.8 appeared. The masses often deviated by 2, 4, 6, or 8 mass units from expected molecular formulas. This can be explained with experiments by Leitner et al. who found that dcypb and bis-(dicyclohexylphosphino)propane (dcypp) ligands at Ru-centers easily dehydrogenate.[50] This thermal activation of sp^3 C−H bonds of bisphosphine Ru−bisallyl complexes leads to η^3-cyclooctenyl bridged Ru-complexes and extrusion of up to three protons from one cyclohexyl ring. We believe that similar dehydrogenation reactions took place under our hydroamidation reaction conditions. This would explain why signals that match $[M]^+ - 2, 4, 6,$ or 8 were detected.

The signal at m/z = 916.6 matched the calculated pattern of a $[Ru(dcypm\text{-}H_2)(hex)_5(H)]^+$ fragment (dcypm-H_2 = $Cy_2P(CH_2)P(Cy)(C_6H_9)$, formed via extrusion of H_2) and was confirmed to be nonidentical with the species at m/z = 915.5, observed in the absence of 1-hexyne (**5b**, Figure 12). The ESI−MS−CID−MS (see Supporting Information) of both signals were completely different. Whereas for the peak at m/z = 915.6, inter alia, the stepwise dissociation of four 1-hexyne (**5b**) molecules was observed, and for the peak at m/z = 915.5, stepwise decay of two phosphine ligands was observed. We believe that the species corresponding to the dominating signal at m/z = 915.6 is formed via dissociation of a 2-pyrrolidinyl anion ($[M\text{-}(pyr)]^+$) of $[Ru(dcypm\text{-}H_2)(hex)_5(pyr)(H)]$ or via protonation and H_2 release ($[M + H]^+\text{-}H_2$)[49] of $[Ru(dcypm)(hex)_5(H)_2]$, both presumably intermediates in alkyne oligomerization side reactions.

The smaller signal at m/z = 1001.7 could be assigned to a $[Ru(dcypm)_2(vinyl)]^+$ fragment likely to originate from a

Scheme 10. Catalytic Cycle for the *E*-Selective Hydroamidation of 1-Hexyne (5b) and 2-Pyrrolidinone (1a), L = ligand ($P(n\text{-}Bu)_3$ or DMAP)

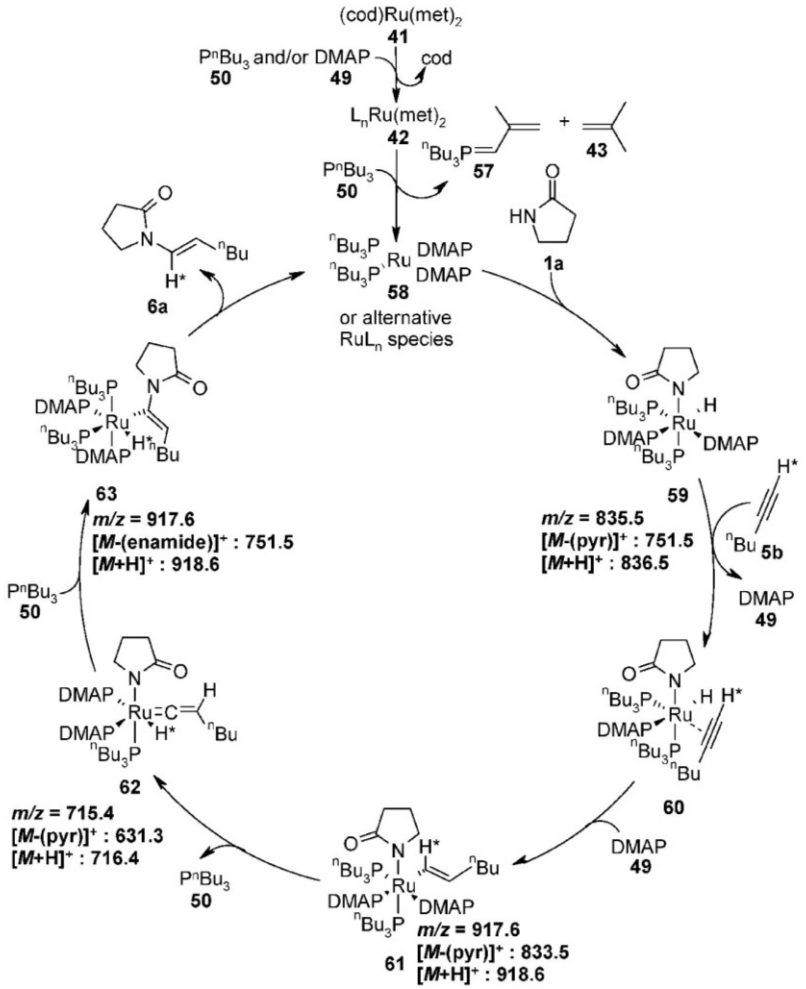

$[Ru(dcypm)_2(vinyl)(pyr)]$ species with the general formula **17**, **18** or **38**, formed by insertion of one 1-hexyne molecule (**5b**) into a Ru−H bond of **16** or **35** (consistent with *Mechanisms A* and *D*). The corresponding Ru−hydride−vinylidene species **39** would show the identical mass and isotope pattern. This is so, since both bidentate phosphine ligands would remain attached to the Ru center even if one of the Ru−P bonds is cleaved during the vinyl/vinylidene rearrangement step (consistent with *Mechanism D*).

Four Ru^{III} species could be assigned to the signals at m/z = 593.4, 649.4, 675.4, and 731.5 matching the calculated patterns of $[Ru(dcypm\text{-}H_2)(pyr)(H)]^+$, $[Ru(dcypm)(pyr)(H)(H_2O)_3]^+$, $[Ru(dcypm)(pyr)(vinyl)]^+$ and $[Ru(dcypm)(pyr)(vinyl)(H_2O)_3]^+$ fragments. These species occur with only low intensities. They are most likely formed by oxidation side reaction during the sample extraction and injection into the ESI−MS instrument. Nevertheless, these Ru^{III} complexes—bearing 2-pyrrolidinyl-, hydrido-, and/or 1-hexenyl ligands—suggest that an oxidative addition step of the amide and an insertion step of the alkyne into a Ru−H bond is involved in the catalytic cycle of the *Z*-selective hydroamidation (consistent with *Mechanisms A* and *D*).

The five signals at m/z = 757.5, 839.6, 859.5, 1083.7, and 1165.8 match the calculated patterns of $[Ru(dcypm)_x(hex)_y(H)]^+$ species bearing one or two dcypm ligands (x = 1 or 2) and up to four 1-hexyne molecules (**5b**, y = 1−4). These species are also likely formed via dissociation of a 2-pyrrolidinyl anion ($[M\text{-}(pyr)]^+$) of $[Ru(dcypm)_x(hex)_y(pyr)(H)]$ or via protonation and H_2 release ($[M+H]^+\text{-}H_2$)[49] of $[Ru(dcypm)_x(hex)_y(H)_2]$. They constitute intermediates of the alkyne oligomerization side reaction.

After 25 min of heating, the intensities of all Ru-species remained at a high level and two new Ru-species at m/z = 865.5 and 947.6 could be detected (see Supporting Information). These new signals matched the calculated pattern of $[Ru(dcypm)(hex)_3(OH)(tol)]^+$ and $[Ru(dcypm)(hex)_4(OH)(tol)]^+$ fragments and are most likely formed via protonation and H_2 release ($[M+H]^+\text{-}H_2$)[49] of $[Ru(dcypm)(hex)_3(H)(OH)(tol)]$.

The intensities of these two signals increased strongly in the spectra obtained after 130 and 360 min of heating, while the intensities of other signals decreased, indicating that the former correspond to oligomerization intermediates which predominate once most of the amide has been consumed.

CONCLUSIONS FROM THE EXPERIMENTAL STUDIES

Overall, most of the mechanisms under consideration were in disagreement with one or more experimental findings. *Mechanism A*, which involves an oxidative addition of the amide followed by an insertion of the alkyne into either the Ru−H or the Ru−N bond, correctly predicted the findings of the deuterium labeling experiments. It is also consistent with the detection of Ru−H species following addition of the amide to the Ru-catalyst and with most species detected by ESI−MS. However, it must be dismissed on the basis that a normal kinetic isotope effect was observed, while *Mechanism A* would have predicted an inverse secondary kinetic isotope effect caused by a change in hybridization of the alkyne-C(1) carbon atom bond from sp to sp^2.

Scheme 11. Selectivity-Determining Step of the Hydroamidation Reaction

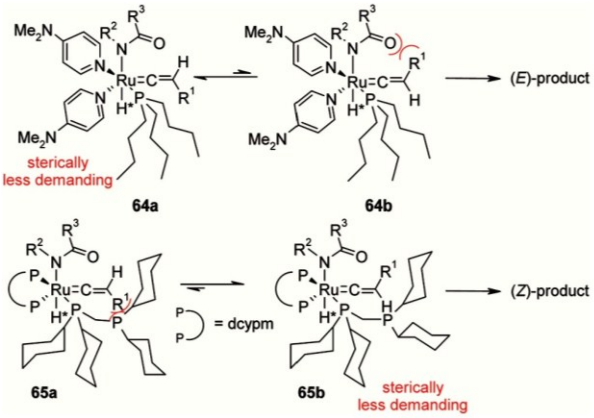

The same experimental findings also rule out the redox-neutral *Mechanism E*, which does not involve Ru−vinylidene intermediates, but instead proceeds via an attack of the amide nucleophile to a π-coordinated alkyne. This pathway is in good agreement with the isotope labeling and the ESI−MS studies, but offers no explanation for the observation of Ru−H-species after the addition of the amide to the catalyst system.

Mechanism B involves the formation of Ru−vinylidene species via 1,2-proton shift followed by an attack of the amide nucleophile. It must be excluded based on the results of the deuterium labeling studies, which unambiguously showed that in contrast to Ru-catalyzed additions of other nucleophiles, hydroamidations do not involve a shift of the terminal alkyne proton to the internal sp-carbon.

Mechanism C, which involves the formation of Ru−vinyl species and their rearrangement to Ru−hydride−vinylidene intermediates, is in agreement with most of the experimental findings. It correctly predicts the results of the deuterium labeling experiments and the observed normal kinetic isotope effect, and is in good agreement with most of the species observed in the ESI−MS studies. However, some of the cationic Ru^{IV} intermediates (**28**, **29** or **31**) should have been easily detectable by ESI−MS. One might also have expected the detection of Ru−H-species in the ^{1}H NMR in the presence of 1-hexyne (**5b**), rather than after the addition of 2-pyrrolidinone (**1a**) to the catalyst system. Moreover, it is unlikely that a protonation step with formation of cationic Ru−vinyl species is a favorable pathway in a nonpolar solvent under almost neutral conditions. The catalytic cycle involves only Ru-species in high oxidation states and offers no

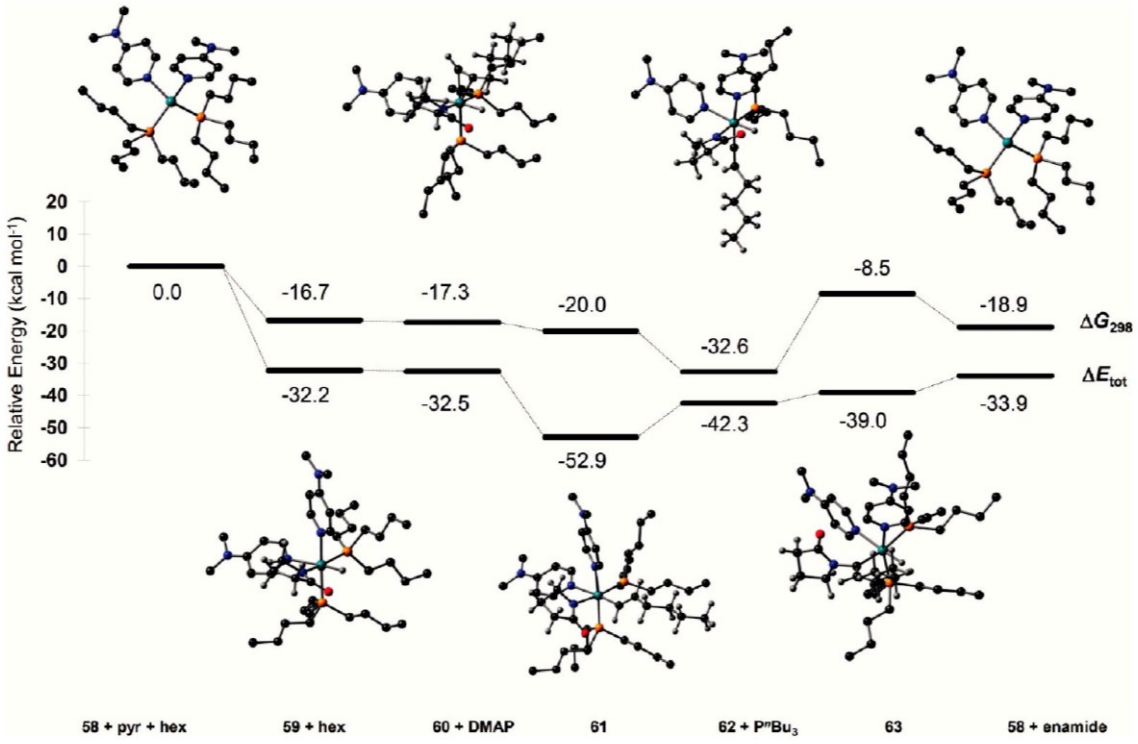

Figure 14. Relative energies and optimized structures of potential hydroamidation intermediates.

explanation for the detection of phosphonium salts known to arise from reductive deallylation processes.

Mechanism D is similar to *Mechanism C* in that it also involves Ru−vinyl intermediates that rearrange to Ru−hydride−vinylidene complexes. It is thus also in full agreement with the deuteration studies and correctly predicts the observed normal kinetic isotope effect. In contrast to *Mechanism C*, it starts from a Ru^0 species and thus offers a good explanation for the detection of phosphonium salts and of many Ru-species in the ESI−MS experiments. Moreover, the findings of the NMR studies are best explained by this mechanism, which starts with the oxidative addition of amides to the Ru-center with formation of Ru−H species. This would explain why after the addition of amides to the catalyst system, ^{1}H NMR signals below 0 ppm were detected, whereas these were not observed when only the alkyne was added to the catalyst.

For these combined reasons, the possible catalytic pathways can be narrowed down to a mechanism closely related to the proposed *Mechansim D*. On the basis of the experimental evidence, we believe that our model reaction, the *E*-selective hydroamidation of 1-hexyne (**5b**) with 2-pyrrolidinone (**1a**), proceeds via the mechanism depicted in Scheme 10.

The catalyst preformation proceeds via a reductive allylation process with release of a phosphorus ylide (**57**) and isobutene (**43**) and formation of a coordinatively unsaturated Ru^0 species bearing several neutral ligands. As the starting point for the depicted catalytic cycle we choose complex **58** with two phosphine and two DMAP ligands on the basis that intermediates with this combination of neutral ligands showed particularly strong signals in the in situ ESI−MS experiments. However, similar catalytic cycles with any combination of DMAP, phosphines, and solvent molecules would also be viable (MS signals at m/z = 751.5 $[M + H]^+$). Oxidative addition of the amide (**1a**) gives rise to an octahedral Ru−hydride complex **59**. This must be a slow step to be in accordance with the KIE of 2.3 found during the kinetic studies. The detection of signals at m/z = 751.5 and 836.5, which would match the $[M\text{-(pyr)}]^+$ and $[M + H]^+$ fragments of complex **59**, is in agreement with this pathway. In the next step, an alkyne (**5b**) coordinates to this species with dissociation of one neutral ligand (**60**). The alkyne then inserts into the Ru−H bond and the open coordination site created in the process is filled with a neutral ligand, leading to Ru^{II}-vinyl intermediate **61**. Signals at m/z = 833.5 and 918.6 can be explained by the presence of $[M\text{-(pyr)}]^+$ and $[M + H]^+$ fragments of species **61**. The high intensity of the signal at m/z = 833.5 along with the observed KIE when using deuterated alkynes, indicates that this step is comparatively slow. 1,2-Hydride shift in Ru^{II}−vinyl complex **61** then gives Ru^{IV}−H−vinylidene species **62**. Only weak ESI−MS signals could be assigned to **62** (m/z = 631.3 $[M\text{-(pyr)}]^+$ and 716.4 $[M + H]^+$). Because of the δ^+ polarization at C(1) of the vinylidene moiety, **62** is susceptible to attack of the amide ligand to afford species **63**. A neutral ligand is likely to coordinate and to refill the empty coordination site. The signals detected at m/z = 751.5 ($[M\text{-(enamide)}]^+$) and 918.6 ($[M + H]^+$) could be assigned to intermediate **63**. Finally, reductive elimination releases the enamide **6a**, regenerating the original catalytic species **58** and closing the catalytic cycle of the hydroamidation.

On the basis of the findings of the deuteration studies and the kinetic investigations, we assume that this pathway is also valid for related hydroamidations with other N−H nucleophiles. The studies presented above did not reveal any fundamental mechanistic differences between the *E*- and *Z*-selective protocols. On the basis of the NMR and ESI−MS studies with reaction mixtures of *Z*-selective hydroamidations, we believe that analogous species as those presented in Scheme 10 (**58**−**63**) are also present. The ligands are dcypm instead of P(*n*-Bu)$_3$ and DMAP before. However, in each step in which a vacant coordination site is required in the catalytic cycle (Scheme 10), one Ru−P bond of the bidentate ligand is cleaved, and therefore, the ligand remains coordinated to the Ru center leading to sterically more demanding Ru complexes. Hence, we conclude that the steric bulk of the ligand sphere is the decisive factor in directing the orientation of the substituent at the vinylidene moiety. As stretched in Scheme 11, the attack of the amide would then lead to enamides with different stereoselectivities depending on the preferred orientation of the vinylidene moiety relative to the amide. More in-depth studies are required to fully understand how the choice of ligands affects the stereoselectivity.

COMPUTATIONAL STUDIES

The Ru intermediates of the proposed catalytic cycle (Scheme 10, *Mechanism D*) have been identified based on ESI−MS and to some extent on NMR data. Since the information on the likely configuration of these intermediates is still limited, we used DFT calculations to look at the stability of each individual structure and possible spatial arrangements of the ligands. All calculations were performed using the Gaussian 03 or Gaussian 09 software package,[51] with B3LYP[52]/6-311+G(2d,p)[53]//B3LYP/6-31G-(d)[54] for H, C, N, O, P and Stuttgart RSC 1997 ECP[55] for Ru. A scaling factor for anharmonic corrections of vibrational frequencies of f = 0.9804 was used.[56]

A stable minimum was found for every postulated intermediate within the catalytic cycle. The calculated structures along with total energies and Gibbs free energies are depicted in Figure 14. The hydrogen atoms of the phosphine and DMAP ligands are omitted for clarity. Larger pictures of the optimized structures are included in the Supporting Information. The oxidative addition of 2-pyrrolidinone (**1a**) to the Ru species **58** with formation of the Ru−hydride complex **59** was calculated to be exothermic by Δ_rE_{tot} = −32.2 kcal mol^{-1} and exergonic by Δ_rG_{298} = −16.7 kcal mol^{-1}. The exchange reaction of DMAP by 1-hexyne (**5b**) to give a π-coordinated complex is almost thermoneutral (Δ_rE_{tot} = −0.3 kcal mol^{-1}, Δ_rG_{298} = −0.6 kcal mol^{-1}). The insertion of the alkyne in the Ru−H bond and refilling of the empty coordination site with one additional DMAP is exothermic and exergonic (Δ_rE_{tot} = −20.4 kcal mol^{-1}, Δ_rG_{298} = −2.7 kcal mol^{-1}). The following formation of vinylidene species **62** with the concomitant release of one phosphine ligand is endothermic (Δ_rE_{tot} = 10.6 kcal mol^{-1}) but exergonic (Δ_rG_{298} = −12.6 kcal mol^{-1}). The subsequent addition of the amide to the vinylidene moiety and the concomitant coordination of a neutral ligand is slightly endothermic (Δ_rE_{tot} = 3.3 kcal mol^{-1}) and highly endergonic (Δ_rG_{298} = 24.2 kcal mol^{-1}). The last reaction step, the reductive elimination of the enamide product requires only a small amount of total energy but releases a large amount of Gibbs free energy (Δ_rE_{tot} = 5.1 kcal mol^{-1}, Δ_rG_{298} = −10.4 kcal mol^{-1}). Overall, the computational studies support the conclusions drawn from the mechanistic studies. They confirm that the proposed catalytic cycle involves stable intermediates with comparable energies. Extensive computational studies using strongly simplified model systems are underway with the goal of calculating the transition states and obtaining reliably predicted kinetic isotope effects.

In summary, the results of our in-depth mechanistic studies of the hydroamidation support a catalytic cycle with ruthenium hydride and vinylidene species as the key intermediates. We thus propose that the reaction proceeds via an oxidative addition of the amide, followed by insertion of a π-coordinated alkyne into a ruthenium−hydride bond, rearrangement to a vinylidene species, nucleophilic attack of the amide, and finally reductive elimination of the product. This catalytic cycle is in agreement with all experimental results and is supported by DFT calculations that confirm the stability of all reaction intermediates.

■ ASSOCIATED CONTENT

Supporting Information. Experimental procedures and full spectroscopic data of the deuterium-labeling, the in situ IR, the in situ NMR, the in situ ESI−MS and the competition experiments. This material is available free of charge via the Internet at http://pubs.acs.org.

■ AUTHOR INFORMATION

Corresponding Author
goossen@chemie.uni-kl.de; gns@chemie.uni-kl.de

■ ACKNOWLEDGMENT

We thank the DFG and NanoKat and OPTIMAS for financial support, Umicore for donating chemicals, Mettler Toledo for giving us access to a ReactIR spectrometer, and the DAAD (K.S. M.S) and Landesgraduiertenförderung Rheinland-Pfalz (M.A. and A.F.) and Hans-Böckler-Stiftung (F.M.) for scholarships, and Dr. M. Blanchot for technical assistance. Part of this work was performed in preparation of the new transregional collaborative research center SFB/TRR 88 3MET.

■ REFERENCES

(1) Yet, L. *Chem. Rev.* **2003**, *103*, 4283–4306.

(2) Sugie, Y.; Dekker, K. A.; Hirai, H.; Ichiba, T.; Ishiguro, M.; Shiomi, Y.; Sugiura, A.; Brennan, L.; Duignan, J.; Huang, L. H.; Sutcliffe, J.; Kojima, Y. *J. Antibiot.* **2001**, *54*, 1060–1065.

(3) (a) McDonald, L. A.; Swersey, J. C.; Ireland, C. M.; Carroll, A. R.; Coll, J. C.; Bowden, B. F.; Fairchild, C. R.; Cornell, L. *Tetrahedron* **1995**, *51*, 5237–5244. (b) Boyd, M. R.; Farina, C.; Belfiore, P.; Gagliardi, S.; Kim, J. W.; Hahakawa, Y.; Beutler, J. A.; Mckee, T. C.; Bowman, B. J.; Bowman, E. J. *J. Pharmacol. Exp. Ther.* **2001**, *297*, 114–120.

(4) Davyt, D.; Entz, W.; Fernandez, R.; Mariezcurrena, R.; Mombrú, A. W.; Saldaña, J.; Domínguez, L.; Coll, J.; Manta, E. *J. Nat. Prod.* **1998**, *61*, 1560–1563.

(5) (a) Vidal, J.-P.; Escale, R.; Girard, J.-P.; Rossi, J.-C. *J. Org. Chem.* **1992**, *57*, 5857–5860. (b) Erickson, K. L.; Beutler, J. A.; Cardellina, J. H.; Boyd, M. R. *J. Org. Chem.* **1997**, *62*, 8188–8192. (c) Jansen, R.; Washausen, P.; Kunze, B.; Reichenbach, H.; Höfle, G. *Eur. J. Org. Chem.* **1999**, 1085–1089.

(6) Carbery, D. R. *Org. Biomol. Chem.* **2008**, *6*, 3455–3460.

(7) (a) Stevenson, P. J.; Graham, I. *ARKIVOC* **2003**, *7*, 139–144. (b) Gaulon, C.; Dhal, R.; Chapin, T.; Maisonneuve, V.; Dujardin, G. *J. Org. Chem.* **2004**, *69*, 4192–4202.

(8) Roff, G. J.; Lloyd, R. C.; Turner, N. J. *J. Am. Chem. Soc.* **2008**, *126*, 4098–4099.

(9) Willans, C. E.; Mulders, J. M. C. A.; de Vries, J. G.; de Vries, A. H. M. *J. Organomet. Chem.* **2003**, *687*, 494–497.

(10) Matsubara, R.; Nakamura, Y.; Kobayashi, S. *Angew. Chem.* **2004**, *116*, 1711–1713; *Angew. Chem. Int. Ed.* **2004**, *43*, 1679–1681.

(11) (a) van den Berg, M.; Minnaard, A. J.; Haak, R. M.; Leeman, M.; Schudde, E. P.; Meetsma, A.; Feringa, B. L.; de Vries, H. M.; Maljaars, E. P.; Wilians, C. E.; Hyett, D.; Boogers, A. F.; Hendricks, J. W.; de Vries, J. G. *Adv. Synth. Catal.* **2003**, *345*, 308–323. (b) Blaser, H.-U.; Malan, C.; Pugin, B.; Spindler, F.; Steiner, H.; Studer, M. *Adv. Synth. Catal.* **2003**, *345*, 103–151.

(12) (a) Dupau, P.; Le Gendre, P.; Bruneau, C.; Dixneuf, P. H. *Synlett* **1999**, 1832–1834. (b) Wang, X.; Porco, J. A., Jr. *J. Org. Chem.* **2001**, *66*, 8215–8221. (c) Bayer, A.; Maier, M. E. *Tetrahedron* **2004**, *60*, 6665–6677. (d) Adam, W.; Bosio, S. G.; Turro, N. J. *J. Org. Chem.* **2004**, *69*, 1704–1715. (e) Burk, M. J.; Casy, G.; Johnson, N. B. *J. Org. Chem.* **1998**, *63*, 6084–6098.

(13) (a) Brettle, R.; Mosedale, A. J. *J. Chem. Soc., Perkin Trans. 1* **1988**, 2185–2195. (b) Kuramochi, K.; Watanabe, H.; Kitahara, T. *Synlett* **2000**, 397–399. (c) Sato, M. *J. Org. Chem.* **1961**, *26*, 770–779.

(14) (a) Ager, D. J. *Synthesis* **1984**, 384–398. (b) Fürstner, A.; Brehm, C.; Cancho-Grande, Y. *Org. Lett.* **2001**, *3*, 3955–3957.

(15) Krompiec, S.; Pigulla, M.; Kuźnik, N.; Krompiec, M.; Marciniec, B.; Chadyniak, D.; Kasperczyk, J. *J. Mol. Catal. A: Chem.* **2005**, *225*, 91–101.

(16) (a) Wallace, D. J.; Klauber, D. J.; Chen, C.-Y.; Volante, R. P. *Org. Lett.* **2003**, *5*, 4749–4752; (b) Jiang, L.; Job, G. E.; Klapars, A.; Buchwald, S. L. *Org. Lett.* **2003**, *5*, 3667–3669; (c) Pan, X.; Cai, Q.; Ma, D. *Org. Lett.* **2004**, *6*, 1809–1812; (d) Brice, J. L.; Meerdink, J. E.; Stahl, S. S. *Org. Lett.* **2004**, *6*, 1845–1848; (e) Han, C.; Shen, R.; Su, S.; Porco, J. A., Jr. *Org. Lett.* **2004**, *6*, 27–30; (f) Tracey, M. R.; Hsung, R. P.; Antoline, J.; Kurtz, K. C. M.; Shen, L.; Slafer, B. W.; Zhang, Y. *Sci. Synth.* **2005**, *21*, 387–475; (g) Klapars, A.; Campos, K. R.; Chen, C.; Volante, R. P. *Org. Lett.* **2005**, *7*, 1185–1188; (h) Bolshan, Y.; Batey, R. A. *Angew. Chem.* **2008**, *120*, 2139–2142; *Angew. Chem. Int. Ed.* **2008**, *47*, 2109–2112.

(17) (a) Goossen, L. J.; Döhring, A. *Adv. Synth. Catal.* **2003**, *345*, 943–947. (b) Goossen, L. J.; Paetzold, J.; Winkel, L. *Synlett* **2002**, *10*, 1721–1723. (c) Goossen, L. J.; Ghosh, K. *Chem. Commun* **2001**, *20*, 2084–2085. (d) Goossen, L. J.; Goossen, K.; Rodríguez, N.; Blanchot, M.; Linder, C.; Zimmermann, B. *Pure Appl. Chem.* **2008**, *80*, 1725–1731.

(18) Heider, M.; Henkelmann, J.; Ruehl, T. EP 646571 **1995** [*Chem. Abstr.* **1995**, *123*, 229254].

(19) Kondo, T.; Tanaka, A.; Kotachi, S.; Watanabe, Y. *J. Chem. Soc. Chem. Commun* **1995**, 413–414.

(20) (a) Tokunaga, M.; Wakatsuki, Y. *Angew. Chem.* **1998**, *110*, 3024–3027; *Angew. Chem. Int. Ed.* **1998**, *37*, 2867–2869; (b) Tokunaga, M.; Suzuki, T.; Koga, N.; Fukushima, T.; Horiuchi, A.; Wakatsuki, Y. *J. Am. Chem. Soc.* **2001**, *123*, 11917–11924; (c) Grotjahn, D. B.; Incarvito, C. D.; Rheingold, A. L. *Angew. Chem.* **2001**, *113*, 4002–4005; *Angew. Chem. Int. Ed.* **2001**, *40*, 3884–3887; (d) Chevallier, F.; Breit, B. *Angew. Chem.* **2006**, *118*, 1629–1632; *Angew. Chem. Int. Ed.* **2006**, *45*, 1599–1602. (e) Labonne, A.; Kribber, T.; Hintermann, L. *Org. Lett.* **2006**, *8*, 5853–5856. (f) Hintermann, L.; Kribber, T.; Labonne, A.; Paciok, E. *Synlett* **2009**, 2412–2416.

(21) (a) Rotem, M.; Shvo, Y. *Organometallics* **1983**, *2*, 1689–1691. (b) Mitsudo, T.; Hori, Y.; Yamakawa, Y.; Watanabe, Y. *J. Org. Chem.* **1987**, *52*, 2230–2239. (c) Ruppin, C.; Dixneuf, P. H. *Tetrahedron Lett.* **1986**, *27*, 6323–6324. (d) Philippot, K.; Devanne, D.; Dixneuf, P. H. *J. Chem. Soc. Chem. Commun.* **1990**, 1199–1200. (e) Neveux, M.; Seiller, B.; Hagedorn, F.; Bruneau, C.; Dixneuf, P. H. *J. Organomet. Chem.* **1993**, *451*, 133–138. (f) Goossen, L. J.; Paetzold, J.; Koley, D. *Chem. Commun.* **2003**, 706–707.

(22) (a) Uchimaru, Y. *Chem. Commun* **1999**, 1133–1134; (b) Tokunaga, M.; Eckert, M.; Wakatsuki, Y. *Angew. Chem.* **1999**, *111*, 3416–3419; *Angew. Chem. Int. Ed.* **1999**, *38*, 3222–3225. (c) Kondo, T.; Okada, T.; Suzuki, T.; Mitsudo, T.-a. *J. Organomet. Chem.* **2001**, *622*, 149–154. (d) Fukumoto, Y.; Dohi, T.; Masaoka, H.; Chatani, N.; Murai, S. *Organometallics* **2002**, *21*, 3845–3847. (e) Shimada, T.; Yamamoto, Y. *J. Am. Chem. Soc.* **2003**, *125*, 6646–6647. (f) Yi, C. S.; Yun, S. Y.; Guzei, I. A. *J. Am. Chem. Soc.* **2005**, *127*, 5782–5783. (g) Li, Y.; Marks, T. J. *Organometallics* **1996**, *15*, 3770–3772. (h) Li, Y.; Marks, T. J. *J. Am. Chem. Soc.* **1998**, *120*, 1757–1771.

(23) Koelle, U.; Rietmann, C.; Tjoe, J.; Wagner, T.; Englert, U. *Organometallics* **1995**, *14*, 703–704.
(24) (a) Gemel, C.; Trimmel, G.; Slugovc, C.; Kremel, S.; Mereiter, K.; Schmid, R.; Kirchner, K. *Organometallics* **1996**, *15*, 3998–4004. (b) Varela-Fernández, A.; González-Rodríguez, C.; Varela, J. A.; Castedo, L.; Saá, C. *Org. Lett.* **2009**, *11*, 5350–5353. (c) Liu, P. N.; Su, F. H.; Wen, T. B.; Sung, H. H.-Y. *Chem.—Eur. J.* **2010**, *16*, 7889–7897.
(25) Goossen, L. J.; Rauhaus, J. E.; Deng, G. *Angew. Chem.* **2005**, *117*, 4110–4113; *Angew. Chem. Int. Ed.* **2005**, *44*, 4042–4045.
(26) Goossen, L. J.; Arndt, M.; Blanchot, M.; Rudolphi, F.; Menges, F.; Niedner-Schatteburg, G. *Adv. Synth. Catal.* **2008**, *350*, 2701–2707.
(27) Goossen, L. J.; Blanchot, M.; Salih, K. S. M.; Karch, R.; Rivas-Nass, A. *Org. Lett.* **2008**, *10*, 4497–4499.
(28) Goossen, L. J.; Blanchot, M.; Brinkmann, C.; Goossen, K.; Karch, R.; Rivas-Nass, A. *J. Org. Chem.* **2006**, *71*, 9506–9509.
(29) (a) Goossen, L. J.; Salih, K. S. M.; Blanchot, M. *Angew. Chem.* **2008**, *120*, 8620–8623; *Angew. Chem. Int. Ed.* **2008**, *47*, 8492–8495. (b) Goossen, L. J.; Blanchot, M.; Salih, K. S. M.; Goossen, K. *Synthesis* **2009**, 2283–2282.
(30) Buba, A. E.; Arndt, M.; Goossen, L. J. *J. Organomet. Chem.* **2010**, *696*, 170–178.
(31) Goossen, L. J.; Blanchot, M.; Arndt, M.; Salih, K. S. M. *Synlett* **2010**, 1685–1687.
(32) (a) Bruneau, C.; Dixneuf, P. H. *Angew. Chem.* **2006**, *118*, 2232–2260; *Angew. Chem. Int. Ed.* **2006**, *45*, 2176–2203. (b) Rigaut, S.; Touchard, D.; Dixneuf, P. H. *Coord. Chem. Rev.* **2004**, *248*, 1585–1601.
(33) Oliván, M.; Clot, E.; Eisenstein, O.; Caulton, K. G. *Organometallics* **1998**, *17*, 3091–3100.
(34) DFT calculations confirmed that the reaction of 2-pyrrolidinone (**1a**) and deprotonated *N*-((*E*)-hex-1-enyl)pyrrolidin-2-one, leading to the 2-pyrrolidinyl anion and the corresponding enamide (**6a**), is both exotherm ($\Delta_r E_{tot} = -30.88$ kcal mol^{-1}) and exergonic ($\Delta_r G_{298} = -30.02$ kcal mol^{-1}).
(35) Although there is no experimental proof in literature that the rehybridisation from sp to sp^2 causes an inverse isotope effect, it must be expected based on the analogy to sp^2/sp^3 rehybridizations. See for example: Carey, F. A.; Sundberg, R. J. *Advanced Organic Chemistry*, Third edition; Plenum Press: New York, London, 1990; pp 216−218. The same assumption was made, e.g., in: Ipaktschi, J.; Mohsseni-Ala, J.; Uhlig, S. *Eur. J. Inorg. Chem.* **2003**, 4313−4320.
(36) Maegawa, T.; Fujiwara, Y.; Inagaki, Y.; Monguchi, Y.; Sajiki, H. *Adv. Synth. Catal.* **2008**, *350*, 2215–2218.
(37) Rigaut, S.; Perruchon, J.; Guesmi, S.; Fave, C.; Touchard, D.; Dixneuf, P. H. *Eur. J. Inorg. Chem.* **2005**, 447–460.
(38) Ryabov, A. D. *Chem. Rev.* **1990**, *90*, 403–424.
(39) Ciardi, C.; Reginato, G.; Gonsalvi, L.; de los Rios, I.; Romerosa, A.; Peruzzini, M. *Organometallics* **2004**, *23*, 2020–2026.
(40) Choe, J.-I.; Choi, H.-S.; Kuczkowski, R. L. *Magn. Reson. Chem.* **1986**, *24*, 1044–1047.
(41) Touchard, D.; Haquette, P.; Pirio, N.; Toupet, L.; Dixneuf, P. H. *Organometallics* **1993**, *12*, 3132–3139.
(42) (a) Bruneau, C.; Dixneuf, P. H. *Acc. Chem. Res.* **1999**, *32*, 311–323. (b) Vijayaraj, T. A.; Sundararajan, G. *J. Mol. Catal. A* **1995**, *99*, 47–54.
(43) Caballero, A.; Jalón, F. A.; Manzano, B. R. *Chem. Commun* **1998**, 1879–1880.
(44) (a) Guerchais, V.; Lapinte, C.; Thepot, J. Y.; Toupet, L. *Organometallics* **1988**, *7*, 604–612. (b) Maurer, J.; Linseis, M.; Sarkar, B.; Schwederski, B.; Niemeyer, M.; Kaim, W.; Zli, S.; Anson, C.; Zabel, M.; Winter, R. F. *J. Am. Chem. Soc.* **2008**, *130*, 259–268. (c) Jung, S.; Ilg, K.; Brandt, C. D.; Wolf, J.; Werner, H. *Eur. J. Inorg. Chem.* **2004**, 469–480. (d) Bassetti, M.; Cadierno, V.; Gimeno, J.; Pasquini, C. *Organometallics* **2008**, *27*, 5009–5016.
(45) Cabeza, J. A.; Riera, V. *J. Organomet. Chem.* **1989**, *376*, C23–C25.
(46) (a) Hinderling, C.; Adlhart, C.; Chen, P. *Angew. Chem.* **1998**, *110*, 2831–2835; *Angew. Chem. Int. Ed.* **1998**, *37*, 2685–2689. (b) Adlhart, C.; Hinderling, C.; Baumann, H.; Chen, P. *J. Am. Chem. Soc.* **2000**, *122*, 8204–8214. (c) Frech, C. M.; Blacque, O.; Schmalle, H. W.; Berke, H.; Adlhart, C.; Chen, P. *Chem.—Eur. J.* **2006**, *12*, 3325–3338.
(47) (a) Markert, C.; Pfaltz, A. *Angew. Chem.* **2004**, *116*, 2551–2554; *Angew. Chem. Int. Ed.* **2004**, *43*, 2498–2500; (b) Markert, C.; Neuburger, M.; Kulicke, K.; Meuwly, M.; Pfaltz, A. *Angew. Chem.* **2007**, *119*, 5996–5999; *Angew. Chem. Int. Ed.* **2007**, *46*, 5892–5895; (c) Markert, C.; Rosel, P.; Pfaltz, A. *J. Am. Chem. Soc.* **2008**, *130*, 3234–3235; (d) Teichert, A.; Pfaltz, A. *Angew. Chem.* **2008**, *120*, 3408–3410; *Angew. Chem. Int. Ed.* **2008**, *47*, 3360–3362. (e) di Lena, F.; Matyjaszewski, K. *Chem. Commun.* **2008**, 6306–6308. (f) di Lena, F.; Matyjaszewski, K. *Dalton Trans.* **2009**, 8884–8890.
(48) Kuran, W.; Musco, A. *Inorg. Chim. Act.* **1975**, *12*, 187–193.
(49) Reinhardt, B. M.; Niedner-Schatteburg, G. *J. Phys. Chem. A* **2002**, *106*, 7988–7992.
(50) Six, C.; Gabor, B.; Görls, H.; Mynott, R.; Philipps, P.; Leitner, W. *Organometallics* **1999**, *18*, 3316–3326.
(51) (a) Gaussian 03, Revision E.01, Gaussian, Inc.: Wallingford CT, 2004. (b) Gaussian 09, Revision A.02, Gaussian, Inc.: Wallingford CT, 2009; for full citations see the Supporting Information.
(52) (a) Lee, C.; Yang, W.; Parr, R. G. *Phys. Rev. B* **1988**, *37*, 785–789. (b) Becke, A. D. *J. Chem. Phys.* **1993**, *98*, 5648–5652. (c) Stephens, P. J.; Devlin, J. F.; Chabalowski, C. F.; Frisch, M. J. *J. Phys. Chem.* **1994**, *98*, 11623–11627.
(53) Krishnan, R.; Binkley, J. S.; Seeger, R.; Pople, J. A. *J. Chem. Phys.* **1980**, *72*, 650–654.
(54) Hariharan, P. C.; Pople, J. A. *Theor. Chim. Acta* **1973**, *28*, 213–222.
(55) Andrae, D.; Häussermann, U.; Dolg, M.; Stoll, H.; Preuss, H. *Theor. Chim. Acta* **1990**, *77*, 123–141.
(56) Wong, M. W. *Chem. Phys. Lett.* **1996**, *256*, 391–399.

IV.1.2. Entwicklung einer Ru/Yb-katalysierten Z-selektiven Methode zur Addition sekundärer Amide und Imide an terminale Alkine

Der rationale Ansatz, auf besserem mechanistischem Verständnis aufbauend die Entwicklung effizienterer und kostengünstigerer Katalysatorsysteme zu stützen, zahlte sich wiederholt aus. Es wurde bereits in einer frühen Phase unserer mechanistischen Studien erkannt, dass die zuvor verwendete, teuere (cod)Ru(met)$_2$-Katalysatorvorstufe für einige Substratklassen gegen einfachere Rutheniumquellen ausgetauscht werden kann, da während der Katalysatorpräformierung sowohl die Cyclookta-1,5-dien- als auch die Methylallyl-Liganden ausgetauscht werden.[37] Auf dieser Grundlage gelang es, eine Rutheniumtrichlorid-Hydrat-basierte Methode zur Hydroamidierung sekundärer Amide zu entwickeln, bei der die katalytisch aktive Spezies alternativ durch eine Phosphin-vermittelte *in situ* Reduktion des Ruthenium(III)salzes generiert und auf diese Weise eine vergleichbare und für einige Substrate sogar erhöhte Aktivität erzielt werden kann.

Einen weiteren Ansatzpunkt zur rationalen Entwicklung effizienterer Katalysatorsysteme konnte direkt aus dem neuen Reaktionsmechanismus abgeleitet werden (Kap. IV.1.1). Es konnten zwei langsame Elementarschritte identifiziert werden, sowohl die oxidative Addition des Amids als auch die Bildung der Ruthenium-Vinyliden-Spezies. Beide Reaktionsschritte sollten durch eine Erhöhung der Elektronendichte am Ruthenium begünstigt werden können. Zusätzlich konnte nachgewiesen werden, dass die Ligandensphäre der involvierten Ruthenium-Vinyliden-Spezies den stereochemischen Verlauf der Hydroamidierung beeinflusst. Der Einsatz sterisch einfacher Phosphinliganden führt bevorzugt zur Bildung des *E*-Produkts, wohingegen sterisch anspruchsvollere Liganden zur Bildung des *Z*-Produkts führen.

In früheren Arbeiten des AK Gooßen erwies sich die *Z*-selektive Addition sekundärer Amide an terminale Alkine als besonders herausfordernd, da lediglich zwei Substrate mit einer (*E*/*Z*)-Selektivität von 1 zu 5 bzw. 1 zu 8 umgesetzt werden konnten.[38] Daher sollte im Folgenden erforscht werden, ob mit Hilfe sterisch anspruchsvoller, elektronenreicher Chelatphosphine sowohl die Katalysatoraktivität als auch die Selektivität zugunsten des Z-Isomers erhöht werden kann. Ferner sollte untersucht werden, ob die N-H-Bindung des Amids durch Zugabe von Lewis-Säuren geschwächt und somit die oxidative Addition des Amids zusätzlich begünstigt werden kann.

In der nachfolgenden Veröffentlichung wird die Entwicklung eines bimetallischen Ruthenium/Ytterbium basierten Katalysatorsytems für die *Z*-selektive Hydroamidierung

sekundärer Amide und Imide inklusiver aller experimentellen Daten beschrieben. Die bimetallische Hydroamidierungsmethode zeigt deutlich höhere Ausbeuten, eine höhere Selektivität für das gewünschte *Z*-Isomer und eine viel größere Anwendungsbreite als frühere Katalysatorsyteme.

Diplom-Chemikerin Annette E. Buba trat diesem Projekt im Rahmen ihrer Diplomarbeit bei, als die Optimierungsarbeiten des Katalysatorsystems bereits weit fortgeschritten waren. Die finalen Katalysatoroptimierungen und die Bestimmung der Anwendungsbreite wurden gemeinsam durchgeführt und veröffentlicht. Dabei wurde Frau Buba von mir als Betreuer der Diplomarbeit unterstützt.

Journal of Organometallic Chemistry 696 (2011) 170–178

Contents lists available at ScienceDirect

Journal of Organometallic Chemistry

journal homepage: www.elsevier.com/locate/jorganchem

Z-Selective hydroamidation of terminal alkynes with secondary amides and imides catalyzed by a Ru/Yb-system

Annette E. Buba, Matthias Arndt, Lukas J. Gooßen*

Fachbereich Chemie, Technische Universität Kaiserslautern, Erwin-Schrödinger-Straße, Building 54, D-67663 Kaiserslautern, Germany

ARTICLE INFO

Article history:
Received 21 July 2010
Received in revised form
12 August 2010
Accepted 24 August 2010

Keywords:
Addition reaction
Bimetallic catalysis
Z-Enamide
Hydroamidation
Lewis acid
Ruthenium

ABSTRACT

A catalyst system formed *in situ* from bis(2-methallyl)cycloocta-1,5-diene-ruthenium(II) [(cod)Ru(met)$_2$], 1,4-bis(dicyclohexylphosphino)butane (dcypb) and ytterbium(III) triflate hydrate (Yb(OTf)$_3$) was found to catalyze the addition of nitrogen nucleophiles to terminal alkynes under mild conditions to stereoselectively form the *Z*-enamide or *Z*-enimide products. Various secondary amides and imides could be added across the triple bond of a range of aliphatic and aromatic alkynes. The new bimetallic catalyst system sets new standards with regard to scope and selectivity for the synthesis of *Z*-configured *anti*-Markovnikov enamides.

1. Introduction

The enamide substructure is abundant in natural products [1] and synthetic drugs with sedative [2], cytotoxic [3], or anti-inflammatory [4] properties. Examples for biologically active enamides with *Z*-configuration are lansiumamides A and B [5], cyclopeptide alkaloids like mucronines or abyssenines [6], aspergillamide A [3], igzamide [7], as well as botryllamide [8,9]. Fig. 1

Enamides are versatile synthetic intermediates that can serve as substrates for heterocycle syntheses [10,11], cross-coupling reactions [12], Heck olefinations [13], enantioselective additions [14], or asymmetric hydrogenations [15]. Established enamide syntheses, such as the condensation of carbonyl derivatives with amides [16], require harsh conditions and yield mixtures of *E*- and *Z*-enamides. Alternative syntheses of enamides are often based on sensitive precursors, e.g. alkoxyallenes [17].

The selective synthesis of the thermodynamically disfavored *Z*-enamide is much harder and has less literature precedent. Preparations *via* Curtius rearrangement [18], Peterson elimination [5c,19], or cross-coupling reactions [20] transfer the selectivity problem to the availability of the starting materials.

In the context of our research on the use of carboxylic acid derivatives as substrates in catalysis [21], and based on related work on the addition of nucleophiles to multiple bonds [22], we developed Ru-catalysts that allow the atom-economic addition of N–H-bonds to terminal alkynes under mild conditions (Scheme 1).

The scope of the initial protocol, in which ruthenium phosphines complexes in combination with auxiliary bases were employed as catalysts, included secondary amides, ureas, lactams, and oxazolidinones [23,24]. The stereoselectivity of the addition reaction was determined by the choice of ligands and bases. In the presence of monodentate ligands and strongly coordinating bases such as 4-dimethylaminopyridine, *E*-products were obtained in high selectivity. The stereoselectivity could be reversed using chelating ligands and small amounts of water instead of the base. However, the scope and the *Z*-selectivity of this second protocol were only moderate. Improved catalyst systems allowed the extension of this reaction concept to imides [25], thioamides [26], and finally primary amides [27].

In this last protocol, the auxiliary bases were replaced by Lewis acid co-catalysts. As a result, the N–H acidity rather than the nucleophilicity of the N–H component determined the reaction outcome. This way, primary amides could chemoselectively be coupled in the presence of secondary amides to give the *Z*-configured enamides in up to 22:1 stereoselectivity. These experiments seemed to suggest that secondary amides are very slow to react

* Corresponding author. Tel.: +49 631 205 2046; fax: +49 631 205 3921.
E-mail address: goossen@chemie.uni-kl.de (L.J. Gooßen).

0022-328X/$ – see front matter © 2010 Elsevier B.V. All rights reserved.
doi:10.1016/j.jorganchem.2010.08.034

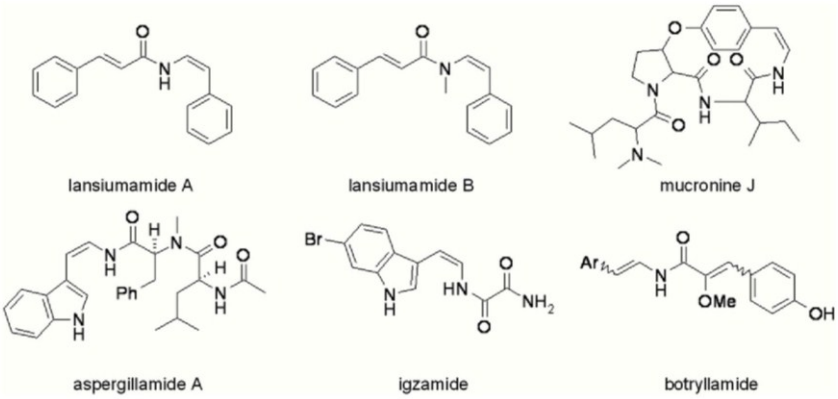

Fig. 1. *Z*-Enamide structure in bioactive molecules.

with such bimetallic catalyst systems. However, we now found that under modified reaction conditions, Yb/Ru-catalysts can also promote the addition of secondary amides and imides to terminal alkynes in high yields and excellent selectivities for the *Z*-configured *anti*-Markovnikov products.

2. Results and discussion

In our search for an effective catalyst for the desired hydroamidation of secondary amides, we chose the reaction of pyrrolidin-2-one (**1a**) with hex-1-yne (**2a**) as a model system to investigate several catalyst systems under various conditions (Table 1). Initially, a combination of (cod)Ru(met)$_2$, dcypb, and Yb(OTf)$_3$ in DMF and 6 equiv of water was employed, which has been the most effective system for the hydroamidation of primary amides (entry 1). Here, the model substrates were converted in 66% yield and a stereoselectivity of 3:1 in favor of the thermodynamically unfavored *Z*-enamide **3aa**. Lowering the catalyst loading to 2 mol% (cod)Ru(met)$_2$ and 3 mol% dcypb led to higher yields with a marginal upgrade of the selectivity, due to less isomerization and polymerization side reactions also catalyzed by ruthenium (entry 2). Without water as the co-solvent, decreased selectivities were obtained (entry 3). A further reduction to 1 mol % of Ru-source and 1.5 mol% phosphine resulted in lower yields and did not enhance the selectivity in favor of the *Z*-enamide (entry 4). Variation of the solvent revealed that nonpolar aromatic solvents such as toluene or chlorobenzene were most effective concerning the selectivity. Moreover, chlorobenzene led to an improved ratio of 9:1 in favor of the *Z*-product (entries 5–10). Although DMF gave a higher total yield, we subsequently focused on chlorobenzene due to the higher selectivity of the catalyst system obtained in this solvent. A smaller amount of 2.25 mol% of dcypb showed further improvement. Under these conditions, 72% yield could be obtained with a satisfactory *Z*/*E*-selectivity of 9:1 (entry 12). Among the ligands investigated, dcypb gave the highest *Z*-selectivity. Bidentate ligands with smaller bite angles or aromatic groups, as well as monodentate phosphines, were less effective (entries 14–18). Without added ligand, no conversion was observed (entry 13). Variation of the Lewis acidic co-catalyst did not improve the yield or the stereoselectivity, and Yb(OTf)$_3$ remained the most effective additive (entries 19–21). A shorter reaction time of 6 h resulted in lower yields (entry 22), and 60 °C reaction temperature was confirmed to be optimal. Decreasing as well as increasing the temperature led to worse yields and selectivities (entries 23–25). Heating a mixture of enamide isomers in the presence of the ruthenium catalyst did not influence the isomeric ratio, indicating that an interconversion between the product isomers, e.g., via reversible amide addition does not take place [28].

After optimizing the catalyst system, we tested the generality of the new *Z*-selective hydroamidation protocol (Table 2). Several reactions had to be carried out in DMF because of an insufficient solubility of some amides in chlorobenzene. We were pleased to find that besides lactams (**1a**–**c**), several carbamates (**1d**–**e**) and linear amides (**1g**–**k**) selectively reacted with hex-1-yne (**2a**) in moderate to high yields to the desired *Z*-enamides. Even chiral auxiliaries can be used as coupling partners (**1e**). Limitations were observed for linear amides with aliphatic substituents on the nitrogen, possibly based on stereoelectronic effects (**1g**, **1i**). Various alkynes were successfully converted into *Z*-enamides, among them are the aliphatic derivatives hept-1-yne (**2b**), oct-1-yne (**2c**), and 3-cyclohexyl-prop-1-yne (**2d**). Alkynes with chloride (**2g**) or aromatic substituents (**2h**–**l**) were tolerated, yielding the *Z*-enamides in good to excellent *Z*/*E*-selectivities. With (trimethylsilyl)acetylene (**2e**) or propargyl chloride (**2f**), none of the desired product could be obtained. Instead, side products, e.g. from oligomerization reactions, were observed.

We also tested this catalyst system in the addition of imides to terminal alkynes and were pleased to find that imides including succinimide, 1,5,5-trimethylhydantoin and phthalimide (**1l**–**n**) could be converted to *Z*-enimides with the same catalyst system in excellent yields and selectivities greater than 20:1. Besides hex-1-yne (**2a**), various aliphatic alkynes reacted with succinimide yielding selectively the corresponding *Z*-enimides.

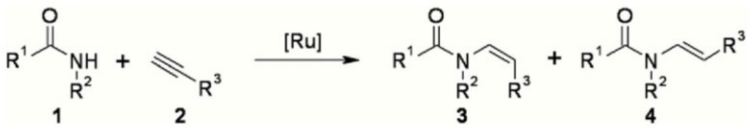

Scheme 1. Ruthenium-catalyzed hydroamidation of terminal alkynes.

Table 1
Optimization of the catalyst and conditions.[a]

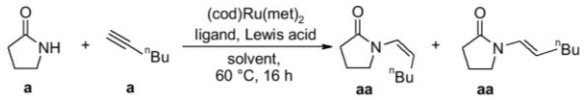

Entry	(cod)Ru(met)$_2$ [mol%]	Ligand [mol%]	Lewis acid [mol%]	Solvent	Yield [%] (ratio (3aa:4aa))
1	5	6 dcypb	4 Yb(OTf)$_3$	DMF/6 equiv H_2O	66 (3:1)
2	2	3	4 Yb(OTf)$_3$	DMF/6 equiv H_2O	86 (4:1)
3	2	3	4 Yb(OTf)$_3$	DMF	86 (3:1)
4	1	1.5	4 Yb(OTf)$_3$	DMF	81 (3:1)
5	2	3	4 Yb(OTf)$_3$	Toluene	70 (7:1)
6	2	3	4 Yb(OTf)$_3$	Chlorbenzene	70 (9:1)
7	2	3	4 Yb(OTf)$_3$	THF	53 (7:1)
8	2	3	4 Yb(OTf)$_3$	Quinoline	52 (2:1)
9	2	3	4 Yb(OTf)$_3$	Acetonitrile	0
10	2	3	4 Yb(OTf)$_3$	Water	0
11	2	2 dcypb	4 Yb(OTf)$_3$	Chlorobenzene	69 (8:1)
12	2	2.25 dcypb	4 Yb(OTf)$_3$	Chlorobenzene	72 (9:1)
13	2	0 dcypb	4 Yb(OTf)$_3$	Chlorobenzene	0
14	2	2.25 dcype	4 Yb(OTf)$_3$	Chlorobenzene	53 (5:1)
15	2	2.25 dcypm	4 Yb(OTf)$_3$	Chlorobenzene	7
16	2	2.25 dppb	4 Yb(OTf)$_3$	Chlorobenzene	66 (1.5:1)
17	2	4.5 PCy_3	4 Yb(OTf)$_3$	Chlorobenzene	0
18	2	4.5 P(^{n}Bu)$_3$	4 Yb(OTf)$_3$	Chlorobenzene	77 (1:1)
19	2	2.25 dcypb	4 Sc(OTf)$_3$	Chlorobenzene	68 (8:1)
20	2	2.25 dcypb	4 Mg(OTf)$_2$	Chlorobenzene	60 (9:1)
21	2	2.25 dcypb	4 AgOTf	Chlorobenzene	0
22[b]	2	2.25 dcypb	4 Yb(OTf)$_3$	Chlorobenzene	57 (9:1)
23[c]	2	2.25 dcypb	4 Yb(OTf)$_3$	Chlorobenzene	66 (6:1)
24[d]	2	2.25 dcypb	4 Yb(OTf)$_3$	Chlorobenzene	48 (8:1)
25[e]	2	2.25 dcypb	4 Yb(OTf)$_3$	Chlorobenzene	27 (6:1)

[a] Reaction conditions: pyrrolidin-2-one (1.00 mmol), hex-1-yne (2.00 mmol), (cod)Ru(met)$_2$, ligand, Lewis acid, solvent (3 mL), GC yields determined using *n*-tetradecane as internal standard. Product ratio determined by GC. dcype = 1,2-di(cyclohexylphosphino)ethane, dcypm = 1,2-di(cyclohexylphosphino)methane, dppb = di(phenylphosphino) butane, PCy_3 = tricyclohexylphosphine, P(^{n}Bu)$_3$ = tri-*n*-butylphosphine.
[b] 6 h reaction time.
[c] 40 °C temperature.
[d] 80 °C temperature.
[e] 100 °C temperature.

3. Conclusion

In summary, a Ru-phosphine catalyst in combination with the Lewis acid Yb(OTf)$_3$ has been found to promote the regio- and stereoselective addition of secondary amides and imides under selective formation of the *Z*-configured *anti*-Markovnikov products. The bimetallic catalyst system is superior to preceding monometallic catalysts in terms of scope and stereoselectivity. The new protocol provides an atom-economic entry to the thermodynamically disfavored *Z*-isomers of various synthetically important enamides and enimides.

4. Experimental

All reactions were performed in oven-dried glassware containing a Teflon-coated stirring bar and dry septum under a nitrogen atmosphere. Solvents were purified by standard procedures prior to use. All reactions were monitored by GC using *n*-tetradecane as an internal standard. Response factors of the products with regard to *n*-tetradecane were obtained experimentally by analyzing known quantities of the substances. GC analyses were carried out using an HP-5 capillary column (phenyl methyl siloxane 30 m × 320 × 0.25, 100/2.3-30-300/3) and a time program beginning with 2 min at 60 °C followed by 30 °C/min ramp to 300 °C, then 3 min at this temperature. Column chromatography was performed using a Combi Flash Companion chromatography system (Isco-Systems) and RediSep prepacked columns (12 g). NMR spectra were obtained on Bruker AMX 400 systems using benzene-d_6 or chloroform-d_1 as solvent, with proton and carbon resonances at 400 MHz and 101 MHz, respectively. Mass spectral data were acquired on a GC–MS Saturn 2100 T (Varian). IR spectra were measured using a Perkin Elmer FT-IR system. Elemental analyses were carried out using a vario Micro tube (Elementar Analysetechnik/Hanau). GC/HRMS spectra were obtained on a GCT Premier (WATERS).

4.1. Synthesis of Z-configured enamides and enimides

4.1.1. General procedure

An oven-dried vessel was charged with *N*-nucleophile **1** (1.00 mmol), bis(2-methallyl)-cycloocta-1,5-diene-ruthenium(II) (6.39 mg, 0.02 mmol), 1,4-bis(dicyclohexylphosphino)butane (10.1 mg, 22.5 μmol) and ytterbium(III) triflate hydrate (24.8 mg, 0.04 mmol). After flushing the vessel with alternating vacuum and nitrogen purge cycles, dry chlorobenzene (3 mL) or dry DMF (3 mL) and the alkyne **2** (2.00 mmol) were added *via* syringe and the resulting mixture was stirred at 60 °C for 16 h. Then, it was allowed to cool to room temperature and the reaction mixture was purified without any work-up by column chromatography (silica gel, ethyl acetate/hexane) to yield the *Z*-product. The identity and purity of the products were confirmed by ^{1}H and ^{13}C NMR spectroscopy, mass spectroscopy, elemental analysis, infrared spectroscopy and, if a solid product was obtained, the melting points were determined.

Table 2
Substrate scope of the enamide and enimide synthesis.[a]

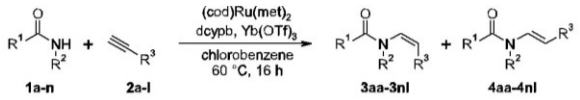

Product	Yield [%] (ratio 3:4)	Product	Yield [%] (ratio 3:4)	Product	Yield [%] (ratio 3:4)
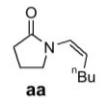 aa	72 (11:1)	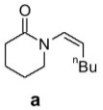 a	43 (>20:1)	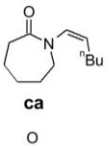 ca	32 (>20:1)
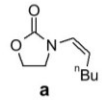 a	88 (17:1)[b]	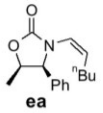 ea	92 (>20:1)[b]	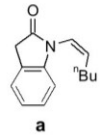 a	86 (10:1)[b]
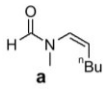 a	16 (>20:1)[b,c]	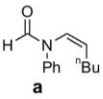 a	85 (3:1)[b]	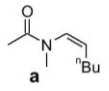 a	5 (>20:1)[b,c]
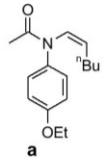 a	84 (>20:1)[b]	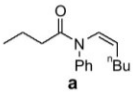 a	45 (1:1)[b]	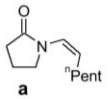 a	74 (8:1)
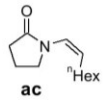 ac	72 (9:1)	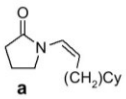 a	74 (12:1)	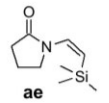 ae	0[c]
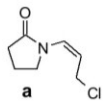 a	0[c]	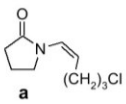 a	87 (4:1)[b]	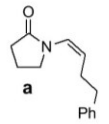 a	75 (9:1)
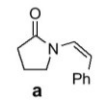 a	74 (>20:1)	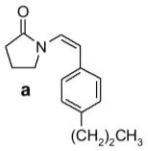 a	73 (>20:1)	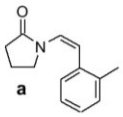 a	83 (>20:1)
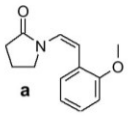 a	86 (4:1)[b]	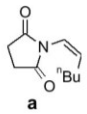 a	89 (>20:1)[b]	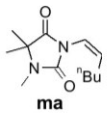 ma	96 (>20:1)[b]

(*continued on next page*)

Table 2 (*continued*)

Product	Yield [%] (ratio 3:4)	Product	Yield [%] (ratio 3:4)	Product	Yield [%] (ratio 3:4)
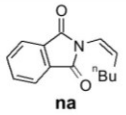 **na**	76 (>20:1)[b]	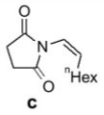 **c**	99 (>20:1)[b]	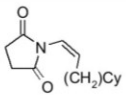	80 (>20:1)[b]
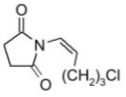	71 (>20:1)[b]	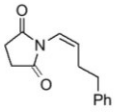	95 (>20:1)[b]		

[a] Reaction conditions: amide (1.00 mmol), alkyne (2.00 mmol), (cod)Ru(met)$_2$ (0.02 mmol), 1,4-bis(dicyclohexylphosphino)butane (22.5 μmol), ytterbium(III) triflate hydrate (0.04 mmol), chlorobenzene (3 mL), 60 °C, 16 h, isolated yields. Product ratio determined by ^{1}H NMR.
[b] DMF as solvent.
[c] GC yields determined using *n*-tetradecane as internal standard. Product ratio determined by GC.

*4.1.2. N-((Z)-Hex-1-enyl)pyrrolidin-2-one (**3aa**)*

Compound **3aa** was synthesized following the general procedure using pyrrolidin-2-one (**1a**) (85.1 mg, 1.00 mmol) and hex-1-yne (**2a**) (234 μL, 2.00 mmol) in chlorobenzene and purified by column chromatography (30:70 ethyl acetate/hexane), yielding the product as a colorless oil (119 mg, 71%) with a (*Z*/*E*)-selectivity of 11:1. ^{1}H NMR (benzene-d_6, 400 MHz): δ = 6.73 (d, ^3J = 10.2 Hz, 1H), 4.54–4.61 (m, 1H), 3.08 (t, ^3J = 7.0 Hz, 2H), 1.97–2.06 (m, 2H), 1.90 (t, ^3J = 8.2 Hz, 2H), 1.15–1.30 (m, 6H), 0.86 (t, ^3J = 6.8 Hz, 3H) ppm. ^{13}C NMR (benzene-d_6, 101 MHz): δ = 173.4, 122.8, 113.3, 47.8, 33.1, 29.9, 27.1, 22.6, 18.3, 14.1 ppm. MS (EI, 70 eV), *m*/*z* (%): 167 (M^+, 9), 124 (100), 96 (63), 94 (10), 86 (46), 79 (22), 41 (36). IR (NaCl) 1662, 1702, 2872, 2927, 2957 cm^{-1}. GC/HRMS-EI *m*/*z* [M^+] calcd. for $C_{10}H_{17}NO$ 167.1310; found: 167.1316.

*4.1.3. N-((Z)-Hex-1-enyl)piperidin-2-one (**3ba**)*

Compound (**3ba**) was synthesized following the general procedure using piperidin-2-one (**1b**) (101 mg, 1.00 mmol) and hex-1-yne (**2a**) (234 μL, 2.00 mmol) in chlorobenzene and purified by column chromatography (30:70 ethyl acetate/hexane), yielding the product as a colorless oil (78 mg, 43%) with a (*Z*/*E*)-selectivity of >20:1. ^{1}H NMR (benzene-d_6, 400 MHz) δ = 7.85 (d, ^3J = 7.9 Hz, 1H), 4.67–4.77 (m, 1H), 2.75 (t, ^3J = 5.5 Hz, 2H), 2.16 (t, ^3J = 5.9 Hz, 2H), 2.01 (q, ^3J = 6.9 Hz, 2H), 1.22–1.38 (m, 4H), 1.02–1.15 (m, 4H), 0.87 (t, ^3J = 6.7 Hz, 3H) ppm. ^{13}C NMR (benzene-d_6, 101 MHz) δ = 166.8, 109.7, 44.8, 33.0, 30.5, 22.6, 22.5, 20.6, 14.1 ppm. MS (EI, 70 eV), *m*/*z* (%): 181 (M^+, 20), 152 (19), 138 (100), 110 (49), 100 (44), 82 (36), 67 (25). IR (NaCl) 1650, 2871, 2927, 3035, 3073 cm^{-1}. GC/HRMS-EI *m*/*z* [M^+] calcd. for $C_{11}H_{19}NO$ 181.1467; found: 181.1474.

*4.1.4. N-((Z)-Hex-1-enyl)azepan-2-one (**3ca**)*

Compound (**3ca**) was synthesized following the general procedure using azepan-2-one (**1c**) (113 mg, 1.00 mmol) and hex-1-yne (**2a**) (234 μL, 2.00 mmol) in chlorobenzene and purified by column chromatography (30:70 ethyl acetate/hexane), yielding the product as a colorless oil (63.2 mg, 32%) with a (*Z*/*E*)-selectivity of >20:1. ^{1}H NMR (benzene-d_6, 400 MHz) δ = 7.60 (d, ^3J = 7.5 Hz, 1H), 4.72–4.82 (m, 1H), 2.98–3.04 (m, 2H), 2.28–2.35 (m, 2H), 1.99 (q, ^3J = 6.9 Hz, 2H), 1.23–1.35 (m, 6H), 1.14–1.21 (m, 4H), 0.85 (t, ^3J = 6.8 Hz, 3H) ppm. ^{13}C NMR (benzene-d_6, 101 MHz) δ = 172.7, 109.2, 44.5, 37, 32.8, 30.2, 29.2, 27.3, 23.4, 22.3, 13.9 ppm. MS (EI, 70 eV), *m*/*z* (%): 195 (M^+, 22), 152 (60), 138 (100), 124 (25), 96 (40), 67 (34), 41 (49). IR (NaCl) 1650, 1761, 2856, 2926, 3070 cm^{-1}. GC/HRMS-EI *m*/*z* [M^+] calcd. for $C_{12}H_{21}NO$ 195.1623; found: 195.1623.

*4.1.5. N-((Z)-Hex-1-enyl)oxazolidin-2-one (**3da**)*

Compound (**3da**) was synthesized following the general procedure using oxazolidin-2-one (**1d**) (87.1 mg, 1.00 mmol) and hex-1-yne (**2a**) (234 μL, 2.00 mmol) in DMF and purified by column chromatography (30:70 ethyl acetate/hexane), yielding the product as a colorless oil (149 mg, 88%) with a (*Z*/*E*)-selectivity of 17:1. ^{1}H NMR (benzene-d_6, 400 MHz) δ = 6.41 (d, ^3J = 9.8 Hz, 1H), 4.45–4.53 (m, 1H), 4.33 (t, ^3J = 8.0 Hz, 2H), 3.90 (t, ^3J = 8.0 Hz, 2H), 2.11 (q, ^3J = 6.8 Hz, 2H), 1.23–1.35 (m, 4H), 0.84 (t, ^3J = 7.0 Hz, 3H) ppm. ^{13}C NMR (benzene-d_6, 101 MHz) δ = 156.5, 123.2, 112.9, 61.5, 44.9, 32.9, 26.3, 22.6, 14.1 ppm. MS (EI, 70 eV), *m*/*z* (%): 169 (M^+, 4), 126 (86), 82 (13), 80 (15), 67 (9), 55 (12), 42 (100). IR (NaCl) 1668, 1752, 2872, 2927, 2958 cm^{-1}. Anal. Calcd. for $C_9H_{15}NO_2$ (169.2): C, 63.88; H, 8.93; N, 8.28. Found: C, 63.71; H, 8.98; N, 8.26.

*4.1.6. (4S,5R)-3-((Z)-Hex-1-enyl)-5-methyl-4-phenyloxazolidin-2-one (**3ea**)*

Compound (**3ea**) was synthesized following the general procedure using (**1e**) (4*S*,5*R*)-5-methyl-4-phenyloxazolidin-2-one (177 mg, 1.00 mmol) and hex-1-yne (**2a**) (234 μL, 2.00 mmol) in DMF and purified by column chromatography (30:70 ethyl acetate/hexane), yielding the product as a colorless solid (239 mg, 92%) with a (*Z*/*E*)-selectivity of >20:1. Mp: 44.6 °C. ^{1}H NMR (benzene-d_6, MHz 400 MHz) δ = 7.02–7.09 (m, 3H), 6.97–7.01 (m, 2H), 6.04 (d, ^3J = 8.8 Hz, 1H), 5.67 (d, ^3J = 7.6 Hz, 1H), 5.10 (q, 1H), 4.33–4.42 (m, 1H), 2.07–2.16 (m, 2H), 1.30–1.45 (m, 4H), 0.90 (t, ^3J = 7.0 Hz, 3H), 0.76 (d, ^3J = 6.6 Hz, 3H) ppm. ^{13}C NMR (benzene-d_6, 101 MHz) δ = 155.6, 135.4, 128.6, 126.2, 121.9, 119.9.6, 78.1, 56.6, 31.9, 27.1, 22.7, 14.2 ppm. MS (EI, 70 eV), *m*/*z* (%): 261 [MH^+] (14), 218 (18), 217 (100), 215 (13), 173 (23), 118 (14), 98 (16). IR (NaCl) 1668, 1731, 2868, 2957, 3038 cm^{-1}. Anal. Calcd. for $C_{16}H_{21}NO_2$ (259.4): C, 74.10; H, 8.16; N, 5.40. Found: C, 74.02; H, 8.28; N, 5.46.

*4.1.7. N-((Z)-Hex-1-enyl)indolidin-2-one (**3fa**)*

Compound (**3fa**) was synthesized following the general procedure using oxindol (**1f**) (137 mg, 1.00 mmol) and hex-1-yne (**2a**) (234 μL, 2.00 mmol) in DMF and purified by column chromatography (50:50 ethyl acetate/hexane), yielding the product as a colorless oil (185 mg, 86%) with a (*Z*/*E*)-selectivity of 10:1. ^{1}H NMR ($CDCl_3$-d_1, 400 MHz) δ = 7.23–7.31 (m, 2H), 7.07 (q, ^3J = 7.7 Hz, 1H), 6.74 (d, ^3J = 7.5 Hz, 1H), 6.04 (d, ^3J = 8.1 Hz, 1H), 5.79 (q, ^3J = 7.5 Hz, 1H), 3.59 (s, 2H), 2.02–2.09 (m, 2H), 1.22–1.31 (m, 2H), 1.17 (m, 2H), 0.76 (t, ^3J = 7.2 Hz, 3H) ppm. ^{13}C NMR ($CDCl_3$-d_1, 101 MHz) δ = 174.0, 144.6, 133.6, 127.9, 124.5, 122.6, 118.9, 109.4, 35.8, 30.9, 27.7, 22.3, 13.9 ppm. MS (EI, 70 eV), *m*/*z* (%): 215 (M^+, 100), 172 (30), 144 (84),

133 (22), 130 (17), 117 (13). IR (NaCl) 1659, 1727, 2870, 2926, 3034, 3053 cm^{-1}. Anal. Calcd. for $C_{14}H_{17}NO$ (215.3): C, 78.10; H, 7.96; N, 6.51. Found: C, 77.70; H, 8.12; N, 6.92.

*4.1.8. N-((Z)-Hex-1-enyl)-N-phenyl-formamide (**3ha**)*

Compound (**3ha**) was synthesized following the general procedure using formanilide (**1h**) (121 mg, 1.00 mmol) and hex-1-yne (**2a**) (234 μL, 2.00 mmol) in DMF and purified by column chromatography (30:70 ethyl acetate/hexane), yielding the product as a colorless oil (173 mg, 85%) with a (*Z*/*E*)-selectivity of 3:1. ^{1}H NMR (benzene-d_6, 400 MHz) δ = 8.17 (s, 1H), 7.50 (d, ^3J = 7.8 Hz, 1H), 7.12 (t, ^3J = 7.6 Hz, 1H), 6.95 (t, ^3J = 7.4 Hz, 1H), 6.87 (t, ^3J = 7.2 Hz, 1H), 6.73 (d, ^3J = 7.4 Hz, 1H), 6.55 (d, ^3J = 9.0 Hz, 1H), 4.98 (q, ^3J = 7.8 Hz, 1H), 1.48–1.57 (m, 2H), 0.97–1.03 (m, 4H), 0.64–0.75 (m, 3H) ppm. ^{13}C NMR (benzene-d_6, 101 MHz) δ = 161.3, 141.5, 129.5, 128.9, 126.7, 123.9, 123.8, 31.7, 31.0, 27.5, 26.3, 22.5, 13.9 ppm. MS (EI, 70 eV), *m*/*z* (%) = 203 (M^+, 30), 160 (54), 132 (100), 130 (31), 121 (32), 117 (64), 77 (55). IR (NaCl) 1554, 1690, 2871, 2927, 2956, 3039 cm^{-1}. Anal. Calcd. for $C_{13}H_{17}NO$ (203.3): C, 76.81, H, 8.43, N, 6.89. Found: C, 76.38; H, 8.38; N, 6.83. GC/HRMS-EI *m*/*z* [M^+] calcd. for $C_{13}H_{17}NO$ 203.1310; found: 203.1313.

*4.1.9. N-(4-Ethoxyphenyl)-N-((Z)-hex-1-enyl)acetamide (**3ja**)*

Compound (**3ja**) was synthesized following the general procedure using *N*-(4-ethoxyphenyl)acetamide (**1j**) (179 mg, 1.00 mmol) and hex-1-yne (**2a**) (234 μL, 2.00 mmol) in DMF and purified by column chromatography (30:70 ethyl acetate/hexane), yielding the product as a colorless oil (219 mg, 84%) with a (*Z*/*E*)-selectivity of >20:1. ^{1}H NMR (benzene-d_6, 400 MHz) δ = 6.73 (d, ^3J = 8.6 Hz, 2H), 6.64 (d, ^3J = 8.6 Hz, 2H), 5.54–5.64 (m, 1H), 5.28–5.37 (m, 1H), 4.31 (d, ^3J = 6.7 Hz, 2H), 3.52 (q, ^3J = 7.0 Hz, 2H), 1.83 (q, ^3J = 7.3 Hz, 2H), 1.78 (s, 3H), 1.16–1.26 (m, 2H), 1.09 (t, ^3J = 7.0 Hz, 3H), 0.75 (t, ^3J = 7.2 Hz, 3H) ppm. ^{13}C NMR (benzene-d_6, 101 MHz) δ = 169.1, 158.5, 136.3, 134.3, 129.7, 125.9, 115.1, 63.5, 51.5, 34.6, 22.6, 14.7, 13.7 ppm. MS (EI, 70 eV), *m*/*z* (%) = 261 (M^+, 55), 219 (43), 176 (100), 137 (50), 109 (25). IR (NaCl) 1651, 2872, 2928, 2958, 3041 cm^{-1}. Anal. Calcd. for $C_{16}H_{23}NO_2$ (261.4): C, 73.53, H, 8.87, N, 5.36. Found: C, 73.02; H, 9.12; N, 5.30. GC/HRMS-EI *m*/*z* [M^+] calcd. for $C_{16}H_{23}NO_2$ 261.17289; found: 261.1718.

*4.1.10. N-((Z)-Hex-1-enyl)-N-phenyl-butanamide (**3ka**)*

Compound (**3ka**) was synthesized following the general procedure using *N*-phenyl-butanamide (**1k**) (163 mg, 1.00 mmol) and hex-1-yne (**2a**) (234 μL, 2.00 mmol) in DMF and purified by column chromatography (30:70 ethyl acetate/hexane), yielding the product as a colorless oil (111 mg, 45%) with a (*Z*/*E*)-selectivity of 1:1. ^{1}H NMR (benzene-d_6, 400 MHz) δ = 6.99–7.09 (m, 3H), 6.89–6.98 (m, 1H), 6.85 (d, ^3J = 6.7 Hz, 1H), 5.23–5.34 (m, 1H), 4.31 (d, ^3J = 5.5 Hz, 1H), 2.02–2.11 (m, 1H), 1.99 (t, ^3J = 7.2 Hz, 1H), 1.80 (q, ^3J = 7.3 Hz, 1H), 1.64–1.76 (m, 2H), 1.44–1.56 (m, 1H), 1.13–1.25 (m, 1H), 1.01 (d, ^3J = 2.7 Hz, 2H), 0.76–0.86 (m, 3H), 0.67–0.76 (m, 3H) ppm. ^{13}C NMR (benzene-d_6, 101 MHz) δ = 171.5, 143.5, 134.3, 129.4, 127.4, 126.1, 51.5, 36.5, 34.5, 26.4, 22.6, 19.2, 18.9, 13.9, 13.7 ppm. MS (EI, 70 eV), *m*/*z* (%) = 245 (M^+, 9), 175 (32), 132 (100), 117 (13), 93 (15), 77 (25), 43 (23). IR (NaCl) 1595, 1659, 2872, 2929, 2959, 3037 cm^{-1}. GC/HRMS-EI *m*/*z* [M^+] calcd. for $C_{16}H_{23}NO$ 245.1780; found: 245.1776.

*4.1.11. N-((Z)-Hept-1-enyl)pyrrolidin-2-one (**3ab**)*

Compound (**3ab**) was synthesized following the general procedure using pyrrolidin-2-one (**1a**) (85.1 mg, 1.00 mmol) and hept-1-yne (**2b**) (269 μL, 2.00 mmol) in chlorobenzene and purified by column chromatography (30:70 ethyl acetate/hexane), yielding the product as a colorless oil (134 mg, 74%) with a (*Z*/*E*)-selectivity of 8:1. ^{1}H NMR (benzene-d_6, 400 MHz) δ = 6.76 (d, ^3J = 9.8 Hz, 1H), 4.54–4.63 (m, 1H), 3.06 (t, ^3J = 7.0 Hz, 2H), 1.19–1.34 (m, 6H), 1.11–1.19 (m, 2H), 0.89 (t, ^3J = 6.8 Hz, 3H) ppm. ^{13}C NMR (benzene-d_6, 101 MHz) δ = 173.2, 122.8, 113.4, 47.8, 31.8, 30.6, 29.9, 27.4, 22.9, 18.2, 14.2 ppm. MS (EI, 70 eV), *m*/*z* (%) = 181 (M^+, 7), 138 (15), 124 (100), 98 (28), 96 (58), 86 (56), 81 (23). IR (NaCl) 1662, 1703, 2857, 2871, 2926, 2956 cm^{-1}. Anal. Calcd. for $C_{11}H_{19}NO$ (181.3): C, 72.88; H, 10.56; N, 7.73. Found: C, 72.30; H, 10.43, N, 7.59.

*4.1.12. N-((Z)-Oct-1-enyl)pyrrolidin-2-one (**3ac**)*

Compound (**3ac**) was synthesized following the general procedure using pyrrolidin-2-one (**1a**) (85.1 mg, 1.00 mmol) and oct-1-yne (**2c**) (298 μL, 2.00 mmol) in chlorobenzene and purified by column chromatography (30:70 ethyl acetate/hexane), yielding the product as a colorless oil (140 mg, 72%) with a (*Z*/*E*)-selectivity of 9:1. ^{1}H NMR (benzene-d_6, 400 MHz) δ = 6.75 (d, ^3J = 9.8 Hz, 1H), 4.60 (q, ^3J = 8.0 Hz, 1H), 3.09 (t, ^3J = 7.0 Hz, 2H), 1.99–2.09 (m, 2H), 1.90 (t, ^3J = 8.2 Hz, 2H), 1.12–1.36 (m, 10H), 0.90 (t, ^3J = 6.5 Hz, 3H) ppm. ^{13}C NMR (benzene-d_6, 101 MHz) δ = 173.3, 122.8, 113.5, 47.9, 32.1, 30.9, 29.9, 29.3, 27.4, 23.0, 18.3, 14.3 ppm. MS (EI, 70 eV), *m*/*z* (%) = 195 (M^+, 9), 138 (30), 98 (100), 96 (41), 86 (73), 81 (22), 67 (35). IR (NaCl) 1661, 1704, 2854, 2924, 2955 cm^{-1}. GC/HRMS-EI *m*/*z* [M^+] calcd. for $C_{12}H_{21}NO$ 195.1623; found: 195.1625.

*4.1.13. N-((Z)-2-Cyclohexylvinyl)pyrrolidin-2-one (**3ad**)*

Compound (**3ad**) was synthesized following the general procedure using pyrrolidin-2-one (**1a**) (85.1 mg, 1.00 mmol) and 3-cyclohexyl-prop-1-yne (**2d**) (290 μL, 2.00 mmol) in chlorobenzene and purified by column chromatography (30:70 ethyl acetate/hexane), yielding the product as a colorless oil (154 mg, 74%) with a (*Z*/*E*)-selectivity of 12:1. ^{1}H NMR (benzene-d_6, 400 MHz) δ = 6.78 (d, ^3J = 9.8 Hz, 1H), 4.58 (q, ^3J = 7.8 Hz, 1H), 3.12 (t, ^3J = 7.0 Hz, 2H), 1.93–1.99 (m, 2H), 1.88–1.93 (m, 2H), 1.67 (d, ^3J = 12.5 Hz, 5H), 1.19–1.28 (m, 3H), 1.08–1.18 (m, 3H), 0.76–0.88 (m, 2H) ppm. ^{13}C NMR (benzene-d_6, 101 MHz) δ = 173.6, 123.7, 112.0, 48.3, 39.5, 35.3, 33.7, 33.5, 30.1, 27.1, 26.9, 18.5 ppm. MS (EI, 70 eV), *m*/*z* (%) = 207 (M^+, 7), 124 (100), 96 (36), 86 (22), 79 (15), 68 (11), 41 (20). IR (NaCl) 1662, 1702, 2850, 2922 cm^{-1}. GC/HRMS-EI *m*/*z* [M^+] calcd. for $C_{13}H_{21}NO$ 207.1623; found: 207.1628.

*4.1.14. N-((Z)-5-Chloropent-1-enyl)pyrrolidin-2-one (**3ag**)*

Compound (**3ag**) was synthesized following the general procedure using pyrrolidin-2-one (**1a**) (85.1 mg, 1.00 mmol) and 5-chloro-pent-1-yne (**2g**) (214 μL, 2.00 mmol) in DMF and purified by column chromatography (30:70 ethyl acetate/hexane), yielding the product as a colorless oil (164 mg, 87%) with a (*Z*/*E*)-selectivity of 4:1. ^{1}H NMR (benzene-d_6, 400 MHz) δ = 6.69 (d, ^3J = 9.8 Hz, 1H), 4.33 (q, ^3J = 7.8 Hz, 1H), 3.15 (t, ^3J = 5.7 Hz, 2H), 3.07 (t, ^3J = 7.2 Hz, 2H), 2.05 (q, ^3J = 7.3 Hz, 2H), 1.89 (t, ^3J = 7.6 Hz, 2H), 1.40–1.50 (m, 2H), 1.15–1.25 (m, 2H) ppm. ^{13}C NMR (benzene-d_6, 101 MHz) δ = 173.7, 124.2, 111.3, 48.0, 44.6, 33.5, 30.1, 24.6, 18.4 ppm. MS (EI, 70 eV), *m*/*z* (%) = 187 (M^+, 22), 152 (15), 124 (100), 96 (53), 69 (16), 41 (22). IR (NaCl) 1701, 2958 cm^{-1}. GC/HRMS-EI *m*/*z* [M^+] calcd. for $C_9H_{14}ClNO$ 187.0764 and 189.0734; found: 187.0770 and 189.0752.

*4.1.15. N-((Z)-4-Phenylbut-1-enyl)pyrrolidin-2-one (**3ah**)*

Compound (**3ah**) was synthesized following the general procedure using pyrrolidin-2-one (**1a**) (85.1 mg, 1.00 mmol) and 4-phenyl-but-1-yne (**2h**) (281 μL, 2.00 mmol) in chlorobenzene and purified by column chromatography (30:70 ethyl acetate/hexane), yielding the product as a colorless oil (161 mg, 75%) with a (*Z*/*E*)-selectivity of 9:1. ^{1}H NMR (benzene-d_6, 400 MHz) δ = 7.14–7.23 (m,

2H), 7.04–7.12 (m, 3H), 6.69 (d, ^3J = 10.2 Hz, 1H), 4.60 (q, ^3J = 7.4 Hz, 1H), 2.92 (t, ^3J = 7.0 Hz, 2H), 2.51 (t, ^3J = 7.6 Hz, 2H), 2.31 (q, ^3J = 7.7 Hz, 2H), 1.87 (t, ^3J = 8.0 Hz, 2H), 1.09–1.19 (m, 2H) ppm. ^{13}C NMR (benzene-d_6, 101 MHz) δ = 173.4, 141.9, 128.8, 128.6, 126.3, 123.1, 112.5, 47.7, 36.9, 29.9, 29.5, 18.18 ppm. MS (EI, 70 eV), *m/z* (%) = 215 (M^+, 1), 124 (100), 96 (39), 91 (13), 79 (12), 69 (12), 41 (16). IR (NaCl) 1698, 2923, 3025, 3059, 3083 cm^{-1}. GC/HRMS-EI *m/z* [M^+] calcd. for $C_{14}H_{17}NO$ 215.1310; found: 215.1305.

4.1.16. *N-((Z)-2-Phenylvinyl)pyrrolidin-2-one (**3ai**)*

Compound (**3ai**) was synthesized following the general procedure using pyrrolidin-2-one (**1a**) (85.1 mg, 1.00 mmol) and phenylacetylene (**2i**) (220 μL, 2.00 mmol) in chlorobenzene and purified by column chromatography (30:70 ethyl acetate/hexane), yielding the product as a yellowish oil (139 mg, 74%) with a (*Z*/*E*)-selectivity of >20:1. [CAS: 6908–67–4]. ^{1}H NMR (benzene-d_6, 400 MHz) δ = 7.06–7.14 (m, 3H), 6.99–7.14 (m, 3H), 5.73 (d, ^3J = 9.8 Hz, 1H), 2.69 (t, ^3J = 7.0 Hz, 2H), 1.87 (t, ^3J = 8.0 Hz, 2H), 0.97–1.08 (m, 2H) ppm. ^{13}C NMR (benzene-d_6, 101 MHz) δ = 174.5, 137.2, 129.7, 126.9, 124.8, 111.8, 47.9, 30.1, 18.6 ppm. MS (EI, 70 eV), *m/z* (%) = 187 (M^+, 100), 159 (11), 132 (52), 130 (52), 117 (26), 115 (24), 77 (20).

4.1.17. *N-((Z)-4-Propylstyryl)pyrrolidin-2-one (**3aj**)*

Compound (**3aj**) was synthesized following the general procedure using pyrrolidin-2-one (**1a**) (85.1 mg, 1.00 mmol) and 1-ethynyl-4-propylbenzene (**2j**) (317 μL, 2.00 mmol) in chlorobenzene and purified by column chromatography (30:70 ethyl acetate/hexane), yielding the product as a yellowish oil (167 mg, 73%) with a (*Z*/*E*)-selectivity of >20:1. ^{1}H NMR (benzene-d_6, 400 MHz) δ = 6.97–7.08 (m, 5H), 5.78 (d, ^3J = 9.8 Hz, 1H), 2.79 (t, ^3J = 7.0 Hz, 2H), 2.43 (t, ^3J = 7.6 Hz, 2H), 1.89 (t, ^3J = 8.0 Hz, 2H), 1.46–1.58 (m, 2H), 1.01–1.11 (m, 2H), 0.84 (t, ^3J = 7.2 Hz, 3H) ppm. ^{13}C NMR (benzene-d_6, 101 MHz) δ = 174.3, 141.1, 134.5, 131.3, 129.6, 124.4, 111.9, 47.7, 37.9, 30.0, 24.8, 18.3, 13.7 ppm. MS (EI, 70 eV), *m/z* (%) = 229 (M^+, 68), 201 (17), 200 (100), 131 (42), 130 (16), 115 (25). IR (NaCl) 1647, 1707, 2871, 2929, 2958 cm^{-1}. Anal. Calcd. for $C_{15}H_{19}NO$ (229.3): C, 78.56; H, 8.35, N, 6.11. Found: C, 77.98; H, 8.00; N, 6.29.

4.1.18. *N-((Z)-2-Methylstyryl)pyrrolidin-2-one (**3ak**)*

Compound (**3ak**) was synthesized following the general procedure using pyrrolidin-2-one (**1a**) (85.1 mg, 1.00 mmol) and 2-ethynyltoluene (**2k**) (260 μL, 2.00 mmol) in chlorobenzene and purified by column chromatography (30:70 ethyl acetate/hexane), yielding the product as a yellowish oil (186 mg, 83%) with a (*Z*/*E*)-selectivity of >20:1. ^{1}H NMR (benzene-d_6, 400 MHz) δ = 7.24 (d, ^3J = 10.2 Hz, 1H), 7.05–7.16 (m, 4H), 5.69 (d, ^3J = 10.2 Hz, 1H), 2.70 (t, ^3J = 7.0 Hz, 2H), 2.19 (s, 3H), 1.95 (t, ^3J = 8.0 Hz, 2H), 1.03–1.14 (m, 2H) ppm. ^{13}C NMR (benzene-d_6, 101 MHz) δ = 174.1, 136.7, 136.5, 130.4, 129.5, 127.3, 125.2, 124.7, 110.0, 47.5, 30.0, 20.2, 18.3 ppm. MS (EI, 70 eV), *m/z* (%) = 201 (M^+, 100), 144 (18), 131 (19), 130 (20), 116 (35), 115 (35). IR (NaCl) 1648, 1706, 2895, 2979, 3019, 3065 cm^{-1}. Anal. Calcd. for $C_{13}H_{15}NO$ (201.3): C, 77.58; H, 7.51; N, 6.96. Found: C, 77.12; H, 7.47; N, 6.92.

4.1.19. *N-((Z)-2-Methoxystyryl)pyrrolidin-2-one (**3al**)*

Compound (**3al**) was synthesized following the general procedure using pyrrolidin-2-one (**1a**) (85.1 mg, 1.00 mmol) and ethynylanisole (**2l**) (259 μL, 2.00 mmol) in DMF and purified by column chromatography (30:70 ethyl acetate/hexane), yielding the product as a yellowish oil (186 mg, 86%) with a (*Z*/*E*)-selectivity of 4:1. ^{1}H NMR (benzene-d_6, 400 MHz) δ = 7.17 (d, ^3J = 9.8 Hz, 1H), 7.07–7.12 (m, 1H), 6.98–7.03 (m, 1H), 6.79–6.85 (m, 1H), 6.57 (d, ^3J = 8.2 Hz, 1H), 5.95 (d, ^3J = 9.8 Hz, 1H), 3.38 (s, 3H), 2.81 (t, ^3J = 7.0 Hz, 2H), 1.88 (t, ^3J = 8.0 Hz, 2H), 1.02–1.11 (m, 2H) ppm. ^{13}C NMR (benzene-d_6, 101 MHz) δ = 174.3, 157.6, 131.4, 128.5, 124.8, 119.9, 110.2, 107.9, 55.0, 47.5, 30.1, 18.5 ppm. MS (EI, 70 eV), *m/z* (%) = 218 (MH^+, 100), 132 (22), 131 (11), 91 (11), 89 (10), 86 (20). IR (NaCl) 1647, 1701, 2836, 2960, 3073 cm^{-1}. GC/HRMS-EI *m/z* [M^+] calcd. for $C_{13}H_{15}NO_2$ 201.1154; found: 201.1153.

4.1.20. *N-((Z)-Hex-1-enyl)succinimide (**3la**)*

Compound (**3la**) was synthesized following the general procedure using succinimide (**1l**) (99.1 mg, 1.00 mmol) and hex-1-yne (**2a**) (231 μL, 2.00 mmol) in DMF and purified by column chromatography (30:70 ethyl acetate/hexane), yielding the product as a colorless oil (162 mg, 89%) with a (*Z*/*E*)-selectivity of >20:1. ^{1}H NMR (benzene-d_6, 400 MHz) δ = 5.86 (d, ^3J = 8.8 Hz, 1H), 5.42 (q, ^3J = 8.6, 7.5 Hz, 1H), 1.97 (qd, ^3J = 7.3, 1.6 Hz, 2H), 1.91 (s, 4H), 1.20–1.31 (m, 4H), 0.81 (t, ^3J = 7.1 Hz, 3H) ppm. ^{13}C NMR (benzene-d_6, 101 MHz) δ = 174.6, 137.0, 113.1, 32.0, 28.8, 27.4, 22.2, 13.7 ppm. MS (EI, 70 eV), *m/z* (%) = 182 (MH^+, 13), 138 (67), 100 (75), 82 (100), 56 (44). IR (NaCl) 1710, 2871, 2931, 2957, 3039 cm^{-1}. Anal. Calcd. for $C_{10}H_{15}NO_2$ (181.2): C, 66.27; H, 8.34; N, 7.73. Found: C, 66.19; H, 8.59; N, 7.89.

4.1.21. *N-((Z)-Hex-1-enyl)-1,5,5-trimethylhydantoin (**3ma**)*

Compound (**3ma**) was synthesized following the general procedure using 1,5,5-trimethylhydantoin (**1m**) (142 mg, 1.00 mmol) and hex-1-yne (**2a**) (234 μL, 2.00 mmol) in DMF and purified by column chromatography (30:70 ethyl acetate/hexane), yielding the product as a yellowish oil (215 mg, 96%) with a (*Z*/*E*)-selectivity of >20:1. ^{1}H NMR ($CDCl_3$-d_1, 400 MHz) δ = 5.85 (d, ^3J = 8.3 Hz, 1H), 5.60 (q, ^3J = 7.3 Hz, 1H), 2.85 (s, 3H), 1.89–1.98 (m, 2H), 1.36 (s, 6H), 1.28–1.34 (m, 2H), 1.21–1.28 (m, 2H), 0.81 (t, ^3J = 7.1 Hz, 3H) ppm. ^{13}C NMR ($CDCl_3$-d_1, 101 MHz) δ = 174.8, 154.2, 132.8, 116.3, 61.2, 30.7, 27.5, 24.5, 22.3, 22.2, 13.8 ppm. MS (EI, 70 eV), *m/z* (%) = 225 (MH^+, 100), 224 (10), 181 (11), 96 (13), 72 (15), 56 (26). IR (NaCl) 1662, 1719, 1777, 2871, 2930, 2956, 3044 cm^{-1}. Anal. Calcd. for $C_{12}H_{20}N_2O_2$ (224.3): C, 64.26; H, 8.99; N, 12.49. Found: C, 63.69, H, 9.08, N, 12.25.

4.1.22. *N-((Z)-Hex-1-enyl)phthalimide (**3na**)*

Compound (**3na**) was synthesized following the general procedure using phthalimide (**1n**) (147 mg, 1.00 mmol) and hex-1-yne (**2a**) (234 μL, 2.00 mmol) in DMF and purified by column chromatography (30:70 ethyl acetate/hexane), yielding the product as a yellowish oil (175 mg, 76%) with a (*Z*/*E*)-selectivity of >20:1. ^{1}H NMR ($CDCl_3$-d_1, 400 MHz) δ = 7.74, 7.84 (m, 2H), 7.61–7.71 (m, 2H), 6.00 (d, ^3J = 8.3 Hz, 1H), 5.67 (q, ^3J = 7.3 Hz, 1H), 1.93–2.05 (m, 2H), 1.28–1.39 (m, 2H), 1.17–1.27 (m, 2H), 0.77 (t, ^3J = 7.2 Hz, 3H) ppm. ^{13}C NMR ($CDCl_3$-d_1, 101 MHz) δ = 166.4, 132.5, 132.0, 123.2, 116.9, 31.3, 28.5, 22.6, 14.0 ppm. MS (EI, 70 eV), *m/z* (%) = 230 (MH^+, 100), 229 (18), 187 (13), 186 (77), 130 (24). IR (NaCl) 1663, 1718, 1764, 1785, 2858, 2956, 3041 cm^{-1}. Anal. Calcd. for $C_{14}H_{15}NO_2$ (229.3): C, 73.34, H, 6.59; N, 6.11. Found: C, 72.88; H, 6.62; N, 5.80.

4.1.23. *N-((Z)-Oct-1-enyl)succinimide (**3lc**)*

Compound (**3lc**) was synthesized following the general procedure using succinimide (**1l**) (99.1 mg, 1.00 mmol) and oct-1-yne (**2c**) (298 μL, 2.00 mmol) in DMF and purified by column chromatography (30:70 ethyl acetate/hexane), yielding the product as a colorless oil (208 mg, 99%) with a (*Z*/*E*)-selectivity of >20:1. ^{1}H NMR (benzene-d_6, 400 MHz) δ = 5.86 (d, ^3J = 8.6 Hz, 1H), 5.43 (q, ^3J = 8.6, 7.3 Hz, 1H), 1.98 (qd, ^3J = 7.4, 1.6 Hz, 2H), 1.91 (s, 4H), 1.27–1.34 (m, 2H), 1.13–1.25 (m, 6H), 0.82 (t, ^3J = 6.8 Hz, 3H) ppm. ^{13}C NMR (benzene-d_6, 101 MHz) δ = 175.0, 174.9, 131.8, 117.7, 32.0, 29.4, 29.1, 28.7, 28.2, 22.9, 14.2 ppm. MS (EI, 70 eV), *m/z* (%) = 210 (MH^+, 100), 138 (43), 110 (65), 82 (29), 81 (30), 56 (42), 55 (30). IR

(NaCl) 1664, 1710, 2856, 2928, 3039 cm^{-1}. Anal. Calcd. for $C_{12}H_{19}NO_2$ (209.3): C, 68.87; H, 9.15; N, 6.69. Found: C, 68.99; H, 9.32; N, 6.67.

*4.1.24. N-((Z)-2-Cyclohexylvinyl)succinimide (**3ld**)*

Compound (**3ld**) was synthesized following the general procedure using succinimide (**1l**) (99.1 mg, 1.00 mmol) and 3-cyclohexyl-prop-1-yne (**2d**) (290 μL, 2.00 mmol) in DMF and purified by column chromatography (30:70 ethyl acetate/hexane), yielding the product as a colorless solid (176 mg, 80%) with a (*Z*/*E*)-selectivity of >20:1. Mp: 106.3 °C. ^{1}H NMR (benzene-d_6, 400 MHz) $\delta = 5.93$ (d, $^3J = 8.6$ Hz, 1H), 5.47 (q, $^3J = 7.4$ Hz, 1H), 1.97 (t, $^3J = 6.5$ Hz, 2H), 1.75 (m, 4H), 1.51–1.70 (m, 5H) 1.20–1.29 (m, 1H), 0.97–1.19 (m, 3H), 0.77–0.90 (m, 2H) ppm. ^{13}C NMR (benzene-d_6, 101 MHz) $\delta = 174.7$, 130.7, 118.4, 37.7, 36.3, 33.4, 28.1, 26.6 ppm. MS (EI, 70 eV), *m*/*z* (%) = 222 [MH^+] (38), 139 (26), 122 (100), 83 (25), 80 (27), 56 (27), 55 (49). IR (NaCl) 1659, 1704, 1765, 2847, 2928, 3029 cm^{-1}. Anal. Calcd. for $C_{13}H_{19}NO_2$ (221.3): C, 70.56, H, 8.65; N, 6.33. Found: C, 70.01; H, 8.99; N, 6.39.

*4.1.25. N-((Z)-5-Chloropent-1-enyl)succinimide (**3lg**)*

Compound (**3lg**) was synthesized following the general procedure using succinimide (**1l**) (99.1 mg, 1.00 mmol) and 5-chloropent-1-yne (**2g**) (214 μL, 2.00 mmol) in DMF and purified by column chromatography (30:70 ethyl acetate/hexane), yielding the product as a colorless oil (143 mg, 71%) with a (*Z*/*E*)-selectivity of >20:1. ^{1}H NMR (benzene-d_6, 400 MHz) $\delta = 5.85$ (d, $^3J = 8.6$ Hz, 1H), 5.21 (q, $^3J = 7.7$ Hz, 1H), 3.15 (t, $^3J = 6.4$ Hz, 2H), 1.96–2.06 (m, 2H), 1.84–1.90 (m, 4H), 1.51 (qd, $^3J = 6.9$, 6.7 Hz, 2H) ppm. ^{13}C NMR (benzene-d_6, 101 MHz) $\delta = 175.0$, 129.9, 118.9, 44.5, 31.3, 28.2, 25.6 ppm. MS (EI, 70 eV), *m*/*z* (%) = 202 (MH^+, 67), 166 (79), 138 (100), 100 (52), 82 (71), 56 (75), 55 (59). IR (NaCl) 1708, 1777, 2942 cm^{-1}. Anal. Calcd. for $C_9H_{12}ClNO_2$ (201.7): C, 53.61; H, 6.00; N, 6.95. Found: C, 53.44; H, 5.98; N, 6.94.

*4.1.26. N-((Z)-2-Phenylbut-1-enyl)succinimide (**3lh**)*

Compound (**3lh**) was synthesized following the general procedure using succinimide (**1l**) (99.1 mg, 1.00 mmol) and 4-phenyl-but-1-yne (**2h**) (281 μL, 2.00 mmol) and purified by column chromatography (30:70 ethyl acetate/hexane), yielding the product as a colorless oil (218 mg, 95%) with a (*Z*/*E*)-selectivity of >20:1. Mp: 63.6 °C. ^{1}H NMR (benzene-d_6, 400 MHz) $\delta = 7.07–7.28$ (m, 5H), 5.93 (d, $^3J = 8.6$ Hz, 1H), 5.45–5.55 (m, 1H), 2.62–2.71 (m, 2H), 2.28–2.38 (m, 2H), 1.91 (s, 4H) ppm. ^{13}C NMR (benzene-d_6, 101 MHz) $\delta = 174.9$, 141.8, 130.3, 128.7, 128.6, 126.2, 118.1, 35.0, 30.7, 28.2 ppm. MS (EI, 70 eV), *m*/*z* (%) = 230 (MH^+, 5), 138 (100), 130 (84), 110 (24), 91 (40), 65 (24), 56 (59), 55 (27). IR (NaCl) 1702, 1764, 2858, 2922, 3024, 3059, 3084 cm^{-1}. Anal. Calcd. for $C_{14}H_{15}NO_2$ (229.3): C, 73.34; H, 6.59; N, 6.11. Found: C, 73.35; H, 6.49; N, 5.64.

Acknowledgements

We thank the Deutsche Forschungsgemeinschaft and NanoKat for financial support and the Landesgraduiertenförderung Rheinland-Pfalz for a scholarship to M.A.

References

[1] L. Yet, Chem. Rev. 103 (2003) 4283–4306.
[2] Y.N. Han, G.-Y. Kim, H.K. Han, B.H. Han, Arch. Pharm. Res. 16 (1993) 289–294.
[3] S.G. Toske, P.R. Jensen, C.A. Kaufman, W. Fenical, Tetrahedron 54 (1998) 13459–13466.
[4] D. Davyt, W. Entz, R. Fernandez, R. Mariezcurrena, A.W. Mombru, J. Saldana, L. Dominguez, J. Coll, E. Manta, J. Nat. Prod. 61 (1998) 1560–1563.
[5] (a) J.-H. Lin, Phytochemistry 28 (1989) 621–622;
(b) I. Stefanuti, S.A. Smith, R.J.K. Taylor, Tetrahedron Lett. 41 (2000) 3735–3738;
(c) A. Fürstner, C. Brehm, Y. Cancho-Grande, Org. Lett. 3 (2001) 3955–3957.
[6] (a) H.-W. Fehlhaber, J. Uhlendorf, S.T. David, R. Tschesche, Liebigs Ann. Chem. 759 (1972) 195–207;
(b) R. Tschesche, S.T. David, R. Zerbes, M. von Radloff, E.U. Kaußmann, G. Eckhardt, Liebigs Ann. Chem. (1974) 1915–1928;
(c) C. Auvin, F. Lezenven, A. Blond, I. Augeven-Bour, L. J-Pousette, B. Bodo, J. Nat. Prod. 59 (1996) 676–678.
[7] E. Dumdei, R.J. Andersen, J. Nat. Prod. 56 (1993) 792–794.
[8] (a) M.R. Rao, D.J. Faulkner, J. Nat. Prod. 67 (2004) 1064–1066;
(b) M.J. McKay, A.R. Carroll, R.J. Quinn, J. Nat. Prod. 68 (2005) 1776–1778;
(c) C.J. Heinrich, R.W. Robey, K. Takada, H.R. Bokesch, S.E. Bates, S. Shukla, S.V. Ambudkar, J.B. McMahon, K.R. Gustafson, ACS Chem. Biol. 4 (2009) 637–647;
(d) K. Takada, N. Imamura, K.R. Gustafson, C.J. Heinrich, Bioorg. Med. Chem. Lett. 20 (2010) 1330–1333;
(e) L.A. McDonald, J.C. Swersey, C.M. Ireland, A.R. Carroll, J.C. Coll, B.F. Bowden, C.R. Fairchild, L. Cornell, Tetrahedron 51 (1995) 5237–5244.
[9] L.J. Gooßen, M. Blanchot, M. Arndt, K.S.M. Salih, Synlett (2010) 1685–1687.
[10] (a) A.R. Katritzky, B. Rachwal, S. Rachwal, J. Org. Chem. 60 (1995) 3993–4001;
(b) C.A. Zezza, M.B. Smith, J. Org. Chem. 53 (1988) 1161–1167;
(c) L.E. Overman, L.A. Clizbe, J. Am. Chem. Soc. 98 (1976) 2352–2354;
(d) P.J. Stevenson, I. Graham, ARKIVOC 7 (2003) 139–144.
[11] C. Gaulon, R. Dhal, T. Chapin, V. Maisonneuve, G. Dujardin, J. Org. Chem. 69 (2004) 4192–4202.
[12] G.J. Roff, R.C. Lloyd, N.J. Turner, J. Am. Chem. Soc. 126 (2004) 4098–4099.
[13] C.E. Wilians, C.A. Mulder, J.G. de Vries, H.M. de Vries, J. Organomet. Chem. 687 (2003) 494–497.
[14] R. Matsubara, Y. Nakamura, S. Kobayashi, Angew. Chem. 116 (2004) 1711–1713; Angew. Chem. Int. Ed. 43(2004) 1679–1681.
[15] (a) T. Sell, A. Meiswinkel, G. Mehler, M.T. Reetz, Tetrahedron Lett. 43 (2002) 7941–7943;
(b) M. van den Berg, A.J. Minnaard, R.M. Haak, M. Leeman, E.P. Schudde, A. Meetsma, B.L. Feringa, H.M. de Vries, E.P. Maljaars, C.E. Wilians, D. Hyett, A.F. Boogers, J.W. Hendricks, J.G. de Vries, Adv. Synth. Catal. 345 (2003) 308–323.
[16] W. Adam, S.G. Bosio, N.J. Turro, J. Org. Chem. 69 (2004) 1704–1715.
[17] (a) M. Brasholz, H.-U. Reißig, R. Zimmer, Acc. Chem. Res. 42 (2009) 45–56;
(b) O. Fögel, J. Dash, I. Brüdgam, H. Hartl, H.-U. Reißig, Chem. Eur. J. 10 (2004) 4283–4290.
[18] (a) R. Brettle, A.J. Mosedale, J. Chem. Soc. Perkin Trans. 1 (1988) 2185–2195;
(b) K. Kuramochi, H. Watanabe, T. Kitahara, Synlett (2000) 397–399.
[19] D. Ager, Synthesis (1984) 384–398.
[20] (a) L. Jiang, G.E. Job, A. Klapars, S.L. Buchwald, Org. Lett. 5 (2003) 3667–3669;
(b) D.J. Wallace, D.J. Klauber, C.-Y. Chen, R.P. Volante, Org. Lett. 5 (2003) 4749–4752;
(c) C. Han, R. Shen, S. Su, J.A. Porco Jr., Org. Lett. 6 (2004) 27–30;
(d) X. Pan, Q. Cai, D. Ma, Org. Lett. 6 (2004) 1809–1812;
(e) J.L. Brice, J.E. Meerdink, S.S. Stahl, Org. Lett. 6 (2004) 1845–1848;
(f) A. Klapars, K.R. Campos, C. Chen, R.P. Volante, Org. Lett. 7 (2005) 1185–1188;
(g) Y. Bolshan, R.A. Batey, Angew. Chem. 120 (2008) 2139–2142;
Angew. Chem., Int. Ed. 47 (2008) 1–5.
[21] (a) L.J. Gooßen, N. Rodríguez, K. Gooßen, Angew. Chem. Int. Ed. 47 (2008) 3100–3120;
(b) L.J. Gooßen, A. Dohring, Adv. Synth. Catal. 345 (2003) 943–947;
(c) L.J. Gooßen, J. Paetzold, L. Winkel, Synlett (2002) 1721–1723;
(d) L.J. Gooßen, L. Winkel, A. Döhring, Ghosh, J. Paetzold, Synlett (2002) 1237–1240.
[22] (a) T.-A. Mitsudo, Y. Hori, Y. Watanabe, J. Org. Chem. 50 (1985) 1566–1568;
(b) H. Doucet, N. Derrien, Z. Kabouche, C. Bruneau, P.H. Dixneuf, J. Organomet. Chem. 551 (1997) 151–157;
(c) L.J. Gooßen, J. Paetzold, D. Koley, Chem. Commun. (2003) 706–707;
(d) F. Pohlki, S. Doye, Chem. Soc. Rev. 32 (2003) 104–114;
(e) R. Severin, S. Doye, Chem. Soc. Rev. 36 (2007) 1407–1420;
(f) F. Alonso, I.P. Beletskaya, M. Yus, Chem. Rev. 104 (2004) 3079–3159;
(g) C. Bruneau, P.H. Dixneuf, Angew. Chem. 118 (2006) 2232–2260;
Angew. Chem. Int. Ed. 45 (2006) 2176–2203.
[23] L.J. Gooßen, J.E. Rauhaus, G. Deng, Angew. Chem. 117 (2005) 4110–4113;
Angew. Chem. Int. Ed. 44 (2005) 4042–4045.
[24] L.J. Gooßen, M. Arndt, M. Blanchot, F. Rudolphi, F. Menges, G. Niedner-Schatteburg, Adv. Synth. Catal. 350 (2008) 2701–2707.
[25] L.J. Gooßen, M. Blanchot, C. Brinkmann, K. Gooßen, R. Karch, A. Rivas-Nass, J. Org. Chem. 71 (2006) 9506–9509.
[26] L.J. Gooßen, M. Blanchot, K.S.M. Salih, R. Karch, A. Rivas-Nass, Org. Lett. 10 (2008) 4497–4499.
[27] (a) L.J. Gooßen, K.S.M. Salih, M. Blanchot, Angew. Chem. 120 (2008) 8620–8623;
Angew. Chem. Int. Ed. 47 (2008) 8492–8495;
(b) L.J. Gooßen, M. Blanchot, K.S.M. Salih, K. Gooßen, Synthesis (2009) 2283–2288.
[28] M. Toumi, F. Couty, G. Evano, J. Org. Chem. 73 (2008) 1270–1281.

Annette Buba was born in 1986 in Ratibor, Poland. In 2005, she started to study chemistry at Universität des Saarlandes. After one year she continued her study at the TU Kaiserslautern. In october 2009, she joined the group of L.J. Gooßen for her diploma research on the *Z-selective Hydroamidation of alkynes*.

Prof. Dr. Lukas J. Gooßen, born 1969 in Bielefeld/Germany, studied chemistry at Universität Bielefeld/University of Michigan, conducted his diploma work with K.P.C. Vollhardt, UC Berkeley and his PhD research with W.A. Herrmann, TU München. After a postdoctoral stay with K.B. Sharpless, Scripps Research Institute and a position as a head of laboratory at Bayer AG, he started his academic career at MPI für Kohlenforschung in the group of M.T. Reetz (2000–2003). In 2004, he moved to RWTH Aachen as a Heisenberg fellow, and in 2005, he was appointed professor at TU Kaiserslautern.

Matthias Arndt was born in 1983 in Koblenz, Germany. In 2003, he started to study chemistry at the TU Kaiserslautern. In 2007 he attended to the Sokrates/Erasmus exchange program and studied at the University of Glasgow for 3 months. In 2008 he joined the group of L.J. Gooßen, finished his diploma work in the same year and started with his PhD research on the *Mechanistic Investigation of Hydroamidation Reactions*.

IV.1.3. Naturstoffsynthese mittels Hydroamidierung terminaler Alkine

Die Ruthenium-katalysierte Hydroamidierung terminaler Alkine ist eine hocheffiziente Methode zur Darstellung einer Vielzahl von Enamiden und Enimiden (vergleiche Kapitel II.2). Je nach verwendetem Katalysatorsystem kann selektiv das *E*- oder *Z*-konfigurierte Enamid aus identischen Alkin- und Amidbaustein zugänglich gemacht werden. In bisherigen Arbeiten stand die Entwicklung der Katalysatorsysteme im Vordergrund. Jede neue Hydroamidierungsmethode wurde auf ihre Anwendungsbreite hin untersucht. Dabei wurden jedoch meist einfache Substrate mit verschiedenen funktionellen Gruppen einer Hydroamidierungsreaktion unterzogen. Unter den Anwendungsbeispielen aus den Veröffentlichungen waren zwar bereits erste strukturell einfache Naturstoffe (Lansiumamid A und Alatamid) und ein wichtiges Intermediat für Castedo's Totalsynthese von Aristolactam,[39] aber es konnte noch nicht hinreichend belegt werden, dass sich die Hydroamidierung zur Synthese komplexer Moleküle eignet, wie z. B. der Totalsynthese von Botryllamiden. Die nachfolgende Veröffentlichung und das darauffolgende Unterkapitel beschreiben die Ergebnisse der Naturstoffsynthese mittels Hydroamidierung terminaler Alkine.

Dieses Projekt wurde in Kooperation mit Dr. Mathieu Blanchot und Dr. Kifah S. M. Salih durchgeführt. Die Naturstoffe Lansiumamid A und B (**Syn-3** und **Syn-4**), Lansamid I (**Syn-6**) sowie Botryllamid C und E (**Syn-11a** und **Syn-11a**) und alle benötigten Startmaterialien wurden in Zusammenarbeit mit Dr. Mathieu Blanchot synthetisiert, vollständig charakterisiert und veröffentlicht. Die Startmaterialien für die Synthese von Coscinamid A und B (**IV.1-1** und **IV.1-2**) sowie Chondriamid A und C (**IV.1-4** und **IV.1-4**) wurden zusammen mit Dr. Kifah S. M. Salih hergestellt und gemeinsam deren Umsetzung in Hydroamidierungs-reaktionen getestet.

Ausgehend von bisherigen Erfahrungen bezüglich der Anwendungsbreite und Gruppentoleranz bestehender Hydroamidierungsverfahren wurden zehn Naturstoffe als mögliche Zielverbindungen identifiziert (Abbildung 3).

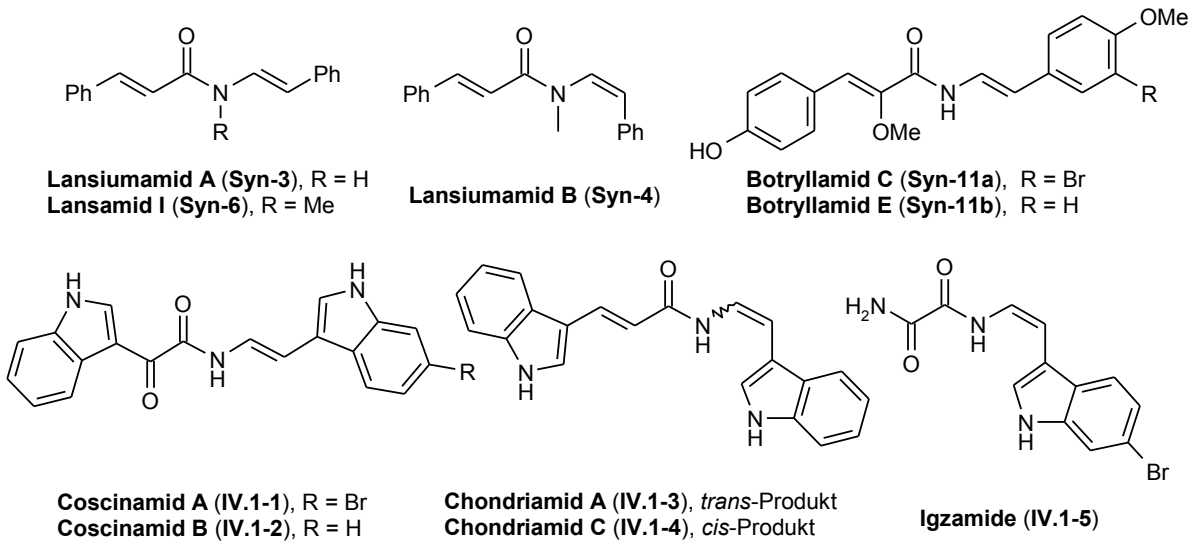

Abbildung 3. Zielverbindungen für Naturstoffsynthese mittels Hydroamidierung terminaler Alkine.

Lansiumamide A und B (**Syn-3** und **Syn-4**), sowie Lansamid I (**Syn-6**) können aus kommerziell erhältlichen Phenylacetylen und Zimtsäureamid synthetisiert werden. Für alle anderen dargestellten Naturstoffe mussten die Alkin- und die Amid-Einheit erst synthetisiert werden, um die Hydroamdierung zu den gewünschten Naturstoffen testen zu können.

Synthese von Botryllamiden und Lansiumamiden mittels Ruthenium-katalysierter Hydroamidierung terminaler Alkine

Synthesis of Botryllamides and Lansiumamides via Ruthenium-Catalyzed Hydroamidation of Alkynes

Lukas J. Gooßen,* Mathieu Blanchot, Matthias Arndt, Kifah S. M. Salih

Institut für Organische Chemie, TU Kaiserslautern, Erwin-Schrödinger-Str., Building 54, 67663 Kaiserslautern, Germany
Fax +49(631)2053921; E-mail: goossen@chemie.uni-kl.de

Received 26 March 2010

In memory of Keith Fagnou

Abstract: Ruthenium-catalyzed hydroamidations of alkynes allow a concise synthetic entry to both *E*- and *Z*-configured enamide natural products. This was demonstrated by the synthesis of botryllamides C and E, lansiumamides A and B, and lansamide I in 1–3 steps and 57–98% yield from simple, commercially available precursors.

Key words: alkyne, botryllamide, hydroamidation, lansamide, lansiumamide, ruthenium

The enamide group is a substructure widely present in natural products with interesting biological activities,[1] as well as fungicides,[2] metabolic drugs,[3] and functional materials.[4] Traditional synthetic entries to this substructure, for example, condensation reactions, require harsh reaction conditions and are usually not stereoselective.[5] Metal-catalyzed coupling reactions offer much milder reaction conditions but suffer from the limited availability of the vinylic precursors, for example, vinyl halides or pseudohalides.[6] Based on pioneering studies by Watanabe[7] and inspired by catalytic additions of other nucleophiles to alkynes,[8,9] we have recently developed ruthenium-catalyzed hydroamidation reactions that allow the *anti*-Markovnikov addition of various N–H nucleophiles to terminal alkynes under selective formation of either *E*- or *Z*-configured enamide derivatives (Scheme 1).[10]

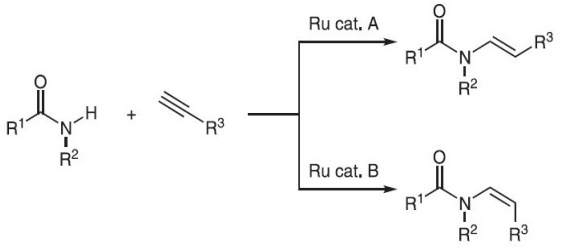

Scheme 1 Hydroamidation of amides and terminal alkynes

The preparative utility of this synthetic strategy has so far been demonstrated only using rather simple model substrates. Based on the encouraging results obtained in these studies, we decided to take the next hurdle and probe the applicability of this methodology in the context of the synthesis of more complex structures, namely lansiumamides, lansamides, and botryllamides (Figure 1).

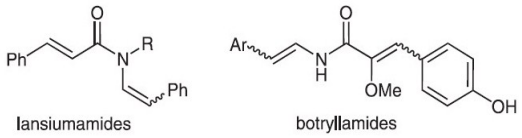

Figure 1 Structures of lansiumamides and botryllamides

Lansiumamides including lansiumamides A and B, and lansamide I have been isolated from the leaves and fruits of *Clausena lansium*, a plant used in traditional chinese medicine for the treatment, for example, of asthma and viral hepatitis.[11] Total syntheses have been reported by Taylor[11b] (4 steps, 8–28% overall yield) and Maier[11d] (5 steps, 11–12% overall yield). Taylor generated the enamide moiety by adding vinylmagnesium reagents to isocyanates obtained via Curtius rearrangement of acyl azides. Maier et al. employed various methods to condense aldehydes with amides. In all the above syntheses, the enamides were obtained as mixtures of *E*- and *Z*-isomers in the key step.

Botryllamides were first isolated from the marine ascidian *Botryllus tyreus* as a complex mixture of ten structurally closely related derivatives.[12] They display activity as selective inhibitors of the ABCG2 multidrug transporter.[12c] While some of them have previously been prepared using traditional methods for enamide synthesis (4 steps, 20% yield),[12d] there are no published syntheses of botryllamides C and E.

The synthesis of the above compounds can greatly be simplified when employing Ru-catalyzed hydroamidation reactions to access the enamide moiety. The key advantage of this strategy is that the stereoselectivity of the reaction is controlled by the catalyst system, so that both (*E*)- and (*Z*)-enamide products can selectively be synthesized from the same, easily accessible amide and alkyne starting materials.

Lansiumamide A (**3**) is thus accessible in a single step from commercially available phenylacetylene (**2**) and cinnamide (**1**) in the presence of a ruthenium catalyst (Scheme 2). We tested various catalyst systems and found that this transformation is most effectively promoted by a bimetallic catalyst generated in situ from bis(2-methallyl)cycloocta-1,5-diene-ruthenium(II), 1,4-bis(dicyclo-

SYNLETT 2010, No. 11, pp 1685–1687
Advanced online publication: 04.06.2010
DOI: 10.1055/s-0029-1219961; Art ID: G10310ST

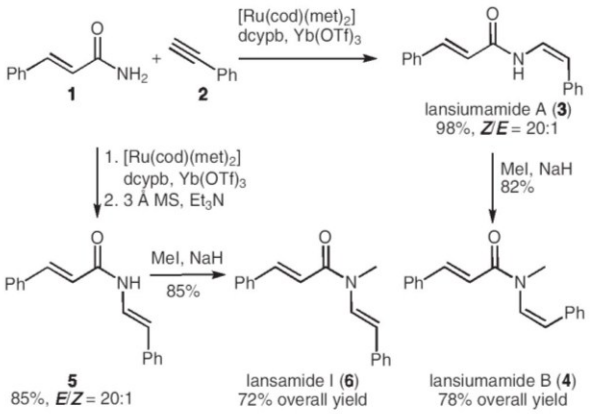

Scheme 2 Syntheses of lansiumamides A and B and lansamide I

hexylphosphino)butane (dcypb), and ytterbium triflate [$Yb(OTf)_3$] in a DMF–water mixture. Within six hours, the desired lansiumamide A (**3**) is formed in 98% yield and a *Z*/*E* ratio of 20:1.[10c] Methylation of **3** according to Maier's protocol[11d] gave lansiumamide B (**4**) in 82% yield. Lansamide I (**6**) was synthesized from the same starting materials using the *E*-selective protocol, in which a hydroamidation under the above conditions is combined with an in situ double-bond isomerization (Scheme 2). This way, the (*E*)-enamide **5** was obtained in 85% yield and an *E*/*Z* ratio in excess of 20:1. The methylation proceeded in 85% yield, so that overall, lansamide I (**6**) was obtained in 72% yield over two steps (Scheme 2).

The hydroamidation strategy was similarly effective for the preparation of botryllamides C and E (**11a**,**b**). In both

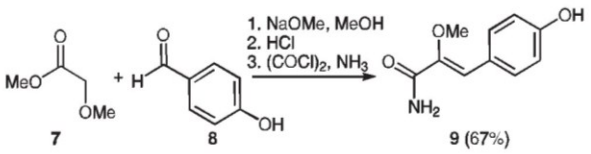

Scheme 3 Synthesis of amide **9**

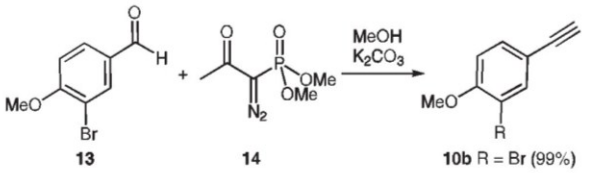

Scheme 4 Synthesis of alkyne **10b**

syntheses, the same primary amide **9** was required. It was obtained via an aldol condensation from commercially available methyl 2-methoxyacetate (**7**) and 4-hydroxybenzaldehyde (**8**). The resulting ester was saponified in situ and converted into the corresponding primary amide **9** in an overall 67% yield (Scheme 3). Its structure was confirmed by X-ray crystal-structure analysis.[13]

Amide **9** was then treated with commercially available 4-methoxyphenylacetylene (**10a**) using the *E*-selective hydroamidation protocol to give botryllamide E (**11a**) in excellent yield (85%, *E*/*Z* = 20:1). We also synthesized the *Z*-configured isomer (**12a**, 98%, *Z*/*E* = 9:1) using the complementary hydroamidation protocol (Scheme 5).

This isomer is sensitive to *E*/*Z*-isomerization under formation of the thermodynamically favored botryllamide E (**11a**). It is thus conceivable that **12a** is also present in *Botryllus tyreus* but isomerizes quantitatively during the isolation procedure. The structure of this unnatural *Z*-configured enamide **12a** was confirmed by X-ray structure analysis (Figure 2).[14]

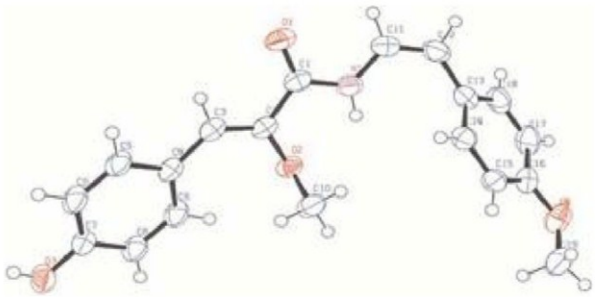

Figure 2 X-ray structure of enamides **12a**

The synthesis of botryllamide C (**11b**) was carried out analogously using the brominated phenylacetylene derivative **10b** (Scheme 4). This was synthesized in near-quantitative yield from 3-bromo-4-methoxybenzaldehyde (**13**) via a Bestmann–Ohira reaction.[15]

Again, the hydroamidation proceeded smoothly, and both the *Z*-configured enamide **12b** (88%, *Z*/*E* = 9:1) and the *E*-configured botryllamide C (**11b**, 88%, *E*/*Z* = 20:1) were obtained in high yields and selectivities (Scheme 5).

In conclusion, short and concise syntheses of lansiumamides A and B, lansamide I, as well as botryllamides C and E are possible using ruthenium-catalyzed hydroamidation reactions. Moreover, the sensitive *Z*-isomers of the

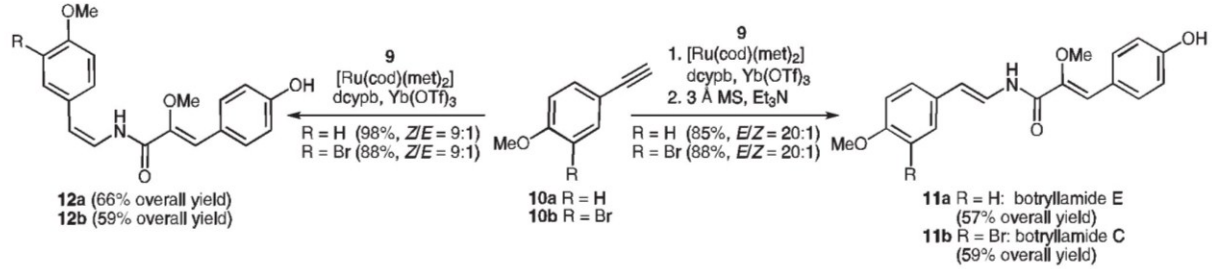

Scheme 5 Synthesis of botryllamides E and C

botryllamides are also accessible in high selectivity. This opens up new opportunities for the investigation of structure–activity relations for this biologically active substrate class.[12c,d]

Hydroamidation of Alkynes

An oven-dried flask was charged with the primary amide **1** or **9** (1.00 mmol), bis(2-methallyl)-cycloocta-1,5-diene-ruthenium(II) (16.0 mg, 0.05 mmol), 1,4-bis(dicyclohexylphosphinobutane (27.0 mg, 0.06 mmol), and ytterbium triflate (24.8 mg, 0.04 mmol) and flushed with nitrogen. Subsequently, dry DMF (3.0 mL), alkyne **2**, **10a**, or **10b** (2.00 mmol), and H_2O (108 μL, 6.00 mmol) were added via syringe. The resulting solution was stirred for 6 h at 60 °C. To access the (*Z*)-enamides, the reaction was worked up at this stage as detailed below. To obtain the (*E*)-enamides, 3 Å MS (500 mg) and Et_3N (200 μL) were added to the reaction mixture, and stirring was continued for 24 h at 110 °C.

For the workup, the reaction mixtures were poured into aq $NaHCO_3$ (30 mL). The resulting mixture was extracted with EtOAc (3 × 20 mL), the combined organic layers were washed with H_2O (20 mL) and brine (20 mL), dried over $MgSO_4$, filtered, and the volatiles were removed in vacuo. The residue was purified by column chromatography (silica gel, EtOAc–hexane gradient). The identity and purity of the enamide products were confirmed by ^1H NMR and ^{13}C NMR spectroscopy.

Supporting Information for this article is available online at http://www.thieme-connect.com/ejournals/toc/synlett. Included are complete experimental procedures and analytical data for compounds **3**–**6**, **9**, **10b**, **11**, and **12**.

Acknowledgment

We thank the Deutsche Forschungsgemeinschaft for financial support and Umicore AG for generous donation of [Ru(cod)(met)$_2$], the Landesgraduiertenförderung Rheinland Pfalz and Deutscher Akademischer Austauschdienst for scholarships to M.A. and K.S.M.S.

References and Notes

(1) (a) Kohno, J.; Koguchi, Y.; Nishio, M.; Nakao, K.; Kuroda, M.; Shimizu, R.; Ohnuki, T.; Komatsubara, S. *J. Org. Chem.* **2000**, *65*, 990. (b) Kunze, B.; Jansen, R.; Höfle, G.; Reichenbach, H. *J. Antibiot.* **1994**, *47*, 881. (c) Ghosh, S.; Datta, D. B.; Sen, N. *Synth. Commun.* **1987**, *17*, 299. (d) Maxwell, A.; Rampersad, D. *J. Nat. Prod.* **1989**, *52*, 411. (e) Estévez, J. C.; Villaverde, M. C.; Estévez, R. J.; Seijas, J. A.; Castedo, L. *Synth. Commun.* **1990**, *20*, 503.

(2) Toske, S. G.; Jensen, P. R.; Kaufman, C. A.; Fenical, W. *Tetrahedron* **1998**, *54*, 13459.

(3) Han, Y. N.; Kim, G.-Y.; Han, H. K.; Han, B. H. *Arch. Pharmacol. Res.* **1993**, *16*, 289.

(4) Yet, L. *Chem. Rev.* **2003**, *103*, 4283.

(5) (a) Dupau, P.; Le Gendre, P.; Bruneau, C.; Dixneuf, P. H. *Synlett* **1999**, 1832. (b) Wang, X.; Porco, J. A. Jr. *J. Org. Chem.* **2001**, *66*, 8215. (c) Bayer, A.; Maier, M. E. *Tetrahedron* **2004**, *60*, 6665. (d) Boeckman, R. K. Jr.; Goldstein, S. W.; Walters, M. A. *J. Am. Chem. Soc.* **1988**, *110*, 8250. (e) Kinderman, S. S.; van Maarseveen, J. H.; Schoemaker, H. E.; Hiemstra, H.; Rutjes, F. P. J. T. *Org. Lett.* **2001**, *3*, 2045.

(6) (a) Pa, X.; Cai, Q.; Ma, D. *Org. Lett.* **2004**, *6*, 1809. (b) Wallace, J.; Klauber, D. J.; Chen, C.; Volante, R. P. *Org. Lett.* **2003**, *5*, 4749. (c) Brice, J. L.; Meerdink, J. E.; Stahl, S. *Org. Lett.* **2004**, *6*, 1845.

(7) Kondo, T.; Tanaka, A.; Kotachi, S.; Watanabe, Y. *J. Chem. Soc., Chem. Commun.* **1995**, 413.

(8) For addition reactions of other hydrogen-bonded nucleophiles to alkynes, see: (a) Mitsudo, T.-A.; Hori, Y.; Watanabe, Y. *J. Org. Chem.* **1985**, *50*, 1566. (b) Doucet, H.; Derrien, N.; Kabouche, Z.; Bruneau, C.; Dixneuf, P. H. *J. Organomet. Chem.* **1997**, *551*, 151. (c) Gooßen, L. J.; Paetzold, J.; Koley, D. *Chem. Commun.* **2003**, 706. (d) Pholki, F.; Doye, S. *Chem. Soc. Rev.* **2003**, *32*, 104. (e) Beller, M.; Seayad, J.; Tillack, A.; Jiao, H. *Angew. Chem. Int. Ed.* **2004**, *43*, 3368; *Angew. Chem.* **2004**, *116*, 3448. (f) Tokunaga, M.; Suzuki, T.; Koga, N.; Fukushima, T.; Horiuchi, A.; Wakatsuki, Y. *J. Am. Chem. Soc.* **2001**, *123*, 11917. (g) Hashmi, A. S. K.; Hutchings, G. J. *Angew. Chem. Int. Ed.* **2006**, *45*, 7896; *Angew. Chem.* **2006**, *118*, 8064.

(9) For recent reviews, see: (a) Alonso, F.; Beletskaya, I. P.; Yus, M. *Chem. Rev.* **2004**, *104*, 3079. (b) Bruneau, C.; Dixneuf, P. H. *Angew. Chem. Int. Ed.* **2006**, *45*, 2176; *Angew. Chem.* **2006**, *118*, 2232.

(10) (a) Gooßen, L. J.; Rauhaus, J. E.; Deng, G. *Angew. Chem. Int. Ed.* **2005**, *44*, 4042; *Angew. Chem.* **2005**, *117*, 4110. (b) Gooßen, L. J.; Blanchot, M.; Brinkmann, C.; Gooßen, K.; Karch, R.; Rivas-Nass, A. *J. Org. Chem.* **2006**, *71*, 9506. (c) Gooßen, L. J.; Salih, K. S. M.; Blanchot, M. *Angew. Chem. Int. Ed.* **2008**, *47*, 8492; *Angew. Chem.* **2008**, *120*, 8620. (d) Gooßen, L. J.; Arndt, M.; Blanchot, M.; Rudolphi, F.; Menges, F.; Niedner-Schatteburg, G. *Adv. Synth. Catal.* **2008**, *350*, 2701. (e) Gooßen, L. J.; Blanchot, M.; Salih, K. S. M.; Gooßen, K. *Synthesis* **2009**, 2283. (f) Gooßen, L. J.; Blanchot, M.; Salih, K. S. M.; Karch, R.; Rivas-Nass, A. *Org. Lett.* **2008**, *10*, 4497.

(11) Isolation: (a) Lin, J.-H. *Phytochemistry* **1989**, *28*, 621; and references cited therein. Synthesis: (b) Stefanuti, I.; Smith, S. A.; Taylor, R. J. K. *Tetrahedron Lett.* **2000**, *41*, 3735. (c) Fürstner, A.; Brehm, C.; Cancho-Grande, Y. *Org. Lett.* **2001**, *3*, 3955. (d) Bayer, A.; Maier, M. E. *Tetrahedron* **2004**, *60*, 6665.

(12) (a) Rao, M. R.; Faulkner, D. J. *J. Nat. Prod.* **2004**, *67*, 1064. (b) McKay, M. J.; Carroll, A. R.; Quinn, R. J. *J. Nat. Prod.* **2005**, *68*, 1776. (c) Henrich, C. J.; Robey, R. W.; Takada, K.; Bokesch, H. R.; Bates, S. E.; Shukla, S.; Ambudkar, S. V.; McMahon, J. B.; Gustafson, K. R. *ACS Chem. Biol.* **2009**, *4*, 637. (d) Takada, K.; Imamura, N.; Gustafson, K. R.; Henrich, C. J. *Bioorg. Med. Chem. Lett.* **2010**, *20*, 1330. (e) McDonald, L. A.; Swersey, J. C.; Ireland, C. M. *Tetrahedron* **1995**, *51*, 5237.

(13) CCDC 768748 contains the supplementary crystallographic data for this paper. These data can be obtained free of charge from The Cambridge Crystallographic Data Centre via www.ccdc.cam.ac.uk/data_request/cif.

(14) CCDC 768747 contains the supplementary crystallographic data for this paper. These data can be obtained free of charge from The Cambridge Crystallographic Data Centre via www.ccdc.cam.ac.uk/data_request/cif.

(15) (a) Ohira, S. *Synth. Commun.* **1989**, *19*, 561. (b) Müller, S.; Liepold, B.; Roth, G. J.; Bestmann, H. J. *Synlett* **1996**, 521. (c) Roth, G. J.; Liepold, B.; Müller, S. G.; Bestmann, H. J. *Synthesis* **2004**, 59. (d) For the synthesis of the Bestmann–Ohira reagent 14, see: Pietruszka, J.; Witt, A. *Synthesis* **2006**, 4266.

Hydroamidierungsexperimente mit 3-Ethinylindolen

Nach der erfolgreichen Synthese von Botryllamid C und E (**Syn-11a** und **Syn-11b**), Lansiumamid A und B (**Syn-3** und **Syn-4**) sowie Lansamid I (**Syn-6**) sollten als nächstes die Synthesen der Indol-substituierten Naturstoffe Coscinamid A und B (**IV.1-1** und **IV.1-2**), Chondriamid A und C (**IV.1-3** und **IV.1-4**) sowie Igzamid (**IV.1-5**) durchgeführt werden.

Einen ersten gangbaren, aber auch aufwendigen Zugang zu allen fünf Naturstoffen konnte von Kuramochi *et al.* entwickelt werden.[40] Die Synthese beinhaltet als Schlüsselschritte eine Curtius-Umlagerung sowie eine Acylierung von Alkenylcarbamaten und liefert die entsprechenden Naturstoffe in 5 bis 6 Stufen in Gesamtausbeuten von 4-46%.

Der in Schema 13 dargestellte retrosynthetische Ansatz zur Darstellung der Zielverbindungen verdeutlicht, dass die Ruthenium-katalysierte Hydroamidierung einen direkten und hundert Prozent atomökonomischen Zugangsweg zu den Naturstoffen eröffnen würde.

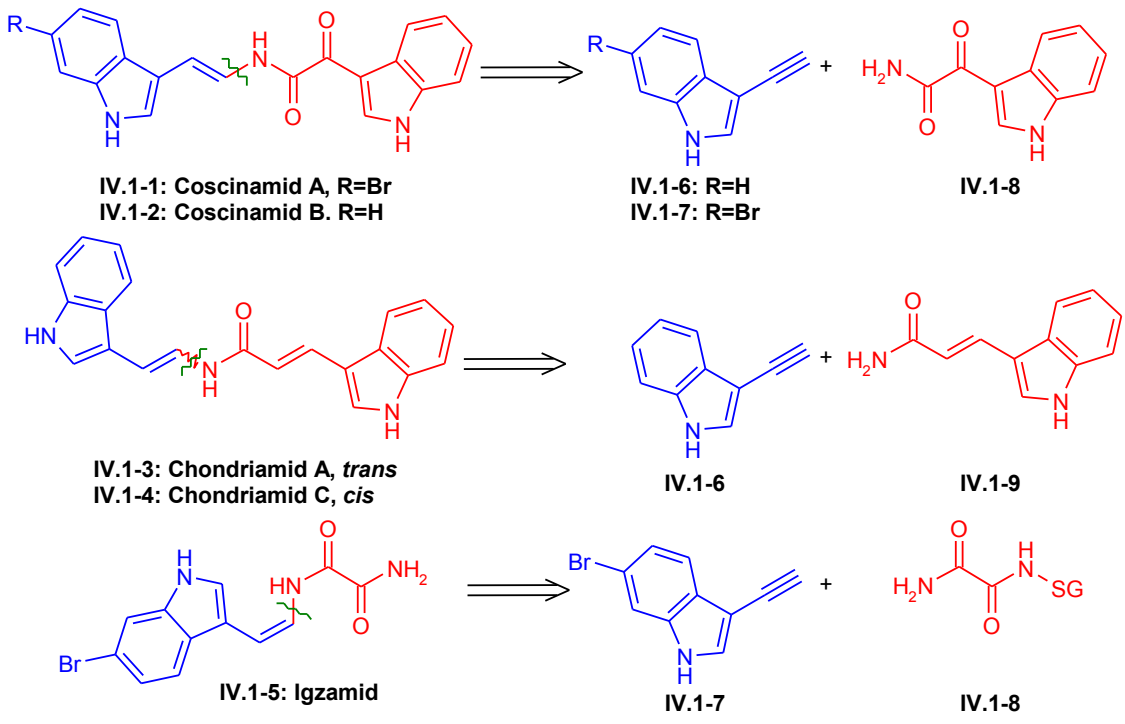

Schema 13. Retrosynthetischer Ansatz zur Darstellung von Coscinamid A und B, Chondriamid A und C sowie Igzamid durch Hydroamidierung von 3-Ethinylindolen (IV.1-6 und IV.1-7).

Da die benötigten Startverbindungen nicht kommerziell erhältlich sind, mussten sie zuerst in ausreichenden Mengen synthetisiert werden, bevor Hydroamidierungsexperimente

durchgeführt werden konnten. Als erstes sollte die Synthese von Coscinamid A und B (**IV.1-1** und **IV.1-2**) getestet werden, da vor allem der Amid-Baustein einfach zugänglich ist.

Die Synthese der benötigten Amid-Einheit (**IV.1-8**) konnte analog zu Schema 14 durchgeführt werden.

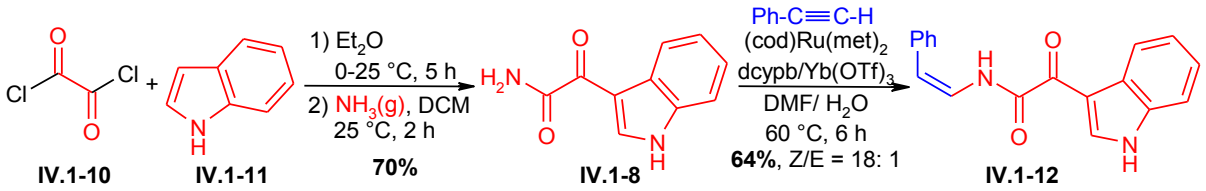

Schema 14. Synthese von Indol-3-glyoxylamid (IV.1-8) und dessen Einsatz in der Hydroamidierung.

Nach der von Garg *et al.* beschriebenen Methode wurde Indol (**IV.1-11**) mit Oxalsäurechlorid (**IV.1-10**) bei Raumtemperatur umgesetzt und anschließend durch Einleiten gasförmigen Ammoniaks in das gewünschte Amid **IV.1-8** umgewandelt.[41] Dieser Reaktionsvorschrift folgend konnte Indol-3-glyoxylamid (**IV.1-8**) auf Anhieb in einer Ausbeute von 70% isoliert und erfolgreich in einem Kontrollexperiment mit Phenylacetylen umgesetzt werden. Unter Standardbedingungen für die Ruthenium-katalysierte Hydroamidierung primärer Amide konnten 64% des *Z*-konfigurierten Additionsprodukt **IV.1-12** erhalten werden.

Die Synthese der benötigten Alkin-Einheiten (**IV.1-6** und **IV.1-7**) erwies sich als deutlich aufwendiger, weil die einzige bekannte Synthese von 3-Ethinylindol (**IV.1-6**) über eine Pyrolyse verläuft, die bei 800 °C in einer speziellen Pyrolyseapparatur durchgeführt werden muss.[42] Da solche Pyrolysepparaturen nicht zur Verfügung standen, wurden zwei allgemeine literaturbekannte Reaktionswege zu funktionalisierten Alkinen geprüft.

Der erste Reaktionsweg verläuft nach einer Vilsmeier-Haack Reaktion. Dabei wird zuerst aus Phosphoroxytrichlorid (**IV.1-13**) und Dimethylformamid bei 0 °C ein reaktives Formylierungsreagenz **IV.1-14** gebildet, das anschließend in α-Stellung zur Carbonyl-Gruppe des Ketons **IV.1-16** angreift. Der dadurch gebildete Chlorvinylaldehyd **IV.1-17** kann unter basischen Bedingungen zu dem entsprechenden Alkin **IV.1-6** umgesetzt werden (Schema 15).[43]

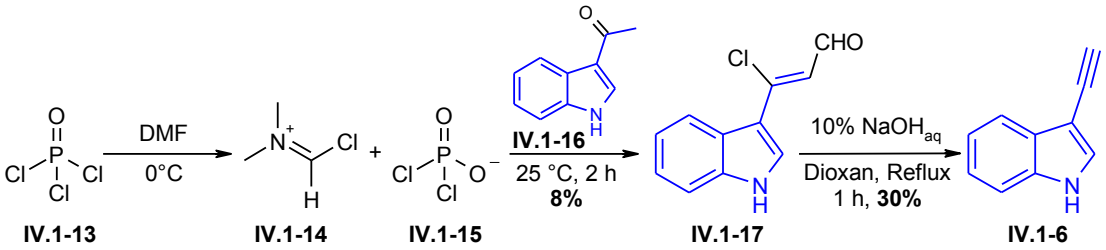

Schema 15. Darstellung von 3-Ethinylindol (IV.1-6) über Vilsmeier-Haack Reaktion.

Nach dieser Methode konnte 3-Ethinylindol (**IV.1-6**) lediglich in einer Ausbeute von weniger als 5% isoliert werden. Besonders die Bildung des Chlorvinylaldehyds **IV.1-17** schien ausgehend von dem Indol-substituierten Keton **IV.1-16** besonders ungünstig zu sein, was sich in unbefriedigenden Ausbeuten von maximal 8% zeigte. Dies scheint daran zu liegen, dass hauptsächlich der elektronenreiche Indol-Rest anstelle der Keto-Gruppe mit dem Formylierungsreagenz **IV.1-14** reagiert und es so anstelle der Bildung des Chlorvinylaldehyds **IV.1-17** zu einer Acylierung des Indol-Substituenten kommt. Das reine, farblose 3-Ethinylindol (**IV.1-6**) erwies sich als sehr temperaturunbeständig und war sogar im Eisfach nicht lange lagerbar, da es zur spontanen Polymerisierung neigte. Da die Ausbeute nicht verbessert werden konnte und somit keine größeren Mengen von 3-Ethinylindol (**IV.1-6**) hergestellt werden konnten, wurde diese Methode verworfen.

Als zweiter Reaktionsweg wurde eine Horner-Wadsworth-Emmons Reaktion unter Verwendung des Bestmann-Ohira-Reagenzes (**IV.1-22**) getestet.[44] Diese besonders milde Methode ermöglicht die Synthese empfindlicher Alkine ausgehend von Aldehyden.

Eine präparativ einfache Synthese des benötigten Bestmann-Ohira-Reagenzes (**IV.1-22**) wurde von Pietruszka *et al.* entwickelt und führt in zwei Stufen mit guten Ausbeuten zum gewünschten Reagenz (Schema 16).[45]

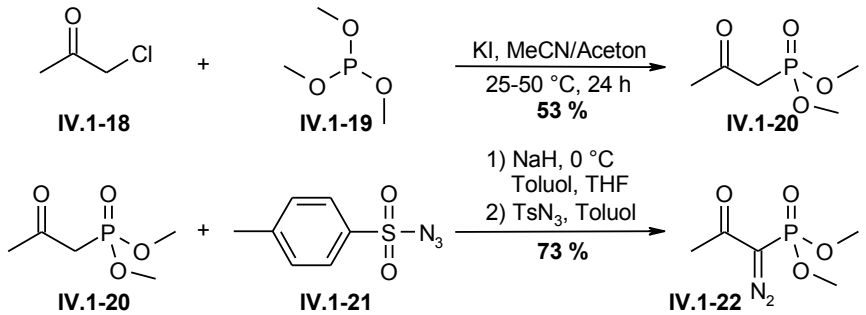

Schema 16. Synthese des Bestmann-Ohira (IV.1-22) Reagenzes nach Pietruszka *et al.*

Die Horner-Wadsworth-Emmons Reaktion des kommerziell erhältlichen, ungeschützten Indol-3-carboxaldehyds (**IV.1-23**) mit Hilfe des Bestmann-Ohira Reagenzes führte nicht zum gewünschten 3-Ethinylindol (**IV.1-6**). Die Deprotonierung der aciden N-H-Gruppe des Indolgerüsts unter den basischen Reaktionsbedingungen führt dazu, dass der anionische Indol-Rest mehr Elektronendichte zur Carbonyl-Gruppe verschieben kann und so die Elektrophilie des Kohlenstoffs verringert wird. Erst nach Einführung einer Tosyl-Schutzgruppe und somit der Verhinderung einer Deprotonierung kann das intermediär gebildete nukleophile Reagenz **IV.1-29** die Carbonyl-Gruppe angreifen. Das entsprechende *N*-Tosyl-3-ethinylindol (**IV.1-25**) konnte in bis zu 42% Ausbeute isoliert werden (Schema 17).

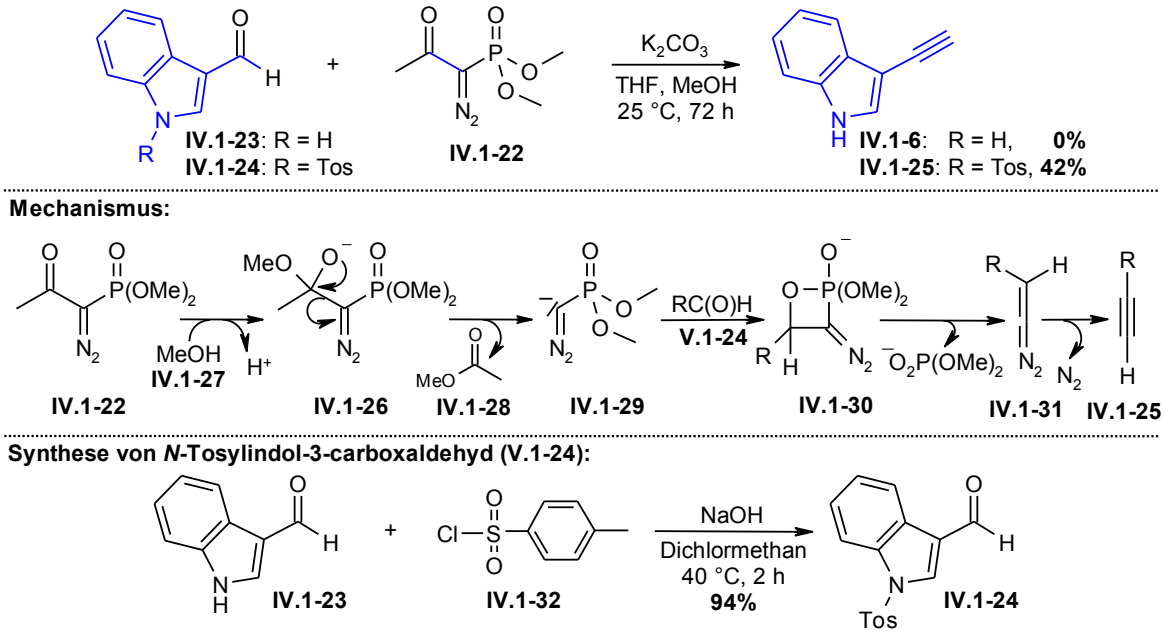

Schema 17. Synthese von *N*-Tosyl-3-Ethinylindol (IV.1-25) durch eine Horner-Wadsworth-Emmons Reaktion.

Nach der erfolgreichen Synthese des Amidbausteins (**IV.1-8**) und des *N*-Tosyl-Alkinbausteins (**IV.1-25**) wurde die Darstellung von Coscinamid B (**IV.1-2**) durch Ruthenium-katalysierte Hydroamidierung getestet (Schema 18).

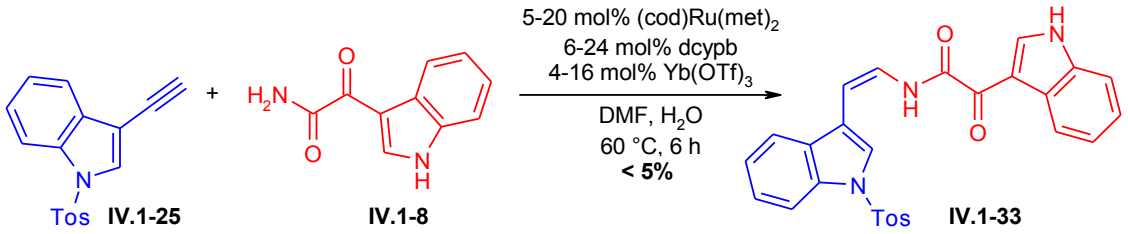

Schema 18. Hydroamidierung von *N*-Tosyl-3-ethinylindol (IV.1-25) und Indol-3-glyoxylamid (IV.1-8).

Die Hydroamidierung von *N*-Tosyl-3-ethinylindol (**IV.1-25**) mit Indol-3-glyoxylamid (**IV.1-8**) führte auch mit deutlich höheren Katalysatorbeladungen von 20 mol% nur in Spuren zum gewünschten *N*-Tosyl-geschützten Coscinamid B (**IV.1-33**), und die Bildung des Produkts konnte einzig durch MALDI-TOF Untersuchungen der Reaktionslösung nachgewiesen werden.

Bestrebungen das Katalysatorsystem für die Hydroamidierung von *N*-Tosyl-3-ethinylindol (**IV.1-25**) zu optimieren waren erfolglos, auch wenn einfachere Amide wie z. B. Benzamid eingesetzt wurden. Scheinbar toleriert das Ruthenium-basierte Katalysatorsystem keine *N*-Tosyl-geschützten Indolalkine, höchstwahrscheinlich wegen der enthaltenen Sulfon-Gruppe. Andere Schutzgruppen konnten nicht in der Hydroamidierung getestet werden, weil die Synthese des entsprechenden Alkins durch eine Horner-Wadsworth-Emmons Reaktion mit anderen Schutzgruppen unmöglich war.

In Hydroamidierungsexperimenten mit freiem 3-Ethinylindol (**IV.1-6**) konnte ebenfalls keine Produktbildung beobachtet werden; stattdessen wurden verschiedene Polymerisierungsprodukte des Indolalkins nachgewiesen. Aufgrund der geringen thermischen Stabilität und hohen Polymerisierungsaktivität von 3-Ethinylindol (**IV.1-6**) scheint eine erfolgreiche Umsetzung des freien Alkins in einer Hydroamidierungsreaktion nicht möglich.

Basierend auf diesen Ergebnisse musste die Synthese Indol-abgeleiteter Naturstoffe durch Ruthenium-katalysierte Hydroamdierung verworfen werden.

IV.2. Direkte Carboxylierung terminaler Alkine mit Kohlenstoffdioxid

Die Forschungsarbeiten bezüglich der Addition von Nukleophilen an Alkine am Beispiel der Ruthenium-katalysierten Hydroamidierung waren sehr erfolgreich und konnten mit der Entwicklung eines neuen Reaktionsmechanismus und eines effizienteren Katalysatorsystems sowie der Darstellung komplexer Naturstoffe abgeschlossen werden. Auf den aus diesen Arbeiten gewonnenen Erfahrungen im Umgang mit Alkinen aufbauend sollte als nächstes die Insertion von Elektrophilen in die terminale C-H Bindung von Alkinen am Beispiel der Münzmetall-katalysierten Carboxylierung terminaler Alkine mit Kohlenstoffdioxid erforscht werden.

IV.2.1. C–H Carboxylierung terminaler Alkine unter CO_2-Normaldruck katalysiert durch geringe Mengen eines Silber(I)/DMSO-Systems

Aufbauend auf den Arbeiten unserer Arbeitsgruppe zur Kupfer(I)-katalysierten Carboxylierung terminaler Alkine mit Kohlenstoffdioxid von Prof. Dr. Nuria Rodríguez Garrido, Diplom-Chemiker Filipe Manjolinho Costa und Dr. Paul P. Lange sowie weiterer literaturbekannter Kupfer- und Silber-katalysierter Carboxylierungsmethoden terminaler Alkine sollten effizientere und kostengünstigere Verfahren entwickelt werden.[31-34]

Die folgende Veröffentlichung beschreibt die Entwicklung einer hocheffizienten Silber/DMSO-katalysierten Methode zur Carboxylierung terminaler Alkine unter CO_2-Normaldruck. Dabei gelang es, die Katalysatorbeladung im Vergleich zu bekannten Verfahren um viele Größenordnungen zu verringern und gleichzeitig ein breites Spektrum terminaler Alkine unter Normaldruck zu den entsprechenden Propiolsäuren umzusetzen. Die verwendete Reaktionsführung ist aus großtechnischer Sichtweise eine deutliche Weiterentwicklung zu bestehenden Methoden, weil eine Umsatzzahl (TON) von mehr als 3000 erzielt werden kann und nur niedrige Reaktionstemperaturen von 50 °C benötigt werden. Schwachpunkt der Methode ist die große Menge an Cäsiumcarbonat (Cs_2CO_3), die benötigt wird, um hohe Umsätze zu erreichen. Die nach der Veröffentlichung durchgeführten Arbeiten hatten daher die Zielsetzung, die teure Base Cs_2CO_3 gegen günstigere Basen zu ersetzen oder eine Möglichkeit zum katalytischen Einsatz einer Base zu entwickeln.

Alle Ergebnisse der nachfolgenden Publikation wurden im Rahmen dieser Doktorarbeit erarbeitet, ausgewertet und veröffentlicht. Die Chemiestudenten Eugen Risto und Thilo Krause unterstützten diese Arbeiten jeweils im Rahmen eines sechswöchigen

Forschungspraktikums, in dem sie unter meiner Betreuung in die Katalysatoroptimierung und die Bestimmung der Anwendungsbreite sowie alle dafür nötigen Arbeitstechniken eingewiesen wurden.

Heterogeneous & Homogeneous & Bio-
CHEMCATCHEM
CATALYSIS

Table of Contents

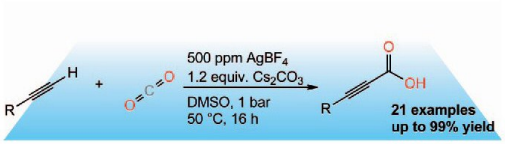

Terminally active: A reaction protocol that permits the C–H carboxylation of alkynes at low temperatures, with mild bases, at ambient CO_2 pressure, in the presence of ppm-quantities of an inexpensive silver catalyst.

CHEMCATCHEM

ChemPubSoc Europe

DOI: 10.1002/cctc.201200047

C–H Carboxylation of Terminal Alkynes Catalyzed by Low Loadings of Silver(I)/DMSO at Ambient CO_2 Pressure

Matthias Arndt, Eugen Risto, Thilo Krause, and Lukas J. Gooßen*[a]

Carbon dioxide is arguably the most attractive C_1 building block for organic synthesis. Dry air contains 0.039% CO_2, and every year, human activity releases 29 billion tons of this greenhouse gas into the atmosphere.[1] It would be desirable to instead utilize at least a small part of the CO_2 for chemical value creation.[2] However, this is a great challenge, owing to its high thermodynamic stability and low reactivity.[3] Traditionally, CO_2 could thus be activated only with reactive organometallic species or strained ring systems.[2]

In the last decades, several catalytic processes for CO_2 fixation have emerged that allow for example, the carboxylation of organometallic reagents, epoxides, the carboxylative cyclization of propargylic amines and alcohols, the reductive carboxylation of alkynes and alkenes, and the hydrosilylation of CO_2 under mild conditions (Scheme 1).[3,4] A substantial advance was recently made in the development of direct C–H carboxylations mediated by coinage metals.[5–7]

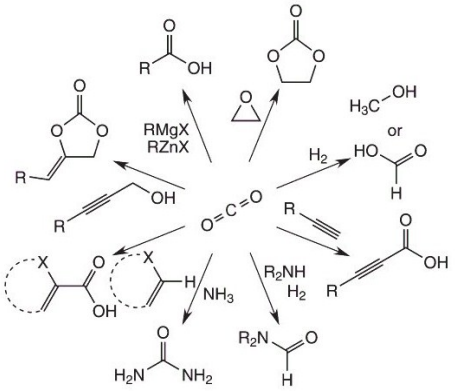

Scheme 1. Overview of direct carboxylation processes.

In 2010, Nolan and co-workers disclosed the first catalytic carboxylations of N–H and C–H bonds in the presence of hydroxide bases to form heterocyclic carboxylic acids.[6] They used copper(I) or gold(I) hydroxides ligated with 1,3-bis(diisopropyl)phenylimidazol-2-ylidene as catalysts.

The problem associated with catalytic carboxylations of terminal alkynes is that the products are thermally so unstable that with most catalysts, high yields can only be obtained when trapping the products by in situ esterification.[8] Our group and that of Zhang disclosed the first catalysts that operate at such low temperatures that the free propiolic acids can be isolated.[9] We employed (4,7-diphenyl-1,10-phenanthroline)bis[tri(4-fluorophenyl)phosphine]-copper(I) nitrate ([Cu^I]) as the catalyst,[9a] and Zhang described the use of *N*-heterocyclic carbene-copper complexes and copper(I) *N,N,N′,N′*-tetramethylethylenediamine complexes (Scheme 2).[9b] Lu et al. recently disclosed a silver(I) iodide-catalyzed protocol.[10] In all three protocols, only mild bases and low reaction temperatures are required.

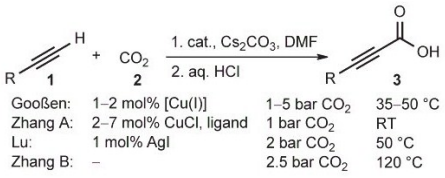

Scheme 2. C–H carboxylation of terminal alkynes.

Both C–H acidic heterocycles[11] and terminal alkynes[12] can be carboxylated also in the absence of a catalyst, but only at substantially higher temperatures and increased CO_2 pressures. As in the metal-catalyzed cases, alkali carbonates, usually Cs_2CO_3, were employed as the base.

The propiolic acids produced in these transformations are valuable synthetic intermediates. They serve as substrates for cycloaddition, hydroarylation and decarboxylative cross-coupling reactions,[13] giving access for example, to coumarins, flavones, aminoalkynes, alkynylarenes, and arylidene-oxindoles.[14] The concept of a C–H carboxylation of terminal alkynes compares favorably with traditional synthetic entries, for example, the addition of alkynes to formaldehyde and subsequent oxidation,[15] the reaction of alkynylmetal species with CO_2 or chloroformate,[16] and the oxidative carbonylation of alkynes.[17] A substantial improvement of catalyst activity, however, is needed before carboxylative C–H activations of alkynes can compete with the established syntheses of arylpropiolic acids on laboratory, and especially on industrial scale.

We herein disclose a reaction protocol that fulfills these requirements by permitting the C–H carboxylation of alkynes at low temperatures, with mild bases, and at ambient CO_2 pressure in the presence of ppm-quantities of an inexpensive silver catalyst.

The carboxylation of 1-octyne (**1a**) was used as a model reaction to systematically study the influence of various parameters on the reaction outcome (Table 1). At ambient CO_2 pres-

[a] *M. Arndt, E. Risto, T. Krause, Prof. Dr. L. J. Gooßen*
FB Chemie - Organische Chemie
TU Kaiserslautern
Erwin-Schrödinger-Str. Geb. 54, 67663 Kaiserslautern (Germany)
Fax: (+49) 631-205-3921
E-mail: goossen@chemie.uni-kl.de

Supporting information for this article is available on the WWW under http://dx.doi.org/10.1002/cctc.201200047.

Table 1. Development of the catalyst system.[a]

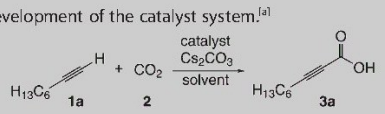

Entry	Catalyst [ppm]	Solvent	Conversion [%]	Yield [%]
1	2500 [Cu^I]	DMF	31	24
2	2500 AgI	DMF	86	82
3	2500 [Cu^I]	DMSO	54	46
4	2500 AgI	DMSO	100	99
5	2500 AgI	MeCN	51	10
6	2500 AgI	PC	64	50
7	2500 AgI	sulfolane	71	65
8	2500 AgI	H_2O	26	0
9[b]	2500 AgI	DMF/DMSO	100	95
10[c]	2500 AgI	DMF/DMSO	93	92
11	1250 Ag_2O	DMSO	100	94
12	2500 $AgNO_3$	DMSO	100	98
13	2500 AgOAc	DMSO	100	96
14	2500 $AgBF_4$	DMSO	100	98
15	5000 [Au^I]	DMSO	9	6
16	500 $AgBF_4$	DMSO	100	99
17	250 $AgBF_4$	DMSO	80	74
18[d]	250 Ag_2O	DMSO	100	98
19	–	DMSO	0	0
20[e]	500 $AgBF_4$	DMSO	100	93
21[f]	500 $AgBF_4$	DMSO	90	83

[a] Reaction conditions: 1-octyne (**1a**, 1.00 mmol), catalyst, Cs_2CO_3 (1.20 mmol), solvent (3.00 mL), 50 °C, 16 h. Yields determined by GC analysis of the α-nonynoic acid hexyl ester (**4a**) generated by treatment of the crude mixture with 1-bromohexane (2.00 mmol), and using *n*-tetradecane as the internal standard. [Cu^I] = (4,7-dichloro-1,10-phenanthroline)-bis(triphenylphosphine) copper(I) nitrate. [Au^I] = chloro[1,3-bis(2,6-diisopropylphenyl) imidazol-2-ylidene]gold(I). PC = propylene carbonate. [b] Solvent ratio 1:1. [c] Solvent ratio 5:1. [d] 1-octyne (**1a**, 10.0 mmol), Cs_2CO_3 (12.0 mmol), catalyst, DMSO (30.0 mL), 50 °C, 16 h, isolated yield. [e] 60 °C. [f] 40 °C.

sure, the performance limit of the copper(I)- or silver(I)-based literature systems was reached when the catalyst loading was reduced to 2500 ppm (entries 1 and 2). The yield could not be improved by variation of the ligand, but we detected a surprisingly strong dependence on the reaction solvent (entries 3–8). Simple copper(I) or silver(I) salts gave high conversions specifically in DMSO as the solvent, or at least a co-solvent (entry 9). At lower DMSO concentrations, the conversion is reduced, indicating that its solvent properties contribute to its beneficial effect (entry 10). A gold(I) complex also showed detectable conversion (entry 15).

The nature of the silver counter-ion was found to have only a limited effect (entries 11–14). The high solubility of $AgBF_4$ allows the preparation of stock solutions useful particularly on small scale. The inexpensive but less soluble silver(I) oxide is advantageous for preparative-scale reactions (entry 18). At 50 °C or above, 500 ppm of silver(I) are sufficient to achieve full conversion in overnight reactions (entries 16, 20, 21), and when reducing the amount to 250 ppm, 80% conversion were still achieved which corresponds to a turnover number of ≈3000 (entry 17). A control experiment revealed that under such mild conditions, C–H carboxylation does not proceed without a metal catalyst (entry 19).

Having thus identified a catalyst system with a new level of efficiency for the carboxylation of alkyl- and aryl-substituted alkynes, we tested the generality of the new protocol by applying it to various terminal alkynes (Table 2). In many cases, full conversion was achieved using 500 ppm of the catalyst within 16 h. For some substrates, especially aryl alkynes, the conversion was incomplete after this time. However, increasing the catalyst loading to 0.25 mol% led to near full conversion also for these substrates. The propiolic acids were isolated in high yields and purity after a simple acidic workup. If desired, alkyl esters can directly be accessed by in situ alkylation. Thus, in method B, 1-bromohexane was added at the end of the reaction. This also allowed isolating ester derivatives of particularly unstable propiolic acids (**3d**, **3g**, and **3r**).

Most functional groups, including halogens, ethers, tertiary amines and trifluoromethyl groups, were tolerated. The isolated yields compare favorably with those previously reported with catalyst loadings of 1–7 mol%.

The unique catalyst performance observed in DMSO, as well as the surprisingly small influence of the silver counter-ion, are best explained by a mechanism in which the catalytically active species is a DMSO-ligated silver(I) carbonate formed in situ from the silver salt, DMSO, and caesium carbonate (Scheme 3). $[Ag(DMSO)_{1\ 2}]^+X$ structures are known to form

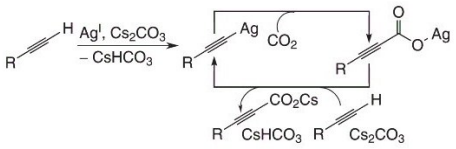

Scheme 3. Proposed reaction mechanism.

upon dissolving silver salts in DMSO.[18] DMSO is known to act as an oxygen donor to Ag^I.[19] The unique efficiency of DMSO as a reaction solvent may partially be explained by the higher solubility of CO_2 in DMSO than in other solvents.[20] There are also several reports that silver nanoparticles form when heating silver salts in DMSO.[21] Although we never observed precipitation of the silver, it cannot be excluded that such silver nanoparticles are involved in the catalytic cycle.

The carboxylation is likely to follow the catalytic cycle proposed by Lu.[10] The reaction of silver salts or nanoparticles with a terminal alkyne is likely to afford a silver acetylide along with caesium bicarbonate.[22] After insertion of CO_2 into the C–Ag bond,[23] caesium propiolate would then be released via salt metathesis with caesium carbonate, regenerating the initial silver species. Further mechanistic studies of this convenient and high-yielding propiolic acid synthesis are underway.

Experimental Section

General procedure for the carboxylation of terminal alkynes (Table 2)

A 10 mL vessel was charged with caesium carbonate (399 mg, 1.20 mmol). Under an atmosphere of carbon dioxide, a solution of

CHEMCATCHEM

ChemPubSoc Europe

Table 2. Carboxylation of terminal alkynes.[a]

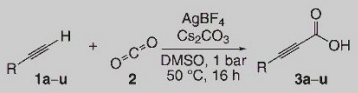

Product	Yield [%]	Product	Yield [%]	Product	Yield [%]
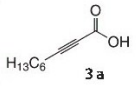 **3a**	**99(94)** 95;[c] 88[e]	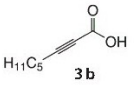 **3b**	**95(99)**	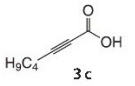 **3c**	**99(97)** 85,[d] 90[f]
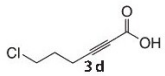 **3d**	**21(52)**[b]	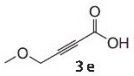 **3e**	**93(83)**[b]	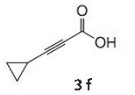 **3f**	**95(97)** 74[e]
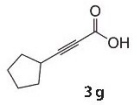 **3g**	**70(99)** 96[e]	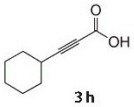 **3h**	**98(93)**	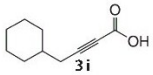 **3i**	**99(97)** 85;[c] 74[e]
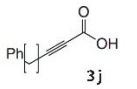 **3j**	**97(99)** 73;[c] 90[e]	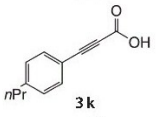 **3k**	**99(91)**[b] 62[c]	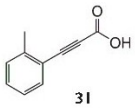 **3l**	**92(99)**[b] 87[c]
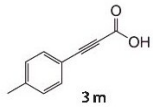 **3m**	**97(96)**[b] 99;[c] 96[f]	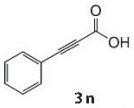 **3n**	**98(91)**[b] 98;[c] 95[f]	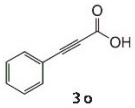 **3o**	**99(96)**[b] 89;[d] 90[f]
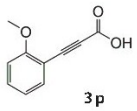 **3p**	**99**[b] 73;[c] 81[d]	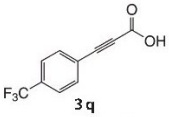 **3q**	**98(99)**[b] 99;[c] 83[e]	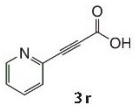 **3r**	**40(92)**[b] 0(75)[c]
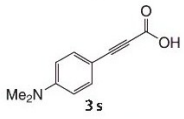 **3s**	**96(95)**[b]	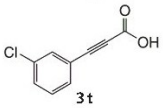 **3t**	**97(99)**[b] 86;[c] 86[d]	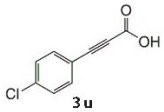 **3u**	**99(96)**[b] 86;[d] 92[f]

[a] Reaction conditions: alkyne **1a–u** (1.00 mmol), $AgBF_4$ (500 ppm), Cs_2CO_3 (1.20 mmol), DMSO (3.00 mL), 50 °C, 16 h; isolated yields. Yields in parentheses correspond to the *n*-hexyl esters **4a–u** generated by treatment of the crude mixture with 1-bromohexane (2.00 mmol). For further details see the Supporting Information. [b] 2500 ppm $AgBF_4$. [c] Isolated yields for method of Gooßen, see Ref. [9a]. [d] Isolated yields for method A of Zhang, see Ref. [9b]. [e] Isolated yields for method of Lu, see Ref. [10]. [f] Isolated yields for method B of Zhang, see Ref. [11].

silver tetrafluoroborate (0.01 mg, 0.50 μmol) in degassed DMSO (3.00 mL) was added, and the mixture was stirred at room temperature for 5 min. After purging the reaction vessel with CO_2, the alkyne **1a–u** (1.00 mmol) was added via syringe. The resulting mixture was stirred for 16 h at 50 °C at ambient CO_2 pressure. At the end of the reaction time, the mixture was cooled down to room temperature and the solvent was removed by lyophilization. The resulting salt was dissolved in H_2O (10.0 mL) and extracted with *n*-hexane (3×20.0 mL). Then the aqueous layer was acidified with aqueous HCl (1N, 2.00 mL) and extracted with ethyl acetate (3× 20.0 mL). The combined organic layers were washed with brine (10.0 mL), dried over $MgSO_4$, filtered and the volatiles were removed under vacuum to afford the corresponding acids **3a–u**.

For full experimental procedures, see the Supporting Information.

Acknowledgements

We thank BASF SE for funding and S. Schäfer, A. W. Jones, C. Matheis, M. Weiland, and S. Brühl for technical support.

Keywords: C–H activation · carbon dioxide fixation · catalysis · propiolic acids · silver

[1] a) C. Federsel, R. Jackstell, M. Beller, *Angew. Chem.* **2010**, *122*, 6392–6395; *Angew. Chem. Int. Ed.* **2010**, *49*, 6254–6257; b) A. Bazzanella, D. Krämer, M. Peters, *Nachr. Chem.* **2010**, *58*, 1226–1230; c) D. M. Dalton, T. Rovis, *Nat. Chem.* **2010**, *2*, 710–711.

[2] a) R. Zevenhoven, S. Eloneva, S. Teir, *Catal. Today* **2006**, *115*, 73–79; b) M. Aresta, A. Dibenedetto, I. Tommasi, *Energy Fuels* **2001**, *15*, 269–273; c) P. Tundo, M. Selva, *Acc. Chem. Res.* **2002**, *35*, 706–716; d) G. A. Olah, *Angew. Chem.* **2005**, *117*, 2692–2696; *Angew. Chem. Int. Ed.* **2005**, *44*, 2636–2639; e) T. Aida, S. Inoue, *Acc. Chem. Res.* **1996**, *29*, 39–48; f) M. Mori, *Eur. J. Org. Chem.* **2007**, 4981–4993; g) M. Aresta, A. Dibenedetto, *Dalton Trans.* **2007**, 2975–2992.

[3] T. Sakakura, J.-C. Choi, H. Yasuda, *Chem. Rev.* **2007**, *107*, 2365–2387.

[4] a) H. Arakawa et al., *Chem. Rev.* **2001**, *101*, 953–996; b) D. J. Darensbourg, *Chem. Rev.* **2007**, *107*, 2388–2410; c) N. Eghbali, C.-J. Li, *Green Chem.* **2007**, *9*, 213–215; d) S. N. Riduan, Y. Zhang, J. Y. Ying, *Angew. Chem.* **2009**, *121*, 3372–3375; *Angew. Chem. Int. Ed.* **2009**, *48*, 3322–3325; e) T. Sakakura, K. Kohno, *Chem. Commun.* **2009**, 1312–1330; f) L. Gu, Y. Zhang, *J. Am. Chem. Soc.* **2010**, *132*, 914–915; g) A. Correa, R. Martín, *Angew. Chem.* **2009**, *121*, 6317–6320; *Angew. Chem. Int. Ed.*

2009, *48*, 6201 – 6204; h) I. Omae, *Catal. Today* **2006**, *115*, 33 – 52; i) T. Kubota, I. Hayakawa, H. Mabuse, K. Mori, K. Ushikoshi, T. Watanabe, M. Saito, *Appl. Organomet. Chem.* **2001**, *15*, 121 – 126; j) M. Cokoja, C. Bruckmeier, B. Rieger, W. A. Herrmann, F. E. Kühn, *Angew. Chem.* **2011**, *123*, 8662 – 8690; *Angew. Chem. Int. Ed.* **2011**, *50*, 8510 – 8537.

[5] For reviews, see: a) S. N. Riduan, Y. Zhang, *Dalton Trans.* **2010**, *39*, 3347 – 3357; b) K. Huang, C.-L. Sun, Z.-J. Shi, *Chem. Soc. Rev.* **2011**, *40*, 2435 – 2452.

[6] a) I. I. F. Boogaerts, G. C. Fortman, M. R. L. Furst, C. S. J. Cazin, S. P. Nolan, *Angew. Chem.* **2010**, *122*, 8856 – 8859; *Angew. Chem. Int. Ed.* **2010**, *49*, 8674 – 8677; b) I. I. F. Boogaerts, S. P. Nolan, *J. Am. Chem. Soc.* **2010**, *132*, 8858 – 8859.

[7] a) L. Zhang, J. Cheng, T. Ohishi, Z. Hou, *Angew. Chem.* **2010**, *122*, 8852 – 8855; *Angew. Chem. Int. Ed.* **2010**, *49*, 8670 – 8673; b) H. Mizuno, J. Takaya, N. Iwasawa, *J. Am. Chem. Soc.* **2011**, *133*, 1251 – 1253; c) M. T. Johnson, J. M. J. van Rensburg, M. Axelsson, M. S. G. Ahlquist, O. F. Wendt, *Chem. Sci.* **2011**, *2*, 2373 – 2377.

[8] a) T. Tsuda, Y. Chujo, T. Saegusa, *J. Chem. Soc. Chem. Commun.* **1975**, 963 – 964; b) Y. Fukue, S. Oi, Y. Inoue, *J. Chem. Soc. Chem. Commun.* **1994**, 2091; c) W.-Z. Zhang, W.-J. Li, X. Zhang, H. Zhou, X.-B. Lu, *Org. Lett.* **2010**, *12*, 4748 – 4751.

[9] a) L. J. Gooßen, N. Rodríguez, F. Manjolinho, P. P. Lange, *Adv. Synth. Catal.* **2010**, *352*, 2913 – 2917; b) D. Yu, Y. Zhang, *Proc. Natl. Acad. Sci. USA* **2010**, *107*, 20184 – 20189.

[10] Y. Dingyi, Z. Yugen, *Green Chem.* **2011**, *13*, 1275 – 1279.

[11] X. Zhang, W.-Z. Zhang, X. Ren, L.-L. Zhang, X.-B. Lu, *Org. Lett.* **2011**, *13*, 2402 – 2405.

[12] O. Vechorkin, N. Hirt, X. Hu, *Org. Lett.* **2010**, *12*, 3567 – 3569.

[13] a) J. Moon, M. Jeong, H. Nam, J. Ju, J. H. Moon, H. M. Jung, S. Lee, *Org. Lett.* **2008**, *10*, 945 – 948; b) J. Moon, M. Jang, S. Lee, *J. Org. Chem.* **2009**, *74*, 1403 – 1406; c) W. Jia, N. Jiao, *Org. Lett.* **2010**, *12*, 2000 – 2003.

[14] a) B. M. Trost, F. D. Toste, K. Greenman, *J. Am. Chem. Soc.* **2003**, *125*, 4518 – 4526; b) T. Kitamura, *Eur. J. Org. Chem.* **2009**, 1111 – 1125; c) M. Bararjanian, S. Balalaie, F. Rominger, B. Movassagh, H. R. Bijanzadeh, *J. Org. Chem.* **2010**, *75*, 2806 – 2812.

[15] a) W. Reppe, *Liebigs Ann. Chem.* **1955**, *596*, 25 – 32; b) J. Stohrer, E. Fritzlanghals, C. Brüninghaus, U.S. Patent 7,173,149B2, **2007**.

[16] L. Brandsma, *Preparative Acetylenic Chemistry, 2nd ed.*, Elsevier, Amsterdam, **1998**.

[17] a) J. Tsuji, M. Takahashi, T. Takahashi, *Tetrahedron Lett.* **1980**, *21*, 849 – 850; b) E. R. H. Jones, G. H. Whitham, M. C. Whiting, *J. Chem. Soc.* **1957**, 4628 – 4633; c) N. Satyanarayana, H. Alper, *Organometallics* **1991**, *10*, 804 – 807; d) J. Li, H. Jiang, M. Chen, *Synth. Commun.* **2001**, *31*, 199 – 202; e) Y. Izawa, I. Shimizu, A. Yamamoto, *Bull. Chem. Soc. Jpn.* **2004**, *77*, 2033 – 2045; f) L. Kollár, *Modern Carbonylation Reactions*, Wiley-VCH, Weinheim, **2008**, pp. 276 – 280.

[18] a) S. Ahrland, N.-O. Björk, *Acta Chem. Scand. A* **1974**, *28*, 823 – 828; b) N.-O. Björk, A. Cassel, *Acta Chem. Scand. A* **1976**, *30*, 235 – 240.

[19] a) G. Gritzner, *J. Mol. Liq.* **2010**, *156*, 103 – 108; b) Y.-F. Song, H. Abbas, C. Ritchie, N. McMillian, D.-L. Long, N. Gadegaard, Leroy Cronin, *J. Mater. Chem.* **2007**, *17*, 1903 – 1908; c) M. Calligaris, O. Carugo, *Coord. Chem. Rev.* **1996**, *153*, 83 – 154; d) J. Cornella, C. Sanchez, D. Banawa, I. Larrosa, *Chem. Commun.* **2009**, 7176 – 7178.

[20] A. Gennaro, A. A. Isse, E. Vianello, *J. Electroanal. Chem.* **1990**, *289*, 203 – 215.

[21] a) G. Rodríguez-Gattorno, D. Díaz, L. Rendón, G. O. Hernández-Segura, *J. Phys. Chem. B* **2002**, *106*, 2482 – 2487; b) C. Tan, F. Wang, J. Liu, Y. Zhao, J. Wang, L. Zhang, K. C. Park, M. Endo, *Mater. Lett.* **2009**, *63*, 969 – 971.

[22] a) J. D. McCowan, *Trans. Faraday Soc.* **1963**, *59*, 1860 – 1864; b) J. Eggert, *Z. Elektrochem.* **1918**, *12*, 150 – 154; c) R. Vestin, E. Ralf, *Acta Chem.* **1949**, *3*, 101 – 124.

[23] Control experiments with non-carbonate bases confirmed that the CO_2 does not originate from the Cs_2CO_3. See the Supporting Information, Table S1, and Ref. 10.

Received: January 27, 2012
Published online on March 1, 2012

IV.2.2. Optimierung der Silber(I)/DMSO-katalysierten Carboxylierung terminaler Alkine für die großtechnische Anwendung

Die hier beschriebenen Arbeiten entstammen einem Forschungs- und Entwicklungsprojekt mit der BASF SE und sind die Grundlage für eine Patentmeldung.

Die hohe katalytische Aktivität der Ag(I)/DMSO-basierten Methode zur Carboxylierung terminaler Alkine und die Möglichkeit sowohl Alkyl- als auch Arylalkine unter Normaldruck umsetzen zu können, waren der optimale Ausgangspunkt für die Entwicklung einer Carboxylierungsmethode in Gegenwart günstigerer oder organischer Basen. Die Verwendung stöchiometrischer Mengen an Cs_2CO_3 ist der Hauptgrund, der gegen eine industrielle Nutzung spricht. Der Austausch der anorganischen gegen eine organische Base erscheint auf den ersten Blick naheliegend, doch die Verwirklichung einer solchen Methode ist mit großen Herausforderungen verbunden.

Die Carboxylierung terminaler Alkine mit CO_2 ist eine Gleichgewichtsreaktion. Die Insertion von CO_2 (Carboxylierung) wird durch geringe Temperaturen und einen erhöhten Reaktionsdruck bevorzugt, wohingegen die Extrusion (Decarboxylierung) durch hohe Temperaturen und einen geringen CO_2-Druck begünstigt wird. Um jedoch überhaupt eine Carboxylierungsreaktion zu ermöglichen, wird eine hohe Aktivierungsenergie benötigt. Dieser Energiebetrag ist erforderlich, um das Alkin zu deprotonieren und den nukleophilen Angriff an das lineare und sehr stabile CO_2-Molekül zu ermöglichen. Mit Hilfe von Metallkatalysatoren kann diese Aktivierungsenergie deutlich verringert werden, indem das Alkin für die Deprotonierung und das CO_2 für die Insertion aktiviert wird. Unglücklicherweise sind die effektivsten Carboxylierungskatalysatoren oft auch sehr effektive Decarboxylierungskatalysatoren. Daher kann in vielen Fällen die Carboxylierung nur bei erhöhtem CO_2-Druck durchgeführt werden.

Die zuvor beschriebene Ag(I)/DMSO-katalysierte Carboxylierungsmethode in Gegenwart von Cs_2CO_3 benötigt erstaunlicherweise keinen erhöhten CO_2-Druck, um hohe Umsatzzahlen zu erreichen. Dies lässt sich durch die intermediäre Bildung schwerlöslicher Cäsiumsalze der Propiolsäurederivate erklären, die während der Reaktion aus dem organischen Lösungsmitteln (z. B. DMSO) ausfallen und so dem Gleichgewicht entzogen werden. Auf diese Weise wird das Gleichgewicht immer weiter auf die Seite der Produkte verschoben, bis hin zu vollständigen Umsätzen. Organische Basen wie z. B. Aminbasen bilden unter den Reaktionsbedingungen jedoch keine schwerlöslichen Salze der Propiolsäurederivate. Daher

wird das Produkt nicht dem Gleichgewicht entzogen und es stellt sich eine Gleichgewichtskonzentration ein, die unabhängig von der Basenmenge und der Katalysatorbeladung ist. Außerdem können Aminbasen sehr stark an Silber und Kupfer koordinieren und somit benötigte Koordinationsstellen blockieren, wodurch der Katalysator deaktiviert wird. Des Weiteren werden Amine in Gegenwart von CO_2 unter Bildung von Carbamaten leicht carboxyliert, wodurch ihre Basizität deutlich verringert wird. Daher gibt es bisher keine literaturbekannten Carboxylierungsmethoden terminaler Alkine mit Aminbasen.

In den folgenden Optimierungsexperimenten wurde versucht, die teuere Base Cs_2CO_3 durch günstigere oder organische Basen zu ersetzen. Dafür wurde analog zu vorherigen Optimierungsexperimenten die Carboxylierung von 1-Oktin (**IV.2-1**) mit CO_2 (**IV.2.2**) als Modellreaktion gewählt (Tabelle 1).

Keine der im Rahmen dieser Optimierungsarbeiten getesteten anorganischen Basen zeigte eine vergleichbare Aktivität zu Cs_2CO_3 (Eintrag 1). Trotz zum Teil deutlich höherer Basizität konnten mit Kalium-*tert*.-butanolat (KO^tBu), Kaliumphosphat (K_3PO_4), Kaliumcarbonat (K_2CO_3) und Kaliummethoxid (KOMe) unter Standardreaktionsbedingungen lediglich Umsätze von maximal 52% bei einer GC-Ausbeute von 41% erzielt werden. Mit Cäsiumhydrogencarbonat und –hydroxid sowie Kaliumacetat konnte überhaupt keine Ausbeute beobachtet wurde (Einträge 2-8). Unter 14 getesteten Aminbasen konnten lediglich mit DBN und DBU Umsätze von 12 bzw. 24% erreicht werden (Einträge 9-24).

Diese Optimierungen belegen, dass nicht die Stärke der Base für die Carboxylierung terminaler Alkine sondern primär das Gegen-Ion der Base entscheidend ist, da mit KO^tBu und KOMe geringere Ausbeuten erzielt wurden im Vergleich zu deutlich weniger basischem Cs_2CO_3. Es ist daher anzunehmen, dass starke Basen aufgrund ihrer hohen Nukleophilie unter den Reaktionsbedingungen mit CO_2 Carboxylat-Addukte bilden und somit ihre Basenstärke deutlich reduziert wird. Beispielsweise bilden sich so aus CO_2 und Hydroxid-Ionen Hydrogencarbonate, die analog zu Acetat- sowie Carboxylat-Anionen über eine zu geringe Basizität verfügen, um das terminale Alkin in Gegenwart von Silber zu deprotonieren und daher keine Umsätze beobachtet werden können. Cäsiumsalze sind in organischen Lösungsmitteln besser löslich als die entsprechenden Kaliumsalze, wodurch sich die höheren Umsätze erklären lassen.

Tabelle 1. Optimierung der Silber-katalysierten Carboxylierung von 1-Oktin (IV.2-1) in Gegenwart verschiedener Basen unter CO_2-Normaldruck.[a]

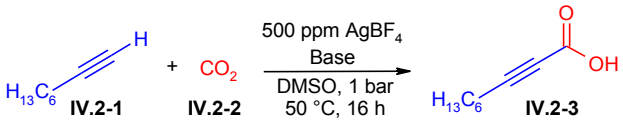

Eintrag	Base [Äquivalente]	Umsatz [%]	Ausbeute [%]	TON
1	1,2 Cs_2CO_3	100	99	2000
2	1,2 $CsHCO_3$	0	0	0
3	1,2 CsOH	0	0	0
4	1,2 KO^tBu	52	41	820
5	1,2 K_3PO_4	52	39	780
6	1,2 K_2CO_3	39	32	640
7	1,2 KOMe	18	6	120
8	1,2 KOAc	12	0	0
9	1,2 NH_3 (*g*)	0	0	0
10	1,2 2,6-Dimethylpyridin	0	0	0
11	1,2 4-*tert*.-Butylpyridin	0	0	0
12	1,2 *N*,*N*-Dimethyl-4-aminopyridin	0	0	0
13	1,2 Piperidin	0	0	0
14	1,2 Morpholin	0	0	0
15	1,2 Ethanolamin	0	0	0
16	1,2 Bis(2-hydroxyethyl)amin	0	0	0
17	1,2 Triethylamin	0	0	0
18	1,2 Dicyclohexylethylamin	0	0	0
19	1,2 Triphenylamin	0	0	0
20	1,2 Penta-*iso*-propylguanidin	0	0	0
21[b]	1,2 DBN	12	11	44
22[b]	1,2 DBU	24	12	49

[a] *Reaktionsbedingungen*: 1,00 mmol 1-Oktin (**IV.2-1**), 500 ppm $AgBF_4$, Base, 3,00 mL DMSO, 50 °C, 16 h. Ausbeuten bestimmt mittels GC-Analyse des *n*-Hexylpropiolsäurehexylesters (**IV.2-4**) hergestellt durch Zugabe von 2,00 mmol 1-Bromhexan zur Reaktionsmischung und mit *n*-Tetradekan als internen Standard. [b] 2500 ppm $AgBF_4$.

Die Tatsache, dass DBN und DBU die einzigen Aminbasen sind, die für die Carboxylierung terminaler Alkine einsetzbar sind, kann erneut nicht nur auf die hohe Basizität der Verbindungen zurückgeführt werden, da alle getesteten Amine eine vergleichbare oder höhere Basizität als Cs_2CO_3 besitzen. Die besondere Aktivität von DBN und DBU könnte auf deren Fähigkeit als reversibler CO_2-Speicher beruhen (Schema 19).[46]

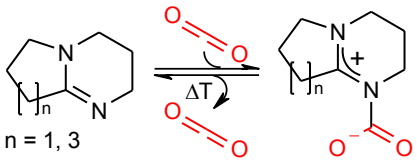

Schema 19. Reversible CO_2-Speicherung mit DBN und DBU.

In den Arbeiten von Endo *et al.* konnte beispielsweise gezeigt werden, dass Tetrahydropyrimidine unter CO_2-Zufuhr bei Raumtemperatur dieses binden und bei Erhöhung der Temperatur und unter Stickstoff-Zufuhr vollständig wieder freisetzen. Somit sind DBN und DBU in der Lage Kohlenstoffdioxid zu binden und die CO_2-Konzentration in der Lösung zu erhöhen.

Tabelle 2. Optimierung der Silber-katalysierten Carboxylierung von 1-Oktin (IV.2-1) in Gegenwart von Aminbasen bei 10 bar CO_2-Druck.[a]

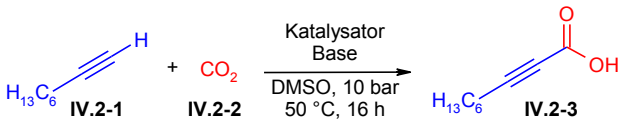

Eintrag	Katalysator [ppm]	Base [Äquiv.]	Umsatz [%]	Ausbeute [%]	TON
23[b]	2500 $AgNO_3$	1,2 DBU	18	7	28
24	"	"	70	39	156
25	"	1,2 Piperidin	0	0	0
26	"	1,2 Morpholin	0	0	0
27	"	1,2 Triethylamin	0	0	0
28	"	4,8 DBU	78	8	32
29	"	1,0 DBU	68	39	156
30	"	0,6 DBU	50	34	136
31	5000 $AgNO_3$	1,2 DBU	69	37	74
32	"	2,4 DBU	77	20	40
33	10000 $AgNO_3$	1,2 DBU	72	35	35
34	1250 $AgNO_3$	"	68	39	312
35	500 $AgNO_3$	"	67	38	760

[a] *Reaktionsbedingungen*: 1,00 mmol 1-Oktin (**IV.2-1**), Katalysator, Base, 3,00 mL DMSO, 50 °C, 16 h, 10 bar. Ausbeuten bestimmt mittels GC-Analyse des *n*-Hexylpropiolsäurehexylesters (**IV.2-4**) hergestellt durch Zugabe von 2,00 mmol 1-Bromhexan zur Reaktionsmischung und mit *n*-Tetradekan als internen Standard. [b] 1 bar CO_2-Druck.

Da ein großes Interesse an der Verwendung von Aminbasen anstelle von Cs_2CO_3 besteht, wurden im Folgenden die Reaktionsbedingungen für die Carboxylierung von 1-Oktin (**IV.2-1**) mit CO_2 (**IV.2.2**) in Gegenwart von Aminbasen optimiert (Tabelle 2).

Entsprechend der Annahme, dass es sich bei der Carboxylierung von Alkinen um eine Gleichgewichtsreaktion handelt, konnte durch Erhöhung des Reaktionsdrucks von 1 auf 10 bar das Gleichgewicht weiter auf die Seite des Produkts verschoben und die GC-Ausbeute von 7 auf 39% erhöht werden (Einträge 23-24). Auch bei 10 bar CO_2-Druck wurde mit anderen Aminbasen wie z. B. Piperidin, Morpholin oder Triethylamin kein Umsatz des Alkins beobachtet (Einträge 25-27). Eine Erhöhung der Basenmengen sowie der Katalysatorbeladung führte wie erwartet zu keiner Steigerung der Ausbeute (Einträge 28-33). Eine Verringerung der Katalysatorbeladung ist ohne Ausbeuteverlust möglich, und so konnte eine maximale TON von 760 für die Carboxylierung von 1-Oktin (**IV.2-1**) mit DBU erzielt werden. (Einträge 34-35).

Der folgenden Mechanismus kann für die Silber-katalysierte Carboxylierung terminaler Alkine mit DBN oder DBU formuliert werden (Schema 20).

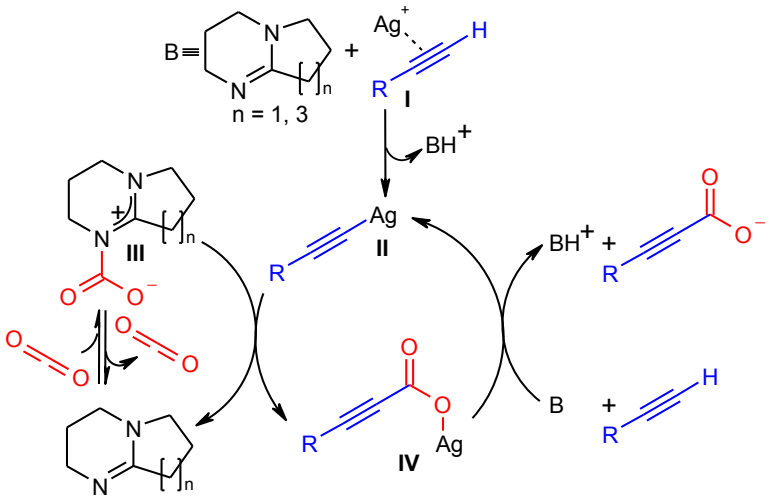

Schema 20. Mechanismus für die Carboxylierung terminaler Alkine in Gegenwart von DBN oder DBU.

Analog zum Mechanismus in Gegenwart anorganischer Basen führt die Koordination des Silber(I)-Salzes an das Alkin zur Erhöhung der Azidität der terminalen C(sp)-H–Bindung, wodurch DBN oder DBU in der Lage ist das Alkin zu deprotonieren und die Bildung eines katalytisch aktiven Silberacetylids **II** zu vermitteln. Das CO_2 für den folgenden Schritt wird aus einem DBU-CO_2-Komplex **III** freigesetzt. Die Insertion von CO_2 in die Ag-C-Bindung des Silberacetylids **II** liefert ein Silberpropiolat **IV**. Der Katalysezyklus wird durch die

Freisetzung eines Ammoniumpropiolats und der Regenerierung des Silberacetylids **II** geschlossen, indem ein weiteres Alkin in Gegenwart von DBN oder DBU deprotoniert und auf das Silber übertragen wird.

Im Rahmen dieser Doktorarbeit konnten keine weiterführenden Carboxylierungsexperimente bei einem CO_2-Druck von mehr als 10 bar durchgeführt werden, da aus Zeitgründen die Entwicklung eines Herstellungsverfahren von Acetylendicarbonsäure (Kap. IV.2.3) priorisiert wurde.

Aufgrund der bisherigen Ergebnisse ist jedoch zu erwarten, dass höhere Umsätze bei deutlich höherem Druck möglich sowie geringere Katalysatorbeladung ausreichend und auf diese Weise noch höhere TONs erreichbar sein sollten. Ferner sollte es möglich sein bei einem höheren CO_2-Druck andere Lösungsmittel zu verwenden, die eine geringere CO_2-Löslichkeit als DMSO besitzen, oder DMSO nur als Co-Solvent in katalytischen Mengen einzusetzen.

Diese Resultate belegen bereits jetzt, dass Aminbasen anstelle von anorganischen Basen für die Carboxylierung terminaler Alkine verwendbar sind. Der Nachteil von Aminbasen gegenüber z. B. Cs_2CO_3, dass die Ammoniumsalze der Propiolsäurederivate nicht während der Reaktion ausfallen und daher das entstehende Produkt nicht dem Gleichgewicht entzogen wird, kann möglicherweise durch einen noch höheren Reaktionsdruck ausgeräumt werden. Für eine großtechnische Anwendung ist dies von großem Vorteil, da kein Salz während der Reaktion anfällt und das Produkt nach der Reaktion gelöst vorliegt und deshalb sehr leicht aus dem Reaktor zur weiteren Aufarbeitung entfernt werden kann. Ferner können in Gegenwart der Aminbase wahlweise Hydrierungen der Mehrfachbindung oder der Carboxy-Gruppe im gleichen Reaktor ohne zusätzlichen Aufarbeitungsschritt durchgeführt werden. In Gegenwart von anorganischen Basen ist dies nicht ohne Aufarbeitungsschritt möglich.

So konnte ein weiterer große Schwachpunkt der katalytischen Carboxylierung terminaler Alkine mit CO_2 überwunden werden, und damit die Grundlage geschaffen werden, um diese Methode in einen großtechnischen Maßstab übertragen zu können.

IV.2.3. Synthese von Acetylendicarbonsäure durch direkte Carboxylierung von Ethin mit CO_2

Auch die hier beschriebenen Arbeiten entstammen dem Forschungs- und Entwicklungsprojekt mit der BASF SE und sind die Basis für eine Patentmeldung.

Nachdem die Grundlage für die Entwicklung einer großtechnischen Methode zur Carboxylierung terminaler Alkine geschaffen werden konnte, sollte als nächstes die Synthese wertvoller Propiolsäurederivate untersucht werden. Ein weiteres Ziel dieses Forschungs- und Entwicklungsprojekts war es daher, eine großtechnisch realisierbare selektive Synthese von Acetylendicarbonsäure ausgehend von Ethin und CO_2 zu entwickeln, um einen alternativen Zugangsweg zu 2-Butin-1,4-diol sowie Butan-1,4-diol zu eröffnen. Wie in Kapitel II.3.1 beschrieben, ist Butan-1,4-diol ein wertvolles chemisches Zwischenprodukt zur Herstellung von z. B. Tetrahydrofuran und γ-Butyrolacton.

Die Übertragung einer Carboxylierungsmethode primärer Alkine auf Ethin ist keineswegs trivial, da Ethin nur schwach in organischen Solventien löslich ist und CO_2 als zweiter Reaktant aufgrund der deutlich höheren Löslichkeit eine Anreicherung von Ethin im Reaktionsmedium zusätzlich erschwert. Auch die zunächst entstehenden Salze der Acetylenmonocarbonsäure sind nur wenig löslich, so dass eine zweite Carboxylierung unter Bildung von Acetylendicarbonsäure deutlich erschwert wird und oftmals Produktgemische der Mono- und Di-Säure entstehen. Diese Säuren, vor allem die Acetylendicarbonsäure, sind in Lösung thermisch instabil und zerfallen unter CO_2-Abspaltung. Solche Decarboxylierungsreaktionen werden zudem durch zahlreiche Silber- und Kupfer-Komplexe katalysiert.

Die Entwicklung einer Carboxylierungsmethode für Ethin wird zusätzlich durch die Gefahr der Metallacetylid-Bildung erschwert. Metallacetylide sind hochexplosive Verbindungen, die bevorzugt bei einem hohen Ethin-Druck entstehen. Daher müssen besondere Vorsichtsmaßnamen getroffen und möglichst geringe Katalysatorbeladungen verwendet werden. Die großtechnische Handhabung von Kupferacetyliden konnte in einigen industriellen Prozessen realisiert werden, wohingegen der Umgang mit Silberacetyliden aufgrund der höheren Detonationsgeschwindigkeiten noch nicht großtechnisch verwirklicht wurde.

Das einzige literaturbekannte Beispiel für eine erfolgreiche Umsetzung von Ethin und CO_2 zur Acetylendicarbonsäure wurde von Gooßen *et al.* patentiert.[47] In diesen Arbeiten wurde

nachgewiesen, dass sich in Gegenwart von 0,02 mmol einer speziellen Klasse von Kupfer(I)-Katalysatoren [z. B. (4,7-Diphenylphenanthrolin)bis[tri-phenylphosphin]-Kupfer(I) nitrat] bei 5 bar Druck (1 bar Ethin und 4 bar CO_2) nach 2 h Rühren bei 60 °C im Autoklaven-Reaktor ein Gemisch aus 10,4 mg Acetylendicarbonsäure und 7,5 mg Acetylenmonocarbonsäure bildet. Dies entspricht einer TON von ca. 2 für die Bildung der Acetylendicarbonsäure. Eine selektive Bildung der Acetylendicarbonsäure konnte bisher nicht erreicht werden und die Säure konnte lediglich in Form des *n*-Hexylesters isoliert werden.

Als nächstes sollte daher getestet werden, ob mit der Silber-katalysierten Carboxylierungsmethode ein Zugang zur Acetylendicarbonsäure (**IV.2-6**) möglich ist.

Erste Testexperimente wurden mit Trimethylsilylacetylen (**IV.2-5**) anstelle von Ethin durchgeführt, weil sich zeigte, dass unter den Reaktionsbedingungen die Trimethylsilyl-Gruppe *in situ* abgespalten wird und so die Acetylendicarbonsäure (**IV.2-6**) dargestellt werden kann. Der Vorteil in der Verwendung von Trimethylsilylacetylen (**IV.2-5**) liegt darin, dass es bei Raumtemperatur flüssig ist und im Gegensatz zu gasförmigen Ethin mit definierten Mengen des Alkins gearbeitet werden kann. So können neben Umsatzzahlen auch HPLC-Ausbeuten bestimmt werden, wodurch eine Anpassung des Katalysatorsystems zur Darstellung von Acetylendicarbonsäure (**IV.2-6**) vielfach erleichtert wurde (Tabelle 3).

Es zeigte sich, dass das Katalysatorsystem für die Umsetzung von Trimethylsilylacetylen (**IV.2-5**) zur Acetylendicarbonsäure (**IV.2-6**) geeignet ist. Da eine doppelte Carboxylierung nötig ist, um das gewünschte Produkt darzustellen, wurde lediglich die Basenmenge verdoppelt. Ohne weitere Anpassung konnten volle Umsätze zur Acetylendicarbonsäure (**IV.2-6**) erzielt werden, was einer TON von 4000 entspricht (Eintrag 1). Eine weitere Erhöhung der Basenmenge führte genau wie eine Erhöhung der Katalysatorbeladung zu keiner Verbesserung der TON, und eine 10 °C höhere oder tiefere Reaktionstemperatur war unvorteilhaft für den Reaktionsumsatz (Einträge 2-7). Eine Halbierung der Katalysatorbeladung führte zu einer Halbierung der Ausbeute (Eintrag 8). Die Reaktion verläuft auch mit CuCN und CuI nahezu vollständig ab, jedoch werden deutlich höhere Katalysatorbeladung benötigt, um vergleichbar hohe Umsätze zu erreichen (Einträge 9-10).

Die optimierten Reaktionsbedingungen wurden schließlich auf die Umsetzung von Ethin (**IV.2-7**) angewendet (Tabelle 4). Dabei wurde ein 1:2 Gasgemisch von Ethin und CO_2 anstelle von Trimethylsilylacetylen (**IV.2-5**) unter Normaldruck eingesetzt (Eintrag 11). Nach 40 h bei 50 °C konnten 250 mg der reinen Acetylendicarbonsäure (**IV.2-6**) isoliert werden. Dies entspricht einer TON von 1244. Im Vergleich zum bekannten Kupfer(I)-Phenanthrolin-

Phosphin-Komplex katalysierten Verfahren zur Carboxylierung von Ethin bei 5 bar CO_2-Druck kann mit dem neuen Silber(I)/DMSO-katalysierte Verfahren eine 622-fach höhere Umsatzzahl bereits bei Normaldruck mit einem 1:2 Ethin-CO_2-Gemisch erzielt werden (Eintrag 12).

Tabelle 3. Optimierung des Katalysatorsystems mit Trimethylsilylacetylen (IV.2-5) für die Darstellung von Acetylendicarbonsäure (IV.2-6).[a]

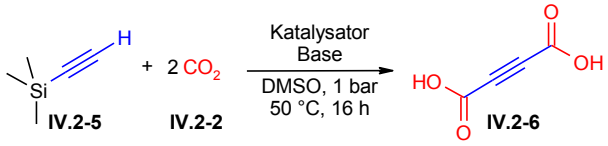

IV.2-5 IV.2-2 IV.2-6

Eintrag	Katalysator [ppm]	Base [Äquivalente]	Ausbeute [%]	TON
1	500 $AgBF_4$	2,4 Cs_2CO_3	100	4000
2	"	3,6 Cs_2CO_3	87	3468
3[b]	"	2,4 Cs_2CO_3	27	1088
4[c]	"	"	91	3632
5	1000 $AgBF_4$	"	93	1860
6	"	4,8 Cs_2CO_3	82	1640
7[d]	2500 $AgBF_4$	2,4 Cs_2CO_3	74	590
8	250 $AgBF_4$	"	46	3648
9	5000 CuCN	"	100	400
10	1500 CuI	"	94	1214

[a] *Reaktionsbedingungen*: 1,00 mmol Trimethylsilylacetylen (**IV.2-5**), Katalysator, Base, 3,00 mL DMSO, 50 °C, 16 h, 1 bar. Ausbeuten bestimmt mittels HPLC-Analyse des Cäsiumsalzes der Acetylendicarbonsäure (**IV.2-6**) mit 100 µL NMP als interner Standard. [b] 30 °C. [c] 60 °C. [d] Isolierte Ausbeute.

Weitere Experimente wurden im Autoklaven-Reaktor bei 10 bar Druck [1 bar Ethin (**IV.2-7**) und 9 bar CO_2 (**IV.2-2**)] durchgeführt. Dabei konnten keine höheren TONs erzielt werden (Einträge 13-16), jedoch konnte die Bildung der Acetylendicarbonsäure (**IV.2-6**) in Gegenwart von DBU und DBN mittels HPLC nachgewiesen werden (Einträge 17-20).

Diese Experimente belegen die erfolgreiche Synthese von Acetylendicarbonsäure (**IV.2-6**) durch katalytische Carboxylierung von Ethin (**IV.2-7**) bei CO_2-Normaldruck. Unter milden Reaktionsbedingungen konnte erstmals die reine Acetylendicarbonsäure (**IV.2-6**) isoliert werden und mit dem hocheffizienten Silber(I)/DMSO-Katalysatorsystem auf Anhieb eine TON von mehr als 1000 erzielt werden. Ferner ist es möglich die Acetylendicarbonsäure

(**IV.2-6**) auch in Gegenwart von Aminbasen darzustellen. Dafür wird jedoch ein Reaktionsdruck von mindestens 10 bar benötigt.

Tabelle 4. Silber-katalysierte Carboxylierung von Ethin (IV.2-7) mit CO_2 (IV.2-2).[a]

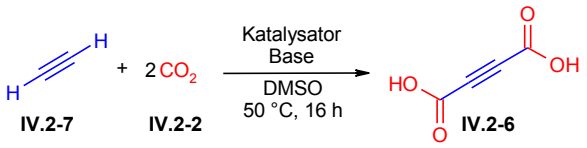

IV.2-7 IV.2-2 IV.2-6

Eintrag	Katalysator [ppm]	Base [Äquivalente]	Druck [bar]	TON
11[b]	500 $AgBF_4$	2,4 Cs_2CO_3	1	1244
12[c]	20000 [Cu(I)]	"	5	2
13	2500 $AgNO_3$	"	10	311
14	"	4,8 Cs_2CO_3	10	114
15	5000 $AgNO_3$	2,4 Cs_2CO_3	10	71
16	"	4,8 Cs_2CO_3	10	110
17	2500 $AgNO_3$	2,4 DBU	10	3
18	"	2,4 DBN	10	18
19	5000 $AgNO_3$	4,8 DBU	10	12
20	"	4,8 DBN	10	11

[a] *Reaktionsbedingungen*: 1 bar Ethin (**IV.2-7**), 9 bar CO_2 (**IV.2-2**), Katalysator, Base, 3,00 mL DMSO, 50 °C, 16 h. TONs wurden anhand der korrigierten HPLC-Ausbeute berechnet mit 100 µL NMP als interner Standard. [b] 3,5 µmol $AgBF_4$, 16,8 mmol Cs_2CO_3, 1 bar Druck, 1:2 Gasgemisch Ethin und CO_2, 15,0 mL DMSO, 50°C, 40 h, isolierte Ausbeute. [c] 1 bar Ethin (**IV.2-7**), Katalysator, 2,40 mmol Cs_2CO_3, 3,00 mL DMF, 50 °C, 16 h. Isolierte Ausbeuten des Acetylendicarbonsäurehexylesters (**IV.2-6**) hergestellt durch Zugabe von 2,00 mmol 1-Bromhexan zur Reaktionsmischung. [Cu(I)] = (4,7-Diphenylphenanthrolin)bis[tri-phenylphosphin]-Kupfer(I) nitrat.

Im Rahmen dieser Doktorarbeit konnte somit auch die Grundlage für ein großtechnisches Herstellungsverfahren von Acetylendicarbonsäure ausgehend von Ethin und CO_2 geschaffen werden. Es wurde gezeigt, dass sowohl bei Normaldruck als auch bei erhöhtem Reaktionsdruck hohe Umsätze erzielt werden können und das prinzipiell auch Aminbasen einsetzbar sind.

IV.3. Literatur des Hauptteils

[37] L. J. Gooßen, M. Arndt, M. Blanchot, F. Rudolphi, F. Menges, G. Niedner-Schatteburg, *Adv. Synth. Catal.* **2008**, *350*, 2701–2707.

[38] L. J. Gooßen, J. E. Rauhaus, G. Deng, *Angew. Chem*. **2005**, *117*, 4110–4113; *Angew. Chem. Int. Ed.* **2005**, *44*, 4042–4045.

[39] L. J. Gooßen, K. S. M. Salih, M. Blanchot, *Angew. Chem.* **2008**, *120*, 8620–8623; *Angew. Chem. Int. Ed.* **2008**, *47*, 8492–8495.

[40] K. Kuramochi, Y. Osada, T. Kitahara, *Tetrahedron* **2003**, *59*, 9447–9454.

[41] N. K. Garg, R. Sarpong, B. M. Stoltz, *J. Am. Chem. Soc.* **2002**, *124*, 13179−13184.

[42] C. Wentrup, H.-W. Winter, *Angew. Chem.* **1978**, *8*, 643−644.

[43] a) A. Chakraborty, J. K. Ray, *Synthetic Commun.* **1995**, *25*, 1869−1876; b) J. Lotzbeyer, K. Bodendorf, *Chem. Ber.* **1967**, *100*, 2620−2624; c) C. Alexander, W. J. Feast, *Synthesis* **1992**, 735−737.

[44] a) S. Müller, B. Liepold, G. J. Roth, H. J. Bestman, *Synlett* **1996**, 521−522; b) G. J. Roth, B. Liepold, S. G. Müller, H. J. Bestmann, *Synthesis* **2004**, *1*, 59–62.

[45] J. Pietruszka, A. Witt, *Synthesis* **2006**, *24*, 4266–4268.

[46] a) E. Haruki, M. Arakawa, N. Matsumura, Y. Otsuji, E. Imoto, *Chem. Lett.* **1974**, 427–428; b) H. Mori, *Bull. Chem. Soc. Jpn.* **1988**, *61*, 435–439; c) T. Endo, D. Nagai, T. Monma, H. Yamaguchi, B. Ochiai, *Macromolecules* **2004,** *37,* 2007–2009; d) B. Ochiai, K. Yokota, A. Fujii, D. Nagai, T. Endo, *Macromolecules* **2008,** *41,* 1229–1236; e) M. Carafa, E. Mesto, E. Quaranta, *Eur. J. Org. Chem.* **2011**, 2458–2465; f) E. J. Beckman, P. Munshi, *Green Chem.* **2011**, *13*, 376–383.

[47] L. J. Gooßen, N. Rodríguez, F. Manjolinho, P. P. Lange, *Patentanmeldung UKL-2010-170*, **2010**.

V. Zusammenfassung und Ausblick

Ruthenium-katalysierte Hydroamidierung terminaler Alkine

Im Rahmen dieser Dissertation wurde der Mechanismus der Ruthenium-katalysierten Addition von Amiden an terminale Alkine eingehend durch eine Kombination von Kontrollexperimenten, kinetischen Studien, spektroskopischen Untersuchungen und theoretischen Berechnungen untersucht. Die dabei gewonnenen Erkenntnisse wurden zur Entwicklung einer neuen Katalysatorgeneration mit ausgesprochen hoher Selektivität für die Bildung wertvoller *Z*-Enamide und *Z*-Enimide genutzt. Das synthetische Potential wurde zudem durch die Darstellung der biologisch aktiven Naturstoffe Lansiumamid A und B, Lansamid I sowie Botryllamid C und E demonstriert.

Vor Beginn unserer mechanistischen Studien wurden nach intensiver Literaturrecherche vier Katalysezyklen identifiziert, die plausible Mechanismen für die Hydroamidierung terminaler Alkine darstellen. Anschließend wurde eine Reihe von Kontrollexperimenten durchgeführt, deren Ausgang den Ausschluss einzelner Elementarschritte dieser Katalysezyklen und folglich auch den Ausschluss der entsprechenden Mechanismen ermöglichte.

Der erste untersuchte Katalysezyklus wurde von Watanabe *et al.* für die Addition von Formaniliden an terminale Alkine beschrieben und besteht aus einer Sequenz von oxidativer Addition des Amids, Insertion des Alkins in die Ru-N- oder Ru-H-Bindung und reduktiver Eliminierung des Enamid-Produkts unter gleichzeitiger Regenerierung der katalytisch aktiven Ru^0-Spezies. Im Verlauf dieses Zyklus wird eine Änderung des Hybridisierungsgrads des terminalen Alkin-Kohlenstoffatoms von sp nach sp^2 beschrieben. In Gegenwart von 1-Deuterioalkinen sollte dies zu einem inversen sekundären Isotopeneffekt führen. Entsprechende Kontrollexperimente zeigten jedoch, dass normale kinetische Isotopeneffekte für Hydroamidierungsreaktionen vorliegen und dieser Mechanismus daher ausgeschlossen werden kann.

Ein von unserer Arbeitsgruppe anfänglich favorisierter redox neutraler Mechanismus musste ebenfalls aufgrund der ermittelten normalen kinetischen Isotopeneffekten verworfen werden. Denn auch dieser Zyklus verläuft über eine Umhybridisierung des terminalen Alkin-Kohlenstoffatoms von sp nach sp^2. Dieser Katalysezyklus startet jedoch von Ru^{II}-Amid-

Spezies, die durch Austauschreaktionen der Methylallyl-Liganden gegen Amid-Anionen generiert werden. In den folgenden Schritten insertiert ein Alkin in die Ru-N-Bindung unter Bildung eines Ru^{II}-Enamid-Komplexes, der nach Protonolyse das Produkt freisetzt und die aktive Ru^{II}-Amid-Spezies regeneriert.

Für die Addition von Carbonsäuren an terminale Alkine wurde ein Katalysezyklus von Dixneuf *et al.* vorgeschlagen, der auch auf die Addition von Amiden an terminale Alkine übertragen werden könnte. In diesem Mechanismus bildet sich eine Ru-Vinyliden-Spezies ausgehend von Ru^{II}-Spezies durch einen 1,2-Protonenshift des terminalen Alkin-Wasserstoffatoms. Diese Ru-Vinyliden-Spezies wird von einem Amid bevorzugt in α-Stellung zum Ruthenium angegriffen. Dabei wird ein Ruthenium-Enamid-Komplex gebildet, der nach Protonolyse das *anti*-Markovnikov Produkt freisetzt und die katalytisch aktive Ru^{II}-Spezies regeneriert. Dieser Zyklus ist im Einklang mit den beobachteten normalen kinetischen Isotopeneffekten in Gegenwart von 1-Deuterioalkinen. In zusätzlichen Kontrollexperimenten mit Deuterium-markierten Alkinen konnten jedoch keine 1,2-Protonenshifts beobachten werden, da im Produkt das Deuterium nahezu vollständig am ursprünglichen, terminalen Kohlenstoffatom des Alkins nachgewiesen werden konnte. Aufgrund dieser Ergebnisse konnte auch dieser Mechanismus für die Hydroamidierung terminaler Alkine ausgeschlossen werden.

Ein vierter denkbarer Katalysezyklus verläuft ebenfalls über Ru-Vinyliden-Spezies und wurde in Anlehnung an den Mechanismus für die Hydratisierung terminaler Alkine von Wakatsuki *et al.* aufgestellt. Im Gegensatz zum Mechanismus von Dixneuf wird die Vinyliden-Spezies durch Protonierung eines π-koordinierten Alkins unter Bildung einer kationischen Ru^{IV}-Vinyl-Spezies erzeugt. Es folgt eine Umlagerung zu einem kationischen Ru^{IV}-Hydrid-Vinyliden-Komplex. Der anschließende selektive Angriff eines Amid-Anions in α-Stellung zum Ruthenium führt zur Bildung einer neutralen Ru^{IV}-Hydrid-Enamid-Spezies, die nach reduktiver Eliminierung das *anti*-Markovnikov Enamid freisetzt und die katalytisch aktive Ru^{II}-Spezies regeneriert. Dieser Mechanismus ist im Einklang mit den kinetischen Untersuchung und den Deuterium-Markierungsexperimenten, allerdings ist die Bildung kationischer Intermediate in Gegenwart basischer Additive und in unpolaren Lösungsmitteln sehr unwahrscheinlich. Keine der postulierten, kationischen Ru^{IV}-Intermediate konnte in ESI-MS-Studien detektiert werden, sodass wir diesen Mechanismus als unwahrscheinlich für die Hydroamidierung terminaler Alkine einstuften.

Nachdem somit alle literaturbekannten Mechanismen ausgeschlossen wurden, stellten wir einen weiteren Mechanismus für die Hydroamidierung terminaler Alkine auf. Dieser wurde auf Grundlage einer Ruthenium-Vinyl-Vinyliden-Umlagerung aufgebaut, die in einem anderen Zusammenhang von Caulton *et al.* belegt wurde (Schema 21).

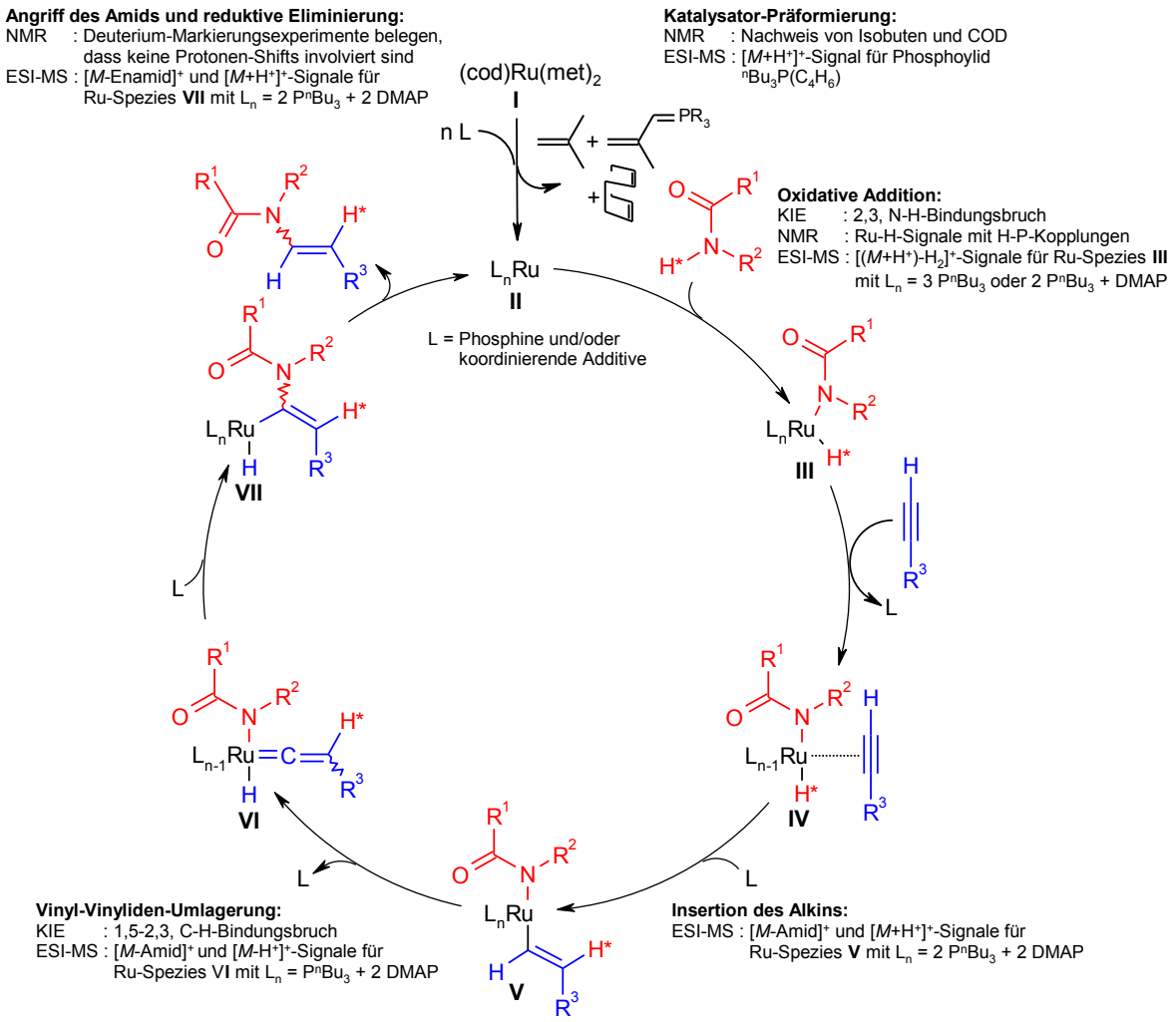

Schema 21. Reaktionsmechanismus für die Ruthenium-katalysierte Hydroamidierung terminaler Alkine.

Die Katalysator-Präformierung verläuft über einen reduktiven Allylierungsprozess, wobei ein Phosphorylid, Isobuten und 1,5-Cyclooktadien freigesetzt werden und eine koordinativ ungesättigte Ru^0-Spezies **II** generiert wird. Im ersten Schritt des Katalysezyklus wird ein Amid oxidativ an diese katalytisch aktive Ru^0-Spezies **II** addiert und bildet die Ru-Hydrid-Spezies **III**. Nach dem Austausch eines Liganden gegen ein Alkin (**III** → **IV**) insertiert dieses in die Ru-H-Bindung. Der so entstandene Ru-Vinyl-Komplex **V** lagert sich im nächsten Schritt zu einem Ru-Vinyliden-Hydrid-Komplex **VI** um. Der folgende interne Angriff des Amid-Anions erfolgt bevorzugt in α-Stellung zum Ruthenium und führt zur Generierung

eines Ru-Enamid-Komplexes **VII**, der nach reduktiver Eliminierung das *anti*-Markovnikov Produkt freisetzt und die katalytisch aktive Ru^0-Spezies **II** regeneriert.

Dieser Mechanismus ist im Einklang mit allen im Rahmen dieser mechanistischen Studien durchgeführten Kontrollexperimenten. So können sowohl die Ergebnisse der kinetischen Studien als auch der Deuterium-Markierungsexperimente erklärt werden, da die terminale C-H Bindung des Alkins gebrochen und das Proton in einem späteren Schritt am gleichen Kohlenstoffatom wieder gebunden wird. Aufgrund der Involvierung von Ru-Vinyliden-Spezies lässt sich sowohl die Limitierung auf terminale Alkine als auch die selektive Bildung von *anti*-Markovnikov Produkten erklären.

Als nächstes versuchten wir, mit Hilfe spektroskopischer Untersuchungen Intermediate des Katalysezyklus nachzuweisen und somit den Mechanismus zusätzlich zu bekräftigen. Dabei konnten wir den Katalysator-Präformierungsschritt mit Hilfe von ESI-MS Untersuchungen aufklären. So wurde in einer Toluol-Lösung aus $(cod)Ru^{II}(met)_2$ und $^nBu_3P$ nach kurzem Erhitzen auf 100 °C das kationische Fragment mit der Summenformel $[^nBu_3P(C_4H_7)]$ (*m/z* = 257,2) detektiert. Dieses Fragment bildet sich durch einen nukleophilen Angriff von $^nBu_3P$ an einen Methylallyl-Liganden der $(cod)Ru^{II}(met)_2$-Vorstufe und gleichzeitiger Reduktion des Rutheniums. Der erste Schritt des Katalysezyklus ist die oxidative Addition des Amids, wobei sich Ru-Hydrid-Spezies bilden. In NMR-Untersuchungen von Reaktionsmischungen ohne Zusatz von Alkinen wurden mehrere Ru-Hydrid-Signale detektiert. Aufgrund deren Aufspaltungsmuster und charakteristischen H-P-Kopplungen sowie mit Hilfe zusätzlicher 2D-NMR Experimente konnten für zwei dieser Ru-Hydrid-Spezies Strukturvorschläge abgeleitet werden. Es handelt sich dabei um einen trigonal bipyramidialen Komplex der Summenformel $[(^nBu_3P)_3Ru(H)(Pyr)]$ mit zwei $^nBu_3P$-Liganden und einem Amid-Ligand (Pyr = $C_4H_6NO^-$) in einer Ebene sowie um einen quadratisch bipyramidialen Komplex der Summenformel $[(^nBu_3P)_3(DMAP)Ru(H)(Pyr)]$ mit drei $^nBu_3P$-Liganden und einem DMAP-Liganden (DMAP = $C_7H_{10}N_2$) in einer Ebene. ESI-MS Experimente von Reaktionsmischungen in Gegenwart aller Startmaterialien ermöglichten die Detektion zahlreicher, kationischer Ru^{II}-Intermediate, die Amide, Alkine sowie Kombinationen von $^nBu_3P$- und DMAP-Liganden enthielten. Durch zusätzliche ESI-MS-CID-MS Experimente konnten neben der Summenformel auch strukturelle Informationen abgeleitet werden. Die Signale mit *m/z* = 833.5 und 918.6 entsprechen beispielsweise den berechneten Mustern für die Ru-Vinyl-Spezies $[Ru(P(^nBu_3)_2(DMAP)_2(Vinyl)]^+$ und $[Ru(P(^nBu_3)_2(DMAP)_2(Pyr)(Vinyl)]+H^+$ (Vinyl = $C_6H_{11}^-$). Beide kationischen Fragmente entstammen dem gleichen

[Ru(P^nBu_3)$_2$(DMAP)$_2$(Pyr)(Vinyl)]-Komplex und werden höchstwahrscheinlich während des Ionisierungsprozesses durch Abspaltung eines Amids ([*M*-(Pyr)]$^+$) und durch Protonierung ([*M*+H]$^+$) erzeugt. Zusätzliche CID-Fragmentierungen dieser Spezies waren in Einklang mit der strukturellen Zuordnung und zeigten hauptsächlich die Abspaltung oder die Zersetzung von DMAP- und $^nBu_3$P-Liganden. Dieser Komplex entspricht dem Ru-Intermediat **V** aus dem Katalysezyklus, das durch Insertion eines Alkins in ein Ru-Hydrid-Intermediat gebildet wird und sich im nächsten Schritt zur einer Ru-Vinyliden-Spezies umlagert. Auf ähnliche Weise konnten zahlreiche Ru-Amid-Vinyl-Spezies eindeutig nachgewiesen werden. Zusätzlich wurden DFT-Berechnungen durchgeführt, die bestätigen, dass es sich bei allen vorgeschlagenen Ru-Intermediaten des Katalysezyklus um stabile Komplexe handelt.

Eine der wichtigsten Erkenntnisse dieser mechanistischen Studien bestand darin, dass trotz deutlich verschiedener Katalysatorsysteme für die einzelnen *E*- und *Z*-selektiven Hydroamidierungsmethoden sehr ähnliche Reaktionsintermediate nachgewiesen werden konnten, die sich lediglich durch die Natur der Liganden unterscheiden. Daher kann davon ausgegangen werden, dass das gleiche Ru-Intermediat aus dem Katalysezyklus den stereochemischen Verlauf der Reaktion bestimmt. Wir haben somit Grund zur Annahme, dass die Ru-Vinyliden-Spezies **VI** entscheidend für die Stereochemie der Reaktion ist. Die relative Ausrichtung des Restes (hier R^3) der Vinyliden-Einheit hat einen direkten Einfluss darauf, ob sich im Folgenden ein *E*- oder *Z*-konfigurierter Ru-Enamid-Komplex **VII** bildet. Wir gehen davon aus, dass der sterische Anspruch der eingesetzten Liganden für die Ausrichtung der R^3-Gruppe verantwortlich ist.

Die kinetischen Untersuchungen zeigten, dass zwei Schritte im Katalysezyklus langsam sind: Die oxidative Addition und die Ru-Vinyl-Vinyliden-Umlagerung. Beide Schritte sollten durch eine hohe Elektronendichte am Ruthenium begünstigt sein. Dies bestätigten experimentelle Beobachtungen, nach denen der Einsatz elektronenreicher Liganden für diese Schritte vorteilhaft ist. Eine Erleichterung des langsamen Aktivierungsschritts der N-H Bindung sollte durch Lewis-azide Verbindungen möglich sein. Basierend auf diesem vertieften mechanistischen Verständnis konnte in weiterführenden Arbeiten ein hocheffizientes, bimetallisches Katalysatorsystem für die *Z*-selektive Hydroamidierung terminaler Alkine entwickelt werden. Ein Katalysatorsystem, bestehend aus (cod)Ru^{II}(met)$_2$, Bis(dicyclohexylphosphino)butan und Ytterbiumtriflat, ermöglicht bereits nach 16 h bei 60 °C hohe Ausbeuten für die Umsetzung zahlreicher sekundärer Amide und Imide zu den entsprechenden Enamiden bzw. Enimiden. Dabei können durch den Einsatz des sterisch anspruchsvollen, chelatisierenden Phosphinliganden (*Z*/*E*)-Verhältnisse größer als 20 zu 1

erzielt und im Vergleich zu vorherigen Methoden eine deutliche größere Anwendungsbreite erreicht werden.

Die synthetische Reife der Ru-katalysierten Hydroamidierung terminaler Alkine wurde anhand der Synthese von Lansiumamid A und B, Lansamid I sowie Botryllamid C und E demonstriert. Alle Verbindungen wurden in ein bis drei Stufen und Gesamtausbeuten zwischen 57 und 98% hergestellt. In literaturbekannten Totalsynthesen für Lansiumamid A und B sowie Lansamid I konnten zuvor über vier bis fünf Schritte lediglich Ausbeuten von 8 bis 28% erhalten werden. Erstmals wurden die Botryllamide C und E sowie deren Z-konfigurierte Isomere synthetisch hergestellt. Bisher konnten durch Extraktion aus *Botryllus tyreus* nur *E*-konfigurierte Botryllamide gewonnen werden, möglicherweise aufgrund unerwünschter Isomerisierungsreaktionen unter den Extraktionsbedingungen.

Ein lohnenswertes Ziel zukünftiger Arbeiten besteht darin, die katalytische Aktivität der Hydroamidierungsverfahren weiter zu erhöhen; bisher werden TONs von maximal 50 erzielt. Ein möglicher Weg dazu wäre die Erforschung effizienterer Methoden zur Aktivierung der N-H-Bindung des Amids. Ferner könnte versucht werden, die Anwendungsbreite der vielfach preiswerteren Rutheniumtrichlorid-katalysierten Hydroamidierungsmethode auf die Umsetzung anderer Amide zu erweitern. Eine große Herausforderung bleibt die Entwicklung eines Markovnikov-selektiven Hydroamidierungsverfahrens. Aufgrund der Ergebnisse der mechanistischen Studien erscheint die Entwicklung einer solchen Hydroamidierungsmethode mit Ru^0/Ru^{II}-Katalysatoren nicht möglich, da die Reaktion über Ru-Vinyliden-Intermediate verläuft, die zur Bildung von *anti*-Markovnikov-Additionsprodukten führen. Durch Verwendung anderer Übergangsmetall-Katalysatoren, beispielsweise Gold- oder Kupfer-Komplexe, oder von Ru-Katalysatoren, die nicht in der Lage sind Vinyliden-Intermediate zu bilden, könnte eine Umkehr der Regioselektivität erzielt werden.

Direkte Carboxylierung terminaler Alkine mit CO_2

Im zweiten Teil dieser Dissertation wurde ein hocheffizientes Silber-katalysiertes Verfahren zur Carboxylierung terminaler Alkine entwickelt. Als Basis für die Entwicklung dieses Verfahrens dienten Katalysatorsysteme von Gooßen und Lu *et al.* Beide Verfahren benötigen hohe Katalysatorbeladungen und einen erhöhten CO_2-Druck, um hohe Umsätze zu den Propiolsäurederivaten zu erreichen. Durch gezielte Katalysatoroptimierung wurde ein Liganden-freies Normaldruck-Verfahren zur Carboxylierung terminaler Alkyl- und Arylalkine mit CO_2 realisiert (Schema 22, Reaktionspfad **a**). Während der Optimierungen

zeigte sich, dass in Abwesenheit von Liganden nicht das Gegenion der eingesetzten Kupfer(I)- oder Silber(I)-Quelle, sondern das Lösungsmittel entscheidend ist, um eine hohe Katalysatoraktivität zu erreichen. In DMSO konnten mit Silber(I)salzen besonders hohe Umsatzzahlen beobachtet werden, da DMSO in der Lage ist, über den Sauerstoff an das Silber(I)-Ion zu koordinieren und auf diese Weise Elektronendichte zu übertragen und die Löslichkeit zu erhöhen. Mit Cäsiumcarbonat als besonders milde Base werden bereits mit 500 ppm verschiedener Silber(I)salze nach 16 Stunden bei 50 °C und CO_2-Normaldruck volle Umsätze für eine Vielzahl von Alkyl- und Arylalkinen erreicht. Die Anwendungsbreite der neuen Methode wurde anhand von 21 Beispielen verdeutlicht, wobei unter anderem Halogen-, Ether-, Dialkylamin- und Trifluormethyl-Gruppen toleriert wurden. Im Vergleich mit allen bekannten Verfahren waren die erzielten Ausbeuten der freien Propiolsäurederivate durchweg höher. Mit einer Umsatzzahl von mehr als 3000 konnte ein neuer Benchmark für katalytische Carboxylierungsreaktionen gesetzt werden.

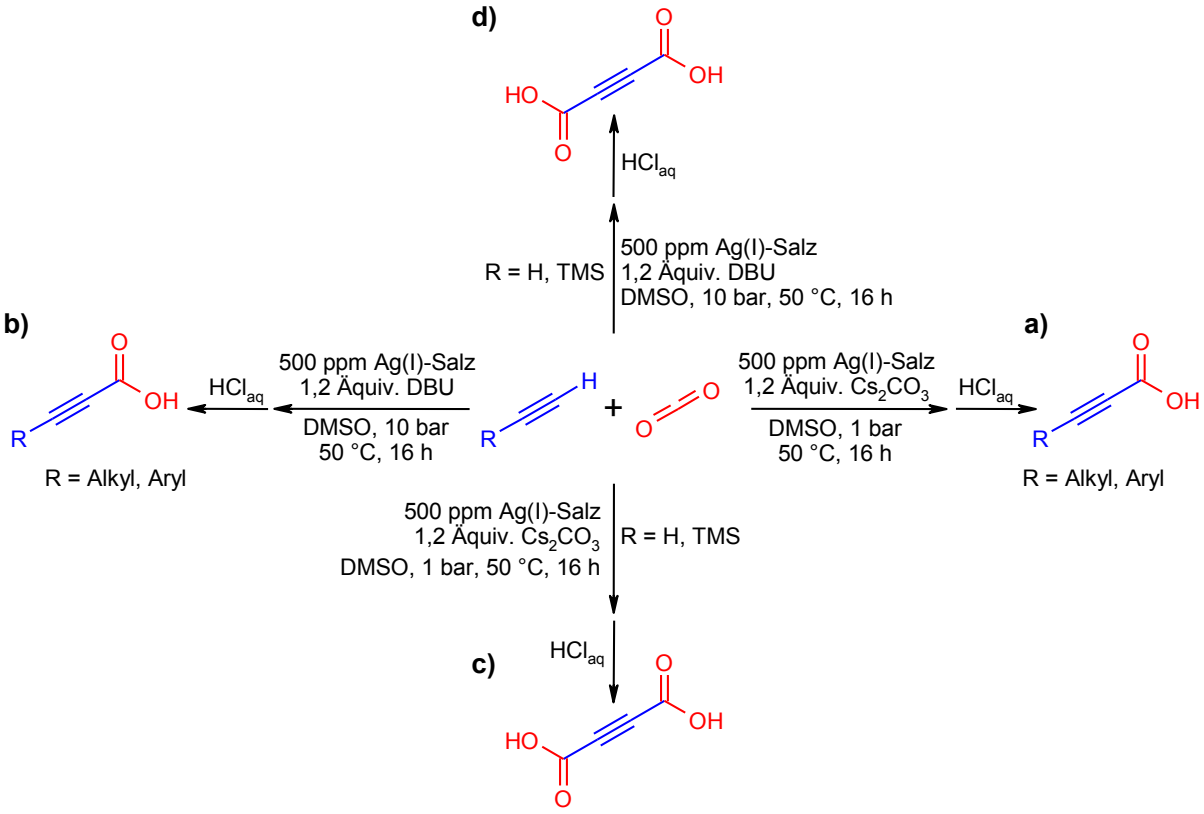

Schema 22. Neue Methoden zur Silber-katalysierten Carboxylierung von Alkyl- und Arylalkinen sowie von Ethin mit CO_2.

Aufbauend auf dieser Silber(I)/DMSO-katalysierten Methode konnte in weiterführenden Arbeiten eine Carboxylierungsmethode in Gegenwart von Aminbasen entwickelt werden

(Schema 22, Reaktionspfad **b**). Die Herausforderung bestand darin, dass sich mit Aminbasen, im Gegensatz zu anorganischen Basen wie Cs_2CO_3, keine schwerlöslichen Metallsalze der Propiolsäurederivate bilden und so das Gleichgewicht der Reaktion nicht durch physikalische Prozesse in Richtung der Produkte verschoben wird. Darüber hinaus reagieren viele Aminbasen mit CO_2 zu Carbamaten, die nur noch eine geringe Basizität besitzen. In Testreaktionen mit 1-Oktin und verschiedenen organischen Basen unter Standardbedingungen konnte nur für DBU und strukturverwandte Basen überhaupt die Produktbildung nachgewiesen werden. Die einzigartige Struktur von DBU ermöglicht eine reversible Speicherung von CO_2. Dadurch kann deutlich mehr CO_2 im Lösungsmittel gelöst werden und es liegt genügend freies DBU vor, damit die Deprotonierung des Alkins erfolgen kann. In Experimenten unter erhöhtem CO_2-Druck konnte eine Verschiebung des Gleichgewichts und somit eine Verbesserung des Umsatzes beobachtet werden. Unter optimalen Bedingungen können mit DBU als Base und 500 ppm eines Silber(I)salzes nach 16 Stunden bei 50 °C und 10 bar CO_2-Druck Umsatzzahlen von bis zu 760 für die Carboxylierung von 1-Oktin erzielt werden.

In Kooperation mit der BASF SE sollte abschließend eine Methode zur Darstellung von Acetylendicarbonsäure entwickelt werden. Die Übertragung einer Carboxylierungsmethode für primäre Alkine auf Ethin ist keineswegs trivial, da Ethin nur schwach in organischen Solventien löslich ist und CO_2 als zweiter Reaktant aufgrund der deutlich höheren Löslichkeit eine Anreicherung von Ethin im Reaktionsmedium zusätzlich erschwert. Auch die zunächst entstehenden Salze der Acetylenmonocarbonsäure sind nur wenig löslich, sodass eine zweite Carboxylierung unter Bildung von Acetylendicarbonsäure erschwert wird und oftmals Produktgemische der Mono- und Di-Säure entstehen. Mit dem neuen Silber(I)/DMSO Katalysatorsystem und Cs_2CO_3 als Base konnten bereits bei Normaldruck mit Ethin-CO_2-Gemischen Umsatzzahlen von bis zu 1240 erzielt werden (Schema 22, Reaktionspfad **c**). Dabei gelang es erstmals, selektiv durch katalytische Umsetzung von Ethin mit CO_2 die freie Acetylendicarbonsäure atomökonomisch darzustellen. Im direkten Vergleich zu dem zuvor einzig bekannten Kupfer-katalysierten Alternativverfahren, mit dem nur ein Gemisch der Mono- und Dicarbonsäurehexylester erhalten werden konnte, wurden mehr als 600fach höhere Umsatzzahlen erreicht.

Bei erhöhtem Reaktionsdruck können auch Aminbasen für die Herstellung von Acetylendicarbonsäure verwendet werden. Mit DBN oder DBU als Base bei 10 bar Druck (1 bar Ethin und 9 bar CO_2) können Umsatzzahlen von bis zu 18 erreicht werden (Schema 22, Reaktionspfad **d**). Der Vorteil von Aminbasen gegenüber anorganischen Basen besteht darin,

Folgereaktionen wie beispielsweise eine Hydrierung ohne weiteren Aufarbeitungsschritt durchführen zu können. So könnte Acetylendicarbonsäure direkt in die industriell wertvollen Basischemikalien 2-Butin-1,4-diol und Butan-1,4-diol überführt werden.

Eine erfolgversprechende Vorgehensweise für zukünftige Arbeiten wäre, analog zur erfolgreichen Weiterentwicklung von Hydroamidierungsverfahren, aufbauend auf umfassenden mechanistischen Studien zur Carboxylierung neue Ansatzpunkte für die Katalysatoroptimierung zu identifizieren. So könnte geklärt werden, ob die hohe katalytische Aktivität in DMSO als Lösungsmittel mit der Funktion als Elektronen-donierender Ligand oder der literaturbekannten *in situ* Bildung von Silber-Nanopartikeln in DMSO zusammenhängt. Mit einem besseren mechanistischen Verständnis könnten noch rationalere Katalysatoroptimierungen erfolgen und noch effizientere Methoden entwickelt werden. Ein möglicher Weg dazu könnte in der Verwendung heterogenisierter Silber(I)- oder Kupfer(I)-Katalysatoren liegen. So wäre eine einfachere Rückgewinnung des Katalysators aus dem Reaktionsansatz möglich und durch mehrfache Wiederverwendung des Katalysators insgesamt noch höhere Umsatzzahlen erzielbar. Ein weiterer lohnenswerter Ansatz besteht in der Entwicklung von Verfahren, die bereits mit katalytischen Mengen an Base vollständige Umsätze ermöglichen, da theoretisch das Propiolatsalz, das während der Reaktion anfällt, in nachfolgenden Zyklen als Base fungieren kann.

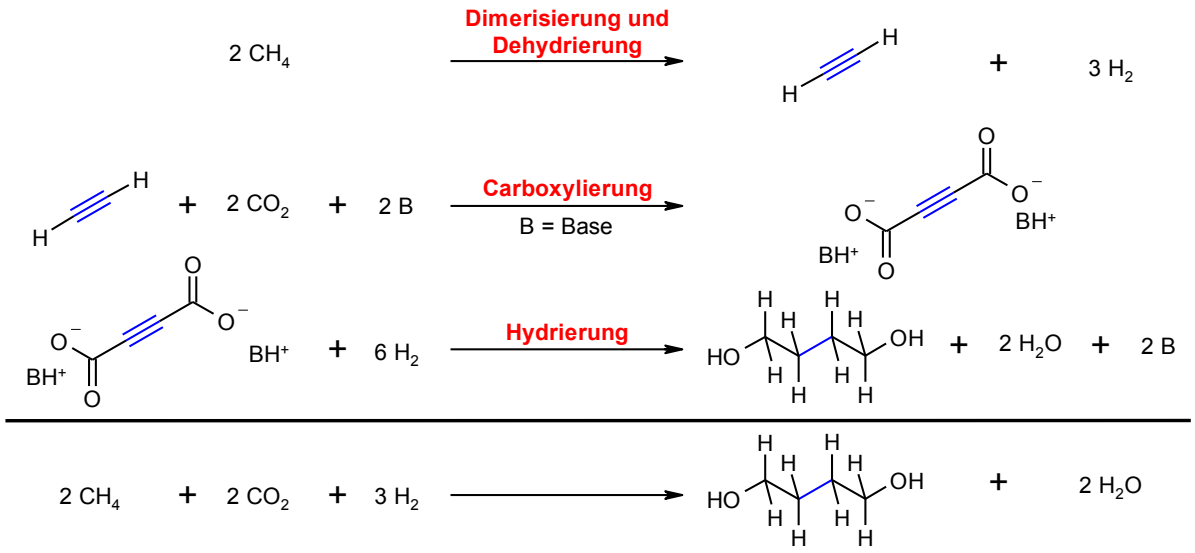

Schema 23. Neuer Syntheseweg zu Butan-1,4-diol ausgehend von Erdgas.

Mit den hier beschriebenen Arbeiten konnte bereits ein großer Schritt in Richtung der industriellen Nutzung von katalytischen Carboxylierungsverfahren terminaler Alkine gemacht werden. In zukünftigen Arbeiten müsste eine deutliche Erhöhung der Katalysatoraktivität

erzielt und ein *in situ* Reduktionsverfahren entwickelt werden. Darauf aufbauend könnte mit einer optimierten Darstellungsmethode von Acetylendicarbonsäure ein neuer industrieller Syntheseweg zu Butan-1,4-diol ausgehend von Erdgas realisiert werden (Schema 23).

Auf diese Weise könnte sowohl Ethin als auch Wasserstoff durch Dimerisierung und Dehydrierung von Methan erzeugt werden. Durch anschließende katalytische Carboxylierung mit CO_2 in Gegenwart einer organischen Base würde ein Acetylendicarboxylat generiert werden. Dieses könnte *in situ* vollständig zu Butan-1,4-diol hydriert werden, wobei die Base regeneriert und als einziges Nebenprodukt Wasser gebildet wird. Die Hälfte des für die Hydrierung benötigten Wasserstoffs würde bei der Dehydrierung von Methan anfallen. Insgesamt würde auf diese Weise ein Verfahren ermöglicht, das aus zwei Äquivalenten Methan mit zwei Äquivalenten CO_2 und drei Äquivalenten H_2 ein Äquivalent Butan-1,4-diol und zwei Äquivalenten Wasser erzeugt. Aus ökonomischer und ökologischer Sicht ist dieses Verfahren bestehenden Synthesewegen gegenüber deutlich überlegen. In Kooperation mit der Industrie soll dieses Verfahren auf die großtechnische Produktion von Butan-1,4-diol übertragen werden.

VI. Experimenteller Teil

VI.1. General Information

VI.1.1. Solvents and Chemicals

All used solvents were purified by generally described procedures.[48] All commercially available reagents were distilled either from CaH_2 or molecular sieves under an inert atmosphere before use. All commercially available compounds with a purity higher than 95% were used without further purification, if not stated otherwise.

VI.1.2. High-throughput experiments

In order to perform a large number of experiments in a minimal amount of time a specially manufactured setup was used. All reactions were carried out in 20, 50 or 100 mL headspace vials that were closed and clamped shut with aluminum caps fitted with a Teflon-coated butyl rubber septum (both commercially available at e.g. *Macherey & Nagel*).

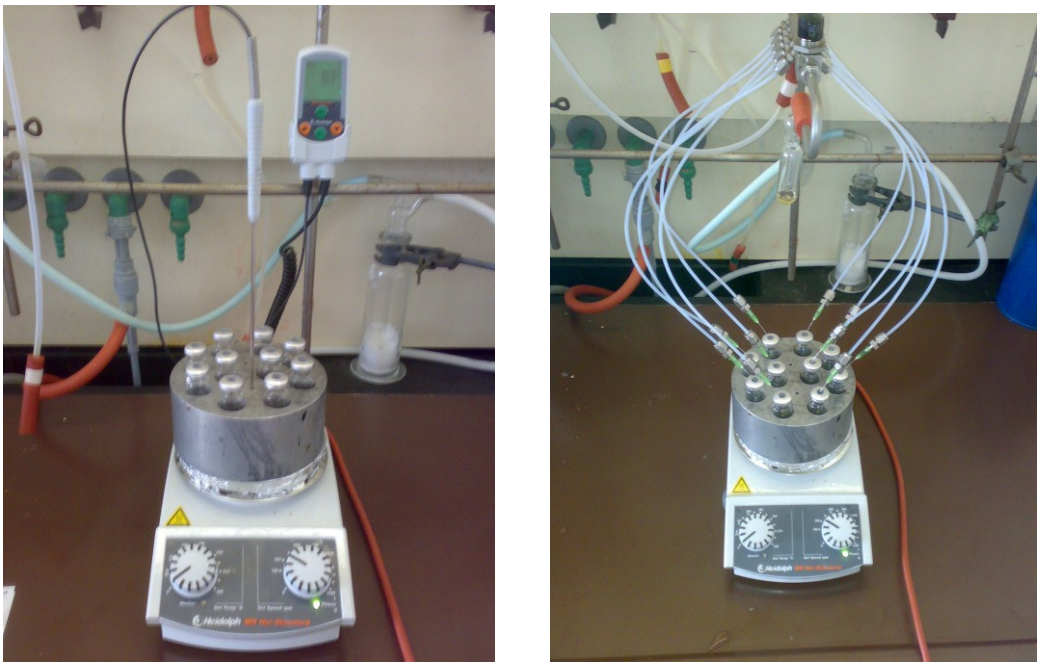

Figure 1. Reaction setup: Aluminum block with 10 reaction vials with and without vacuum distributor.

In 8 cm high round aluminum blocks, which fit the hot plate of a regular laboratory heater (e.g. *Heidolph Hei-Standard*) in diameter, 10 prepared 20 mL headspace vials (10 of 50 mL

and 5 of 100 mL headspace vials) can be tempered between 25°C and 180 °C. A smaller hole drilled in the middle of the case creates room to hold the thermometer of the heater (Figure 1, left).

Special vacuum distributors were manufactured and connected to the Schlenk-line to correctly evacuate and refill 10 reaction vessels with inert gas simultaneously (Figure 1, right). A steel tubing is linked to ten 3 mm Teflon tubes, which are equipped on the opposite end with adaptors for Luer-Lock syringe needles. This way the steel tubing can be connected to the Schlenk-line *via* a steel olive and vacuum tubing.

In order to perform ten or more reactions in parallel the following protocol was used. All solid compounds were weighed in oven-dried reaction vessels, oven-dried 20 mm stirring bars were added and each vessel was closed with a separate cap using flanging pliers. All ten vessels were transferred to one of the aforementioned aluminum blocks and evacuated using syringe needles connected to the vacuum steel tubing.

The reaction vessels were evacuated and refilled with nitrogen three times. An oil bubbling valve at the top of the steel tubing was used to guarantee a pressure release. Using standard sterile and Hamilton syringes all liquid reagents, stock solutions of reagents, solvents and the internal standard (*n*-tetradecane) were added. After removal of the needles, the aluminum block was tempered to the desired temperature, which only differs by maximum 2°C from the actual reaction media temperature.

Figure 2. Modified reaction setup for carboxylation reactions: 1200 mL CO_2 glass container.

For carboxylation reactions at normal pressure the same procedure was performed but the needles of the vacuum distributors remained connected to the vials for the entire reaction time. This way a 1200 mL glass container filled with CO_2 was connected to the reaction vials *via* the Schlenk-line and the vacuum distributors (Figure 2). The atmosphere of the reaction mixture was exchanged another three times with CO_2 to enrich the solvent with the gaseous reactant, and then the aluminum block was heated to the desired temperature.

For carboxylation reactions at 10 bar pressure the needles were removed and the vessels were transferred into an autoclave-reactor (Figure 3). Long twisted needles were pierced into the septa of the reaction vials, the reactor was closed and the atmosphere was exchanged 3 times by alternating vacuum-CO_2 cycles. Then the autoclave-reactor was pressurized with 1 bar of acetylene and 9 bar of CO_2 or 10 bar of CO_2 (if 1-octyne was used), and the reaction mixtures were stirred for 16 h at 50 °C.

Figure 3. Autoclave-reactor manufactured by the Max-Planck-Institut für Kohlenforschung.

After stirring the reaction mixtures at the required temperature for the necessary reaction time the reaction vials were cooled down to room temperature and opened carefully. The internal standard (*n*-tetradecane; if not added before) and 2 to 4 mL of ethyl acetate were added to dilute the reaction mixture. The mixture was thoroughly mixed with a disposable pipette to ensure a high homogeneity. Then a 0.25 mL sample was withdrawn and filled in a 10 mL work-up vial filled with 2 mL of ethyl acetate and 2 mL of saturated potassium carbonate solution or water. The mixture was also thoroughly mixed with the disposable pipette and after phase separation the organic layer was removed with the disposable pipette,

filtered into a GC-vial through a glass pipette filled with a cotton plug and magnesium sulfate, and analyzed *via* GC.

Figure 4. Combi Flash Companion-Chromatography.

For HPLC-analysis the cooled-down reactions mixtures were filtered and washed with acetonitrile (10.0 mL). The resulting crude was dissolved in cold water (1.00 mL) and the internal standard (NMP) was added. A sample (0.10 mL) was abstracted and transferred into a HPLC-vial, diluted in water (1.90 mL) and analyzed *via* HPLC.

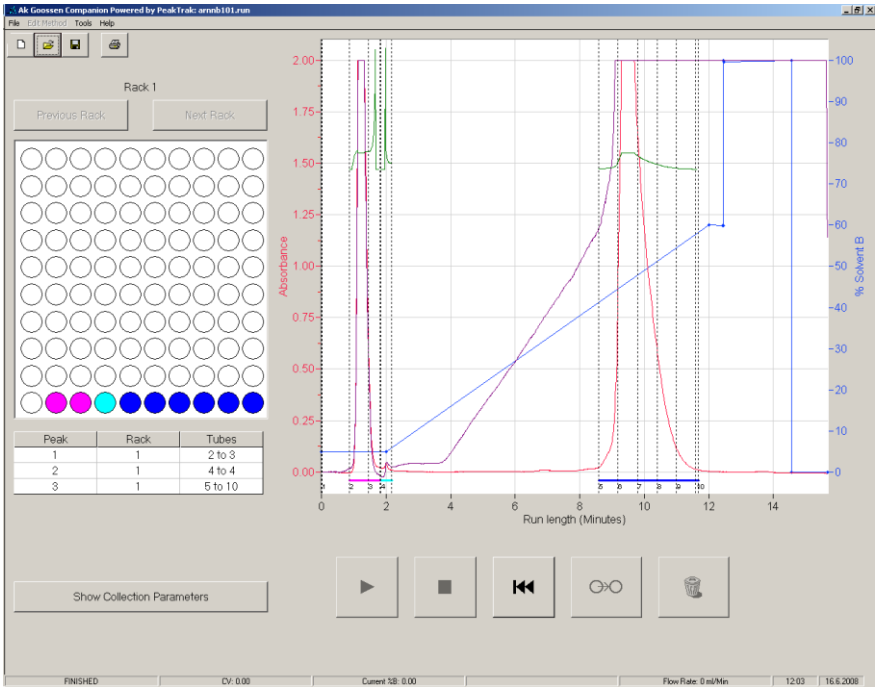

Figure 5. Screenshot of the *PeakTrak* control software.

After evaluating them *via* GC analysis and if necessary *via* GC-MS, the contents of all reaction, work-up and analysis vials were recombined and the product isolated using standard procedures, deposed on silica-gel and purified by flash chromatography (Figure 4).

Column chromatography was performed using a *Combi Flash Companion-Chromatography-System* (*Isco-Systems*) with DAD and *RediSep*® packed column (12 g). The instrument was controlled by the *PeakTrak* software (Figure 5).

Preparative scale reactions were performed mostly in standard laboratory oven-dried glassware.

The described reaction setups supported by the highly efficient electronic laboratory journal and inventory system *open enventory* (Figure 6) allowed to perform a substantial amount of reactions during the course of this work. More than 2500 reactions would have consumed a much longer period of time using standard laboratory techniques.

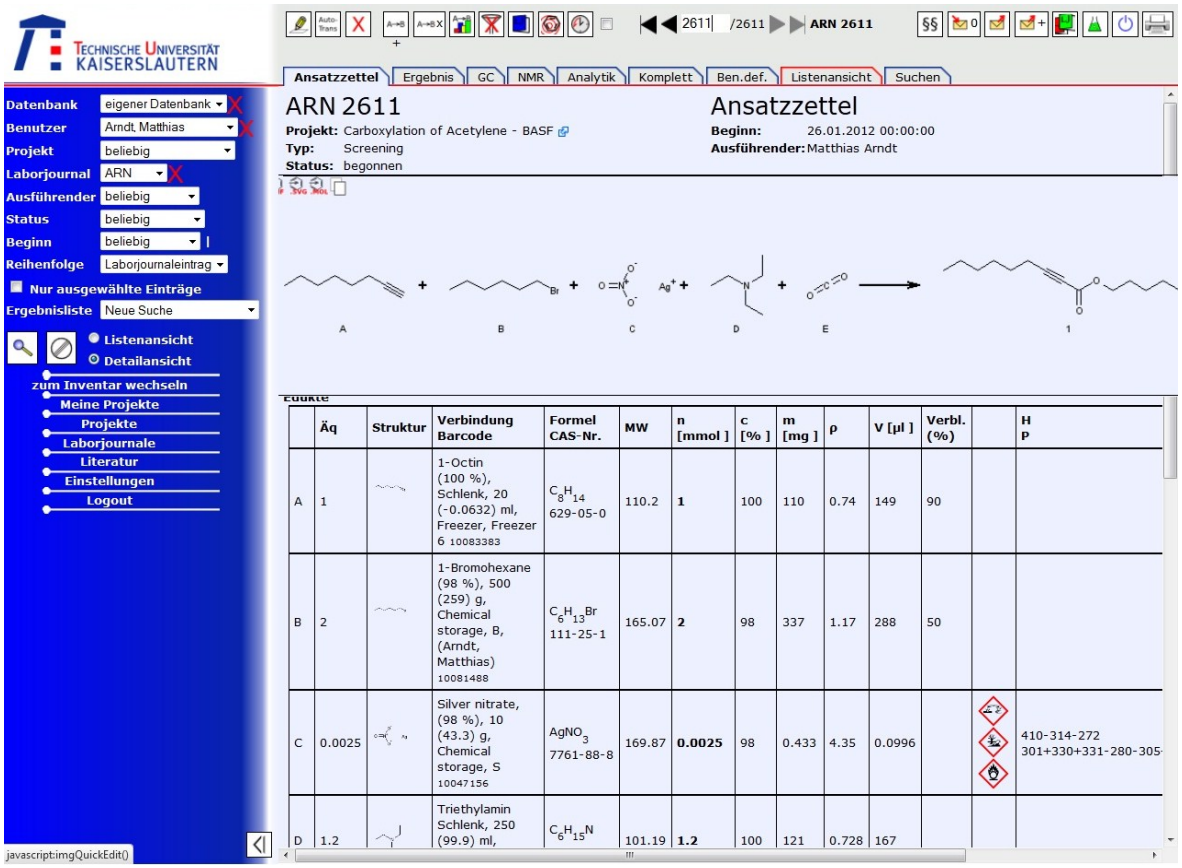

Figure 6. Screenshot of the electronic laboratory journal *open enventory*.

The following experimental section describes all reactions mentioned in the sections above. Yields are isolated yields if not stated otherwise. All known compounds were analyzed by proton and carbon NMR, as well as GC-MS, GC/HRMS and elemental analysis.

VI.2. Analytical methods

VI.2.1. Nuclear Magnetic Resonance

Proton- and decoupled carbon-NMR spectra were recorded with a *Bruker FT-NMR DPX 200*, *DPX 400* and a *Bruker Avance 600*. The frequency and solvent used is described separately for each substance. Chemical shifts are given in units of the δ-scale in ppm. Shifts for ^{1}H-spectra are given respectively to the proton signal of the solvent used (chloroform: 7.25 ppm, dimethyl sulfoxide: 2.50 ppm, methanol: 3.35 ppm, water: 4.75 ppm), for ^{13}C-spectra respectively to the deuterated solvent (chloroform: 77.0 ppm, dimethyl sulfoxide: 37.7 ppm, methanol: 49.3 ppm). *The atom numbering within products is not according to the IUPAC rules*. The multiplicity of the signals is abbreviated by the following letters: s = singlet, d = doublet, dd = doublet of doublets, ddd = doublet of doublet of doublets, dt = doublet of triplets, t = triplet, q = quartet, quin = quintet.

Coupling constants are given in Hertz (Hz). Processing and interpretation was performed with *ACD-Labs 12.0* (Advanced Chemistry Development Inc.).

VI.2.2. Gas-Chromatography

For GC-analysis a *Hewlett Packard 5890* or a *Hewlett Packard 6980* chromatograph was used. The gas carrier was nitrogen with a flow rate of 149 mL/min (0.5 bar pressure). The temperature of the injector was 220 °C. The split-ratio was 1:100. For separation an Agilent HP-5-column with 5% phenyl-methyl-siloxane (30 x 320 µm x 1.0 µm, 100/ 2.3-30-300/ 3) was used. The following temperature program was implemented: starting temperature 60 °C (2min), linear temperature increase (30 °C min^{-1}) to 300 °C, end temperature 300 °C (13min).

VI.2.3. Elemental Analysis

CHN-elemental analysis was performed with a *Perkin-Elmer Elemental Analyzer EA 2400 CHN*.

VI.2.4. High-Performance-Liquid-Chromatography

A *Shimadzu LC-2010A* High Performance Liquid Chromatograph with a Merck Reversed Phase LiChroCat© PAH C 18 column with a particle diameter of 5 µm was used at a constant oven temperature of 50 °C and a column pressure of 125 bar. The eluents used were water and acetonitrile with a flow rate of 1.5 mL/min. Gradient: 5% acetonitrile for 1 min, linear increase to 90% acetonitrile during the course of 5 min, constant gradient for 2 min, decrease to 5% within 0.2 min and constant for 1.8 min. The standard configuration injected 5 µL of the sample. This amount could be manually changed with the control and interpretation program *Shimadzu Class-VP* (Figure 7).

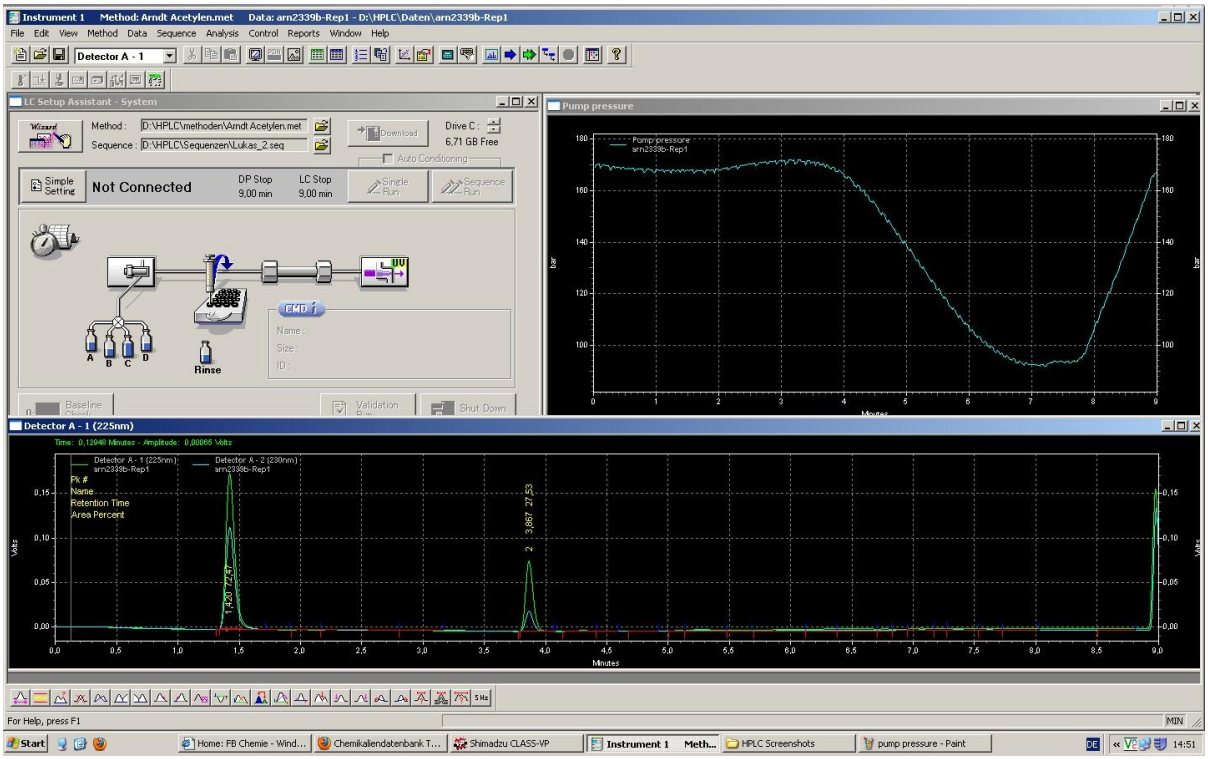

Figure 7. Screenshot of the *Shimadzu Class-VP* control software.

VI.2.5. Mass Spectrometry

Mass spectrometry was performed with a *GC-MS Varian Saturn 2100 T*. The ionization was done by EI AGC. The intensities of the signals are relative to the highest peak. For fragments with isotopomers only the most intensive peak of the isotopomer is given.

VI.2.6. High Resolution Mass Spectrometry (HRMS)

GC/HRMS analysis was performed with a *Waters GCT Premier*.

VI.2.7. Electrospray Ionization Mass Spectrometry (ESI-MS)

In situ ESI-MS experiments were performed with a *Bruker Esquire 3000plus* ion trap instrument. The ion source was used in positive electrospray ionization mode. Scan speed was 13000 *m/z* / s in normal resolution scan mode (0.3 FWHM / *m/z*), scan range was at least 50 to 1500 *m/z*. All spectra were accumulated for at least one minute. Sample solutions in toluene at concentrations of 0.007 M were continuously infused into the ESI chamber at a flow rate of 4 µL/min using a syringe pump. Nitrogen was used as drying gas with flow rate of 3.0 L/min at 300 °C. The solutions were sprayed at a nebulizer pressure of 4 psi (275.8 mbar) and the electrospray needle was typically held at 4.5 kV. The instrument was controlled by *Bruker Esquire Control 5.3* software and data analysis was performed using *Bruker Data Analysis 3.4 software* (Figure 8).

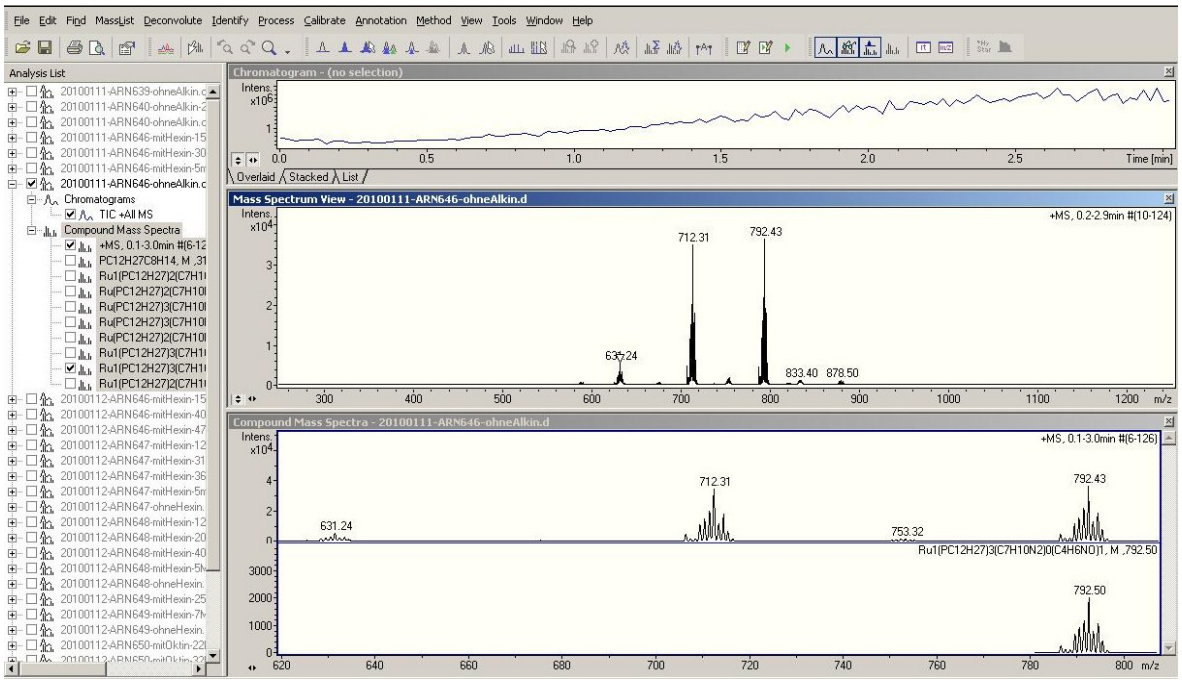

Figure 8. Screenshot of the *Bruker Data Analysis 3.4 software.*

VI.2.8. Infrared Spectroscopy

Infrared spectra were recorded with a *Perkin*-Elmer Fourier Transform Infrared Spectrometer FT/IR or a *Perkin Elmer Spectrum 100 FT-IR spectrometer* equipped with an *Universal ATR Accessory* (UATR). Solids were thoroughly grounded and mixed with potassium bromide and pressed into a pellet or directly measured with the ATR Accessory. Liquids were measured as a thin film in between sodium chloride plates or with the ATR

Accessory. Absorbance-bands are shown in wave numbers (cm^{-1}). Intensities are abbreviated: s (strong), m (medium) and b (broad).

VI.2.9. In situ Infrared Spectroscopy

In situ IR experiments were performed using a *Mettler Toledo ReactIR 45m FT-IR* spectrometer equipped with a multiplexing unit and a DS-SiComp-1.5m (length)-AgX-9.5mm (rod diameter) fiber conduit. All spectra were recorded over a wavelength range from 2800 cm^{-1} to 650 cm^{-1}, at a resolution of 8 cm^{-1}, using a MCT (Mercury Cadmium Telluride) detector and the Happ-Genzel apodization. Every 10 seconds, a spectrum was recorded with 32 scans per spectrum (Figure 9).

Figure 9. Experimental set-up for *in-situ* hydroamidation experiments.

The system was controlled and the raw data were collected and analyzed by the *iC IR reaction analysis software* (version 4.1 and 4.2, Figure 10).

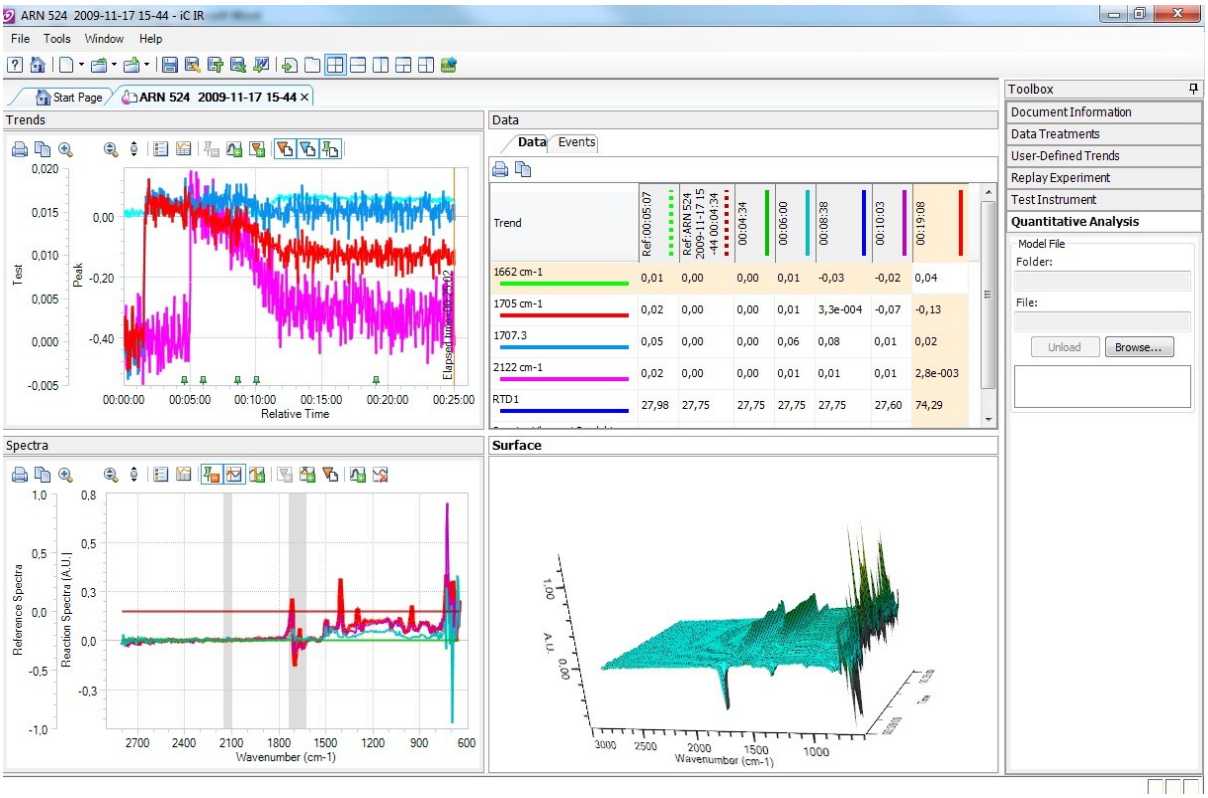

Figure 10. Screenshot of the *iC IR* reaction analysis control software.

VI.3. Mechanistic investigation of the Ru-Catalyzed hydroamidation of terminal alkynes: experimental procedures and spectroscopic data

VI.3.1. General Methods

Reactions were performed in oven-dried glassware containing a Teflon-coated stirrer bar and dry septum under a nitrogen atmosphere. Solvents were freshly distilled from CaH_2. All commercially available reagents were distilled either from CaH_2 or molecular sieves under an inert atmosphere before use. Deuterated amides were prepared by exchange reactions in ethanol-d_1. 1-[*D*]-hex-1-yne was prepared according to a literature procedure.[49] GC analyses were carried out using an HP-5 capillary column (Phenyl Methyl Siloxane 30 m x 320 x 0.25, 100/2.3-30-300/3) and a time program beginning with 2 min at 60 °C followed by 30 °C/min ramp to 300 °C, then 3 min at this temp. Column chromatography was performed using Combi Flash Companion-Chromatography-Systems (Isco-Systems) and RediSep packed column (12 g). NMR spectra were obtained on Bruker Avance 600 systems using $CDCl_3$, DMF-d_7, benzene-d_6 or toluene-d_8 as the solvents, with proton, carbon and phosphorus resonances at 600.3 MHz, 150.9 MHz, and 242.9 MHz, respectively; on Bruker DPX 400 systems using $CDCl_3$, benzene-d_6 or toluene-d_8 as the solvents, with proton, deuterium, carbon

and phosphorus resonances at 400.1 MHz, 61.4 MHz, 101.6 MHz, and 162.0 MHz. Mass spectral data were acquired on a GC-MS Saturn 2100 T (Varian). Electrospray ionization mass spectrometry (ESI-MS) was performed with a Bruker Esquire 3000plus ion trap instrument. The ion source was used in positive electrospray ionization mode. Scan speed was 13000 *m/z* / s in normal resolution scan mode (0.3 FWHM / *m/z*), scan range was at least 50 to 1500 *m/z*. All spectra were accumulated for at least one minute. Sample solutions in toluene at concentrations of 0.007 M were continuously infused into the ESI chamber at a flow rate of 4 µL/min using a syringe pump. Nitrogen was used as drying gas with flow rate of 3.0 L/min at 300 °C. The solutions were sprayed at a nebulizer pressure of 4 psi (275.8 mbar) and the electrospray needle was typically held at 4.5 kV. The instrument was controlled by Bruker Esquire Control 5.3 software and data analysis was performed using Bruker Data Analysis 3.4 software. In situ IR experiments were performed using a ReactIR 45m FT-IR spectrometer equipped with a multiplexing unit and a DS-SiComp-1.5m (length)-AgX-9.5mm (rod diameter) fiber conduit. All spectra were recorded over a wavelength range from 2800 cm^{-1} to 650 cm^{-1}, at a resolution of 8 cm^{-1}, using a MCT (Mercury Cadmium Telluride) detector and the Happ-Genzel apodization. Every 10 seconds, a spectrum was recorded with 32 scans per spectrum. The system was controlled and the raw data were collected and analyzed by the iC IR reaction analysis software (version 4.1 and 4.2).

VI.3.2. Catalytic hydroamidation of terminal alkynes.

Hydroamidation of secondary amides, exemplified by the reaction of 1-hexyne (JACS-5b) with 2-pyrrolidinone (JACS-1a):

Synthesis of *N*-((*E*)-hex-1-enyl)pyrrolidin-2-one (JACS-6a) [CAS: 863709-29-9]: Method A: An oven-dried flask was charged with bis-(2-methallyl)-cycloocta-1,5-diene-ruthenium(II) (6.4 mg, 0.02 mmol) and DMAP (4.99 mg, 0.04 mmol) and flushed with argon. Subsequently, tri-*n*-butylphosphine (15 µL, 0.06 mmol), 2-pyrrolidinone (**JACS-1a**) (85.1 mg, 1.00 mmol), 1-hexyne (**JACS-5b**) (229 µL, 2.00 mmol), and dry toluene (3.00 mL) were added via syringe. The resulting green solution was stirred for 15 h at 100 °C and was then poured into aqueous $NaHCO_3$ solution (30 mL). The resulting mixture was extracted repeatedly with 20 mL portions of ethyl acetate, the combined organic layers were washed with water and brine, dried over $MgSO_4$, filtered, and the volatiles were removed in vacuo. The residue was purified by column chromatography (silica gel, ethyl acetate / hexane 3:1)) yielding a 28:1 mixture of **JACS-6a** and **JACS-7a** as a colorless oil (158.9 mg, 95 % yield).

Method B: An oven-dried flask was charged with potassium carbonate (20.7 mg, 0.15 mmol), and a stock solution containing ruthenium(III) chloride hydrate (7.8 mg, 0.03 mmol), 4-dimethylaminopyridine (11.0 mg, 0.09 mmol) and acetone (1.0 mL). The acetone was removed in vacuo and the flask flushed with nitrogen. Subsequently, tri-*n*-butylphosphine (22 µL, 0.09 mmol), pyrrolidin-2-one (**JACS-1a**, 77 µL, 1.00 mmol), 1-hexyne (**JACS-5b**, 229 µL, 2.00 mmol), water (7 µL, 0.40 mmol) and dry toluene (3.00 mL) were added via syringe. The resulting solution was stirred for 15 h at 100 °C, then poured into an aqueous $NaHCO_3$ solution (30 mL). The resulting mixture was extracted repeatedly with 20 mL portions of ethyl acetate, the combined organic layers were washed with water and brine, dried with $MgSO_4$, filtered, and the volatiles were removed in vacuo. The residue was purified by column chromatography (silica gel, ethyl acetate/hexane 2:3) yielding a 32:1 mixture of **JACS-6a** and **JACS-7a** as a yellowish oil (165.6 mg, 99%). ^{1}H-NMR (600.3 MHz, $CDCl_3$): δ = 6.70 (d, ^3J = 14.5 Hz, 1H), 4.79 (dt, ^3J = 14.4 Hz, 7.2 Hz, 1H), 3.34 (t, ^3J = 7.2 Hz, 2H), 2.31 (t, ^3J = 8.2 Hz, 2H), 1.87–1.99 (m, 4H), 1.12-1.27 (m, 4H), 0.74 (t, ^3J = 7.2 Hz, 3H) ppm. ^{13}C-NMR (150.9 MHz, $CDCl_3$): δ = 172.3, 123.2, 112.1, 44.9, 31.9, 30.9, 29.4, 21.7, 17.1, 13.5 ppm. MS (EI, 70 eV): *m/z* (%) = 168 (12, [M^+]), 124 (100), 96 (44), 86 (23), 69 (11), 41 (14).

Synthesis of *N*-((*Z*)-hex-1-enyl)pyrrolidin-2-one (JACS-7a) [CAS: 863709-30-2]: Method A: An oven-dried flask was charged with bis-(2-methallyl)-cycloocta-1,5-diene-ruthenium(II) (6.4 mg, 0.02 mmol), DMAP (4.99 mg, 0.04 mmol), bis(dicyclohexylphosphino)methane (12.3 mg, 0.03 mmol) and flushed with argon. Subsequently, 2-pyrolidinone (**JACS-1a**, 85.1 mg, 1.00 mmol), 1-hexyne (**JACS-5b**, 229 µL, 2.00 mmol), dry toluene (3.00 mL) and deoxygenated water (144 mL, 8 mmol) were added via syringe. The resulting green solution was stirred for 15 h at 100 °C and was then poured into aqueous $NaHCO_3$ solution (30 mL) and the resulting mixture was extracted repeatedly with 20 mL portions of ethyl acetate. The combined organic layers were washed with water and brine, dried over $MgSO_4$, filtered, and the volatiles were removed in vacuo. The residue was purified by column chromatography (silica gel, ethyl acetate / hexane 3:1) yielding a 5:1 mixture of **JACS-7a** and **JACS-6a** (166.1 mg, 99 %) as a colorless oil. **Method B**: An oven-dried flask was charged with bis(2-methallyl)-cycloocta-1,5-diene-ruthenium(II) (6.39 mg, 0.02 mmol), 1,4-bis(dicyclohexylphosphino)butane (10.1 mg, 22.5 µmol) and ytterbiumtriflatehydrate (24.8 mg, 0.04 mmol) and flushed with nitrogen. Subsequently, 2-pyrolidinone (**JACS-1a**, 85.1 mg, 1.00 mmol), 1-hexyne (**JACS-5b**, 229 µL, 2.00 mmol) and dry chlorobenzene (3.00 mL) were added via syringe. The resulting mixture was stirred for

16 h at 60 °C. Then, it was allowed to cool down to room temperature and the reaction mixture was purified without further work-up by column chromatography (silica gel, ethyl acetate/hexane 3:7) yielding a 11:1 mixture of **JACS-7a** and **JACS-6a** (119.0 mg, 71 %) as a colorless oil.. ^{1}H-NMR (benzene-d_6, 400.1 MHz): δ = 6.73 (d, ^{3}J = 10.2 Hz, 1H), 4.54−4.61 (m, 1H), 3.08 (t, ^{3}J = 7.0 Hz, 2H), 1.97−2.06 (m, 2H), 1.90 (t, ^{3}J = 8.2 Hz, 2H), 1.15−1.30 (m, 6H), 0.86 (t, ^{3}J = 6.8 Hz, 3H). ^{13}C-NMR (benzene-d_6, 101.6 MHz): δ = 173.4, 122.8, 113.3, 47.8, 33.1, 29.9, 27.1, 22.6, 18.3, 14.1. MS (EI, 70 eV), *m/z* (%): 168 (100, [M^+]), 167 (9), 124 (53), 96 (32), 94 (6). IR (NaCl): = 1662 cm^{-1}, 1702, 2872, 2927, 2957. Anal. Calcd. for $C_{10}H_{17}NO$ (167.3): C, 71.81; H, 10.25; N, 8.37. Found: C, 70.81; H, 10.47; N, 8.29.

Hydroamidation of imides, exemplified by the reaction of 1-hexyne (JACS-5b) with succinimide (JACS-2a):

Synthesis of *N*-((*E*)-hex-1-enyl)succinimide (JACS-8a) [CAS: 888973-40-8]: An oven-dried flask was charged with bis-(2-methallyl)-cycloocta-1,5-diene-ruthenium(II) (16 mg, 0.05 mmol), scandium triflate (19.7 mg, 0.04 mmol) and succinimide (**JACS-2a**, 99.1 mg, 1.00 mmol) and flushed with argon. Subsequently, tri-isopropylphosphine (29 µL, 0.15 mmol), 1-hexyne (**JACS-5b**, 229 µL, 2.00 mmol), and dry DMF (3.00 mL) were added via syringe. The resulting colorless solution was stirred for 15 h at 60 °C, then poured into an aqueous $NaHCO_3$ solution (30 mL). The resulting mixture was extracted repeatedly with 20 mL portions of ethyl acetate, the combined organic layers were washed with water and brine, dried with $MgSO_4$ and filtered, and the volatiles were removed in vacuo. The residue was purified by column chromatography (silica gel, ethyl acetate/hexanes 3:1) yielding a 15:1 mixture of **JACS-8a** and **JACS-9a** (135.5 mg, 75 %) as a yellowish oil. ^{1}H-NMR (400.1 MHz, $CDCl_3$): δ = 6.52 (d, ^{3}J = 14.7 Hz, 1H), 6.36 (dt, ^{3}J = 15.0 Hz, 14.7 Hz, 1H), 2.66 (s, 4H), 2.05 (dt, ^{3}J = 14.6, 7.2 Hz, 2H), 1.37 (m, 2H), 1.24–1.31 (m, 4H), 0.83 (t, ^{3}J = 7.2 Hz, 3H) ppm. ^{13}C-NMR (101.6 MHz, $CDCl_3$): δ = 175.4, 124.5, 117.8, 31.2, 30.5, 27.6, 22.0, 13.7 ppm. MS (EI, 70 eV): *m/z* (%) = 182 (30, [M^+]), 138 (100), 100 (75), 82 (94), 56 (53). Anal. Calcd for $C_{10}H_{15}NO_2$: C, 66.2; H, 8.3; N, 7.7. Found: C, 66.4; H, 8.5; N, 7.9.

Synthesis of *N*-((*Z*)-hex-1-enyl)succinimide (JACS-9a) [CAS: 863709-33-5]: An oven-dried flask was charged with bis-(2-methallyl)-cycloocta-1,5-diene-ruthenium(II) (6.4 mg, 0.02 mmol), scandium triflate (19.7 mg, 0.04 mmol) and succinimide (**JACS-2a**, 99.1 mg, 1.00 mmol) and flushed with argon. Subsequently, tri-*n*-butylphosphine (15 µL, 0.06 mmol), 1-hexyne (**JACS-5b**, 229 µL, 2.00 mmol), and dry DMF (3.00 mL) were added via syringe. The resulting colorless solution was stirred for 15 h at 60 °C, then poured into an aqueous

$NaHCO_3$ solution (30 mL). The resulting mixture was extracted repeatedly with 20 mL portions of ethyl acetate, the combined organic layers were washed with water and brine, dried with $MgSO_4$, and filtered, and the volatiles were removed in vacuo. The residue was purified by column chromatography (silica gel, ethyl acetate/hexanes 3:1) yielding a 8:1 mixture of **JACS-9a** and **JACS-8a** (177.6 mg, 98%) as a yellowish oil. ^{1}H-NMR (400.1 MHz, $CDCl_3$): δ = 5.82 (d, ^3J = 8.6 Hz, 1H), 5.68 (dt, ^3J = 15.0 Hz, 7.5 Hz, 1H), 2.74 (s, 4H), 1.89 (dt, ^3J = 14.6, 7.3, 1.6 Hz, 2H), 1.25–1.36 (m, 4H), 0.83 (t, ^3J = 7.1 Hz, 3H) ppm. ^{13}C-NMR (101.6 MHz, $CDCl_3$): δ = 175.6, 133.6, 116.7, 30.7, 28.4, 27.7, 22.3, 13.8 ppm. MS (EI, 70 eV): *m/z* (%) = 182 (13, [M^+]), 138 (67), 100 (75), 82 (100), 56 (44). Anal. Calcd for $C_{10}H_{15}NO_2$: C, 66.2; H, 8.3; N, 7.7. Found: C, 66.3; H, 8.4; N, 7.7.

Hydroamidation of primary amides, exemplified by the reaction of 1-hexyne (JACS-5b) with benzamide (3a):

Synthesis of *N*-((*Z*)-hex-1-en-1-yl)benzamide (JACS-10a) [CAS: 1095320-48-1]: An oven-dried flask was charged with bis(2-methallyl)-cycloocta-1,5-diene-ruthenium(II) (16.0 mg, 0.05 mmol), 1,4-bis(dicyclohexylphosphino) butane (27.0 mg, 0.06 mmol) and ytterbium triflate (24.8 mg, 0.04 mmol), benzamide (**JACS-3a**, 121.1 mg, 1.00 mmol) and flushed with nitrogen. Subsequently, dry DMF (3.00 mL), 1-hexyne (**JACS-5b**, 229 µL, 2.00 mmol) and water (108 µL, 6.00 mmol) were added via syringe. The resulting solution was stirred for 6 h at 60 °C, then poured into an aqueous $NaHCO_3$ solution (30 mL). The resulting mixture was extracted repeatedly with 20 mL portions of ethyl acetate, the combined organic layers were washed with water and brine, dried with $MgSO_4$, filtered, and the volatiles were removed in vacuo. The residue was purified by column chromatography (silica gel, ethyl acetate/hexane 1:9) yielding a 18:1 mixture of **JACS-10a** and **JACS-11a** (191.1 mg, 94%) as a yellowish oil. ^{1}H-NMR (600.3 MHz, $CDCl_3$, 25 °C): δ = 7.78 (d, ^3J = 7.2 Hz, 2H), 7.64 (d, ^3J = 8.4 Hz, 1H), 7.52 (t, ^3J = 7.4 Hz, 1H), 7.45 (t, ^3J = 7.6 Hz, 2H), 6.90 (dd, ^3J = 10.8, 9.2 Hz, 1H), 4.83–4.88 (m, 1H), 2.08 (qd, ^3J = 7.3, 1.5 Hz, 2H), 1.40–1.44 (m, 2H), 1.34–1.39 (m, 2H), 0.92 ppm (t, ^3J = 7.2 Hz, 3H). ^{13}C-NMR (150.9 MHz, $CDCl_3$, 25 °C): δ = 164.3, 134.0, 131.9, 128.7, 127.0, 121.1, 112.3, 31.4, 25.5, 22.3, 14.0 ppm. MS (EI, 70 eV): *m/z* (%) = 203 (8, [M^+]), 160 (10), 122 (27), 105 (100), 77 (39), 51 (11). Anal. Calcd for $C_{13}H_{17}NO$: C, 76.81; H, 8.43; N, 6.89. Found: C, 76.73; H, 8.49; N, 6.88.

Synthesis of *N*-((*E*)-hex-1-en-1-yl)benzamide (JACS-11a) [CAS: 474352-83-5]: An oven-dried flask was charged with bis(2-methallyl)-cycloocta-1,5-diene-ruthenium(II) (16.0 mg, 0.05 mmol), 1,4-bis(dicyclohexylphosphino) butane (27.0 mg, 0.06 mmol) and

ytterbium triflate (24.8 mg, 0.04 mmol), benzamide (**JACS-3a**, 121.1 mg, 1.00 mmol) and flushed with nitrogen. Subsequently, dry DMF (3.00 mL), 1-hexyne (**JACS-5b**, 229 µL, 2.00 mmol) and water (108 µL, 6.00 mmol) were added via syringe. The resulting solution was stirred for 6 h at 60 °C. After cooling down to ambient temperature 3 Å molecular sieves (500 mg) and triethylamine (200 µL) were added to the reaction mixture, and stirring was continued for 24 h at 110 °C, then poured into an aqueous $NaHCO_3$ solution (30 mL). The resulting mixture was extracted repeatedly with 20 mL portions of ethyl acetate, the combined organic layers were washed with water and brine, dried with $MgSO_4$, filtered, and the volatiles were removed in vacuo. The residue was purified by column chromatography (silica gel, ethyl acetate/hexane 1:9) yielding a 4:1 mixture of **JACS-11a** and **JACS-10a** (180.9 mg, 89%) as a white solid. ^{1}H-NMR (600.3 MHz, $CDCl_3$, 25 °C): δ = 7.78 (d, ^3J = 7.4 Hz, 2H), 7.69 (d, ^3J = 8.4 Hz, 1H), 7.50 (t, ^3J = 7.3 Hz, 1H), 7.43 (t, ^3J = 7.7 Hz, 2H), 6.94 (dd, ^3J = 14.0, 10.6 Hz, 1H), 5.30 (dt, ^3J = 14.3, 7.2 Hz, 1H), 2.07 (q, ^3J = 6.8 Hz, 2H), 1.30–1.38 (m, 4H), 0.89 ppm (t, ^3J = 7.2 Hz, 3H). ^{13}C-NMR (150.9 MHz, $CDCl_3$, 25 °C): δ = 164.3, 133.9, 131.9, 128.7, 127.0, 121.1, 112.3, 31.4, 25.5, 22.3, 13.9 ppm. MS (EI, 70 eV): *m/z* (%) = 203 (17, [M^+]), 122 (26), 105 (100), 77 (41), 51 (12), 44 (15).

VI.3.3. Deuterium-labeling experiments and experimental data:

N-[1'-Deutero-(*E*)-hex-1-en-1-yl]-2-pyrrolidinone (**JACS-6aa**) was synthesized following the *E*-selective method for the addition of secondary amides to terminal alkynes using 2-pyrrolidinone (**JACS-1a**, 77 µL, 1.00 mmol) and 1-[*D*]-hex-1-yne (**JACS-5a**, 234 µL, 2.00 mmol, DG = 92%) and purified by column chromatography (silica gel, ethyl acetate/hexane 1:3), yielding the product **JACS-6aa** as a colorless oil (155.7 mg, 93%). ^{1}H-NMR (400.1 MHz, $CDCl_3$): δ = 4.83 (t, ^3J = 7.0 Hz, 1H), 3.37–3.43 (m, 2H), 2.37 (t, ^3J = 8.2 Hz, 2H), 1.94–2.03 (m, 4H), 1.19–1.30 (m, 4H), 0.80 (t, ^3J = 7.2 Hz, 3H) ppm. ^{13}C-NMR (101.6 MHz, $CDCl_3$): δ = 172.4, 123.2 (t, $J_{C\text{-}D}$ = 25.9 Hz), 112.0, 45.1, 32.1, 31.1, 29.5, 21.9, 17.3, 13.7 ppm. ^{2}H-NMR (61.4 MHz, $CHCl_3$): δ = 6.82 (br, 1D) ppm. MS (EI, 70 eV): *m/z* (%) = 169 (66, [M^+]), 139 (7), 125 (100), 97 (43), 81 (3). Anal. Calcd for $C_{10}H_{16}NOD$: C, 71.38; H, 9.58; N, 8.32. Found: C, 71.15; H, 9.79; N, 8.02.

N-[2'-Deutero-(*E*)-hex-1-en-1-yl]-2-pyrrolidinone (**JACS-6ab**) was synthesized following the *E*-selective method for the addition of secondary amides to terminal alkynes using *N*-[*D*]-2-pyrrolidinone (**JACS-1b**, 86.1 mg, 1.00 mmol, DG = 85%) and 1-hexyne (**JACS-5b**, 229 µL, 2.00 mmol) and purified by column chromatography (silica gel, ethyl acetate/hexane 1:3), yielding the product **JACS-6ab** as a colorless oil (152.5 mg, 91%). ^{1}H-NMR

(400.1 MHz, $CDCl_3$): δ = 6.77 (s, 1H), 3.38–3.43 (m, 2H), 2.38 (t, ^3J = 8.2 Hz, 2H), 1.95–2.04 (m, 4H), 1.19–1.30 (m, 4H), 0.80 (t, ^3J = 7.2 Hz, 3H) ppm. ^{13}C-NMR (101.6 MHz, $CDCl_3$): δ = 172.4, 123.4, 111.8 (t, $J_{C\text{-}D}$ = 23.1 Hz,), 45.1, 32.1, 31.1, 29.4, 21.9, 17.3, 13.7 ppm. ^{2}H-NMR (61.4 MHz, $CHCl_3$): δ = 4.91 (br, 1D) ppm. MS (EI, 70 eV): *m/z* (%) = 169 (62, [M^+]), 139 (8), 125 (100), 97 (45), 81 (5). Anal. Calcd for $C_{10}H_{16}NOD$: C, 71.38; H, 9.58; N, 8.32. Found: C, 71.19; H, 9.79; N, 7.97.

N-[1'-Deutero-(*Z*)-hex-1-en-1-yl]-2-pyrrolidinone (**JACS-7aa**) was synthesized following the *Z*-selective method for the addition of secondary amides to terminal alkynes using 2-pyrrolidinone (**JACS-1a**, 77 µL, 1.00 mmol) and 1-[*D*]-hex-1-yne (**JACS-5a**, 234 µL, 2.00 mmol, DG = 92%) and purified by column chromatography (silica gel, ethyl acetate/hexane 1:3), yielding the product **JACS-7aa** as a colorless oil (148.1 mg, 89%). ^{1}H-NMR (600.3 MHz, $CDCl_3$): δ = 4.77–4.82 (m, 1H), 3.71 (td, ^3J = 7.1, 2.1 Hz, 2H), 2.36 (t, ^3J = 8.1 Hz, 2H), 2.13 (q, ^3J = 7.5 Hz, 2H), 2.00–2.07 (m, 2H), 1.26–1.34 (m, 4H), 0.82–0.87 (m, 3H) ppm. ^{13}C-NMR (150.9 MHz, $CDCl_3$): δ = 174.5, 121.8 (t, $J_{C\text{-}D}$ = 26.8 Hz), 116.5, 48.6, 32.3, 30.1, 26.8, 22.2, 18.5, 13.8 ppm. ^{2}H-NMR (61.4 MHz, $CHCl_3$): δ = 6.38 (br, 1D) ppm. MS (EI, 70 eV): *m/z* (%) = 168 (10, [M^+]), 139 (27), 125 (100), 97 (50), 83 (39). Anal. Calcd for $C_{10}H_{16}NOD$: C, 71.38; H, 9.58; N, 8.32. Found: C, 71.23; H, 9.75; N, 7.99.

N-[2'-Deutero-(*Z*)-hex-1-en-1-yl]-2-pyrrolidinone (**JACS-7ab**) was synthesized following the *Z*-selective method for the addition of secondary amides to terminal alkynes using 1-[*D*]-2-pyrrolidinone (**JACS-1b**, 86.1 mg, 1.00 mmol, DG = 85%) and 1-hexyne (**JACS-5b**, 229 µL, 2.00 mmol) and purified by column chromatography (silica gel, ethyl acetate/hexane 1:3), yielding the product **JACS-7ab** as a colorless oil (151.2 mg, 90%). ^{1}H-NMR (600.3 MHz, $CDCl_3$): δ = 6.38 (s, 1H), 3.76–3.79 (m, 2H), 2.43 (t, ^3J = 8.22 Hz, 2H), 2.19 (t, ^3J = 7.13 Hz, 2H), 2.06–2.13 (m, 2H), 1.32–1.40 (m, 4H), 0.89–0.93 (m, 3H) ppm. ^{13}C-NMR (150.9 MHz, $CDCl_3$): δ = 174.5, 122.1, 116.6 (t, $J_{C\text{-}D}$ = 23.5 Hz,), 48.6, 32.3, 30.3, 26.8, 22.3, 18.6, 13.9 ppm. ^{2}H-NMR (61.4 MHz, $CHCl_3$): δ = 4.86 (br, 1D) ppm. MS (EI, 70 eV): *m/z* (%) = 168 (12, [M^+]), 139 (28), 125 (100), 97 (49), 81 (35). Anal. Calcd for $C_{10}H_{16}NOD$: C, 71.38; H, 9.58; N, 8.32. Found: C, 71.15; H, 9.72; N, 7.95.

N-[1'-Deutero-(*E*)-hex-1-en-1-yl]succinimide (**JACS-8aa**) [CAS: 919083-08-2] was synthesized following the *E*-selective method for the addition of imides to terminal alkynes using succinimide (**JACS-2a**, 99.1 mg, 1.00 mmol), 1-[*D*]-hex-1-yne (**JACS-5b**, 234 µL, 2.00 mmol, DG = 92%) and DMF-d_7 (1.00 mL) and purified by column chromatography (silica gel, ethyl acetate/hexane 1:3), yielding the product **JACS-8aa** as a yellowish oil

(136.0 mg, 75%). ^{1}H-NMR (400.1 MHz, $CDCl_3$): δ = 6.53 (t, ^{3}J = 7.3 Hz, 1H) 2.67 (s, 3H) 2.07 (td, ^{3}J = 7.5 Hz, 2H) 1.22–1.43 (m, 4H) 0.85 (t, ^{3}J = 7.2 Hz, 3H) ppm. ^{13}C-NMR (101.6 MHz, $CDCl_3$): δ = 175.3, 124.3, 117.6 (t, $J_{C\text{-}D}$ = 27.1 Hz), 31.2, 30.4, 27.6, 21.9, 13.6 ppm. ^{2}H-NMR (61.4 MHz, $CHCl_3$): δ = 6.43 (br, 1D) ppm. MS (EI, 70 eV): *m/z* (%) = 182 (8, [M^+]), 139 (83), 100 (93), 83 (100), 68 (65). Anal. Calcd for $C_{10}H_{14}NO_2D$: C, 65.91; H, 7.74; N, 7.69. Found: C, 65.81; H, 8.00; N, 7.49.

N-[2'-Deutero-(*E*)-hex-1-en-1-yl]succinimide (**JACS-8ab**) was synthesized following the *E*-selective method for the addition of imides to terminal alkynes using *N*-[*D*]-succinimide (**JACS-2b**, 100.1 mg, 1.00 mmol, DG = 81%) and 1-hexyne (**JACS-5b**, 229 µL, 2.00 mmol) and purified by column chromatography (silica gel, ethyl acetate/hexane 1:3), yielding the product **JACS-8ab** as a yellowish oil (131.0 mg, 72%). ^{1}H-NMR (600.3 MHz, $CDCl_3$): δ = 6.39 (s, 1H), 2.69 (s, 4H), 2.08 (t, ^{3}J = 7.3 Hz, 2H), 1.35–1.41 (m, 2H), 1.27–1.34 (m, 2H), 0.87 (t, ^{3}J = 7.3 Hz, 3H) ppm. ^{13}C-NMR (150.9 MHz, $CDCl_3$): δ = 175.6, 124.5 (t, $J_{C\text{-}D}$ = 24.5 Hz), 117.8, 31.3, 30.6, 27.8, 22.2, 13.9 ppm. ^{2}H-NMR (61.4 MHz, $CHCl_3$): δ = 6.61 (br, 1D) ppm. MS (EI, 70 eV): *m/z* (%) = 182 (9, [M^+]), 139 (80), 100 (95), 83 (100), 68 (62). Anal. Calcd for $C_{10}H_{14}NO_2D$: C, 65.91; H, 7.74; N, 7.69. Found: C, 65.71; H, 8.05; N, 7.40.

N-[1'-Deutero-(*Z*)-hex-1-en-1-yl]succinimide (**JACS-9aa**) [CAS: 919086-95-6] was synthesized following the *Z*-selective method for the addition of imides to terminal alkynes using succinimide (**JACS-2a**, 99.1 mg, 1.00 mmol) and 1-[*D*]-hex-1-yne (**JACS-5a**, 234 µL, 2.00 mmol, DG = 92%) and purified by column chromatography (silica gel, ethyl acetate/hexane 1:3), yielding the product **JACS-9aa** as a yellowish oil (169.5 mg, 94%). ^{1}H-NMR (400.1 MHz, $CDCl_3$): δ = 5.67 (s, 1H), 2.73 (s, 4H), 1.85–1.91 (m, 2H), 1.23–1.36 (m, 4H), 0.81 (t, ^{3}J = 7.3 Hz, 3H) ppm. ^{13}C-NMR (101.6 MHz, $CDCl_3$): δ = 175.5, 133.4, 116.4 (t, $J_{C\text{-}D}$ = 27.7 Hz), 30.6, 28.3, 27.6, 22.2, 13.7 ppm. ^{2}H-NMR (61.4 MHz, $CHCl_3$): δ = 5.87 (br, 1D) ppm. MS (EI, 70 eV): *m/z* (%) = 183 (100, [M^+]), 139 (30), 111 (14), 83 (25), 57 (17). Anal. Calcd for $C_{10}H_{14}NO_2D$: C, 65.91; H, 7.74; N, 7.69. Found: C, 65.81; H, 8.00; N, 7.49.

N-[2'-Deutero-(*Z*)-hex-1-en-1-yl]succinimide (**JACS-9ab**) was synthesized following the *Z*-selective method for the addition of imides to terminal alkynes using *N*-[*D*]-succinimide (**JACS-2b**, 100.1 mg, 1.00 mmol, DG = 81%) and 1-hexyne (**JACS-5b**, 229 µL, 2.00 mmol) and purified by column chromatography (silica gel, ethyl acetate/hexane 1:3), yielding the product **JACS-9ab** as a yellowish oil (165.2 mg, 91%). ^{1}H-NMR (400.1 MHz, $CDCl_3$): δ = 5.81 (s, 1H), 2.73 (s, 4H), 1.88 (t, ^{3}J = 7.3 Hz, 2H), 1.23–1.35 (m, 4H), 0.82 (t, ^{3}J = 7.2 Hz, 3H) ppm. ^{13}C-NMR (101.x MHz, $CDCl_3$): δ = 175.5, 133.3 (t, $J_{C\text{-}D}$ = 21.3 Hz), 116.6,

30.5, 28.3, 27.6, 22.2, 13.7 ppm. ^{2}H-NMR (61.4 MHz, $CHCl_3$): δ = 5.76 (br, 1D) ppm. MS (EI, 70 eV): *m/z* (%) = 183 (100, [M^+]), 139 (30), 111 (14), 83 (25), 57 (17). Anal. Calcd for $C_{10}H_{14}NO_2D$: C, 65.91; H, 7.74; N, 7.69. Found: C, 65.81; H, 8.00; N, 7.49.

N-[1'-Deutero-(*Z*)-hex-1-en-1-yl]benzamide (**JACS-10aa**) [CAS: 1095320-68-5] was synthesized following the *Z*-selective method for the addition of primary amides to terminal alkynes using benzamide (**JACS-3a**, 121.1 mg, 1.00 mmol) and 1-[*D*]-hex-1-yne (**JACS-5a**, 234 µL, 2.00 mmol, DG = 92%) in the absence of water and purified by column chromatography (silica gel, ethyl acetate/hexane 1:9), yielding the product **JACS-10aa** as a yellowish oil (182.8 mg, 90%). ^{1}H-NMR (400.1 MHz, $CDCl_3$): δ = 7.76 (d, ^{3}J = 7.2 Hz, 3H), 7.49 (t, ^{3}J = 7.3 Hz, 1H), 7.41 (t, ^{3}J = 7.5 Hz, 2H), 4.38 (t, ^{3}J = 7.2 Hz, 1H), 2.08 (q, ^{3}J = 7.4 Hz, 2H), 1.31–1.43 (m, 4H), 0.90 (t, ^{3}J = 7.0 Hz, 3H) ppm. ^{13}C-NMR (101.6 MHz, $CDCl_3$): δ = 164.3, 134.0, 131.7, 128.6, 126.9, 120.9 (t, $J_{C\text{-}D}$ = 27.7 Hz), 112.1, 31.4, 25.4, 22.2, 13.8, ppm. ^{2}H-NMR (61.4 MHz, $CHCl_3$): δ = 6.96 (br, 1D) ppm. MS (EI, 70 eV): *m/z* (%) = 205 (67, [M^+]), 187 (24), 161 (3), 105 (100), 77 (2). Anal. Calcd for $C_{13}H_{16}NOD$: C, 76.43; H, 7.89; N, 6.86. Found: C, 76.73; H, 8.60; N, 6.87.

N-[2'-Deutero-(*Z*)-hex-1-en-1-yl]benzamide (**JACS-10ab**) [CAS: 1095320-67-4] was synthesized following the *Z*-selective method for the addition of primary amides to terminal alkynes using *N*,*N*-[D_2]-benzamide (**JACS-3b**, 123.2 mg, 1.00 mmol, DG = 75%) and 1-hexyne (**JACS-5b**, 229 µL, 2.00 mmol) in the absence of water and purified by column chromatography (silica gel, ethyl acetate/hexane 1:9), yielding the product **JACS-10ab** as a yellowish oil (182.8 mg, 90%). ^{1}H-NMR (400.1 MHz, $CDCl_3$): δ = 7.81 (d, ^{3}J = 7.2 Hz, 2H), 7.72 (s, 1H), 7.51–7.56 (m, 1H), 7.47 (t, ^{3}J = 7.3 Hz, 2H), 6.92 (dd, ^{3}J = 6.3, 4.6 Hz, 1H), 2.10 (t, ^{3}J = 7.2 Hz, 2H), 1.35–1.47 (m, 4H), 0.94 (t, ^{3}J = 7.2 Hz, 3H), ppm. ^{13}C-NMR (101.6 MHz, $CDCl_3$): δ = 164.3, 134.0, 131.8, 128.7, 127.0, 121.1, 112.1 (t, $J_{C\text{-}D}$ = 24.5 Hz), 31.4, 25.4, 22.3, 13.8 ppm. ^{2}H-NMR (61.4 MHz, $CHCl_3$): δ = 4.93 (br, 1D) ppm. MS (EI, 70 eV): *m/z* (%) = 205 (52, [M^+]), 187 (20), 161 (2), 105 (100), 77 (2). Anal. Calcd for $C_{13}H_{16}NOD$: C, 76.43; H, 7.89; N, 6.86. Found: C, 76.73; H, 8.59; N, 6.87.

VI.3.4. In situ IR experiments and experimental data:

In situ IR experiment with 1-hexyne (JACS-5b) and 2-pyrrolidinone (JACS-1a):

An oven-dried schlenk tube was charged with bis-(2-methallyl)-cycloocta-1,5-diene-ruthenium(II) (12.8 mg, 0.04 mmol) and 4-dimethylaminopyridine (9.77 mg, 0.08 mmol) and was flushed with nitrogen. Dry toluene (3.00 mL) was added via syringe and the schlenk tube

was equipped with the fiber conduit. The in-situ IR measurement was started after 15 minutes of stirring at room temperature. Subsequently, tri-*n*-butylphosphine (31 µL, 0.12 mmol), 2-pyrrolidinone (**JACS-1a**, 170.0 mg, 2.00 mmol) and 1-hexyne (**JACS-5b**, 463 µL, 4.00 mmol) were added. The resulting green solution was stirred in a pre-heated heating block for 15 minutes at 100 °C. The measurement was stopped after an overall reaction time of 30 minutes. The experimental data was analyzed with the iC IR reaction analysis software.

Reference spectra1:

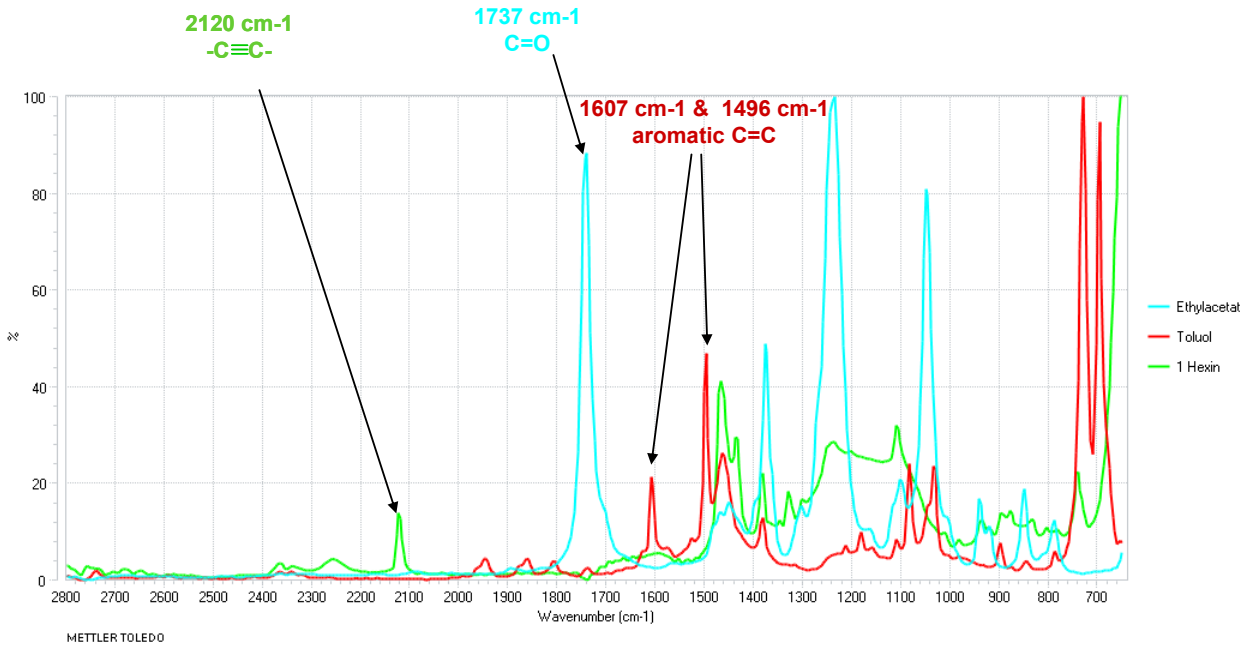

Reference spectra 2:

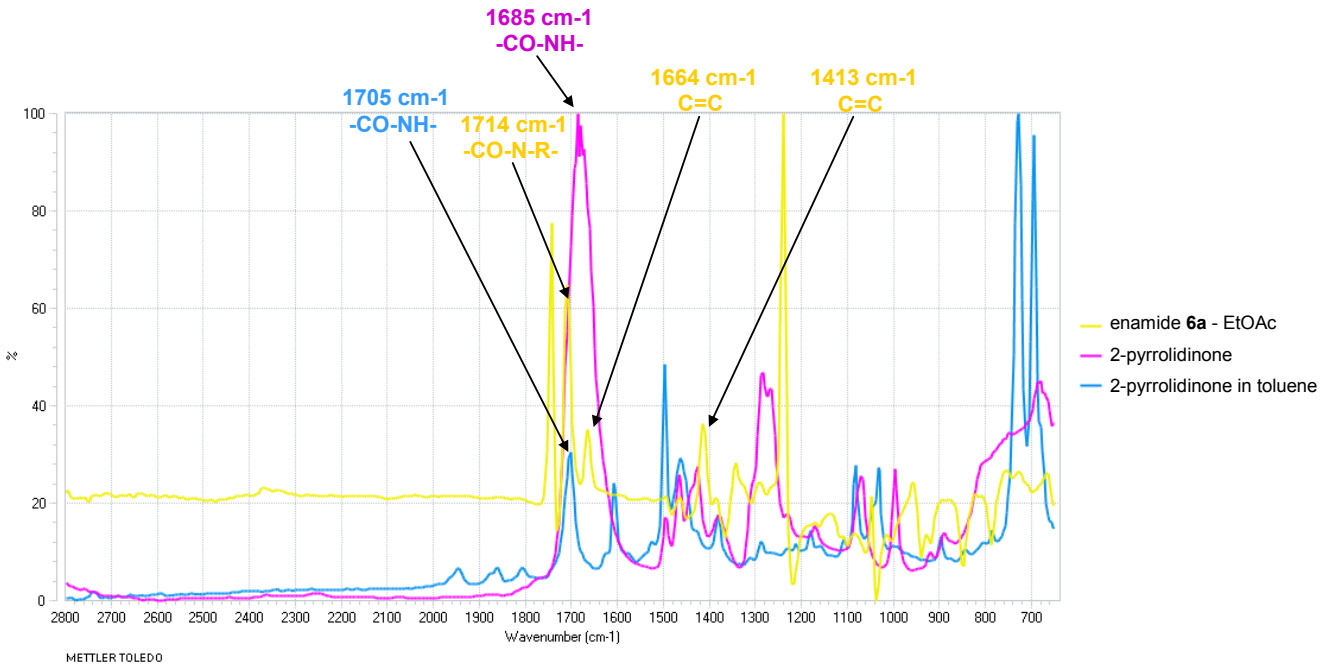

Time resolved spectrum:

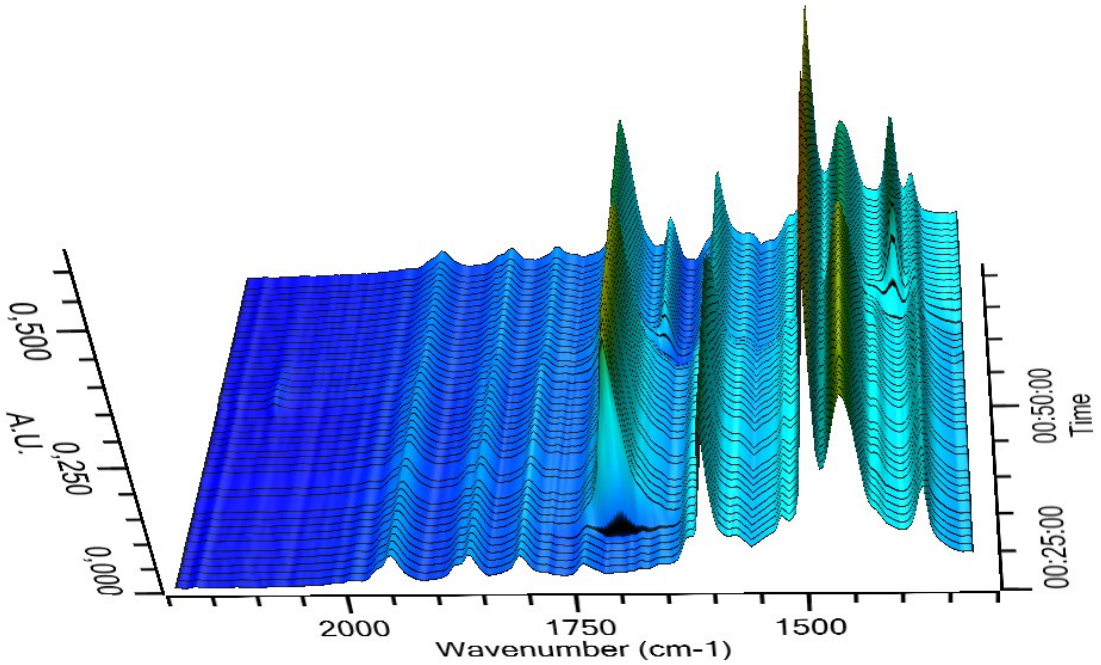

Profile of reaction compounds:

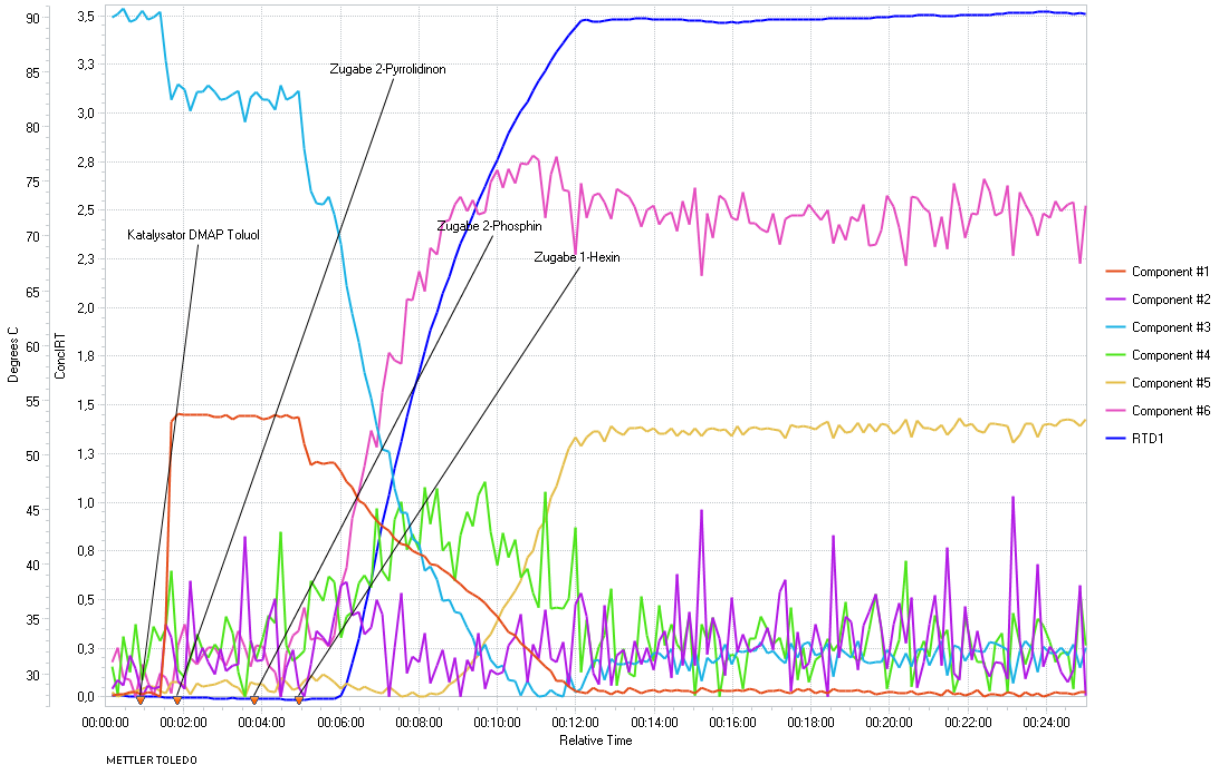

Spectrum compound 1:

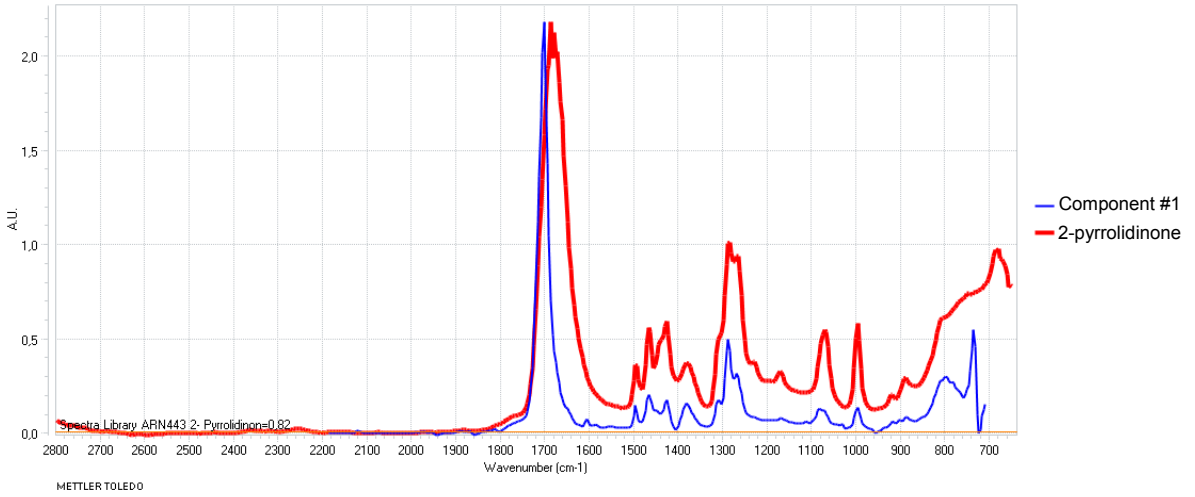

Spectrum compound 2:

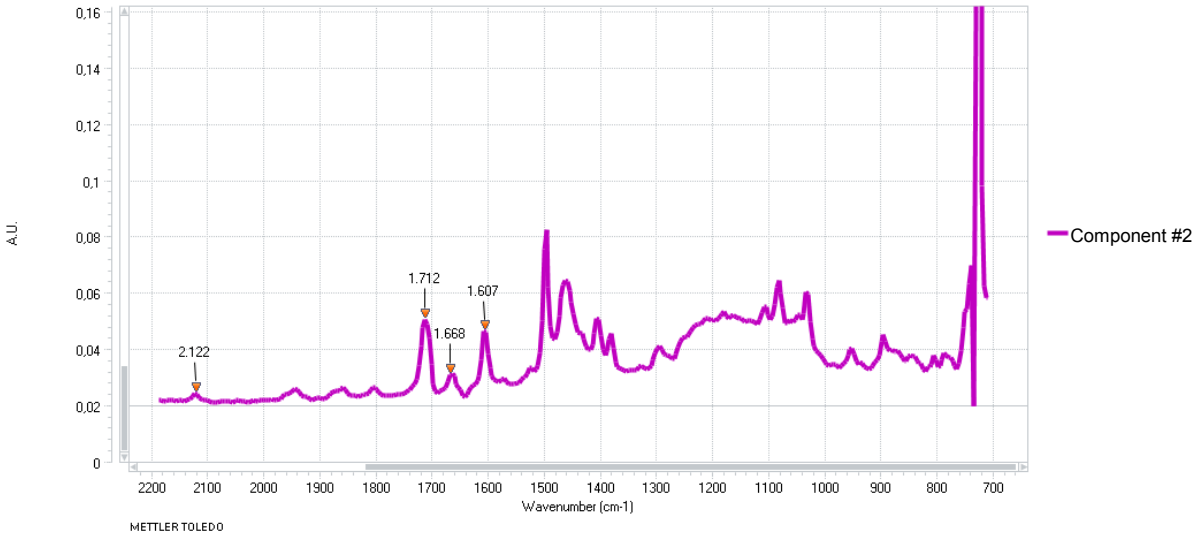

Spectrum compound 3:

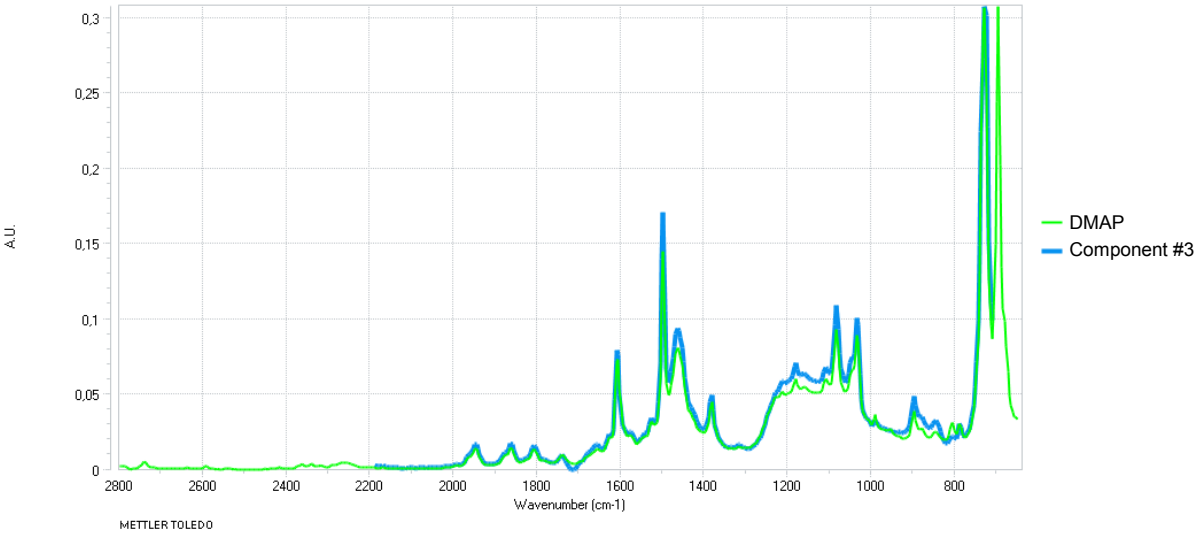

Spectrum compound 4:

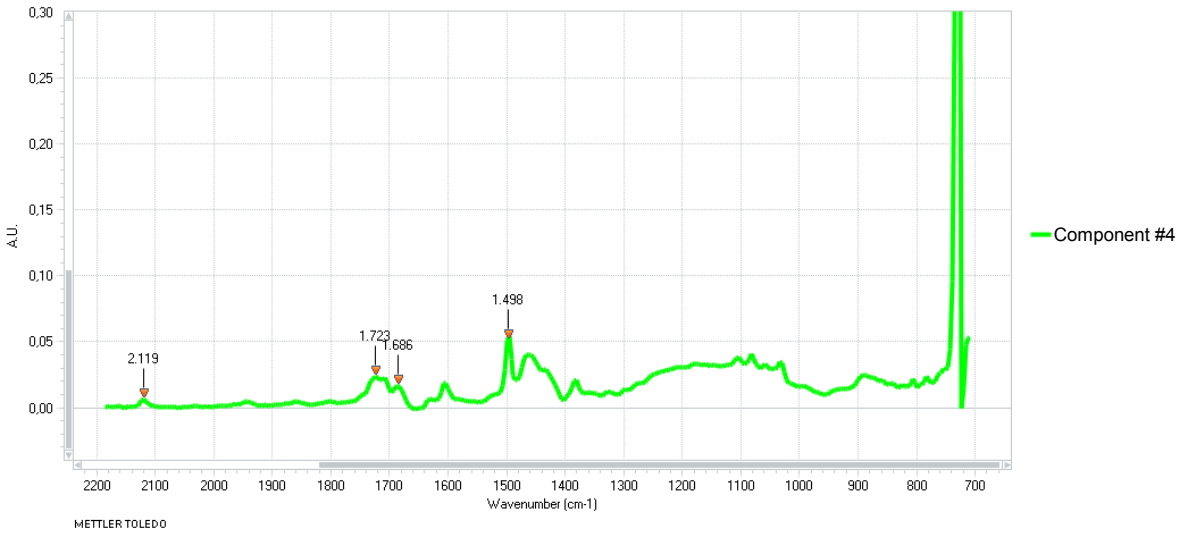

Spectrum compound 5 and 6:

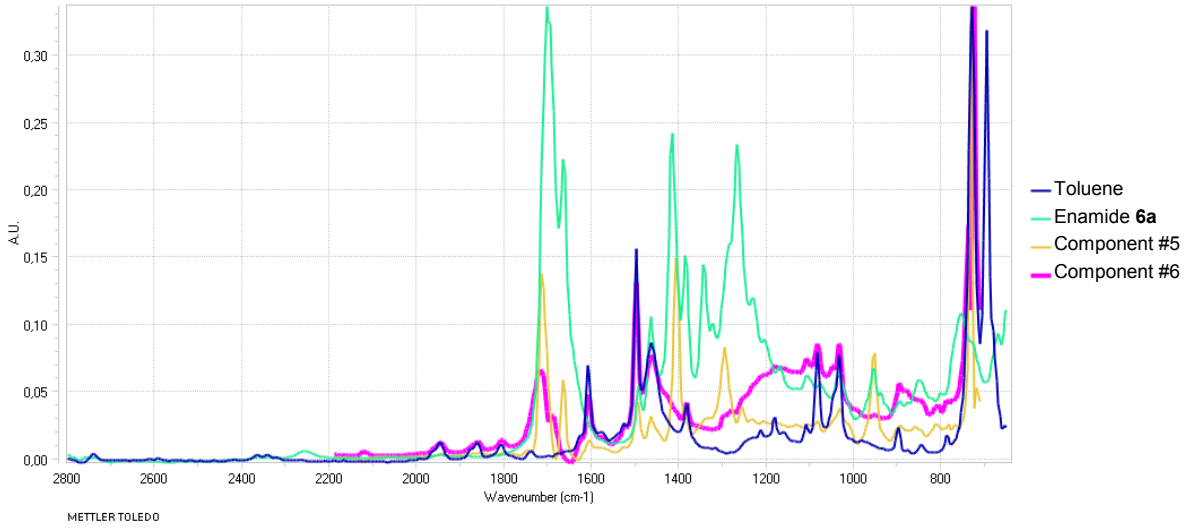

VI.3.5. Determination of kinetic isotope effects.

Hydroamidation competition reactions of secondary amides:

Competition reactions with 1-hexyne (JACS-5b) and 1-[*D*]-hex-1-yne (JACS-5a): An oven-dried flask was charged with bis(2-methallyl)-cycloocta-1,5-diene-ruthenium(II) (6.4 mg, 0.02 mmol) and DMAP (4.99 mg, 0.04 mmol) and flushed with nitrogen. Subsequently, tri-*n*-butylphosphine (15 µL, 0.06 mmol), 2-pyrrolidinone (**JACS-1a**, 77 µL, 1.00 mmol), 1-hexyne (**JACS-5b**, 229 µL, 2.00 mmol), 1-[*D*]-hex-1-yne (**JACS-5a**, 234 µL, 2.00 mmol, DG = 96%) and dry toluene (3.00 mL) were added via syringe. The resulting green solution was stirred for 15 h at 100 °C and was then poured into aqueous $NaHCO_3$ solution (30 mL). The resulting mixture was extracted repeatedly with 20 mL portions of ethyl acetate, the combined organic layers were washed with water and brine, dried with $MgSO_4$, filtered, and the volatiles were removed in vacuo. A kinetic isotope effect of 1.56 was determined by NMR (determined by the ratio of non-deuterated to deuterated product).

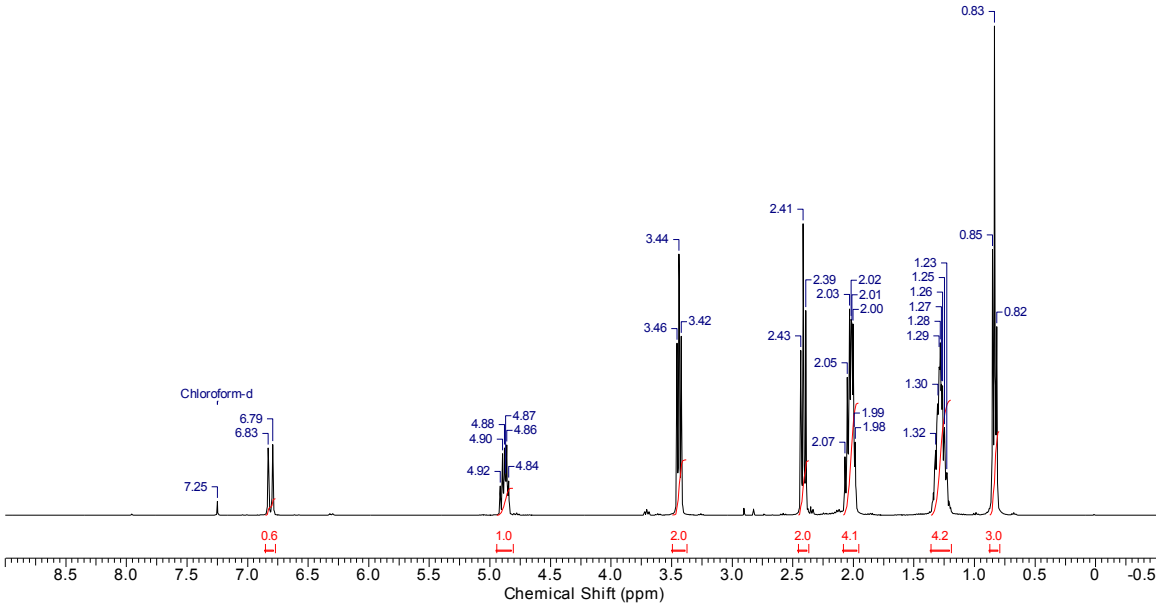

Competition reactions with 2-pyrrolidinone (JACS-1a) and 1-[*D*]-2-pyrrolidinone (JACS-1b): An oven-dried flask was charged with bis(2-methallyl)-cycloocta-1,5-diene-ruthenium(II) (6.4 mg, 0.02 mmol) and DMAP (4.99 mg, 0.04 mmol) and flushed with nitrogen. Subsequently, tri-*n*-butylphosphine (15 µL, 0.06 mmol), 2-pyrrolidinone (**JACS-1a**, 154 µL, 2 mmol), 1-[*D*]-2-pyrrolidinone (**JACS-1b**, 172.2 mg, 2.00 mmol, DG = 85%) 1-hexyne (**JACS-5b**, 115 µL, 1.00 mmol), and dry toluene (3.00 mL) were added via syringe. The resulting green solution was stirred for 15 h at 100 °C and was then poured into aqueous $NaHCO_3$ solution (30 mL). The resulting mixture was extracted repeatedly with 20 mL portions of ethyl acetate, the combined organic layers were washed with water and brine, dried with $MgSO_4$, filtered, and the volatiles were removed in vacuo. A kinetic isotope effect of 2.33 was determined by NMR (determined by the ratio of non-deuterated to deuterated product).

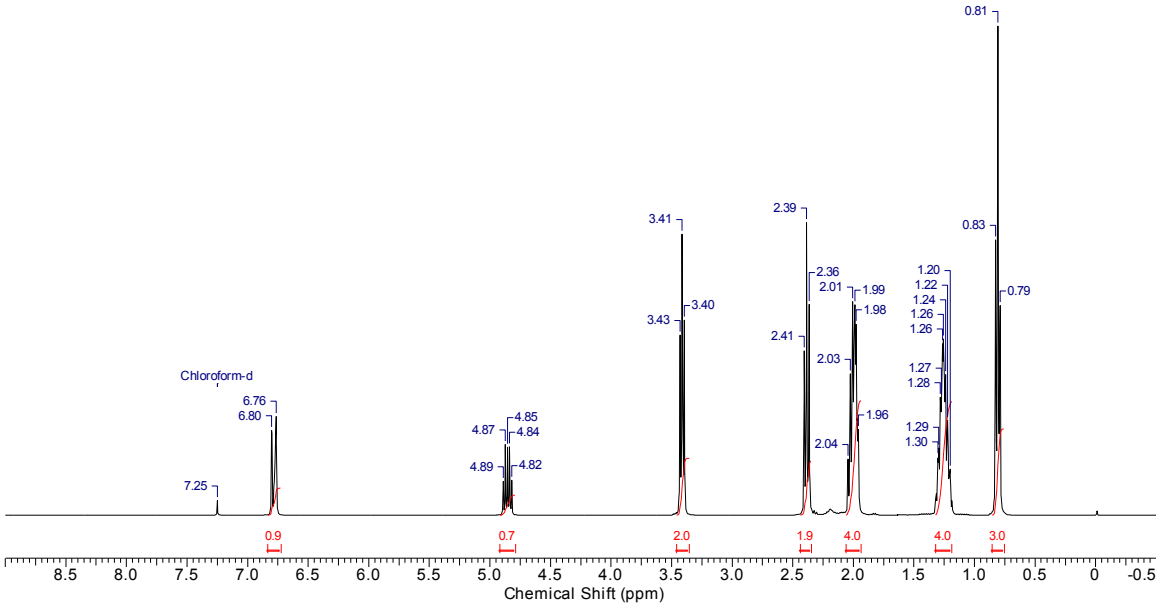

Hydroamidation competition reactions of imides:

Competition reactions with 1-hexyne (JACS-5b) and 1-[*D*]-hex-1-yne (JACS-5a): An oven-dried flask was charged with bis(2-methallyl)-cycloocta-1,5-diene-ruthenium(II) (6.4 mg, 0.02 mmol), scandium triflate (19.7 mg, 0.04 mmol) and succinimide (**JACS-2a**, 99.1 mg, 1.00 mmol) and flushed with nitrogen. Subsequently, tri-*n*-butylphosphine (15 µL, 0.06 mmol), 1-hexyne (**JACS-5b**, 229 µL, 2.00 mmol), 1-[*D*]-hex-1-yne (**JACS-5a**, 234 µL, 2.00 mmol, DG = 96%) and dry DMF (3.00 mL) were added via syringe. The resulting colorless solution was stirred for 15 h at 60 °C, then poured into an aqueous $NaHCO_3$ solution (30 mL). The resulting mixture was extracted repeatedly with 20 mL portions of ethyl acetate, the combined organic layers were washed with water and brine, dried with $MgSO_4$, and filtered, and the volatiles were removed in vacuo. A kinetic isotope effect of 2.23 was determined by NMR (determined by the ratio of non-deuterated to deuterated product).

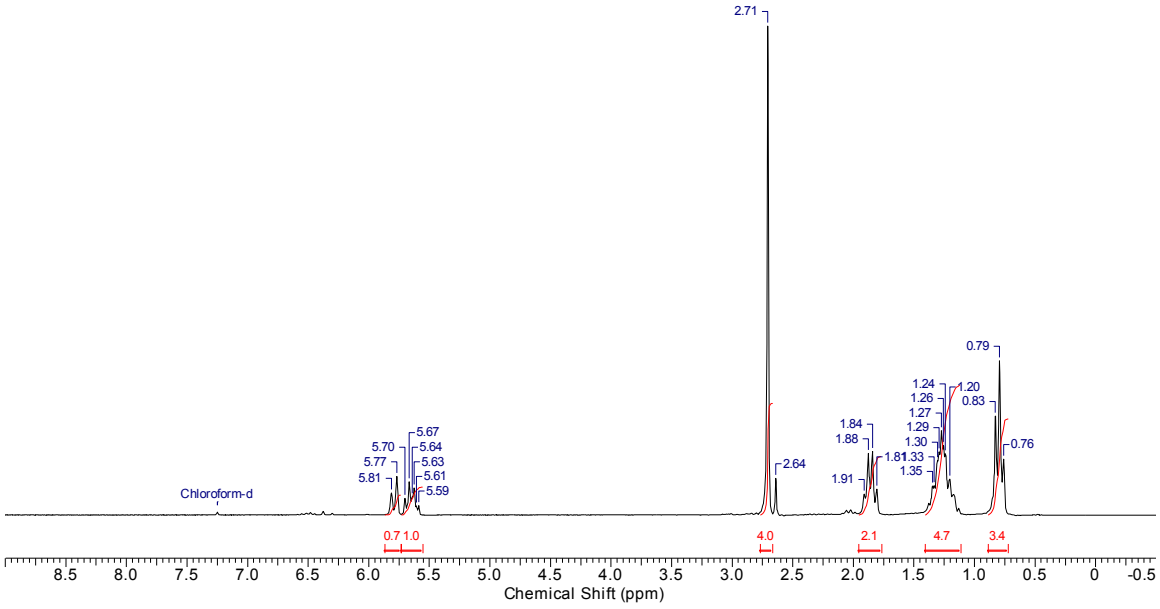

Hydroamidation competition reactions of primary amides:

Competition reactions with 1-hexyne (JACS-5b) and 1-[*D*]-hex-1-yne (JACS-5a): An oven-dried flask was charged with benzamide (**JACS-3a**, 121.1 mg, 1.00 mmol), bis(2-methallyl)-cycloocta-1,5-diene-ruthenium(II) (16.0 mg, 0.05 mmol), 1,4-bis(dicyclohexylphosphino) butane (27.0 mg, 0.06 mmol) and ytterbium triflate (24.8 mg, 0.04 mmol) and flushed with nitrogen. Subsequently, 1-hexyne (**JACS-5b**, 229 µL, 2.00 mmol), 1-[*D*]-hex-1-yne (**JACS-5a**, 234 µL, 2.0 mmol, DG = 96%) and dry DMF (3.00 mL) were added via syringe. The resulting solution was stirred for 6 h at 60 °C, then poured into an aqueous $NaHCO_3$ solution (30 mL). The resulting mixture was extracted repeatedly with 20 mL portions of ethyl acetate, the combined organic layers were washed with water and brine, dried with $MgSO_4$, filtered, and the volatiles were removed in vacuo. A kinetic isotope effect of 1.50 was determined by NMR (determined by the ratio of non-deuterated to deuterated product).

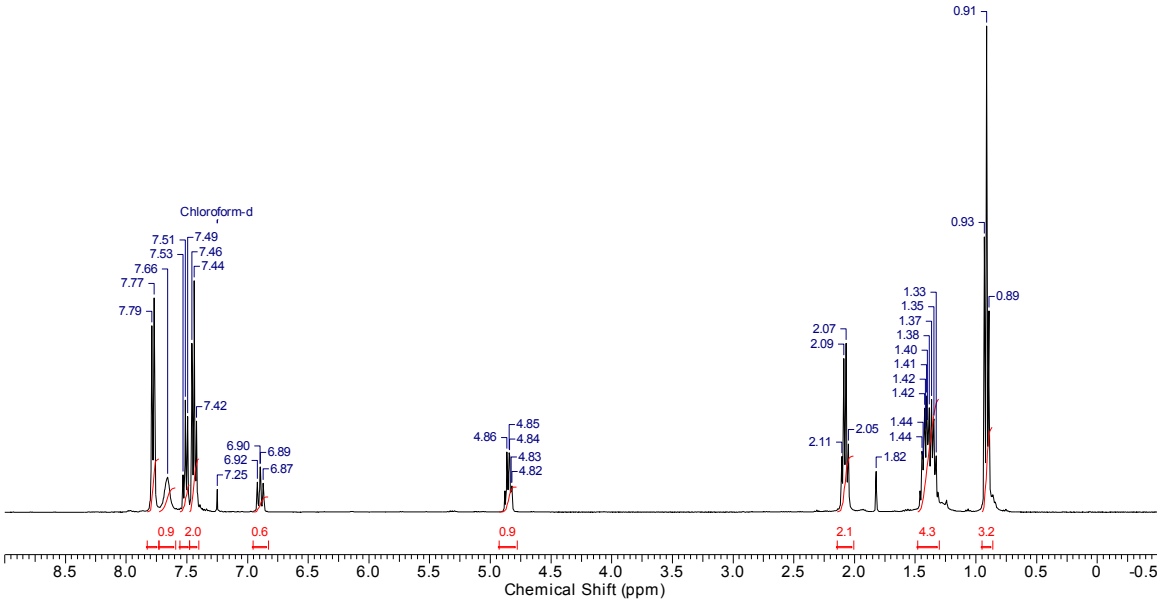

VI.3.6. In situ NMR experiments and experimental data.

_E_-selective hydroamidation protocol:

***In situ* NMR experiments with 1-[*D*]-2-pyrrolidinone (JACS-1b):** A 5 mm NMR tube was charged with bis-(2-methallyl)-cycloocta-1,5-diene-ruthenium(II) (31.9 mg, 0.10 mmol) and DMAP (24.4 mg, 0.20 mmol). The tube was sealed with a rubber septum and purged with alternating vacuum and nitrogen cycles. Subsequently, tri-*n*-butylphosphine (77 µL, 0.30 mmol), 1-[*D*]-2-pyrrolidinone (**JACS-1b**, 20 µL, 0.25 mmol, DG = 85%), benzene-d_6 (5 µL, 0.06 mmol) and dry toluene (0.50 mL) were added via syringe and placed in an ultrasonic bath for 15 min to give a clear yellow solution. Spectra 1h/1d/1p{h} were recorded at 22 °C. The sample was heated to 100 °C for 5 min and spectra 2h/2d/2p{h} were recorded. After cooling down the sample to 22 °C spectra 3h/3d/3p{h} was recorded. 1-[D]-hexyne (**JACS-5a**, 59 µL, 0.5 mmol, DG = 96%) was added and spectrum 4d was taken at 22°C, spectrum 5d at 100°C and spectrum 6d after cooling down the sample to 22°C.

spectrum 1h: ^{1}H-NMR (400.1 MHz, 295 K):

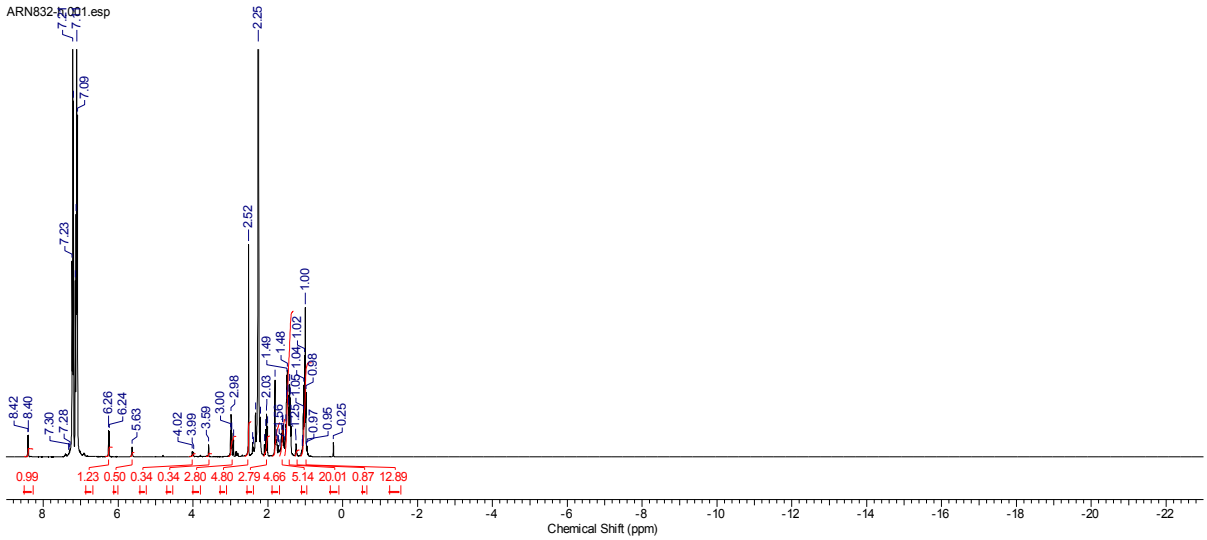

spectrum 1d: ^{2}H-NMR (61.4 MHz, 295 K):

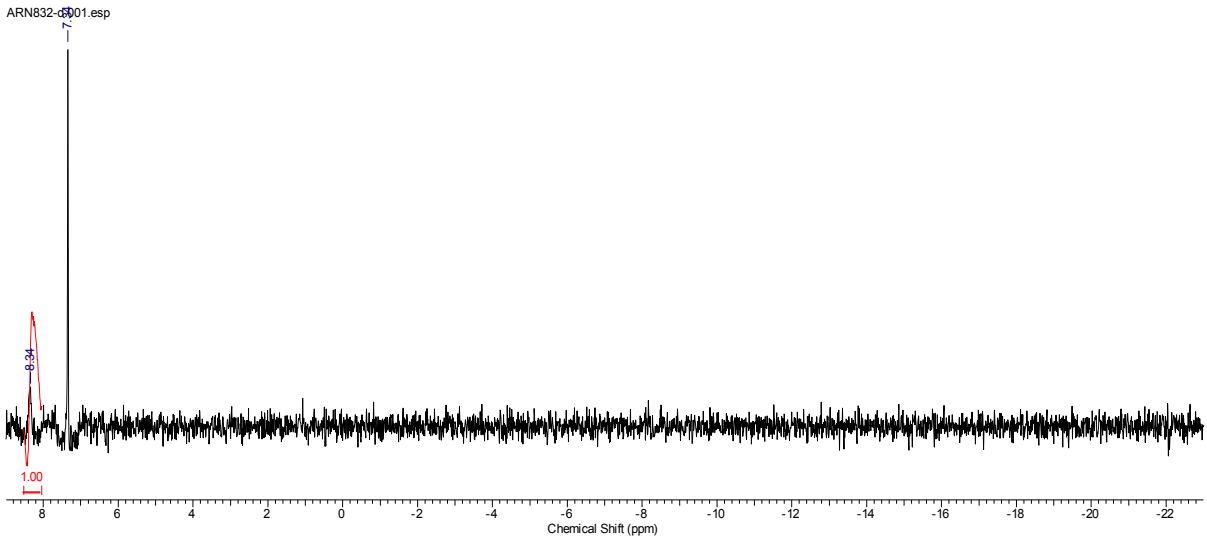

spectrum 1p{h}: ^{31}P-NMR (162.0 MHz, 295 K):

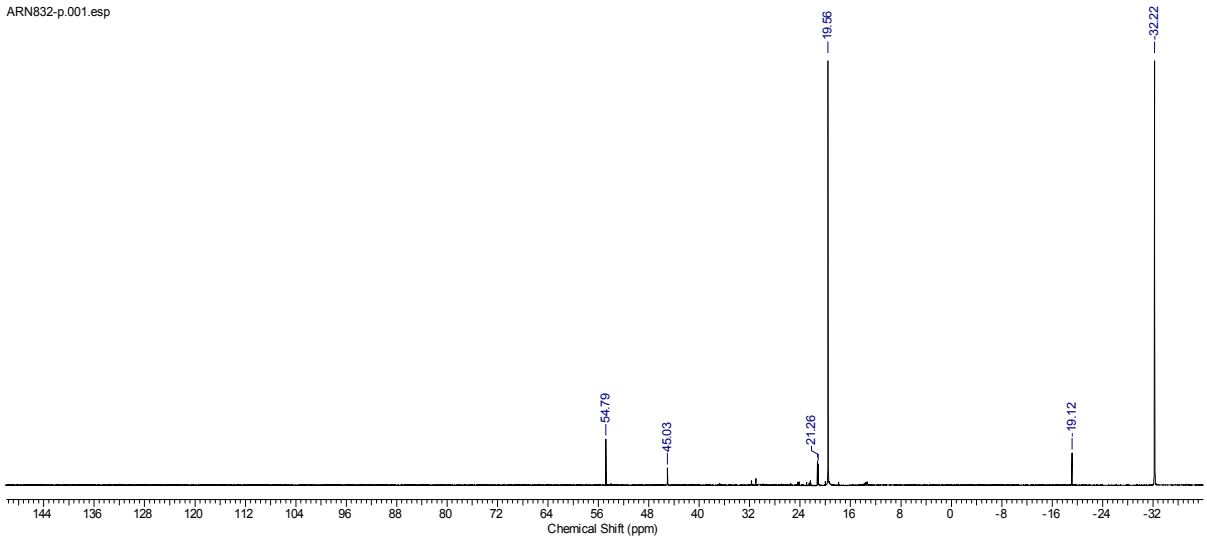

spectrum 2h: ^{1}H-NMR (400.1 MHz, 373 K):

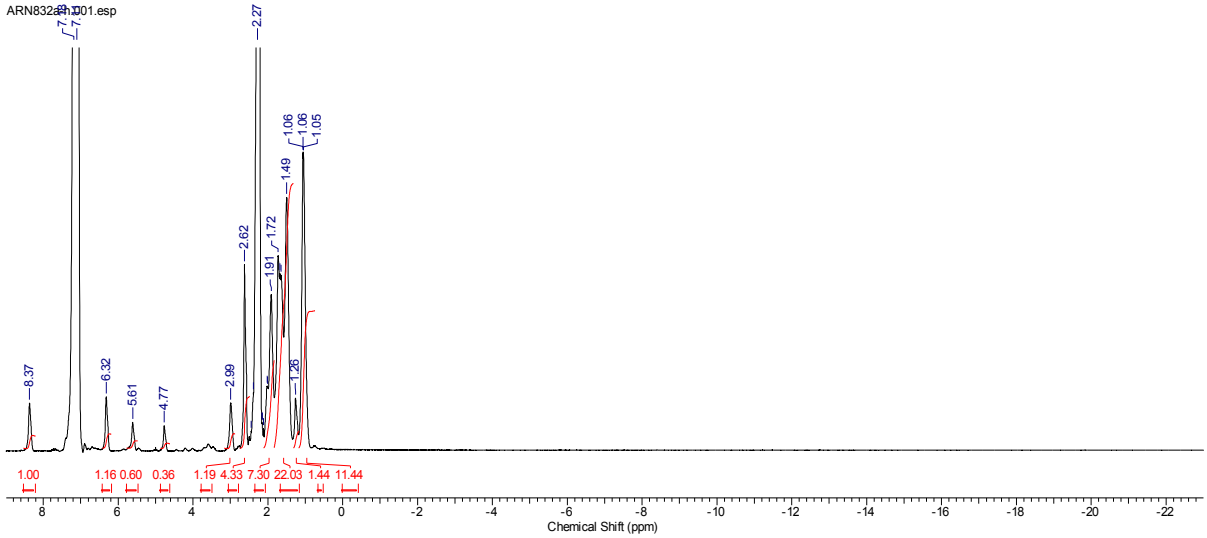

spectrum 2d: ^{2}H-NMR (61.4 MHz, 373 K):

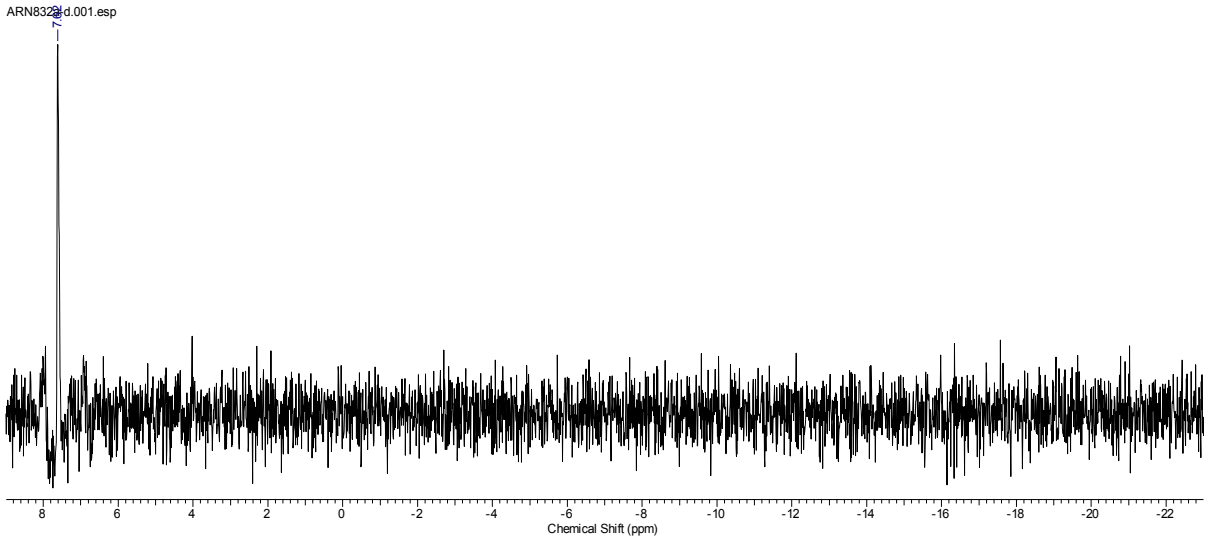

spectrum 2p{h}: ^{31}P-NMR (162.0 MHz, 373 K):

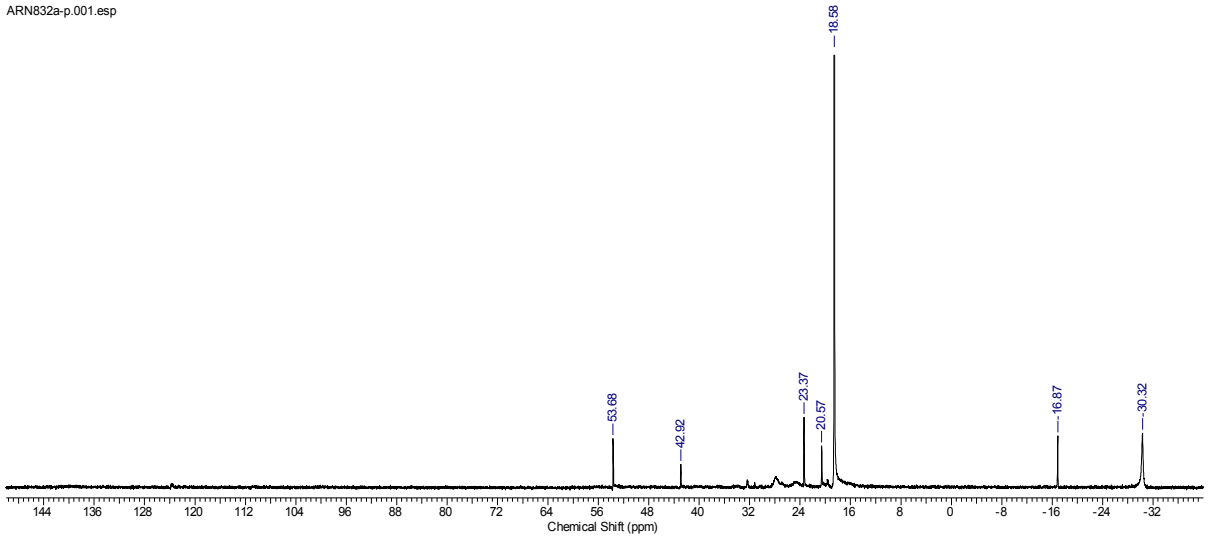

spectrum 3h: ^{1}H-NMR (400.1 MHz, 295 K):

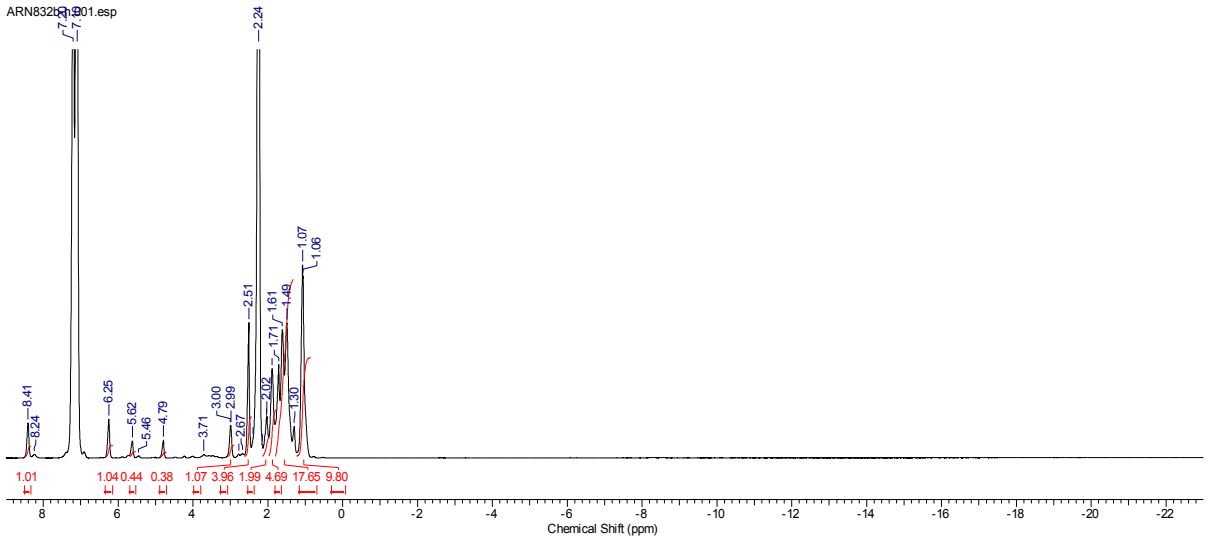

spectrum 3d: ^{2}H-NMR (61.4 MHz, 295 K):

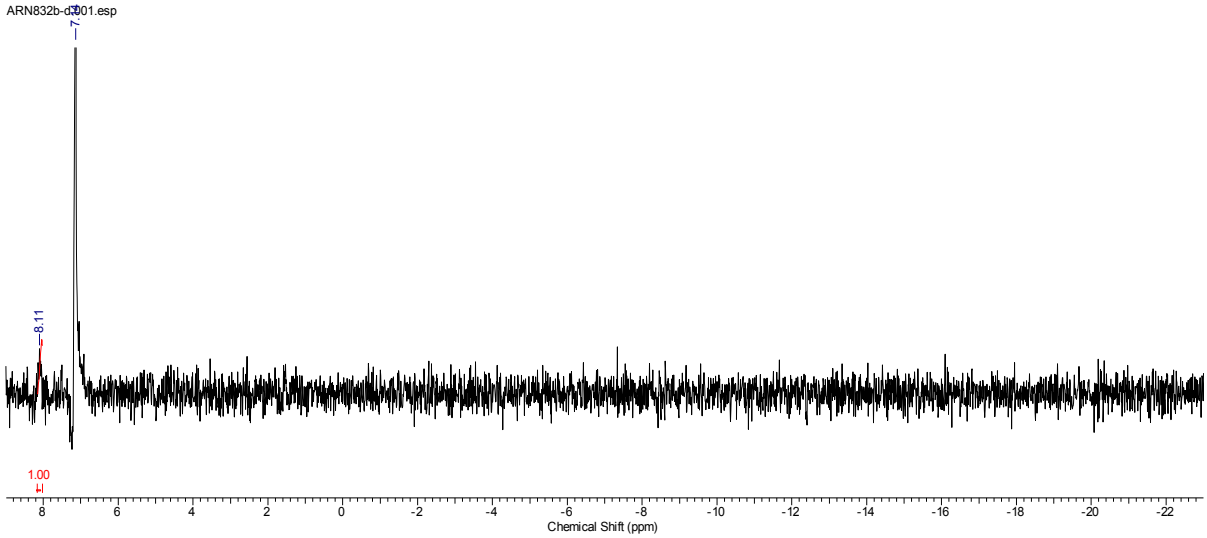

spectrum 3p{h}: ^{31}P-NMR (162.0 MHz, 295 K):

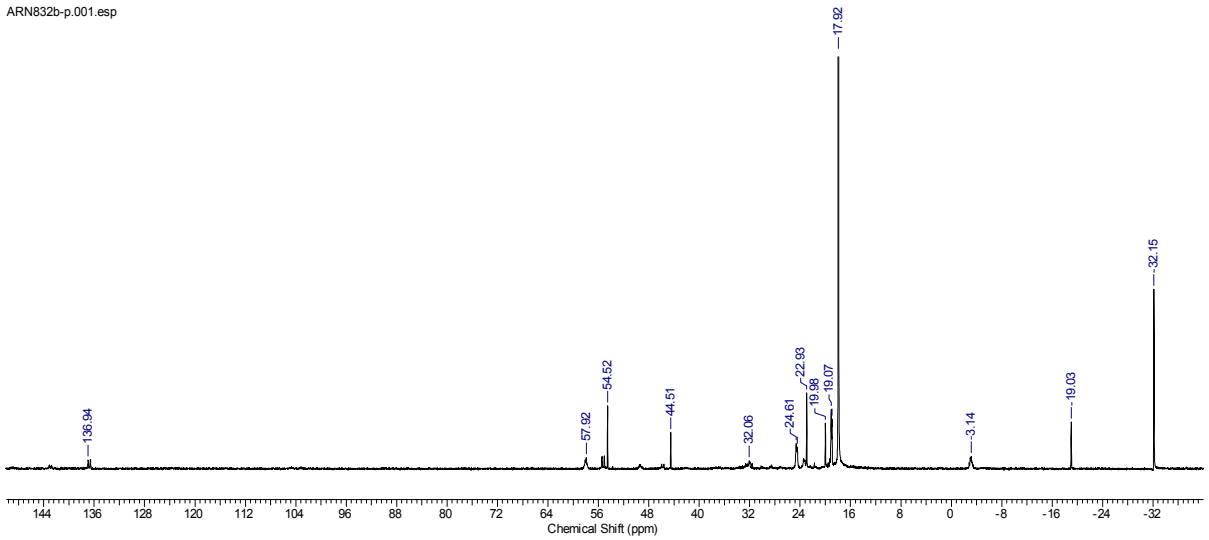

spectrum 4d: ^{2}H-NMR (61.4 MHz, 295 K):

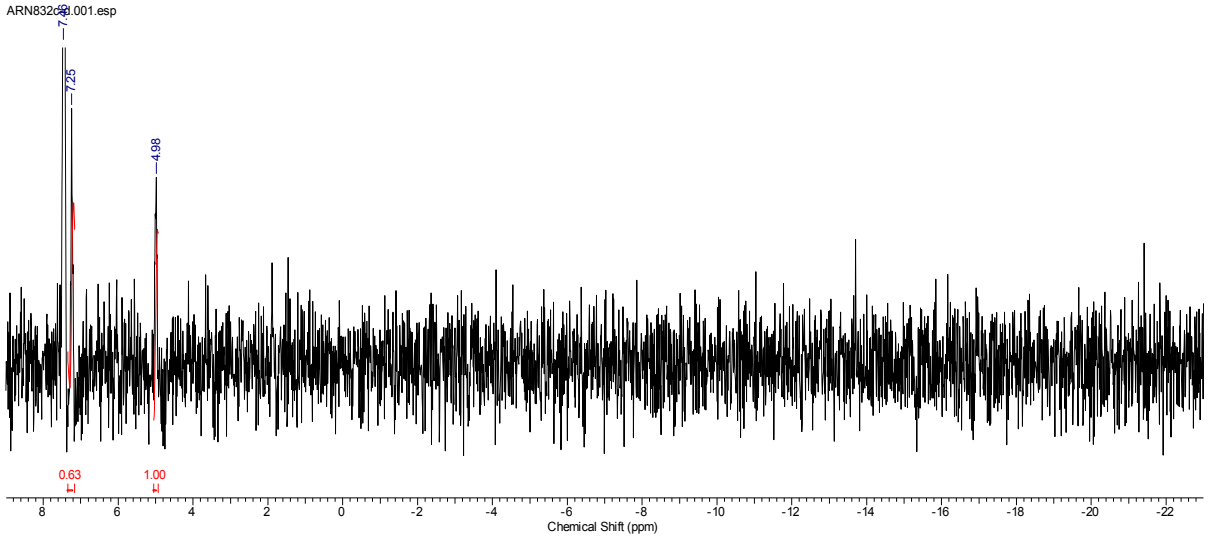

spectrum 5d: ^{2}H-NMR (61.4 MHz, 373 K):

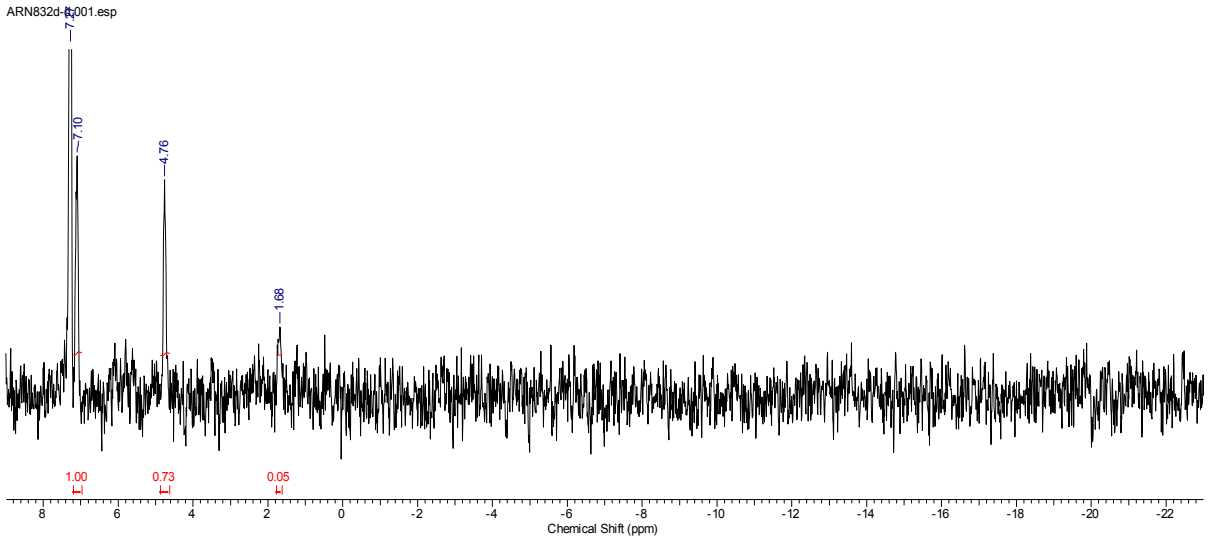

spectrum 6d: ^{2}H-NMR (61.4 MHz, 295 K):

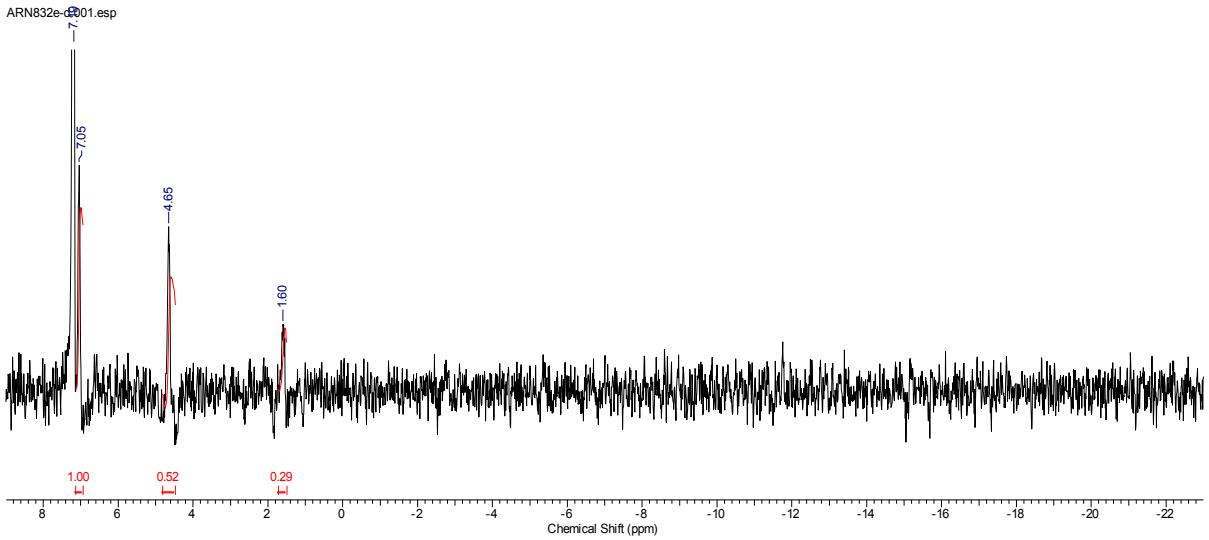

***In situ* NMR experiments with 1-[*D*]-hex-1-yne (JACS-5a):** A 5 mm NMR tube was charged with bis-(2-methallyl)-cycloocta-1,5-diene-ruthenium(II) (31.9 mg, 0.10 mmol) and DMAP (18.3 mg, 0.15 mmol). The tube was sealed with a rubber septum and purged with alternating vacuum and nitrogen cycles. Subsequently, tri-*n*-butylphosphine (77 µL, 0.30 mmol), 1-[*D*]-hex-1-yne (**JACS-5a**, 59 µL, 0.5 mmol, DG = 96%), benzene-d_6 (20 µL, 0.24 mmol) and dry toluene (0.50 mL) were added via syringe and placed in an ultrasonic bath for 15 min to give a clear yellow solution. Spectrum 7d was recorded at 22 °C. The sample was heated to 100 °C for 5 min and after cooling down to 22°C spectrum 8d was recorded.

spectrum 7d: ^{2}H-NMR (61.4 MHz, 295 K):

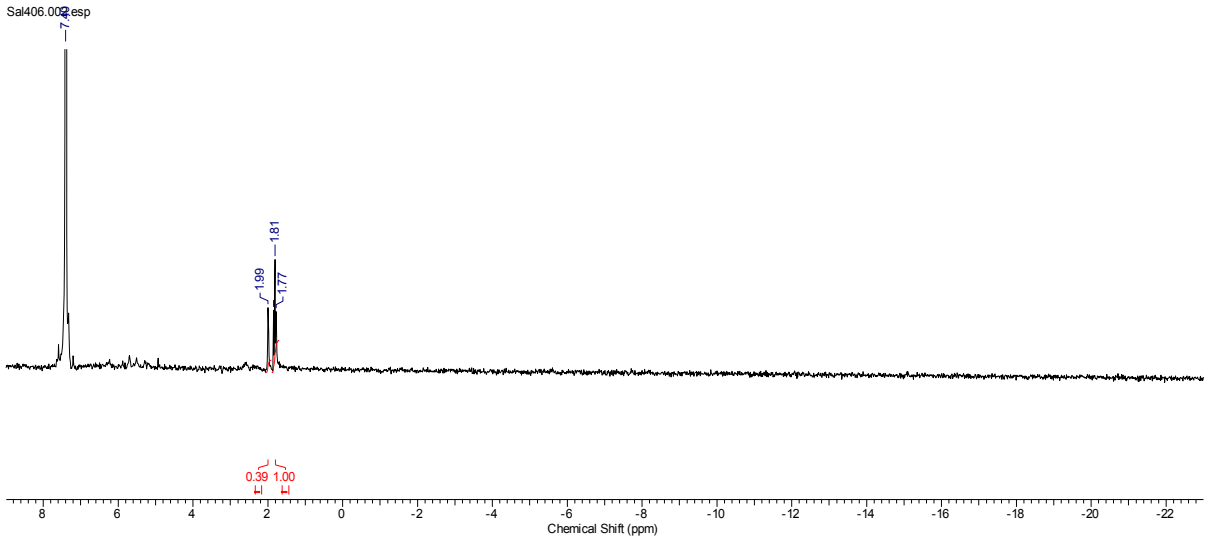

spectrum 8d: ^{2}H-NMR (61.4 MHz, 373 K):

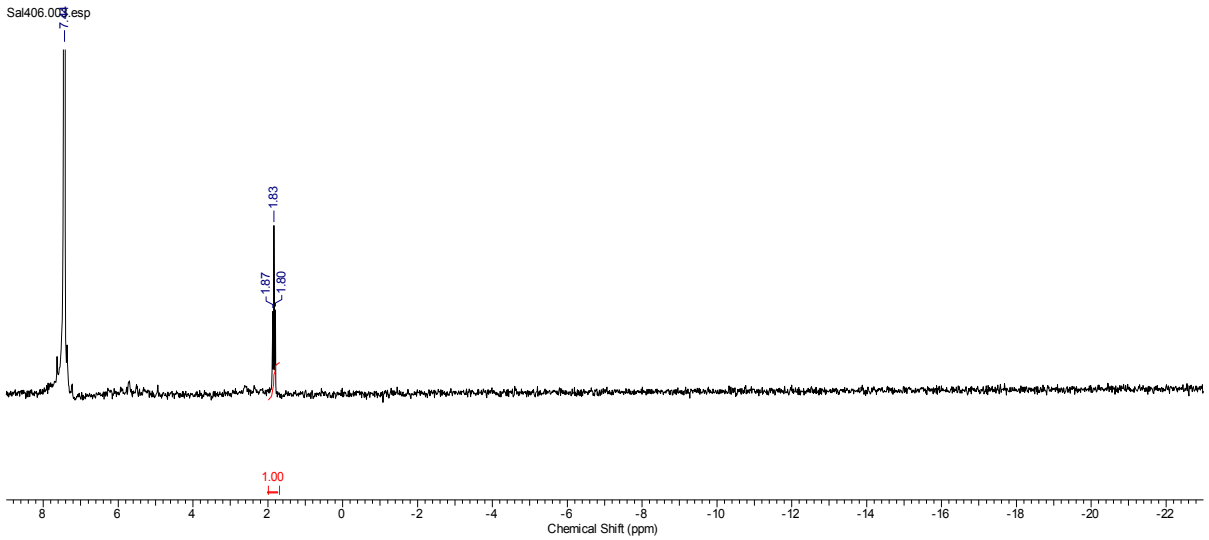

***In situ* NMR experiments with 1-[*D*]-hex-1-yne (JACS-5a) and 2-pyrrolidinone (JACS-1a):** A 5 mm NMR tube was charged with bis-(2-methallyl)-cycloocta-1,5-diene-ruthenium(II) (31.9 mg, 0.10 mmol) and DMAP (18.3 mg, 0.15 mmol). The tube was sealed with a rubber septum and purged with alternating vacuum and nitrogen cycles. Subsequently, tri-*n*-butylphosphine (77 µL, 0.30 mmol), 2-pyrrolidione (**JACS-1a**, 19 µL, 0.25 mmol), 1-[*D*]-hex-1-yne (**JACS-5a**, 59 µL, 0.5 mmol, DG = 96%), benzene-d_6 (20 µL, 0.24 mmol) and dry toluene (0.50 mL) were added via syringe and placed in an ultrasonic bath for 15 min to give a clear yellow solution. The sample was heated to 100 °C for 10 min and after cooling down to 22°C spectrum 9d was recorded.

spectrum 9d: ^{2}H-NMR (61.4 MHz, 295 K):

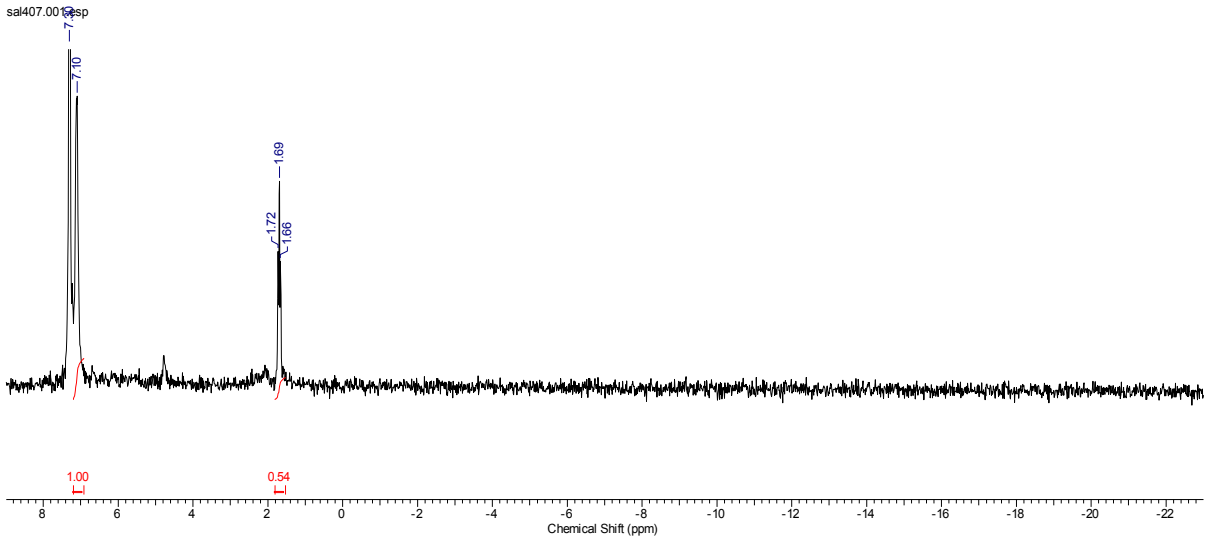

***In situ* NMR experiments with 2-pyrrolidinone (JACS-1a):** A 5 mm NMR tube was charged with bis-(2-methallyl)-cycloocta-1,5-diene-ruthenium(II) (31.9 mg, 0.10 mmol) and DMAP (24.4 mg, 0.20 mmol). The tube was sealed with a rubber septum and purged with alternating vacuum and nitrogen cycles. Subsequently, tri-*n*-butylphosphine (77 µL, 0.30 mmol), 2-pyrrolidinone (**JACS-1a**, 19 µL, 0.25 mmol) and toluene-d_8 (0.50 mL) were added via syringe and placed in an ultrasonic bath for 15 min to give a clear yellow solution. Spectra 10h/10p{h} were recorded at 22 °C. The sample was heated to 100 °C for 5 min and spectra 11h/11p{h} were recorded. After cooling down the sample to 22 °C spectra 12h/12p{h}/12h{p}/12p/12ppCOSY/12hpHMQC were recorded.

spectrum 10h: ^{1}H-NMR (400.1 MHz, 295 K):

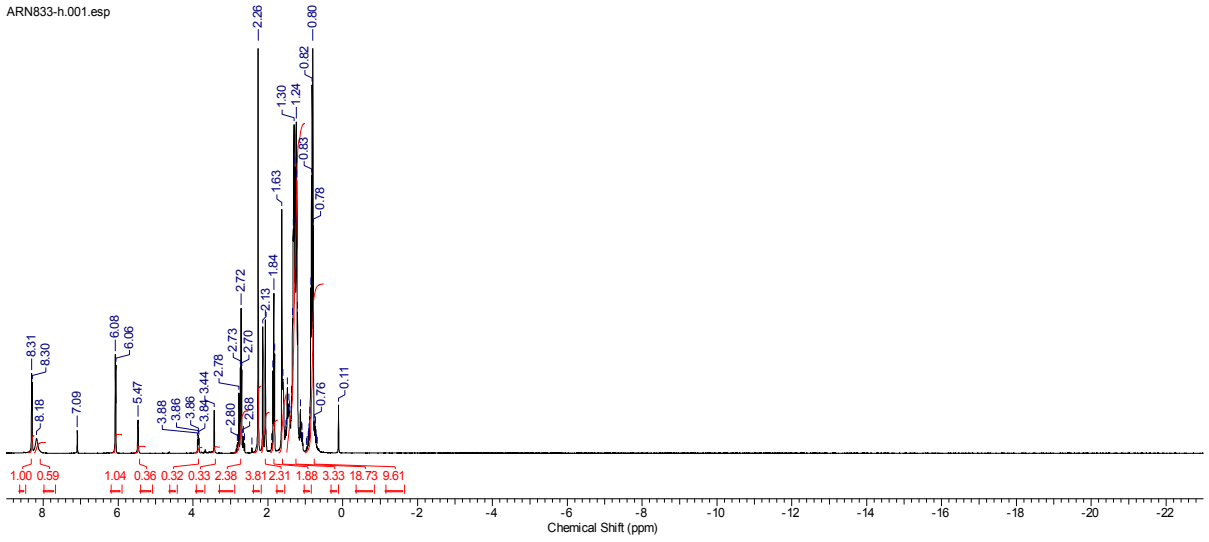

spectrum 10p{h}: ^{31}P-NMR (162.0 MHz, 295 K):

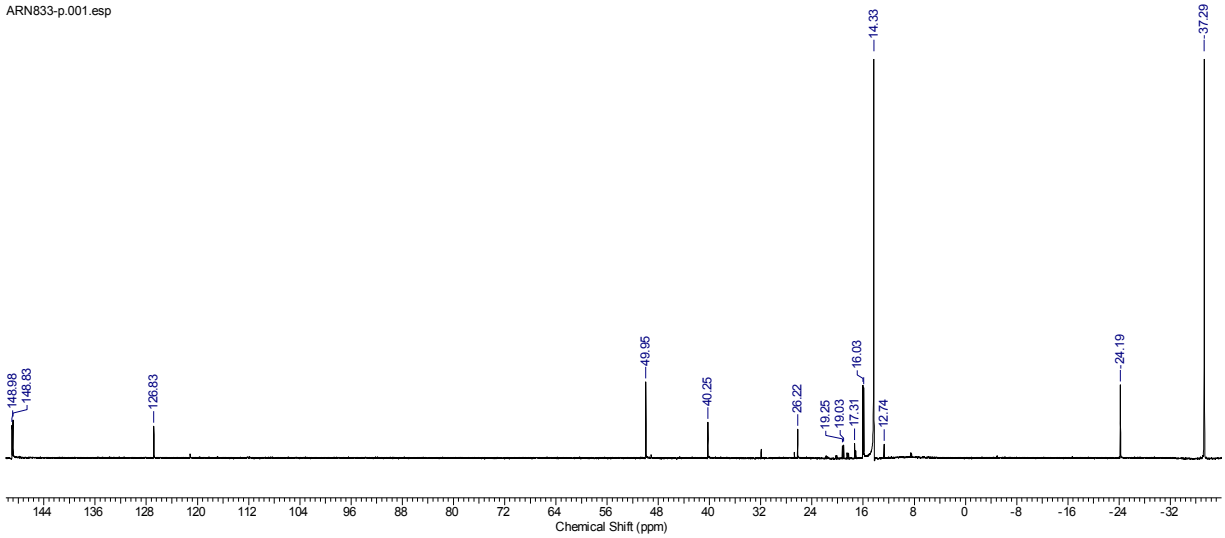

spectrum 11h: ^{1}H-NMR (400.1 MHz, 373 K):

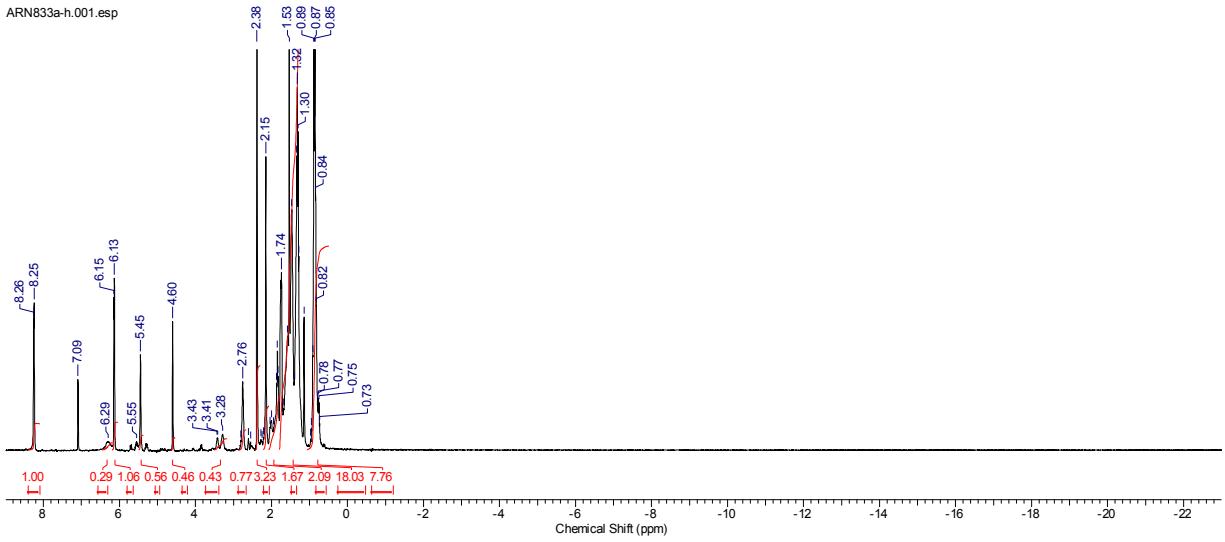

spectrum 11p{h}: ^{31}P-NMR (162.0 MHz, 373 K):

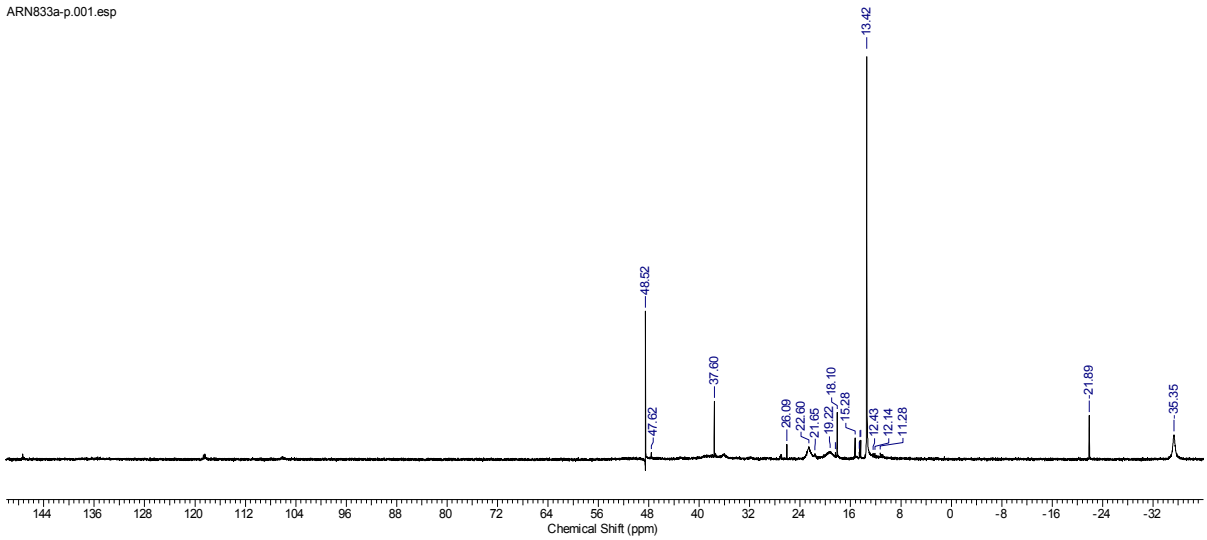

spectrum 12h: ^{1}H-NMR (600.3 MHz, 295 K):

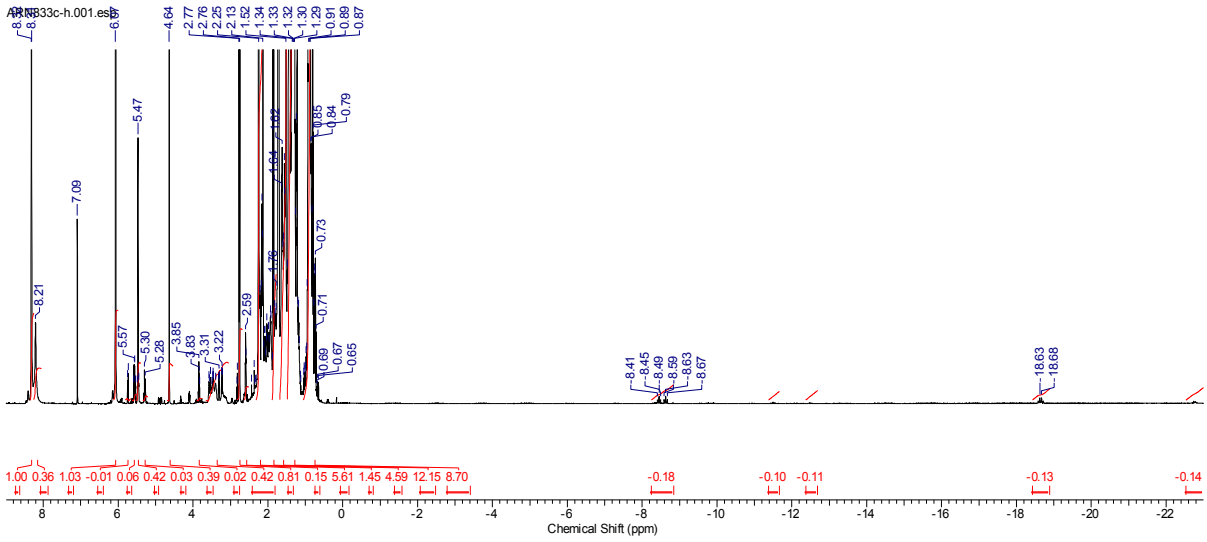

spectrum 12p{h}: ^{31}P-NMR (242.9 MHz, 295 K):

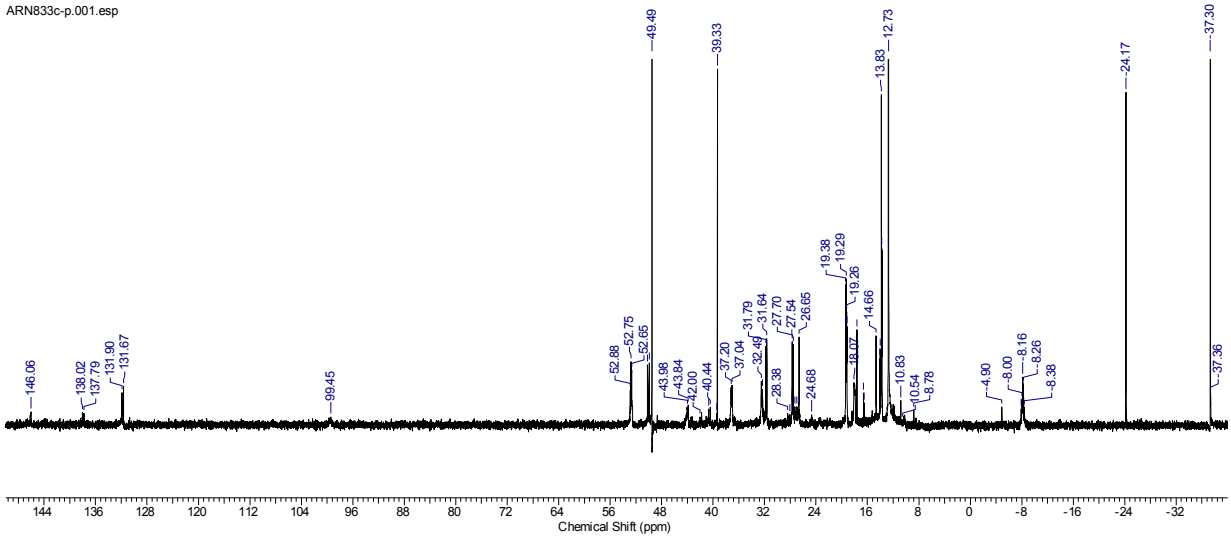

spectrum 12h{p}: ^{1}H-NMR (400.1 MHz, 295 K):

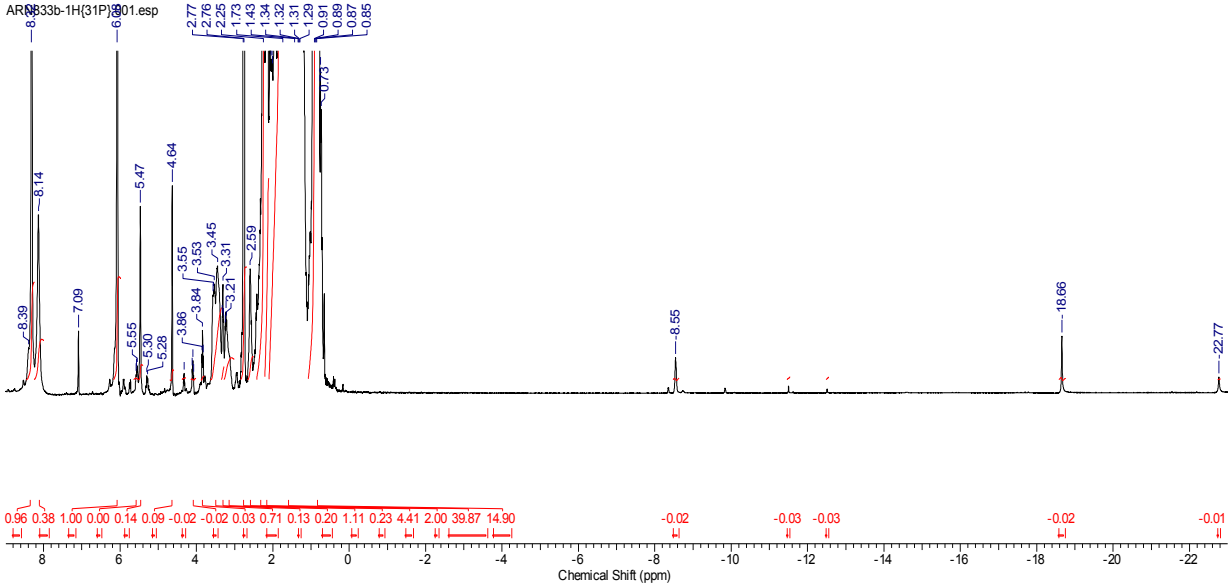

spectrum 12p: ^{31}P-NMR (242.9 MHz, 295 K):

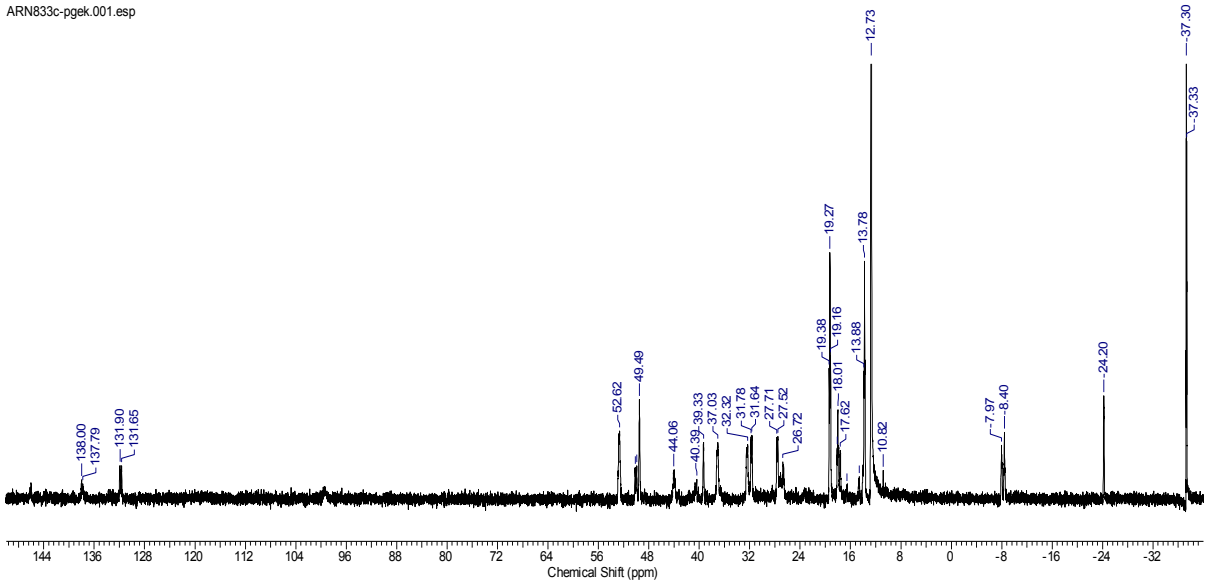

spectrum 12hpHMQC: (600.3 MHz, 242.9 MHz, 295 K):

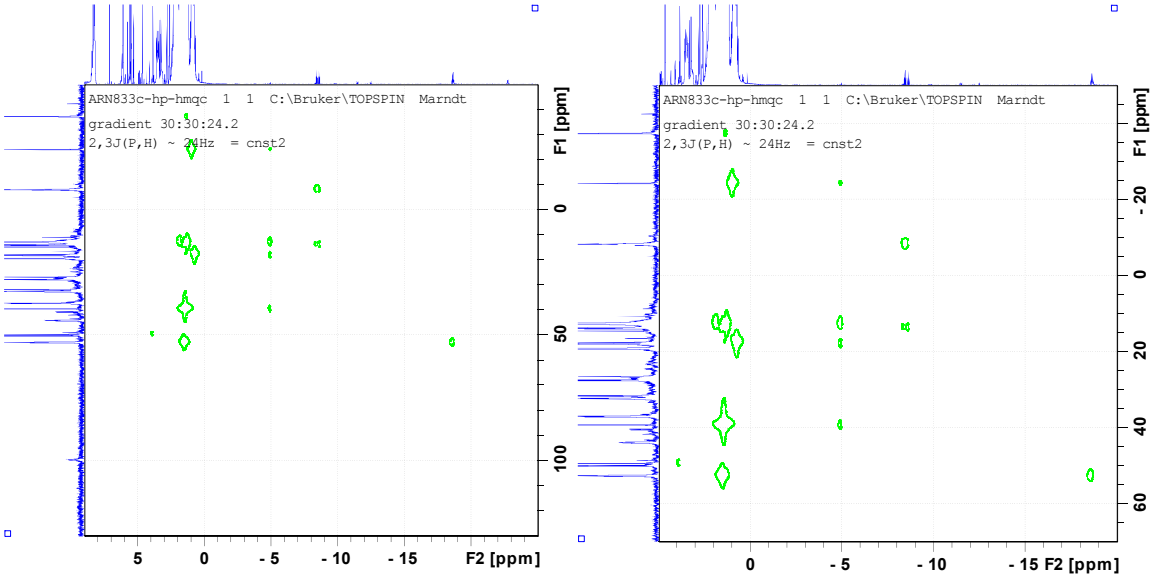

spectrum 12ppCOSY: (242.9 MHz, 295 K):

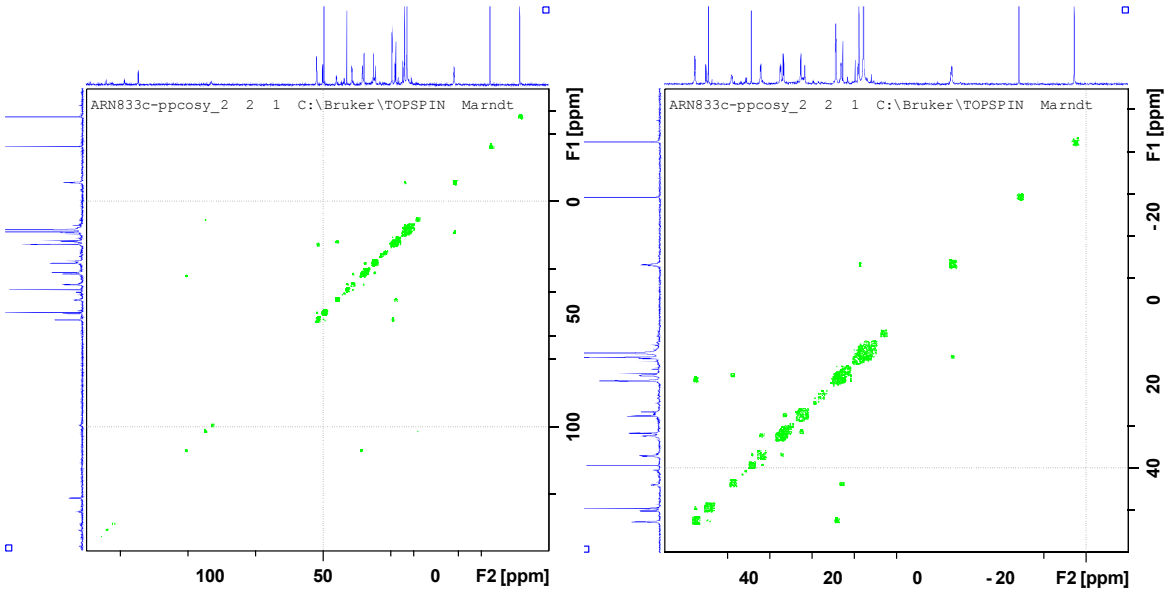

***In situ* NMR experiments with 1-hexyne (JACS-5b):** A 5 mm NMR tube was charged with bis-(2-methallyl)-cycloocta-1,5-diene-ruthenium(II) (31.9 mg, 0.10 mmol) and DMAP (18.3 mg, 0.15 mmol). The tube was sealed with a rubber septum and purged with alternating vacuum and nitrogen cycles. Subsequently, tri-*n*-butylphosphine (77 µL, 0.30 mmol), 1-hexyne (**JACS-5b**, 59 µL, 0.5 mmol) and dry toluene-d_8 (0.50 mL) were added via syringe and placed in an ultrasonic bath for 15 min to give a clear yellow solution. Spectra 12h/13p{h} were recorded at 22 °C. The sample was heated to 100 °C for 5 min and spectra 14h/14p{h} were recorded. After cooling down the sample to 22 °C spectra 15h/15p{h} were recorded.

spectrum 13h: ^{1}H-NMR (600.3 MHz, 295 K):

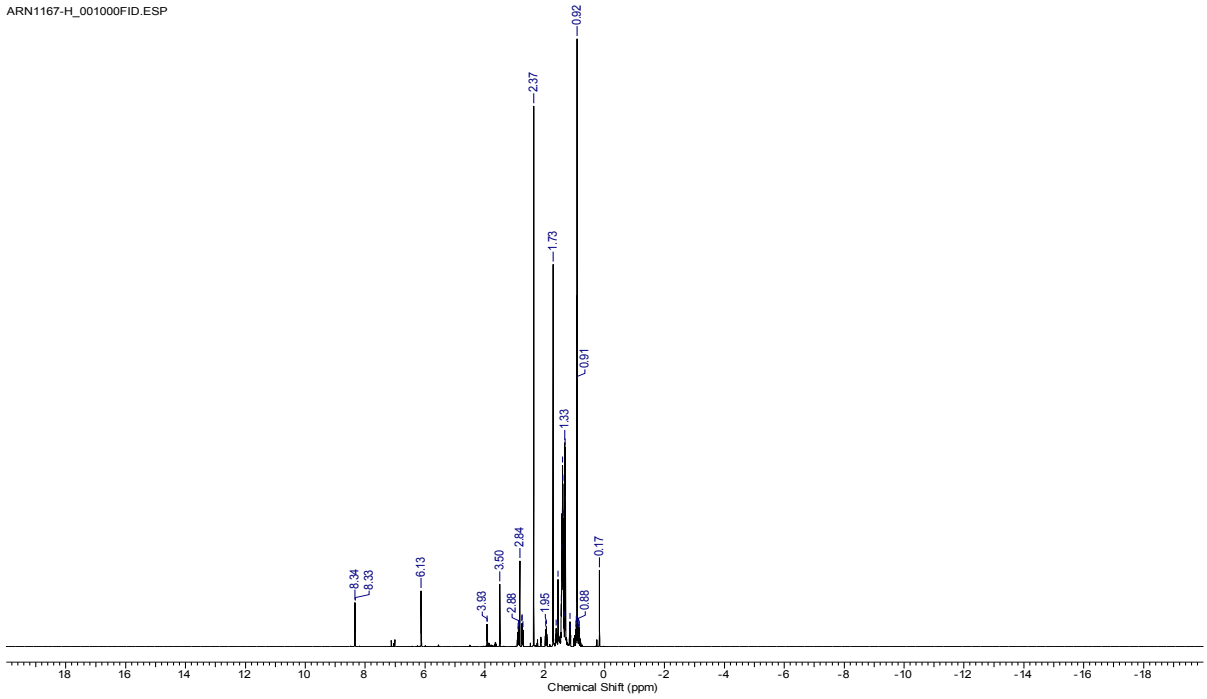

spectrum 13p: ^{31}P-NMR (242.9 MHz, 295 K):

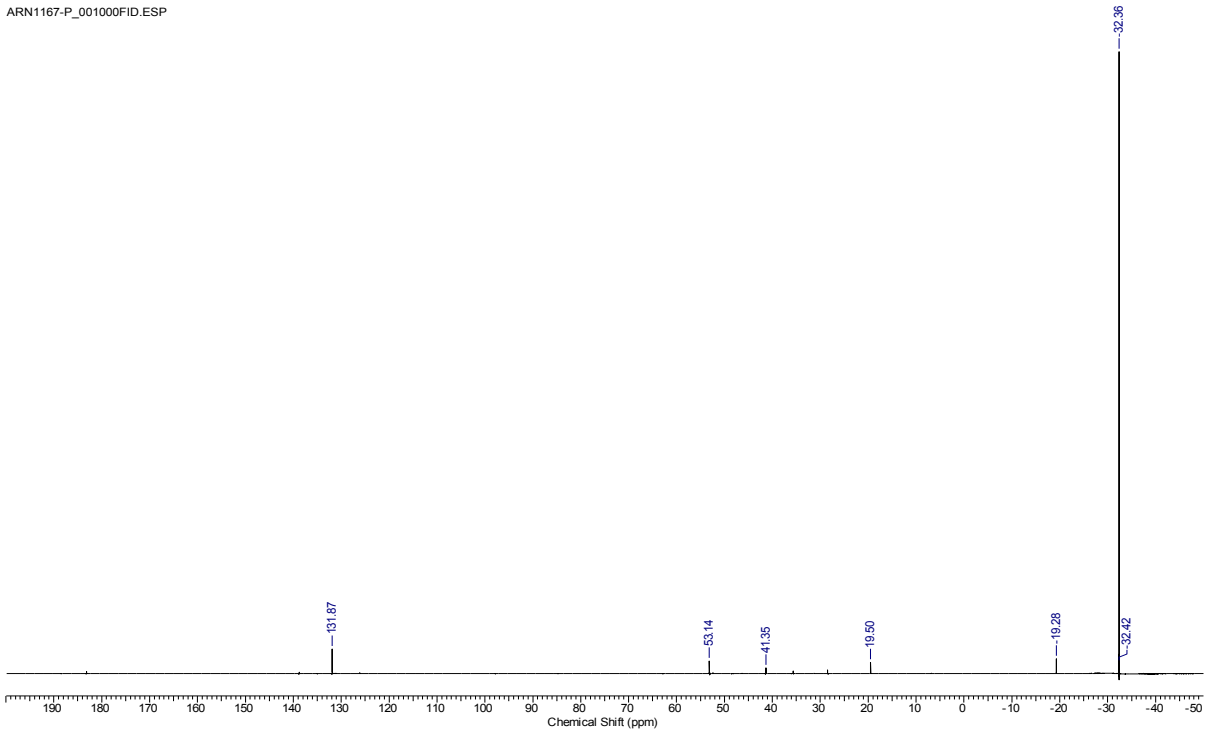

spectrum 14h: ^{1}H-NMR (600.3 MHz, 373 K):

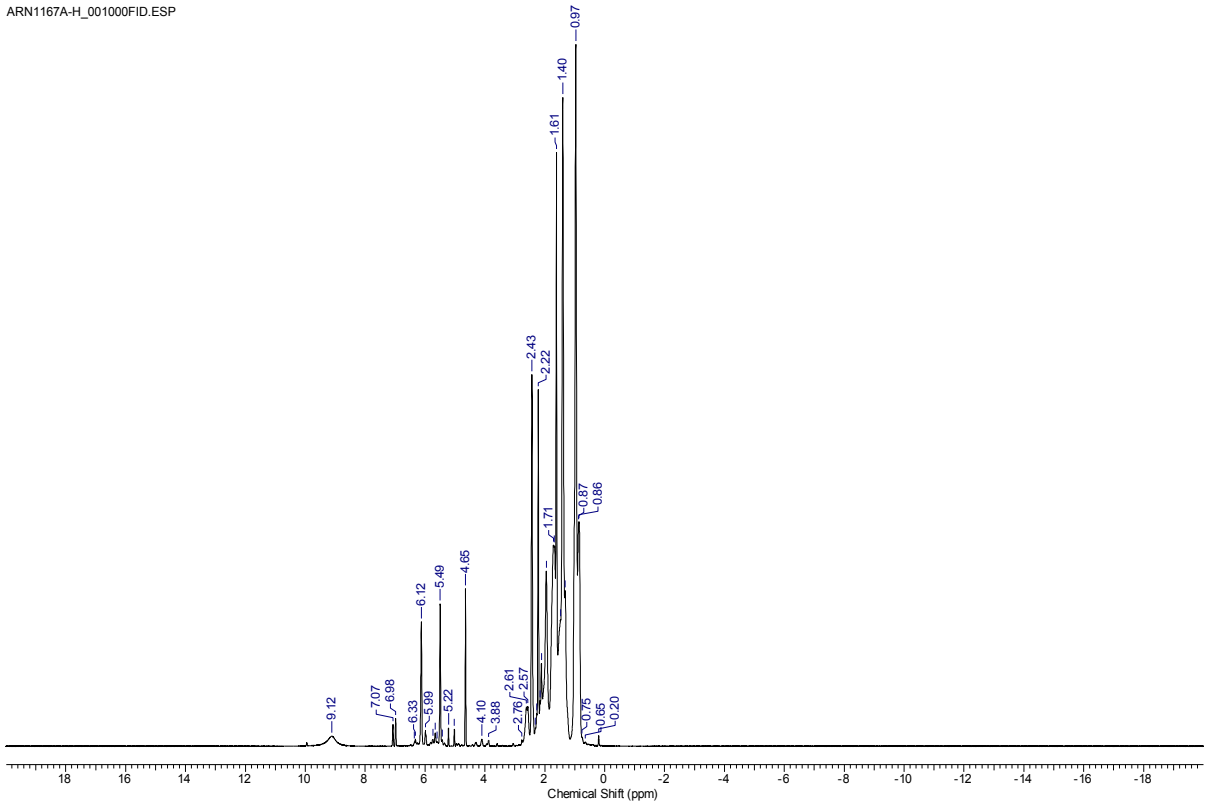

spectrum 14p: ^{31}P-NMR (242.9 MHz, 373 K):

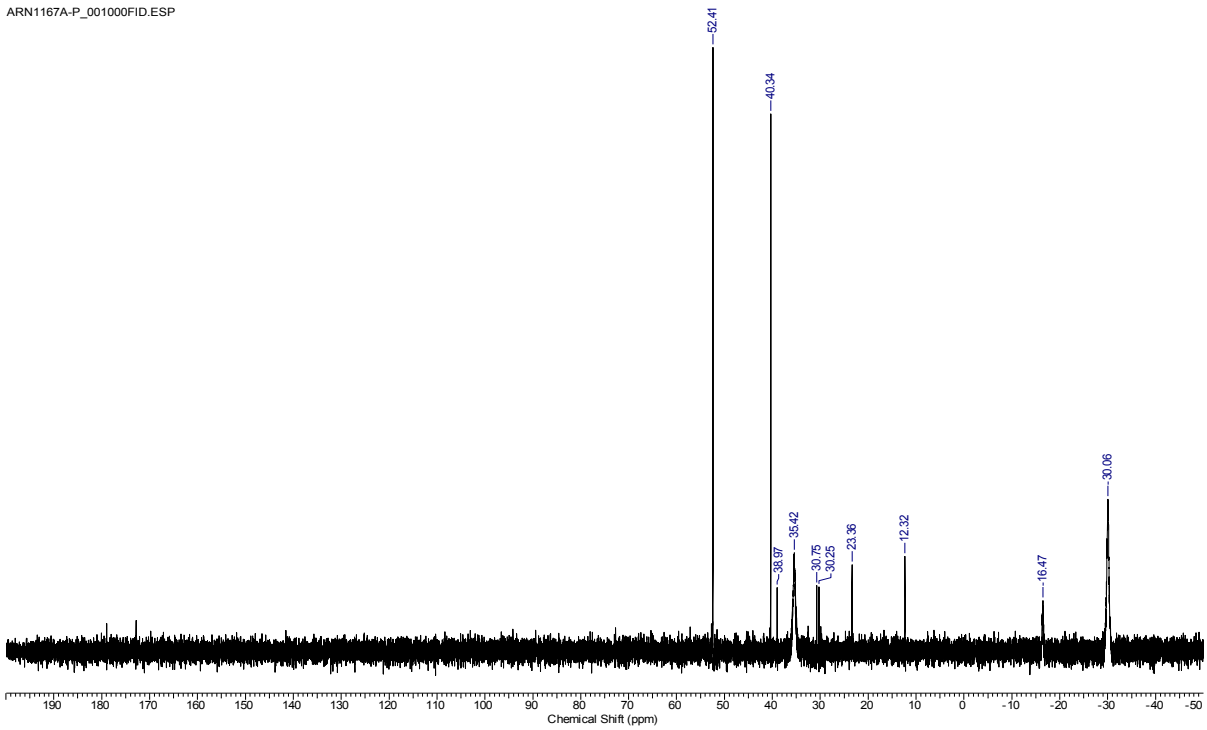

spectrum 15h: ^{1}H-NMR (600.3 MHz, 295 K):

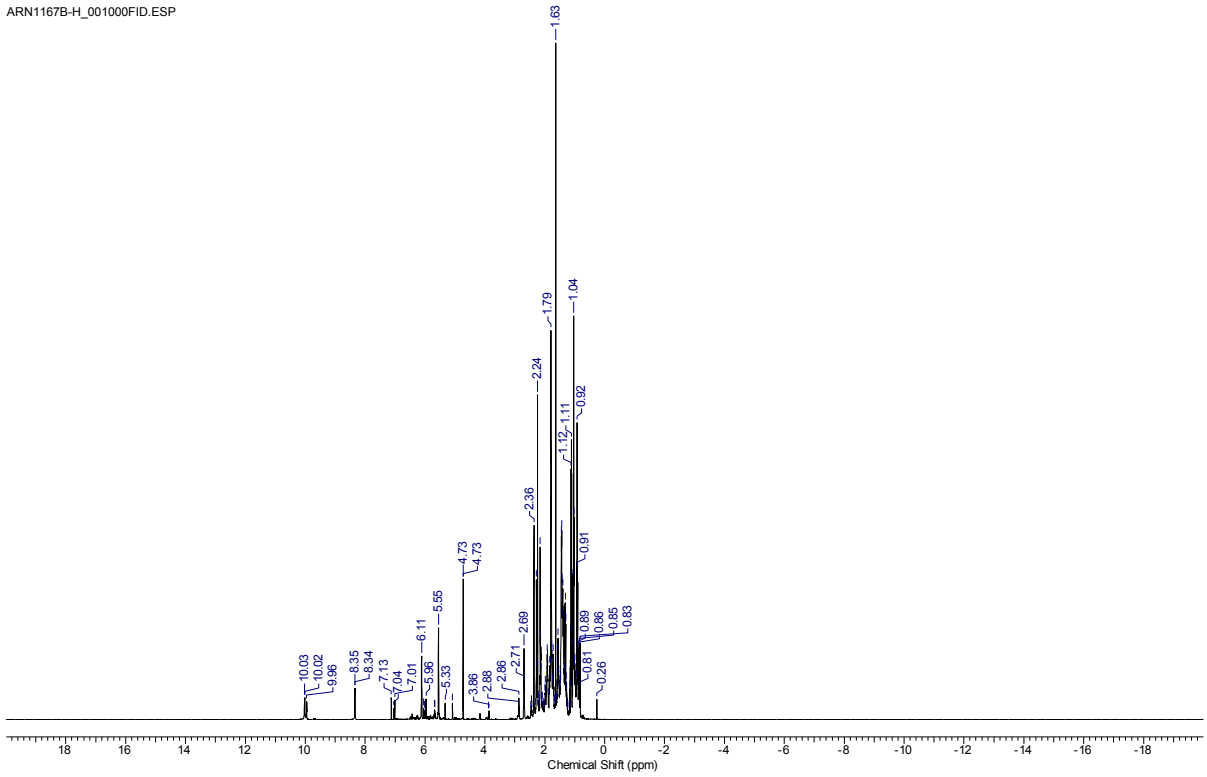

spectrum 15p: ^{31}P-NMR (242.9 MHz, 295 K):

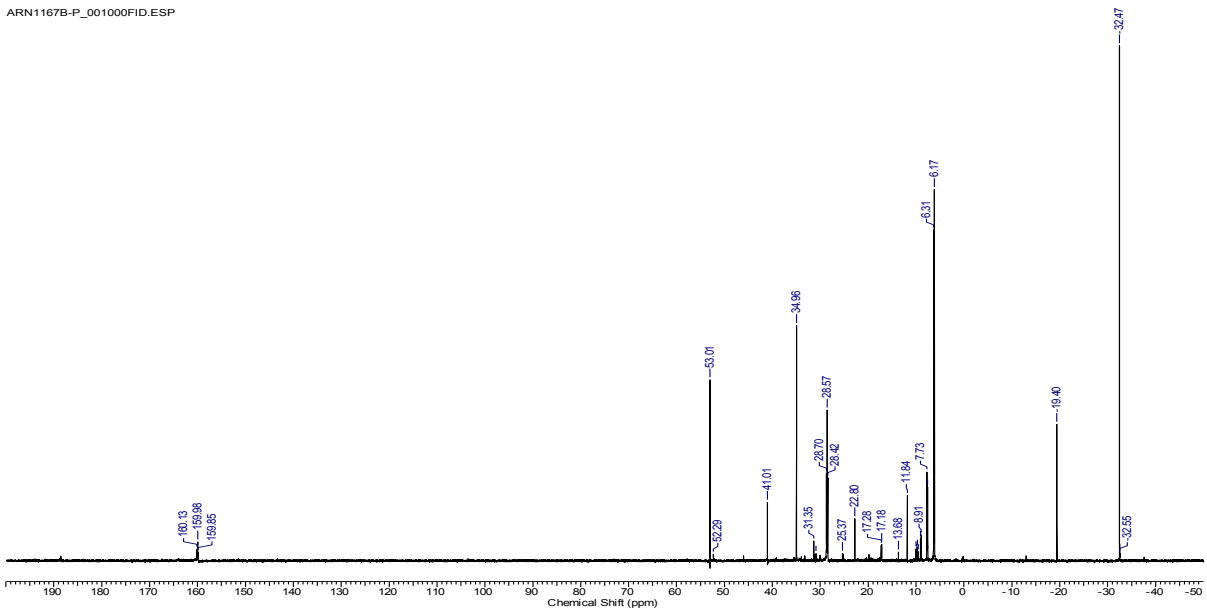

***In situ* NMR experiments with 2-pyrrolidinone (JACS-1a) and phenylacetylene-2-^{13}C (JACS-5c):** A 5 mm NMR tube was charged with bis-(2-methallyl)-cycloocta-1,5-diene-ruthenium(II) (31.9 mg, 0.10 mmol) and DMAP (24.4 mg, 0.20 mmol). The tube was sealed with a rubber septum and purged with alternating vacuum and nitrogen cycles. Subsequently,

tri-*n*-butylphosphine (77 µL, 0.30 mmol), 2-pyrrolidinone (**JACS-1a**, 19 µL, 0.25 mmol) and toluene-d_8 (0.50 mL) were added via syringe and placed in an ultrasonic bath for 15 min to give a clear yellow solution. The sample was heated to 100 °C for 5 min and phenylacetylene-2-^{13}C (**JACS-5c**, 56.0 µL, 0.5 mmol) was added. Spectra 16h/16c were recorded at 22 °C. The sample was heated to 100 °C for 5 minutes and after cooling down the sample spectra 17h/17c were recorded at 22 °C.

spectrum 16h: ^{1}H-NMR (600.3 MHz, 295 K):

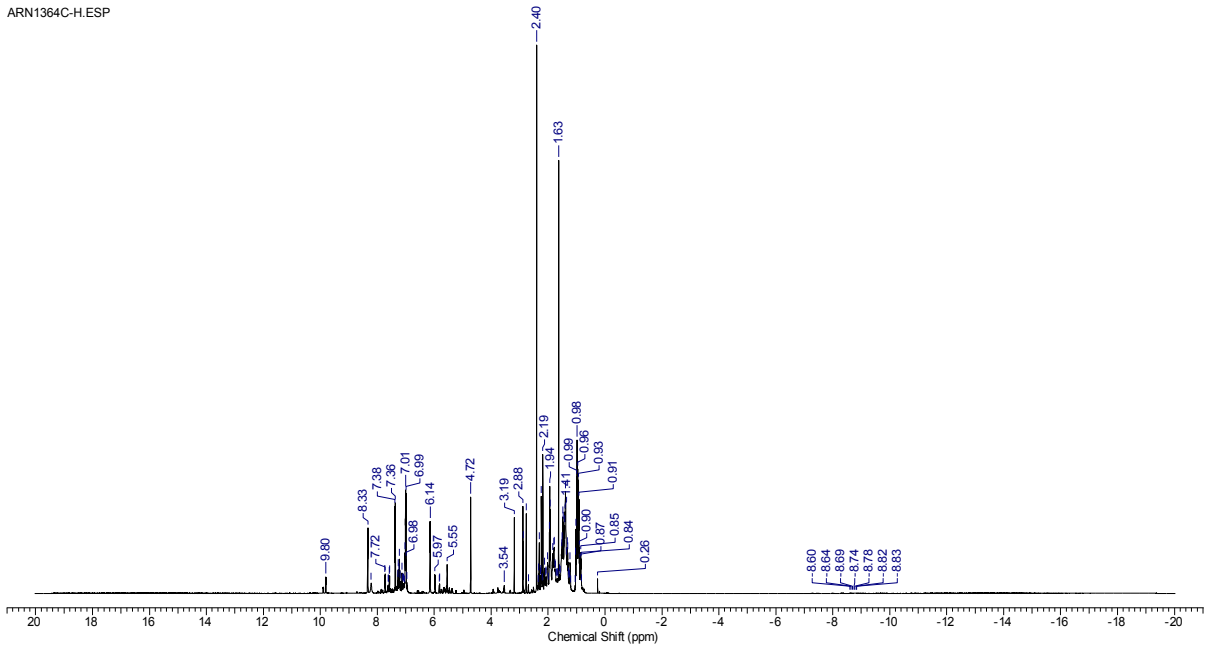

zoom:

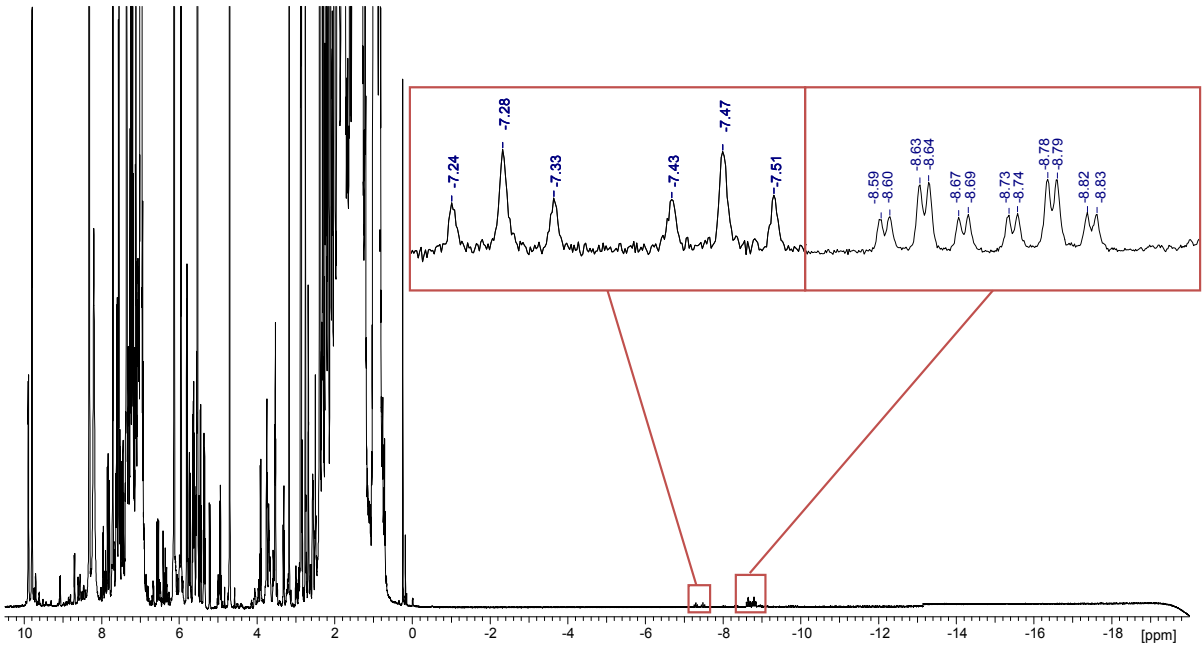

spectrum 16c: ^{13}C-NMR (150.9 MHz, 295 K):

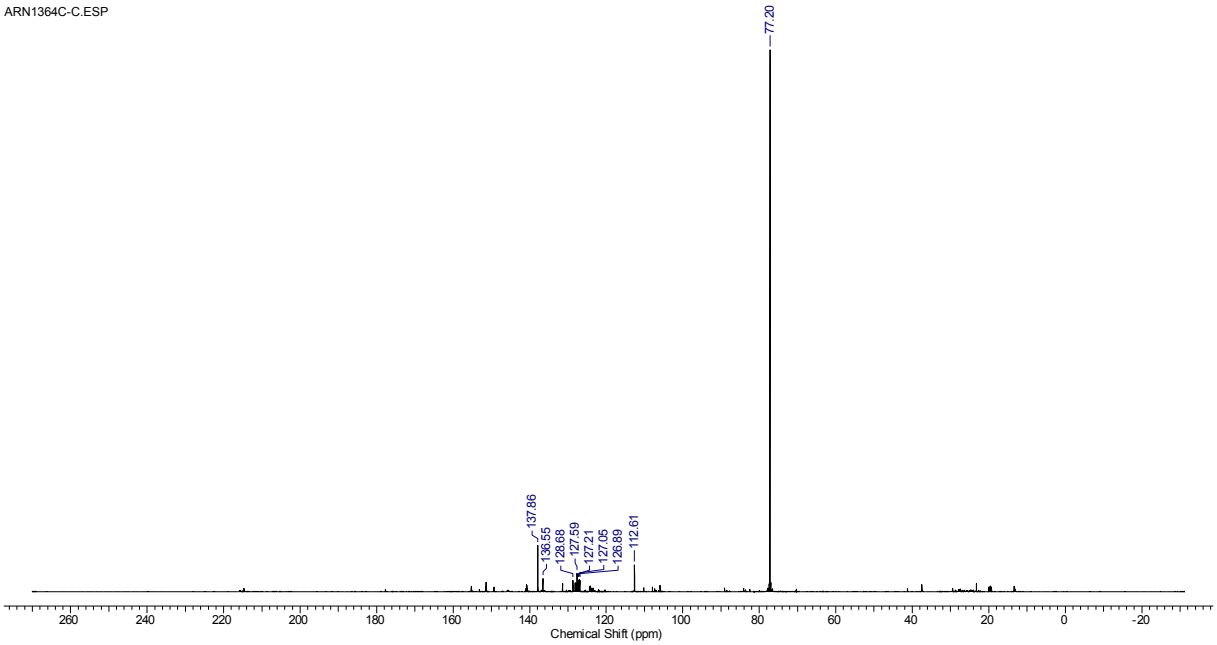

zoom:

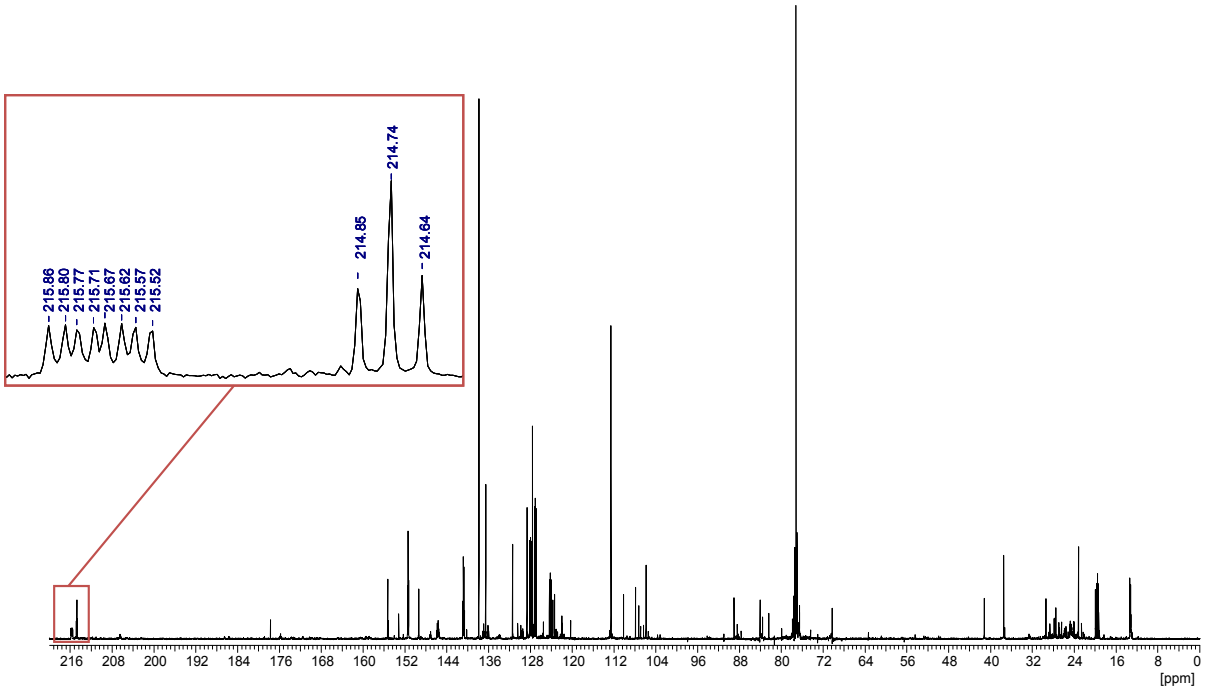

spectrum 17h: ^{1}H-NMR (600.3 MHz, 295 K):

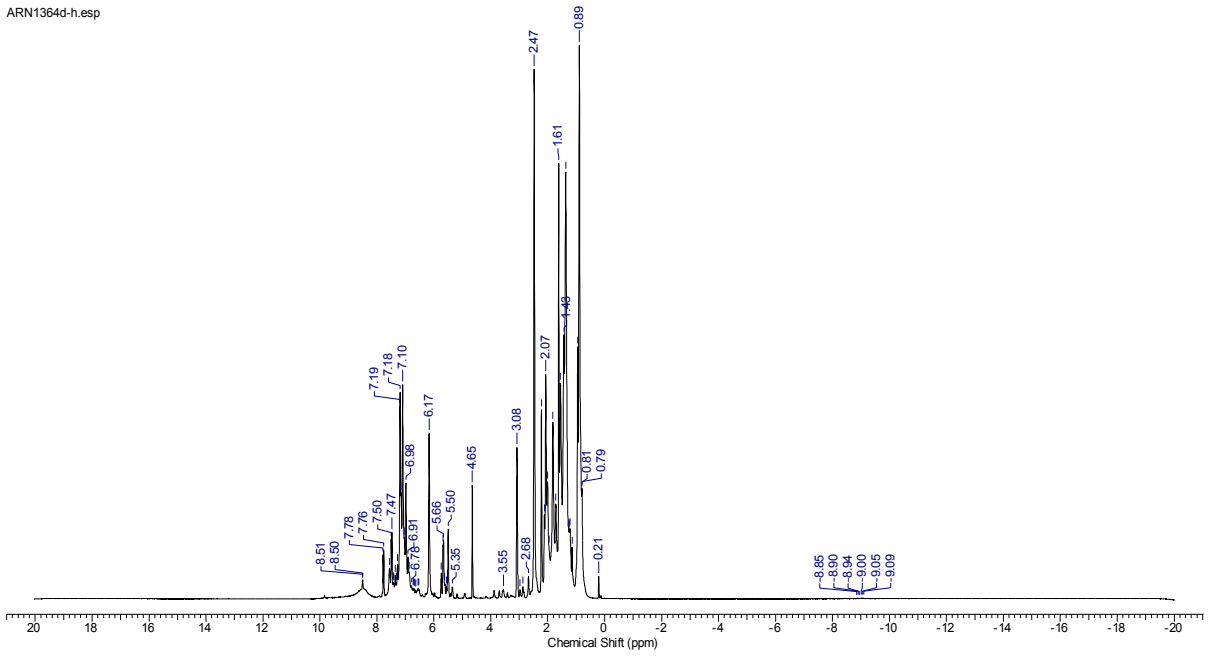

spectrum 17c: ^{13}C-NMR (150.9 MHz, 295 K):

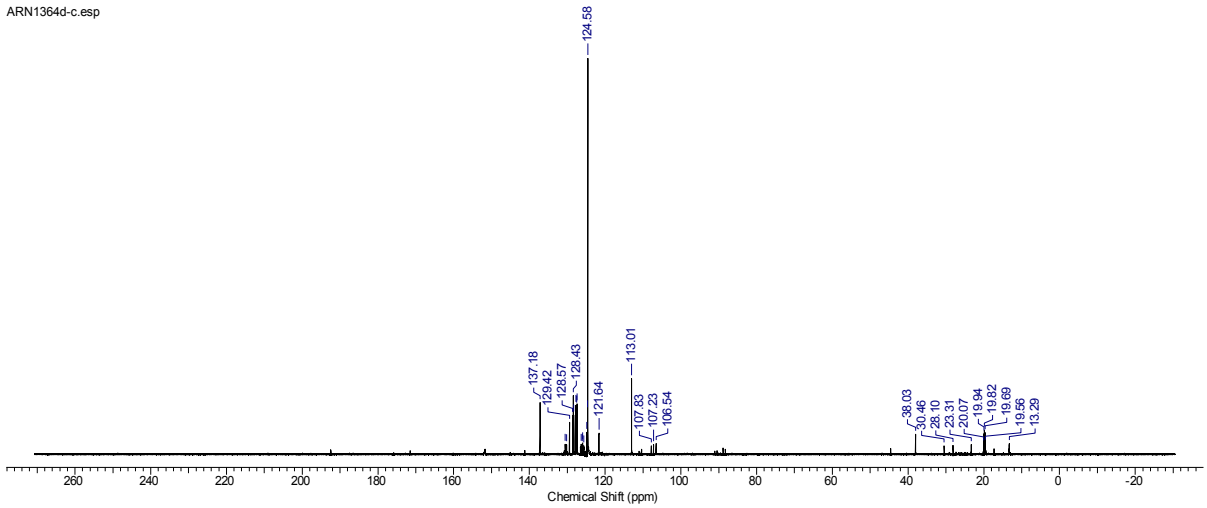

***Z*-selective hydroamidation protocol:**

***In situ* NMR experiments with 2-pyrrolidinone (JACS-1a):** A 5 mm NMR tube was charged with bis-(2-methallyl)-cycloocta-1,5-diene-ruthenium(II) (31.9 mg, 0.10 mmol), 1,4-bis(dicyclohexylphosphino) butane (50.7 mg, 0.11 mmol) and scandium triflate (100.0 mg, 0.2 mmol). (Ytterbium(III) is paramagnetic, therefore we used Scandium(III) triflate, which is diamagnetic and shows a similar activity in hydroamidation experiments) The tube was sealed with a rubber septum and purged with alternating vacuum and nitrogen cycles. Subsequently, 2-pyrrolidinone (**JACS-1a**, 19 µL, 0.25 mmol) and DMF-d_7 (0.80 mL) were added via syringe and placed in an ultrasonic bath for 30 min to give a cloudy suspension. Spectra 18h/18p were recorded at 22 °C. The sample was heated in a water bath to 60 °C for 15 min, afterwards the sample was centrifuged for 15 min, resulting in a clear yellow organic phase at the bottom of the tube and a white solid phase on top. Spectra 19h/19h{p}/19p/19c/19ppCOSY/19hpHMQC were recorded at 22 °C.

spectrum 18h: ^{1}H-NMR (600.3 MHz, 295 K):

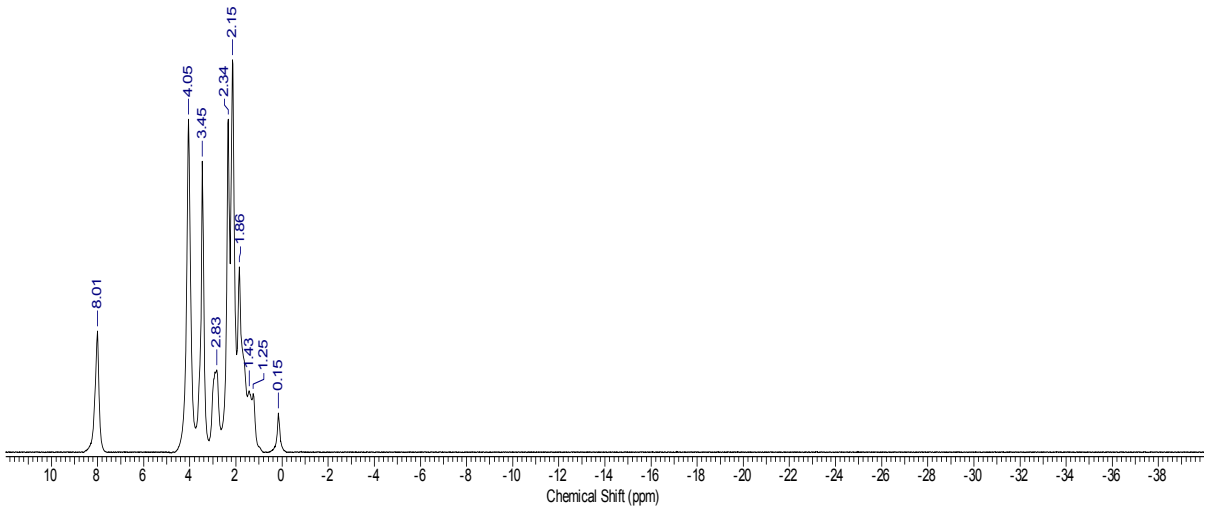

spectrum 18p: ^{31}P-NMR (242.9 MHz, 295 K):

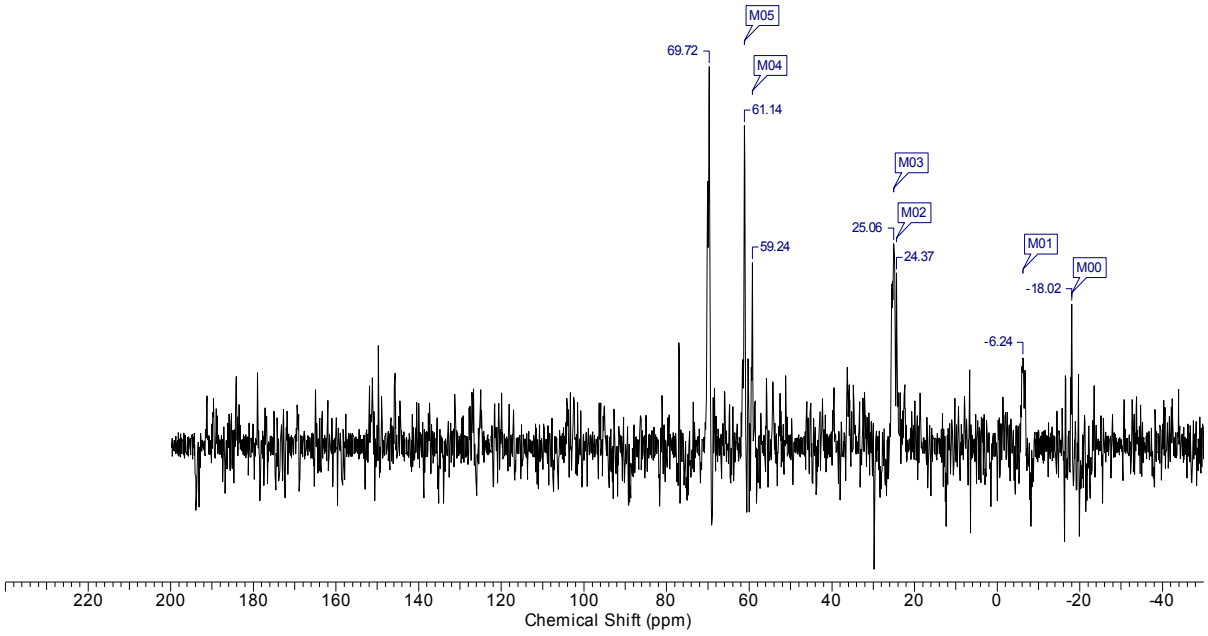

spectrum 19h: ^{1}H-NMR (600.3 MHz, 295 K):

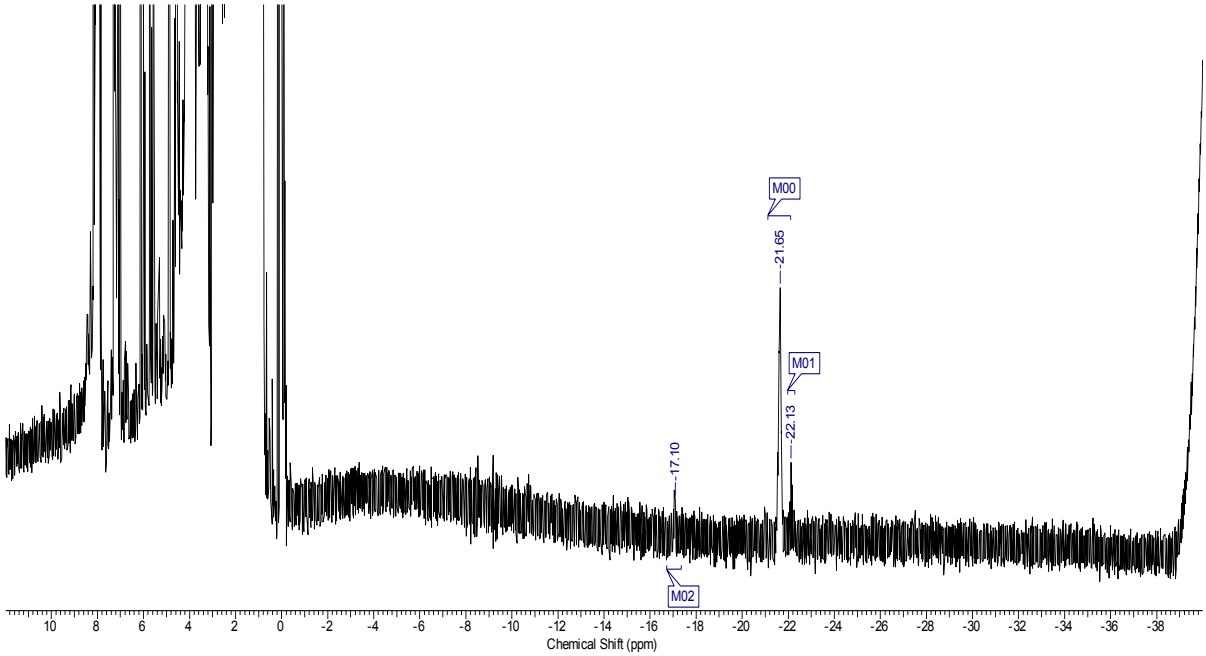

spectrum 19h{p}: ^{1}H-NMR (600.3 MHz, 295 K):

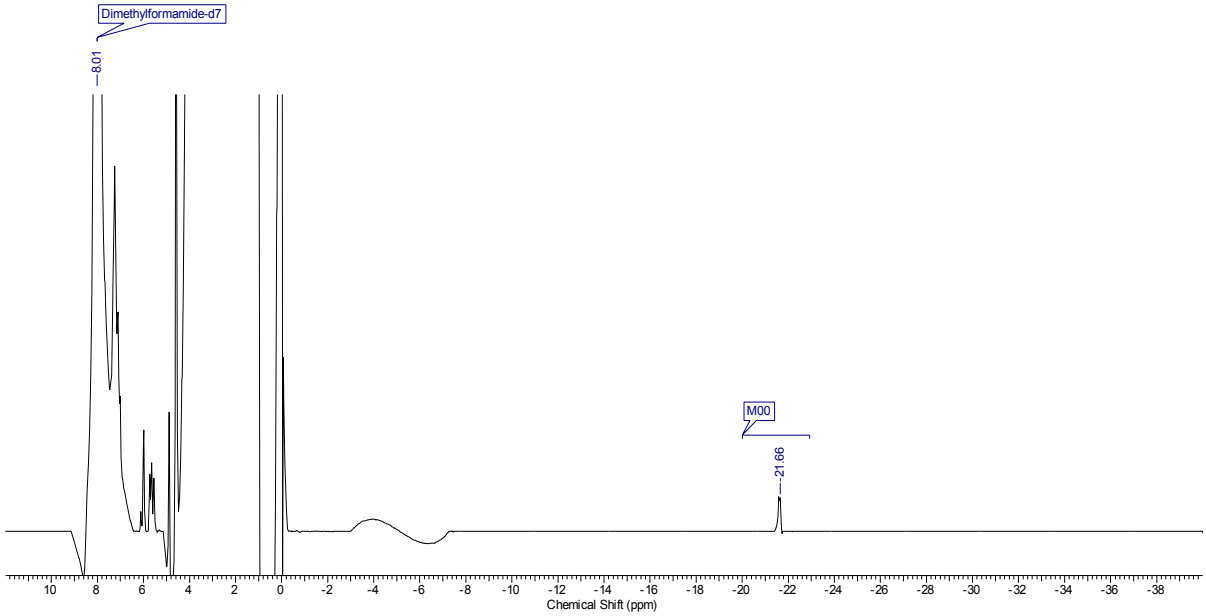

spectrum 19p: ^{31}P-NMR (242.9 MHz, 295 K):

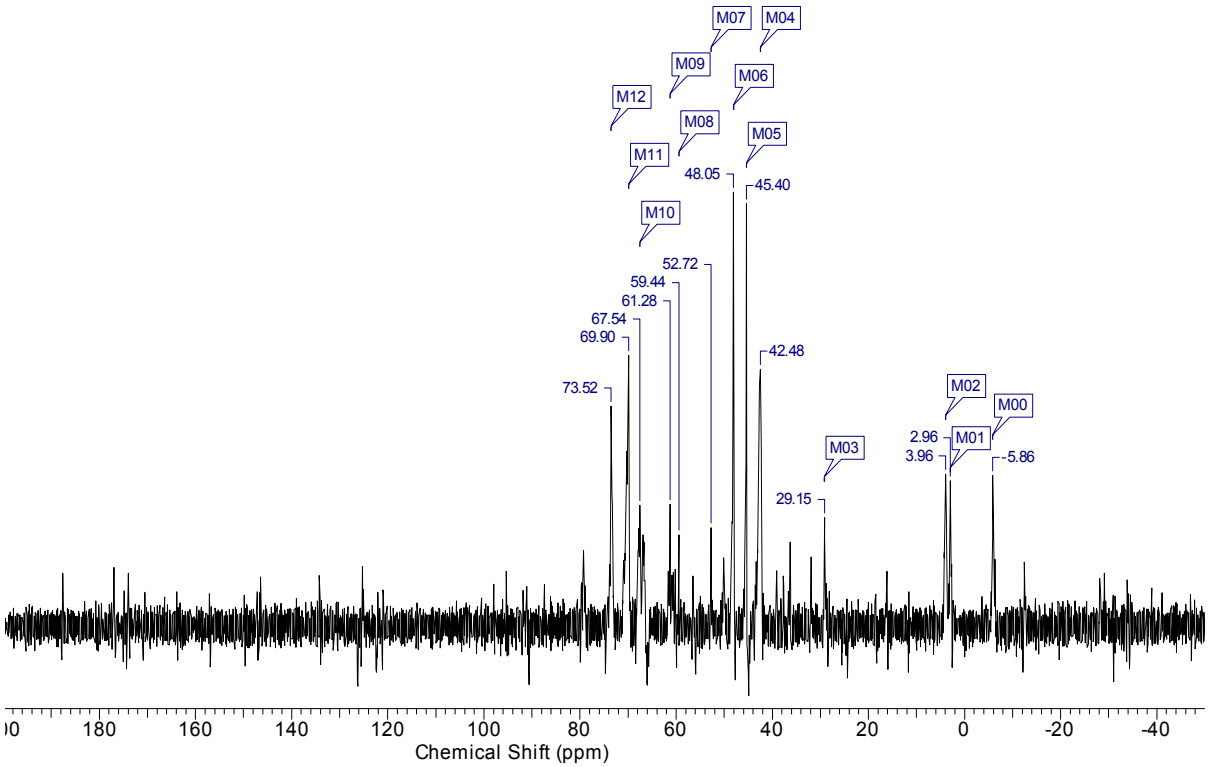

spectrum 19c: ^{13}C-NMR (150.9 MHz, 295 K):

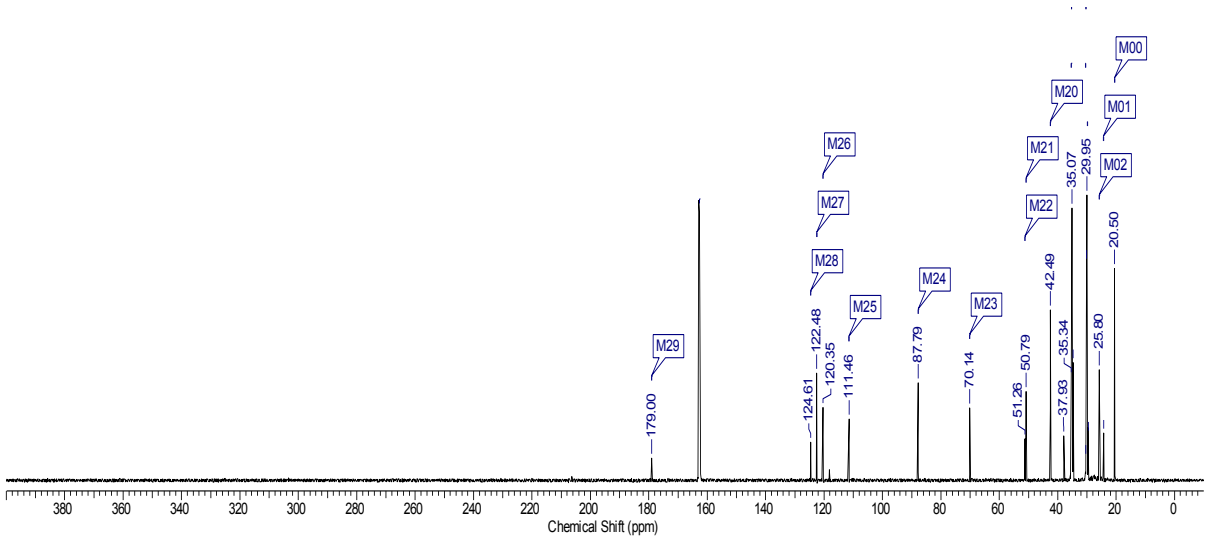

spectrum 19pp-COSY: (242.9 MHz, 295 K):

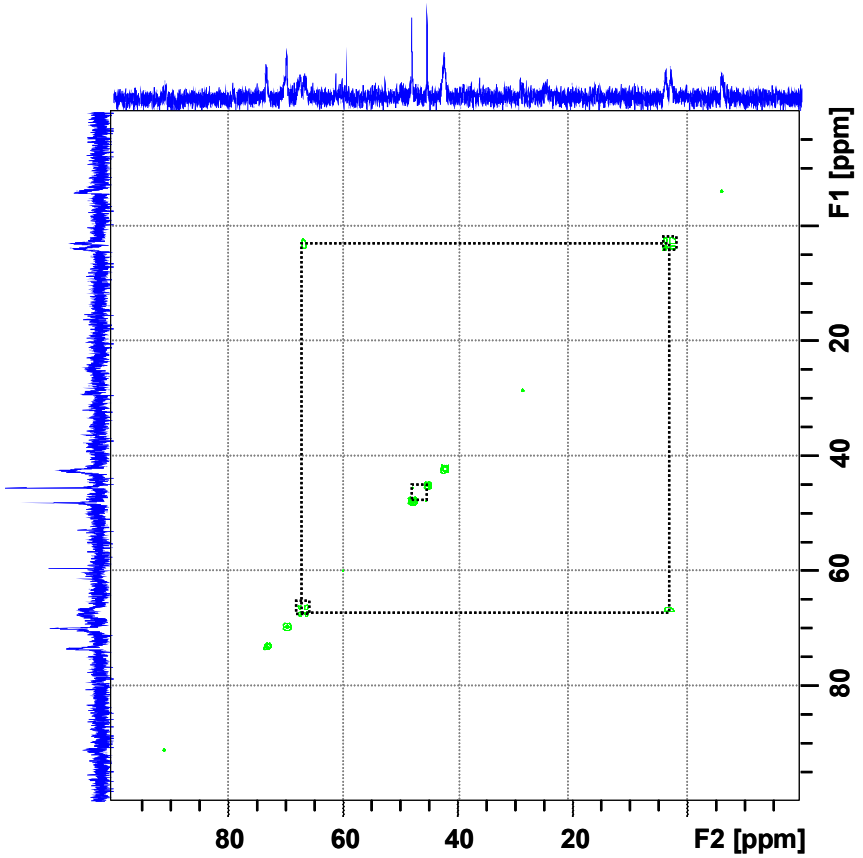

VI.3.7. ESI-MS experiments and experimental data.

***E*-selective hydroamidation protocol:**

***In situ* ESI-MS experiments with 1-hexyne (JACS-5b) and 2-pyrrolidinone (JACS-1a):** An oven-dried flask was charged with bis-(2-methallyl)-cycloocta-1,5-diene-ruthenium(II) (6.4 mg, 0.02 mmol) and 4-dimethylaminopyridine (4.9 mg, 0.04 mmol) and flushed with nitrogen. Subsequently, tri-*n*-butylphosphine (15 µL, 0.06 mmol), 2-pyrrolidinone (**JACS-1a**, 77 µL, 1.00 mmol) and dry toluene (3.00 mL) were added via syringe. The resulting solution was stirred at 100 °C for 5 min and spectrum 1esi was recorded. After adding 1-hexyne (**JACS-5b**, 231 µL, 2.00 mmol) the solution was stirred at 100 °C for 5 min and spectrum 2esi was recorded. Spectra 3esi, 4esi, 5esi, 6esi and 7esi were recorded after stirring at 100°C for 15, 30, 40, 150 and 470 min.

spectrum 1esi:

overview:

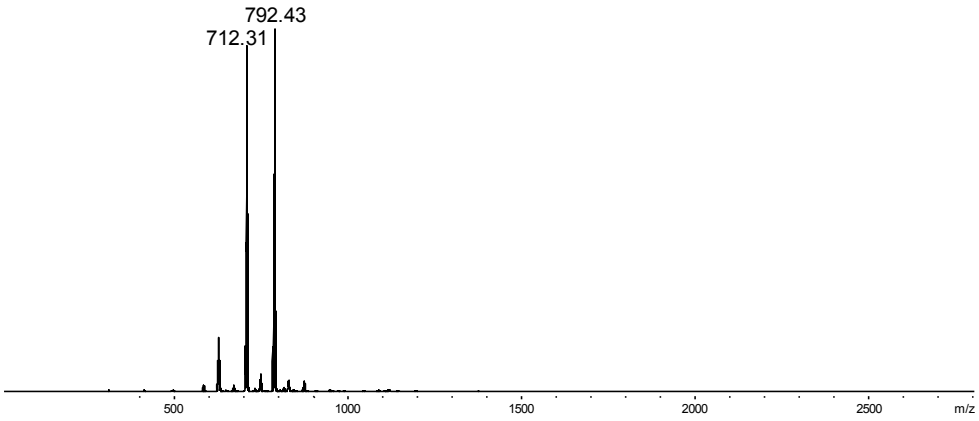

assignment m/z = 712.31:

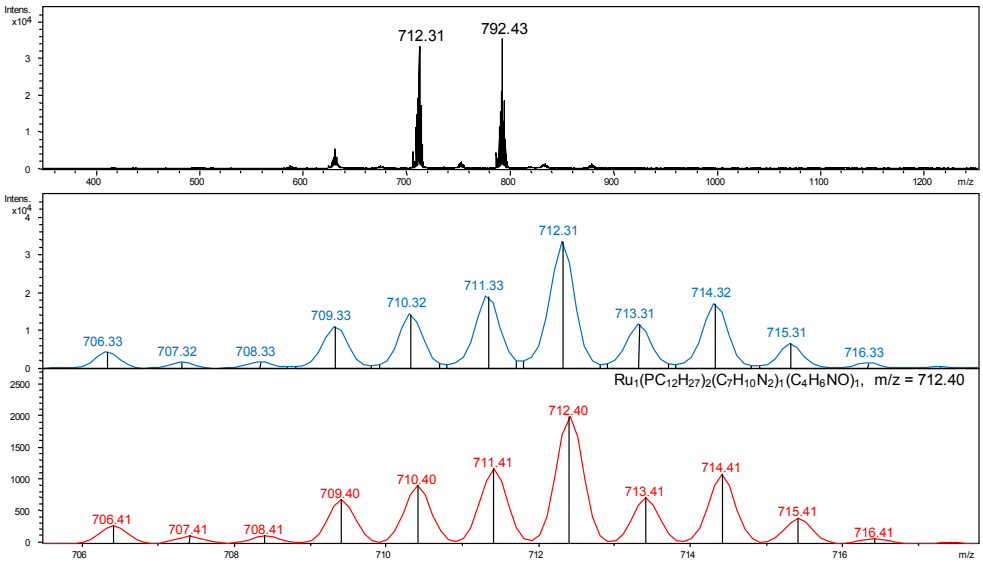

m/z (% relative to peak at 712.31) = 706.33 (13), 707.32 (5), 708.33 (5), 709.33 (33), 710.32 (43), 711.33 (57), 712.31 (100), 713.31 (35), 714.32 (51), 715.31 (20), 716.33 (4), Calc.: 706.41 (14), 707.41 (6), 708.41 (6), 709.40 (34), 710.40 (45), 711.41 (59), 712.40 (100), 713.41 (36), 714.41 (54), 715.41 (20), 716.41 (4).

assignment m/z = 792.43:

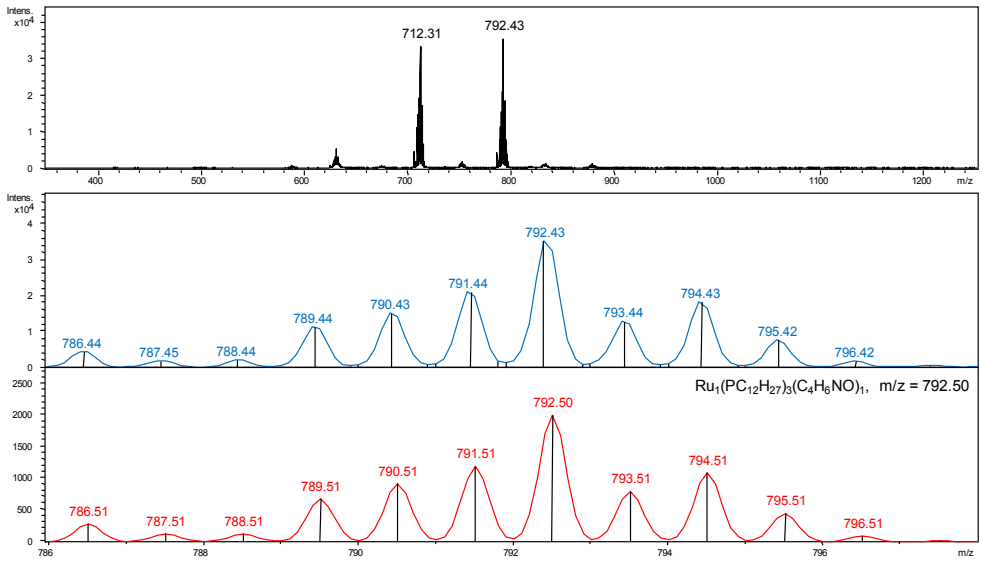

m/z (% relative to peak at 792.43) = 786.44 (13), 787.45 (5), 788.44 (6), 789.44 (32), 790.43 (43), 791.44 (60), 792.43 (100), 793.44 (37), 794.43 (52), 795.42 (22), 796.42 (5), Calc.: 786.51 (14), 787.51 (6), 788.51 (6), 789.51 (34), 790.51 (45), 791.51 (60), 792.50 (100), 793.51 (40), 794.51 (54), 795.51 (22), 796.51 (4).

spectrum 2esi:

overview:

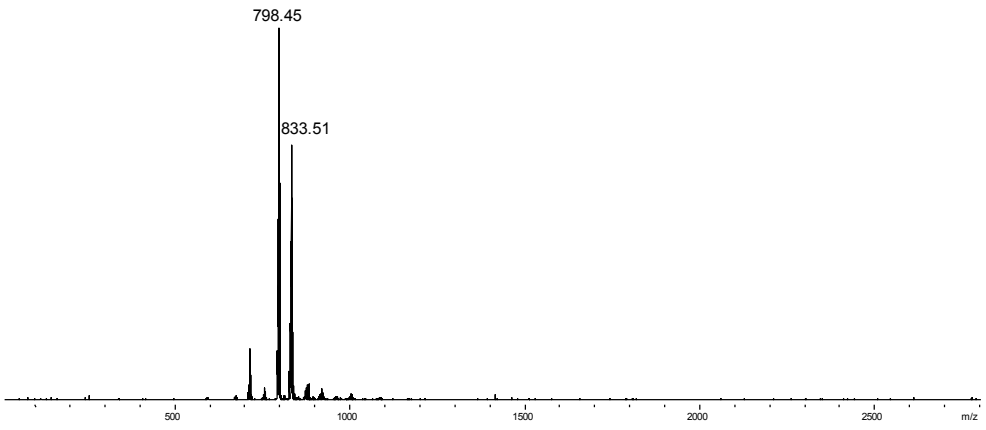

assignment m/z = 798.45:

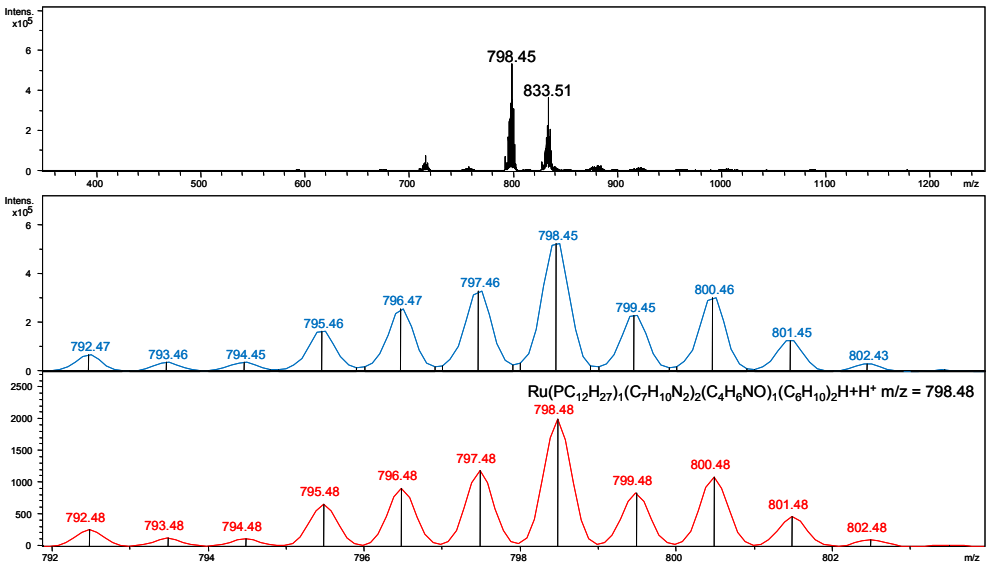

m/z (% relative to peak at 798.45) = 792.47 (13), 793.46 (7), 794.45 (7), 795.46 (32), 796.47 (49), 797.46 (63), 798.45 (100), 799.45 (44), 800.46 (58), 801.45 (24), 802.43 (6), Calc.: 792.48 (13), 793.48 (7), 794.48 (6), 795.48 (33), 796.48 (45), 797.48 (60), 798.48 (100), 799.48 (42), 800.48 (54), 801.48 (24), 802.48 (5).

CID-fragmentation of species at m/z = 798.45:

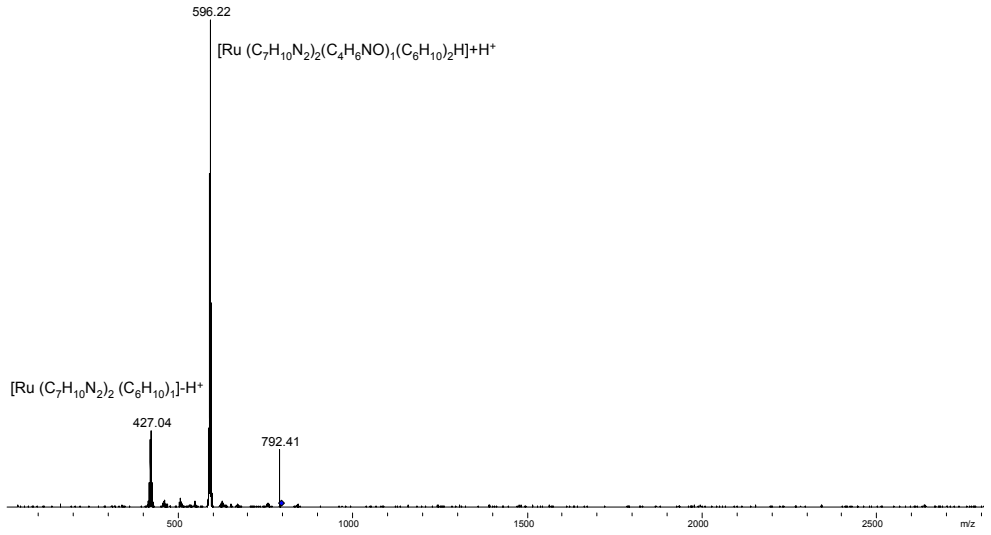

assignment m/z = 833.51:

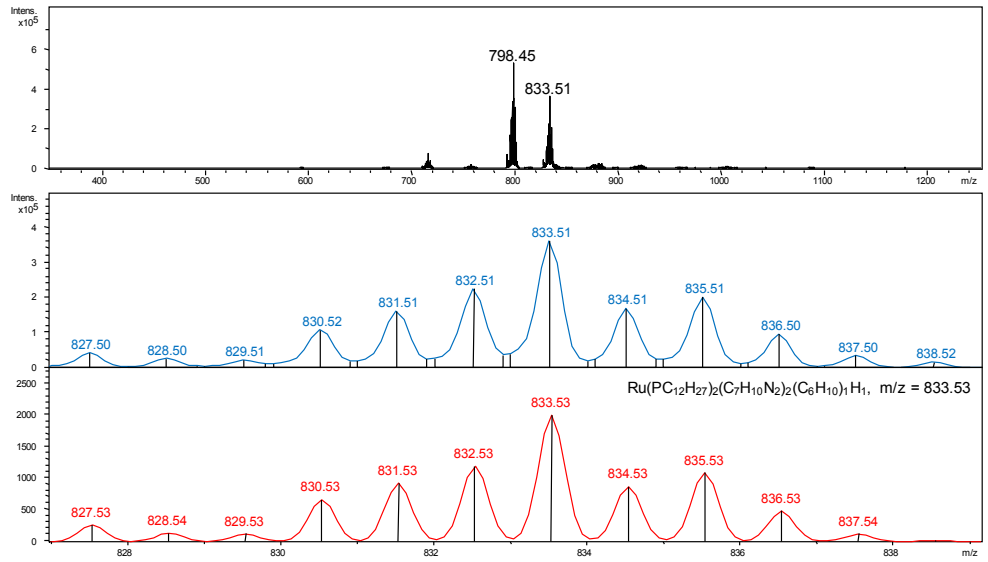

m/z (% relative to peak at 833.51) = 827.50 (12), 828.50 (8), 829.51 (6), 830.52 (30), 831.51 (45), 832.51 (62), 833.51 (100), 834.51 (47), 835.51 (56), 836.50 (26), 837.50 (10), 838.52 (4), Calc.: 827.53 (13), 828.54 (7), 829.53 (6), 830.53 (33), 831.53 (46), 832.53 (60), 833.53 (100), 834.53 (43), 835.53 (54), 836.53 (24), 837.54 (6), 838.54 (1).

spectrum 3esi:

overview:

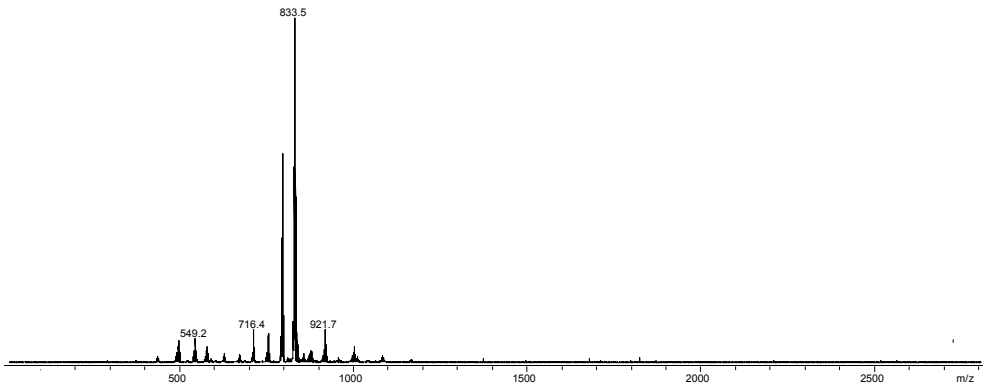

spectrum 4esi:

overview:

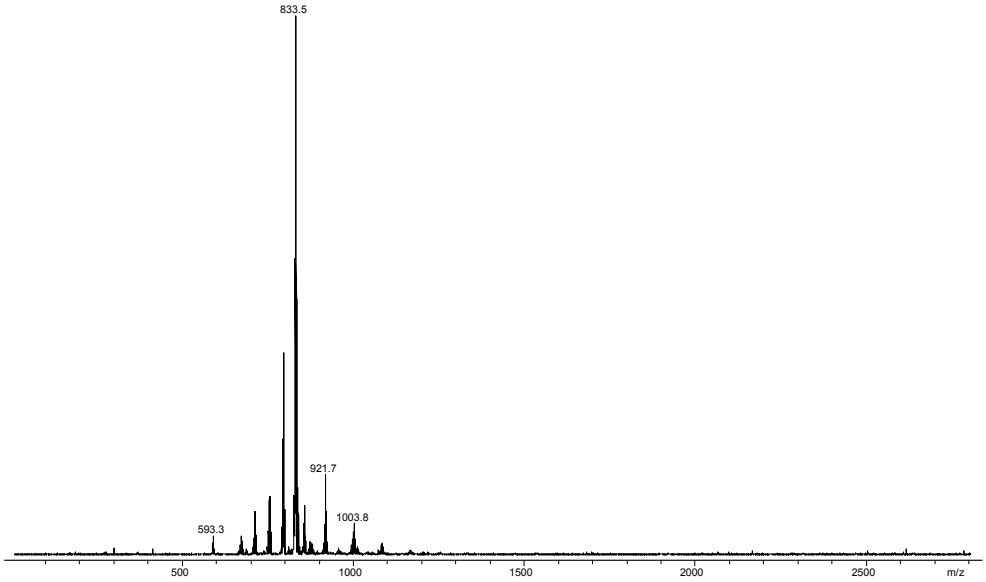

spectrum 5esi:

overview:

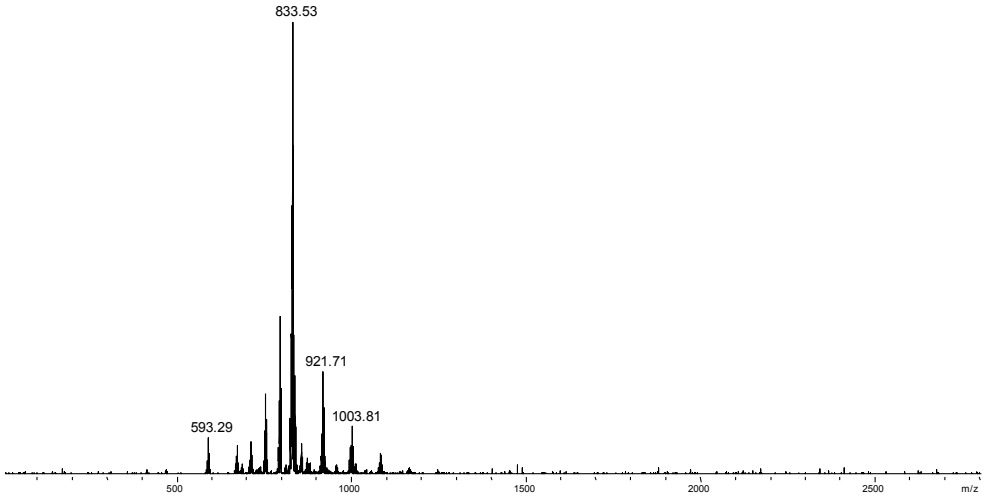

assignment m/z = 593.28:

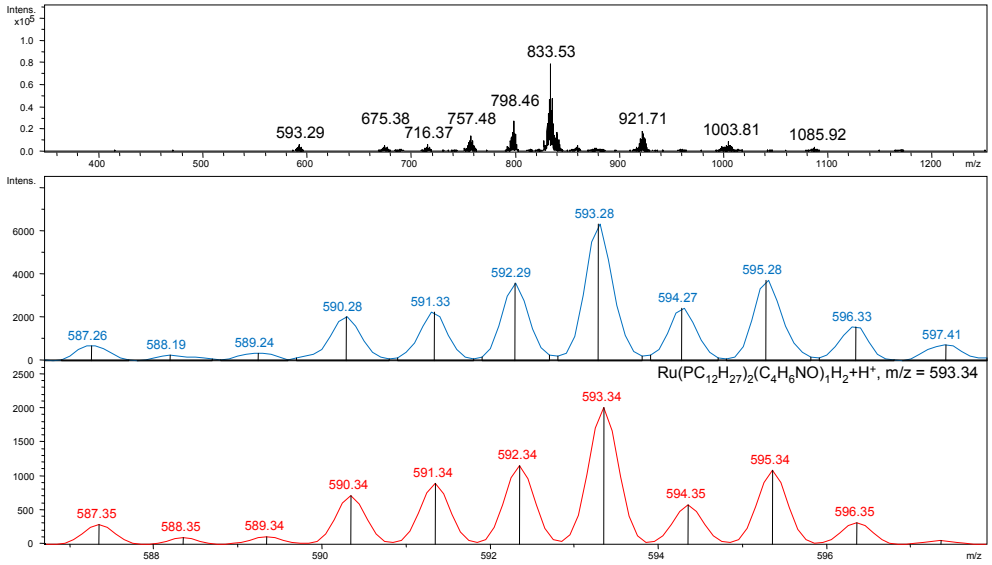

m/z (% relative to peak at 593.28) = 587.26 (11), 588.19 (4), 589.24 (5), 590.28 (32), 591.33 (36), 592.29 (57), 593.28 (100), 594.27 (38), 595.28 (59), 596.33 (25), 597.41 (12), Calc.: 587.35 (14), 588.35 (5), 589.34 (5), 590.34 (36), 591.34 (45), 592.34 (57), 593.34 (100), 594.35 (29), 595.34 (54), 596.35 (16), 597.35 (3).

assignment m/z = 675.38:

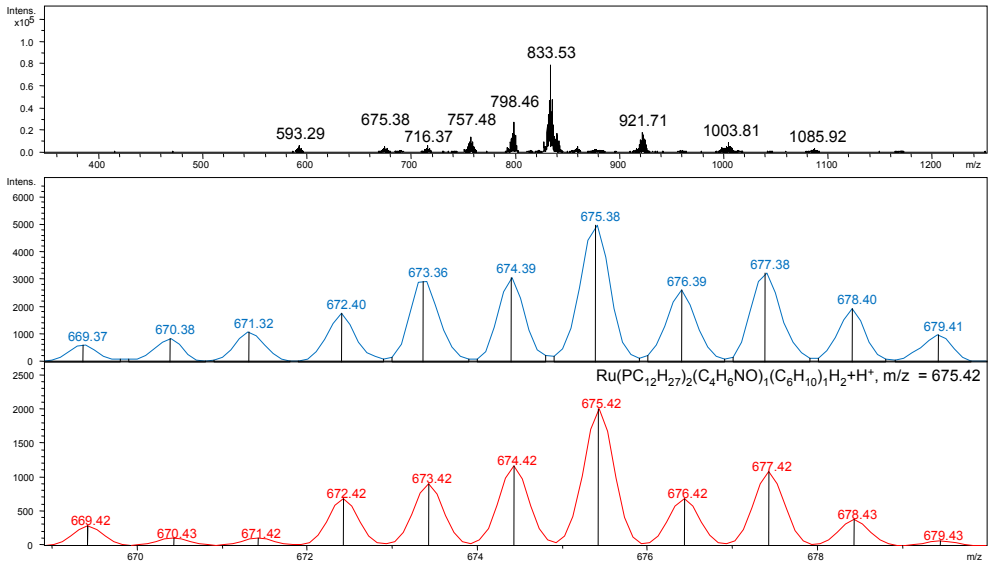

m/z (% relative to peak at 675.38) = 669.37 (12), 670.38 (17), 671.32 (22), 672.40 (36), 673.36 (59), 674.39 (62), 675.38 (100), 676.39 (53), 677.38 (65), 678.40 (39), 679.41 (20), Calc.: 669.42 (14), 670.43 (5), 671.42 (5), 672.42 (34), 673.42 (45), 674.42 (58), 675.42 (100), 676.42 (34), 677.42 (54), 678.43 (19), 679.43 (3).

assignment m/z = 716.38:

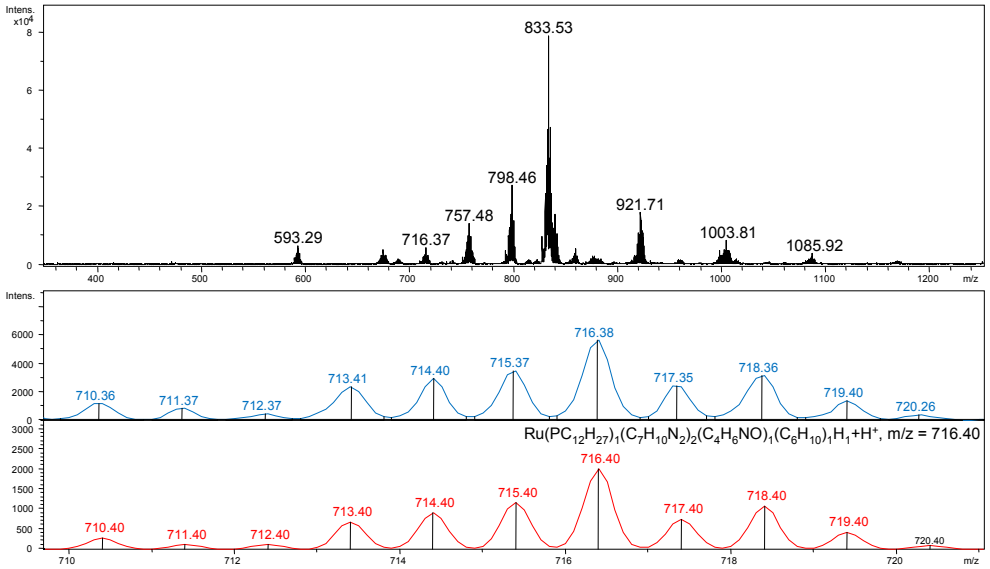

m/z (% relative to peak at 716.38) = 710.36 (21), 711.37 (15), 712.37 (8), 713.41 (42), 714.40 (36), 715.37 (62), 716.38 (100), 717.35 (43), 718.36 (56), 719.40 (24), 720.26 (7), Calc.: 710.40 (14), 711.40 (6), 712.40 (6), 713.40 (34), 714.40 (45), 715.40 (58), 716.40 (100), 717.40 (37), 718.40 (54), 719.40 (21), 720.26 (5).

assignment m/z = 757.48:

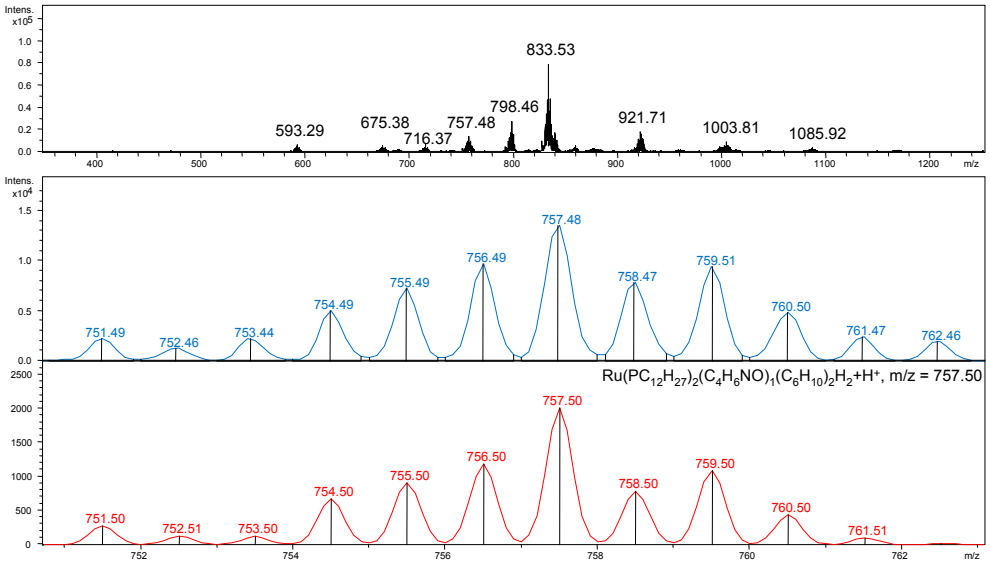

m/z (% relative to peak at 757.48) = 751.49 (16), 752.46 (10), 753.44 (16), 754.49 (37), 755.49 (54), 756.49 (71), 757.48 (100), 758.47 (58), 759.51 (69), 760.50 (36), 761.47 (18), 762.46 (14), Calc.: 751.50 (14), 752.51 (6), 753.50 (6), 754.50 (34), 755.50 (45), 756.50 (59), 757.50 (100), 758.50 (39), 759.50 (54), 760.50 (22), 761.51 (5), 762.50 (0).

assignment m/z = 798.45:

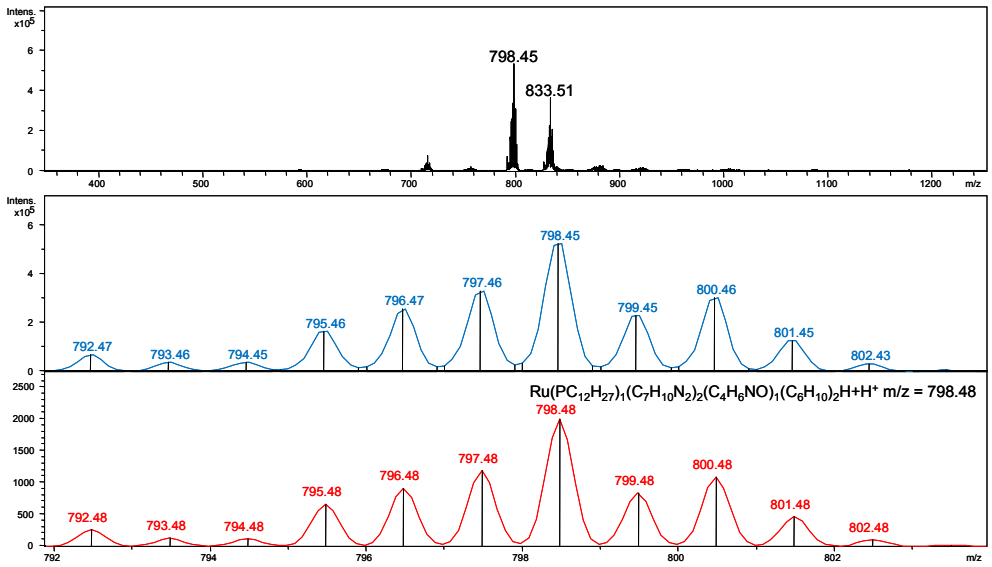

m/z (% relative to peak at 798.45) = 792.47 (16), 793.48 (12), 794.52 (11), 795.49 (35), 796.47 (46), 797.47 (62), 798.46 (100), 799.48 (43), 800.47 (56), 801.48 (21), 802.49 (7), Calc.: 792.48 (13), 793.48 (7), 794.48 (6), 795.48 (33), 796.48 (45), 797.48 (60), 798.48 (100), 799.48 (42), 800.48 (54), 801.48 (24), 802.48 (5).

assignment m/z = 833.51 (827.53–843.58):

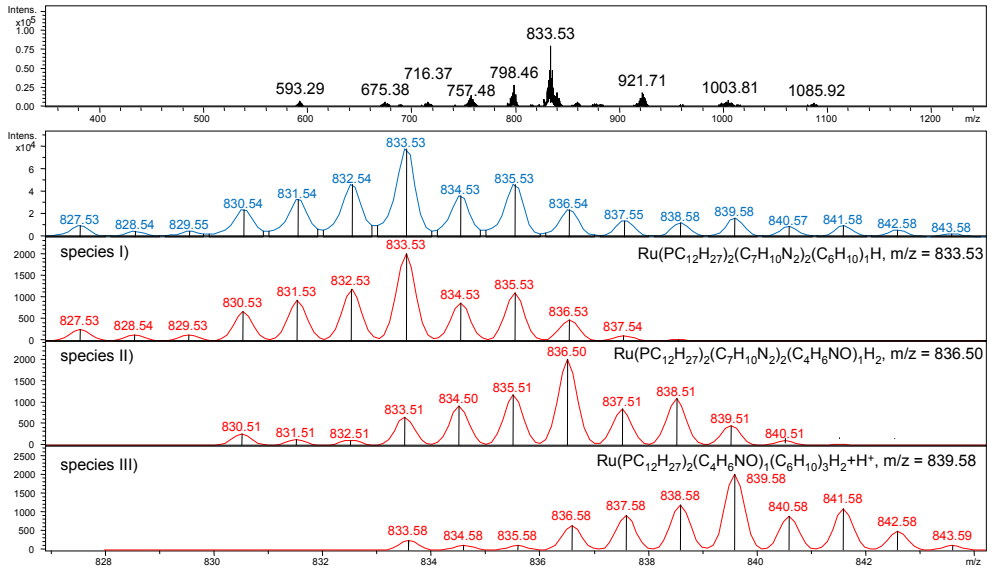

m/z (% relative to peak at 833.53) = 827.53 (13), 828.54 (6), 829.55 (6), 830.54 (31), 831.54 (43), 832.54 (60), 833.53 (100), 834.53 (47), 835.53 (60), 836.54 (31), 837.55 (18), 838.58 (16), 839.58 (21), 840.57 (12), 841.58 (13), 842.58 (8), 843.58 (3), Calc. [species I (75%) + species II (5%) + species III (20%)]: 827.53 (12), 828.54 (6), 829.53 (6), 830.53

(33), 831.53 (45), 832.53 (57), 833.53 (100), 834.53 (46), 835.53 (57), 836.53 (36), 837.54 (18), 838.58 (17), 839.58 (23), 840.58 (10), 841.58 (12), 842.58 (5), 843.59 (1).

CID-fragmentation of species at m/z = 833.53:

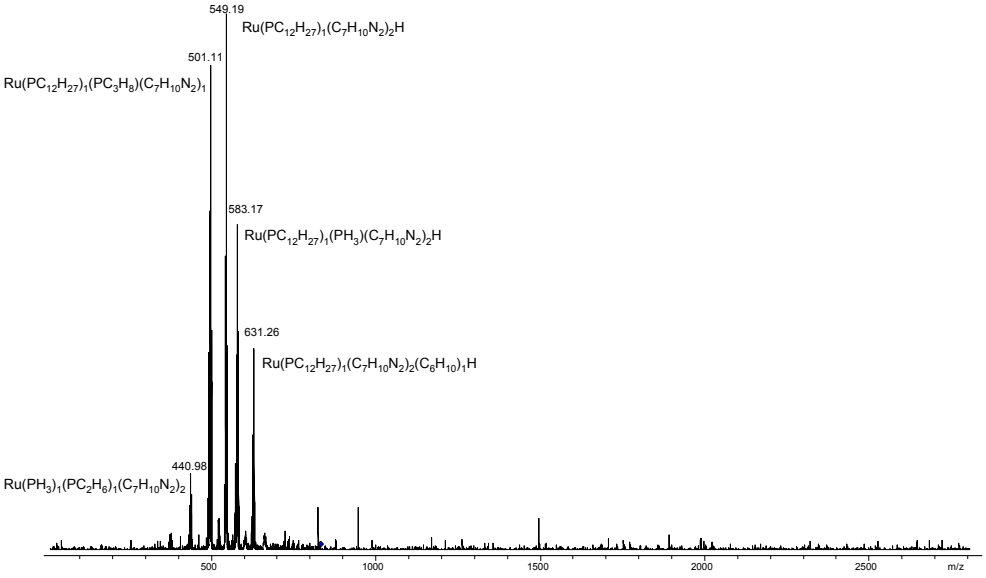

CID-fragmentation of species at m/z = 501:

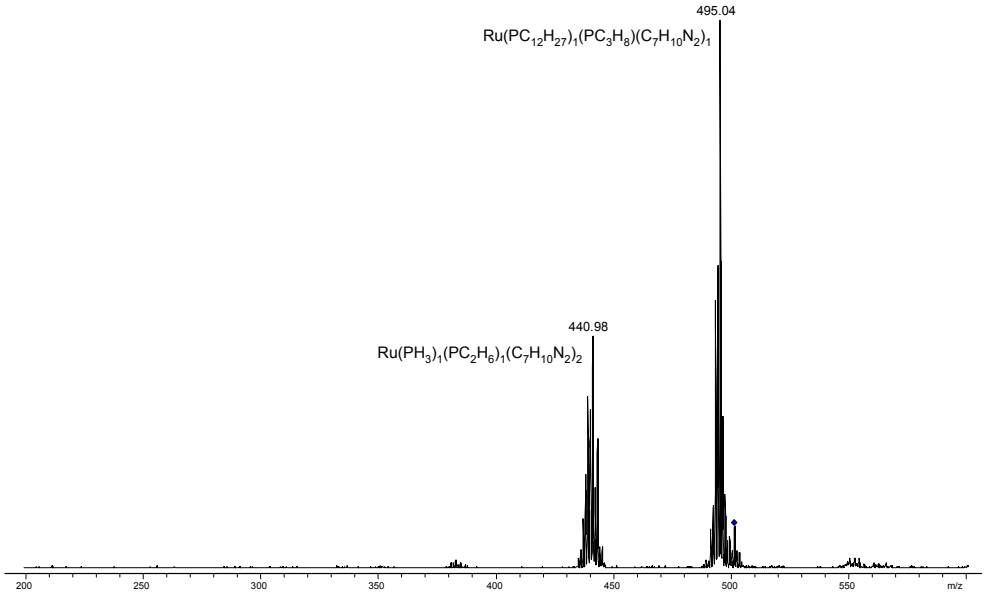

CID-fragmentation of species at m/z = 549:

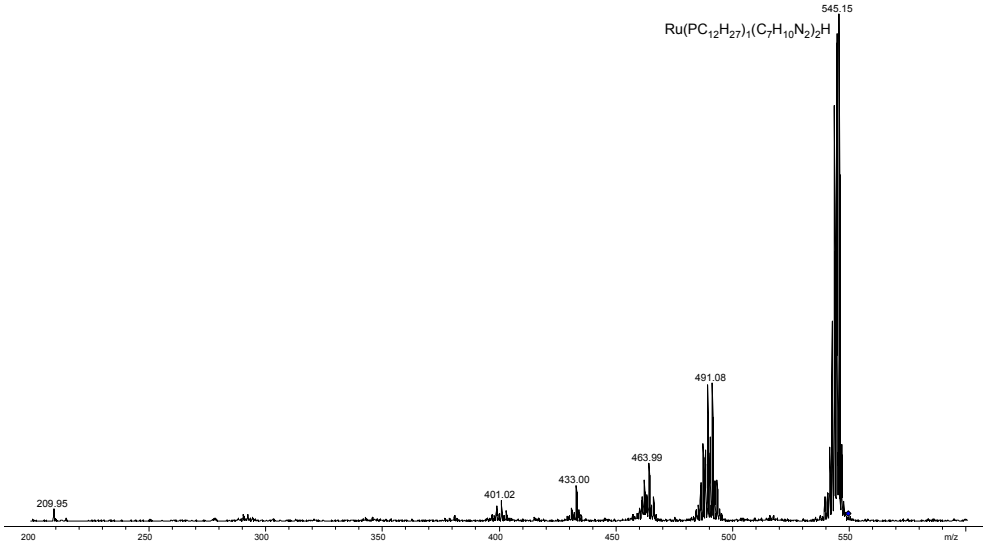

CID-fragmentation of species at m/z = 582:

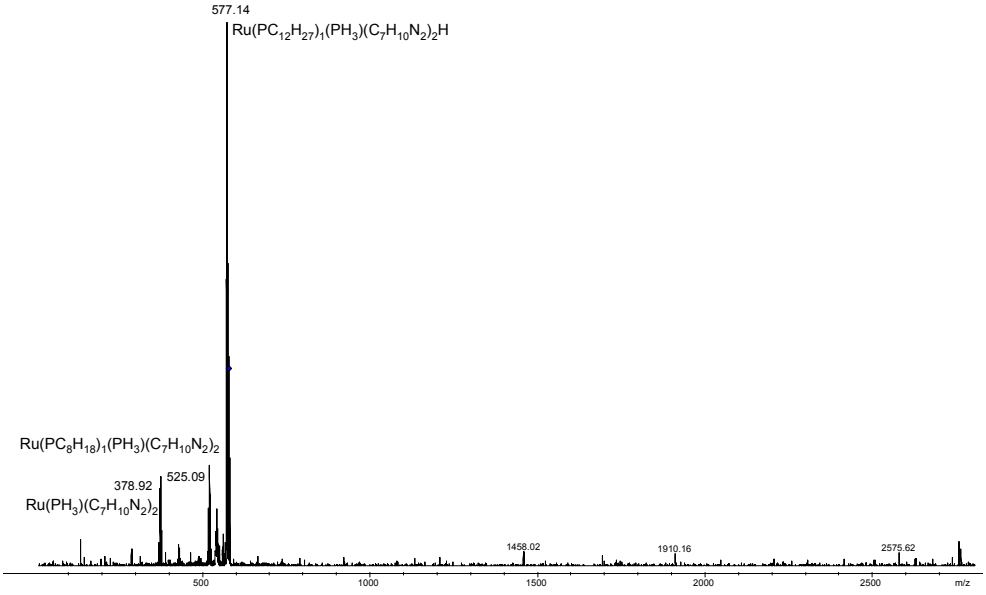

CID-fragmentation of species at m/z = 631:

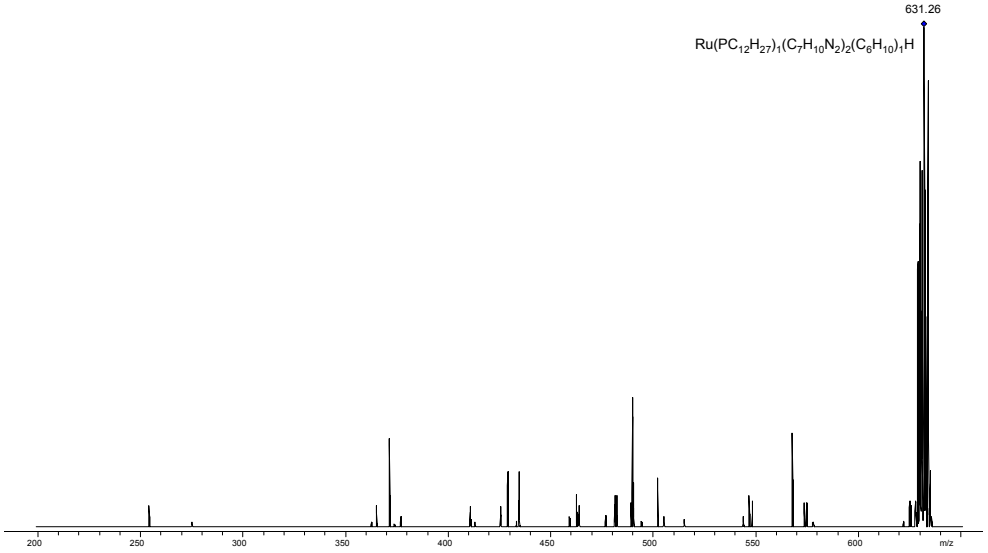

assignment m/z = 867.59–887.52:

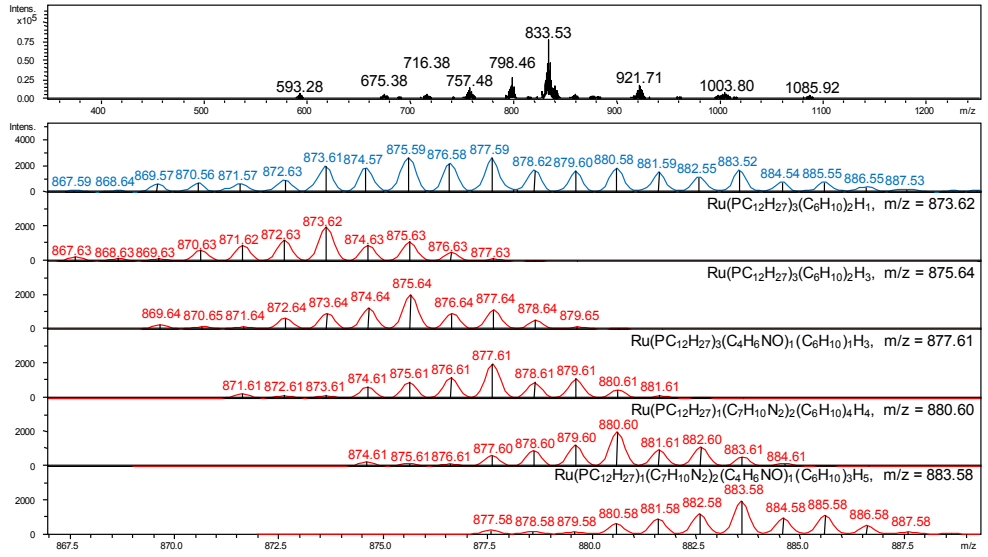

m/z (% relative to peak at 875.59) = 867.59 (5), 868.64 (5), 869.57 (25), 870.56 (28), 871.57 (25), 872.63 (36), 873.61 (76), 874.57 (70), 875.59 (100), 876.58 (84), 877.59 (100), 878.62 (64), 879.60 (62), 880.58 (70), 881.59 (59), 882.55 (43), 883.52 (64), 884.54 (30), 885.55 (30), 886.55 (16), 887.53 (8), Calc. [species I (18%) + species II (23%) + species III (18%) + species IV (18%) + species V (23%)]: 867.63 (6), 868.63 (3), 869.63 (10), 870.63 (18), 871.61 (30), 872.61 (47), 873.61 (70), 874.61 (72), 875.61 (100), 876.61 (64), 877.61 (96), 878.61 (57), 879.61 (59), 880.61 (71), 881.61 (48), 882.58 (57), 883.58 (64), 884.58 (29), 885.58 (30), 886.58 (15), 887.58 (4).

spectrum 6esi:

overview:

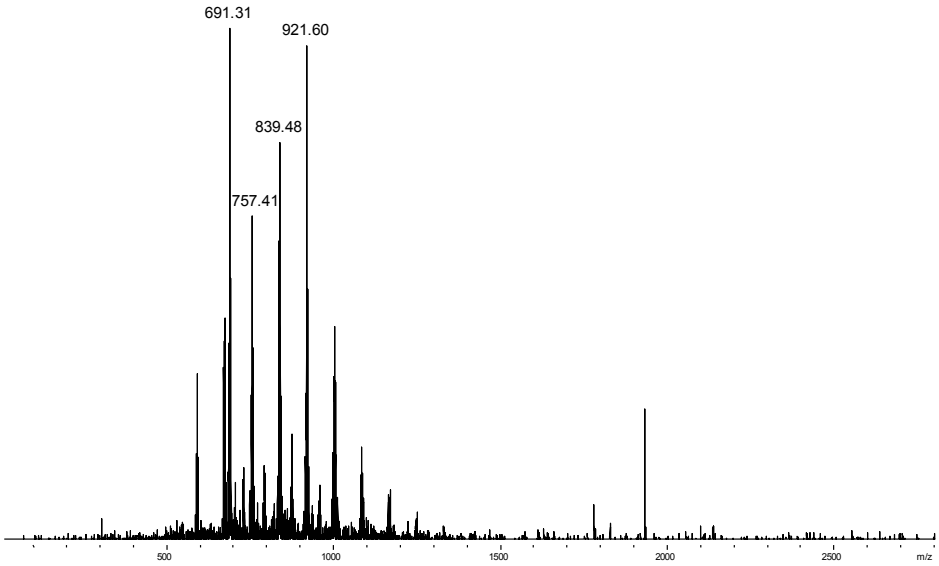

assignment m/z = 593.20:

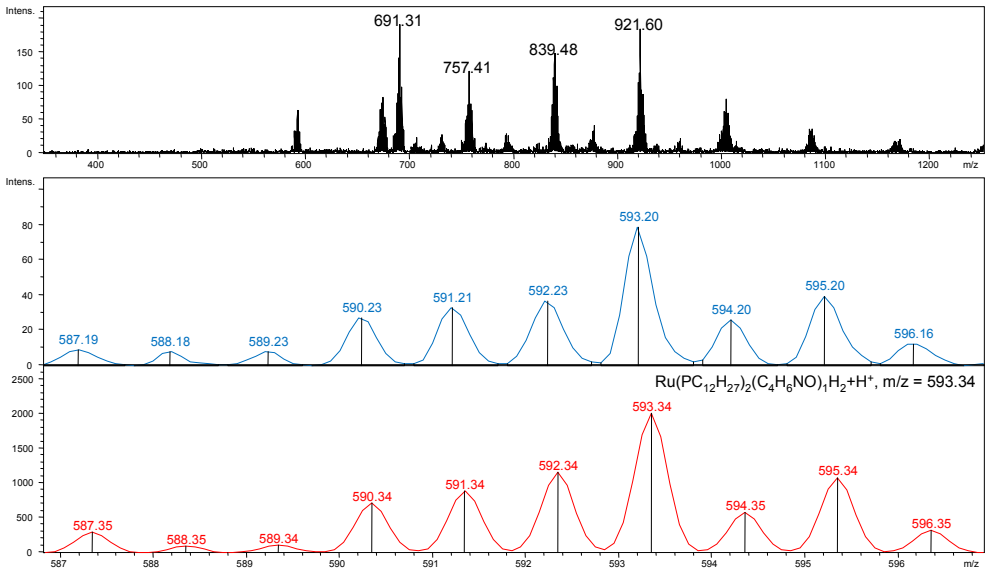

m/z (% relative to peak at 593.20) = 587.19 (12), 588.18 (10), 589.23 (10), 590.23 (35), 591.21 (42), 592.23 (47), 593.20 (100), 594.20 (33), 595.20 (50), 596.16 (15), Calc.: 587.35 (15), 588.35 (5), 589.34 (5), 590.34 (36), 591.34 (44), 592.34 (58), 593.34 (100), 594.35 (29), 595.34 (54), 596.35 (16).

assignment m/z = 675.38:

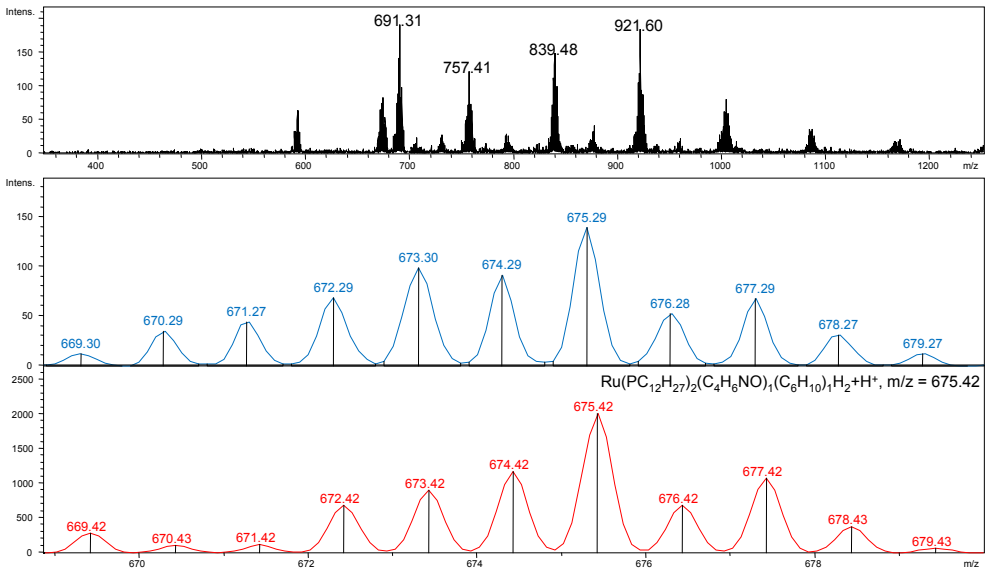

m/z (% relative to peak at 675.29) = 669.30 (9), 670.29 (25), 671.27 (32), 672.29 (49), 673.30 (71), 674.29 (65), 675.29 (100), 676.28 (38), 677.29 (49), 678.27 (22), 679.27 (9), Calc.: 669.42 (14), 670.43 (5), 671.42 (5), 672.42 (34), 673.42 (45), 674.42 (58), 675.42 (100), 676.42 (34), 677.42 (54), 678.43 (19), 679.43 (3).

assignment m/z = 757.40:

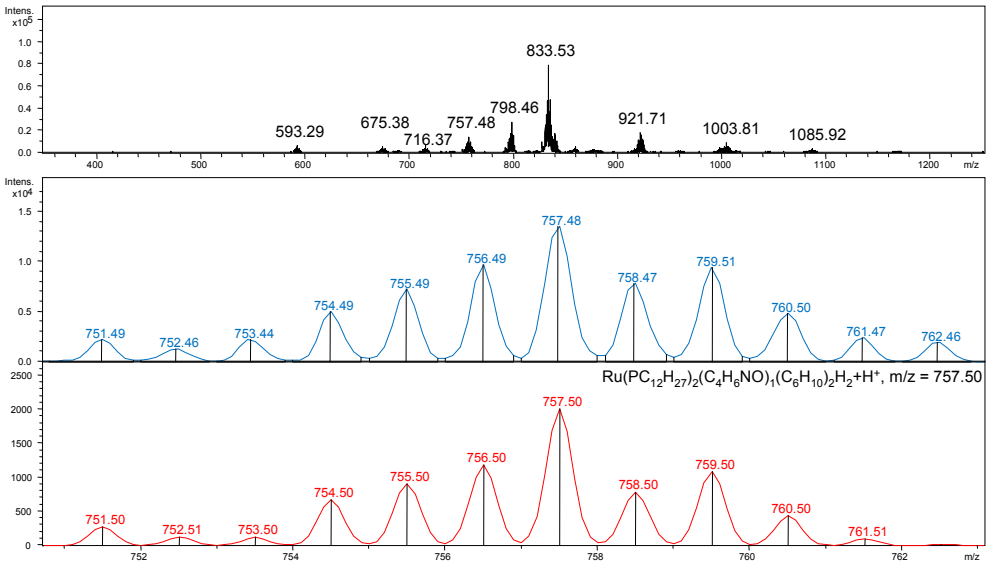

m/z (% relative to peak at 757.40) = 751.41 (10), 752.39 (8), 753.37 (12), 754.39 (34), 755.39 (46), 756.41 (60), 757.40 (100), 758.38 (54), 759.42 (60), 760.38 (42), 761.40 (17), Calc.: 751.50 (14), 752.51 (6), 753.50 (6), 754.50 (34), 755.50 (45), 756.50 (59), 757.50 (100), 758.50 (39), 759.50 (54), 760.50 (22), 761.51 (5).

assignment m/z = 839.50:

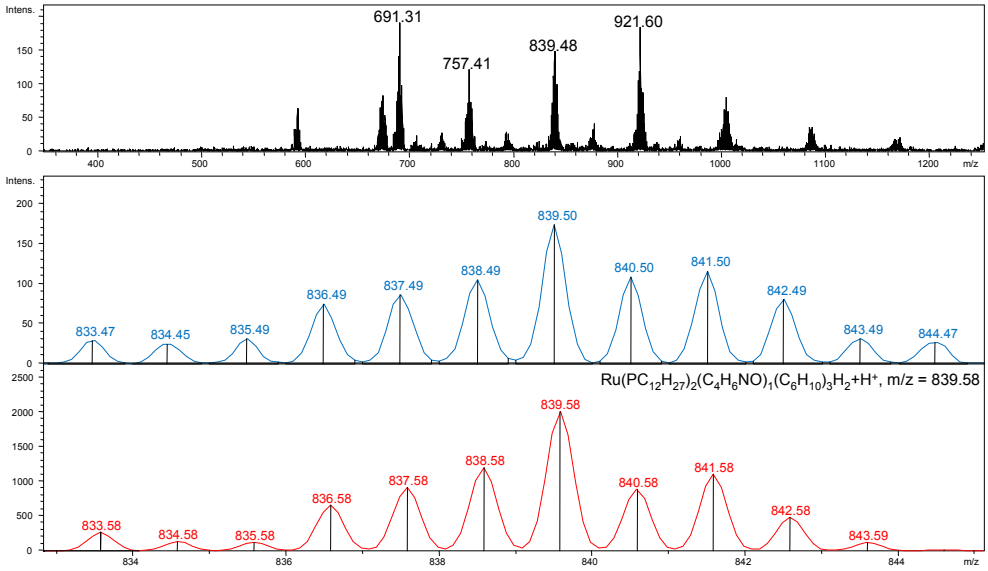

m/z (% relative to peak at 839.50) = 833.47 (17), 834.45 (14), 835.49 (18), 836.49 (43), 837.49 (50), 838.49 (60), 839.50 (100), 840.50 (64), 841.50 (66), 842.49 (46), 843.49 (18), 844.47 (15), Calc.: 833.58 (13), 834.58 (7), 835.58 (6), 836.58 (33), 837.58 (45), 838.58 (60), 839.58 (100), 840.58 (44), 841.58 (55), 842.58 (24), 843.59 (6), 844.58 (1).

assignment m/z = 921.60:

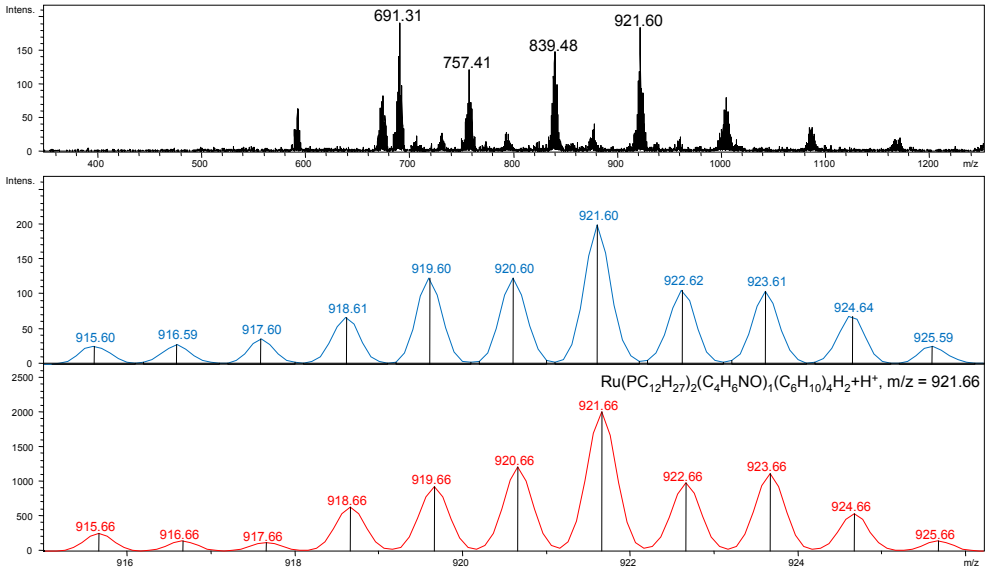

m/z (% relative to peak at 921.60) = 915.60 (13), 916.59 (14), 917.60 (18), 918.61 (34), 919.60 (62), 920.60 (62), 921.60 (100), 922.61 (53), 923.61 (52), 924.64 (34), 925.59 (13), Calc.: 915.66 (13), 916.66 (8) 917.66 (6), 918.66 (32), 919.66 (46), 920.66 (60), 921.66 (100), 922.66 (49), 923.66 (56), 924.66 (27), 925.66 (8).

assignment m/z = 1003.72:

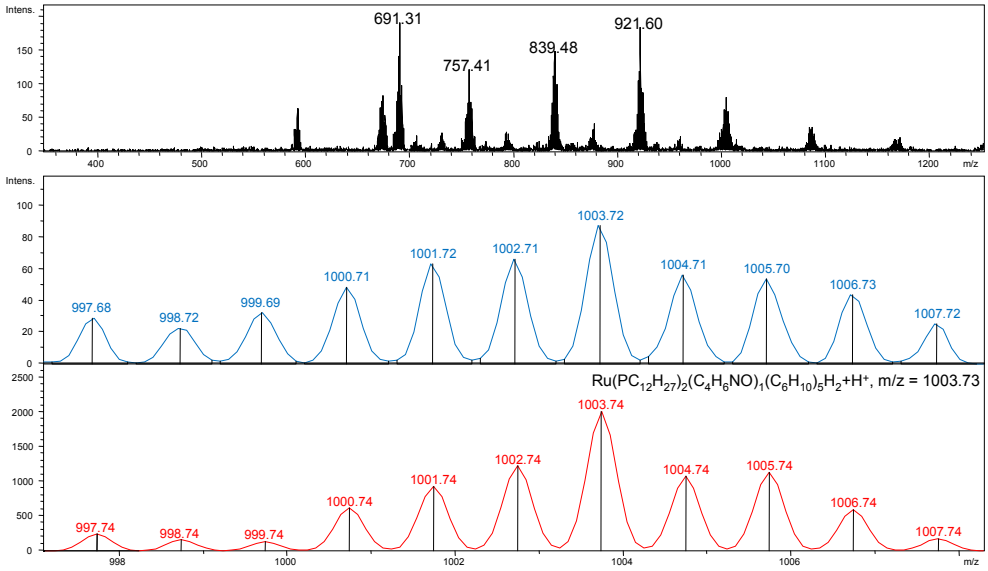

m/z (% relative to peak at 1003.72) = 997.68 (33), 998.72 (26), 999.69 (37), 1000.71 (56), 1001.72 (72), 1002.71 (76), 1003.72 (100), 1004.71 (64), 1005.70 (62), 1006.73 (50), 1007.72 (29), Calc.: 997.68 (12), 998.72 (8), 999.69 (7), 1000.71 (31), 1001.74 (46), 1002.71 (61), 1003.72 (100), 1004.71 (54), 1005.70 (56), 1006.73 (29), 1007.72 (9).

assignment m/z = 1085.50:

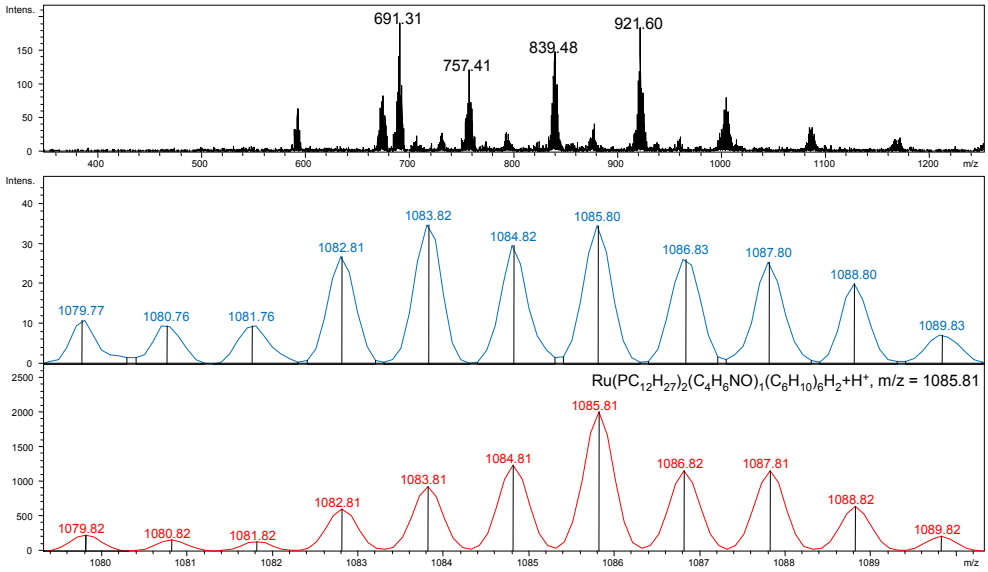

m/z (% relative to peak at 1085.50) = 1079.77 (32), 1080.76 (28), 1081.76 (28), 1082.81 (78), 1083.82 (100), 1084.82 (86), 1085.80 (100), 1086.83 (76), 1087.80 (74), 1088.80 (58), 1089.83 (21), Calc.: 1079.82 (11), 1080.82 (8), 1081.82 (7), 1082.81 (30), 1083.81 (46), 1084.81 (62), 1085.81 (100), 1086.82 (58), 1087.81 (58), 1088.82 (32), 1089.82 (11).

spectrum 7esi:

overview:

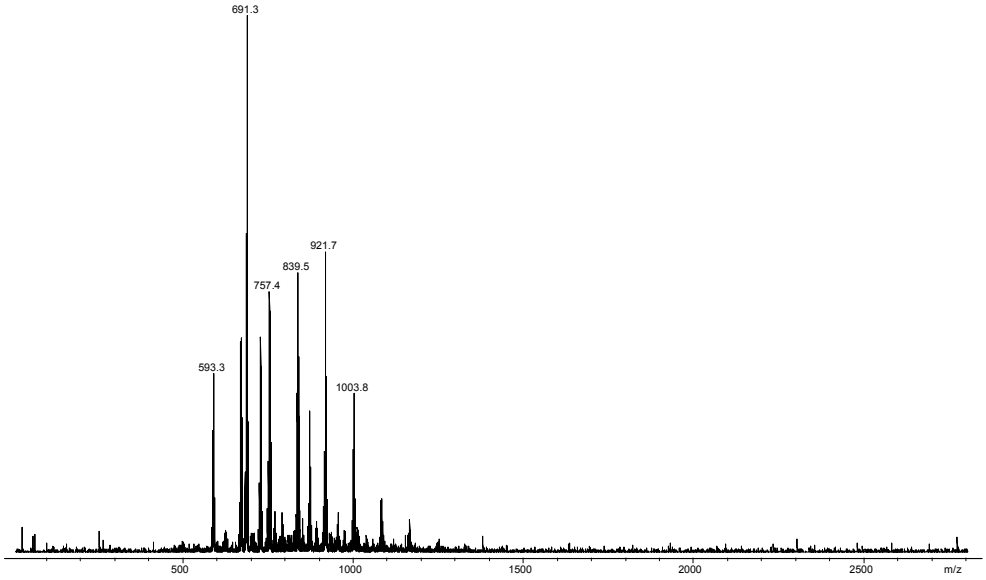

In situ **ESI-MS experiments with [2-(Dicyclohexylphosphino)ethyl] trimethylammonium chloride:** An oven-dried flask was charged with bis-(2-methallyl)-cycloocta-1,5-diene-ruthenium(II) (6.4 mg, 0.02 mmol), 4-dimethylaminopyridine (4.9 mg, 0.04 mmol) and [2-(Dicyclohexylphosphino)ethyl]trimethylammonium chloride (19.6 mg, 0.06 mmol) and flushed with nitrogen. Subsequently, 2-pyrrolidinone (**JACS-1a**, 1a, 77 µL, 1.00 mmol) and dry toluene (3.00 mL) were added via syringe. The resulting solution was stirred at 100 °C for 5 min and spectrum 8esi was recorded. After adding 1-hexyne (**JACS-5b**, 231 µL, 2.00 mmol) the solution was stirred at 100 °C for 5 min and spectrum 9esi was recorded.

spectrum 8esi:

overview:

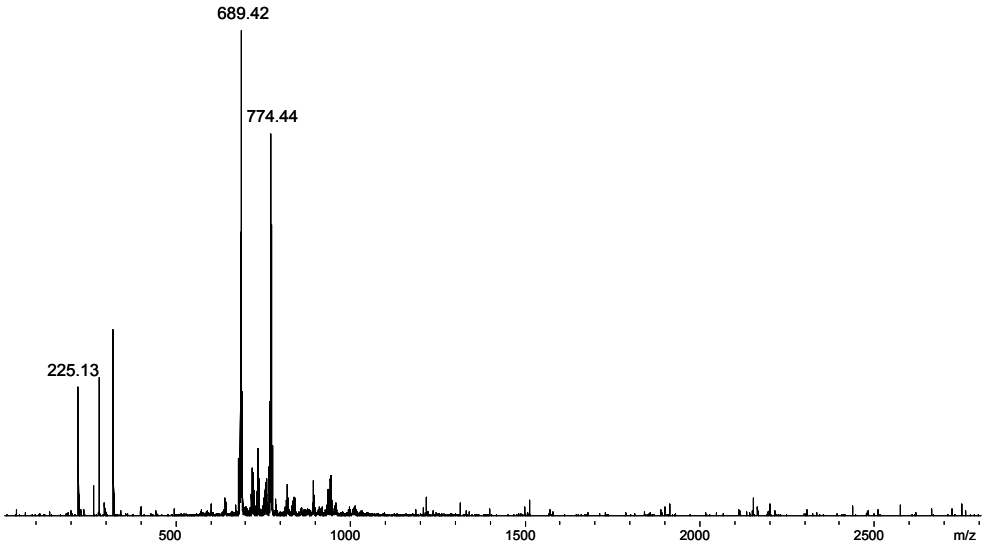

assignment m/z = 225.13:

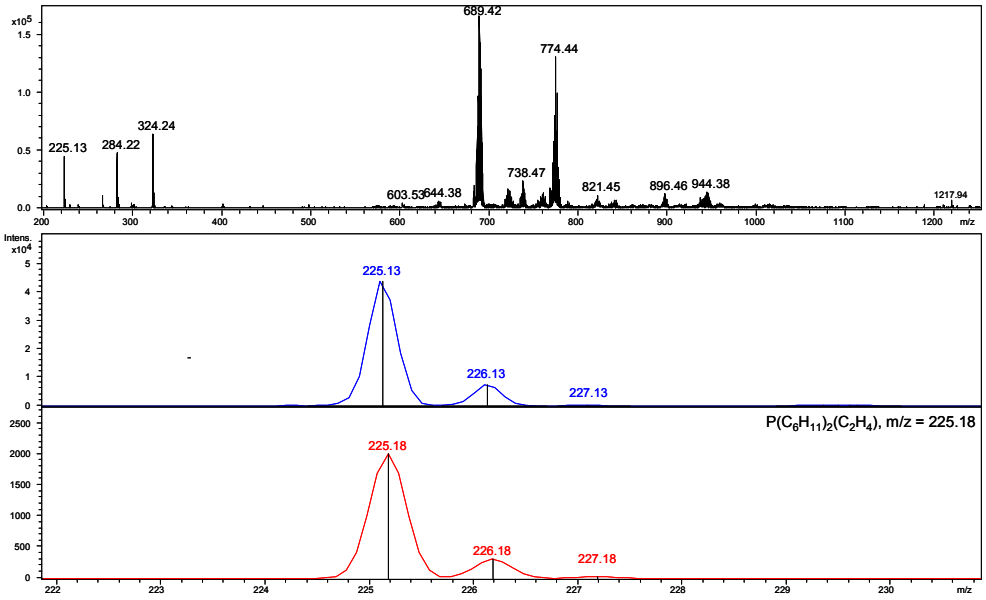

m/z (% relative to peak at 225.13) = 225.13 (100), 226.13 (17), 227.13 (1), Calc.: 225.18 (100), 226.18 (16), 227.18 (1).

spectrum 9esi:

overview:

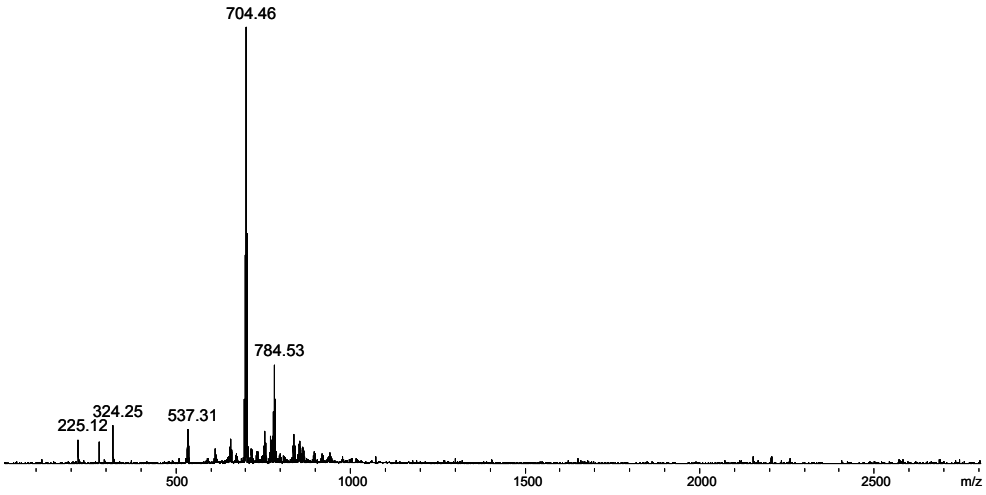

***In situ* ESI-MS experiments with (cod)Ru(met)$_2$:** An oven-dried flask was charged with bis-(2-methallyl)-cycloocta-1,5-diene-ruthenium(II) (6.4 mg, 0.02 mmol) and flushed with nitrogen. Dry toluene (3.00 mL) was added and the resulting solution was stirred at room temperature for 15 min. Spectrum 10esi was recorded. Then the solution was heated to 100°C for 5 min and spectrum 11esi was recorded.

spectrum 10esi:

overview:

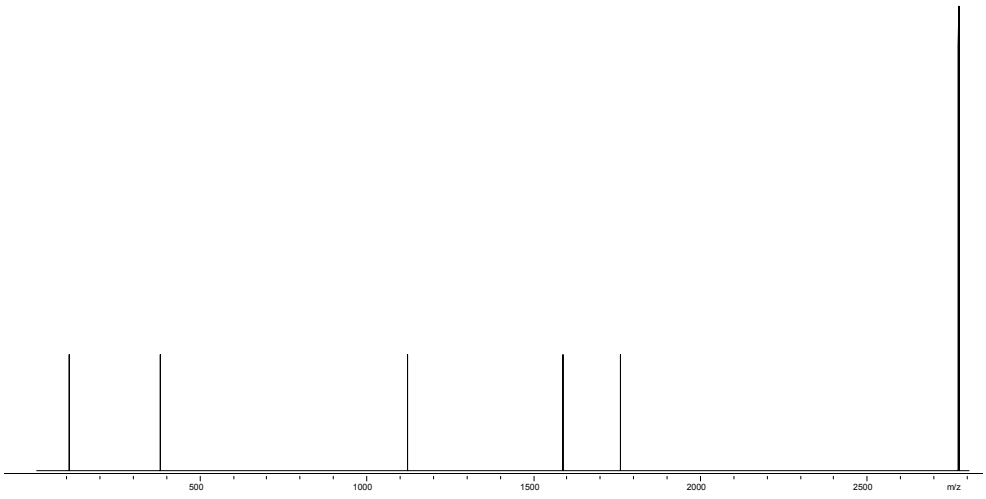

spectrum 11esi:

overview:

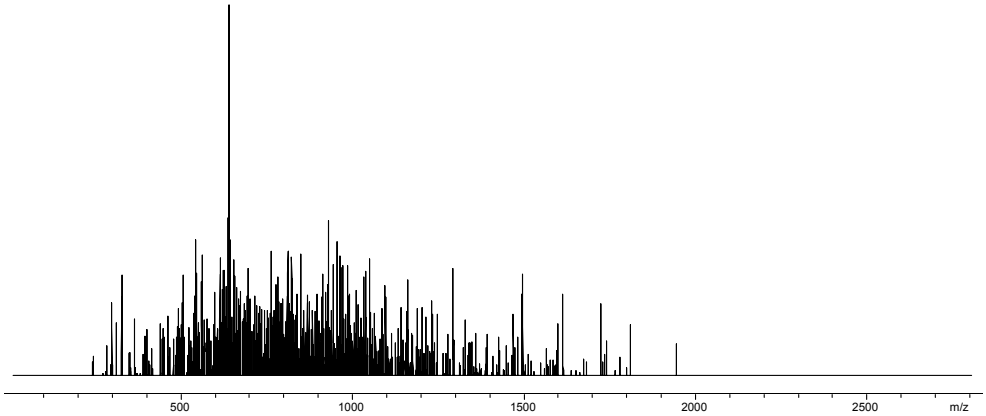

***In situ* ESI-MS experiments with (cod)Ru(met)$_2$ and DMAP:** An oven-dried flask was charged with bis-(2-methallyl)-cycloocta-1,5-diene-ruthenium(II) (6.4 mg, 0.02 mmol) and 4-dimethylaminopyridine (4.9 mg, 0.04 mmol) and flushed with nitrogen. Dry toluene (3.00 mL) was added and the resulting solution was stirred for 15 min at room temperature. Spectrum 12esi was recorded. Then the solution was heated to 100°C for 5 min and spectrum 13esi was recorded.

spectrum 12esi:

overview:

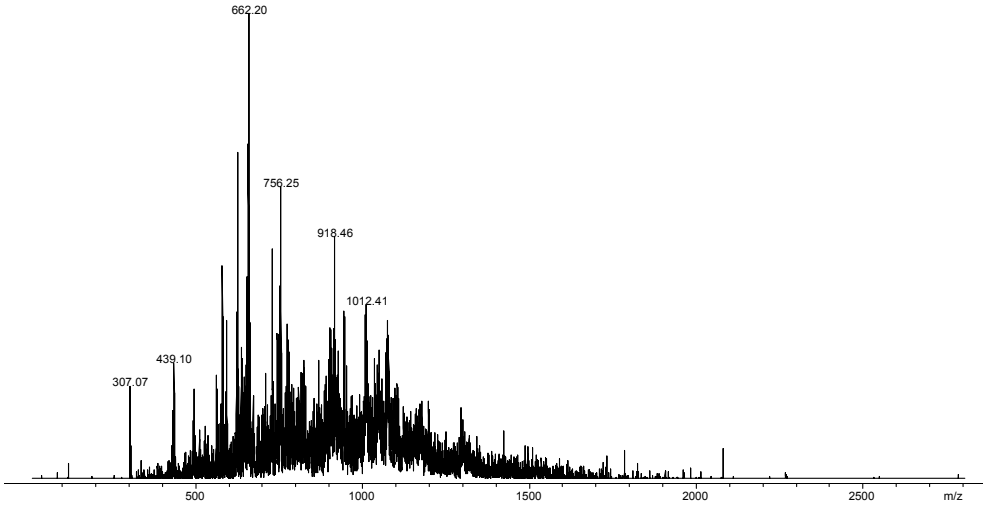

spectrum 13esi:

overview:

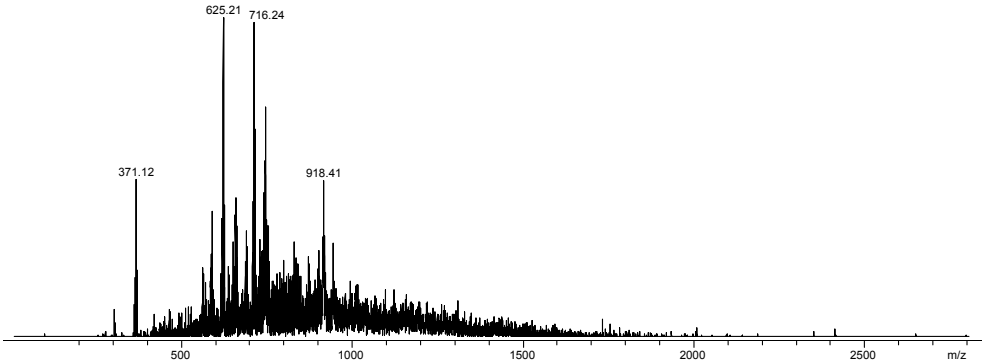

assignment m/z = 371.12:

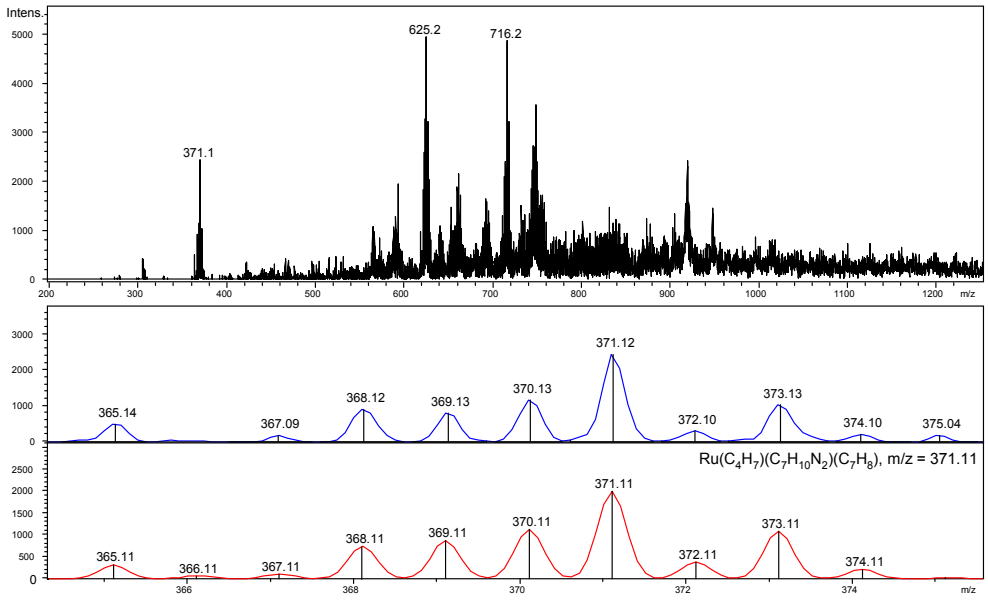

m/z (% relative to peak at 371.12) = 365.14 (20), 366.14 (1), 367.09 (8), 368.12 (37), 369.13 (33), 370.13 (48), 371.12 (100), 372.10 (13), 373.13 (43), 374.10 (9), 375.04 (8); Calc.: 365.11 (16), 366.11 (3), 367.11 (6), 368.11 (37), 369.11 (44), 370.11 (19), 371.11 (100), 372.11 (19), 373.11 (55), 374.11 (11), 375.11 (5).

assignment m/z = 625.21:

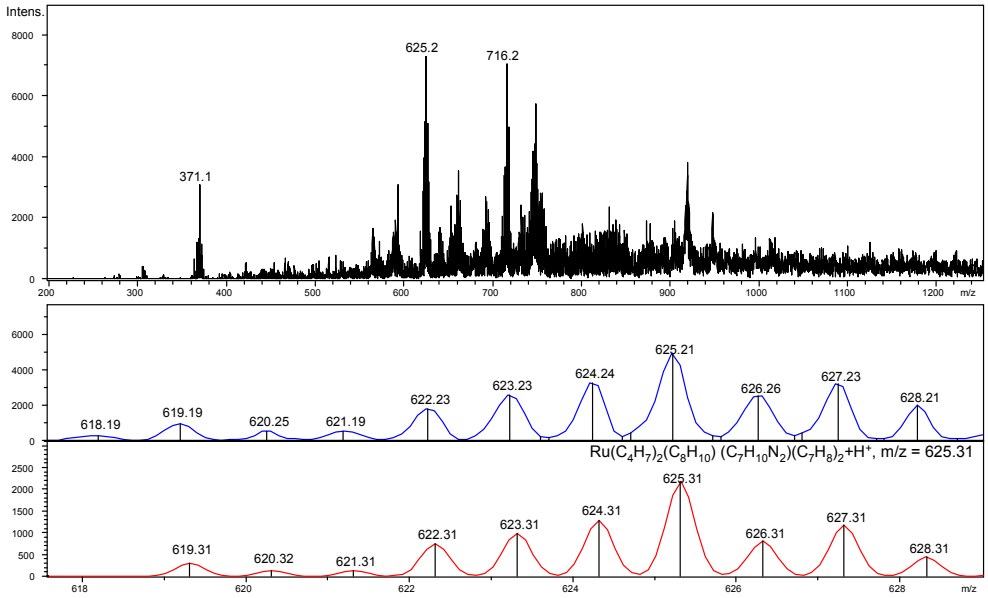

m/z (% relative to peak at 625.21) = 619.19 (20), 620.25 (11), 621.19 (11), 622.23 (37), 623.23 (53), 624.24 (66), 625.21 (100), 626.26 (52), 627.23 (65), 628.21 (41); Calc.: 619.31 (19), 620.32 (6), 621.31 (6), 622.31 (34), 623.31 (49), 624.31 (62), 625.31 (100), 626.31 (49), 627.31 (54), 628.31 (21).

assignment m/z = 716.25:

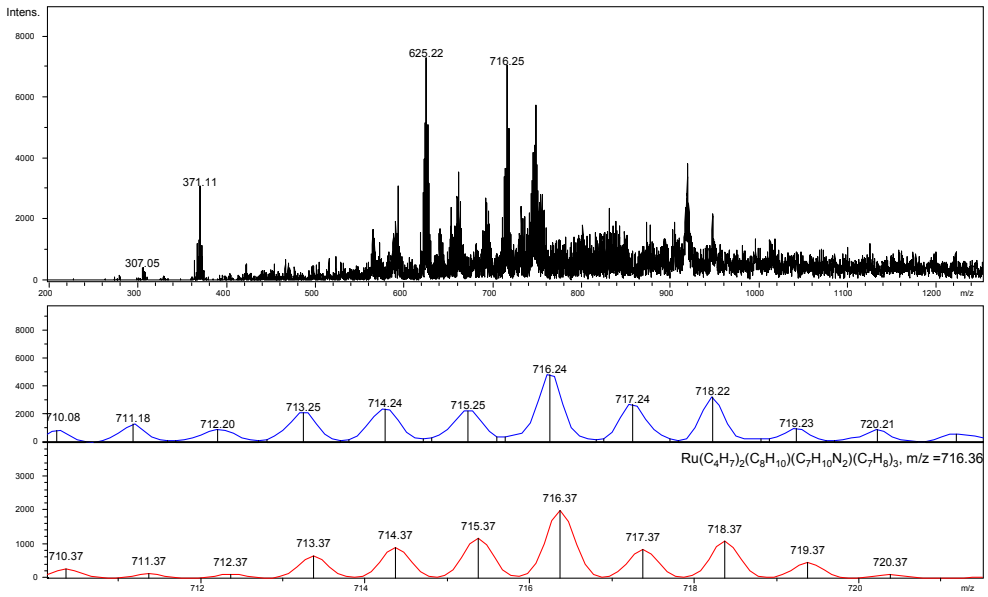

m/z (% relative to peak at 716.25) = 710.08 (18), 711.18 (28), 712.20 (19), 713.25 (44), 714.24 (49), 715.25 (46), 716.24 (100), 717.24 (56), 718.22 (67), 719.23 (20), 720.21 (19);

Calc.: 710.37 (13), 711.37 (6), 712.37 (5), 713.37 (33), 714.37 (45), 715.37 (59), 716.37 (100), 717.37 (42), 718.37 (55), 719.37 (23), 720.37 (5).

***In situ* ESI-MS experiments with (cod)Ru(met)$_2$ and P*n*Bu$_3$:** An oven-dried flask was charged with bis-(2-methallyl)-cycloocta-1,5-diene-ruthenium(II) (6.4 mg, 0.02 mmol) and flushed with nitrogen. Subsequently, tri-*n*-butylphosphine (15 µL, 0.06 mmol) and dry toluene (3.00 mL) were added and the resulting solution was stirred for 15 min at room temperature. Spectrum 14esi was recorded. Then the solution was heated to 100°C for 5 min and spectrum 15esi was recorded.

spectrum 14esi:

overview:

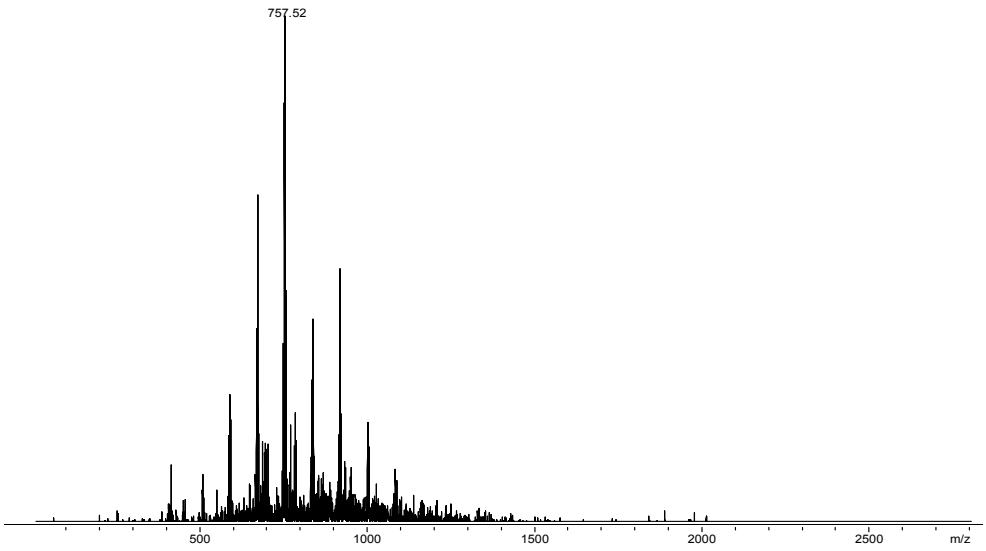

spectrum 15esi:

overview:

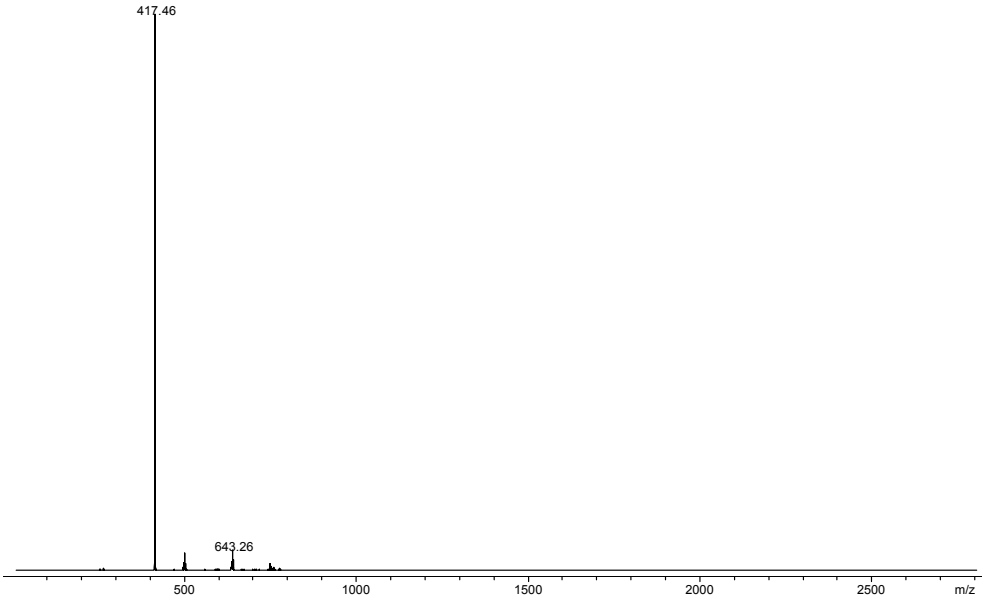

assignment m/z = 505.25:

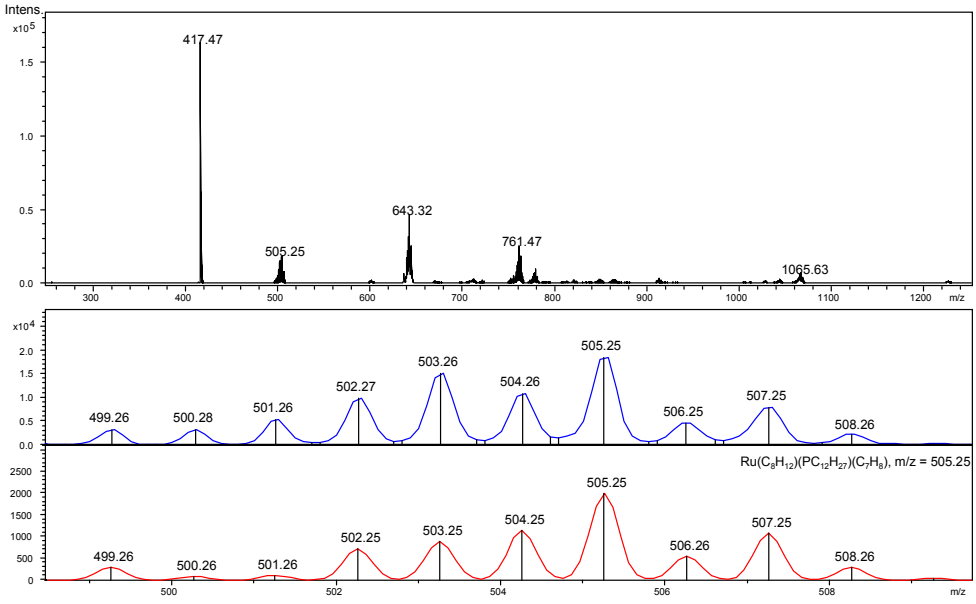

m/z (% relative to peak at 505.25) = 499.26 (18), 500.28 (18), 501.26 (29), 502.27 (53), 503.26 (82), 504.26 (59), 505.25 (100), 506.25 (25), 507.25 (43), 508.26 (13); Calc.: 499.26 (15), 500.26 (4), 501.26 (5), 502.25 (36), 503.26 (45), 504.26 (57), 505.25 (100), 506.25 (28), 507.25 (54), 508.26 (15).

assignment m/z = 761.47

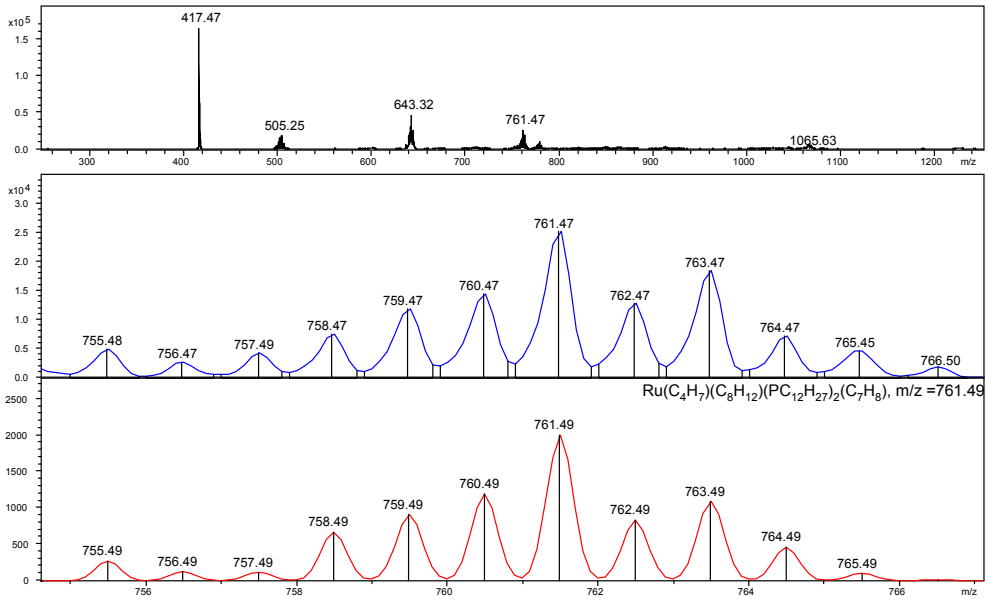

m/z (% relative to peak at 761.47) = 755.48 (20), 756.47 (11), 757.49 (17), 758.47 (30), 759.47 (47), 760.47 (74), 761.47 (100), 762.47 (51), 763.47 (73), 782.49 (29), 783.46 (19); Calc.: 755.49 (14), 756.49 (6), 757.49 (6), 758.49 (33), 759.49 (45), 760.49 (59), 761.49 (100), 762.49 (41), 763.49 (54), 764.49 (23), 765.49 (5).

assignment m/z = 779.47

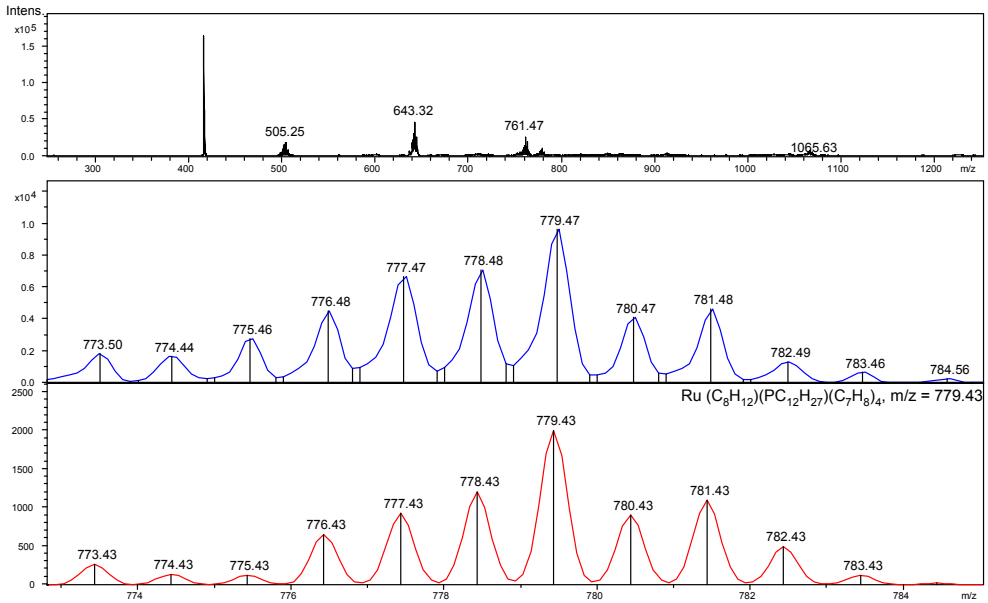

m/z (% relative to peak at 779.47) = 773.50 (20), 774.44 (18), 775.46 (29), 776.48 (47), 777.47 (69), 778.48 (74), 779.47 (100), 780.47 (43), 781.48 (48), 782.49 (14), 783.46 (7);

Calc.: 773.43 (13), 774.43 (7), 775.43 (6), 776.43 (32), 777.43 (46), 778.43 (60), 779.43 (100), 780.43 (45), 781.43 (55), 782.43 (25), 783.43 (6).

***In situ* ESI-MS experiments with (cod)Ru(met)$_2$, P*n*Bu$_3$ and DMAP:** An oven-dried flask was charged with bis-(2-methallyl)-cycloocta-1,5-diene-ruthenium(II) (6.4 mg, 0.02 mmol) and 4-dimethylaminopyridine (4.9 mg, 0.04 mmol) and flushed with nitrogen. Subsequently, tri-*n*-butylphosphine (15 µL, 0.06 mmol) and dry toluene (3.00 mL) were added and the resulting solution was stirred for 15 min at room temperature. Spectrum 16esi was recorded. Then the solution was heated to 100°C for 5 min and spectrum 17esi was recorded.

Spectrum 16esi:

overview:

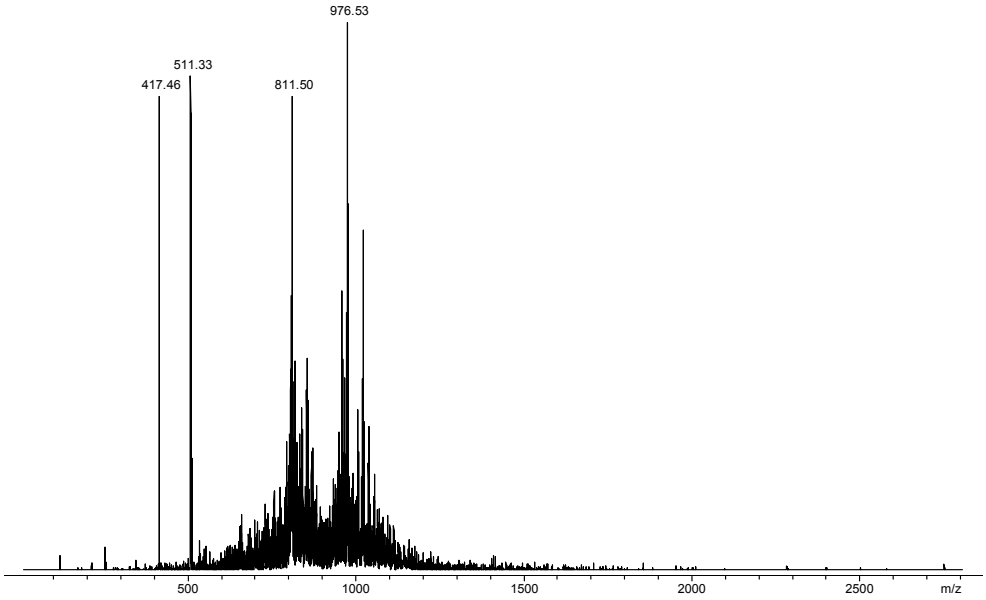

assignment m/z = 257.20:

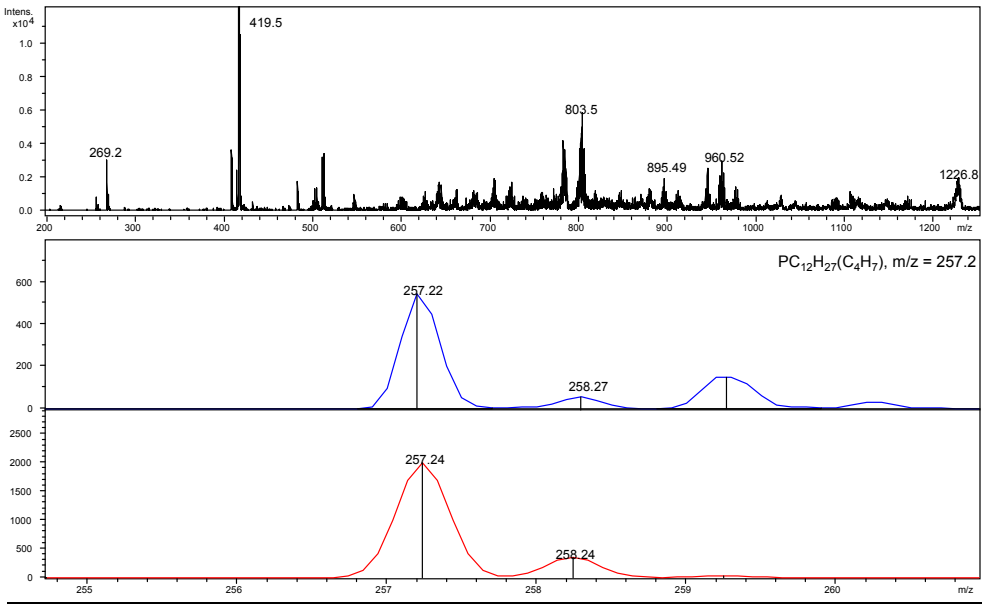

m/z (% relative to peak at 257.22) = 257.22 (100), 258.27 (12), Calc.: 257.24 (100), 258.24 (18).

spectrum 17esi:

overview:

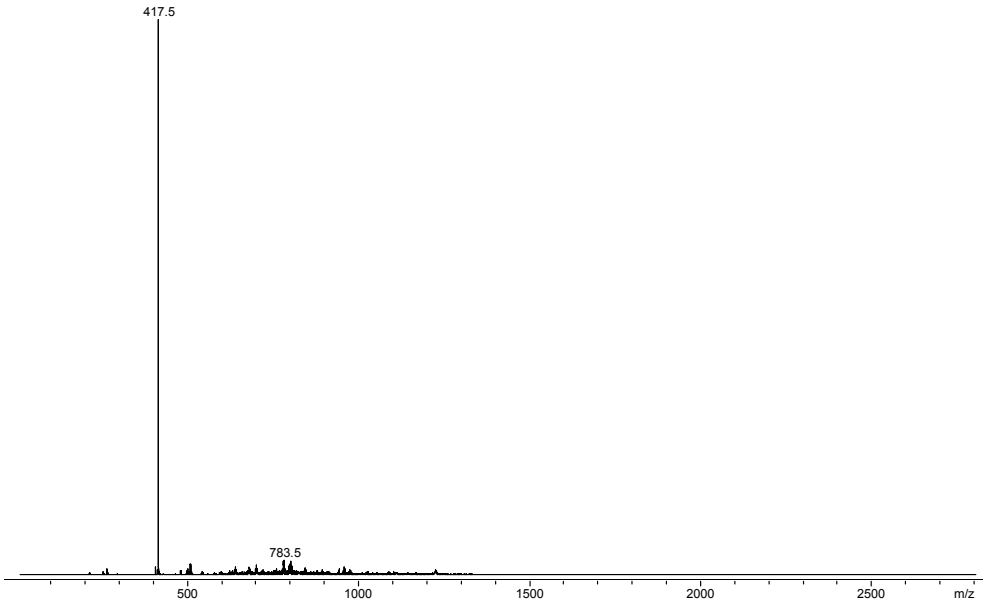

assignment m/z = 783.46:

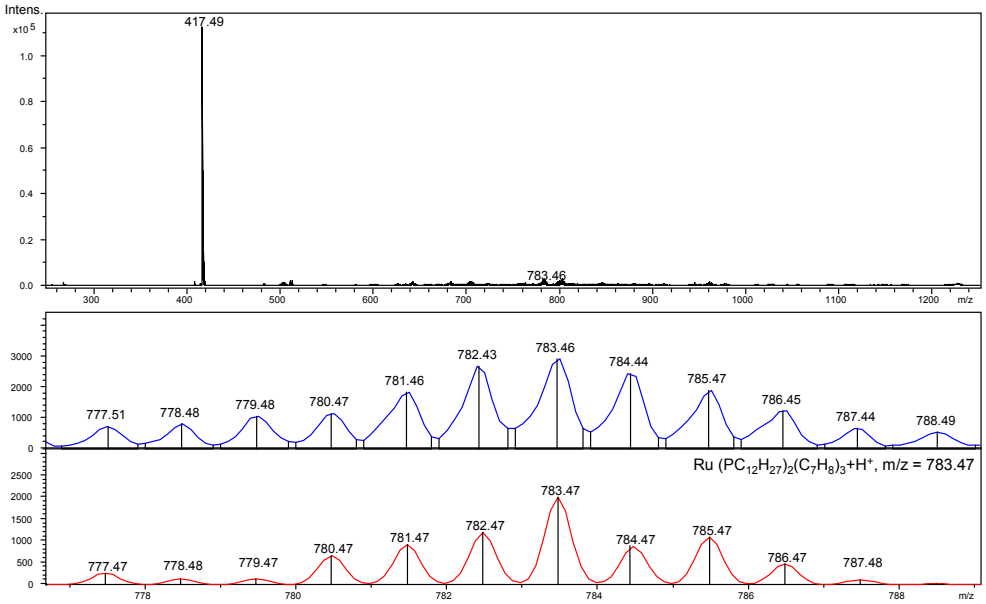

m/z (% relative to peak at 783.46) = 777.51 (25), 778.48 (28), 779.48 (36), 780.47 (39), 781.46 (63), 782.43 (92), 783.46 (100), 784.44 (83), 785.47 (65), 786.45 (42), 787.44 (23); Calc.: 777.47 (13), 778.48 (6), 779.47 (6), 780.47 (33), 781.47 (46), 782.47 (60), 783.47 (100), 784.47 (44), 785.47 (54), 786.47 (23), 787.48 (5).

assignment m/z = 803.51:

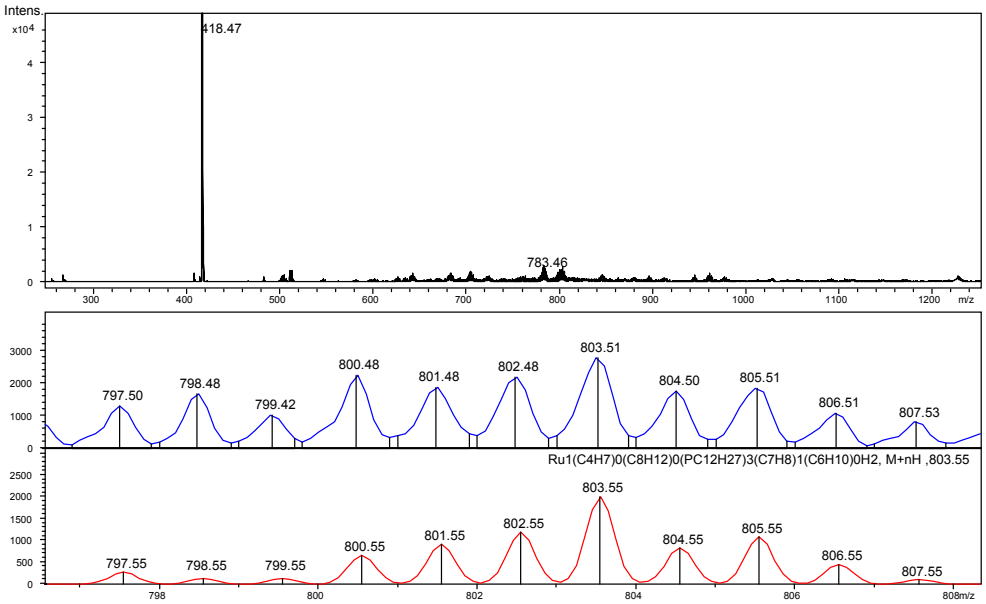

m/z (% relative to peak at 783.46) = 797.50 (47), 798.48 (60), 799.42 (37), 800.48 (81), 801.48 (68), 802.48 (79), 803.51 (100), 804.50 (63), 805.51 (67), 806.51 (39), 807.53 (29); Calc.: 797.55 (14), 798.55 (6), 799.55 (6), 800.55 (33), 801.55 (46), 802.55 (59), 803.55 (100), 804.55 (41) 805.55 (54), 806.55 (22), 807.55 (5).

***In situ* ESI-MS experiments with (cod)Ru(met)$_2$, P*n*Bu$_3$, DMAP and [2-(Dicyclohexylphosphino)ethyl]trimethyl-ammonium chloride:** An oven-dried flask was charged with bis-(2-methallyl)-cycloocta-1,5-diene-ruthenium(II) (6.4 mg, 0.02 mmol) and 4-dimethylaminopyridine (4.9 mg, 0.04 mmol) and flushed with nitrogen. Subsequently, tri-*n*-butylphosphine (15 µL, 0.06 mmol) and dry toluene (3.00 mL) were added and the resulting solution was stirred for 15 min at 100°C. The resulting yellow stock solution was transferred in a second oven-dried flask, which was charged with [2-(Dicyclohexylphosphino)ethyl]trimethyl-ammonium chloride (9.8 mg, 0.03 mmol) and flushed with nitrogen. The resulting suspension was sonicated for 15 minutes, stirred at room temperature for 30 minutes and spectrum 18esi was recorded. Then the solution was heated to 40°C for 5 min and spectrum 19esi was recorded.

spectrum 18esi:

overview:

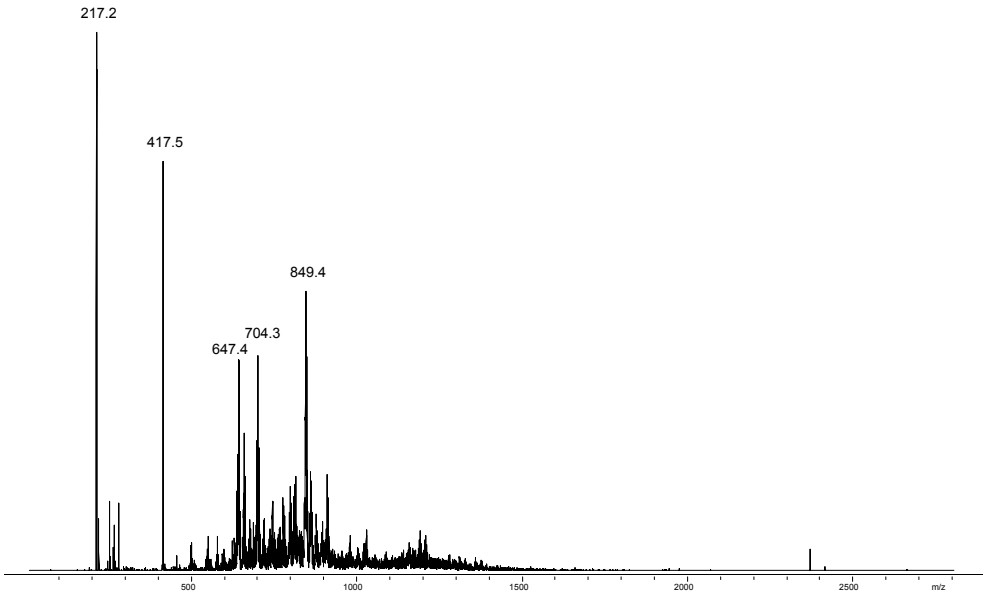

spectrum 19esi:

overview:

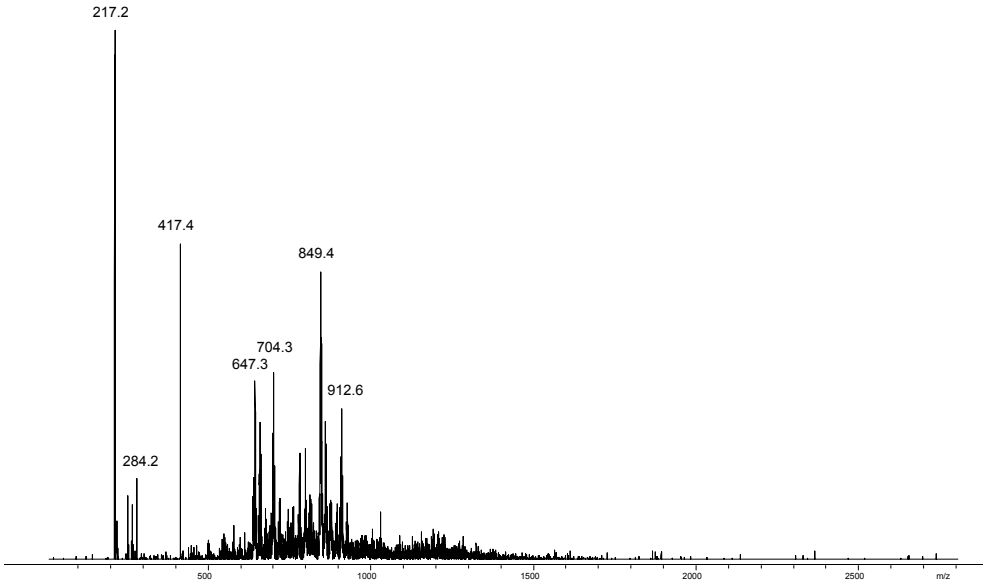

***Z*-selective hydroamidation protocol:**

***In situ* ESI-MS experiments with 1-hexyne (JACS-5b) and 2-pyrrolidinone (JACS-1a):** An oven-dried flask was charged with bis-(2-methallyl)-cycloocta-1,5-diene-ruthenium(II) (6.4 mg, 0.02 mmol) and bis(dicyclohexylphosphino) methane (12.3 mg, 0.03 mmol) and flushed with nitrogen. Subsequently, 2-pyrrolidinone (**JACS-1a**, 77 µL, 1.00 mmol), water (144 µL, 8.00 mmol) and dry toluene (3.00 mL) were added via syringe. The resulting solution was stirred at 100 °C for 5 min and spectrum 20esi was recorded. After adding 1-hexyne (**JACS-5b**, 231 µL, 2.00 mmol) the solution was stirred at 100 °C for 5 min and spectrum 21esi was recorded. Spectra 22esi, 23esi and 24esi were recorded after stirring at 100°C for 25, 130 and 360 min.

spectrum 20esi:

overview:

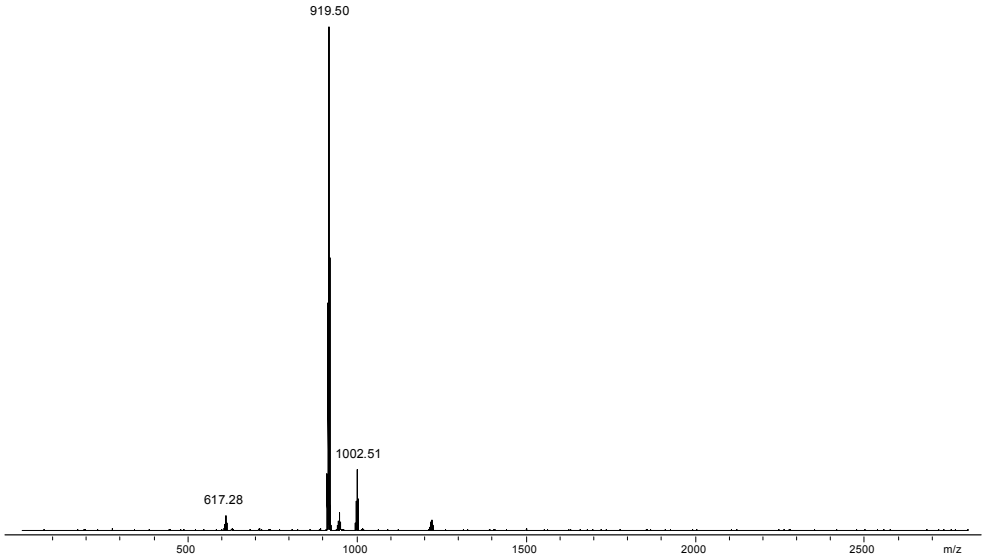

assignment m/z = 617.25

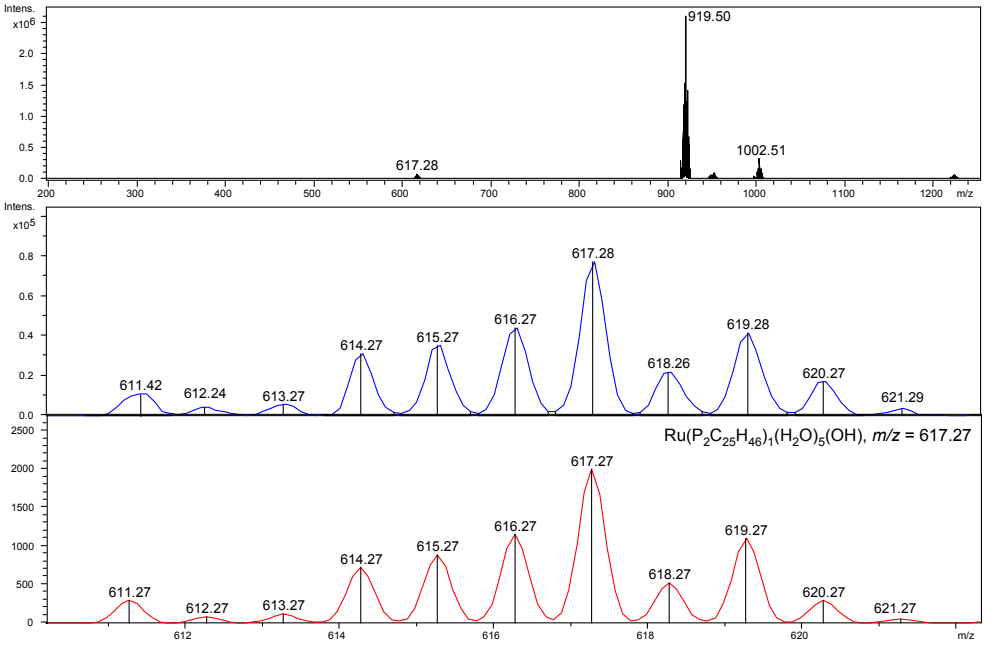

m/z (% relative to peak at 617.25) = 611.42 (14), 612.24 (5), 613.27 (7), 614.27 (40), 615.27 (46), 616.27 (57), 617.28 (100), 618.26 (28), 619.28 (54), 620.27 (22), 621.29 (5); Calc.: 611.27 (15), 612.27 (4), 613.27 (6), 614.27 (36), 615.27 (44), 616.27 (58), 617.27 (100), 618.27 (26), 619.27 (55), 620.27 (15), 621.27 (3).

assignment m/z = 919.50:

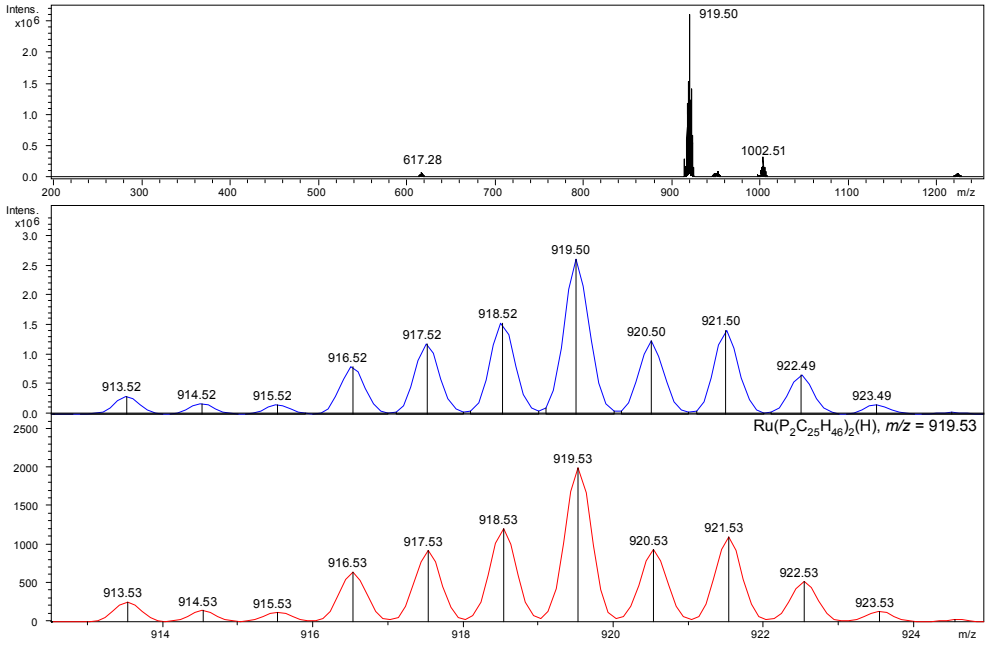

m/z (% relative to peak at 919.50) = 913.53 (11), 914.52 (7), 915.52 (6), 916.52 (31), 917.52 (45), 918.52 (61), 919.50 (100), 920.50 (47), 921.50 (54), 922.49 (25), 923.49 (6); Calc.: 913.53 (13), 914.53 (8), 915.53 (6), 916.53 (32), 917.53 (46), 918.53 (61), 919.53 (100), 920.53 (47), 921.53 (55), 922.53 (26), 923.53 (7).

CID-fragmentation of species at m/z = 919.50:

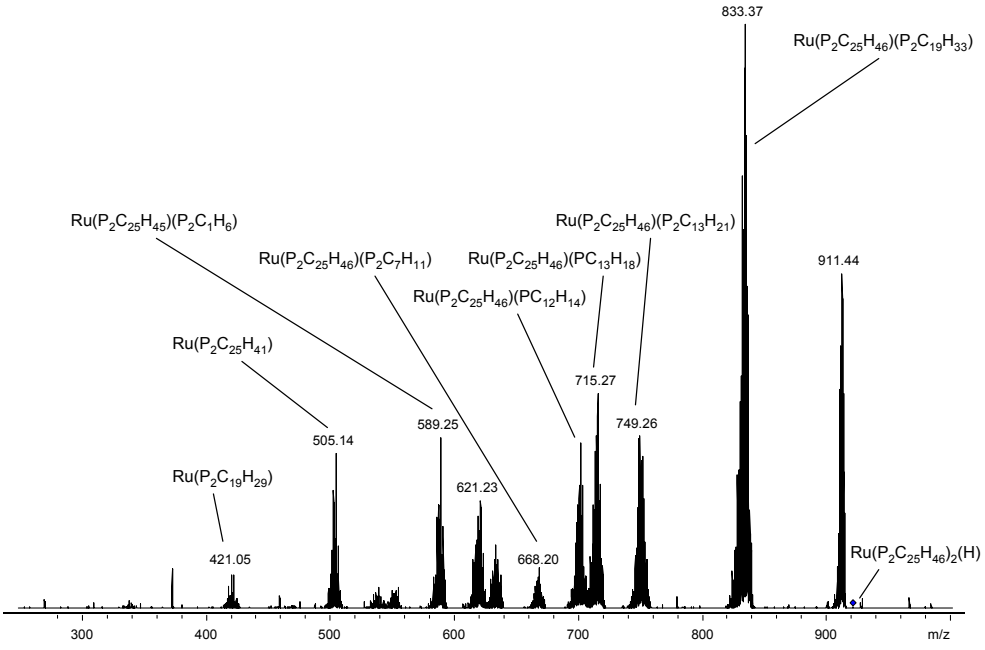

assignment m/z = 1002.51:

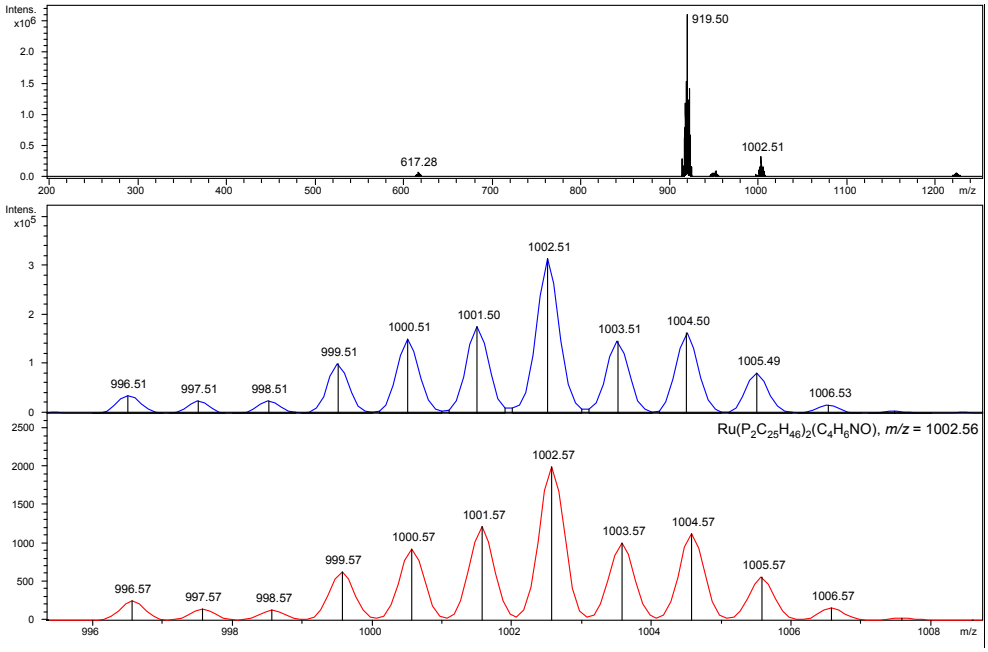

m/z (% relative to peak at 1002.51) = 996.51 (11), 997.51 (8), 998.51 (8), 999.51 (32), 1000.51 (48), 1001.51 (56), 1002.51 (100), 1003.51 (47), 1004.50 (52), 1005.49 (26), 1006.53 (5); Calc.: 996.57 (13), 997.57 (7), 998.57 (7), 999.57 (32), 1000.57 (47), 1001.57 (61), 1002.57 (100), 1003.57 (50), 1004.57 (56), 1005.57 (28), 1006.57 (8).

CID-fragmentation of species at m/z = 1002.51:

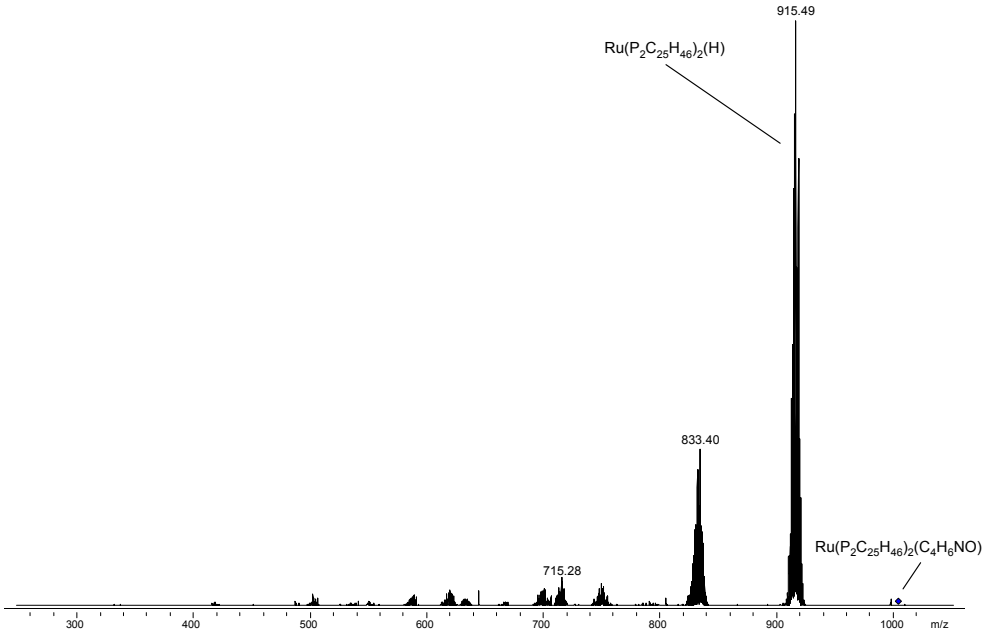

spectrum 21esi:

overview:

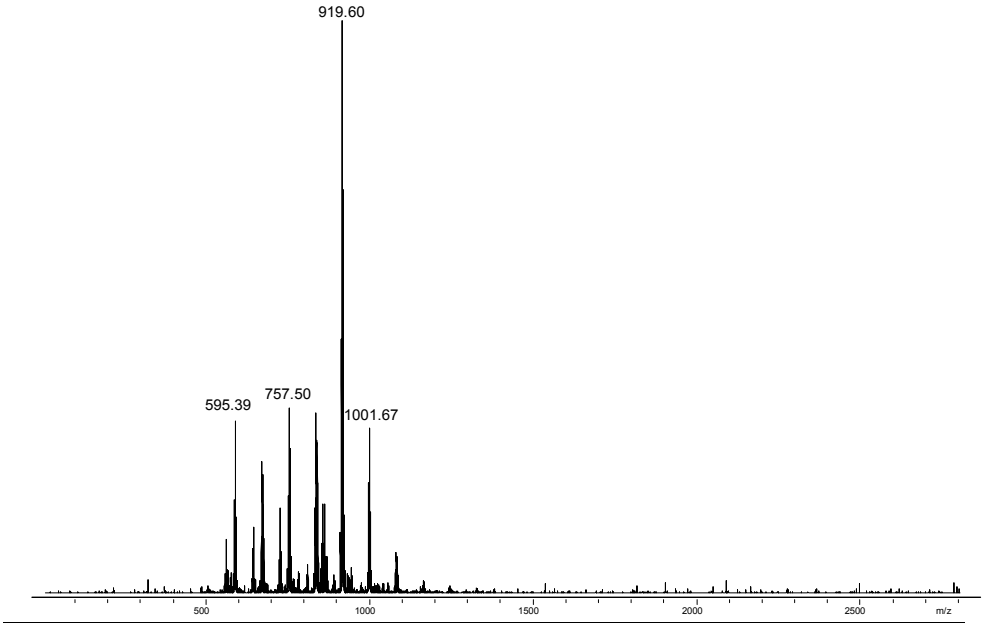

assignment m/z = 593.38:

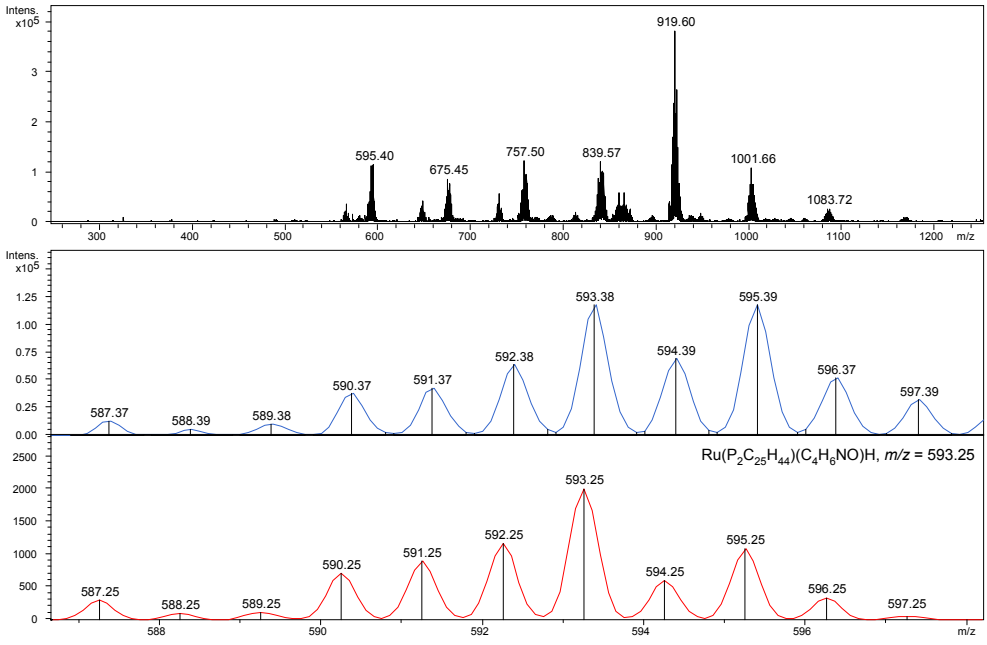

m/z (% relative to peak at 593.38) = 587.37 (11), 588.39 (5), 589.38 (9), 590.37 (32), 591.37 (36), 592.38 (54), 593.38 (100), 594.39 (59), 595.39 (100), 596.37 (44), 597.39 (27); Calc.: 587.25 (15), 588.25 (5), 589.25 (5), 590.25 (36), 591.25 (45), 592.25 (58), 593.25 (100), 594.25 (30), 595.25 (54), 596.25 (17), 597.25 (2).

assignment m/z = 649.43:

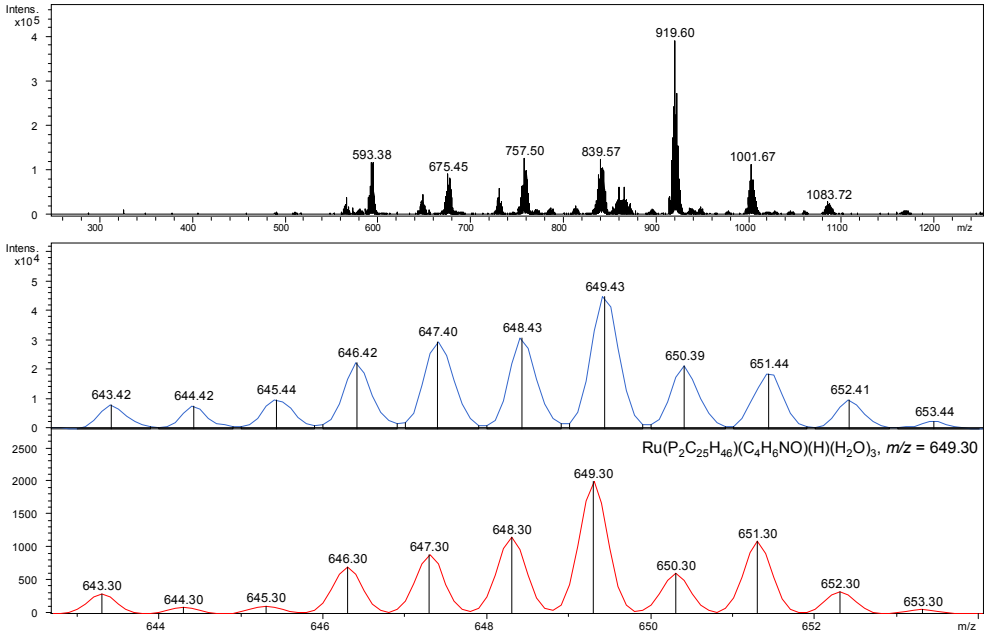

m/z (% relative to peak at 649.43) = 643.42 (18), 644.42 (17), 645.44 (22), 646.42 (50), 647.40 (66), 648.43 (69), 649.43 (100), 650.39 (47), 651.44 (41), 652.41 (22), 653.44 (5); Calc.: 643.30 (15), 644.30 (5), 645.30 (6), 646.30 (35), 647.30 (45), 648.30 (58), 649.30 (100), 650.30 (31), 651.30 (55), 652.30 (16), 653.30 (3).

assignment m/z = 677.34:

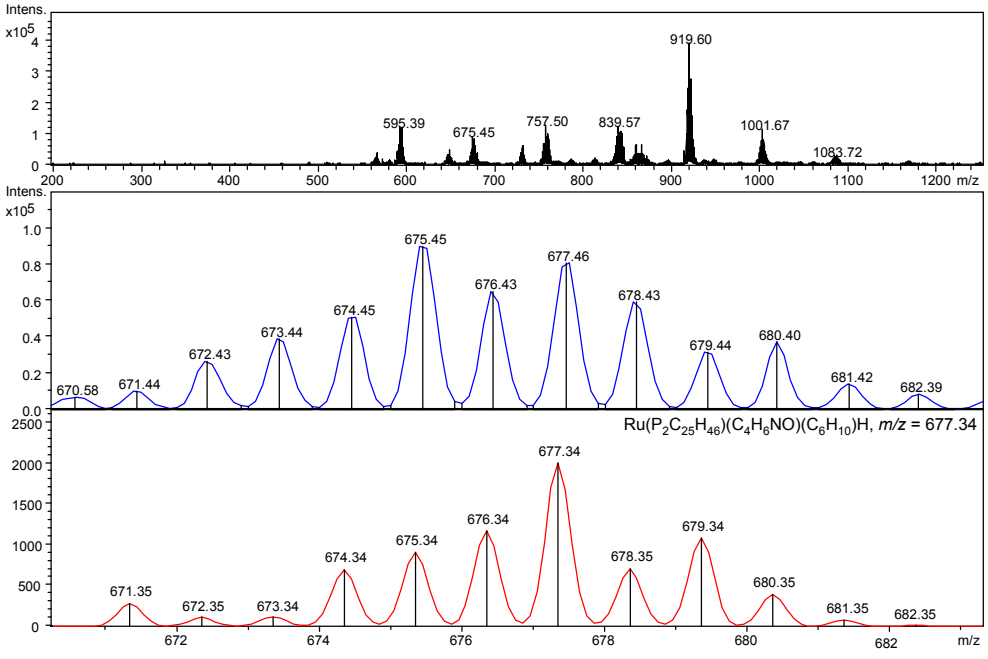

m/z (% relative to peak at 677.34) = 671.44 (11), 672.43 (30), 673.44 (43), 674.45 (56), 675.45 (100), 676.43 (72), 677.46 (90), 678.43 (66), 679.44 (35), 680.40 (42), 681.42 (16),

682.39 (9); Calc.: 671.35 (14), 672.35 (6), 673.34 (6), 674.34 (35), 675.34 (45), 676.34 (59), 677.34 (100), 678.35 (35), 679.34 (54), 680.35 (19), 681.35 (4), 682.35 (0).

assignment m/z = 731.49:

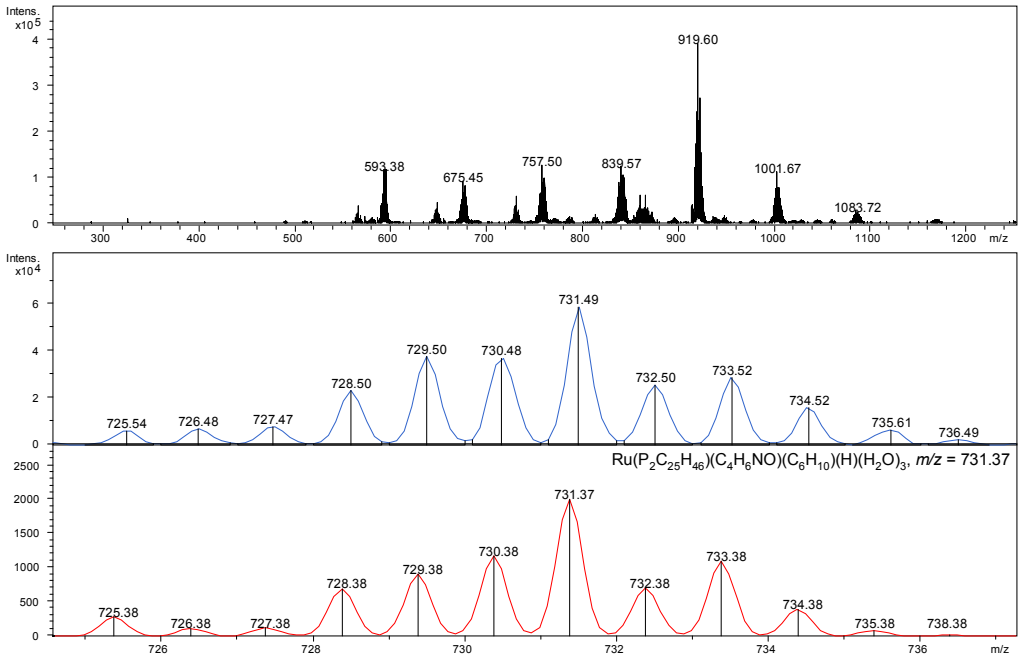

m/z (% relative to peak at 731.49) = 725.54 (10), 726.48 (12), 727.47 (13), 728.50 (40), 729.50 (64), 730.48 (63), 731.49 (100), 732.50 (43), 733.52 (49), 734.52 (27), 735.61 (11), 736.49 (4); Calc.: 725.38 (14), 726.38 (5), 727.38 (6), 728.38 (34), 729.38 (45), 730.38 (59), 731.37 (100), 732.38 (35), 733.38 (55), 734.38 (19), 735.38 (4), 736.38 (1).

assignment m/z = 757.50:

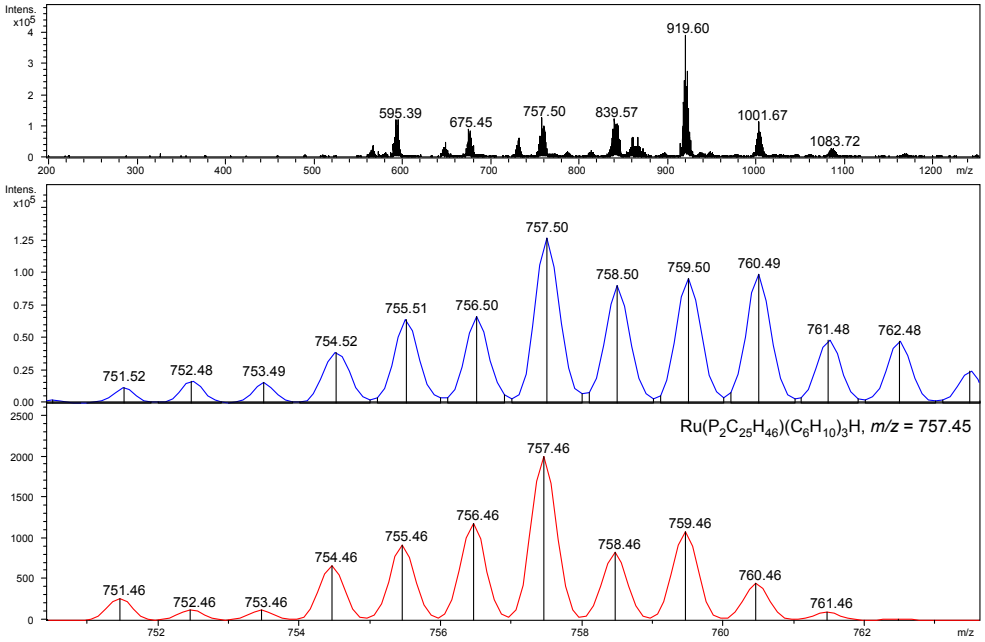

m/z (% relative to peak at 757.50) = 751.52 (9), 752.48 (13), 753.49 (13), 754.52 (31), 755.51 (51), 756.50 (52), 757.50 (100), 758.50 (71), 759.50 (76), 760.49 (78), 761.48 (38), 762.48 (38); Calc.: 751.46 (13), 752.46 (6), 753.46 (6), 754.46 (33), 755.46 (46), 756.46 (59), 757.46 (100), 758.46 (42), 759.46 (54), 760.46 (23), 761.46 (5), 762.46 (0).

assignment m/z = 839.57:

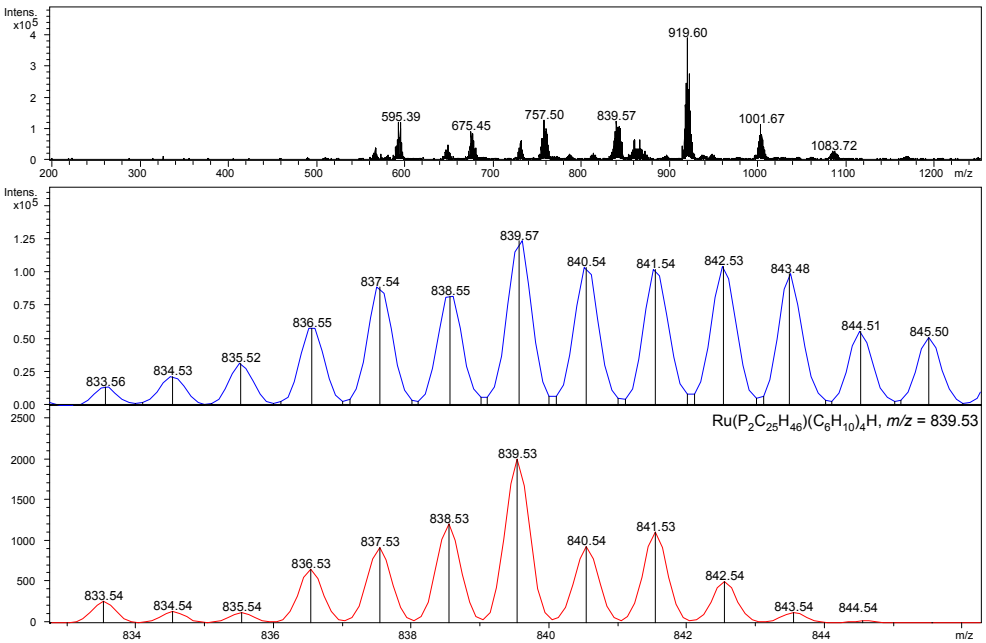

m/z (% relative to peak at 839.57) = 833.56 (11), 834.53 (18), 835.52 (26), 836.55 (47), 837.54 (72), 838.55 (66), 839.57 (100), 840.54 (84), 841.54 (83), 842.53 (84), 843.48 (80),

844.51 (44); Calc.: 833.54 (13), 834.54 (7), 835.54 (6), 836.53 (33), 837.53 (46), 838.53 (60), 839.53 (100), 840.54 (47), 841.53 (55), 842.54 (25), 843.54 (6), 844.54 (1).

assignment m/z = 859.45:

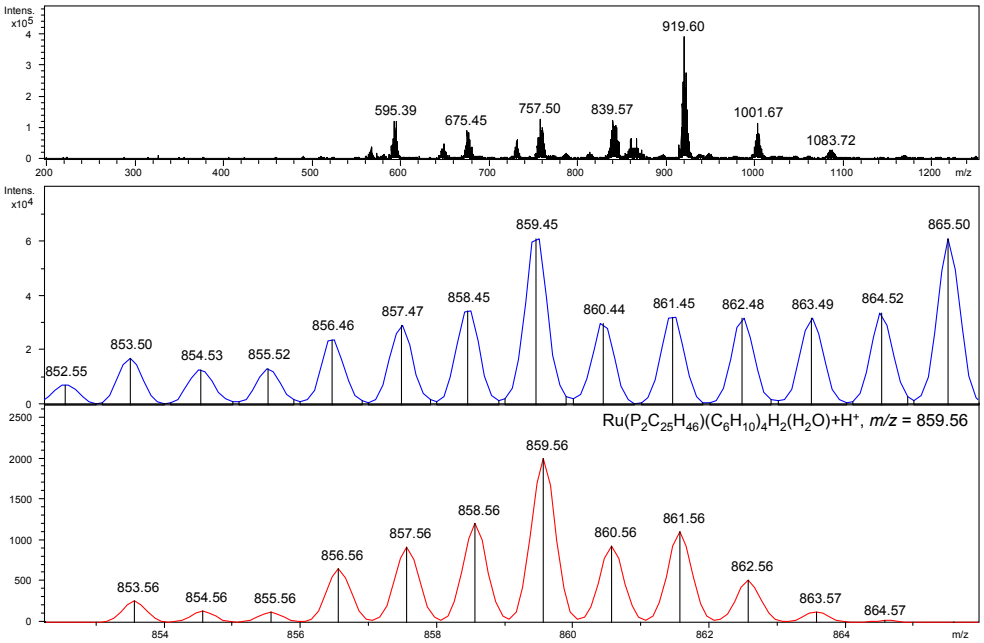

m/z (% relative to peak at 859.45) = 853.50 (28), 854.53 (21), 855.52 (22), 856.46 (39), 857.47 (48), 858.45 (57), 859.45 (100), 860.44 (49), 861.45 (53), 862.48 (52), 863.49 (52); Calc.: 853.56 (13), 854.56 (7), 855.56 (6), 856.56 (33), 857.56 (46), 858.56 (60), 859.56 (100), 860.56 (47), 861.56 (55), 862.57 (26), 863.57 (6).

assignment m/z = 919.60:

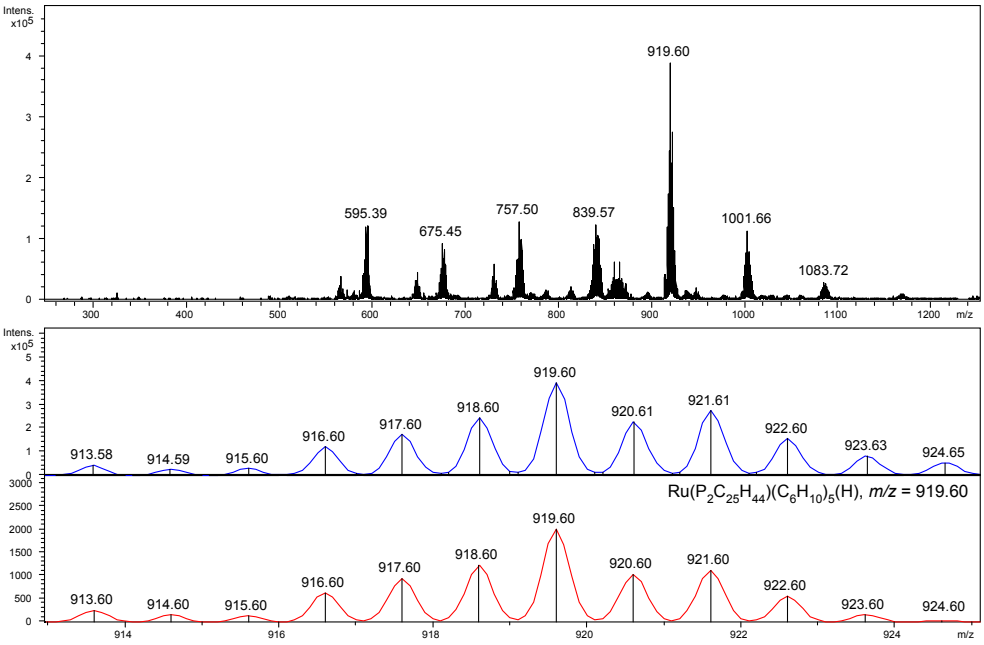

m/z (% relative to peak at 919.60) = 913.58 (11), 914.59 (7), 915.60 (8), 916.60 (31), 917.60 (45), 918.60 (62), 919.60 (100), 920.61 (58), 921.61 (70), 922.60 (40), 923.63 (21), 924.65 (14); Calc.: 913.60 (12), 914.60 (8), 915.60 (7), 916.60 (31), 917.60 (47), 918.60 (61), 919.60 (100), 920.60 (52), 921.60 (56), 922.60 (28), 923.60 (8), 924.60 (1).

CID-fragmentation of species at m/z = 919.60:

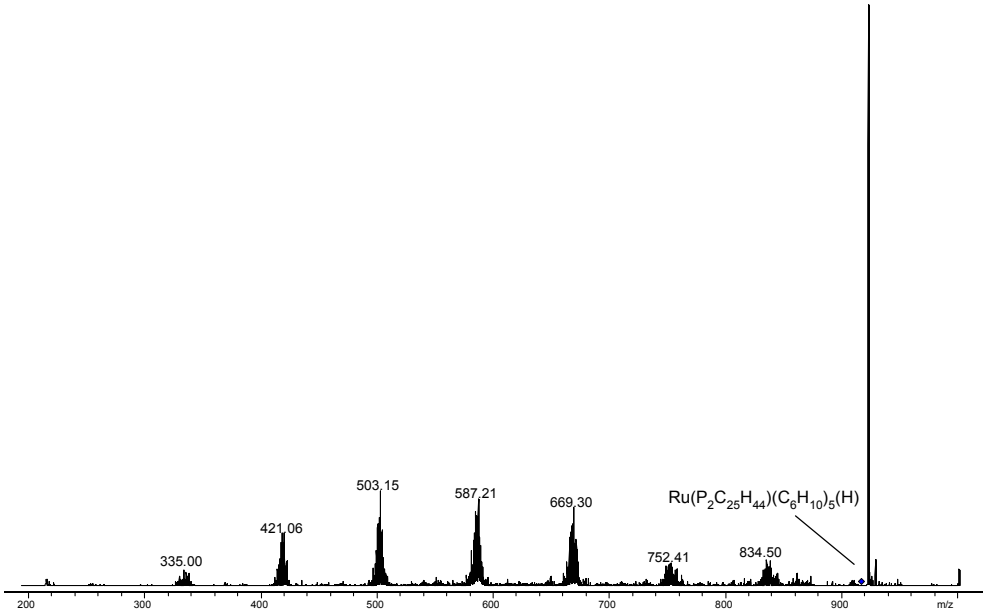

assignment m/z = 1001.67:

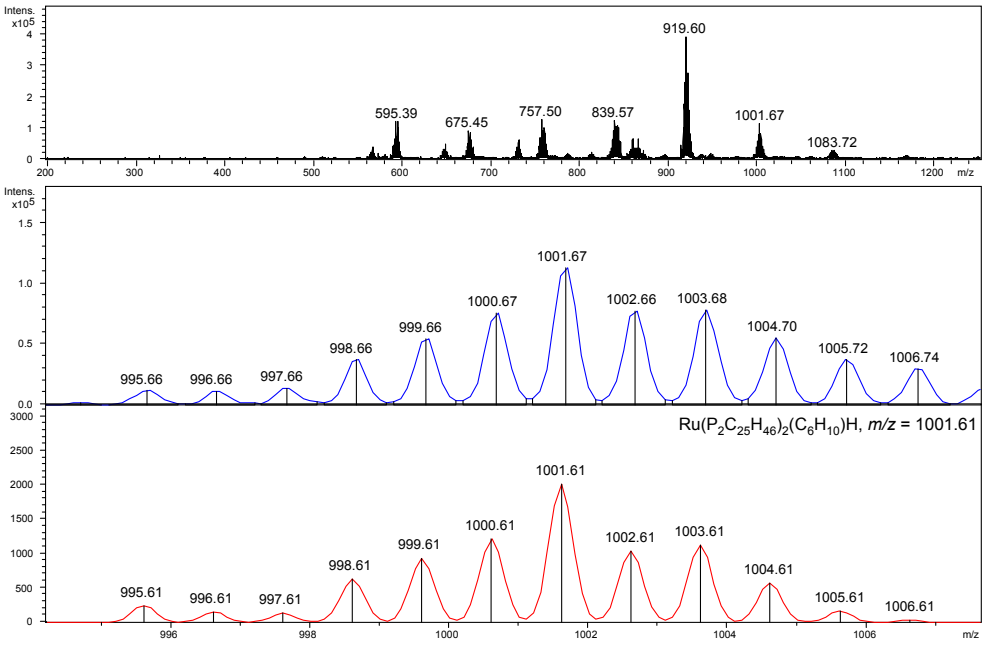

m/z (% relative to peak at 1001.67) = 995.66 (11), 996.66 (10), 997.66 (12), 998.66 (33), 999.66 (48), 1000.67 (67), 1001.67 (100), 1002.66 (68), 1003.68 (68), 1004.70 (69), 1005.72

(33), 1006.74 (26); Calc.: 995.61 (12), 996.61 (7), 997.61 (7), 998.61 (31), 999.61 (46), 1000.61 (61), 1001.61 (100), 1002.61 (51), 1003.61 (56), 1004.61 (29), 1005.62 (8), 1006.61 (1).

CID-fragmentation of species at m/z = 1001.67:

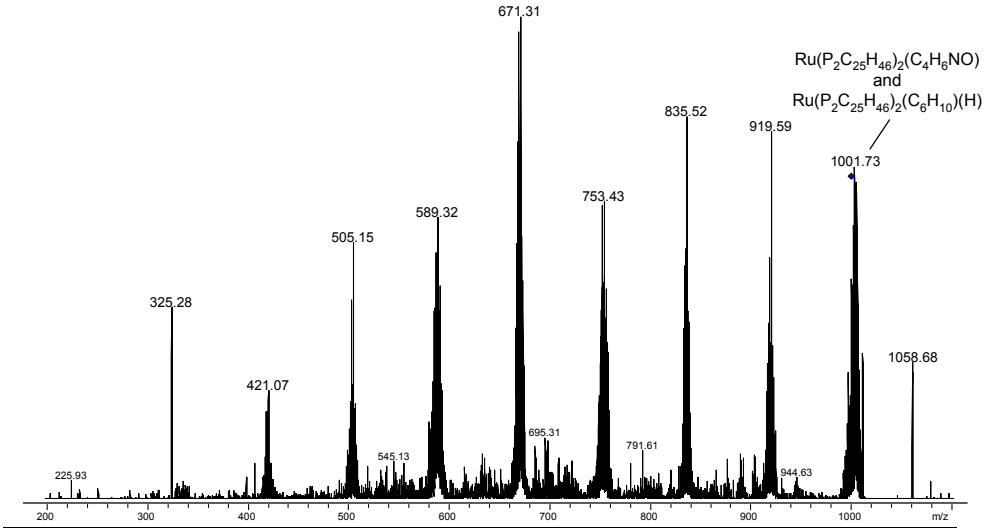

assignment m/z = 1083.72:

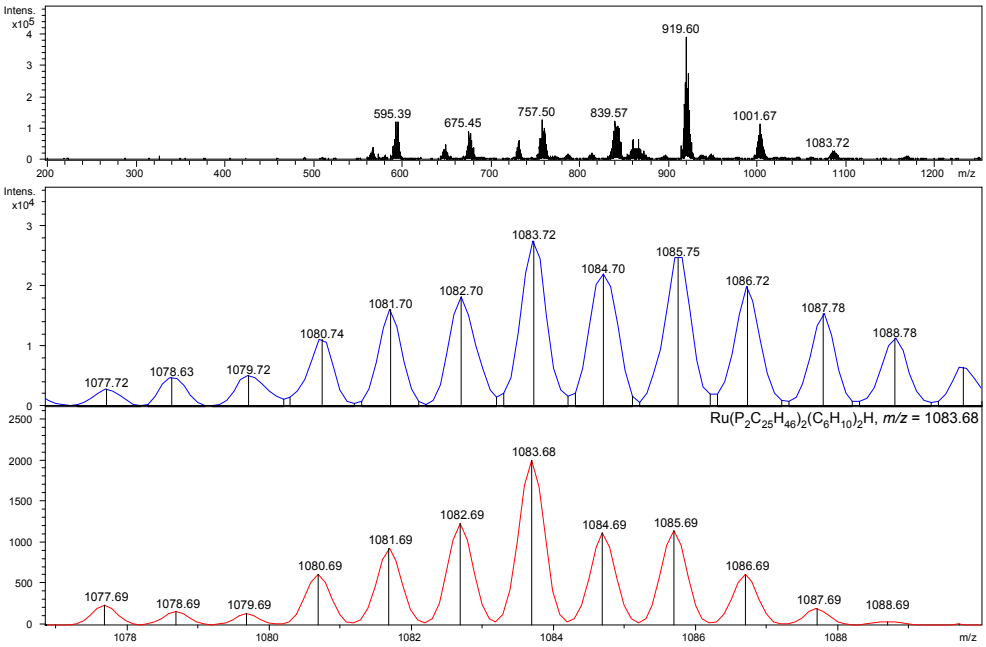

m/z (% relative to peak at 1083.72) = 1077.72 (11), 1078.63 (17), 1079.72 (19), 1080.74 (41), 1081.70 (61), 1082.70 (66), 1083.72 (100), 1084.70 (80), 1085.75 (90), 1086.72 (73), 1087.78 (56), 1088.78 (41); Calc.: 1077.69 (12), 1078.69 (8), 1079.69 (7), 1080.69 (31), 1081.69 (47), 1082.69 (62), 1083.69 (100), 1084.69 (56), 1085.69 (57), 1086.69 (31), 1087.69 (10), 1088.69 (2).

assignment m/z = 1165.83:

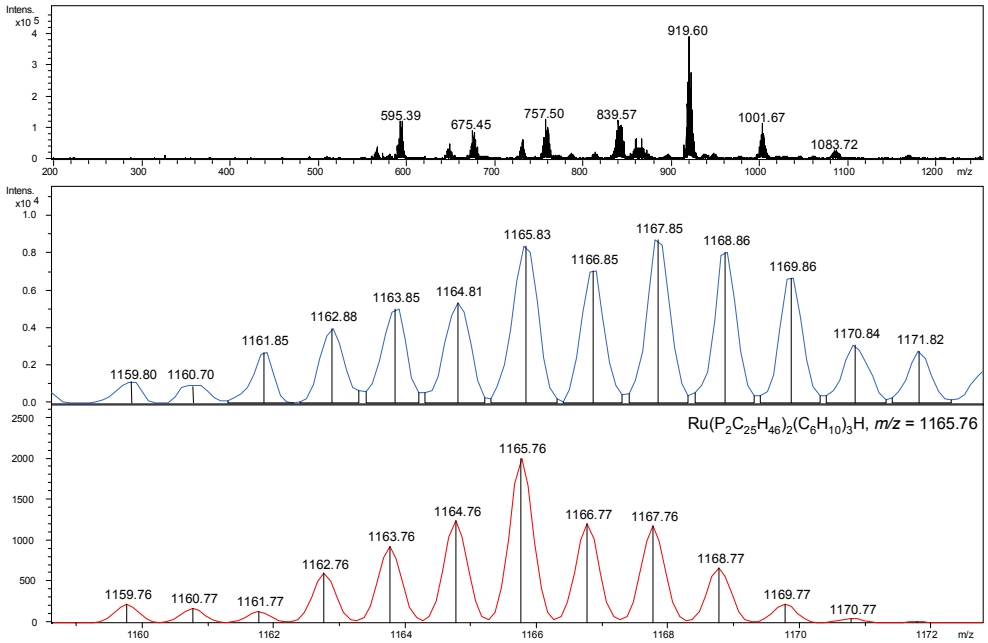

m/z (% relative to peak at 1167.85) = 1159.80 (13), 1160.70 (10), 1161.85 (31), 1162.88 (46), 1163.85 (58), 1164.81 (61), 1165.83 (96), 1166.85 (81), 1167.85 (100), 1168.86 (92), 1169.86 (77), 1170.84 (35), 1171.82 (32); Calc.: 1159.76 (11), 1160.77 (9), 1161.77 (7), 1162.76 (30), 1163.76 (47), 1164.76 (62), 1165.76 (100), 1166.77 (60), 1167.76 (59), 1168.77 (34), 1169.77 (11), 1170.77 (3), 1171.78 (1).

spectrum 22esi:

overview:

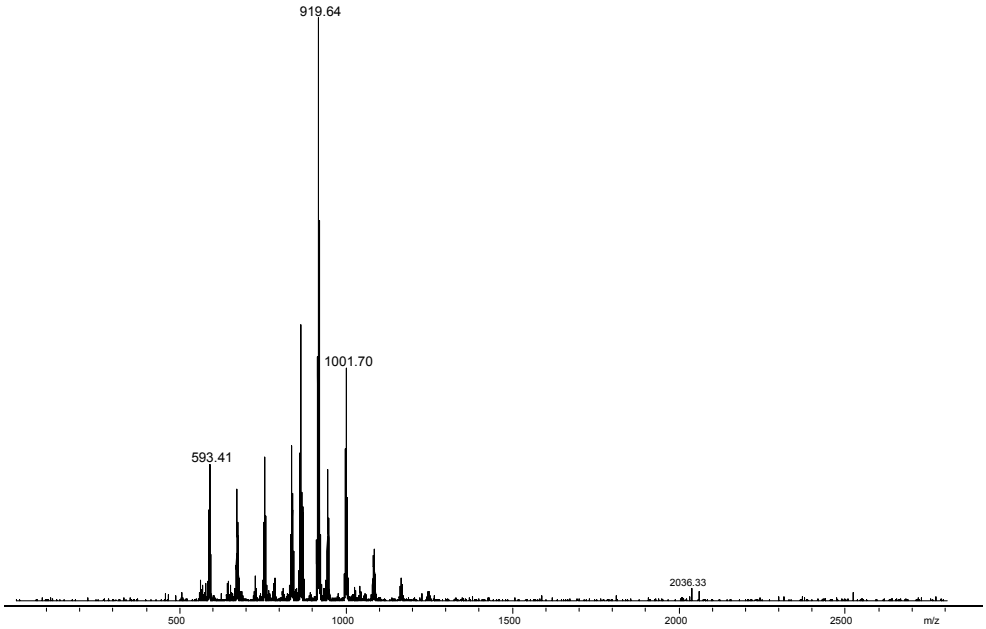

assignment m/z = 865.53:

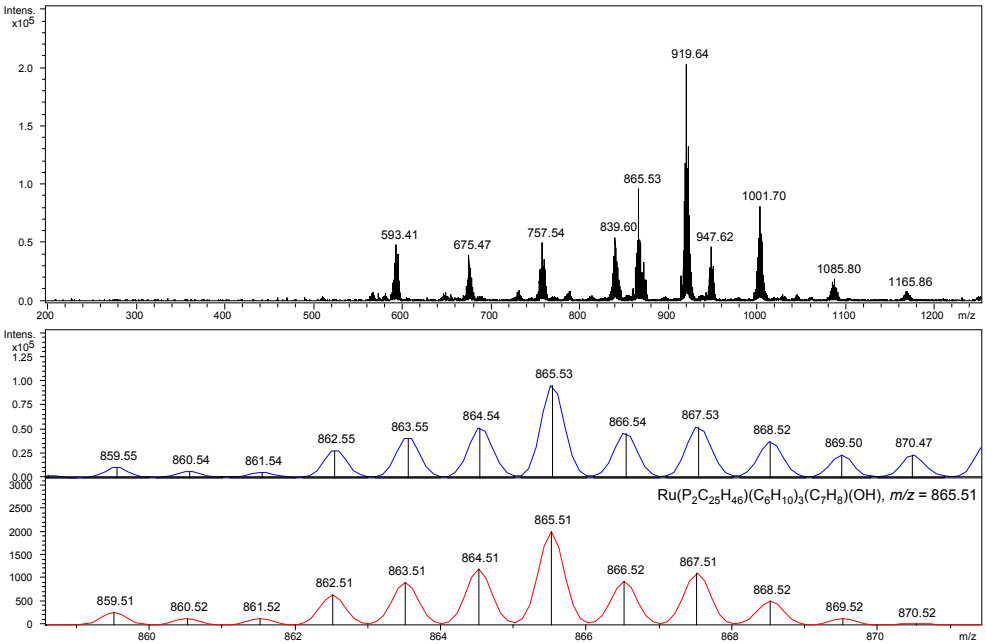

m/z (% relative to peak at 865.53) = 859.55 (11), 860.54 (7), 861.54 (6), 862.55 (29), 863.55 (43), 864.54 (54), 865.53 (100), 866.54 (48), 867.53 (55), 868.52 (39), 869.50 (25), 870.47 (25); Calc.: 859.59 (13), 860.59 (7), 861.59 (7), 862.59 (32), 863.59 (46), 864.59 (60), 865.59 (100), 866.59 (47), 867.59 (55), 868.59 (26), 869.60 (7), 870.60 (1).

assignment m/z = 947.62:

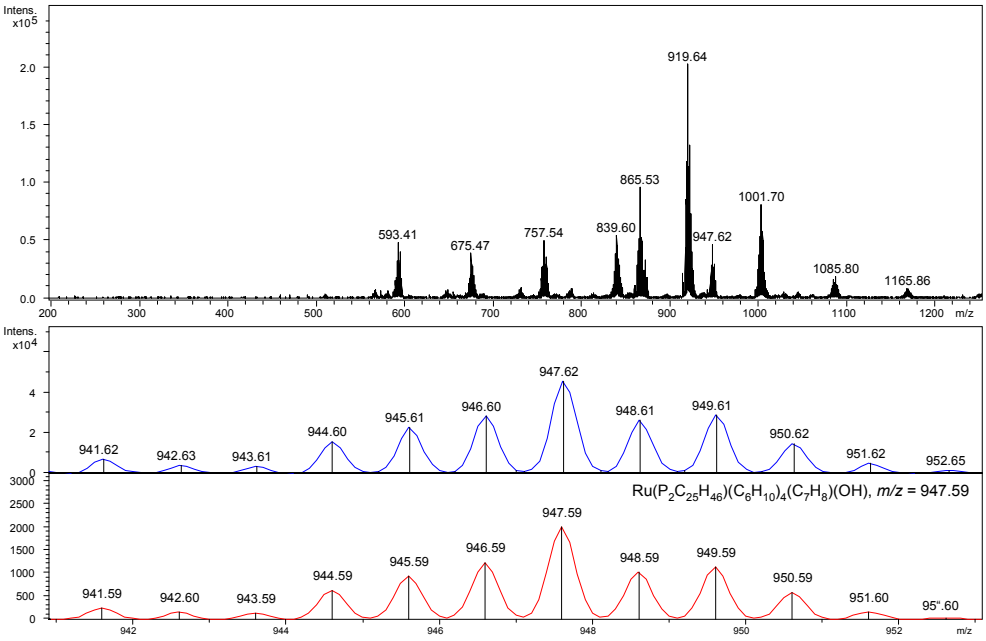

m/z (% relative to peak at 947.62) = 941.62 (16), 942.63 (9), 943.61 (8), 944.60 (35), 945.61 (50), 946.60 (62), 947.62 (100), 948.61 (58), 949.61 (63), 950.62 (32), 951.62 (11), 952.62 (3); Calc.: 941.59 (13), 942.60 (7), 943.59 (7), 944.59 (32), 945.59 (46), 946.59 (60), 947.59 (100), 948.59 (47), 949.59 (55), 950.59 (26), 951.60 (7), 952.60 (1).

spectrum 23esi:

overview:

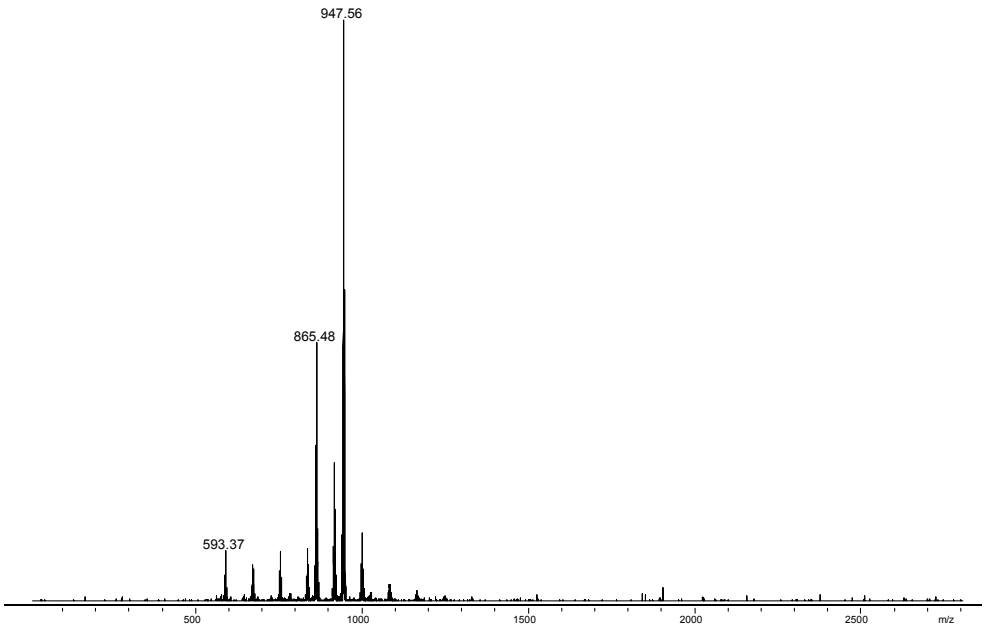

spectrum 24esi:

overview:

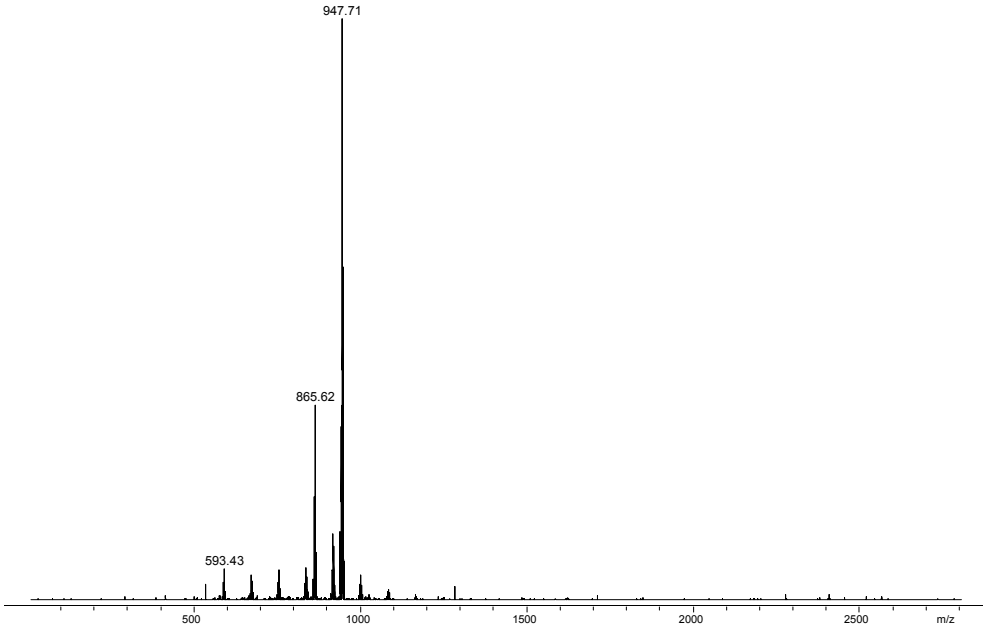

VI.3.8. Quantum chemical calculations.

All calculations were performed with the Gaussian 03[50] or the Gaussian 09[51] program package and the B3LYP density functional.[52] The atoms H, C, N, O and P were described by the 6-31G(d) basis,[53] while the Stuttgart RSC 1997 ECP pseudopotential was used to represent Ru.[54] All geometries were fully optimized. Harmonic force constants were calculated for the optimized geometries to characterize the stationary points as minima. Thermal corrections from the frequency calculations were scaled with Wong's scaling factor (f = 0.9804) for B3LYP/6-31G(d).[55] Additional single point energy calculation were performed on all structures employing the 6-311+G(2d,p) basis[56] for the atoms H, C, N, O and P. All ball and stick models were rendered with GaussView 5.[57]

Table 1. Total energies (hartree) from B3LYP/6-311+G(2d,p) single point energy calculations, unscaled thermal corrections (hartree) from B3LYP/6-31G(d) frequency calculations at 298.15 K and page numbers for the optimized coordinates.

Structure	Total energy	*E*298	*U*298	*H*298	*G*298
$P(^nBu)_3$	-815.08978125	0.371767	0.390658	0.391602	0.323444
(DMAP)	-382.36912707	0.162737	0.171342	0.172287	0.128985
(COD)	-312.12427441	0.181199	0.188622	0.189566	0.149678
(*iso*butene)	-157.27902867	0.108530	0.113823	0.114767	0.081892
$(^nBu_3PC_4H_6)$	-971.12063974	0.459616	0.483934	0.484878	0.403891
1a (2-pyrrolidone)	-286.72485760	0.111580	0.116986	0.117930	0.082739
5b (1-hexyne)	-234.67093414	0.142273	0.149898	0.150842	0.110837
6a (*N*-((*E*)-hex-1-enyl)pyrrolidin-2-one)	-521.44987506	0.259114	0.272208	0.273152	0.218077
58 $[Ru(P^nBu_3)_2(DMAP)_2]$	-2489.84987265	1.075194	1.136119	1.137064	0.969675
59 $[Ru(P^nBu_3)_2(DMAP)_2(C_4H_6NO)H]$	-2776.62606340	1.188433	1.255323	1.256268	1.077557
60 $[Ru(P^nBu_3)_2(DMAP)(C_4H_6NO)(C_6H_{10})H]$	-2628.92829811	1.167439	1.233047	1.233991	1.058926
61 $[Ru(P^nBu_3)_2(DMAP)_2(C_4H_6NO)(C_6H_{11})]$	-3011.33001403	1.336707	1.411763	1.412707	1.216711
62 $[Ru(P^nBu_3)(DMAP)_2(C4H_6NO)(C_6H_{10})H]$	-2196.22332751	0.956649	1.012749	1.013693	0.855549
63 $[Ru(P^nBu_3)_2(DMAP)_2(C_{10}H_{16}NO)H]$	-3011.30785048	1.334305	1.409406	1.410350	1.212932

E_{298} unscaled zero-point vibrational energy correction at 298.15 K
U_{298} unscaled thermal correction to energy at 298.15 K
H_{298} unscaled thermal correction to enthalpy at 298.15 K
G_{298} unscaled thermal correction to Gibbs free enthalpy at 298.15 K

VI.4. Synthesis of natural products *via* hydroamidation of terminal alkynes

VI.4.1. General methods

Commercially available reagents and solvents were used as received unless otherwise noted. All solvents were purified according to standard procedures. Phenyl acetylene and DMF were distilled from CaH_2 under an inert atmosphere before use. Reactions were performed in oven-dried glassware containing a Teflon-coated stir bar, degassed, and purged with nitrogen.

HPLC analyses were performed on a Shimadzu High Performance Liquid Chromatograph using a Merck Reversed Phase LiChroCat© PAH C 18 column; particle diameter: 5 µm; oven temperature: 60°C; column pressure: 125 bar; eluent A: water, B: acetonitrile; gradient: 15% B for 2 min, linear increase to 85% B within 8 min, hold for 3.5 min, decrease to 15% B within 0.1 min, hold for 3 min; flow rate 1 mL/min.

Melting points are uncorrected.

NMR spectra were recorded on a Bruker FT-NMR DPX 200, DPX 400, or Bruker Avance 600 using $CDCl_3$ or DMSO-d_6 as solvents, with proton and carbon resonances at 200 MHz, 400 MHz or 600 MHz and 50 MHz, 101 MHz or 151 MHz, respectively. Chemical shifts are reported relative to the residual solvent peaks.

Mass spectra were acquired on a GC-MS Varian Saturn 2100 T with EI AGC ionization. The intensities of the signals are reported relative to the highest peak. High resolution mass spectra were acquired on a GC/HR-MS Waters GCT Premier. The ionization was done by EI AGC. The intensities of the signals are reported relative to the highest peak. Elemental analyses were measured on a Hanau Elemental Analyzer vario Micro cube.

VI.4.2. General procedures

Hydroamidation

An oven-dried flask was charged with the primary amide **Syn-1** or **Syn-9** (1.00 mmol), bis(2-methallyl)-cycloocta-1,5-diene-ruthenium(II) (16.0 mg, 0.05 mmol), 1,4-bis(dicyclohexylphosphinobutane (27.0 mg, 0.06 mmol) and ytterbium triflate (24.8 mg,

0.04 mmol) and flushed with nitrogen. Subsequently, dry DMF (3.0 mL), alkyne **Syn-2**, **Syn-10a** or **Syn-10b** (2.00 mmol), and water (108 μL, 6.00 mmol) were added *via* syringe. The resulting solution was stirred for 6 h at 60 °C.

To access the *Z*-enamides (**method A**), the reaction was worked up at this stage as detailed below.

To obtain the *E*-enamides (**method B**), 3 Å molecular sieves (500 mg) and triethylamine (200 μL) were added to the reaction mixture, and stirring was continued for 24 h at 110 °C, then the reaction was worked up as detailed below.

For the workup, the reaction mixtures were poured into aqueous sodium bicarbonate (30 mL). The resulting mixture was extracted with ethyl acetate (3 × 20 mL), the combined organic layers were washed with water (20 mL) and brine (20 mL), dried over magnesium sulfate, filtered, and the volatiles were removed in vacuo. The residue was purified by column chromatography (silica gel, ethyl acetate/hexane gradient).

Methylation of enamides

Sodium hydride (4 equiv.) was added portionwise at 0 °C to a solution of the enamide (1 equiv.) in dry THF (3 mL / mmol of enamide). The resulting mixture was stirred for 1 h at 0 °C, methyl iodide (2 equiv.) was added, and stirring was continued at room temperature overnight. The reaction was quenched with water, the layers were separated, and the aqueous layer was extracted with ethyl acetate (3 × 20 mL). The combined organic layers were washed with water (20 mL) and brine (20 mL), dried over magnesium sulfate, filtered, and the volatiles were removed *in vacuo*. The residue was purified by column chromatography (silica gel, ethyl acetate/hexane gradient).

Bestmann-Ohira reaction

Dimethyl-1-diazo-2-oxopropylphosphonate (1.2 equiv.) was added to a solution of the aldehyde (1 equiv.) and K_2CO_3 (2 equiv.) in dry MeOH (15 mL). The resulting mixture was stirred for 8 h at room temperature, diluted with Et_2O (25 mL), washed with aqueous sodium bicarbonate (10 mL), dried over magnesium sulfate, filtered, and the volatiles were removed *in vacuo*. The alkynes were obtained in analytically pure form.

VI.4.3. Syntheses of lansiumamides, lansamide and botryllamides

Synthesis of (*E*)-3-phenyl-*N*-[(*Z*)-2-phenylvinyl]acrylamide (lansiumamide A) (Syn-3) [CAS: 121817-36-5]

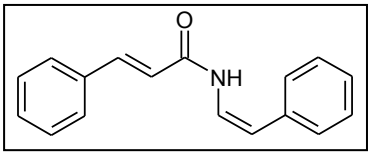

Compound **Syn-3** was synthesized following method A using 3-phenylacrylamide (**Syn-1**, 147 mg, 1.00 mmol) and ethynylbenzene (**Syn-2**, 220 µL, 2.00 mmol) and purified by column chromatography (1:8 ethyl acetate/hexane), yielding the product as a white solid (244 mg, 98%).

The spectroscopic data (NMR, GC-MS) matched those reported in the literature for lansiumamide A [CAS: 121817-36-5].[58]

^{1}H-NMR (600 MHz, $CDCl_3$): δ = 5.82 (d, *J* = 9.5 Hz, 1 H), 6.40 (d, *J* = 15.6 Hz, 1 H), 7.12 (dd, *J* = 11.3, 9.7 Hz, 1 H), 7.27 (t, *J* = 7.4 Hz, 1 H), 7.41 (t, *J* = 7.7 Hz, 2 H), 7.31–7.37 (m, 5 H), 7.50 (dd, *J* = 6.5, 2.7 Hz, 2 H), 7.71 (d, *J* = 15.6 Hz, 1 H), 7.87 (d, *J* = 11.0 Hz, 1 H).

^{13}C-NMR (151 MHz, $CDCl_3$): δ = 110.6, 119.4, 122.2, 127.0, 127.9, 128.0, 128.8, 129.1, 130.1, 134.4, 135.7, 143.0, 163.1.

MS (EI, 70 eV): *m/z* (%) = 249 (44, [M^+]), 131 (100), 119 (35) 103 (50), 77 (23), 51 (10).

IR (KBr) 3246, 3023, 1644, 1625, 1511, 1202 cm^{-1}.

Synthesis of (2*E*)-*N*-methyl-3-phenyl-*N*-[(*E*)-2-phenylvinyl]-acrylamide (lansiumamide B) (Syn-4) [CAS: 121817-37-6]

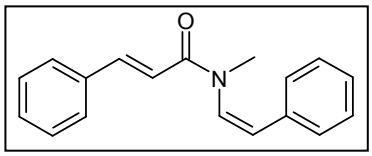

Compound **Syn-4** was synthesized following the general procedure for the methylation of enamides using enamide **Syn-3** (244 mg, 0.98 mmol) and methyl iodide (122 µL, 1.96 mmol) and purified by column chromatography (1:4 ethyl acetate/hexane), yielding the product as a yellow solid (216 mg, 82%).

The spectroscopic data (NMR, GC-MS) matched those reported in the literature for lansiumamide A [CAS: 121817-37-6].[58]

^{1}H-NMR (600 MHz, $CDCl_3$): δ = 3.08 (s, 3 H), 6.23 (d, *J* = 8.7 Hz, 1 H), 6.49 (d, *J* = 8.7

Hz, 1 H), 6.93 (d, *J* = 15.6 Hz, 1H), 7.20–7.25 (m, 1 H), 7.28–7.35 (m, 7 H), 7.44 (s, 1 H), 7.45 (d, *J* = 2.6 Hz, 1 H), 7.63 (d, *J* = 15.6 Hz, 1 H).

^{13}C-NMR (151 MHz, $CDCl_3$): δ = 34.6, 118.3, 125.0, 127.9, 128.0, 128.6, 128.7, 128.8, 129.6, 134.4, 135.1, 142.6, 166.4.

MS (EI, 70 eV): *m/z* (%) = 263 (26, [M^+]), 131 (100), 103 (63), 91 (10), 77 (33), 51 (13).

IR (NaCl) 3056, 3025, 1659, 1614, 1448, 1362 cm^{-1}.

Synthesis of (*E*)-3-phenyl-*N*-[(*E*)-2-phenylvinyl]acrylamide (Syn-5)

Compound **Syn-5** was synthesized following method B using 3-phenylacrylamide (147 mg, 1.00 mmol) and ethynylbenzene (220 µL, 2.00 mmol). Standard workup yield **Syn-5** as a crude product (85% yields determined by gas chromatography). Product **Syn-5** was used in the next reaction without further purifications.

Synthesis of (2*E*)-*N*-methyl-3-phenyl-*N*-[(*E*)-2-phenylvinyl]-acrylamide (lansamide I) (Syn-6) [CAS: 77527-97-0]

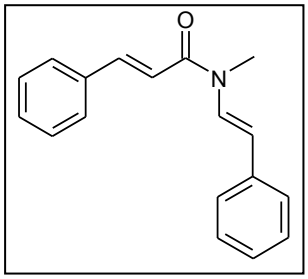

Compound **Syn-6** was synthesized following the general procedure for the methylation of enamides using enamide **Syn-5** (212 mg, 0.85 mmol) and methyl iodide (106 µL, 1.70 mmol) and purified by column chromatography (1:4 ethyl acetate/hexane), yielding the product **Syn-6** as a yellow solid (190 mg, 85%).

The spectroscopic data (NMR, GC-MS) matched those reported in the literature for lansiumamide A [CAS: 77527-97-0].[58]

^{1}H-NMR (200 MHz, $CDCl_3$): δ = 3.36 (s, 3 H), 6.06 (d, *J* = 14.5 Hz, 1 H), 7.02 (d, *J* = 15.5 Hz, 1 H), 7.19–7.43 (m, 8 H), 7.48–7.62 (m, 3 H), 7.76 (d, *J* = 15.2 Hz, 1 H).

^{13}C-NMR (50 MHz, $CDCl_3$): δ = 32.0, 112.6, 117.8, 126.2, 127.0, 128.4, 128.8, 128.9, 129.0, 129.2, 129.3, 130.4, 135.6, 137.2, 144.6, 166.0.

MS (EI, 70 eV): *m/z* (%) = 263 (26, [M^+]), 131 (100), 103 (65), 91 (11), 77 (35), 51 (13).

IR (KBr) 3079, 3023, 1635, 1607, 1380, 1113 cm^{-1}.

Synthesis of (*Z*)-3-(4-hydroxyphenyl)-2-methoxyacrylic acid [CAS: 690258-63-0]

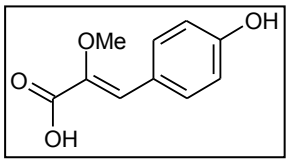

To a solution of sodium methanolate (10.81 g, 0.20 mol) in methanol (30% solution of NaOMe in MeOH, 40 mL) was added methyl 2-methoxyacetate (**7**, 11.9 mL, 0.12 mol) and the solution was stirred for 1 h at room temperature. 4-Hydroxybenzaldehyde (**Syn-8**, 4.89 g, 0.04 mol) dissolved in methanol (20 mL) was added dropwise to the reaction mixture, and the mixture was heated for 6 h under gentle reflux. After reaction completion, water (100 mL) was added and the methanol was removed *via* distillation. The reaction was acidified with concentrated hydrochloric acid until pH = 2 was reached. The product directly started to participate and the suspension was stirred for 1 h. The solid was then filtered and dried under high vacuum to yield (*Z*)-3-(4-hydroxyphenyl)-2-methoxyacrylic acid as a white solid (7.49 g, 96%).

^{1}H-NMR (600 MHz, DMSO) δ = 3.67 (s, 3 H), 6.79 (d, *J* = 8.7 Hz, 2 H), 6.86 (s, 1 H), 7.61 (d, *J* = 8.7 Hz, 2 H).

^{13}C-NMR (151 MHz, DMSO) δ = 58.5, 115.7, 123.2, 124.5, 131.8, 143.7, 158.5, 165.5.

MS (EI, 70 eV): *m/z* (%) = 194 (100, [M^{+}]), 151 (21), 123 (29), 107 (26), 77 (19), 51 (8).

Synthesis of (*Z*)-3-(4-hydroxyphenyl)-2-methoxyacrylamide (Syn-9)

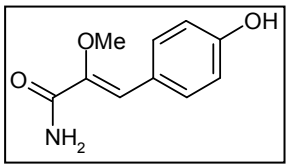

Oxalylchloride (1.1 ml, 21 mmol) diluted in dry methylene chloride (10 mL) was added dropwise to a solution of (*Z*)-3-(4-hydroxyphenyl)-2-methoxyacrylic acid (1.00 g, 10.3 mmol) in dry methylene chloride (15 mL). The reaction mixture was stirred under nitrogen at room temperature for 1 h. Solvent removal under vacuum gave a pale brown solid, which was immediately used for the next reaction without further purification. Methylene chloride (5 mL) and aqueous ammonia (12 mL) were added to the solution dropwise at room temperature. After 1 h water was added (15 ml) and the resulting two phases were separated. The aqueous layer was extracted with methylene chloride (3 × 60 mL), the combined organic layers were washed with water (60 mL), aqueous sodium bicarbonate (60 mL) and brine (60 mL), dried over $MgSO_4$, filtered and the solvent was removed under reduced pressure.

The residue was purified by column chromatography (silica gel, methanol) to yield the amide **Syn-9** as a white solid (753 mg, 70%). The structure of compound **Syn-9** was confirmed by X-ray crystal structure analysis.[59]

^{1}H-NMR (600 MHz, DMSO) δ = 3.57 (s, 3 H), 6.69 (s, 1 H), 6.79 (d, *J* = 8.7 Hz, 2 H), 7.32 (s, 1 H), 7.54 (d, *J* = 8.7 Hz, 2 H), 7.58 (s, 1 H), 9.79 (s, 1 H).

^{13}C-NMR (151 MHz, DMSO) δ = 39.5, 58.6, 115.6, 118.6, 124.5, 131.2, 147.4, 157.8, 165.7.

MS (EI, 70 eV): *m/z* (%) = 221 (100, [M^+]), 206 (19), 149 (29), 134 (86), 106 (29), 72 (44).

Synthesis of (*Z*)-3-(4-hydroxyphenyl)-2-methoxy-*N*-((*Z*)-4-methoxystyryl)acrylamide (Syn-12a)

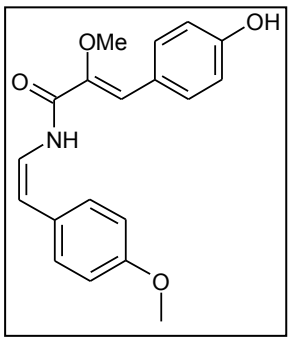

Compound **Syn-12a** was synthesized following method A using amide **Syn-9** (193 mg, 1.00 mmol) and 1-ethynyl-4-methoxybenzene (**Syn-10a**, 259 µL, 2.00 mmol) and purified by column chromatography (1:1 ethyl acetate/hexane), yielding the product as a white solid (318 mg, 98%). It was then recrystallized from ethanol/water.

The structure of compound **Syn-12a** was confirmed by X-ray crystal structure analysis.[60]

Mp 160-158°C

^{1}H-NMR (600 MHz, DMSO) δ = 3.64 (s, 3 H), 3.78 (s, 3 H), 5.82 (d, *J* = 9.6 Hz, 1 H), 6.85–6.74 (m, 3 H), 6.89 (s, 1 H), 7.01 (d, *J* = 8.7 Hz, 2 H), 7.35 (d, *J* = 8.7 Hz, 2 H), 7.59 (d, *J* = 8.7 Hz, 2 H), 9.15 (d, *J* = 10.8 Hz, 1 H), 9.91 (s, 1 H).

^{13}C-NMR (151 MHz, DMSO) δ = 55.2, 59.1, 111.3, 114.4, 115.7, 120.4, 120.5, 123.8, 127.9, 129.2, 131.7, 145.5, 158.1, 158.4, 161.4, 162.3.

EA Anal. Calcd for $C_{19}H_{19}NO_4$: C, 4.30; H, 70.14; N, 5.89.

Found: C, 4.32; H, 69.94; N, 5.94.

GC/HRMS-EI *m/z* [M^+] calcd for $C_{19}H_{19}NO_4$ 325.1314; found: 325.1301.

MS (EI, 70 eV): *m/z* (%) = 105 (5), 106 (17), 134 (100), 149 (74), 325 (61, [M^+]), 326 (13).

IR(KBr) 3321, 2932, 1602, 1511, 1487, 1252 cm^{-1}.

Synthesis of (*Z*)-3-(4-hydroxyphenyl)-2-methoxy-*N*-((*E*)-4-methoxystyryl)acrylamide (Botryllamide E) (Syn-11a) [CAS: 724434-03-1]

Compound **Syn-11a** was synthesized following method B using amide **Syn-9** (193 mg, 1.00 mmol) and 1-ethynyl-4-methoxybenzene (**Syn-10a**, 259 µL, 2.00 mmol) and purified by column chromatography (1:1 ethyl acetate/hexane), yielding the product **Syn-11a** as a yellow solid (190 mg, 85%).

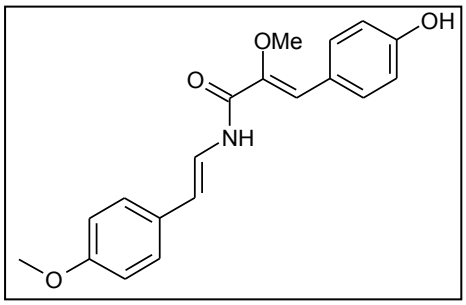

The spectroscopic data (NMR, GC-MS, IR) matched those reported in the literature for Botryllamide E [CAS: 724434-03-1].[61]

Mp 148-150°C

^{1}H-NMR (400 MHz, DMSO) δ = 3.61 (s, 3 H), 3.74 (s, 3 H), 6.50 (d, *J* = 14.7 Hz, 1 H), 6.91–6.79 (m, 5 H), 7.29 (d, *J* = 8.6 Hz, 2 H), 7.37 (dd, *J* = 14.7, 10.1 Hz, 1 H), 7.59 (d, *J* = 8.5 Hz, 2 H), 9.98 (s, *J* = 6.3 Hz, 1 H), 10.26 (d, *J* = 10.1 Hz, 1 H).

^{13}C-NMR (101 MHz, DMSO) δ = 55.1, 58.9, 113.1, 113.7, 114.2, 115.6, 119.8, 121.9, 124.1, 126.4, 129.1, 131.4, 146.3, 158.0, 158.2, 161.3.

EA Anal. Calcd for $C_{19}H_{19}NO_4$: C, 4.30; H, 70.14; N, 5.89.

Found: C, 4.44; H, 70.22; N, 6.08.

GC/HRMS-EI *m/z* [M^+] calcd for $C_{19}H_{19}NO_4$ 325.1314; found: 325.1339.

MS (EI, 70 eV): *m/z* (%) = 77 (13), 106 (18), 134 (100), 149 (61), 219 (10), 325 (45, [M^+]).

IR (KBr) 3327, 2932, 1605, 1511, 1246, 1171 cm^{-1}.

Synthesis of 2-bromo-4-ethynyl-1-methoxybenzene (Syn-10b) [CAS: 724434-03-1]

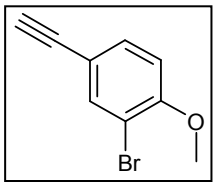

Compound **Syn-10b** was synthesized following the method for the synthesis of alkynes from aldehydes using 3-bromo-4-methoxybenzaldehyde (**Syn-13**, 2.15 g, 10.00 mmol), potassium carbonate (2.76 g, 20.00 mmol) and dimethyl-1-diazo-2-oxopropylphosphonate (**Syn-14**, 2.38 g, 12.00 mmol), yielding the product as a white solid (2.16 g, 99%).

^{1}H-NMR (400 MHz, $CDCl_3$) δ = 3.02 (s, 1 H), 3.89 (s, 3 H), 6.81 (d, *J* = 8.5 Hz, 1 H), 7.40 (dd, *J* = 8.5, 2.0 Hz, 1 H), 7.67 (d, *J* = 2.0 Hz, 1 H).

^{13}C-NMR (101 MHz, $CDCl_3$) δ = 56.3, 76.8, 82.1, 111.4, 111.5, 115.7, 132.6, 136.8, 156.5.

MS (EI, 70 eV): *m/z* (%) = 212 (100, [M^+]), 197 (17), 169 (26), 116 (12), 88 (24), 62 (16).

Synthesis of (*Z*)-*N*-((*Z*)-3-bromo-4-methoxystyryl)-3-(4-hydroxyphenyl)-2-methoxyacrylamide (Syn-12b)

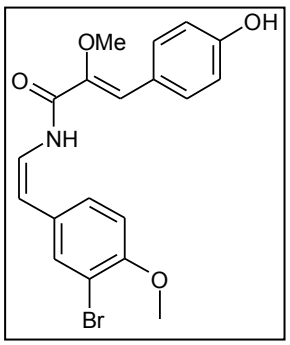

Compound **Syn-12b** was synthesized following method A using amide **Syn-9** (193 mg, 1.00 mmol) and 2-bromo-4-ethynyl-1-methoxybenzene (**Syn-10b**, 422 mg, 2.00 mmol) and purified by column chromatography (1:1 ethyl acetate/hexane), yielding the product as a colorless oil (357 mg, 88%).

^{1}H-NMR (400 MHz, DMSO) δ = 3.67 (s, 3 H), 3.87 (s, 3 H), 5.79 (d, *J* = 9.6 Hz, 1 H), 6.90–6.75 (m, 4 H), 7.17 (d, *J* = 8.6 Hz, 1 H), 7.39 (dd, *J* = 8.5, 1.8 Hz, 1 H), 7.59 (d, *J* = 8.6 Hz, 2 H), 7.66 (d, *J* = 1.8 Hz, 1 H), 9.30 (d, *J* = 10.5 Hz, 1 H), 9.90 (s, 1 H).

^{13}C-NMR (101 MHz, DMSO) δ = 56.3, 59.0, 110.1, 110.9, 112.9, 115.7, 120.5, 121.6, 123.8, 128.6, 129.6, 131.7, 132.2, 145.6, 154.1, 158.3, 161.6.

EA Anal. Calcd for $C_{19}H_{18}BrNO_4$: C, 3.46; H, 56.45; N, 4.49.

Found: C, 3.14; H, 56.07; N, 4.78.

GC/HRMS-EI *m/z* [M^+] calcd for $C_{19}H_{18}BrNO_4$ 403.0419 and 405.0399; found: 403.0410 and 405.0392.

MS (EI, 70 eV): *m/z* (%) = 106 (20), 134 (100), 227 (17), 229 (17), 403 (23,

[M^+]), 405 (23, [M^+]).

IR (KBr) 3306, 2932, 1657, 1600, 1513, 1477 cm^{-1}.

Synthesis of (*Z*)-*N*-((*E*)-3-bromo-4-methoxystyryl)-3-(4-hydroxyphenyl)-2-methoxyacrylamide (Botryllamide C) (Syn-11b) [CAS: 163564-66-7]

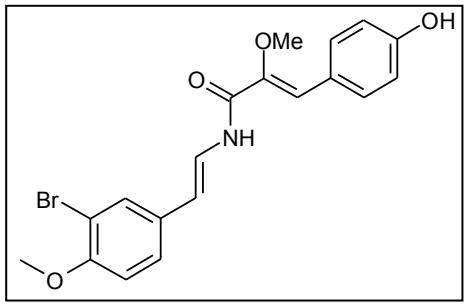

Compound **Syn-11b** was synthesized following method B using amide **Syn-9** (193 mg, 1.00 mmol) and 2-bromo-4-ethynyl-1-methoxybenzene (**Syn-10b**, 422 mg, 2.00 mmol) and purified by column chromatography (1:1 ethyl acetate/hexane), yielding the product as a white solid (357 mg, 88%). The spectroscopic data (NMR, GC-MS, IR) matched those reported in the literature for Botryllamide C [CAS: 163564-66-7].[62]

Mp 169-173°C

^{1}H-NMR (400 MHz, DMSO) δ = 3.62 (s, 3 H), 3.83 (s, 3 H), 6.44 (d, *J* = 14.6 Hz, 1 H), 6.81 (d, *J* = 6.6 Hz, 3 H), 7.04 (d, *J* = 8.6 Hz, 1 H), 7.50–7.28 (m, 2 H), 7.65–7.51 (m, 3 H), 9.86 (s, 1 H), 10.31 (d, *J* = 10.1 Hz, 1 H).

^{13}C-NMR (101 MHz, DMSO) δ = 56.2, 58.8, 111.1, 111.5, 113.0, 115.6, 119.8, 123.2, 124.1, 125.6, 129.3, 130.9, 131.3, 146.2, 153.8, 158.0, 161.4.

EA Anal. Calcd for $C_{19}H_{18}BrNO_4$: C, 3,46; H, 56.45; N, 4.49.

Found: C, 3.18; H, 56.15; N, 4.72.

GC/HRMS-EI *m/z* [M^+] calcd for $C_{19}H_{18}BrNO_4$ 403.0419 and 405.0399; found: 403.0387 and 405.0370.

MS (EI, 70 eV): *m/z* (%) = 134 (100), 149 (16), 227 (16), 229 (16), 403 (31, [M^+]), 405 (31, [M^+]).

IR (KBr) 3153, 2943, 1600, 1512, 1488, 1257 cm^{-1}.

VI.4.4. Preparation of starting materials for synthesis of coscinamide A & B, and chondriamide A & C

Synthesis of indole-3-glyoxylamide (IV.1-8) (CAS NO.: 58117-28-5)

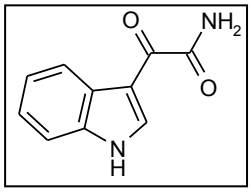

To a solution of indole (3.00 g, 25.6 mmol) in dry ether (100 mL) cooled to 0 °C, oxallylchloride (2.82 mL, 29.7 mmol) was added dropwise over 30 min. The reaction mixture was stirred at 0 °C for 3 h, and then allowed to warm to room temperature for 1 h. The resulting yellow crystals were collected by filtration under nitrogen, washed with cold ether (2 x 30 mL) and dried under vacuum. Gaseous ammonia was bubbled through a suspension of the yellow crystals in dry chloroform (40 mL) over 15 min. After stirring for 1 h, the solvent was removed under reduced pressure. The resulting crude was suspended in water (100 mL) and extracted with ethyl acetate. The combined organic layers were dried over $MgSO_4$, filtered and the solvent was removed under reduced pressure. The crude was washed with cold ethyl acetate and dried under high vacuum to yield the product (3.35 g, 70%) which was used without further purification.

^{1}H-NMR (400 MHz, DMSO): δ = 7.22–7.27 (m, 2H), 7.50–7.54 (m, 1H),. 7.70 (s, 1H), 8.08 (s, 1H), 8.19–8.23 (m, 1H) , 8.67 (s, 1H).

^{13}C-NMR (101 MHz, DMSO): δ = 112.1, 112.4, 121.2, 122.4, 123.3, 126.1, 136.2, 138.1, 166.0, 182.8.

MS (EI, 70 eV): *m/z* (%) = 63 (12), 89 (24), 116 (32), 144 (100), 188 (17, [M^+]).

Synthesis of 1*H*-indol-3-yl-*N*-[(*Z*)-2-phenylvinyl]glyoxylamide (IV.1-12)

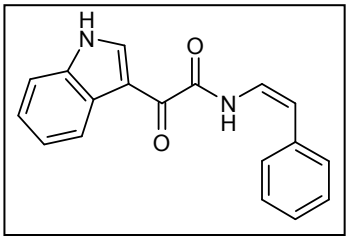

Compound **IV.1-12** was synthesized following method A using indole-3-glyoxylamide (**IV.1-8)**, 188.0 mg, 1.00 mmol) and phenyl acetylene (220 µL, 2.00 mmol) and purified by column chromatography (1:3 ethyl acetate/hexane), yielding the product as a greenish solid (18:1 mixture with the *E*-isomer, 185.0 mg, 64%).

^{1}H-NMR (400 MHz, $CDCl_3$): δ = 5.99 (d, *J* = 9.4 Hz, 1H), 6.99 (dd, *J* = 11.9, 9.6 Hz, 1H), 7.27–7.35 (m, 4H), 7.36–7.46 (m, 5H), 8.41 (d, *J* = 7.4 Hz, 1H), 9.28 (s, 1H), 9.06 (s, 1H), 9.82 (d, *J* = 11.7 Hz, 1H).

^{13}C-NMR (101 MHz, $CDCl_3$): δ = 111.7, 113.3, 113.7, 120.4, 122.4, 123.6, 124.4, 126.5, 127.3, 128.0, 129.2, 135.2, 135.7, 138.4, 159.5, 179.4.

MS (EI, 70 eV): *m/z* (%) = 63 (9), 89 (24), 116 (28), 144 (100), 290 (49, [M^+]).

EA Anal. Calcd for $C_{18}H_{14}N_2O_2$: C, 74.47; H, 4.86; N, 9.65.

Found: C, 74.56; H, 5.05; N, 9.61.

Two step synthesis of dimethyl-1-diazo-2-oxopropylphosphonate (IV.1-22, Bestmann-Ohira reagent) (CAS NO.: 90965-06-3)[63]

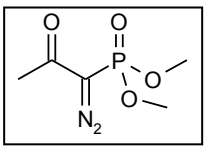

To a stirred suspension of potassium iodide (33.2 g, 200 mmol) in acetone (40mL) and MeCN (50 mL) was added chloroacetone (16.1 mL, 200 mmol). Stirring was continued for 1 h at r.t. Trimethyl phosphite (24.4 mL, 200 mmol) was slowly added. After 12 h at r.t., the mixture was heated to 50 °C to ensure complete conversion. Filtration through a pad of Celite and evaporation of the solvents under reduced pressure yielded the crude product. Distillation under vacuum (0.5 mbar) furnished the product **IV.1-20** as a colorless liquid (17.7 g, 53%).

^{1}H-NMR (400 MHz, $CDCl_3$): δ = 2.26 (s, 3H), 3.05 (d, *J* = 22.9 Hz, 2H), 3.72 (s, 3H), 3.74 (s, 3H).

^{13}C-NMR (101 MHz, $CDCl_3$): δ = 31.1, 41.3, 42.9, 52.6 (d, *J* = 6.5 Hz), 200.1.

MS (EI, 70 eV): *m/z* (%) = 79 (48), 94 (53), 109 (46), 124 (61), 167 (100, [M^+]).

A 250 mL, three-necked flask was equipped with a stirrer and an addition funnel. To a ice cold solution of NaH (2.20 g of 60% in paraffin, 55 mmol) in toluene (125 mL) and THF (25 mL) phosphonate **IV.1-20** (8.31 g, 50 mmol) is slowly added.; 35 mmol). After the gas evolution had ceased, a solution of tosylazide (9.86 g, 50 mmol) in toluene (25 mL) was added dropwise; the highly viscous suspension slowly discolored to yellow-brown and stirring became easier. After 2 h the mixture is filtered through a pad of Celite, the solvent was removed under reduced pressure and the crude was further purified by chromatography (1:4 ethyl acetate/hexane), yielding the product as yellow oil (7.0 g, 73%).

^{1}H-NMR (400 MHz, $CDCl_3$): δ = 2.25 (s, 3H), 3.81 (s, 3H), 3.84 (s, 3H).

^{13}C-NMR (101 MHz, $CDCl_3$): δ = 53.48, 53.54, 127.9 (d, *J* = 323.7 Hz), 189.8 (d, *J* = 13.0 Hz).

^{31}P-NMR (162 MHz, $CDCl_3$): δ = 15.5.

Synthesis of 1-tosyl-1*H*-indole-3-carbaldehyde (IV.1-24) (CAS NO.: 50562-79-3)

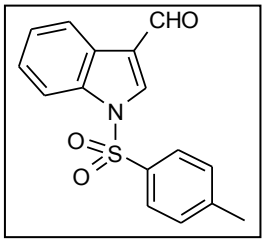

A mixture of 3-formyl-indole (20.0 g, 138 mmol) and sodium hydroxide (12.2 g, 305 mmol) in DCM (700 mL) was stirred for 15 min, and then toluenesulfonyl chloride (32.0 g, 168 mmol) was added. The reaction mixture was heated to 40 °C and stirred for 2 h. The solution was quenched with ammonia solution (25%, 75 mL) and water (75 mL) and stirred for 2 h at 35 °C. The organic layer was separated and washed with water (200 mL). The combined organic layers were dried over $MgSO_4$, filtered and the solvent was removed under reduced pressure to yield the product as red solid (38.3 g, 92,7%).

^{1}H-NMR (400 MHz, $CDCl_3$): δ = 2.34 (s, 3H), 7.27 (d, *J* = 8.2 Hz, 2H), 7.32–7.41 (m, 2H), 7.84 (d, *J* = 8.6 Hz, 2H), 7.94 (d, *J* = 7.8 Hz, 1H), 8.22–8.25 (m, 2H), 10.08 (s, 1H).

^{13}C-NMR (101 MHz, $CDCl_3$): δ = 21.5, 113.2, 122.4, 122.5, 125.0, 126.2, 126.3, 127.2, 130.3, 134.4, 135.2, 136.1, 146.1, 185.2.

MS (EI, 70 eV): *m/z* (%) = 65 (25), 91 (100), 116 (22), 155 (77), 299 (86, $[M^+]$).

Synthesis of 3-ethynyl-1-tosyl-1*H*-indole (IV.1-25) (CAS NO.: 765914-04-3) ARN202,211,218

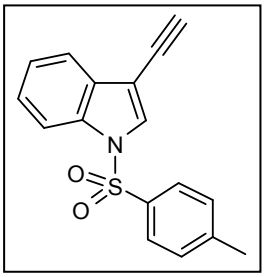

Dimethyl 1-diazo-2-oxopropylphosphonate **IV.1-22** (12.1 g, 9.48 mL, 60 mmol) was added to a solution of aldehyde **IV.1-24** (15.8 g, 50 mmol), potassium carbonate (13.8, 100.0 mmol) and methanol (16.0 g, 20.3 mL, 500 mmol) in THF (100 mL) and stirring was continued for 72 h. The solvent was removed under reduced pressure and the resulting crude was extracted with a solution of ethyl acetate: hexane (3:7, 400 mL). The solution was dried over magnesium sulfate, filtered, and the volatiles were removed in vacuo.

The residue was purified by column chromatography (1:9 ethyl acetate/hexane), yielding the product as a white solid (5.90 g, 42%).

^{1}H-NMR (400 MHz, $CDCl_3$): δ = 2.33 (s, 3H), 3.25 (s, 1H), 7.22 (d, *J* = 8.3 Hz, 2H), 7.29 (t, *J* = 7.0 Hz, 1H), 7.35 (t, *J* = 7.2 Hz, 1H), 7.63 (d, *J* = 7.6 Hz, 1H), 7.75–7.79 (m, 3H), 7.96 (d, *J* = 8.3 Hz, 1H).

^{13}C-NMR (101 MHz, $CDCl_3$): δ = 21.5, 75.0, 81.5, 104.1, 113.6, 120.5, 123.8, 125.5, 127.0, 130.0, 130.0, 130.8, 134.2, 135.1, 145.4.

MS (EI, 70 eV): *m/z* (%) = 91 (43), 113 (22), 140 (51), 155 (30), 295 (100, $[M^+]$).

EA Anal. Calcd for $C_{17}H_{13}NO_2S$: C, 69.13; H, 4.44; N, 4.74; S, 10.86.

Found: C, 69.15; H, 4.39; N, 4.50; S, 10.97.

VI.5. Silver(I)/DMSO catalyzed carboxylation of terminal alkynes

VI.5.1. General Methods

Reactions were performed in oven-dried glassware under a carbon dioxide atmosphere containing a teflon-coated stirrer bar and dry septum. For the exclusion of atmospheric oxygen from the reaction media, the solvent was degassed with nitrogen before the reagents were mixed. Solvents were purified by standard procedures prior to use. All reactions were monitored by GC using *n*-tetradecane as an internal standard. Response factors of the products with regard to *n*-tetradecane were obtained experimentally by analyzing known quantities of the substances. GC analyses were carried out using an HP-5 capillary column (Phenyl Methyl Siloxane 30 m x 320 x 0.25, 100/2.3-30- 300/3) and a time program beginning with 2 min at 60 °C followed by 30 °C/min ramp to 300 °C, then 3 min at this temp. Column chromatography was performed using a Combi Flash Companion-Chromatography-System (Isco-Systems) and Redi*Sep* packed columns (12 g). NMR spectra were obtained on Bruker AMX 400 or on Bruker Avance 600 systems using $CDCl_3$, methanol-d_4 and DMSO-d_6 as solvents, with proton and carbon resonances at 400/600 MHz and 101/151 MHz, respectively. Mass spectral data were acquired on a GC-MS Saturn 2100 T (Varian). IR spectra were measured using a Perkin Elmer FT-IR system or a Perkin Elmer Spectrum 100 FT-IR spectrometer equipped with an Universal ATR Accessory (UATR). Elemental analyses were carried out using a vario Micro tube (Elementar Analysetechnik/Hanau). GC/HRMS spectra were obtained on a GCT Premier (WATERS).

DMSO, DMF and all alkynes were dried using CaH_2 followed by fractioned distillation prior to use. Copper and silver salts were dried *in vacuo* at 80 °C prior to use. The cesium salt was dried for 1 hour *in vacuo* at 125 °C prior to use. CO_2 was supplied by Air Liquide with a purity of 4.5. All other commercially available compounds were used without further purification.

VI.5.2. Experimental Procedures

Standard procedure for the carboxylation of terminal alkynes.

A vessel was charged with cesium carbonate (399 mg, 1.20 mmol). To this, a solution of silver tetrafluoroborate (0.1 mg, 0.50 µmol) in DMSO (0.10 mL) and DMSO (2.90 mL) were added. The reaction vessel was purged with CO_2 using 3 alternate cycles of vacuum and CO_2, and the alkyne (**CCC-1a**−**CCC-1u**) (1.00 mmol) was added *via* syringe. The resulting mixture was stirred for 16 h at 50 °C at ambient CO_2 pressure. The reaction mixture was cooled down to room temperature and the solvent was removed by lyophilization. The resulting salt was dissolved in H_2O (10.0 mL) and extracted with *n*-hexane (3 x 20.0 mL). Then the aqueous layer was acidified with aqueous HCl (1N, 2.00 mL) and extracted with ethyl acetate (3x30 mL). The combined organic layers were washed with brine (10.0 mL), dried over $MgSO_4$, filtered and the volatiles were removed *in vacuo* to afford the corresponding acids **CCC-3a**−**CCC-3u**.

Synthesis of 2-nonynoic acid (CCC-3a): Compound **CCC-3a** was prepared following the standard procedure, starting from 1-octyne (1a) (110 mg, 149 µL, 1.00 mmol). After purification **CCC-3a** was isolated as a colorless liquid (152 mg, 99%). ^{1}H NMR (400 MHz, $CDCl_3$) δ= 9.90 (br. s., 1 H), 2.34 (t, *J*=7.2 Hz, 2 H), 1.57 (quin, *J*=7.3 Hz, 2 H), 1.22 − 1.43 (m, 6 H), 0.88 (t, *J*=6.9 Hz, 3 H) ppm. ^{13}C NMR (101 MHz, $CDCl_3$) δ= 158.4 (s), 92.7 (s), 72.6 (s), 31.1 (s), 28.4 (s), 27.3 (s), 22.4 (s), 18.6 (s), 13.9 (s) ppm. IR (ATR) 2930, 2236, 1683, 1276, 1232 cm^{-1}. GC/HRMS-EI m/z [M^+] calcd. for $C_9H_{14}O_2$ 154.0994; found: 154.1000.

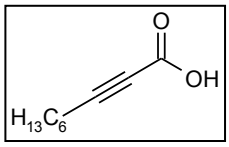

The spectroscopic data (NMR, IR) matched those reported in the literature for 2-nonynoic acid (**CCC-3a**) [CAS: 1846-70-4].

Synthesis of 2-octynoic acid (CCC-3b): Compound **CCC-3b** was prepared following the standard procedure, starting from 1-heptyne (**CCC-1b**) (98.1 mg, 134 µL, 1.00 mmol). After purification **CCC-3b** was isolated as a colorless liquid (133 mg, 95%). ^{1}H NMR (400 MHz, $CDCl_3$) δ= 10.23 (br. s., 1 H), 2.34 (t, *J*=7.2 Hz, 2 H), 1.58 (quin, *J*=7.3 Hz, 2 H), 1.26 − 1.42 (m, 4 H), 0.84 − 0.93 (m, 3 H) ppm. ^{13}C NMR (101 MHz, $CDCl_3$) δ= 158.5 (s), 92.7 (s), 72.6 (s), 30.9 (s), 27.0 (s), 22.0 (s), 18.6 (s), 13.7 (s) ppm. IR (ATR) 2931, 2235, 1709, 1244, 1077 cm^{-1}. GC/HRMS-EI m/z [M^+] calcd. for $C_8H_{12}O_2$ 140.0837; found: 140.0836.

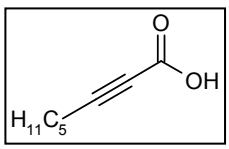

The spectroscopic data (NMR, IR) matched those reported in the literature for 2-octynoic acid (**CCC-3b**) [CAS: 5663-96-7].

Synthesis of 2-heptynoic acid (CCC-3c): Compound **CCC-3c** was prepared following the standard procedure, starting from 1-hexyne (**CCC-1c**) (82.2 mg, 116 µL, 1.00 mmol). After purification **CCC-3c** was isolated as a colorless liquid (126 mg, 97%). ^{1}H NMR (400 MHz, $CDCl_3$) δ= 10.46 (br. s., 1 H), 2.35 (t, *J*=7.2 Hz, 2 H), 1.50 − 1.62 (m, 2 H), 1.33 − 1.48 (m, 2 H), 0.91 (t, *J*=7.3 Hz, 3 H) ppm. ^{13}C NMR (101 MHz, $CDCl_3$) δ= 158.5 (s), 92.7 (s), 72.5 (s), 29.3 (s), 21.8 (s), 18.3 (s), 13.3 (s) ppm. IR (ATR) 2935, 2235, 1682, 1232, 757 cm^{-1}. GC/HRMS-EI m/z [M^+] calcd. for $C_7H_{10}O_2$ 126.0681; found: 126.0670.

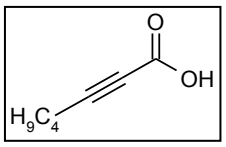

The spectroscopic data (NMR, IR) matched those reported in the literature for 2-heptynoic acid (**CCC-3c**) [CAS: 1483-67-6].

Synthesis of 6-chloro-hex-2-ynoic acid (CCC-3d): Compound **CCC-3d** was prepared following the standard procedure, starting from 5-chloropent-1-yne (**CCC-1d**) (105 mg, 109 µL, 1 mmol) using 0.25 mol% $AgBF_4$ and stirring for 16 h at 40 °C at ambient CO_2 pressure. After purification **CCC-3d** was isolated as a yellow liquid (31 mg, 21%). ^{1}H NMR (400 MHz, methanol-d_4) δ= 3.63 − 3.71 (m, 2 H), 2.51 − 2.60 (m, 2 H), 2.01 (quin, *J*=6.7 Hz, 2 H) ppm. ^{13}C NMR (151 MHz, methanol-d_4) δ= 156.4 (s), 88.3 (s), 65.5 (s), 44.3 (s), 31.8 (s), 16.7 (s) ppm. IR (ATR) 2970, 2237, 1685, 1231, 751 cm^{-1} GC/HRMS-EI m/z [M^+] calcd. for $C_6H_7ClO_2$ 146.0135; found: 146.0134.

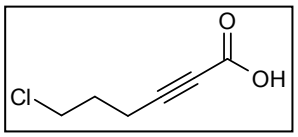

Synthesis of 4-methoxy-but-2-ynoic acid (CCC-3e): Compound **CCC-3e** was prepared following the standard procedure, starting from methylpropargylether (**CCC-1e**) (70.1 mg, 84.4 µL, 1.00 mmol) using 0.25 mol% $AgBF_4$. After purification **CCC-3e** was isolated as a colorless liquid (106 mg, 93%). ^{1}H NMR (400 MHz, $CDCl_3$) δ= 9.23 (br. s., 1 H), 4.27 (s, 2 H), 3.43 (s, 2 H) ppm. ^{13}C NMR (101 MHz, $CDCl_3$) δ= 156.2 (s), 85.1 (s), 77.9 (s), 59.3 (s), 58.0 (s) ppm. IR (ATR) 2939, 2239, 1695, 1229, 1092 cm^{-1}. GC/HRMS-EI m/z [M^+] calcd. for $C_5H_6O_3$ 114.0317; found: 114.0312.

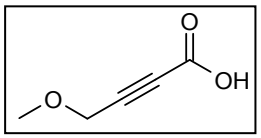

The spectroscopic data (NMR, IR) matched those reported in the literature for 4-methoxy-but-2-ynoic acid (**CCC-3f**) [CAS: 24303-64-8].

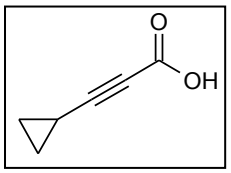

Synthesis of 3-cyclopropyl-prop-2-ynoic acid (CCC-3f): Compound **CCC-3f** was prepared following the standard procedure, starting from cyclopropylacetylene (**CCC-1f**) (68.1 mg, 1.00 mmol). After purification **CCC-3f** was isolated as a white solid (104 mg, 95%, m.p. 56.7 °C). ^{1}H NMR (400 MHz, DMSO-d_6) δ= 1.49 (tt, *J* =8.3, 5.0 Hz, 1 H), 0.87 – 0.97 (m, 2 H), 0.75 – 0.85 (m, 2 H) ppm. ^{13}C NMR (101 MHz, DMSO-d_6) δ= 154.2 (s), 92.1 (s), 69.5 (s), 8.9 (s), -1.2 (s) ppm. IR (ATR) 2216, 1663, 1411, 1280, 857 cm^{-1}. GC/HRMS-EI m/z [M^+] calcd. for $C_6H_6O_2$ 110.0368; found: 110.0363.

The spectroscopic data (NMR, IR) matched those reported in the literature for 3-cyclopropylprop-2-ynoic acid (**CCC-3f**) [CAS: 7358-93-2].

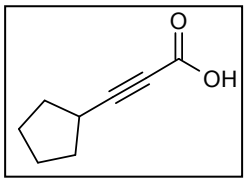

Synthesis of 3-cyclopentyl-prop-2-ynoic acid (CCC-3g): Compound **CCC-3g** was prepared following the standard procedure, starting from cyclopentylacetylene (**CCC-1g**) (99.1 mg, 122 µL, 1.00 mmol). After purification **CCC-3g** was isolated as a white solid (96 mg, 70%, m.p. 48.0 °C). ^{1}H NMR (400 MHz, DMSO-d_6) δ= 2.66 – 2.93 (m, 1 H), 1.86 – 1.98 (m, 2 H), 1.49 – 1.70 (m, 6 H) ppm. ^{13}C NMR (101 MHz, DMSO-d_6) δ= 154.4 (s), 91.9 (s), 73.7 (s), 32.7 (s), 28.9 (s), 24.8 (s) ppm. IR (ATR) 2969, 2233, 1670, 1408, 1268 cm^{-1}. GC/HRMS-EI m/z [M^+] calcd. for $C_8H_{10}O_2$ 138.0681; found: 138.0680.

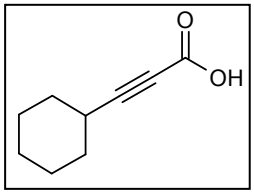

Synthesis of 3-cyclohexyl-prop-2-ynoic acid (CCC-3h): Compound **CCC-3h** was prepared following the standard procedure, starting from cyclohexylacetylene (**CCC-1h**) (110 mg, 133 µL, 1.00 mmol). After purification **CCC-3h** was isolated as a yellow liquid (149 mg, 98%). ^{1}H NMR (400 MHz, $CDCl_3$) δ= 7.42 (br. s., 1 H), 2.47 − 2.72 (m, 1 H), 1.65 − 1.88 (m, 4 H), 1.44 − 1.59 (m, 3 H), 1.24 − 1.44 (m, 3 H) ppm. ^{13}C NMR (101 MHz, $CDCl_3$) δ= 158.1 (s), 95.9 (s), 72.6 (s), 31.3 (s), 28.9 (s), 25.5 (s), 24.6 (s) ppm. IR (ATR) 2931, 2228, 1681, 1235, 755 cm^{-1}. GC/HRMS-EI m/z [M^+] calcd. for $C_9H_{12}O_2$ 152.0837; found: 152.0837.

The spectroscopic data (NMR, IR) matched those reported in the literature for 3-cyclohexyl-prop-2-ynoic acid (**CCC-3h**) [CAS: 4361-27-7].

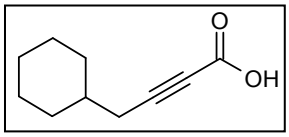

Synthesis of 4-cyclohexyl-2-butynoic acid (CCC-3i): Compound **CCC-3i** was prepared following the standard procedure, starting from 3-cyclohexyl-1-propyne (**CCC-1i**) (126 mg, 149 µL, 1.00 mmol). After purification **CCC-3i** was isolated as a white solid (166 mg, 99%, m.p.

72.1 °C). ^{1}H NMR (400 MHz, $CDCl_3$) δ= 11.18 (br. s., 1 H), 2.25 (d, *J* =6.6 Hz, 2 H), 1.54 − 1.82 (m, 5 H), 1.11 − 1.30 (m, 3 H), 0.96 − 1.06 (m, 2 H) ppm. ^{13}C NMR (101 MHz, $CDCl_3$) δ= 158.7 (s), 91.9 (s), 73.4 (s), 36.5 (s), 32.5 (s), 26.4 (s), 25.9 (s), 25.9 (s) ppm. IR (ATR) 2922, 2233, 1669, 1422, 1275 cm^{-1}. Anal. Calcd. for $C_{10}H_{14}O_2$: C, 72.3%; H, 8.5%. Found: C, 72.2%; H, 8.3%. GC/HRMS-EI m/z [M^+] calcd. for $C_{10}H_{14}O_2$ 166.0994; found: 166.0991.

The spectroscopic data (NMR, IR) matched those reported in the literature for 4-cyclohexyl-2-butynoic acid (**CCC-3i**) [CAS: 5962-81-2].

Synthesis of 5-phenyl-pent-2-ynoic acid (CCC-3j): Compound **CCC-3j** was prepared following the standard procedure, starting from 4-phenyl-1-butyne (**CCC-1j**) (133 mg, 144 µL, 1.00 mmol). After purification **CCC-3j** was isolated as a yellow solid (169 mg, 97%, m.p. 54.7 °C). ^{1}H NMR (400 MHz, $CDCl_3$) δ= 10.18 (br. s., 1 H), 7.28 − 7.40 (m, 3 H), 7.25 (s, 1 H), 2.89 − 2.98 (m, 2 H), 2.62 − 2.75 (m, 2 H) ppm. ^{13}C NMR (101 MHz, $CDCl_3$) δ= 158.1 (s), 139.3 (s), 128.5 (s), 128.2 (s), 126.6 (s), 91.4 (s), 73.2 (s), 33.5 (s), 20.8 (s) ppm. IR (ATR) 2237, 1674, 1406, 1270, 697 cm^{-1}. Anal. Calcd. for $C_{11}H_{10}O_2$: C, 75.8%; H, 5.8%. Found: C, 75.5%; H, 5.9%.

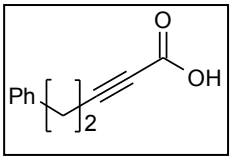

The spectroscopic data (NMR, IR) matched those reported in the literature for 5-phenyl-pent-2-ynoic acid (**CCC-3j**) [CAS: 3350-93-4].

Synthesis of (4-propylphenyl)propynoic acid (CCC-3k): Compound **CCC-3k** was prepared following the standard procedure, starting from 1-ethynyl-4-propylbenzene (**CCC-1k**) (144 mg, 158 µL, 1.00 mmol) using 0.25 mol% $AgBF_4$. After purification **CCC-3k** was isolated as a white solid (187 mg, 99%, m.p. 111.3 °C). ^{1}H NMR (400 MHz, DMSO-d_6) δ= 7.49 (m, *J*=8.2 Hz, 2 H), 7.23 (m, *J* =8.2 Hz, 2 H), 1.54 (sxt, *J* =7.4 Hz, 2 H), 0.79 − 0.91 (m, 3 H) ppm. ^{13}C NMR (101 MHz, DMSO-d_6) δ= 154.6 (s), 145.7 (s), 132.7 (s), 129.1 (d, *J* =20.9 Hz) 116.4 (s) 84.9 (s) 81.6 (s) 37.3 (t, *J* =22.3 Hz) 23.8 (t, *J* =37.7 Hz) 13.6 (q, *J* =20.0 Hz) ppm. IR (ATR) 2959, 2200, 1667, 1307, 1213 cm^{-1}. GC/HRMS-EI m/z [M^+] calcd. for $C_{12}H_{12}O_2$ 188.0837; found: 188.0836.

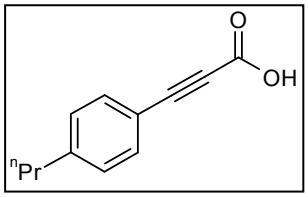

Synthesis of (2-methylphenyl)propynoic acid (CCC-3l): Compound **CCC-3l** was prepared following the standard procedure, starting from 2-ethynyltouluene (**CCC-1l**) (120 mg, 130 µL, 1.00 mmol) using 0.25 mol% $AgBF_4$. After purification **CCC-3l** was isolated as a white solid (147 mg, 92%, m.p. 94.0 °C). ^{1}H NMR (400 MHz, methanol-d_4) δ= 7.50 − 7.53

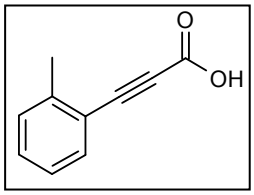

(m, 1 H), 7.36 (dd, *J*=7.6, 1.5 Hz, 1 H), 7.29 (d, *J*=7.6 Hz, 1 H), 7.21 (t, *J*=7.6 Hz, 1 H), 2.46 (s, 3 H) ppm. ^{13}C NMR (101 MHz, methanol-d_4) δ= 156.9 (s), 143.3 (s), 134.4 (s), 132.0 (s), 131.1 (s), 127.2 (s), 120.8 (s), 85.9 (s), 85.7 (s), 20.7 (s) ppm. IR (ATR) 2193, 1685, 1362, 1205, 758 cm^{-1}. Anal. Calcd. for $C_{10}H_8O_2$: C, 75.0%; H, 5.0%. Found: C, 75.0%; H, 5.2%.

The spectroscopic data (NMR, IR) matched those reported in the literature for (2-methylphenyl)propynoic acid (**CCC-3l**) [CAS: 7515-27-7].

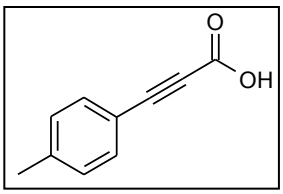

Synthesis of (4-methylphenyl)propynoic acid (CCC-3m): Compound **CCC-3m** was prepared following the standard procedure, starting from 4-ethynyltouluene (**CCC-1m**) (116 mg, 127 µL, 1.00 mmol) using 0.25 mol% $AgBF_4$. After purification **CCC-3m** was isolated as a white solid (155 mg, 97%, m.p. 148.2 °C). ^{1}H NMR (400 MHz, DMSO-d_6) δ= 7.44 − 7.51 (m, 2 H), 7.24 (m, *J*=8.3 Hz, 2 H), 2.31 (s, 3 H) ppm. ^{13}C NMR (101 MHz, DMSO-d_6) δ= 154.6 (s), 141.3 (s), 132.7 (t, *J* =32.2 Hz) 129.8 (d, *J* =17.6 Hz), 116.1 (s), 85.0 (s), 81.6 (s), 21.3 (q, *J* =25.0 Hz) ppm. IR (ATR) 2229, 2196, 1667, 1295, 1178 cm^{-1}. Anal. Calcd. for $C_{10}H_8O_2$: C, 75.0%; H, 5.0%. Found: C, 74.5%; H, 5.0%.

The spectroscopic data (NMR, IR) matched those reported in the literature for (4-methylphenyl)propynoic acid (**CCC-3m**) [CAS: 2227-58-9].

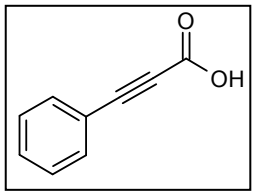

Synthesis of 3-phenyl-prop-2-ynoic acid (CCC-3n): Compound **CCC-3n** was prepared following the standard procedure, starting from phenyl acetylene (**CCC-1n**) (105 mg, 113 µL, 1.00 mmol) using 0.25 mol% of $AgBF_4$. After purification **CCC-3n** was isolated as a white solid (143 mg, 98%, m.p. 133.3 °C). ^{1}H NMR (400 MHz, DMSO-d_6) 7.56 − 7.64 (m, 2 H), 7.48 − 7.56 (m, 1 H), 7.39 − 7.48 (m, 2 H) ppm. ^{13}C NMR (101 MHz, DMSO-d_6) δ= 154.5 (s), 132.8 (s), 132.6 (s), 131.0 (s), 129.1 (s), 119.2 (s), 84.6 (s), 81.9 (s) ppm. IR (ATR) 2825, 2202, 1664, 1301, 1206 cm^{-1}. Anal. Calcd. for $C_9H_6O_2$: C, 74.0%; H, 4.1%. Found: C, 73.6%; H, 4.3%.

The spectroscopic data (NMR, IR) matched those reported in the literature for 3-phenyl-prop-2-ynoic acid (**CCC-3n**) [CAS: 637-44-5].

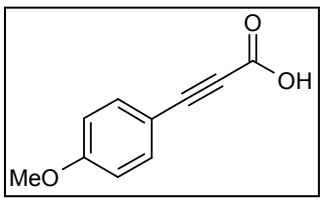

Synthesis of (4-methoxyphenyl)propynoic acid (CCC-3o): Compound **CCC-3o** was prepared following the standard procedure, starting from 1-eth-1-ynyl-4-methoxybenzene (**CCC-1o**) (136 mg, 134 µL, 1.00 mmol) using 0.25 mol% $AgBF_4$. After

purification **CCC-3o** was isolated as a white solid (177 mg, 99%, m.p. 140.8 °C). ^{1}H NMR (400 MHz, DMSO-d_6) δ= 7.51 − 7.58 (m, 2 H), 6.94 − 7.02 (m, 2 H), 3.78 (s, 3 H) ppm. ^{13}C NMR (101 MHz, DMSO-d_6) δ= 161.4 (s), 154.8 (s), 134.8 (d, *J*=16.9 Hz), 114.8 (d, *J*=38.2 Hz), 110.8 (s), 85.5 (s), 81.2 (s), 55.5 (d, *J*=47.0 Hz) ppm. IR (ATR) 2198, 1666, 1215, 1024, 831 cm^{-1}. Anal. Calcd. for $C_{10}H_8O_3$: C, 68.2%; H, 4.6%. Found: C, 68.1%; H, 4.5%.

The spectroscopic data (NMR, IR) matched those reported in the literature for (4-methoxy)propynoic acid (**CCC-3o**) [2227-57-8].

Synthesis of (2-methoxyphenyl)propynoic acid (CCC-3p): Compound **CCC-3p** was prepared following the standard procedure, starting from 1-eth-1-ynyl-2-methoxybenzene (**CCC-1p**) (136 mg, 133 µL, 1.00 mmol) using 0.25 mol% $AgBF_4$. After purification **CCC-3p** was isolated as a yellow solid (177 mg, 99%, m.p. 122.0 °C). ^{1}H NMR (600 MHz, methanol-d_4) δ= 7.40 − 7.48 (m, 2 H), 7.01 (d, *J*=8.5 Hz, 1 H), 6.94 (t, *J*=7.6 Hz, 1 H), 5.16 (br. s., 1 H), 3.86 (s, 3 H) ppm. ^{13}C NMR (151 MHz, methanol-d_4) δ= 163.0 (s), 157.1 (s), 135.8 (s), 133.8 (s), 121.7 (s), 112.3 (s), 110.0 (s), 85.8 (s), 84.2 (s), 56.4 (s) ppm. IR (ATR) 2199, 1660, 1490, 1251, 1198 cm^{-1}. Anal. Calcd. for $C_{10}H_8O_3$: C, 68.2%; H, 4.6%. Found: C, 68.2%; H, 4.8%. GC/HRMS-EI m/z [M^+] calcd. for $C_{10}H_8O_3$ 176.0473; found: 176.0474.

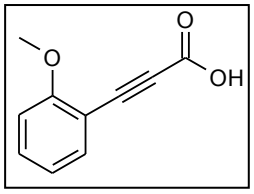

The spectroscopic data (NMR, IR) matched those reported in the literature for (4-methoxy)propynoic acid (**CCC-3p**) [7342-00-9].

Synthesis of (4-triflouromethylphenyl)-propynoic acid (CCC-3q): Compound **CCC-3q** was prepared following the standard procedure, starting from 4-ethynyl-a,a,a-trifluorotoluene (**CCC-1q**) (175 mg, 168 µL, 1.00 mmol) using 0.25 mol% $AgBF_4$. After purification **CCC-3q** was isolated as a white solid (210 mg, 98%, 151.7 °C). ^{1}H NMR (400 MHz, DMSO-d_6) δ= 7.78 (q, *J*=8.7 Hz, 4 H) ppm. ^{13}C NMR (101 MHz, DMSO-d_6) δ= 154.2 (s), 132.8 − 134.0 (m), 130.7 (q, *J*=32.3 Hz), 125.4 − 126.2 (m), 123.5 (s), 123.8 (q, *J*=272.3 Hz), 99.7 (s), 83.6 (s), 82.4 (s) ppm. IR (ATR) 2231, 2205, 1687, 1317, 1064 cm^{-1}. Anal. Calcd. for $C_{10}H_5F_3O_2$: C, 56.1%; H, 2.4%. Found: C, 55.9%; H, 2.6%.

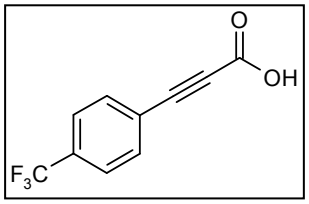

The spectroscopic data (NMR, IR) matched those reported in the literature for (4-triflouromethylphenyl)-propynoic acid (**CCC-3q**) [CAS: 3792-88-9].

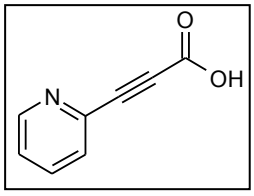

Synthesis of (pyridin-2-yl)propynoic acid (CCC-3r): Compound **CCC-3r** was prepared following the standard procedure, starting from pyridin-2-ylacetylene (**CCC-1r**) (105 mg, 103 µL, 1.00 mmol) using 0.25 mol% $AgBF_4$. After purification **CCC-3r** was isolated as a white solid (59.0 mg, 40%, m.p. 129.3 °C). ^{1}H NMR (600 MHz, methanol-d_4) δ= 8.61 (ddd, *J*=5.2, 1.7, 1.0 Hz, 1 H), 7.93 (td, *J*=7.8, 1.7 Hz, 1 H), 7.72 − 7.76 (m, 1 H), 7.53 (ddd, *J*=7.8, 4.9, 1.2 Hz, 1 H) ppm. ^{13}C NMR (151 MHz, methanol-d_4) δ= 155.8 (s), 151.4 (s), 141.4 (s), 139.0 (s), 130.3 (s), 126.7 (s), 83.5 (s), 81.4 (s) ppm. IR (ATR) 3079, 2215, 1687, 1432, 1221 cm^{-1}. GC/HRMS-EI m/z [M^+] calcd. for $C_8H_5NO_2$ 147.0320; found: 147.0315.

The spectroscopic data (NMR, IR) matched those reported in the literature for (pyridin-2-yl)propynoic acid (**CCC-3r**) [CAS: 858678-71-4].

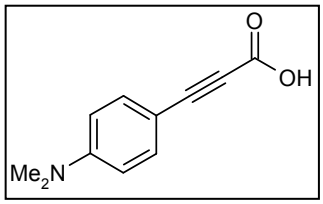

Synthesis of (4-dimethylamin)propynoic acid (CCC-3s): Compound **CCC-3s** was prepared following the standard procedure, starting from 4-ethynyl-*N*,*N*-dimethylaniline (**CCC-1s**) (145 mg, 1.00 mmol) using 0.25 mol% $AgBF_4$. After purification **CCC-3s** was isolated as a brown solid (181 mg, 96%, m.p. 87.9 °C). ^{1}H NMR (400 MHz, DMSO-d_6) δ= 7.40 (m, *J*=9.0 Hz, 2 H), 6.67 (m, *J*=9.0 Hz, 2 H), 2.94 (s, 6 H) ppm. ^{13}C NMR (101 MHz, DMSO-d_6) δ= 155.0 (s), 151.5 (s), 134.3 (s), 111.7 (s), 104.1 (s), 87.9 (s), 81.3 (s), 39.5 (br. s) ppm. IR (ATR) 2179, 1657, 1596, 1225, 819 cm^{-1}. GC/HRMS-EI m/z [M^+] calcd. for $C_{11}H_{11}NO_2$ 189.0790; found: 189.0788.

The spectroscopic data (NMR, IR) matched those reported in the literature for (4-dimethylamin)propynoic acid (**CCC-3s**) [CAS: 35283-06-8].

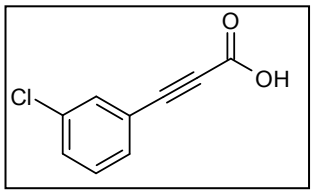

Synthesis of (3-chlorophenyl)propynoic acid (CCC-3t): Compound **CCC-3t** was prepared following the standard procedure, starting from 3-chloro-1-ethynylbenzene (**CCC-1t**) (141 mg, 127 µL, 1.00 mmol) using 0.25 mol% $AgBF_4$. After purification **CCC-3t** was isolated as a white solid (175 mg, 97%, m.p. 146.2 °C). ^{1}H NMR (400 MHz, DMSO-d_6) δ= 7.69 (t, *J*=1.9 Hz, 1 H), 7.55 − 7.62 (m, 2 H), 7.43 − 7.53 (m, 1 H) ppm. ^{13}C NMR (101 MHz, DMSO-d_6) δ= 154.1 (s), 133.6 (d, *J*=4.5 Hz), 132.2 (br. s.), 131.1 − 131.8 (m), 131.0 (br. s.), 130.6 (d, *J*=12.7 Hz), 121.1 (d, *J*=3.6 Hz), 82.6 (s), 82.5 (s) ppm. IR (ATR) 2214, 1670, 1295, 1203, 730 cm^{-1}. Anal. Calcd. for $C_9H_5ClO_2$: C, 59.9%; H, 2.8%. Found: C, 59.7%; H, 3.0%.

The spectroscopic data (NMR, IR) matched those reported in the literature for (2-methylphenyl)propynoic acid (**CCC-3t**) [CAS: 7396-28-3].

Synthesis of (4-chlorophenyl)propynoic acid (CCC-3u): Compound **CCC-3u** was prepared following the standard procedure, starting from 1-chloro-4-ethynylbenzene (**CCC-1u**) (139 mg, 1 mmol) using 0.25 mol% $AgBF_4$. After purification **CCC-3u** was isolated as a yellow solid (180 mg, 99%, m.p. 193.7 °C). ^{1}H NMR (400 MHz, DMSO-d_6) δ= 7.69 (t, *J*=1.9 Hz, 1 H), 7.55 − 7.62 (m, 2 H), 7.43 − 7.53 (m, 1 H) ppm. ^{13}C NMR (101 MHz, DMSO-d_6) δ= 154.1 (s), 133.6 (d), 132.2 (br. s.), 131.1 − 131.9 (m), 130.4 − 131.1 (m), 121.1 (d), 82.6 (s), 82.5 (s) ppm. IR (ATR) 2214, 1670, 1295, 1203, 730 cm^{-1}. Anal. Calcd. for $C_{15}H_{17}ClO_2$: C, 59.9%; H, 2.8%. Found: C, 59.7%; H, 3.0%.

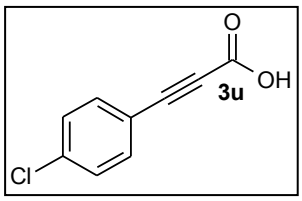

The spectroscopic data (NMR, IR) matched those reported in the literature for (4-chlorophenyl)propynoic acid (**CCC-3u**) [CAS: 3240-10-6].

Standard procedure for the carboxylation of terminal alkynes and transformation to the corresponding esters.

A vessel was charged with cesium carbonate (399 mg, 1.20 mmol). To this, a solution of silver tetrafluoroborate (0.1 mg, 0.50 µmol) in DMSO (0.1 mL) and DMSO (2.90 mL) were added. The reaction vessel was purged with CO_2 using 3 alternate cycles of vacuum and CO_2, and the alkyne (**CCC-1a**-**CCC-1u**) (1.00 mmol) was added *via* syringe. The resulting mixture was stirred for 16 h at 50 °C at ambient CO_2 pressure. Once the reaction time was completed, the crude mixture is treated with 1-bromohexane (337 mg, 282 µL, 2.00 mmol). After 30 min stirring at room temperature, the reaction mixture was diluted with H_2O (10.0 mL) and extracted with ethyl acetate (3 x 20.0 mL). The combined organic layers were washed with brine (10.0 mL), dried over $MgSO_4$, filtered and the volatiles were removed *in vacuo*. The residue was purified by column chromatography (SiO_2, ethyl acetate/*n*-hexane gradient), yielding the corresponding esters **CCC-4a** to **CCC-4u**.

Synthesis of 2-nonynoic acid hexyl ester (CCC-4a): Compound **CCC-4a** was prepared following the standard procedure, starting from 1-octyne (**1a**) (110 mg, 149 µL, 1.00 mmol). After purification **CCC-4a** was isolated as a colorless liquid (225 mg, 94%). ^{1}H NMR (400 MHz, $CDCl_3$) δ= 4.03 − 4.10 (m, 2 H), 2.25 (t, *J*=7.2 Hz 2 H), 1.55 − 1.63 (m, 2 H), 1.46 − 1.55 (m, 2 H), 1.31 (d, *J*=7.0 Hz 1 H), 1.20 − 1.28 (m, 9 H), 0.88 (t, *J*=6.9 Hz, 6 H) ppm. ^{13}C NMR (101 MHz,

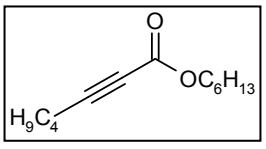

$CDCl_3$) δ= 153.8, 89.1, 73.0, 65.7, 31.2, 31.1, 28.4, 27.4, 25.3, 22.4, 22.3, 18.5, 13.8 ppm. IR (ATR) 2929, 2236, 1710, 1243, 1073 cm^{-1}. MS (Ion trap, EI): m/z (%) = 236 (3, [M^+]), 155 (100), 109 (22), 67 (49), 41 (35). Anal. Calcd. for $C_{15}H_{26}O_2$: C, 75.6%; H, 11.0%. Found: C, 75.4%; H, 10.7%.

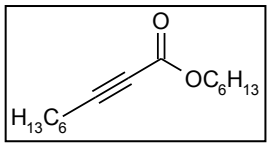

Synthesis of 2-octynoic acid hexyl ester (CCC-4b): Compound **CCC-4b** was prepared following the standard procedure, starting from 1-heptyne (**CCC-1b**) (98.1 mg, 134 µL, 1.00 mmol). After purification **CCC-4b** was isolated as a colorless liquid (227 mg, 99%). ^{1}H NMR (400 MHz, $CDCl_3$) δ= 4.12 (t, *J*=6.8 Hz, 2 H), 2.30 (t, *J*=7.2 Hz, 2 H), 1.51 − 1.71 (m, 4 H), 1.24 − 1.41 (m, 10 H), 0.81 − 0.93 (m, 6 H) ppm. ^{13}C NMR (101 MHz, $CDCl_3$) δ= 153.9 (s), 89.3 (s), 73.1 (s), 65.8 (s), 31.3 (s), 30.9 (s), 28.3 (s), 27.2 (s), 25.4 (s), 22.4 (s), 22.0 (s), 18.6 (s), 13.9 (s), 13.8 (s) ppm. MS (Ion trap, EI): m/z (%) = 224 (5, [M^+]), 141 (100), 123 (40), 95 (27), 67 (43). IR (ATR) 2931, 2235, 1709, 1244, 1077 cm^{-1}. Anal. Calcd. $C_{14}H_{24}O_2$: C, 75.0%; H, 10.8%. Found: C, 74.6%; H, 10.6%.

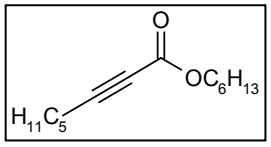

Synthesis of 2-heptynoic acid hexyl ester (CCC-4c): Compound **CCC-4c** was prepared following the standard procedure, starting from 1-hexyne (**CCC-1c**) (82.2 mg, 116 µL, 1.00 mmol). After purification **CCC-4c** was isolated as a colorless liquid (204 mg, 97%). ^{1}H NMR (400 MHz, $CDCl_3$) δ= 4.09 (t, *J*=6.8 Hz, 2 H), 2.28 (t, *J*=7.0 Hz, 2 H), 1.56 − 1.65 (m, 2 H), 1.46 − 1.56 (m, 2 H), 1.22 − 1.43 (m, 8 H), 0.80 − 0.90 (m, 6 H) ppm. ^{13}C NMR (101 MHz, $CDCl_3$) δ= 153.8 (s), 89.1 (s), 73.0 (s), 65.7 (s), 31.2 (s), 29.4 (s), 28.2 (s), 25.3 (s), 22.4 (s), 21.8 (s), 18.2 (s), 13.8 (s), 13.3 (s) ppm. IR (NaCl) 2959, 2237, 1713, 1248, 1078 cm^{-1}. MS (Ion trap, EI): m/z (%) = 210 (1, [M^+]), 127 (100), 127 (64), 109 (51), 79 (30). Anal. Calcd. for $C_{13}H_{22}O_2$: C, 74.2%; H, 10.5%. Found: C, 74.2%; H, 10.6%. GC/HRMS-EI m/z [M^+] calcd. for $C_{13}H_{22}O_2$ 216.1620; found: 216.1627.

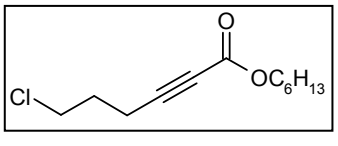

Synthesis of 6-chloro-hex-2-ynoic acid hexyl ester (CCC-4d): Compound **CCC-4d** was prepared following the standard procedure, starting from 5-chloropent-1-yne (**CCC-4d**) (105 mg, 109 µL, 1 mmol), using 0.25 mol% $AgBF_4$ and stirring for 16 h at 40 °C at ambient CO_2 pressure. After purification **CCC-4d** was isolated as a colorless liquid (120 mg, 52%). ^{1}H NMR (400 MHz, $CDCl_3$) δ= 4.13 (t, *J*=6.7 Hz, 2 H), 3.63 (t, *J*=6.2 Hz, 2 H), 2.53 (t, *J*=6.9 Hz, 2 H), 2.02 (quin, *J*=6.6 Hz, 2 H), 1.57 − 1.70 (m, 2 H), 1.23 − 1.39 (m, 6 H), 0.83 − 0.92 (m, 3 H) ppm. ^{13}C NMR (101 MHz, $CDCl_3$) δ= 153.6 (s), 86.9 (s), 73.8 (s), 66.0 (s), 43.1 (s),

31.3 (s), 30.2 (s), 28.3 (s), 25.4 (s), 22.4 (s), 16.0 (s), 13.9 (s) ppm. IR (ATR) 2930, 2239, 1707, 1245, 1079 cm^{-1}. MS (Ion trap, EI): m/z (%) = 230 (1, [M^+]), 129 (100), 111 (23), 69 (40), 56 (54). Anal. Calcd. for $C_{12}H_{19}ClO_2$: C, 62.5%; H, 8.3%. Found: C, 62.1%; H, 8.1%.

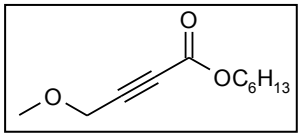

Synthesis of 4-methoxy-but-2-ynoic acid hexyl ester (CCC-4e): Compound **CCC-4e** was prepared following the standard procedure, starting from methylpropargylether (**CCC-1e**) (70.1 mg, 84.4 µL, 1.00 mmol) using 0.25 mol% $AgBF_4$. After purification **CCC-4e** was isolated as a colorless liquid (165 mg, 83%). ^{1}H NMR (400 MHz, $CDCl_3$) δ= 4.19 (s, 2 H), 4.14 (t, *J*=6.7 Hz, 2 H), 3.38 (s, 3 H), 1.59 − 1.67 (m, 2 H), 1.23 − 1.37 (m, 6 H), 0.83 − 0.89 (m, 3 H) ppm. ^{13}C NMR (101 MHz, $CDCl_3$) δ= 153.1 (s), 82.8 (s), 78.1 (s), 78.1 (s), 66.1 (s), 59.3 (s), 57.9 (s), 31.2 (s), 28.2 (s), 25.3 (s), 22.4 (s), 13.8 (s) ppm. IR (ATR) 2931, 2236, 1712, 1241, 1106 cm^{-1}. MS (Ion trap, EI): m/z (%) = 115 (35), 97 (99), 84 (33), 69 (100), 56 (78). Anal. Calcd. for $C_{11}H_{18}O_3$: C, 66.6%; H, 9.2%. Found: C, 66.2%; H, 9.1%.

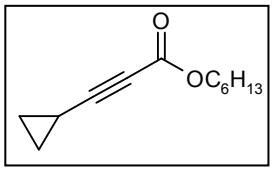

Synthesis of 3-cyclopropyl-prop-2-ynoic acid hexyl ester (CCC-4f): Compound **CCC-4f** was prepared following the standard procedure, starting from cyclopropylacetylene (**CCC-1f**) (68.1 mg, 1.00 mmol). After purification **CCC-4f** was isolated as a colorless liquid (189 mg, 97%). ^{1}H NMR (400 MHz, $CDCl_3$) δ= 4.12 (t, *J*=6.7 Hz, 2 H), 1.60 − 1.69 (m, 2 H), 1.25 − 1.41 (m, 7 H), 0.86 − 0.95 (m, 7 H) ppm. ^{13}C NMR (101 MHz, $CDCl_3$) δ= 153.9 (s), 93.0 (s), 68.5 (s), 65.8 (s), 31.3 (s), 28.4 (s), 25.4 (s), 22.5 (s), 13.9 (s), 9.1 (s) -0.6 (s) ppm. IR (ATR) 2931, 2225, 1704, 1251, 1182 cm^{-1}. MS (Ion trap, EI): m/z (%) = 194 (3, [M^+]), 111 (70), 93 (100), 65 (61), 41 (19). Anal. Calcd. for $C_{12}H_{18}O_2$: C, 74.2%; H, 9.3%. Found: C, 73.8%; H, 9.3%. GC/HRMS-EI m/z [M^+] calcd. for $C_{12}H_{18}O_2$ 194.1307; found: 194.1307.

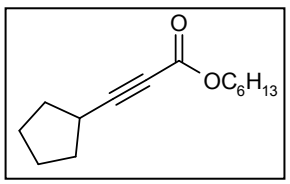

Synthesis of 3-cyclopentyl-prop-2-ynoic acid hexyl ester (CCC-4g): Compound **CCC-4g** was prepared following the standard procedure, starting from cyclopentylacetylene (**CCC-1g**) (99.1 mg, 122 µL, 1.00 mmol). After purification **CCC-4g** was isolated as a colorless liquid (222 mg, 99%). ^{1}H NMR (400 MHz, $CDCl_3$) δ= 4.12 (t, *J*=6.8 Hz, 2 H), 2.72 (quin, *J*=7.5 Hz, 1 H), 1.90 − 2.01 (m, 2 H), 1.54 − 1.77 (m, 8 H), 1.24 − 1.38 (m, 6 H), 0.84 − 0.91 (m, 3 H) ppm. ^{13}C NMR (101 MHz, $CDCl_3$) δ= 154.1 (s), 93.2 (s), 72.6 (s), 65.8 (s), 33.0 (s), 31.3 (s), 29.7 (s), 28.3 (s), 25.4 (s), 25.1 (s), 22.4 (s), 13.9 (s) ppm. IR 2956, 2230,

1707, 1243, 1088 cm^{-1}. MS (Ion trap, EI): m/z (%) = 220 (2, [M^+]), 139 (100), 121 (59), 91 (31), 77 (25). Anal. Calcd. for $C_{14}H_{22}O_2$: C, 75.6%; H, 10.0%. Found: C, 75.2%; H, 9.8%.

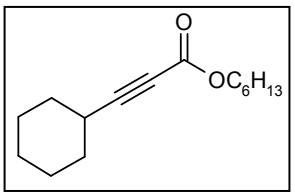

Synthesis of 3-cyclohexyl-prop-2-ynoic acid hexyl ester (CCC-4h): Compound **CCC-4h** was prepared following the standard procedure, starting from cyclohexylacetylene (**CCC-1h**) (110 mg, 133 µL, 1.00 mmol). After purification **CCC-4h** was isolated as a colorless liquid (220 mg, 93%). ^{1}H NMR (400 MHz, $CDCl_3$) δ= 4.14 (t, *J*=6.8 Hz, 2 H), 2.47 − 2.55 (m, 1 H), 1.78 − 1.92 (m, 2 H), 1.61 − 1.76 (m, 4 H), 1.45 − 1.58 (m, 3 H), 1.26 − 1.40 (m, 9 H), 0.86 − 0.93 (m, 3 H) ppm. ^{13}C NMR (101 MHz, $CDCl_3$) δ= 154.2 (s), 92.8 (s), 73.1 (s), 65.9 (s), 31.4 (s), 31.4 (s), 28.9 (s), 28.4 (s), 25.6 (s), 25.5 (s), 25.3 (s), 24.6 (s), 22.5 (s), 13.9 (s) ppm. IR (ATR) 2930, 2230, 1708, 1241, 1089 cm^{-1}. MS (Ion trap, EI): m/z (%) = 236 (5, [M^+]), 153 (100), 135 (43), 107 (19), 79 (33). Anal. Calcd. for $C_{15}H_{24}O_2$: C, 76.2%; H, 10.2%. Found: C, 76.2%; H, 10.3%. GC/HRMS-EI m/z [M^+] calcd. for $C_{15}H_{24}O_2$ 236.1776; found: 236.1782.

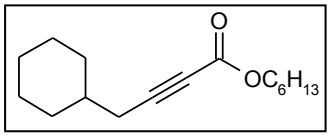

Synthesis of 4-cyclohexyl-2-butynoic acid hexyl ester (CCC-4i): Compound **CCC-4i** was prepared following the standard procedure, starting from 3-cyclohexyl-1-propyne (**CCC-1i**) (126 mg, 149 µL, 1.00 mmol). After purification **CCC-4i** was isolated as a colorless liquid (242 mg, 97%). ^{1}H NMR (400 MHz, $CDCl_3$) δ= 4.12 (t, *J*=6.8 Hz, 2 H), 2.20 (d, *J*=6.6 Hz, 2 H), 1.76 − 1.83 (m, 2 H), 1.51 − 1.74 (m, 6 H), 1.10 − 1.38 (m, 9 H), 0.94 − 1.07 (m, 2 H), 0.83 − 0.91 (m, 3 H) ppm. ^{13}C NMR (101 MHz, $CDCl_3$) δ= 153.9 (s), 88.4 (s), 74.0 (s), 65.8 (s), 36.6 (s), 32.6 (s), 31.3 (s), 28.3 (s), 26.3 (s), 25.9 (s), 25.9 (s), 25.4 (s), 22.4 (s), 13.9 (s) ppm. IR (ATR) 2924, 2234, 1709, 1242, 1075 cm^{-1}. MS (Ion trap, EI): m/z (%) = 250 (2, [M^+]), 167 (100), 149 (40), 84 (99), 55 (72). Anal. Calcd. for $C_{16}H_{26}O_2$: C, 76.8%; H, 10.5%. Found: C, 76.6%; H, 10.3%.

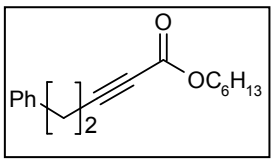

Synthesis of 5-phenyl-pent-2-ynoic acid hexyl ester (CCC-4j): Compound **CCC-4j** was prepared following the standard procedure, starting from 4-phenyl-1-butyne (**CCC-1j**) (133 mg, 144 µL, 1.00 mmol). After purification **CCC-4j** was isolated as a colorless liquid (270 mg, 99%). ^{1}H NMR (400 MHz, $CDCl_3$) δ= 7.09 − 7.24 (m, 5 H), 4.05 (t, *J*=6.7 Hz, 2 H), 2.80 (t, *J*=7.6 Hz, 2 H), 2.47 − 2.57 (m, 2 H), 1.49 − 1.63 (m, 2 H), 1.16 − 1.32 (m, 6 H), 0.75 − 0.87 (m, 3 H) ppm. ^{13}C NMR (101 MHz, $CDCl_3$) δ= 153.7 (s), 139.5 (s), 128.4 (s), 128.2 (s), 126.5 (s), 88.1 (s), 73.7 (s), 65.8 (s), 33.7 (s), 31.3 (s), 28.3 (s), 25.4 (s), 22.4 (s), 20.8 (s), 13.9 (s) ppm. IR

(ATR) 2930, 2236, 1707, 1244, 1070 cm^{-1}. MS (Ion trap, EI): m/z (%) = 258 (1, [M^+]), 174 (29), 157 (23), 129 (57), 91 (100). Anal. Calcd. for $C_{17}H_{22}O_2$: C, 79.0%; H, 8.6%. Found: C, 78.7%; H, 8.6%.

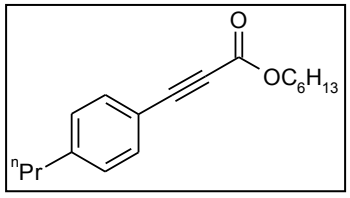

Synthesis of (4-propylphenyl)propynoic acid hexyl ester (CCC-4k): Compound **CCC-4k** was prepared following the standard procedure, starting from 1-ethynyl-4-propylbenzene (**CCC-1k**) (144 mg, 158 µL, 1.00 mmol) using 0.25 mol% $AgBF_4$. After purification **CCC-4k** was isolated as a yellow liquid (249 mg, 91%). ^{1}H NMR (400 MHz, $CDCl_3$) δ= 7.48 − 7.53 (m, 2 H), 7.16 − 7.20 (m, 2 H), 4.23 (t, *J*=6.8 Hz, 2 H), 2.58 − 2.63 (m, 2 H), 1.59 − 1.75 (m, 4 H), 1.28 − 1.44 (m, 6 H), 0.87 − 0.96 (m, 6 H) ppm. ^{13}C NMR (101 MHz, $CDCl_3$) δ= 154.3 (s), 145.9 (s), 132.9 (s), 128.7 (s), 116.7 (s), 86.6 (s), 80.3 (s), 66.1 (s), 66.1 (s), 38.0 (s), 31.3 (s), 28.4 (s), 25.4 (s), 24.1 (s), 22.5 (s), 13.9 (s), 13.9 (s), 13.6 (s) ppm. IR (ATR) 2930, 2216, 1705, 1286, 1168 cm^{-1}. MS (Ion trap, EI): m/z (%) = 272 (1, [M^+]), 188 (25), 171 (52), 144 (100), 115 (51). Anal. Calcd. for $C_{18}H_{24}O_2$: C, 79.4%; H, 8.9%. Found: C, 79.3%; H, 8.8%. GC/HRMS-EI m/z [M^+] calcd. for $C_{18}H_{24}O_2$ 272.1776; found: 272.1777.

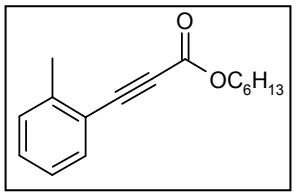

Synthesis of (2-methylphenyl)propynoic acid hexyl ester (CCC-4l): Compound **CCC-4l** was prepared following the standard procedure, starting from 2-ethynyltouluene (**CCC-1l**) (120 mg, 130 µL, 1.00 mmol) using 0.25 mol% $AgBF_4$. After purification **CCC-4l** was isolated as a yellow solid (244 mg, 99%, m.p. 94.0 °C). ^{1}H NMR (400 MHz, $CDCl_3$) δ= 7.52 − 7.57 (m, 1 H), 7.30 − 7.37 (m, 1 H), 7.15 − 7.27 (m, 2 H), 4.24 (t, *J*=6.7 Hz, 2 H), 2.50 (s, 3 H), 1.66 − 1.77 (m, 2 H), 1.29 − 1.47 (m, 7 H), 0.88 − 0.96 (m, 3 H) ppm. ^{13}C NMR (101 MHz, $CDCl_3$) δ= 154.3 (s), 142.2 (s), 133.3 (s), 130.5 (s), 129.7 (s), 125.7 (s), 119.5 (s), 85.1 (s), 84.4 (s), 66.2 (s), 31.4 (s), 28.4 (s), 25.5 (s), 22.5 (s), 20.5 (s), 14.0 (s) ppm. IR (ATR) 2929, 2214, 1706, 1274, 1179 cm^{-1}. MS (Ion trap, EI): m/z (%) = 244 (3, [M^+]), 160 (28), 143 (76), 115 (100), 89 (17). Anal. Calcd. for $C_{16}H_{20}O_2$: C, 78.7%; H, 8.3%. Found: C, 78.3%; H, 8.2%. GC/HRMS-EI m/z [M^+] calcd. for $C_{16}H_{20}O_2$ 244.1463; found: 244.1462.

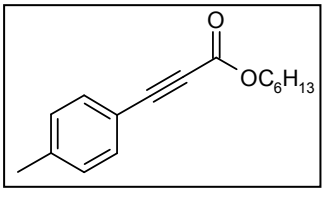

Synthesis of (4-methylphenyl)propynoic acid hexyl ester (CCC-4m): Compound **CCC-4m** was prepared following the standard procedure, starting from 4-ethynyltouluene (**CCC-1m**) (116 mg, 127 µL, 1.00 mmol) using 0.25 mol% $AgBF_4$. After purification **CCC-4m** was isolated as a colorless liquid (233 mg, 96%). ^{1}H NMR (400 MHz,

$CDCl_3$) δ= 7.45 (m, *J*=8.3 Hz, 2 H), 7.15 (m, *J*=7.8 Hz, 2 H), 4.20 (t, *J*=6.8 Hz, 2 H), 2.35 (s, 3 H), 1.62 − 1.83 (m, 2 H), 1.25 − 1.42 (m, 6 H), 0.83 − 0.94 (m, 3 H) ppm. ^{13}C NMR (101 MHz, $CDCl_3$) δ= 154.1 (s), 141.0 (s), 132.8 (s), 129.2 (s), 116.4 (s), 86.3 (s), 80.3 (s), 65.9 (s), 31.2 (s), 28.3 (s), 25.4 (s), 22.4 (s), 21.5 (s), 13.8 (s) ppm. IR (ATR) 2929, 2214, 1705, 1288, 1167 cm^{-1}. MS (Ion trap, EI): m/z (%) = 244 (1, [M^+]), 160 (55), 143 (100), 116 (82), 89 (16). Anal. Calcd. for $C_{16}H_{20}O_2$: C, 78.7%; H, 8.3%. Found: C, 78.5%; H, 8.1%. GC/HRMS-EI m/z [M^+] calcd. for $C_{16}H_{20}O_2$ 244.1463; found: 244.1460.

Synthesis of 3-phenyl-prop-2-ynoic acid hexyl ester (CCC-4n): Compound **CCC-4n** was prepared following the standard procedure, starting from phenyl acetylene (**CCC-1n**) (105 mg, 113 µL, 1.00 mmol) using 0.25 mol% of $AgBF_4$. After purification **CCC-4n** was isolated as a colorless liquid (210 mg, 91%). ^{1}H NMR (400 MHz, $CDCl_3$) δ= 7.53 − 7.60 (m, 2 H), 7.32 − 7.44 (m, 3 H), 4.21 (t, *J*=6.7 Hz, 2 H), 1.62 − 1.76 (m, 2 H), 1.25 − 1.42 (m, 6 H), 0.79 − 0.94 (m, 3 H) ppm. ^{13}C NMR (101 MHz, $CDCL_3$) δ= 154.0 (s), 132.8 (s), 130.4 (s), 128.4 (s), 119.5 (s), 85.8 (s), 80.6 (s), 66.0 (s), 31.3 (s), 28.3 (s), 25.4 (s), 22.4 (s), 13.9 (s) ppm. IR (NaCl) 2931, 2221, 1709, 1286, 1188 cm^{-1}. MS (Ion trap, EI): m/z (%) = 230 (1, [M^+]), 146 (31), 129 (100), 102 (69), 75 (18). Anal. Calcd. for $C_{15}H_{18}O_2$: C, 78.2%; H, 7.9%. Found: C, 77.9%; H, 7.9%.

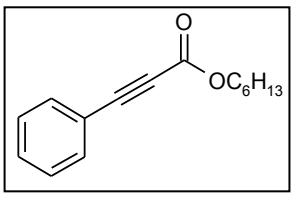

Synthesis of (4-methoxy)propynoic acid hexyl ester (CCC-4o): Compound **CCC-4o** was prepared following the standard procedure, starting from 1-eth-1-ynyl-4-methoxybenzene (**CCC-1o**) (136 mg, 134 µL, 1.00 mmol) using 0.25 mol% $AgBF_4$. After purification **CCC-4o** was isolated as a colorless liquid (249 mg, 96%). ^{1}H NMR (400 MHz, $CDCl_3$) δ= 7.45 − 7.52 (m, 2 H), 6.80 − 6.87 (m, 2 H), 4.18 (t, *J*=6.8 Hz, 2 H), 3.78 (s, 3 H), 1.61 − 1.71 (m, 2 H), 1.23 − 1.40 (m, 6 H), 0.80 − 0.92 (m, 3 H) ppm. ^{13}C NMR (101 MHz, $CDCl_3$) δ= 161.3 (s), 154.2 (s), 134.7 (s), 114.1 (s), 111.2 (s), 86.6 (s), 80.0 (s), 65.8 (s), 55.1 (s), 31.2 (s), 28.3 (s), 25.3 (s), 22.4 (s), 13.8 (s) ppm. IR (ATR) 2931, 2210, 1701, 1509, 1160 cm^{-1}. MS (Ion trap, EI): m/z (%) = 260 (4, [M^+]), 176 (17), 132 (100), 116 (11), 62 (5). Anal. Calcd. for $C_{16}H_{20}O_3$: C, 73.8%; H, 7.7%. Found: C, 73.8%; H, 7.8%.

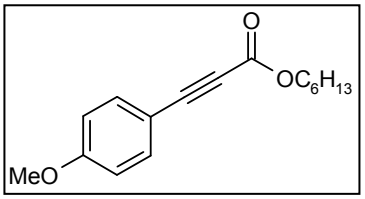

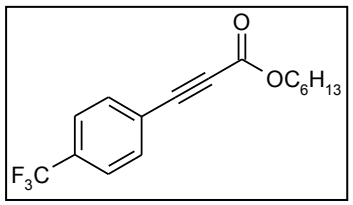

Synthesis of (4-triflouromethylphenyl)-propynoic acid hexyl ester (CCC-4q): Compound **CCC-4q** was prepared following the standard procedure, starting from 4-ethynyl-a,a,a-trifluorotoluene (**CCC-1q**) (175 mg, 168 µL, 1.00 mmol) using 0.25 mol% $AgBF_4$. After purification **CCC-4q** was isolated as a colorless liquid (298 mg, 99%). ^{1}H NMR (400 MHz, $CDCl_3$) δ= 7.58 − 7.69 (m, 4 H), 4.23 (t, *J*=6.8 Hz, 2 H), 1.62 − 1.74 (m, 2 H), 1.25 − 1.43 (m, 6 H), 0.81 − 0.93 (m, 3 H) ppm. ^{13}C NMR (101 MHz, $CDCl_3$) δ= 153.6 (s), 133.0 (s), 132.0 (q, *J*=33.0 Hz), 125.4 (q, *J*=4.2 Hz), 123.5 (d, *J*=1.5 Hz), 124.8 (t, *J*=272.3 Hz), 83.6 (s), 82.3 (s), 66.4 (s), 31.3 (s), 28.3 (s), 25.4 (s), 22.4 (s), 13.8 (s) ppm. IR (ATR) 2933, 2229, 1710, 1321, 1066 cm^{-1}. MS (Ion trap, EI): m/z (%) = 215 (30), 197 (100), 170 (35), 69 (15), 56 (19). Anal. Calcd. for $C_{16}H_{17}F_3O_2$: C, 64.4%; H, 5.7%. Found: C, 64.3%; H, 5.8%.

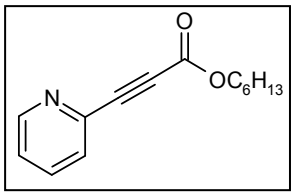

Synthesis of (pyridin-2-yl)propynoic acid hexyl ester (CCC-4r): Compound **CCC-4r** was prepared following the standard procedure, starting from pyridin-2-ylacetylene (**CCC-1r**) (105 mg, 103 µL, 1.00 mmol) using 0.25 mol% $AgBF_4$. After purification **CCC-4r** was isolated as a yellow liquid (212 mg, 92%). ^{1}H NMR (400 MHz, $CDCl_3$) δ= 8.53 − 8.58 (m, 1 H), 7.66 (td, *J*=7.8, 1.8 Hz, 1 H), 7.50 (d, *J*=7.8 Hz, 1 H), 7.28 (ddd, *J*=7.7, 4.9, 1.3 Hz, 1 H), 4.15 (t, *J*=6.8 Hz, 2 H), 1.52 − 1.66 (m, 2 H), 1.17 − 1.34 (m, 6 H), 0.75 − 0.85 (m, 3 H) ppm. ^{13}C NMR (101 MHz, $CDCl_3$) δ= 153.3 (s), 150.2 (s), 140.2 (s), 136.1 (s), 128.3 (s), 124.4 (s), 83.5 (s), 78.9 (s), 66.2 (s), 31.1 (s), 28.1 (s), 25.2 (s), 22.2 (s), 13.7 (s) ppm. IR (ATR) 2930, 2229, 1707, 1279, 1191 cm^{-1}. MS (Ion trap, EI): m/z (%) = 231 (1, [M^+]), 148 (31), 130 (100), 103 (35), 78 (20). Anal. Calcd. for $C_{14}H_{17}NO_2$: C, 72.7%; H, 7.4%; N, 6.1%. Found: C, 72.4%; H, 7.4%; N, 6.0%. GC/HRMS-EI m/z [M^+] calcd. for $C_{14}H_{17}NO_2$ 231.1259; found: 231.1254.

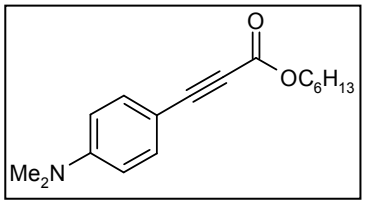

Synthesis of (4-dimethylamin)propynoic acid hexyl ester (CCC-4s): Compound **CCC-4s** was prepared following the standard procedure, starting from 4-ethynyl-*N*,*N*-dimethylaniline (**CCC-1s**) (145 mg, 1.00 mmol) using 0.25 mol% $AgBF_4$. After purification **CCC-4s** was isolated as a red liquid (259 mg, 95%). ^{1}H NMR (400 MHz, $CDCl_3$) δ= 7.38 − 7.46 (m, 2 H), 6.53 − 6.61 (m, 2 H), 4.18 (t, *J*=6.7 Hz, 2 H), 2.97 (s, 6 H), 1.68 (dd, *J*=8.3, 6.7 Hz, 2 H), 1.25 − 1.42 (m, 6 H), 0.83 − 0.94 (m, 3 H) ppm. ^{13}C NMR (101 MHz, $CDCl_3$) δ= 154.6 (s), 151.3 (s), 134.5 (s), 111.2 (s), 104.9 (s), 89.3

(s), 80.0 (s), 65.6 (s), 39.7 (s), 31.2 (s), 28.3 (s), 25.3 (s), 22.3 (s), 13.8 (s) ppm. IR (ATR) 2928, 2192, 1695, 1601, 1148 cm^{-1}. MS (Ion trap, EI): m/z (%) = 273 (44, [M^+]), 188 (17), 172 (44), 145 (100), 77 (4). Anal. Calcd. for $C_{17}H_{23}NO_2$: C, 74.7%; H, 8.5%; N, 5.1%. Found: C, 74.3%; H, 8.4%; N, 5.2%.

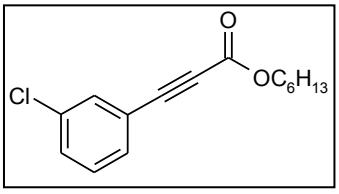

Synthesis of (3-chlorophenyl)propynoic acid hexyl ester (CCC-4t): Compound **CCC-4t** was prepared following the standard procedure, starting from 3-chloro-1-ethynylbenzene (**CCC-1t**) (141 mg, 127 µL, 1.00 mmol) using 0.25 mol% $AgBF_4$. After purification **CCC-4t** was isolated as a colorless liquid (263 mg, 99%). ^{1}H NMR (400 MHz, $CDCl_3$) δ= 7.56 (t, *J*=1.9 Hz, 1 H), 7.39 − 7.49 (m, 2 H), 7.26 − 7.36 (m, 1 H), 4.23 (t, *J*=6.7 Hz, 2 H), 1.62 − 1.76 (m, 2 H), 1.27 − 1.44 (m, 6 H), 0.83 − 0.95 (m, 3 H) ppm. ^{13}C NMR (101 MHz, $CDCl_3$) δ= 153.8 (s), 134.4 (s), 132.6 (s), 130.9 (s), 130.8 (s), 129.8 (s), 121.4 (s), 84.0 (s), 81.4 (s), 66.3 (s), 31.3 (s), 28.3 (s), 25.4 (s), 22.5 (s), 13.9 (s) ppm. IR 2930, 2223, 1707, 1285, 1180 cm^{-1}. MS (Ion trap, EI): m/z (%) = 264 (4, [M^+]), 181 (25), 153 (100), 152 (10), 135 (27). Anal. Calcd. for $C_{15}H_{17}ClO_2$: C, 68.1%; H, 6.5%. Found: C, 67.9%; H, 6.6%.

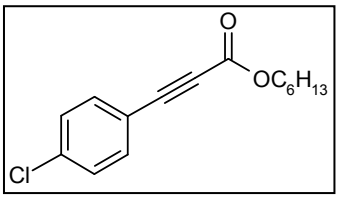

Synthesis of (4-chlorophenyl)propynoic acid hexyl ester (CCC-4u): Compound **CCC-4u** was prepared following the standard procedure, starting from 1-chloro-4-ethynylbenzene (**CCC-1u**) (139 mg, 1 mmol) using 0.25 mol% $AgBF_4$. After purification **CCC-4u** was isolated as a yellow liquid (255 mg, 96%). ^{1}H NMR (400 MHz, $CDCl_3$) δ= 7.48 − 7.56 (m, 2 H), 7.32 − 7.39 (m, 2 H), 4.23 (t, *J*=6.8 Hz, 2 H), 1.59 − 1.76 (m, 2 H), 1.27 − 1.44 (m, 6 H), 0.86 − 0.95 (m, 3 H) ppm. ^{13}C NMR (101 MHz, $CDCl_3$) δ= 154.0 (s), 137.0 (s), 134.1 (s), 129.0 (s), 118.1 (s), 84.7 (s), 81.5 (s), 66.4 (s), 31.4 (s), 28.4 (s), 25.5 (s), 22.5 (s), 14.0 (s) ppm. IR (ATR) 2930, 2221, 1705, 1284, 1184 cm^{-1}. MS (Ion trap, EI): m/z (%) = 264 (1, [M^+]), 180 (60), 163 (100), 136 (94), 99 (16). Anal. Calcd. for $C_{15}H_{17}ClO_2$: C, 68.1%; H, 6.5%. Found: C, 68.1%; H, 6.6%. GC/HRMS-EI m/z [M^+] calcd. for $C_{15}H_{17}ClO_2$ 264.0917; found: 264.0918.

Synthesis of acetylendicarboxylic acid (IV.2-6) via carboxylation of acetylene

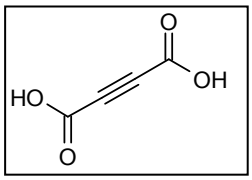

A oven-dried flask was charged with Cs_2CO_3 (5.61 g, 16.9 mmol) and $AgBF_4$ (0.70 mg, 3.50 µmol) and a stirring bar was added. The atmosphere was exchange

two times with alternating vacuum-nitrogen cycles and one time with an alternating vacuum-CO_2 cycle. Then DMSO (15.0 mL) was added *via* syringe and the stirring suspension was saturated with CO_2 (**IV.2-2**) *via* two alternating vacuum-CO_2 cycle. A 1500 mL gas tank containing a 1:2 acetylene (**IV.2.7**) and CO_2 (**IV.2-2**) mixture was connected to the flask. The suspension was saturated one last time with an alternating vacuum-acetylene/CO_2 cycle and stirred for 40 h at 50 °C. During this period 1200 mL of the gas mixture were consumed.

After cooling down to room temperature the resulting crude was filtered and washed with acetonitrile (3 x 10.0 mL). The solid was dissolved in water (5.00 mL) under ice-bath cooling and acidified to pH < 1 with H_2SO_4. The aqueous layer was saturated with NaCl and extracted with ethyl acetate (4 x 50.0 mL). The organic layer was dried over $MgSO_4$ and the solvent was removed under reduced pressure yielding the product as a white solid (250 mg, 2.19 mmol, TON = 1244, m.p. 170.0 °C).

^{1}H NMR (600 MHz, MeOD) δ= 5.34 (s, 2H) ppm. ^{13}C NMR (151 MHz, MeOD) δ= 152.9 (s), 74.5 (s) ppm.

The spectroscopic data (NMR) matched those reported in the literature for acetylendicarboxylic acid [CAS: 142-45-0].[64]

VI.6. Literatur des experimentellen Teils

[48] D. D. Perrin, W. L. F. Armarego, D. R. Perrin, *Purification of Laboratory Chemicals 2nd Ed.* Pergamon Press, Oxford **1980**.

[49] L. J. Gooßen, M. Blanchot, C. Brinkmann, K. Gooßen, R. Karch, A. Rivas-Nass, *J. Org. Chem.* **2006**, *71*, 9506–9509.

[50] Gaussian 03, Revision E.01, Frisch, M. J.; Trucks, G. W.; Schlegel, H. B.; Scuseria, G. E.; Robb, M. A.; Cheeseman, J. R.; Montgomery, Jr., J. A.; Vreven, T.; Kudin, K. N.; Burant, J. C.; Millam, J. M.; Iyengar, S. S.; Tomasi, J.; Barone, V.; Mennucci, B.; Cossi, M.; Scalmani, G.; Rega, N.; Petersson, G. A.; Nakatsuji, H.; Hada, M.; Ehara, M.; Toyota, K.; Fukuda, R.; Hasegawa, J.; Ishida, M.; Nakajima, T.; Honda, Y.; Kitao, O.; Nakai, H.; Klene, M.; Li, X.; Knox, J. E.; Hratchian, H. P.; Cross, J. B.; Bakken, V.; Adamo, C.; Jaramillo, J.; Gomperts, R.; Stratmann, R. E.; Yazyev, O.; Austin, A. J.; Cammi, R.; Pomelli, C.; Ochterski, J. W.; Ayala, P. Y.; Morokuma, K.; Voth, G. A.; Salvador, P.; Dannenberg, J. J.; Zakrzewski, V. G.; Dapprich, S.; Daniels, A. D.; Strain, M. C.; Farkas, O.; Malick, D. K.; Rabuck, A. D.; Raghavachari, K.; Foresman, J. B.; Ortiz, J. V.; Cui, Q.; Baboul, A. G.; Clifford, S.; Cioslowski, J.; Stefanov, B. B.; Liu, G.; Liashenko, A.; Piskorz, P.; Komaromi, I.; Martin, R. L.; Fox, D. J.; Keith, T.; Al-Laham, M. A.; Peng, C. Y.; Nanayakkara, A.; Challacombe, M.; Gill, P. M. W.; Johnson, B.; Chen, W.; Wong, M. W.; Gonzalez, C.; Pople, J. A. Gaussian, Inc., Wallingford CT, **2004**.

[51] Gaussian 09, Revision A.02, Frisch, M. J.; Trucks, G. W.; Schlegel, H. B.; Scuseria, G. E.; Robb, M. A.; Cheeseman, J. R.; Scalmani, G.; Barone, V.; Mennucci, B.; Petersson, G. A.; Nakatsuji, H.; Caricato, M.; Li, X.; Hratchian, H. P.; Izmaylov, A. F.; Bloino, J.; Zheng, G.; Sonnenberg, J. L.; Hada, M.; Ehara, M.; Toyota, K.; Fukuda, R.; Hasegawa, J.; Ishida, M.; Nakajima, T.; Honda, Y.; Kitao, O.; Nakai, H.; Vreven, T.; Montgomery, Jr., J. A.; Peralta, J. E.; Ogliaro, F.; Bearpark, M.; Heyd, J. J.; Brothers, E.; Kudin, K. N.; Staroverov, V. N.; Kobayashi, R.; Normand, J.; Raghavachari, K.; Rendell, A.; Burant, J. C.; Iyengar, S. S.; Tomasi, J.; Cossi, M.; Rega, N.; Millam, J. M.; Klene, M.; Knox, J. E.; Cross, J. B.; Bakken, V.; Adamo, C.; Jaramillo, J.; Gomperts, R.; Stratmann, R. E.; Yazyev, O.; Austin, A. J.; Cammi, R.; Pomelli, C.; Ochterski, J. W.; Martin, R. L.; Morokuma, K.; Zakrzewski, V. G.; Voth, G. A.; Salvador, P.; Dannenberg, J. J.; Dapprich, S.; Daniels, A. D.; Farkas, O.; Foresman, J. B.; Ortiz, J. V.; Cioslowski, J.; Fox, D. J. Gaussian, Inc., Wallingford CT, **2009**.

[52] (a) C. Lee, W. Yang, R. G. Parr, *Phys. Rev. B* **1988**, *37*, 785–789. (b) A. D. Becke, *J. Chem. Phys.* **1993**, *98*, 5648–5652. (c) P. J. Stephens, J. F. Devlin, C. F. Chabalowski, M. J. Frisch, *J. Phys. Chem.* **1994**, *98*, 11623–11627.

[53] P. C. Hariharan, J. A. Pople, *Theor. Chim. Acta* **1973**, *28*, 213–222

[54] D. Andrae, U. Häußermann, M. Dolg, H. Stoll, H. Preuss, *Theor. Chim. Acta* **1990**, *77*, 123–141.

[55] M. W. Wong, *Chem. Phys. Lett.* **1996**, *256*, 391–399.

[56] R. Krishnan, J. S. Binkley, R. Seeger, J. A. Pople, *J. Chem. Phys.* **1980**, *72*, 650–654.

[57] GaussView 5.0.8, Gaussian, Inc., Wallingford CT, **2008**.

[58] A. Bayer, M. E. Maier, *Tetrahedron* **2004**, *60*, 6665–6677.

[59] CCDC 768748 contains the supplementary crystallographic data for this paper. These data can be obtained free of charge from The Cambridge Crystallographic Data Centre via www.ccdc.cam.ac.uk/data_request/cif.

[60] CCDC 768747 contains the supplementary crystallographic data for this paper. These data can be obtained free of charge from The Cambridge Crystallographic Data Centre via www.ccdc.cam.ac.uk/data_request/cif.

[61] M. R. Rao, D. J. Faulkner, *J. Nat. Prod.* **2004**, *67*, 1064–1066.

[62] L. A. McDonald, J. C. Swersey, C. M. Ireland, *Tetrahedron* **1995**, *51*, 5237–5244.

[63] J. Pietruszka, A. Witt, *Synthesis* **2006**, *24*, 4266–4268.

[64] R. I. Gelb, L. M. Schwartz, D. A. Laufer, *J. Am. Chem. Soc.* **1981**,*103*, 5664–5673.

VII. Curriculum vitae

Schulbildung

08.06.2012	Doktor der Naturwissenschaften, Gesamtnote: ausgezeichnet
Feb. 2009 – Jun. 2012	Promotionsstudium im Arbeitskreis von Prof. Dr. L. J. Gooßen (Technischen Universität Kaiserslautern)
Feb. 2009 − Jan. 2011	Stipendium nach dem Landesgraduiertenförderungsgesetz (LGFG)
01.09.2008	Diplom in Chemie, Gesamtnote: sehr gut (1,1): • Steinhoferpreis des Fachbereichs Chemie der Technischen Universität Kaiserslautern für Jahrgangsbeste
Dez. 2007 − Sep. 2008	Diplomarbeit im Arbeitskreis von Prof. Dr. L. J. Gooßen (Technische Universität Kaiserslautern): *"Entwicklung eines Ruthenium-trichloridhydrat basierten Katalysators für die Addition von N-Nucleophilen an Alkine"*
Apr. − Jun. 2007	Auslandsaufenthalt, Forschungspraktikum im Rahmen des Sokrates/Erasmus-Programms an der University of Glasgow, im Arbeitkreis von Prof. Dr. P. Kočovský
26.08.2005	Abschluss des Vordiploms (sehr gut): • Procter&Gamble Förderpreis 2005 für bestes Vordiplom • Jahresabo von Wiley-VCH “Chemie in unserer Zeit“
Okt. 2003 − Sep. 2008	Chemiestudium an der Technischen Universität Kaiserslautern
Jul. 2002 − Apr. 2003	Zivildienst: Ambulante Dienste im Heinrich-Haus (Neuwied)
1993 − 2002	Werner-Heisenberg-Gymnasium (Neuwied). Abschluss: Abitur, Gesamtnote: 1,7

Berufserfahrung

Feb. 2009 − Apr. 2012	Wissenschaftlicher Mitarbeiter (TU Kaiserslautern) im Arbeitskreis von Prof. Dr. L. J. Gooßen
Sep. 2008 − Jan. 2009	Industriepraktikum in der Medizinischen Chemie bei Merck KGaA (Darmstadt)
Apr. 2002 − Okt. 2005	Ferienbeschäftigter bei der Rasselstein GmbH (Andernach) im Team TPA-Veredelung 1 und im Team Energie und Umwelt